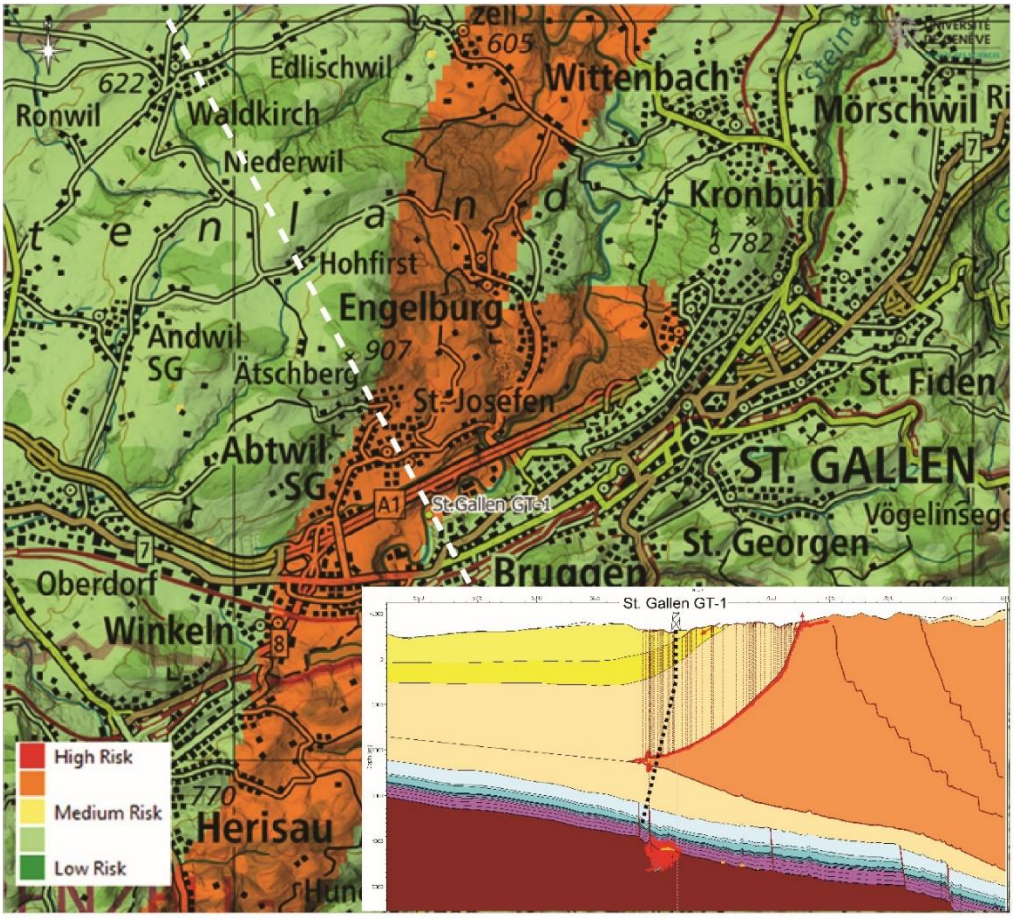
Final report dated 19.08.2025

UNCONGEO

Evaluation of the risk for the geothermal exploration associated with the presence of hydrocarbons in the subsurface of the Swiss Plateau



Source: This report

Date: 19.08.2025

Location: Bern

Publisher:
Swiss Federal Office of Energy SFOE
Energy Research and Cleantech
CH-3003 Bern
www.bfe.admin.ch

Co-financed by:
Federal Office of Topography, Swisstopo,
Seftigenstrasse 264
CH-3084 Berne
www.swisstopo.ch

Etat de Genève, Département du territoire
Rue de l'Hôtel-de-Ville, 14
CH-1204 Genève
www.ge.ch

Etat de Vaud, Direction générale de l'environnment
Rue du Valentin 10
CH-1015
www.vd.ch

NAGRA, Nationale Genossenschaft für die Lagerung radioaktiver Abfälle
Hardstrasse 73,
CH-5430 Wettingen
www.nagra.ch

Agent:
Department of Earth Sciences, University of Geneva
CH-1205 Genève
http://www.unige.ch/sciences/terre/en/

Authors:
Silvia Omodeo Salé, University of Geneva, silvia.omodeosale@unige.ch
Yasin Makhloufi, University of Geneva, yasin.makhloufi@unig.ch
Ovie Emmanuel Eruteya, University of Geneva, ovie.eruteya@unige.ch
Andrea Moscariello, University of Geneva, andrea.moscariello@unige.ch

SFOE project coordinators:
Christian Minnig, christian.minnig@bfe.admin.ch;
Florence Bégué, Florence.begue@bfe.admin.ch
SFOE contract number: SI/501536-01

The author of this report bears the entire responsibility for the content and for the conclusions drawn there from Zusammenfassung

Summary

In sedimentary basins, geothermal resources often coexist with hydrocarbon fluids that can represent a risk to geothermal exploration. Unexpected occurrence of substantial amounts of hydrocarbons could delay, or even halt drilling operations and damage the social perception of deep geothermal exploration activities. Geothermal exploration projects therefore need to be supported by a full understanding of the evolution of the sedimentary basin and specifically the generation, migration, accumulation, preservation potential and physical properties of hydrocarbon fluids. Resolving the origin of possible hydrocarbons alongside evaluating the processes controlling the active petroleum system(s) in the area targeted for geothermal exploration is therefore key.

The Swiss Plateau, part of the more extensive Northern Alpine foreland basin (NAFB), is characterised by widespread occurrences of hydrocarbon seepages, which attest to a complex active petroleum system characterised by multiple plays. Since the last century, oil and gas indications have been regularly found as seepages in deep and shallow wells drilled throughout the Plateau. Nevertheless, in most cases, hydrocarbons have not been found in economically attractive quantities (the exception being, the only short-lived gas field found in the Entlebuch-1 well). Thus, over time, Switzerland has been excluded as a potential hydrocarbon exploration region. However, the geothermal wells drilled during the last twenty years have encountered some oil and gas (e.g. Schlattingen-1; St Gallen; GEo-01; etc.), which in some cases have had both short and long-term negative economic and social impacts on the geothermal exploration projects, both locally and nationally.

Objective 1 of the UNCONGEO project is to evaluate the presence and potential distribution of hydrocarbons in the subsurface of the Swiss Plateau region. To achieve this objective, the first essential step was to understand the active petroleum system in the Swiss Plateau. This required the identification, characterization and quantification of the elements and processes controlling the generation, expulsion, accumulation and preservation of oil and gas in the subsurface through the study area.

The petroleum system of the basin was investigated using the well-established industry-standard thermal and petroleum system modelling approach. A large regional basin analysis study aimed at reconstructing the thermal and structural history of the basin, thus the thermal maturity of the hydrocarbon source rocks was carried out first. In this context, the main variables controlling the temperature reached by the basin infill over time were identified and quantified when possible. The latter are the paleo-heat flow, the sedimentary lithology and facies distribution, the burial history, and the magnitude and timing associated with the most relevant structural and erosional events. Secondly, the timing of the hydrocarbon generation and expulsion was reconstructed and the areas where migration and accumulation are most likely to occur were identified using industry-standard modelling software.

Constraints on the project work and deliverables were dictated by the complexity of the geological system of the Swiss Plateau, the data availability, the computational capacity and the available time for this study. The petroleum system analyses were, thus, carried out along a series of 2D regional geological sections. However, the generation, expulsion migration, and accumulation of hydrocarbons are controlled by the three-dimensional geometry, distribution, and modification of each petroleum system element over time. Therefore, the results of 2D modelling are strongly limited by a non-realistic representation of the subsurface complexity and petroleum system processes, especially regarding the analysis of migration routes and shapes and locations of possible hydrocarbon traps.

The thermal/petroleum system modelling workflow encompasses the construction of a geological model, which defines the thickness and geometry of the main stratigraphic units. Five 2D models were constructed, based on five regional geological sections, representative of the structure and stratigraphy of the Swiss Plateau. The ages of depositional and erosional events, the lithology and facies of each unit, and the geochemical properties of the potential hydrocarbon source rocks were used as input for the models. Finally, the boundary conditions that control the heat transfer in the basin, the sediment-water interface temperature and the basal heat flow, were assigned to the model.

Thermal modelling was used to calculate the timing of maturation for the main source rocks: the Posidonia Black Shales (Toarcian), which are located both in the immature and oil window thermal conditions, the Autunian shales (Permian) and the Carboniferous coal and shales (Carboniferous in age) which are in the wet and dry gas windows. Where available, calibration data (such as borehole temperature, porosity and vitrinite reflectance) were used to validate the modelling results. For each section, the generation, migration and accumulation processes, and relative timing concerning the structural trap development, were simulated through geological time, defining the areas with the highest probability of encountering hydrocarbons. Hydrocarbons generated by the Posidonia shale source rock (mostly oil) generally accumulated in Upper Jurassic and/or Cretaceous units, migrating along faults and accumulating in structural traps formed in the latest Alpine deformation phases. Hydrocarbons generated by the Permian and Carboniferous source rocks (mostly gas) accumulated in upper Permian and lower Mesozoic sandy deposits (mainly Buntsandstein, Muschelkalk units). Hydrocarbons mostly migrated along deep faults, extensional/trastensional faults reactivated during the Alpine collision, connecting the Permo-Carboniferous grabens to the Mesozoic cover, and they were sealed by the evaporitic Triassic units. Several hydrocarbon migration pathways formed in the Mesozoic and Cenozoic (Molasse) units, mainly along faults, mostly normal and transfer faults, and permeable lithologies.

The petroleum system models reconstructed in this study are based on several assumptions. Subsurface data are scarce and scattered throughout the basin. Interpolation and/or extrapolation of data has been necessary. Therefore, uncertainties in the results presented in this study must be considered. The most relevant uncertainties in terms of their impact on the modelling outcomes are the following: i) distribution and properties of the source rocks, especially of the Permian and Carboniferous deposits, which is barely known; ii) fault location, geometry, activity timing and sealing properties (i.e. degree of cementation, juxtaposition, transmissibility, etc.); iii) porosity and permeability properties throughout the entire basin; iv) geometry of the basin (traps); v) lithology and sedimentary facies distribution of both source, reservoir and seal rocks throughout the entire basin; vi) geochemical properties of the hydrocarbon source rocks; vii) timing of thrusting phase(s); viii) magnitude and timing of syn and post-orogenic erosion.

Objective 2 of the UNCONGEO project is to evaluate the risk associated with the presence of hydrocarbons in the subsurface throughout the entire Plateau and graphically represent it in Common Risk Segment (CRS) maps. CRS maps illustrate the spatial distribution of geological risk associated with a "working petroleum system" within a wider active Petroleum Play.These maps aim to define the likelihood of encountering hydrocarbon accumulation in the Swiss Plateau where a future deep (> 0.5 km) geothermal well could be drilled. The definition of “risk”, as it is intended throughout the text of this report, explicitly refers to the likelyhood of encountering hydrocarbons in the subsurface. In the past 80 years of subsurface exploration, in Switzerland, occurrences of hydrocarbon proved to be small. Therefore, the word “risk” in this report does not by any means translate into the overall risk that a geothermal project might have if located in a zone defined “medium/high risk” in the CRS maps, but on the likelihood that hydrocarbons are found during the exploration and exploitation activities. Hydrocarbon presence is manageable by adapting adequate technology such BOP and appropriate mud control at the rig side during the critical phases of drilling operations.

CRS maps were obtained for each of the main Petroleum Plays of the Swiss Plateau: Lower Cretaceous, Malm, Dogger, Lias, Muschelkalk and Permo-Carboniferous. To simplify, in the CRS maps, the accumulations of oil and gas were not distinguished, and gas refers only to thermogenic gas. The risk of encountering biogenic gas in the shallower stratigraphic units (Quaternary and Molasse) was not considered because of the lack of data. The maps were generated firstly by assessing the quality of the petroleum system elements hence source rocks, reservoir, and seal. This was done by integrating the existing available data with the petroleum system modelling results obtained in the first part of this work. CRS maps indicate that in most plays, the highest risk of encountering hydrocarbons is related to the distribution of the source rocks. The risk is suggested to be highest on top of Permo-Carboniferous grabens and in the west-northern sectors of the Plateau, where the Posidonia shale source rock is distributed, but uncertainties in distribution, properties and thicknesses of the source rocks need to be considered. Fault zones also represent risk areas, as hydrocarbons can flow from the source rock/reservoir to the uppermost units.

Understanding the cementation state of the fault is key to properly evaluating the risk in these areas.

In addition to the CRS maps, for each play element, a set of data availability and data quality assessment maps are also provided. These maps illustrate the type of data used to assess the quality of petroleum elements. They are useful to understand better how the CRS maps are produced and identify data gaps. Because of the generally poor subsurface data coverage, the final CRS maps can have a certain degree of uncertainties, as frequently the data used to build them were extrapolated from other areas and/or from our geological knowledge and understanding of the petroleum system of the basin. Therefore, in a specific area of interest, special attention needs to be paid to the occurrence, density and reliability of subsurface data. Poor data coverage could tremendously increase risk evaluation uncertainties. Thus, in most cases, further investigations and data gathering shall be put in place, to improve the evaluation of the uncertainties associated with hydrocarbon occurrence.

The CRS maps produced are useful tools for planners and decision-makers. They can be used to establish a first assessment of the risk of encountering hydrocarbon at depth. These sets of maps can be further used to propose the necessary mitigation measures (i.e. further subsurface studies, reprocessing of existing data, new data acquisition, use of adapted technologies during drilling, etc.) thus securing the geothermal exploration activity.

Zusammenfassung

In Sedimentbecken treten geothermische Ressourcen häufig gemeinsam mit Kohlenwasserstoffen auf, was potenzielle Risiken für geothermische Explorationsvorhaben mit sich bringt. Das unerwartete Auftreten signifikanter Mengen an Kohlenwasserstoffen kann Bohrarbeiten verzögern oder zum Erliegen bringen und die öffentliche Wahrnehmung von Tiefengeothermieprojekten negativ beeinflussen. Daher erfordert die Planung geothermischer Explorationen ein fundiertes Verständnis der Beckenentwicklung – insbesondere der Bildung, Migration, Akkumulation, Erhaltungsbedingungen und physikalisch-chemischen Eigenschaften kohlenwasserstoffhaltiger Fluide. Die Herkunft potenzieller Kohlenwasserstoffe zu klären sowie die geodynamischen Prozesse, die ein oder mehrere aktive Erdölsysteme in einem geplanten geothermischen Zielgebiet steuern, zu bewerten, ist essenziell..

Das Schweizer Mittelland, ein Teil des Nordalpinen Vorlandbeckens (NAFB), weist zahlreiche natürliche Kohlenwasserstoffaustritte auf, die auf ein komplexes, aktives Erdölsystem mit mehreren Vorkommen hindeuten. Seit dem frühen 20. Jahrhundert wurden Öl- und Gasvorkommen sowohl in tiefen als auch in flacheren Bohrungen nachgewiesen. Allerdings wurden nur in wenigen Fällen wirtschaftlich verwertbare Mengen identifiziert – mit Ausnahme des kurzlebigen Gasfeldes bei der Bohrung Entlebuch-1. Daher wurde die Schweiz im Laufe der Zeit als potenzielles Gebiet für die Produktion von Kohlenwasserstoffen ausgeschlossen. Dennoch kam es in den letzten zwei Jahrzehnten bei geothermischen Tiefbohrungen immer wieder zum unerwarteten Antreffen von Öl und Gas (z. B. Schlattingen-1, St. Gallen, GEo-01). In einigen Fällen führten diese Funde zu kurzfristigen wie auch langfristigen wirtschaftlichen und gesellschaftlichen Beeinträchtigungen auf lokaler und nationaler Ebene.

Ziel 1 des UNCONGEO-Projekts war es daher, das Vorkommen und die potenzielle räumliche Verteilung von Kohlenwasserstoffen im Untergrund des Schweizer Mittellandes zu bewerten. Zunächst musste das aktive Erdölsystem charakterisiert werden. Dazu gehörte die Identifikation, Beschreibung und Quantifizierung jener Schlüsselelemente und -prozesse, die die Generierung, Migration, Akkumulation und Konservierung von Kohlenwasserstoffen kontrollieren.

Zur Analyse wurde ein Beckenmodell gemäß dem in der Erdölindustrie etablierten Standard für thermische und petroleumsystemanalytische Modellierungen eingesetzt. Eine umfassende regionale Beckenanalyse hatte zum Ziel, die thermische und strukturelle Entwicklung des Beckens zu rekonstruieren und die Reife der Muttergesteine zu bestimmen. Wichtige Steuergrößen – wie Paläowärmefluss, Sedimentlithologie und Faziesverteilung, Versenkungsgeschichte sowie der Zeitpunkt und Umfang tektonischer und erosiver Ereignisse – wurden identifiziert und, soweit möglich, quantifiziert.

Anschließend wurde der zeitliche Ablauf der Kohlenwasserstoffgeneration und -migration rekonstruiert. Potenzielle Akkumulationsräume wurden mittels branchentypischer Modellierungssoftware lokalisiert.

Die geologische Komplexität des Schweizer Mittellands, die eingeschränkte Datenverfügbarkeit sowie begrenzte Rechenressourcen und Projektlaufzeit bestimmten die methodischen Rahmenbedingungen. Die Modellierung des Erdölsystems erfolgte daher entlang mehrerer regionaler geologischer 2D-Schnitte. Allerdings kann die räumlich-zeitliche Entwicklung eines Erdölsystems nur unzureichend in zwei Dimensionen dargestellt werden – insbesondere hinsichtlich der Migrationspfade sowie Form und Lage potenzieller Kohlenwasserstofffallen. Die Ergebnisse der 2D-Modellierung sind daher mit Einschränkungen zu interpretieren.

Im nächsten Schritt wurde ein geologisches Modell erstellt, das Mächtigkeit und Geometrie der wichtigsten stratigrafischen Einheiten abbildet. Fünf 2D-Modelle basieren auf repräsentativen regionalen Profilen des Mittellands. Eingangsparameter umfassten Ablagerungsalter, Lithologie und Fazies der Einheiten sowie die geochemischen Eigenschaften potenzieller Muttergesteine. Randbedingungen, welche den Wärmetransport kontrollieren wie die Temperatur an der Sediment-Wasser-Grenzfläche und der basale Wärmefluss, wurden ebenfalls berücksichtigt

Die thermische Reife der Muttergesteine wurde modelliert, u. a. für den Posidonienschiefer (Toarcium), der sich im Reifestadium zwischen unverändert und Ölfenster befindet, sowie für Autun-Schiefer (Perm) und karbonische Kohle/Schiefer, die im feuchten bzw. trockenen Gasfenster liegen. Zur Kalibrierung wurden – soweit verfügbar – Daten wie Bohrlochtemperaturen, Porositäten und Vitrinitreflexionen herangezogen.

Für jede Profillinie wurden die Prozesse der Erzeugung, Migration und Akkumulation simuliert und deren zeitliche Entwicklung im Kontext der strukturellen Fallenbildung dargestellt. Kohlenwasserstoffe aus dem Posidonienschiefer (vorwiegend Öl) migrierten typischerweise entlang von Störungen und sammelten sich in Oberjura- oder Kreideeinheiten. Diese strukturellen Fallen entstanden während der späten alpinen Deformationsphasen. Gasförmige Kohlenwasserstoffe aus dem Perm und Karbon reichern sich vorzugsweise in sandigen Ablagerungen des oberen Perms und unteren Mesozoikums an (z. B. Buntsandstein, Muschelkalk). Die Migration erfolgte entlang tiefreichender, alpin reaktivierter Störungen, die die Perm-Karbon-Gräben mit der mesozoischen Überlagerung verbinden. Abdichtungen erfolgten durch evaporitische Trias-Einheiten. Weitere Migrationspfade verlaufen entlang normaler und transferierter Störungen sowie durch durchlässige Lithologien in mesozoischen und känozoischen Einheiten (Molasse).

Die Modelle basieren zwangsläufig auf zahlreichen Annahmen, da untertägige Daten rar und räumlich ungleich verteilt sind. Folgende Unsicherheiten beeinflussen die Ergebnisse maßgeblich: i) Verteilung und Eigenschaften der Muttergesteine, v. a. permisch und karbonisch; ii) Geometrie, Aktivitätszeitpunkt und Abdichtungspotenzial von Störungen; iii) Porositäts-und Permeabilitätsverteilungen; iv) Strukturgeometrien potenzieller Fallen; v) Mutter-, Speicher und Deckgesteinen; vi) Geochemische Eigenschaften der Muttergesteine; vii) Zeitliche Abfolge tektonischer Phasen (Überschiebungen); viii) Ausmaß und Zeitpunkt erosiver Prozesse während und nach der Orogenese.

Ziel 2 des UNCONGEO-Projekts ist die Bewertung des Kohlenwasserstoff-Risikos im Untergrund des Mittellandes und dessen Visualisierung mittels "Common Risk Segment (CRS)"-Karten. Diese Karten zeigen die räumliche Verteilung geologischer Risiken durch ein funktionierendes Erdölsystem und sollen helfen, Gebiete mit potenzieller Kohlenwasserstoffakkumulation bei zukünftigen Tiefbohrungen (> 500 m) zu identifizieren.

Der Risikobegriff bezieht sich hier auf die Wahrscheinlichkeit des Auftretens von Kohlenwasserstoffen im Untergrund. Es ist explizit nicht als Risikoevaluation von konkreten Geothermieprojekten zu verwenden, was eine unzulässige Verallgemeinerung wäre. Das Risiko kann durch geeignete Maßnahmen wie Blowout-Preventer (BOP) und angepasste Bohrspülungssteuerung während der kritischen Bohrphasen beherrscht werden.

CRS-Karten wurden für die wichtigsten potenziellen Lagerstätten im Mittelland erstellt: Unterkreide, Malm, Dogger, Lias, Muschelkalk und Permokarbon. Eine Differenzierung zwischen Öl und Gas

erfolgte nicht; berücksichtigt wurde ausschließlich thermogenes Gas. Biogenes Gas in flacheren Einheiten (Molasse, Quartär) wurde mangels Daten nicht berücksichtigt.

Die Qualität der Systemelemente – Muttergestein, Speicher und Deckschicht – wurde auf Basis vorhandener Daten und der vorherigen Modellierungen bewertet. Die Karten zeigen, dass das Risiko meist stark von der Verteilung des Muttergesteins abhängt. Besonders hohes Risiko wird für den Permokarbon-Graben und die westlich-nördlichen Bereiche des Plateaus angenommen, wo der Posidonienschiefer häufig vorkommt – allerdings unter großer Unsicherheit hinsichtlich Verteilung, Eigenschaften und Mächtigkeit der Muttergesteine.

Auch Störungszonen bergen erhöhtes Risiko, da sie potenzielle Migrationswege für Kohlenwasserstoffe darstellen. Der Zementationsgrad von Störungen ist hierbei ein entscheidender Parameter zur Risikobewertung.

Zusätzlich wurden Karten zur Datenverfügbarkeit und -qualität erstellt, um Rückschlüsse auf die Verlässlichkeit der CRS-Karten zu ermöglichen. Aufgrund der geringen untertägigen Datenlage können diese Karten mit Unsicherheiten behaftet sein. Daten wurden teilweise aus benachbarten Regionen extrapoliert, was die Notwendigkeit weiterer lokaler Untersuchungen unterstreicht.

Die CRS-Karten stellen ein wichtiges Werkzeug für Planer und Entscheidungsträger dar. Sie unterstützen die erste Risikoabschätzung und helfen bei der Planung zusätzlicher Maßnahmen (z. B. neue Erkundungen, Datenaufbereitung, angepasste Bohrtechnologien), um geothermische Explorationsvorhaben sicher umzusetzen.

Résumé

Dans les bassins sédimentaires, les ressources géothermiques apparaissent fréquemment en association avec des hydrocarbures, ce qui présente des risques potentiels pour les projets d'exploration géothermique. La présence inattendue de quantités significatives d'hydrocarbures peut retarder, voire interrompre les opérations de forage et nuire à la perception publique des projets de géothermie profonde. Les projets d'exploration géothermique doivent donc s'appuyer sur une connaissance approfondie de l'évolution du bassin sédimentaire et plus particulièrement de la génération, de la migration, de l'accumulation, du potentiel de conservation et des propriétés physiques des fluides hydrocarbonés. Il est donc essentiel de déterminer l'origine des hydrocarbures potentiels et d'évaluer les processus géodynamiques contrôlant un ou plusieurs systèmes pétroliers actifs dans la zone géothermique.

Le Plateau suisse, qui fait partie du bassin de l'avant-pays des Alpes du Nord (NAFB), présente de nombreuses manifestations naturelles d'hydrocarbures indiquant un système pétrolier actif complexe caractérisé par plusieurs occurrences. Depuis le siècle dernier, des indices de pétrole et de gaz ont été identifiés lors de forages profonds et peu profonds. Néanmoins, dans la plupart des cas, les quantités d'hydrocarbures découvertes n'ont pas révélé des quantités exploitables sur le plan économique (à l'exception du seul champ de gaz éphémère de Entlebuch-1). Ainsi, la Suisse a progressivement été exclue en tant que région potentielle pour la production d'hydrocarbures. Néanmoins, ces deux dernières décennies, des forages géothermiques profonds ont rencontré de manière inattendue du pétrole et du gaz (par exemple Schlattingen-1 ; St Gallen ; GEo-01). Dans certains cas, ces découvertes ont entrainé des répercussions économiques et sociales à court et à long terme aux niveaux local et national.

L'objectif 1 du projet UNCONGEO est d'évaluer la présence et la distribution spatiale potentielle des hydrocarbures dans le sous-sol du Plateau suisse. Pour atteindre cet objectif, il est d'abord nécessaire de caractériser le système pétrolier actif. Cela inclue l'identification, la caractérisation et la quantification des éléments et des processus clés contrôlant la génération, la migration, l'accumulation et la conservation des hydrocarbures

Pour l'analyse, un modèle de bassin conforme aux standards établis dans l'industrie pétrolière pour la modélisation thermique et des systèmes pétroliers est utilisé. Une analyse régionale complète du bassin vise à reconstruire l'évolution thermique et structurelle du bassin, et à déterminer la maturité thermique des roches mères. Dans ce contexte, les principales variables contrôlant la température atteinte par le remplissage du bassin au fil du temps ont été identifiées et quantifiées

dans la mesure du possible, tel que le paléo-flux de chaleur, la lithologie sédimentaire et la distribution des faciès, l'histoire de l'enfouissement, ainsi que l'ampleur et la chronologie des événements structuraux et érosifs les plus importants. Ensuite, la chronologie de la production et de l'expulsion des hydrocarbures a été reconstituée. Les zones de migration et d'accumulation potentielles ont été identifiées à l'aide d'un logiciel de modélisation standard de l'industrie.

La complexité géologique du Plateau suisse, la disponibilité limitée des données, ainsi que les ressources informatiques et la durée du projet ont défini le cadre méthodologique. La modélisation du système pétrolier a donc été réalisée le long d'une série de coupes géologiques régionales en 2D. Toutefois, le développement spatio-temporel d'un système pétrolier ne peut être représenté de manière adéquate en deux dimensions – notamment en ce qui concerne les chemins de migration et la forme et la position des pièges à hydrocarbures potentiels. Les résultats de la modélisation 2D doivent donc être interprétés avec prudence. Le processus de modélisation du système thermique/pétrolier consiste à établir un modèle géologique représentant l'épaisseur et la géométrie des principales unités stratigraphiques. Cinq modèles 2D ont été construits, basés sur des profils régionaux représentatifs. Les paramètres initiaux incluent l'âge des événements de dépôt et d'érosion, la lithologie et le faciès de chaque unité, ainsi que les propriétés géochimiques des roches mères potentielles. Enfin, les conditions aux limites qui contrôlent le transfert de chaleur dans le bassin, telles que la température à l'interface sédiments-eau et le flux de chaleur basal, ont été assignées au modèle. La maturité thermique des principales roches mères a été modélisée, notamment pour les schistes noirs de Posidonie (Toarcien), se situant à la fois dans des conditions thermiques de la fenêtre immature et de la fenêtre pétrolière, ainsi que pour les schistes autuniens (Permien) et le charbon et les schistes du Carbonifère, situés, respectivement, dans les fenêtres gazières humides et sèches. Des données telles que les températures de forage, les porosités et la réflectance de la vitrinite ont été utilisées pour la calibration, lorsqu'elles étaient disponibles. Pour chaque section, les processus de génération, migration et accumulation, ainsi que la chronologie relative du développement des pièges structuraux, ont été simulés au cours des temps géologiques, ce qui a permis de définir les zones où la probabilité de rencontrer des hydrocarbures est la plus élevée. Les hydrocarbures issus des schistes de Posidonie (principalement du pétrole) se sont généralement accumulés dans les unités du Jurassique supérieur et/ou du Crétacé, migrant le long des failles et s'accumulant dans les pièges structuraux formés lors des dernières phases de la déformation alpine. Les hydrocarbures issus du Permien et du Carbonifère (essentiellement du gaz) se sont accumulés dans les dépôts sableux du Permien supérieur et du Mésozoïque inférieur (principalement dans les unités du Buntsandstein et du Muschelkalk). Les hydrocarbures ont principalement migré le long de failles extensionnelles/trastensionnelles profondes, réactivées au cours de l'orogenèse alpine, reliant les grabens permo-carbonifères à la couverture sédimentaire mésozoïque, et scellés par les unités triasiques évaporitiques. D'autres chemins de migration des hydrocarbures se sont formés dans les unités mésozoïques et cénozoïques (Molasse), principalement le long de failles normales et transversales, et de lithologies perméables.

Les modèles de systèmes pétroliers reconstitués dans cette étude reposent sur plusieurs hypothèses, en raison de la rareté et la distribution spatiale inégale des données du sous-sol. L'interpolation et/ou l'extrapolation des données ont été nécessaires, et il faut donc tenir compte des incertitudes suivantes qui influencent fortement les résultats :i) Distribution et propriétés des roches mères, en particulier permiennes et carbonifères; ii) Géométrie, période d'activité et propriétés de scellement des failles (c'est-à-dire le degré de cimentation, la juxtaposition, la transmissibilité, etc.) ; iii) Distribution et propriétés de porosité et de perméabilité dans l'ensemble du bassin ; iv) Géométries structurales des pièges potentiels ; v) Lithologie et répartition des faciès sédimentaires des roches mères, réservoirs et couverture ; vi) Proprieté géochimiques des roches mères ; vii) Séquence temporelle des épisodes tectoniques (chevauchement) ; viii) Ampleur et chronologie des processus érosifs syn et post-orogénique.

L'objectif 2 du projet UNCONGEO est d'évaluer le risque associé à la présence d'hydrocarbures dans le sous-sol du Plateau et de le représenter graphiquement à l'aide de cartes « Common Risk Segment (CRS)». Ces cartes illustrent la distribution spatiale du risque géologique associé à un système pétrolier actif et visent à identifier les zones à potentiel d'accumulation d'hydrocarbures lors de futurs forages profonds (> 500 m). Le terme de risque se réfère ici à la probabilité de présence d'hydrocarbures dans le sous-sol. Il ne doit en aucun cas être interprété comme une

évaluation des risques pour des projets géothermiques concrets – ce qui constituerait une généralisation inadmissible. Le risque peut être maîtrisé par des mesures appropriées telles que les dispositifs anti-éruption (BOP) et un contrôle adapté des fluides de forage durant les phases critiques.La

Des cartes CRS ont été établies pour les principales zones pétrolières du Plateau suisse : Crétacé inférieur, Malm, Dogger, Lias, Muschelkalk et Permo-Carbonifère. Pour simplifier, les accumulations de pétrole et de gaz n'ont pas été distinguées, et le gaz se réfère uniquement au gaz thermogénique. Le risque de rencontrer du gaz biogénique dans les unités stratigraphiques moins profondes (Quaternaire et Molasse) n'a pas été pris en compte faute de données. La qualité des éléments du système pétrolier, à savoir les roches mères, réservoir et couverture, a été évaluée sur la base des données disponibles et des modélisations précédentes. Les cartes CRS montrent que, le risque dépend souvent fortement de la distribution des roches mères. Le risque serait le plus élevé là où il y a des grabens permo-carbonifères et dans les secteurs ouest-nord du plateau, où les schistes de Posidonie sont présents, mais avec de grandes incertitudes quant à leur distribution, propriétés et épaisseur. Les zones de faille présentent également un risque accru, car elles peuvent constituer des chemins de migration pour les hydrocarbures. Le degré de cimentation des failles est ici un paramètre déterminant pour évaluer correctement les risques dans ces zones.

Des cartes supplémentaires sur la disponibilité et la qualité des données ont été établies, permettant d'évaluer la fiabilité des cartes CRS. En raison de la faible quantité de données du sous-sol disponible, ces cartes comportent de larges incertitudes. Certaines données ont été extrapolées à partir de régions voisines, ce qui souligne la nécessité d'études locales supplémentaires.

Les cartes CRS constituent un outil important pour les planificateurs et les décideurs. Elles peuvent être utilisées pour établir une première évaluation des risques et aide à planifier des mesures complémentaires (p.ex.nouvelles études d'exploration du sous-sol, traitement des données existantes, technologies de forage adaptées) afin de mettre en œuvre des projets d'exploration géothermique en toute sécurité.

Main findings

- This study evaluates the risk associated with the presence of hydrocarbons (oil and thermogenic gas) in the Swiss Plateau, where medium to large-depth geothermal projects may develop in the future.
- Three main hydrocarbon source rocks were identified: the Posidonia black shales (Toarcian), mostly located in the western and northern parts of the Plateau, the Permian shales (Autunian) and the Carboniferous shales and coal deposits, both confined in the grabens segmenting the crystalline basement of the basin.
- Petroleum system modelling estimated immature to oil window thermal conditions for the Posidonia shale source rock and wet to dry gas window conditions for the Permian and Carboniferous source rocks.
- Hydrocarbons generated by the Posidonia shale source rock (mostly oil) generally accumulated in Upper Jurassic and/or Cretaceous units, whereas hydrocarbons generated by the Permian and Carboniferous source rocks (mostly gas) accumulated in the upper Permian and lower Mesozoic sandy deposits (mainly Buntsandstein and Muschelkalk units), sealed by the evaporitic Triassic units.
- Qualitative Common Risk Segment (CRS) maps were generated for the entire Plateau, indicating the potential risk of encountering hydrocarbons in the subsurface. The highest risk category was not achieved anywhere. The highest qualitative risk achieved (mid to high risk) is in areas where the hydrocarbon source rocks are present: on the top of the Permo-Carboniferous grabens and in the western-northern sectors of the Plateau, where the Posidonia shale source rock is mostly present. Faulted areas also present a mid to high risk, as they facilitate the circulation and upwelling of potential hydrocarbons generated at depth.

- A GIS database is provided, where CRS maps can be consulted by future geothermal users.
- Uncertainties in the results presented in this study are highlighted, related to the scarce data coverage and/or the poor assumptions of constraints. Further data acquisition and/or research on the stratigraphic, structural and thermal evolution of the basin would improve the outcomes obtained herein.

Contents

1 Introduction 12

1.1 Geothermal energy exploration in Switzerland: background information and known risks 12

1.2 Purpose of the project 1312

1.3 Objectives 13

1.4 Geographical and geological setting 14

1.4.1 Stratigraphic Evolution 16

1.4.2 Erosional unconformities 18

1.5 The Swiss Plateau petroleum system 19

1.5.1 Source rocks 20

1.5.1.1 The Posidonia black shales source rock 20

1.5.1.2 Permian and Carboniferous source rocks 23

1.5.2 Reservoirs and seals 26

1.5.3 Traps 28

1.5.4 Generation/Migration/Accumulation processes 29

1.5.5 Preservation 29

2 Methodology and Data 29

2.1 Petroleum system modelling 30

2.1.1 Reconstruction of the geometry of the basin 33

2.1.1.1 Stratigraphic horizons and faults 33

2.1.1.2 Permo-Carboniferous grabens 34

2.1.1.3 Erosion 34

2.1.2 Structural model 34

2.1.2.1 Single vergence thrust plane 35

2.1.2.2 Opposite vergence thrust plane 35

2.1.3 Facies distribution 36

2.1.4 Source rock characterization 36

2.1.5 Boundary conditions 36

2.1.5.1 The basal heat flow 37

2.1.6 Calibration of the model 40

2.1.6.1 Porosity 40

2.1.6.2 Temperature 40

2.1.6.3 Thermal maturity conditions 41

2.1.7 Simulation of the hydrocarbon generation, migration, accumulation processes 42

2.1.8 Evaluation of the uncertainties 42

2.2 Common Risk Segment (CRS) maps 42

2.2.1 Geothermal plays definition 45

2.2.2 Class definition 45

2.2.3 Source rocks occurrence and properties. 46

2.2.4 Reservoir occurrence and properties 46

2.2.5 Seal occurrence and properties. 47

2.2.6 GIS Based CRS mapping 48
2.2.7 GIS CRS map production 48
3 Results 49
3.1 Petroleum System Modelling - Section 2 49
3.1.1 Data 49
3.1.1.1 Geological Model 50
3.1.1.2 Wells 51
3.1.1.3 Deposition and erosional events 52
3.1.1.4 Facies 53
3.1.1.5 Calibration data 54
3.1.1.6 Source rocks parameters 54
3.1.2 Boundary Conditions 55
3.1.3 Results 56
3.1.3.1 Restoration to the pre-Alpine thrusting phase 56
3.1.3.2 Geological conceptual model evolution 58
3.1.3.3 Thermal model calibration 60
3.1.3.3.1 Porosity 60
3.1.3.3.2 Present-day temperature 62
3.1.3.3.3 Thermal conditions / Source rocks maturity 64
3.1.3.4 Simulation of the hydrocarbon generation, migration and accumulation processes 67
3.1.3.5 Comparison between the hydrocarbons findings and the modelling results 73
3.1.4 Uncertainties 75
3.2 Petroleum System Modelling - Section 3 83
3.2.1 Data 83
3.2.1.1 Geological Model 83
3.2.1.2 Wells 84
3.2.1.3 Deposition and erosional events 84
3.2.1.4 Facies 86
3.2.1.5 Calibration data 87
3.2.1.6 Source rock parameters 87
3.2.2 Boundary conditions 88
3.2.3 Results 89
3.2.3.1 Restoration to the pre-Alpine thrusting 89
3.2.3.2 Geological conceptual model evolution 90
3.2.3.3 Thermal model calibration 92
3.2.3.3.1 Porosity 92
3.2.3.3.2 Present-day temperature 94
3.2.3.3.3 Thermal conditions / Source rocks maturity 96
3.2.3.4 Simulation of the hydrocarbon generation, migration and accumulation processes 97
3.2.3.5 Hydrocarbons findings and modelling results comparison 104
3.2.4 Uncertainties 106
3.3 Petroleum System Modelling - Section 4 113
3.3.1 Data 113
3.3.1.1 Geological Model 113
3.3.1.2 Wells 114
3.3.1.3 Deposition and erosional events 114
3.3.1.4 Facies 116
3.3.1.5 Calibration data 116
3.3.1.5 Source rock parameters 117

3.3.2 Boundary conditions 118
3.3.3 Results 119
3.3.3.1 Restoration to the pre-Alpine deformation phases 119
3.3.3.2 Geological conceptual model evolution 119
3.3.3.3 Thermal model calibration 121
3.3.3.3.1 Porosity 121
3.3.3.3.2 Present-day temperature 123
3.3.3.3.3 Thermal conditions / Source rocks maturity 126
3.3.3.4 Simulation of the hydrocarbon generation, migration and accumulation processes 128
3.3.3.5 Comparison between the hydrocarbons findings and the modelling results 135
3.3.4 Uncertainties 136
3.4 Petroleum System Modelling - Section 5 143
3.4.1 Data 143
3.4.1.1 Geological Model 143
3.4.1.2 Wells 144
3.4.1.3 Deposition and erosional events 144
3.4.1.4 Facies 146
3.4.1.5 Calibration data 147
3.4.1.6 Source rock parameters 147
3.4.2 Boundary conditions 149
3.4.3 Results 150
3.4.3.1 Restoration to the pre-Alpine deformation phases 150
3.4.3.2 Geological conceptual model evolution 150
3.4.3.3 Thermal model calibration 151
3.4.3.3.1 Porosity 151
3.4.3.3.2 Present-day temperature 153
3.4.3.3.3 Thermal conditions / Source rocks maturity 155
3.4.3.4 Simulation of the hydrocarbon generation, migration and accumulation processes 158
3.4.4 Comparison between the hydrocarbons findings and the modelling results 165
3.4.5 Uncertainties 166
3.5 Petroleum System Modelling - Section 6 174
3.5.1 Data 174
3.5.1.1 Geological Model 174
3.5.1.2 Wells 175
3.5.1.3 Deposition and erosional events 175
3.5.1.4 Facies 177
3.5.1.5 Calibration data 178
3.5.1.5 Source rock parameters 179
3.5.2 Boundary conditions 180
3.5.3 Results 181
3.5.3.1 Restoration to the pre-Alpine deformation phases 181
3.5.3.2 Geological conceptual model evolution 181
3.5.3.3 Thermal model calibration 183
3.5.3.3.1 Porosity 183
3.5.3.3.2 Present-day temperature 185
3.5.3.3.3 Thermal conditions / Source rocks maturity 187
3.5.3.4 Simulation of the hydrocarbon generation, migration and accumulation processes 190
3.5.3.5 Comparison between the Hydrocarbons findings and the modelling results 198
3.5.4 Uncertainties 201

3.6 CRS maps 208
3.6.1 Source rocks maps 210
3.6.2 Lower Cretaceous Play 218
3.6.3 Malm Play 225
3.6.4 Dogger Play 233
3.6.5 Lias Play 241
3.6.6 Muschelkalk Play 249
3.6.7 Permo-Carboniferous Play 257
3.6.8 Accumulations simulated by petroleum system modelling 265
3.6.9 Data occurrence map 266
4 How to use the CRS maps: examples 268
4.1 Zurich airport, example of a high-risk prospect. 269
4.1.3 Seal 273
4.1.4 Uncertainty and data occurrence 274
4.1.5 Recommendations 278
4.2 Bern, example of low data density 279
4.2.1 Play components evaluation 280
4.2.2 Data availability 282
4.2.3 Recommendations 283
4.3 Langenthal, example of a prospect area in the vicinity of a deep borehole 284
4.3.1 Play components evaluation 286
4.3.2 Data availability 286
4.3.3 Recommendations 288
4.4 Yverdon-Les-Bains, example of deviated well into a medium to high-risk area. 288
4.4.1 Recommendations 291
5 Results summary and discussion 292
5.1 Petroleum system modelling part 292
5.2 Common Risk Segment mapping 292
5.3 Uncertainties and assumptions 294
6 Conclusions 297
7 Outlook and next steps 298
8 National and international cooperation 299
9 Authors contribution 300
10 Publications 300
10.1 Peer-reviewed publications in international scientific journals 300
10.2 Reports 301
10.3 Contributions to international conferences 302
11 References 303
12 Appendixes 310
12.1 Lias Rock-Eval data 310
12.2 Permian and Carboniferous Rock-Eval data (Weiach-1 well) 313

12.3 List of the wells and data used in this study 316
12.4 Wells stratigraphy 321
12.5 Wells facies 327
12.6 Porosity data 334
12.7 Temperature data 356
12.8 Vitrinite Reflectance (%Ro) data 361
12.9 TOC data (Hermrigen-1 and Thun-1 wells) 366

Abbreviations

NAFB – Northern Alpine Foreland Basin

UFM – Upper Freshwater Molasse, geological unit

UMM – Upper Marine Molasse, geological unit

LFM – Lower Freshwater Molasse, geological unit

LMM – Lower Marine Molasse, geological unit

Gwh – Gigawatt/hours, energy unit

mW/mq – Miliwatt/meter square, heat transfer unit

T – Temperature

°C – Celsius grade

m - meters

%Ro – Vitrinite reflectance data

Phi - Porosity

AFT – Apatite fission tracks data

TAI – Thermal alteration index data

RE – Rock-Eval analysis

TOC- Total Organic Carbon (from Rock-Eval analysis)

HI – Hydrogen Index (from Rock-Eval analysis)

OI – Oxygen Index (from Rock-Eval analysis)

T_{max} –Maximum temperature measured during the pyrolisis (from Rock-Eval analysis)

CRS – Common Risk Segment maps

1 Introduction

1.1 Geothermal energy exploration in Switzerland: background information and known risks

Geothermal energy is an essential part of the Swiss Federal «energy strategy 2050» (Bundesamt für Energie BFE, 2020) This strategy aims at restructuring Switzerland's overall energy system with the commitment to reduce net greenhouse gas emissions to zero, by discouraging the use of fossil energies and by promoting the investment in renewable energy technologies[1]. Among the available renewable energy sources, geothermal energy has been identified as having significant potential, and the exploration of this resource has received increasing support. Furthermore, recent geopolitical scenarios and conflicts highlight the urgency of developing local renewable energy sources as geothermal, to handle potential energy supply crises.

The development and use of shallow geothermal energy in Switzerland has a long history, thanks to its numerous thermal baths and natural spas known at least since Roman times. Since the 1970s, shallow geothermal technologies have been strongly developed, and today, Switzerland has one of the highest densities of ground-source heat pump systems in the world (Link and Minnig, 2022). In 2023, the heating energy produced by geothermal systems amounted to 4'531 GWh, with a share of geothermal and, thus, renewable energy of 3'418.4 GWh (74.4%) (Link, 2023). The heating energy produced came mainly from heat pump systems (96.0%). Other geothermal energy uses corresponded to 4% of the total heating energy produced. The latter were produced via thermal baths, deep aquifer use (Riehn system) and direct tunnel water use (Link, 2023).

In addition to shallow geothermal systems, the development of deep geothermal systems can be key to electricity production and direct heat supply. According to the Swiss Geothermal Association, geothermal energy could provide by 2050 a quarter of the annual heat demand (Geothermie-Schweiz, 2020). Such heat and power production by geothermal energy can be realised only if there are adequate framework conditions, national policies and an efficient geothermal industry (Link and Minnig, 2022).

At present, in Switzerland, few deeper geothermal plants for heat utilisation exist and none for electricity production. A major obstacle is the scarce knowledge about the subsurface at depth below 2000 meters, and the associated risk of not finding a commercial resource (Link and Minnig, 2022). Additional risks that must be considered when a deep geothermal well is planned are the induced seismicity and the presence of hydrocarbons, especially gas, which could interfere with drilling activities (Spada et al., 2021). In Switzerland, this risk is well-known. In 2006, during the drilling of a deep geothermal well, which aims at exploiting the geothermal potential of crystalline rock below the city of Basel, a 3.4 magnitude earthquake was induced during and following a hydraulic stimulation (Baisch et al., 2009; Mignan et al., 2015). In 2013, during the drilling of a deep geothermal well (over 4000 meters) in the St. Gallen area (St. Gallen GT-1), a 3.5 magnitude earthquake was triggered while containing the overpressure in the drill pipes and annulus induced by natural gas kick (Diehl et al., 2017; Moeck et al., 2015; Omodeo-Salé et al., 2020a; Wolfgramm et al., 2015). The origin of this gas has been considered thermogenic, most likely generated by Permian and/or Carboniferous source rocks, located in deep sedimentary throughs that segmented the basement of the basin (Eichinger, 2014; Jurisch, 2013; Omodeo-Salé et al., 2020a; Wolfgramm et al., 2015). These unfortunate incidents resulted in the loss of several million Swiss francs (CHF) and a negative perception of the safety of geothermal energy among the local population, both representing important obstacles to the future development of geothermal energy.

[1] (https://www.bfe.admin.ch/bfe/en/home/policy/energy-strategy-2050.html/).

1.2 Purpose of the project

The UNCONGEO project aims to carry out a regional assessment of the distribution of potential hydrocarbon occurrences throughout the Swiss Plateau, to identify the areas where hydrocarbons may be encountered in the subsurface and represent a potential risk to geothermal exploration.

The main research questions of the UNCONGEO projects are summarised as follows:

- What types of petroleum systems are active in the Swiss Plateau?

- Which are the areas in the Swiss Plateau and stratigraphic units with the highest risk of holding hydrocarbons in the subsurface?

This study mostly focuses on the thermogenic hydrocarbons, which include oil and gas formed because of the thermal transformation of the organic matter contained in the rocks at temperatures in the range of 60-200 °C (Fig. 1). These hydrocarbons generally form at depths greater than 1,5 kilometres Once generated, they migrate to shallower depths, up to the surface. This study does not consider biogenic gas, produced at low temperatures and shallow depths, by the decomposition of organic matter by anaerobic microorganisms (Fig. 1). This is because there is currently no detailed map of the distribution of the organic matter-rich facies from which biogenic gas can be produced in the shallowest units of the basin (Quaternary, Molasse).

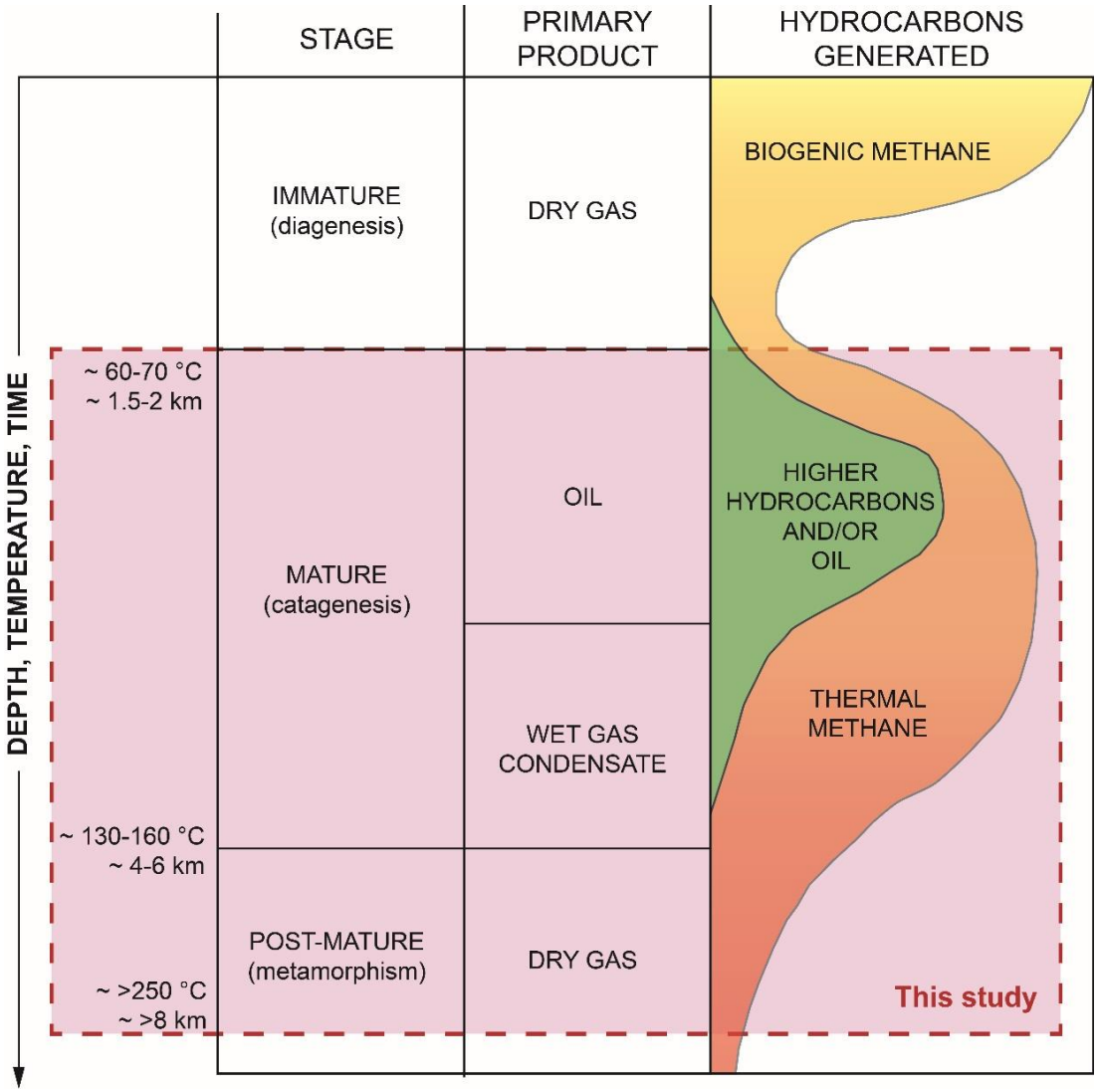


Fig. 1: Biogenic and thermogenic hydrocarbon generation conditions in the sedimentary basins. This study focuses on the thermogenic hydrocarbons. Modified from Rice and Claypool, 1981

1.3 Objectives

The main objectives of the UNCONGEO project are:

- To identify the areas and stratigraphic units where there is the highest risk of encountering thermogenic hydrocarbons during the geothermal drilling operations.
- To highlight the uncertainties in the resulting outputs of the project due to the partial or complete lack of subsurface data and/or to the poor understanding of the geological evolution of the basin.
- To create a GIS map-based tool to evaluate the risks associated with the presence of thermogenic hydrocarbons and a set of maps describing the petroleum system assessment and the data availability for a specific area.
- To offer recommendations to potential geothermal exploration companies to reduce the uncertainties and related risks associated with hydrocarbon occurrences in specific areas in the Swiss Plateau.
- To propose a robust methodology to help in the assessment of hydrocarbon occurrence in the Swiss Plateau.

To achieve the objectives proposed by this study, modern analytical methods and state-of-the-art petroleum industry modelling technology were applied to existing deep seismic lines and borehole material collected over the last 50 years in the Swiss region. The study results in an unprecedented overview of hydrocarbon systems across the entire Swiss Plateau.

The workflow proposed in this project has already been locally applied for some current deep geothermal projects in Switzerland, such as the St. Gallen project (Omodeo-Salé et al., 2020a), La Côte/Vinzel project (Canton of Vaud) (Omodeo-Salé et al., 2020b), Altendorf project (Canton of Schwyz) (Omodeo-Salé and Moscariello, 2020) and is planned in 3D, at a high-resolution for geothermal exploration activities in the Canton of Geneva.

1.4 Geographical and geological setting

The UNCONGEO project focuses on the area morphologically defined as Swiss Plateau, or Central Plateau (Fig. 2). It stretches from Lake Léman in the southwest to Lake Constance in the northeast. It is one of Switzerland's three geographical regions and covers 30% of the country and it is the most densely populated region. The northern part of the Plateau is flanked by the Jura Mountains and the Rhine River, the south by Lake Léman and the Alps.

From a geological point of view, the Swiss Plateau forms part of the North Alpine Foreland Basin (NAFB), which was formed during the Paleogene and Neogene, as a consequence of the flexural bending of the European plate under the thrusts and crustal thickening of the Alpine orogeny (Burkhard and Sommaruga, 1998; Dickinson, 1974; Joachim Kuhlemann and Kempf, 2002; Pfiffner, 2014; Price, 1973; Stampfli et al., 2002; Turcotte and Schubert, 2014). The foreland was filled by Eocene-Miocene siliciclastic deposits, eroded from the uplifting of the Alpine nappes (Berger et al., 2005; Joachim Kuhlemann and Kempf, 2002; Pfiffner, 2014).

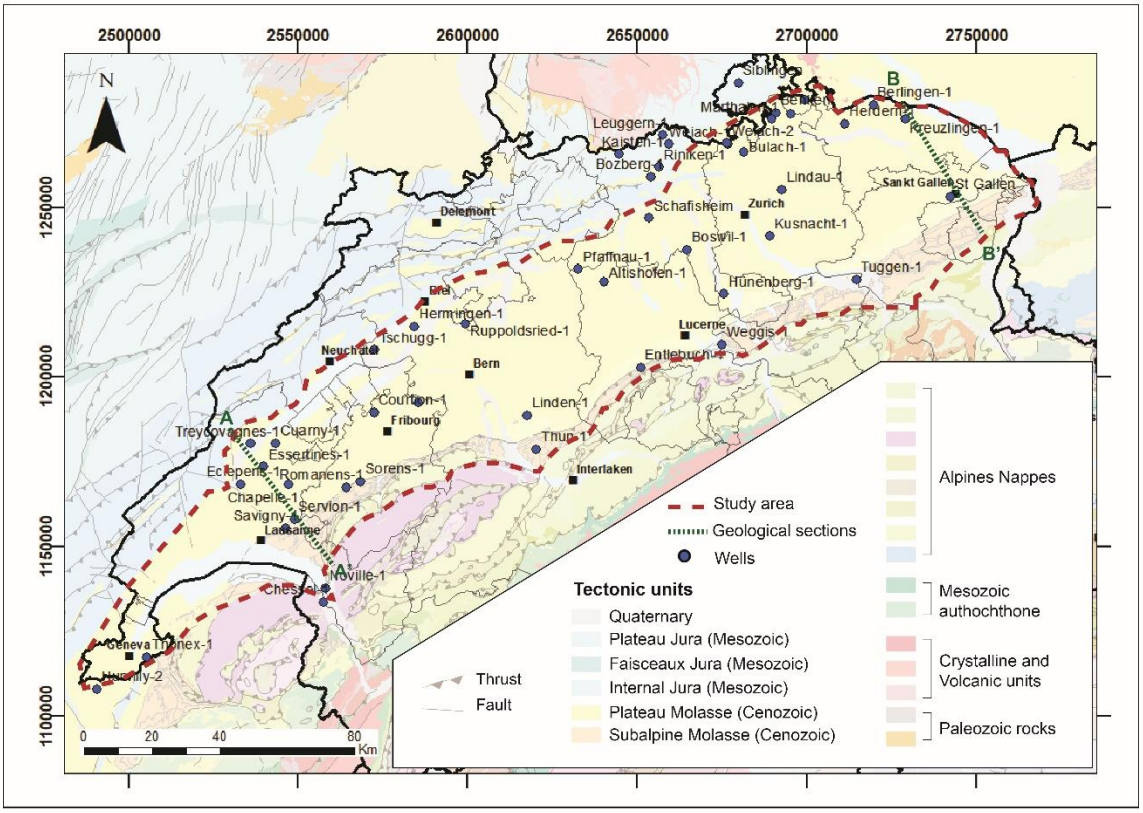


Fig. 2: Geological map of the studied area, showing the area of interest about the main tectonic units. Geographic and geological data from https://map.geo.admin.ch

The Molasse basin is bounded to the northwest by the Jura fold-and-thrust belt and to the southeast by the more external Alpine Nappes. It is separated into the northern external, slightly tilted Plateau Molasse, and the southern internal Subalpine Molasse, characterised by thrust sheets and folds (Pfiffner, 1986) (Fig. 2). Since the latest Alpine thrusting phases, from the Miocene up into the Pliocene, part of the NAFB was gradually uplifted and eroded, forming a diachronous hiatus with the Quaternary cover of approximately 10 My (Kuhlemann and Kempf, 2002). In the western NAFB most of the younger Molasse units are missing, whereas they are still present in the eastern sector (Trümpy et al., 1980).

The internal boundary of the NAFB is characterised by two main structural styles (Fig. 3). In the western part, simple vergent thrust planes overthrust the Subalpine Molasse and the Plateau Molasse deposits in a northwest direction, whereas in the eastern part, the Subalpine Molasse is bounded by partially blind thrust planes with opposite vergence, forming a triangular zone structural style. This structure has been identified from the central part of the basin, up to the Austrian foreland basin (Berge and Veal, 2005; Ortner et al., 2015; Pfiffner, 1986; von Hagke and Malz, 2018). Its formation has been dated as late Miocene (10-6 Ma), during the Subalpine deformation phases, and it can be linked to the Jura mountain formation and to the inner Alps exhumation events (Von Hagke et al., 2012). In Switzerland, the internal geometry and composition of the triangular zone have been poorly constrained because of the poor seismic resolution along this structure and because only a few wells penetrate it entirely. From the existing data, the geometry appears as formed by stacked thrusting slides, mostly southern dipping. Because of the strong deformation affecting the triangular zone area, the age of the deposits composing this structural unit is hard to identify, most likely Oligocene-Miocene (LFM in most of the wells, LMM and LFM in the Weggis-1 well) (Greber et al., 1994; Kopp, 1937; Naef and Schlanke, 2014; Vollmayr and Wendt, 1987) and or older foreland units (Pfiffner, 1986; Sommaruga et al., 2012).

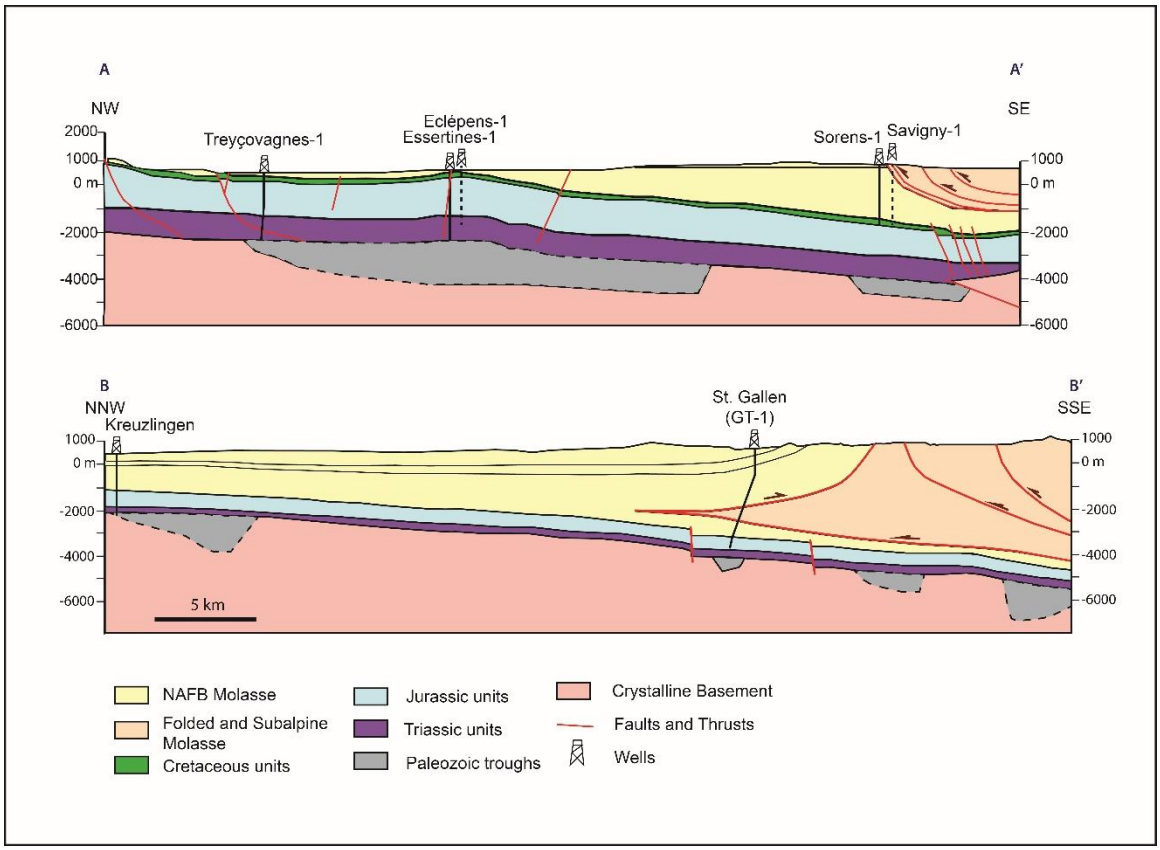


Fig. 3: Representative geological cross-sections of the Plateau Molasse and Subalpine Molasse area, showing stratigraphic thickness and structural style variation throughout the basin: (a) section in the western part of the basin; (b) section in the eastern part of the basin. See Fig.2 for the section trace location.

1.4.1 Stratigraphic Evolution

The stratigraphic record constituting the NAFB and its substratum can be grouped into four mega-sequences, corresponding to the geodynamic evolutionary cycles of the area (Burkhard and Sommaruga, 1998) (Fig. 4).

- The crystalline basement. The crystalline basement of the Molasse Basin formed during three major orogeneses: the Pan-African Cycles on Gondwana, the Caledonian orogeny in northwestern Europe and the Variscan orogeny in central Europe (Pfiffner, 2014; Ziegler et al., 2004).
- The post-Variscan sequence. The Variscan orogeny ends in the Upper Carboniferous (Ziegler et al., 2004). The following dextral translation of Gondwana and Laurussia and the reorganisation of the asthenospheric flow patterns resulted in the collapse of the orogeny and thinning of the lithosphere (Cortesogno et al., 1998; Von Raumer, 1998; Von Raumer and Neubauer, 1993; Ziegler et al., 2004). The transtensional and transpressional tectonic regime and the strong regional thermal subsidence controlled the formation of a narrow and elongated array of pull-apart basins, mostly oriented ESE-WNW, which were rapidly filled by coarse siliciclastic deposits from the eroded orogen relief, Permian and Carboniferous in age (Ziegler et al., 2004). In the transgression phases, coal and carbonaceous shales were deposited in floodplain and swamp depositional environments (Capuzzo and Wetzel, 2004). An intensive intrusive and extrusive magmatic activity characterised this period (Schönlaub, 1997), which was followed by a long-term thermal subsidence up into the Triassic.
- The Mesozoic sequence. The Mesozoic sequence represents the substratum of the Cenozoic foreland basin, and it records the European plate boundary evolution from the rift to passive margin settings. The Permo-Triassic thermal subsidence was overprinted by the Mesozoic rift events related to the opening of the Tethys Ocean between the Eurasian and African plates

(Ziegler et al., 2004). On the European plate, where the study area is located, a rift in the passive margine sequence develops. The Triassic sediments record the transition from continental to shallow marine conditions. They consist of continental sandstone deposits (Buntsandstein facies), intertidal dolomites, limestones and evaporites (Muschelkalk facies) and marine and lagoonal sandstones, marls and shales (Keuper facies). Toward the central-western part of the NAFB, the Keuper is composed of dolomite, anhydrite and salt, making this unit a decollement layer for the last Alpine thrust sheets. The Jurassic succession is mostly composed of shallow water platform facies and is subdivided into the lower Jurassic (Lias), middle Jurassic (Dogger) and upper Jurassic (Malm) units. The Lias and Dogger deposits are marls, shale limestones and sandstones, whereas the Malm deposits are predominantly micritic limestone. The Lias is poorly represented in the southern-eastern NAFB (Bachmann et al., 1987) and is absent southward in the Helvetic realm. The presence of a structural high, the Zurich High (Trümpy et al., 1980), could be the cause of this stratigraphic hiatus. The Cretaceous record is limited to the Early Cretaceous in the western part of the basin, whereas it is completely missing in the eastern part (Lemcke, 1974; Schegg and Leu, 1998; Wildi et al., 1989). The depositional hiatus or erosional nature of this unconformity is still unclear.

- The Cenozoic-Quaternary sequence. It represents the proper infill of the Northern Alpine foreland basin, composed of Molasse deposits. During the Alpine orogeny, the European Plate, where the Paleozoic and Mesozoic sequence overlaid, was tilted to form a foreland basin, filled by mostly siliciclastic deposits, eroded from the forming Alpine nappes. In the internal part of the foreland, Paleocene-Eocene aged flysch sediments were deposited, followed by the Oligocene-Miocene marine to freshwater Molasse deposits (Bachmann et al., 1987; Pfiffner, 2014, 1986). The Molasse deposits are subdivided into four units, representing two under-filling/over-filling megacycles composed of two marine sequences, each followed by sequences of mostly terrestrial deposits (Bachmann and Müller, 1992; Homewood et al., 1986; Joachim Kuhlemann and Kempf, 2002; Lemcke, 1988; Schlunegger et al., 1997; Schlunegger and Willett, 1999). In the NAFB, the four Molasse units and their ages have been defined by Kuhlemann and Kempf, 2002 as follows (Fig. 4): the lower marine Molasse unit (LMM, in German UMM), Rupelian in age; the lower freshwater Molasse (LFM, in German USM), Chattian-Aquitanian in age; the upper marine Molasse (UMM, in German OMM), Burdigalian in age; and the upper freshwater Molasse (UFM, in German OSM), Langhian-Tortonian in age.

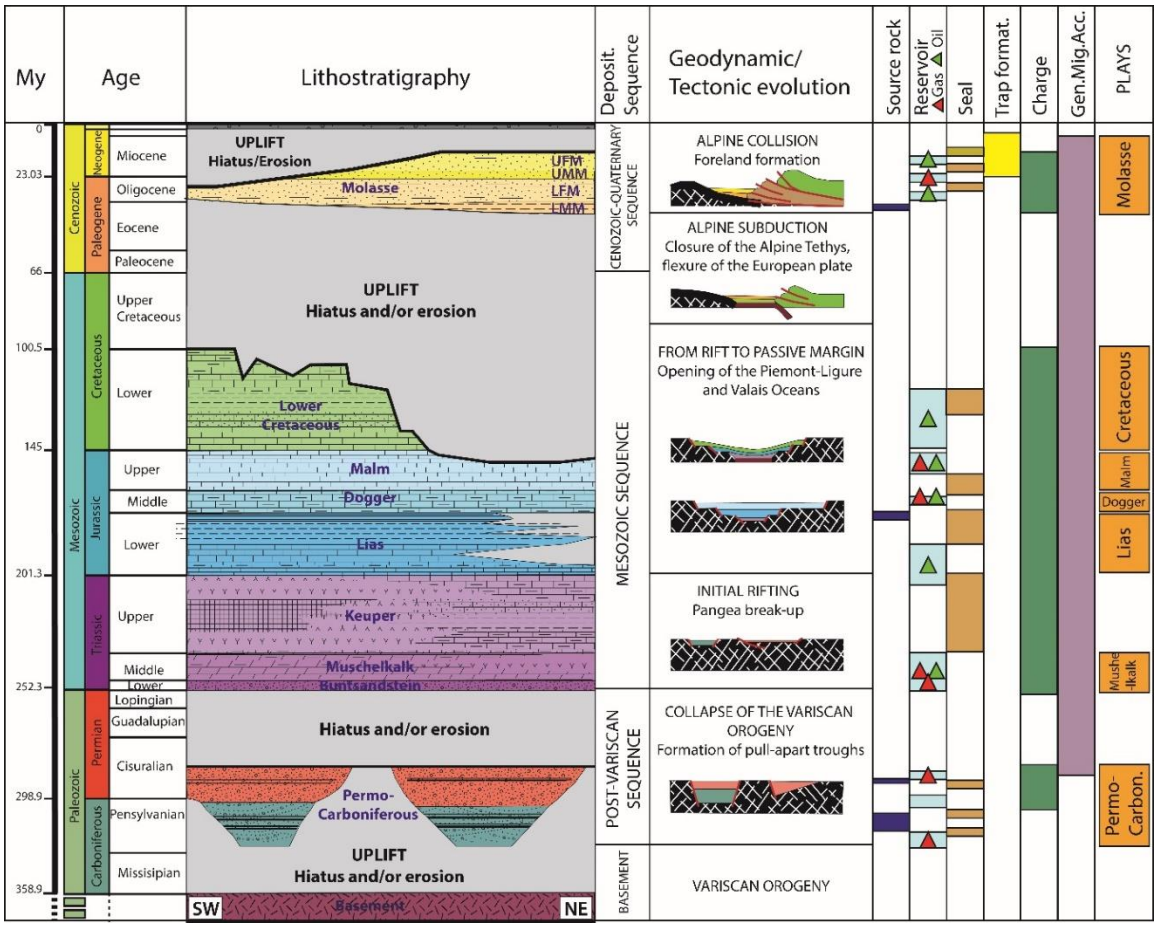


Fig. 4: Stratigraphic chart of the NAFB. Stratigraphic variations throughout the basin have been recognized for the Mesozoic sequence, mostly from the western to the eastern sectors, and for the Cenozoic sequence, mostly from the southwestern to the northeastern sectors of the basin. Absolute ages from ICS chart 2022. The Swiss Plateau petroleum system elements (source rock, reservoir and seal) and processes (Gen.Mig.Acc., generation, migration and accumulations) are indicated, as well as the main Plays considered in this work. Oil and gas indications marked for each reservoir mostly refer to hydrocarbon traces and/or accumulations found in the wells drilling operations.

1.4.2 Erosional unconformities

In the NAFB, three main erosional unconformities are described: 1) Permo-Triassic; 2) Mesozoic-Eocene; 3) Pliocene-Quaternary (Table 4). For the Permo-Triassic unconformity, very few data are available. The magnitude of the missing section could be estimated only for the Weiach-1 well, where the complete sequence Paleozoic to Mesozoic sequence has been penetrated. In this well, a change of the VR value with depth trend at the Permian stratigraphic level could be related to the presence of an erosional unconformity. In Diebold (1988) and Schegg and Leu (1998), a missing section of nearly 1000 meters on the top of the lower Permian debris fan series was estimated from VR data. Most recently, by combining VR and AFT data with the thermal modelling approach, suppose that the increase of the VR with depth trend in the Paleozoic section is most likely related to a high basal heat flow in the Permian time than to a great erosion (Omodeo-Salé et al., 2021). According to this work, in the Weiach-1 well area, a missing section of only 200 meters is estimated for the Permian-Triassic unconformity.

The Mesozoic-Eocene unconformity is observed throughout the entire basin, and its stratigraphic gap increases from west to east. The lower Cretaceous deposits are preserved in the western sector of the NAFB, whereas they are completely absent in the eastern part (Bachmann et al., 1987; Lemcke, 1974; Schegg and Leu, 1998; Wildi et al., 1989). The magnitude of this erosional event has engendered much debate. In Schegg and Leu (1998), by combining different methods and literature data, they estimate, throughout the entire NAFB, an erosion over 1000 meters up to

1800 meters. In the western sector of the NAFB, combining VR data and thermal modelling an erosion thickness of around 500 meters has been estimated (Omodeo-Salé and Moscariello, 2019). The hypothesis of very little or no extra sedimentation and erosion in the Cretaceous-Eocene time has also been considered (Burkhard and Sommaruga, 1998; Lemcke, 1988; Todorov et al., 1993; Wildi et al., 1989). However, the lack of a timing constraint, makes most of these estimates very uncertain, as it is hard to properly differentiate the amount of erosion for each of the main erosional event (Cretaceous-Eocene and Pliocene-Quaternary). In a recent study focused on the northern sector of the NAFB, this issue has been addressed by integrating apatite fission tracks (AFT) data to VR and thermal modelling (Omodeo-Salé et al., 2021). The results of this work support the deposition of 600-1000 meters of deposits in the Cretaceous, which was likely eroded in the Late Cretaceous to Paleocene time when the basin was uplifted.

The Pliocene-Quaternary unconformity surface is located at the top of the Cenozoic foreland sequence (Molasse deposits), separating these from the Quaternary unit. The unconformity is diachronous throughout the NAFB basin, as the Quaternary deposits lie on Molasse deposits, which get older going westward (J. Kuhlemann and Kempf, 2002) Previous studies have estimated a significant variation of the eroded thickness throughout the NAFB, from 1500-3000 meters in the SW to 0-700 meters in the NE (Cederbom et al., 2011; Lemcke, 1974; Monnier, 1982; Schegg and Leu, 1998). Greater values have been estimated in the internal part of the basin, toward the subalpine nappes: 2700 meters in the St. Gallen area (Omodeo-Salé et al., 2020) and 2700 to 4400 meters in the Weggis well area (Schegg and Leu, 1998; Ceberdom et al., 2011). However, these values can be overestimated if the hypothesis of a high paleo geothermal gradient in the eroded section, which could cause a perturbation of the paleotemperature profile by later transfer of heat by fluids, is assumed (Schegg, 1992; Schegg and Leu, 1998).

1.5 The Swiss Plateau Petroleum System

Since the last century, it has been known that in the Swiss Plateau a petroleum system is active (Lahusen and Wyss, 1995; Leu, 2012). Several oil and gas indications were found at the surface, in lakes, in tunnels and galleries (seepages), as well as in boreholes. A graphical synthesis of the oil and gas indications found up to the present day in the Swiss Plateau is shown in Fig. 5.

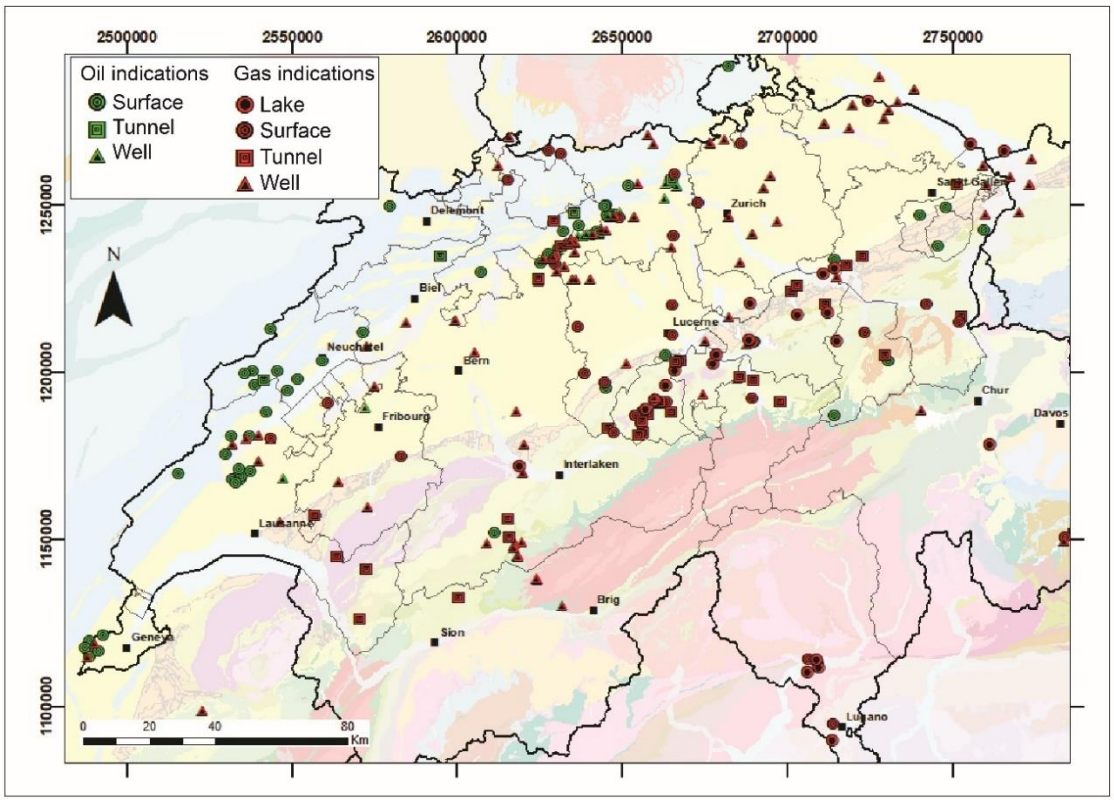


Fig. 5: Oil and gas indications in Swizterland. Modified from Leu (2012). Legend of the geological units, see Fig. 2.

Hydrocarbon exploration in Switzerland started one century ago in the search for local oil and gas resources. In that time, 37 deep wells were realised, up to 2012, when the last exploration well was carried out (Noville-1, Canton of Vaud). The exploration target was changing and deepening over time, from the Cenozoic to the Mesozoic and Permo-Carboniferous units, thanks to the integration of more and more modern and high-resolution geophysical exploration tools (reflection to refraction seismic) and drilling technology (Greber et al., 2007; Leu, 2012). Despite the numerous good oil and gas indications occurring along the entire stratigraphic sequence, only one semi-commercial gas field was discovered in the 80s, in the Entlebuch-1 well, with the production of 2.65 bcf in the upper Jurassic unit (Malm). More recently, a gas play in the Permo-Carboniferous deposits was found in 2000 in the Weiach-2 well and in 2012 in the Noville-1 well. However, in none of these wells was hydrocarbon production carried out, because the quantities discovered were too small to be considered commercially viable. A more exhaustive summary of the hydrocarbon exploration activity in Switzerland can be found in Lahusen and Wyss (1995) and Leu (2012).

A petroleum system is firstly defined by elements (source rock, reservoir, seal and trap) and processes (generation, migration and accumulation) (Magoon and Dow, 1994). The petroleum system elements are generally determined by considering the stratigraphic, sedimentological and geochemical data of the main units forming the basin infill. The petroleum system processes are individuated by knowing the thermal history of the basin, the porosity/permeability and the geometry of the stratigraphic units and the presence and permeability of the faults.

In this work, in addition to the petroleum system concept, the term Play is used. In the literature, there are several definitions of the Play concept. This study refers to Play as a group of rocks formed in similar circumstances (age, depositional setting), which combine a reservoir, a petroleum charge system, a regional top seal and traps, able to produce petroleum accumulations.

In this section, a summary of the most relevant data, acquired in previous studies as well as in the UNCONGEO study, is provided to define the main elements forming the petroleum system of the Swiss Plateau.

1.5.1 Source rocks

The most relevant source rocks identified in the Swiss Plateau petroleum system are the following (Fig. 4): i) the marine Posidonia black shales (Toarcian in age, formerly also defined as Lias z), mostly composed by a Type II kerogen; ii) the lacustrine and terrestrial Autunian shales (Permian in age), composed by a mixed Type I and Type III kerogen; and iii) the terrestrial Carboniferous coal and shales (Carboniferous in age), composed by a Type III kerogen (Brink et al., 1992; Greber et al., 2011; Leu, 2012; Misch et al., 2017; Schegg and Leu, 1998). Less relevant source rocks are the Eocene-Lower Oligocene shales (Rupelian in age, LMM unit), composed of marine Type II kerogen and that may be present in the most internal part of the Subalpine Molasse and beneath the Alpine nappes of Switzerland; and the Opalinus shales (Aalanian in age), composed by Type III kerogen (Greber et al., 2011). The LMM source rock was not considered in this study because of the lack of data on its areal distribution, thickness and geochemical properties. Also, the Opalinus shales source rock was discarded because of the very low hydrocarbon potential reconstructed for this unit (average TOC of 0.7% and maturity values ≤ 0.6 %Ro) (Leu and Gautschi, 2014).

1.5.1.1 The Posidonia black shales source rock

The distribution of the Posidonia black shales is not completely constrained throughout the Plateau, as the Lias unit has been penetrated by a limited number of wells (Table 1). Furthermore, there are several cases where, even if the Lias unit has been penetrated, it has not been clearly defined the presence of the Posidonia shale deposits in the report. This could be a consequence of a too-large sampling rate (considering that the Posidonia shale have an average thickness of 5-7 meters), and/or because of that, geochemical analyses have not been carried out along these deposits.

Well	Posidonia shale presence	Thickness (m)	Geochemical data availability	Observations
Altishofen	Yes	3	No	Described in the well report
Benken-1	Yes	9	No	Described in the well report
Berlingen-1	Likely	9	No	Lias z present, but not clearly defined as Posidonia shale
Boswil-1	Unknown	Unknown	No	The Lias has not been penetrated
Bottstein-1	No	0	No	Eroded
Bozberg-1	Yes	5	No	Described as Rietheim Member
Bulach-1	Yes	6	No	Described as Rietheim Member
Chapelle-1	Unknown	Unknown	No	The Lias has not been penetrated
Courtion-1	Unknown	Unknown	No	Well report not available
Cuarny-1	Unknown	Unknown	No	The Lias has not been penetrated
Eclépens-1	Yes	5	Yes	Rock-Eval Data published in this report
Entlebuch-1	No	0	No	Not evidences in the report
Essertines-1	Yes	3	Yes	Rock-Eval Data published in this report
Fendringen-1	Unknown	Unknown	No	Not accessible
Faucigny-1	Yes	34	Yes	Rock-Eval Data published in Do Couto et al., 2021
Herdern-1	Yes	10	No	Lias z + Lias ἐ described as bituminous shales
Hermingen-1	Unlikely	0	Yes	Considered as unlikely because of that TOC < 1% measured one a set of Lias unit samples; Rock-Eval data published in Elf Aquitaine, 1983
Humilly-2	Yes	8	Yes	Rock-Eval Data published in Do Couto et al., 2021
Hunenberg-1	Unknown	Unknown	No	The Lias has not been penetrated
Kaisten-1	No	0	No	Eroded
Kreuzlingen-	Yes	6	No	Described in the well report
Kusnacht-1	Unknown	Unknown	No	The Lias has not been penetrated
Leuggern-1	No	0	No	Eroded
Lindau-1	Unlikely	0	No	Not evidences in the report
Linden-1	Yes	4	No	Described in the well report
Noville-1	No	0	No	The Lias unit is not present in this area
Marthalen-1	Yes	9	No	Described as Rietheim Member
Pfaffnau-1	Unlikely	0	No	Not evidences in the report. It can be supposed that it is present because recognized in closest wells (Altishofen-1 and Schafisheim-1)
Riniken-1	Yes	5	Yes	Rock-Eval Data published in this report
Romanens-1	Yes	10	No	Described in the well report
Ruppoldsried-1	Unknown	Unknown	No	The Lias has not been penetrated
Savigny-1	Unknown	Unknown	No	The Lias has not been penetrated
Schafisheim-1	Unlikely	0	Yes	Considered as unlikely because of that TOC < 1% measured one a set of Lias unit samples; Rock-Eval data published in this report
Schlattingen-1	Yes	Unknown	Yes	Described in the well report
Sibilingen-1	Yes	7	No	Outcropping in the area
Sorens-1	Unknown	Unknown	No	The Lias has not been penetrated
St. Gallen GT-1	Unknown		No	The Lias has not been penetrated
Thônex-1	Unknown	Unknown	No	The Lias has not been penetrated
Thun-1	Unknown	Unknown	No	The Lias has been only partially penetrated. Not evidences in the report
Treyçovagnes-1	Yes	5	Yes	Rock-Eval Data, published in this report
Tschugg-1	Unknown	Unknown	No	The Lias has not been penetrated
Truellikon-1	Yes	10	No	Described as Rietheim Member
Tuggen-1	Unknown	Unknown	No	The Lias has not been penetrated

Well	Posidonia shale presence	Thickness (m)	Geochemical data availability	Observations
Tuggen-1	Unknown	Unknown	No	The Lias has not been penetrated
Weggis-1	Unknown	Unknown	No	The Lias has not been penetrated
Weggis-1	Unknown	Unknown	No	The Lias has not been penetrated
Weiach-1	Yes	7	Yes	Rock-Eval Data published in this report

Table 1: Wells where the presence of the Posidonia shale unit has been individuated. The availability of geochemical data characterizing this unit and the related source is indicated.

From the data collected in Table 1, the possible areal distribution of the Posidonia shale unit throughout the Plateau is shown in Fig. 6. Because of the scarce and in some cases, uncertain data used, potential inaccuracies of this map must be considered. Further data must be collected to constrain it.

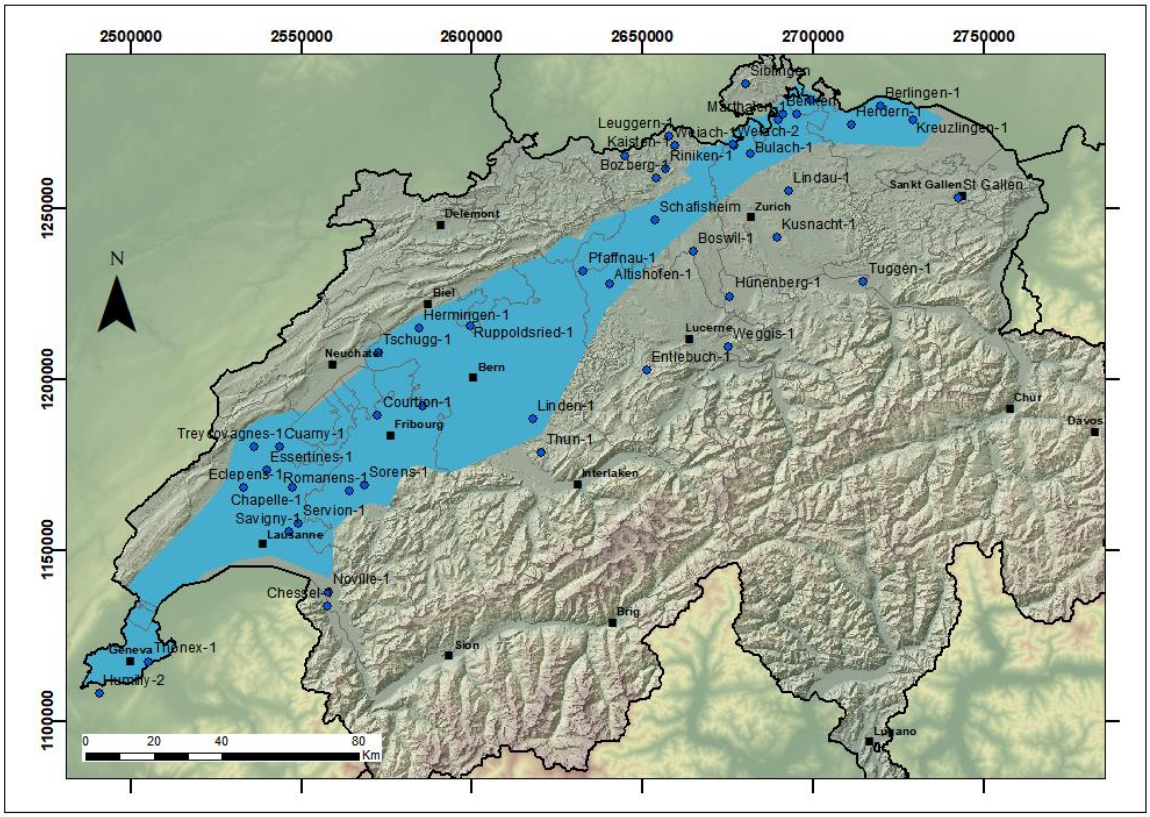


Fig. 6: Posidonia shale distribution throughout the Swiss Plateau, based on well data.

The geochemical properties of the Posidonia shale source rock are available only for some areas: Geneva, Vaud and Northern Switzerland. Geochemical parameters in these areas are summarised in Table 2. The complete Rock-Eval data available for the Lias unit is collected in Appendix 1. Interpolation of these geochemical data permits to reconstruction of their thermal maturity throughout the entire basin, ranging from immature to early oil window conditions in the distal northernmost part of the NAFB, middle oil window conditions in the western part, to late oil window conditions in the southern proximal part of the basin (Greber et al., 2011).

Area	Reference wells	Average thickness (m)	TOC (%)	HI (mgHC/gTOC)	Tmax (°C)	%Ro range
Geneva Basin	Humilly-2; Faucigny-1 and others western Jura French area	20	Min-Max: 0.2-4.3 Avg. 1.18	Min-Max: 22-505 Avg. 147	Min-Max: 422-529 Avg. 458	0.7-2.21
Vaud area	Eclépens-1; Essertines-1; Treyçovagnes-1	4	Min-Max: 0.3-2.7 Avg. 0.86	Min-Max: 57-479 Avg. 170	Min-Max: 429-433 Avg. 435	0.65-0.88
Northern CH	Weiach-1; Riniken-1 and Shafisheim-1	6	Min-Max: 0.3-9 Avg. 3.9	Min-Max: 75-673 Avg. 446	Min-Max: 413-435 Avg. 426	0.43-0.7

Table 2: Posidonia shale source rock geochemical parameters for the areas where data are available. Only in few cases the Posidonia shale deposit could be differentiated from the Toarcian and/or the Lias unit. The source of the Rock-Eval data is indicated in the previous table. Vitrinite reflectance data are from Do Couto et al. (2021) in the Geneva area, from Schegg et al, (1997) in the Vaud area and from Omodeo-Salé et al. (2021) and references herein in Northern Switzerland.

1.5.1.2 Permian and Carboniferous source rocks

The Permian and Carboniferous source rocks represent an important unknown in the petroleum system of the Swiss Plateau. That is because the presence of Permo-Carboniferous grabens under the Mesozoic cover is poorly constrained, as very few high-resolution subsurface data are available. Most of the available data are confined in the North-eastern part of the Plateau, where the Permo-Carboniferous grabens geometry has been reconstructed with good detail, thanks to the availability of several 2D and 3D seismic data and deep wells (Madritsch et al., 2018 and references). A second area where the Permo-Carboniferous grabens geometry has been reconstructed in detail is the St. Gallen area, where a high-resolution 3D seismic survey has been acquired in the planning phase of the St. Gallen GT-1 geothermal well (Heuberger et al., 2016; Omodeo-Salé et al., 2020). In the rest of the basin, the distribution and the geometry of the Permo-Carboniferous grabens were reconstructed by combining gravity data with medium to low-resolution seismic data and data from the few wells penetrating these deposits. The combination of these scattered data provides the map presented by (Leu, 2008). Even though, at present, this map is the most accurate synthesis of the Permo-Carboniferous grabens available data, there still exist several uncertainties. In this work, the data provided in Omodeo-Salé et al. (2020b) and Vranovci (2022) on the distribution of the Permo-Carboniferous graben in the Vaud and Geneva areas were integrated to this map, resulting in the map shown in Fig. 7,.

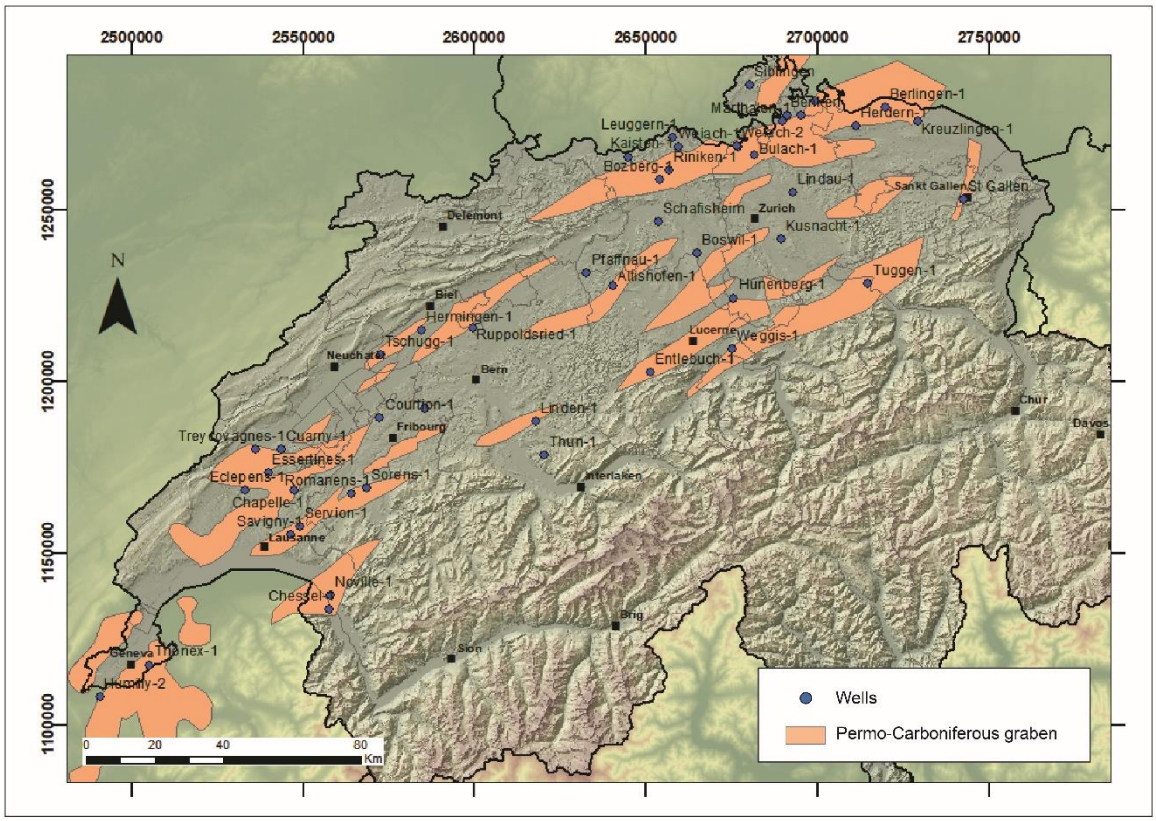


Fig. 7: Permo-Carboniferous troughs distribution in the NAFB

Only in a few cases the Permian and Carboniferous units were penetrated by wells (Table 3) and in even lesser cases, they have been identified layers rich in organic matter, which can be considered as hydrocarbon source rocks. These are the cases of the Weiach-1, Entlebuch-1 and Noville-1 wells. At present, data are publicly available only for the Weiach-1 well (Ajuaba et al., 2021). Few data are also available in the Western Jura and Geneva area (France), where the Permian (and/or Carboniferous) unit has been partially penetrated (Chaleyriat-1; Charmont-1; La Chandelière-1, Chatillon-1D and Humilly-2 wells) (Do Couto et al., 2021). However, because of that, this area is not included in this work, and relatively far from the modelled sections, these data were not considered.

Well	P-C graben identified by geophysical data	Permian presence	Thickness (m)	Carboniferous presence	Thickness (m)	Geochemical data availability	Final depth unit
Altishofen-1		No	0	No	0		Final depth Muschelkalk unit
Benken-1	No	No	0	No	0		Final depth Basement
Berlingen-1	Yes	Unknown		Unknown			Final depth Buntsandstein unit
Boswil-1	No	Unknown		Unknown			Final depth Malm
Bottstein-1	No	No	0	No	0		Final depth Basement
Chapelle-1	Yes	Unknown		Unknown			Final depth Barremian
Bozberg-1	Yes	Yes	48	Unnknown		No	Final depth Permian
Bulach-1	Yes	Yes	50	Unknown		No	Final depth Permian
Courtion-1	No	Unknown		Unknown			Final depth Muschelkalk
Cuarny-1	Yes	Unknown		Unknown			Final depth Lias unit

Well	P-C graben identified by geophysical data	Permian presence	Thickness (m)	Carboniferous presence	Thickness (m)	Geochemical data availability	Final depth unit
Eclépens-1	No	Unknown		Unknown			Final depth Keuper unit
Entlebuch-1	Yes	No	0	Yes	200	No	Final depth Carboniferous unit
Essertines-1	Yes	Unknown		Unknown			Final depth Keuper unit
Faucigny-1	Yes	Yes	363	Unknown		No	Final depth Permian unit
Fendringen-1	No	Unknown		Unknown			Unknown
Herdern-1	No	No	0	No	0		Final depth Basement
Hermingen-1	No	Unknown		Unknown			Final depth Muschelkalk
Humilly-2	Yes	Unknown	110	Yes	110	Yes	Final depth Permian or Carboniferous units (still uncertain)
Hünenberg-1	Yes	Unknown		Unknown			Final depth Malm unit
Kaisten-1	No	Yes	171	No		No	Final depth Basement
Kreuzlingen-	Yes	Yes	18	Unknown		No	Final depth Permian unit
Kusnacht-1	No	Unknown		Unknown			Final depth Malm unit
Leuggern-1	No	No	0	No	0		Final depth Basement
Lindau-1	No	No	0	No	0		Final depth Basement
Linden-1	Yes	Unknown		Unknown			Final depth Keuper unit
Noville-1	Yes	Yes	868	Yes	538	No	Final depth Carboniferous unit
Marthalen-1	No/yes	Yes	56	No	0	No	Final depth Basement unit
Pfaffnau-1	Yes	Yes	12	No	0	No	Final depth Basement
Riniken-1	Yes	Yes	802	Unknown		No	Final depth Permian unit unit
Romanens-1	Yes/No	Unknown		Unknown			Final depth Keuper unit
Ruppoldsried-1	No	Unknown		Unknown			Final depth Cretaceous unit
Savigny-1	Yes	Unknown		Unknown			Final depth Cretaceous unit
Schafisheim-1	No	No	0	No	0		Final depth Basement
Schlattingen-1	Yes	Yes	0	No	0		Final depth Basement
Sibilingen-1	No	No	0	No	0		Final depth Basement
Sorens-1	Yes/No	Unknown		Unknown			Final depth Cretaceous unit
St. Gallen GT-1	Yes	Likely		Likely			Final depth Dogger
Thônex-1	No	Unknown		Unkonown			Final depth Malm unit
Thun-1	Unknown	Unknown		Unknown			Final depth Lias unit
Treyçovagnes-1	Yes	Yes	478	Unknown		No	Final depth Permian unit
Tschugg-1	Yes	Unknown		Unknown			Final depth Cretaceous
Truellikon-1	Yes	Yes	13	No	0	No	Final depth Basement
Tuggen-1	Yes	Unknown		Unknown			Final depth LFM unit
Weggis-1	Yes	Unknown		Unknown			Final depth LFM unit
Weiach-1	Yes	Yes	456	Yes	572	Yes	Final depth Basement

Table 3: Wells where the presence of the Permian and Carboniferous units has been individuated. Thickness and geochemical data availability is also indicated.

The Weiach-1 well is the only case where the Permian and Carboniferous units have been completely penetrated, permitting the realization of a detailed geochemical screening of the potential Permian and Carboniferous source rocks (Ajuaba et al., 2023; Leu et al., 2001; Matter, 1987; NAGRA, 2002). Geochemical parameters of the Permian and Carboniferous source rocks in the Weiach-1 well are summarized in Table 4. The complete Rock-Eval data measured along the well is presented in Appendix 2. The thermal maturity of the Permian and Carboniferous source rocks has been calculated throughout the entire Plateau (Greber et al., 2011), and it ranges from the late oil window in the northernmost distal edge of the basin to the gas window in the south.

Source rock	**TOC (%) Min and Max and average (*) values**	**HI (mgHC/gTOC) range and (*) average**	**Tmax (°C) range**	**%Ro range**
Permian lacustrine shales	0.95-10 *4.3	24-488 *171	435-460	0.56-0.71
Carboniferous coal	51-77 *63	143-227 *215	440-461	0.78-1.28
Carboniferous shales	2-28 *8	37-205 *92	443-480	

Table 4: Permian and Carboniferous source rocks geochemical parameters. Rock-Eval data from Ajuaba et al., (2023); vitrinite reflectance data from NAGRA, 2002 and Ajuaba et al., 2023

1.5.2 Reservoirs and seals

Several potential reservoirs and seals were identified in the NAFB, based on stratigraphic, sedimentological and petrophysical properties, (Chevalier et al., 2010; Greber et al., 2011; Keller, 1992, among others). Based on previous literature and unpublished borehole data (SEAG), (Chevalier et al., (2010) proposed a review of the lithologic sequence of the NAFB, identifying several suitable aquifer and seal pairs in the Permo-Carboniferous, Mesozoic and Cenozoic stratigraphic sequences. Some of them could represent potential hydrocarbon reservoirs (Greber et al., 2011). However, because of the scattered available data (few deep wells cross these targets throughout the entire basin), the regional variations of the reservoirs and seal properties throughout the basin are not fully understood. Thus, there are several uncertainties on the potential capacity of these rocks to store and seal hydrocarbons in the subsurface throughout the basin.

In this study, the potential reservoir units are classified into plays, where a play is a pack of rocks where hydrocarbon reserves can be found. There are several ways to define a play, based on a geographical region, an age, a depositional environment, etc…(Stoneley, 1995). In the Swiss Plateau, plays were defined based on the stratigraphic setting of the Swiss Plateau (Table 5). Each play contains the three elements defining a petroleum system: reservoir, seal, and source rocks. In this study, seven hydrocarbon plays were considered (Table 5). The name assigned to each play refers to the reservoir unit composing the play.

- Cenozoic play. In the Cenozoic foreland deposits (Molasse), the dominant sandy UMM and LMM units can be considered as potential reservoirs, with porosity ranging between 10 and 20% and 2 and 20%, respectively. Nevertheless, the large facies and permeability vertical variation, together with the scarce low-permeability rocks (shales) superimposed and/or interfingered with the sandstone bodies (potential seals), makes the formation of a large hydrocarbon reservoir in the Molasse units unlikely. However, small to medium hydrocarbon accumulations can be expected if local stratigraphic and structural traps are present. In the Cenozoic deposits, oil shows at the surface and tunnels are numerous, especially in the distal edge of the NAFB, mostly in the area from Geneva to Yverdon, in the Jura Mountains and within the subalpine unit in the triangle zone structure, east of Lake Thün (Leu, 2012; Schegg et al., 1999 and references herein). Non-commercial oil impregnations in the Oligocene units were also found in the wells Peissy, La Pleine (Geneva area) and Cuarny-1 (Vaud area) (Dolivo, 2007; Leu, 2012), among others.

- Lower Cretaceous play. The lower Cretaceous units are represented only in the western sector of the basin, reaching their maximum thickness in the Geneva area, whereas they are completely missing in the eastern half. They are mostly composed of limestones and marls. Porosity can be very heterogeneous, up to 15%, depending on the degree of karstification (Leu, 2012). The seal can be the low permeability deposits of the uppermost Molasse LFM unit (Cenozoic in age). Structural traps can be formed in the latest Alpine deformation (Pliocene-late Miocene) when the Jura Mountain belt was also structured. Oil shows in the Cretaceous were mostly found in the Jura Mountain, Geneva areas and the Eclepens-1, Savigny-1 and Hermrigen-1 wells (Leu, 2012, 2008; NAGRA, 2008).

- Malm play. The Upper Malm (late Jurassic in age) reservoir unit is present along the entire basin, and it consists of micritic limestones, reef and argillaceous limestones (late Oxfordian to Kimmeridgian in age). Seals and traps are like what is described above for the lower Cretaceous units. The matrix porosity and permeability of the Malm unit are rather low (1-2%). Nevertheless, karstification and fracking processes can considerably improve their reservoir properties. The only semi-commercial gas field found in Switzerland (Entlebuch-1 well, 1980, 2.65 bcf or 74 Mio. m^3) was produced from karstified Malm limestones (Leu, 2012). Non-commercial gas shows were found in the Malm and in the Linden-1 and Thun-1 wells. Oil shows were found in the Eclepens-1 well.

- Dogger play. The Dogger oolitic limestone unit (middle Jurassic in age) is a potential reservoir, especially in the central part of the basin (Yverdon-Entlebuch-Aarau area) (Chevalier et al., 2010). Porosity can vary from 1 to 6%. The overlying marls and shaly limestones composing the Malm unit (late Jurassic in age) can be the correspondent sealing unit. In the Dogger unit, gas shows were found in the Cuarny-1, Linden-1 and Hermrigen-1 wells, and oil shows in the Eclépens-1 well.

- Lias play. The Rhaetian and Liassic sandstones (late Triassic-early Jurassic in age) are potential reservoirs with medium to good properties (porosity of 5-15%). Lower Jurassic mudstones and the overlying Opalinus clays deposits (middle Jurassic in age) represent the corresponding seals of this reservoir. These units are oil-bearing in the Eclépens-1 and Essertines-1 wells, however, with non-commercial quantities. Hydrocarbon shows in these units have also been found in wells located in central-eastern Switzerland (Leu, 2012).

- Muschelkalk play. In the uppermost part of the Muschelkalk deposits (middle Triassic in age), the dolomite Trigonodus unit represents a potential reservoir with a porosity of 10 to 20% (Chevalier et al., 2010). Porosity is mostly determined by dissolution, faulting and karstification processes. Therefore, permeability can considerably change along the basin, depending on the intensity of these processes. This potential reservoir is sealed by anhydrite and salt (mostly in the SW) deposits, alternated with clay and marl, forming the Gipskeuper unit (late Triassic in age). The thickness of this seal increases from 40 meters in the NE of the basin, to 100 meters near Olten, to more than 200 meters in the SW. The low permeability of this unit can be reduced by dissolution, karstification and faulting processes, similar to what is described for the lowermost Anhydrite Group. In this unit, oil and gas shows have been found in the Treyçovagnes-1 and Hermrigen-1 wells, respectively.

- Lower Triassic play. The basal Triassic sequence is formed by sandstone deposits, 10-20 meters thick and with porosity up to 18%, that can be very good hydrocarbon reservoirs. The lowermost unit is the Buntsandstein sandstone, quartz dominant and present mostly in the NE of the basin and to the SW, presumably also north of the line Olten-Bern-Lausanne. Following, the Melser coarse quartz sandstones (Muschelkalk) presumably cover most of the basin, except for the NE, where it becomes dolomitic and argillaceous (Chevelier et al., 2010). These sandstone units are not easily distinguished throughout the basin; thus, they have been frequently considered as a unique unit. The overlying low-permeable and regional extended anhydrite sequence of the middle Muschelkalk, the Anhydrite Group (middle Triassic in age), composed of anhydrite intercalated with dolomite, mudstones and minor rock, can represent an excellent seal of these reservoirs. However, the high aqueous solubility of anhydrite and gypsum can lead to dissolution, erosion and karstification. Furthermore, as the anhydrite rheological behaviour is more brittle, the seal can be fractured, thus less efficient. That could explain why, at present, only a few oil/gas accumulations have been found in the lower Triassic

deposits: non-commercial gas shows were found in the Buntsandstein and lower Muschelkalk units in the Treyçovagnes-1 well.

Permo-Carboniferous play: In the Permo-Carboniferous sequence, different deposits have potential reservoir properties. These units have been mostly characterised in the northern sector of the NAFB, where the Permo-Carboniferous troughs have been largely explored (Diebold et al., 1991; Madritsch et al., 2018) and references herein). The porosity of the Permian coarse-grained sandstones (Rotliegend facies) and Carboniferous sandstones (Stephanian) ranges from 3 to 12%. The permeability properties are very low due to the great depths at which these deposits have been buried (Chevalier et al., 2010). However, they can be a target for tight reservoirs (Kempter, 1999). The seal of these potential reservoirs are the shaly deposits, which are intercalated and the overlying low-permeable Triassic deposits (Muschelkalk and Keuper anhydrite intervals). Furthermore, the Carboniferous coal deposits, intercalated in the sandstones and shales, can be coal-bed methane play(Lahusen and Wyss, 1995). Gas shows were found in the Noville-1, where a tight gas accumulation was discovered (Leu, 2012), and in non-commercial quantities in the Entlebuch-1 and Weiach-2 wells. In the rest of the NAFB, due to the lack of data, these potential targets remain completely unexplored.

Play	Reservoir	Seal	Wells
Cenozoic	Sandstone bodies (Molasse, UMM and LMM units)	Shales intercalated (Molasse units), Quaternary	• Geneva area, Yverdon area, Jura Mountain, east of Lake Thün (oil shows at surface and tunnels) • Peissy-1 (oil shows) • La Pleine-1 (oil shows) • Cuarny-1 (oil shows)
Lower Cretaceous	Karstified and/or fractured limestones and marls (Lower Cretaceous) in the western part of the NAFB	Shales and marls of the Molasse (LFM)	• Eclépens-1 (oil shows) • Savigny-1 (oil shows) • Hermrigen-1 (oil shows) • Western Jura and Geneva Basin (oil shows)
Malm	Karstified and/or fractured micritic limestones and reef (Malm)	Intercalated argillaceous limestones (Malm) or Cretaceous marls, shales and marls of the Molasse (LMM, LFM)	• Entlebuch-1 (semi-commercial gas field) • Eclépens-1 (oil shows)Entlebuch-1 (semi-commercial gas field) • Linden-1 (gas, non-commercial quantity) • Thun-1(gas, non commercial quantity)
Dogger	Oolitic limestones (Dogger) in the central part of the NAFB	Marls and shaly limestones (Malm)	• Eclépens (oil shows) • Cuarny-1 (gas shows) • Linden-1 (gas shows) • Hermrigen-1 (gas shows)
Lias	Rhaetian and Liassic sandstones	Mudstones (Lias) and Opalinus clays (Dogger)	• Eclépens-1 (oil, non-commercial quantity) • Essertines-1 (oil, non-commercial quantity) • Wells in the central part of the NAFB (?) (oil shows)
Muschelkalk	Muschelkalk (Trigonodus dolomite)	Anhydrite and sault alternated with shales and marls (Gypskeuper)	• Hermrigen-1 (oil shows) • Treyçovagnes-1 (gas shows)
Lower Triassic	Buntsandstein and Muschelkalk (Melser sandstones)	Anhydrite (Middle Muschelkalk)	• Treyçovagnes-1 (gas shows)

Play	Reservoir	Seal	Wells
Permo-Carboniferous	Permian and Carboniferous sandstones	Intercalated shales and Triassic anhydrite deposits	• Noville-1 (gas) • Weiach-2 (gas shows, non-commercial quantity) • Entlebuch-1 (gas shows, non-commercial quantity)

Table 5: Hydrocarbons are defined in the NAFB. For each play, the wells where hydrocarbon traces were encountered in the potential reservoir are also indicated.

1.5.3 Traps

From previous investigations and literature data (Brink et al., 1992; Greber et al., 2011; Kempter, 1994), the most relevant features that can act as traps in the Swiss Plateau are the following: 1) extensional tilted fault blocks, occurring in the Permo-Carboniferous, Mesozoic and Cenozoic unit; 2) compressional tilted fault blocks, occurring in the same units as above, mostly in the distal part of the basin and near the frontal Alpine thrusts; 3) thrusted units, also in the subalpine thrusted area and in the distal part of the NAFB, where the Jura thrust-fold belt starts to form; 4) anticlines structures, in the Jura fold-and-thrust belt domain, in the Alpine front, and along the entire basin; 5) stratigraphic traps, mostly in the Permo-Carboniferous sequence and in the Cenozoic Molasse units. However, the poor volumetrically significant hydrocarbon accumulations found throughout the basin suggest that these traps are scarce and/or breached.

1.5.4 Generation/Migration/Accumulation processes

Very few studies were done in the past to quantify the hydrocarbon generation, migration and accumulation processes in the Swiss Plateau. Schegg et al. (1999) realized a 2D petroleum system model in the Vaud area and Greber et al. (2007) provided several 1D models throughout the entire Plateau. By these works, it has been reconstructed that the hydrocarbon generation and expulsion occurred in the late Jurassic to Cretaceous times in the northern distal part of the basin and in the Cenozoic, when the foreland basin formed in the entire basin. Accumulations form in the clastic Molasse unit and Jurassic carbonates, sourced mostly by the Posidonia black shales. Accumulations in the Triassic reservoirs are sourced by the Permian and Carboniferous source rocks. Migration occurs for overpressure in the proximal thrusted part of the basin, with fluids migrating northward, toward the distal part of the basin. Faults also play an important role in hydrocarbon migration. To estimate the efficiency of a fault to conduct fluids, the fault cementation state must be considered. Cementation depends on the tectonic activity and diagenetic processes, which are difficult to quantify, especially in a basin-scale study. Therefore, assumptions and scenario cases are necessary.

1.5.5 Preservation

To be found in a basin, the hydrocarbons must be accumulated and preserved until the present day in a stratigraphic and/or structural trap. Reservoir leakage, due to reactivation of faults, folding, uplift and erosion of the basin, could impede the preservation. This is why, to predict the hydrocarbon preservation in a basin, it is important to consider parameters such as the age of the main tectonic events and the fault activity. In the Northern Alpine Foreland Basin, uncertainty on these parameters is large. Thermal modelling can calculate the preservation state of the potential hydrocarbon accumulations based on the assumptions made (fault cementation state, fault ages, etc). To take into consideration these uncertainties, different scenarios were run.

2 Methodology and Data

To achieve the UNCONGEO project objectives, two main work phases were envisaged (Fig. 8). In the first phase, the petroleum system modelling of the Swiss Plateau was analysed using the state-of-the-art and industry-standard petroleum system modelling tool. Five 2D thermal models were realised along key geological transects throughout the basin. The thermal models were validated

by calibration data (porosity, temperature, vitrinite reflectance) measured in wells. Modelling results provide an estimate of the thermal maturity of the potential hydrocarbon source rocks. Furthermore, the model estimates the potential hydrocarbon migration paths and the areas and stratigraphic units where hydrocarbon accumulations are likely along the sections. For each section, the uncertainties related to the software limitations and the lack of data were highlighted.

The second phase aims to visually represent in maps the risk of encountering hydrocarbons in the subsurface of the Swiss Plateau. These cartographic representations were generated following the well-established workflow in use in the hydrocarbon industry (Petroleum System Analysis and Combined Common Segment maps). This methodology provides Common Risk Segment maps (CRS) representing the probabilities of hydrocarbon occurrence, which, from the geothermal exploration perspective, is the risk of hydrocarbon occurrence in the subsurface. This approach is applied to each identified hydrocarbon Play. All the available information regarding the distribution and quality of reservoir rock, seal and hydrocarbon source rock was integrated into the map. For each play, the final map obtained by this work offers an overview of the risk of finding hydrocarbons in a specific stratigraphic unit throughout the entire Swiss Plateau area. A final map showing the availability of data (seismic, wells, analytical data, etc) was also realised to identify the areas where uncertainties must be considered because of poor data quality and/or lack of data.

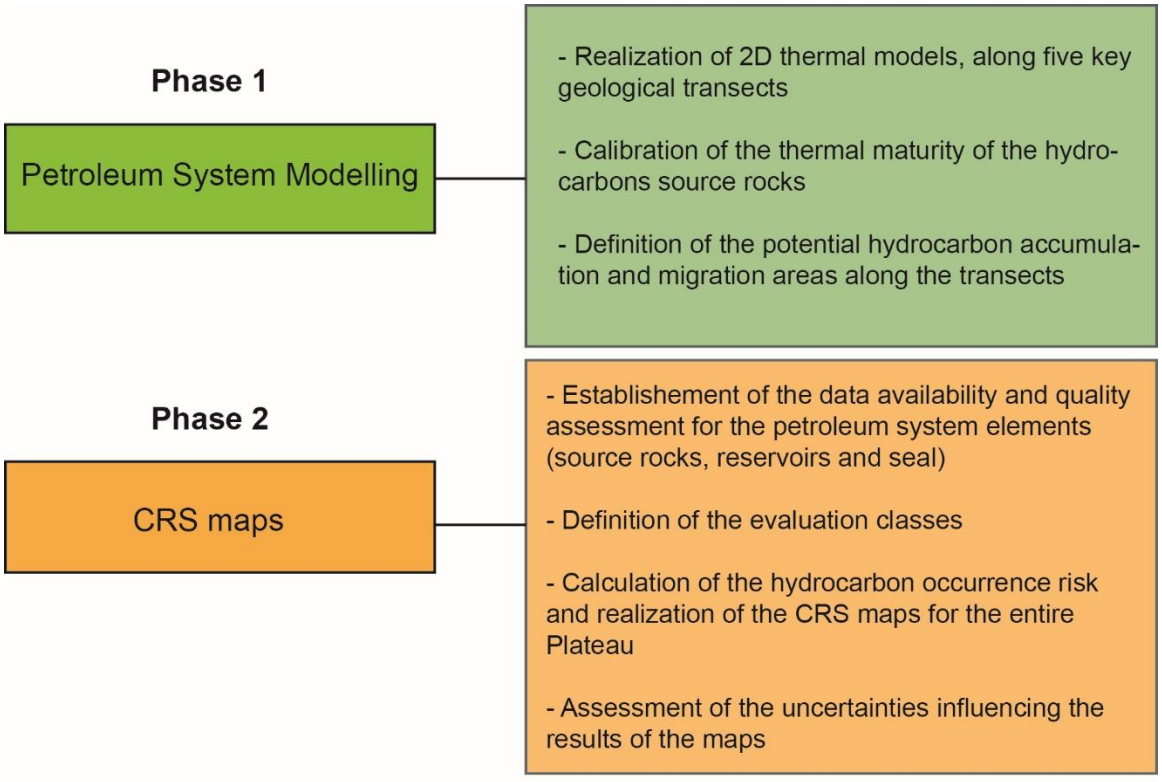


Fig. 8: General workflow adopted in the UNCONGEO project

2.1 Petroleum system modelling

The petroleum system modelling is based on the thermal modelling approach, a basin-scale workflow that aims at reconstructing the thermal history of a basin, taking into account most of the variables influencing the thermal evolution of a basin (Poelchau et al., 1997; Welte and Yalcin, 1987; Welte and Yukler, 1981; Wygrala, 1988; Yalçin, 1991; Yalçin et al., 1997; Yalçin and Welte, 1988). Thermal modelling can consider most of the stratigraphic, sedimentological, geochemical, structural and geodynamic data of a sedimentary basin and calculate their effect on the temperature evolution over time of the basin infill. To carry out this workflow, a specific computational software is used. In this project, the PetroMod software (Version 2022, SLB) was used.

The application of the thermal modelling approach is crucial in determining the hydrocarbon potential of an area. Thermal modelling provides an estimate of the thermal maturity state of

potential hydrocarbon source rocks hosted in the basin and of the timing when hydrocarbon could start to be expelled. Because of that, the model considers the facies and geometry of the stratigraphic units and faults, as well as their evolution over time, it also estimates the areas of the basin where hydrocarbon migration and accumulation could occur.

Petroleum system modelling can have different grades of resolution, which depend on the data and time availability. In the case of 1D model, the geological conceptual model corresponds to a stratigraphic log, generally from a well or, less frequently, from a section measured in the field. In the case of the 2D model, the conceptual model is based on a cross-section of the basin, interpreted from a depth-converted seismic line or a geological cross-section of the basin. In the case of the 3D model, the conceptual model is based on the interpretation of a depth-converted 3D seismic block or from a 3D geological model. In the UNCONGEO project, the 2D model complexity was chosen mostly because of a matter of available time.

Five 2D petroleum system models (Section 2 to Section 6) were realised based on five geological cross-sections representative of the geometry of the Swiss Plateau basin (Fig. 9). Section 1, passing from the Geneva area, was planned in the first phase of the project, but finally, it was not carried out. That is because, soon, a 3D geological model is going to be realised for this part of the basin based on high-resolution 3D seismic data recently acquired in the area. Therefore, for the Geneva area, a 3D petroleum system model will be realised, with greater resolution than what it could be obtained by a 2D section model.

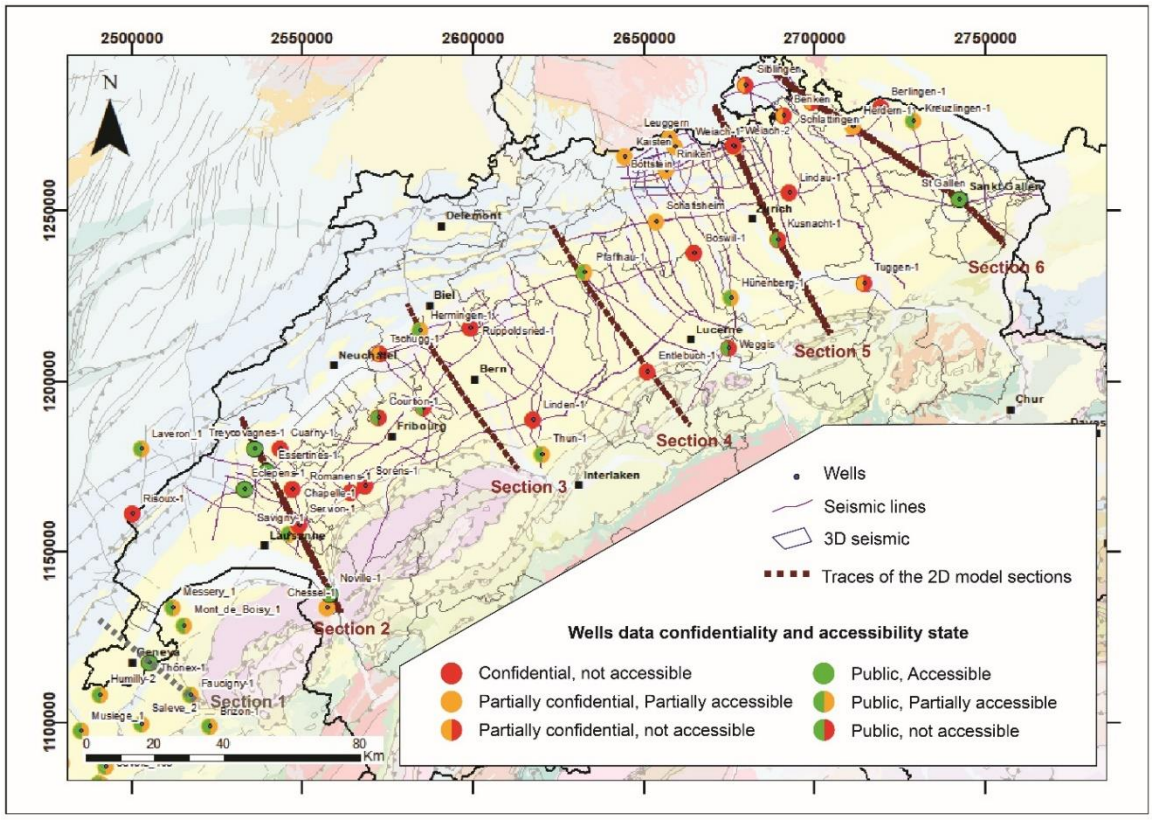


Fig. 9: Traces of the regional sections used for modelling. The distribution of the subsurface data in the study are also shown. The wells data confidentiality and accessibility are indicated. For the geological map legend see Fig. 2

The geological sections used for modelling were extracted from the GeoMol 2021 project, a 3D geological model of the entire Swiss Plateau, realized by swisstopo (Fig. 10) (https://www.swisstopo.admin.ch/de/wissen-fakten/geologie/geologische-daten/3d-geologie/tief/geomol.html). GeoMol is composed by the surfaces of the main geological units and the most relevant faults, converted in depth. It is based on geological maps, digital elevation model, more than 5000 km of seismic data and more than 60 deep wells (Allenbach et al., 2017).

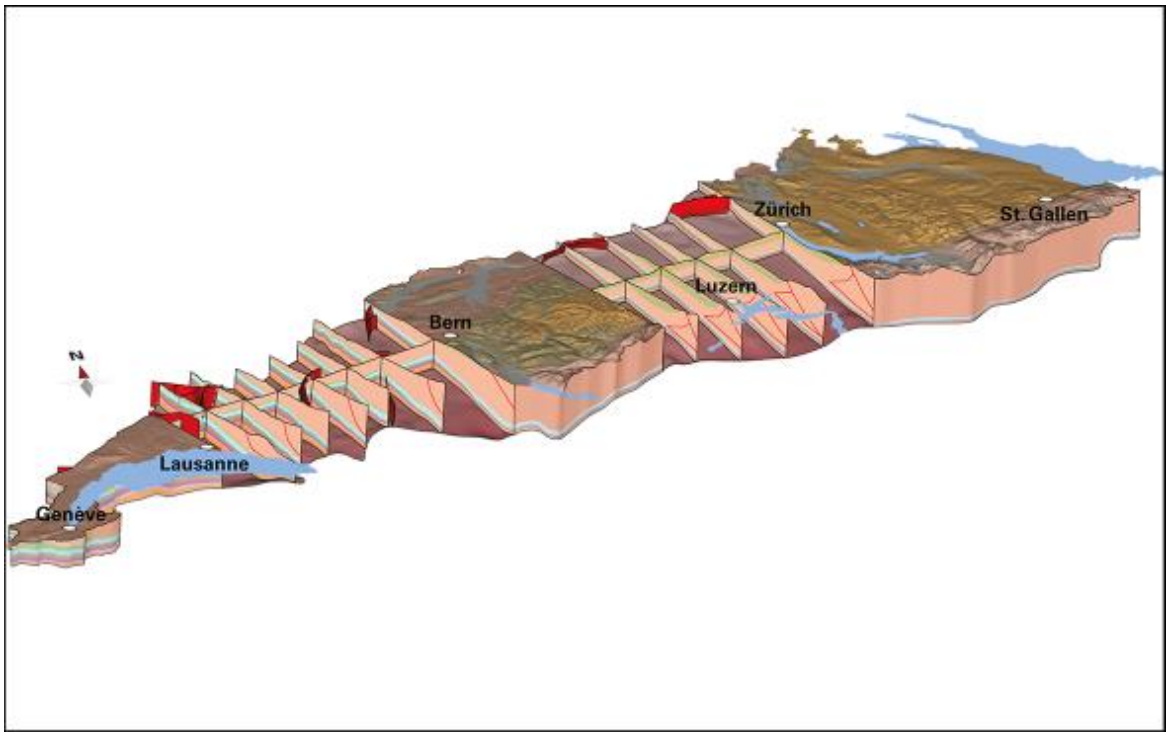


Fig. 10: GeoMol 3D project and 2D sections extracted (from https://www.swisstopo.admin.ch/de/wissen-fakten/geologie/geologische-daten/3d-geologie/tief/geomol.html)

The workflow used to produce the five 2D petroleum system models is shown in Table 6. It is composed of eight steps, aiming at providing the software with all the data necessary to simulate the petroleum potential along a section. In Step 1, the present-day geometry of the basin in depth is defined. Step 2 aims at reconstructing the structural evolution of the basin over time. Step 3 aims to populate the model with the lithological properties of the stratigraphic units composing the basin infill. Step 4 aims at assigning geochemical properties to the source rocks, thus their initial hydrocarbon potential. Step 5 aims to define the upper and lower boundary conditions of the model, controlling the temperature distribution in the basin infill. Step 6 aims at calibrating the modelling results with data directly measured in the rocks. In this phase, the variables controlling the temperature and porosity distribution in the basin are interactively changed to fit the calibration data. Step 7 aims at simulating the generation, migration and accumulation of the hydrocarbons in the basin, thus estimating the areas where hydrocarbons could be present. Step 8 aims to evaluate the main uncertainties of the data and assumptions used to build the model and to indicate their impact on the reliability of the modelling results. In Table 6, for each task, they are indicated the set of data necessary to accomplish it and the main data source. The distribution of the subsurface data available in the studied area is shown in Fig. 9. The list of the wells considered to carry out the petroleum system modelling of the five transects, and the related data collected for each well, are summarised in Appendix 3. The stratigraphic log of the wells is shown in Appendix 4.

PETROLEUM SYSTEM MODELLING workflow		
	Task	Data
1	**Reconstruction of the geometry of the basin**	
a	Stratigraphic horizons and faults	GeoMol, extraction of 2D sections from the 3D model of the basin (in depth)
b	Permo-Carboniferous grabens location and geometry	Leu, (2008) Marchant et al., (2016)
c	Estimate of the missing eroded section	Literature
2	**Structural model**	
a	Single vergent thrust plane: Restoration of the Alpine thrusting (Move software)	Literature, geological map
b	Opposite vergence thrust planes (Triangular zone): Simulation of the formation of the thrusting with the paleo thickness tool (directly in the Petromod software)	GeoMol surfaces
3	**Facies distribution**	
a	Litologic characterization of the stratigraphic units along the section	Wells reports, Stratigraphic logs
4	**Source rocks characterization**	
	Estimating and assigning the initial hydrocarbon potential of each source rock and the kinetic	Rock-Eval data (TOC, HI, Type of kerogen) measured along wells
5	**Boundary conditions**	
a	Heat flow	Present-day heat flow calculated from borehole temperature data throughout the basin. Paleo-heat flow trend over the time estimated from the geodynamic evolution of the basin
b	Paleo water depth	Estimated from the depositional setting of the stratigraphic units composing the basin infill
c	Sediment water interface temperature	From the software library
6	**Calibration of the model**	
a	Porosity Variables changed in the model up to fit the calibration data: initial porosity of the facies assigned to the stratigraphic units	Porosity data measured along wells
b	Present-day temperature Variables changed in the model up to fit the calibration data: present-day heat flow	Temperature data measured along wells
c	Thermal maturity conditions Variables changed in the model up to fit the calibration data: magnitude of the erosion and paleo-heat flow values	%Ro data measured along wells AFT data TAI data
7	**Simulation of the hydrocarbon generation, migration and accumulation processes**	
a	Estimate of the source rocks thermal maturity and timing of hydrocarbon generation	Modelling results
b	Estimate of the hydrocarbon migration paths and potential accumulation	Modelling results
c	Balance of the hydrocarbons generated and accumulated	Modelling results
d	Reconstruction of the petroleum system charts for each source rock	Modelling results
8	**Evaluation of the uncertainties**	All data

Table 6: Workflow followed to reconstruct the petroleum system modelling of five sections of the Swiss Plateau. For each step, the tasks and the data necessary to accomplish it are indicated.

2.1.1 Reconstruction of the geometry of the basin

2.1.1.1 Stratigraphic horizons and faults

The input data necessary to define the basin geometry in the software are:

- The present-day thickness and geometry of the main stratigraphic units.
- The ages of the deposition and erosional events.

- The faults' geometry and age.

The thickness and geometries were defined from the geological cross-sections used to build the model (GeoMol data). The ages of the deposition and erosion events were assigned considering the literature data.

The fault geometry was also defined from the cross-section (GeoMol data). The basement faults, bounding the Permo-Carboniferous grabens, are not included in the GeoMol project, except the Constance-Frick graben in the north-eastern part of the Plateau. Therefore, the geometry and extension of these faults were interpreted by considering the geometry of the grabens (see the source of the latter in the following paragraph). To make the migration most likely and efficient, in most of cases, it has been tested the option that the basement faults continue into the Mesozoic sequence and are active until the present day. The type of faults was defined based on the classification provided by the GeoMol database. For each section, the fault type is indicated with different colours in the section extracted from GeoMol.

The fault activity age was defined by considering its location and nature. Three main groups were defined (Table 7): i) the Jura normal faults and thrusts, which bounded the fold and thrusts structure in the northern part of the sections, toward the Jura Mountain; ii) the Molasse basin thrust planes, which bounded the Alpine and subalpine nappes over thrusting the foreland basin in the southern part of the sections; iii) the Permo-Carboniferous/Basement normal faults, which bounded the Permo-Carboniferous grabens. In this study, it has been considered that the Permo-Carboniferous faults have been reactivated during the Alpine deformation phase up to the present day. Thus, they could be efficient fluid conductors, permitting the hydrocarbons generated by the Permian and Carboniferous source rocks to flow to the uppermost units.

Fault group	Age From (My)	Age To (My)
Jura faults and thrusts	5	0
Molasse Basin thrust planes	11-7	0
Permo-Carboniferous/Basement faults	323	0

Table 7: Fault families and age activities are defined in the models

The permeability of the faults, thus their efficiency as a fluid conductor, depends on the cementation state, which is unknown in most cases. Because of that, for each section, two scenarios were tested: open and closed faults, which they considered respectively not cemented and cemented states.

2.1.1.2 Permo-Carboniferous grabens

The GeoMol project did not include the crystalline basement or the Palaeozoic grabens due to the poor data quality at that depth. An exception is the northeastern area of the basin, where a 3D reconstruction of the geometry of these grabens was possible, thanks to the availability of a newly acquired 2D seismic survey combined with reprocessed previous 2D seismic data (Madritsch et al., 2017 and reference herein). For the rest of the Plateau, we considered what has been proposed by Leu (2008), corroborated by other data when available (e.g., 3D seismic in the St. Gallen area, presented in Naef and Schlanke, 2014; Heuberger et al., 2016; Omodeo-Salé et al., 2020).

2.1.1.3 Erosion

To calculate the maximum burial depth of the basin infill and the maximum temperature attained by these rocks, it is crucial to consider the thickness of the stratigraphic section eroded. The age of the erosional events is also relevant, as it determines the burial timing, which also controls the maturation process. These types of data cannot be directly measured, they need to be estimated from indirect data. Paleotemperature data (such as vitrinite reflectance, apatite fission tracks, clays, etc) are indicators of the maximum temperature/thermal conditions attained by the basin infill at a specific depth, thus they provide essential data to estimate the erosion magnitude and timing.

These data are used to validate the thermal modelling results, which calculate the maximum depth and time necessary to attain these temperatures in a specific geodynamic context.

2.1.2 Structural model

When the geological cross-section presents duplication by thrusts and inverted faults, it cannot be simply imported into the petroleum system modelling software as is, because the thermal modelling software cannot handle multiple z-values (the same unit repeated along a depth z-point).

To deal with this software limitation, it is necessary to introduce the compressive deformation steps; thus, a sequence of paleo sections, representing the evolution of the basin geometry, from the present-day geometry up to pre-deformed geometry. The paleo sections are combined by applying the TecLink-Petromod workflow, which consists of cutting each section into individual blocks, where inverted faults and/or thrust planes are present. Each block is simulated by the software as a separate 2D model. Blocks were enumerated in a sequential order, to provide information to the simulator on how to rebuild the structural evolution of the modelled area. The block with the lowest number is the first in the sequence, and the one with the highest number is the last in the sequence. In each section, parent blocks were defined, in case different blocks were formed from a unique block of a previous stage.

In the NAFB, the most relevant inverted faults are located firstly in its southern border, where the more external thrusts of the Subalpine Nappes are present, and secondly in the northern area, where the most internal fold-and-thrust structures of the Jura Mountains appear. To the south, two structural styles were distinguished (Fig. 3). The first style is characterised by single-vergent thrust planes, and it is observed in the western-central part of the basin (area of Section 2 and Section 3) (Section A-A' in Fig. 3). The second style is characterised by opposite vergence thrust planes, forming in between a triangular zone. It is observed in the central-eastern part of the basin (Section 4, Section 5 and Section 6 area) (Section B-B' in Fig. 3). Because of that, these two settings present different grades of complexity, and two different workflows were envisaged.

2.1.2.1 Single vergence thrust plane

When a single-vergent thrust plane is present, the reconstruction of the basin geometry to the pre-Alpine thrusting phase was done using structural restoration. The Move software (IPM 12.5) was used, applying the Simple Shear and Fault Bend Fold methods (Mitra and Namson, 1989; Rouby et al., 1996; Suppe, 1983). The thrusted area was shifted back (southward) to find the geometry of the basin before the compressive deformation. The amount of shifting is hardly constrainable as there are very poor stratigraphic key horizons in the thrusted deposits. Thus, in this work, a representative length of 10-15 km is considered. To constrain this data, in the future, a more detailed structural restoration will be necessary, which is beyond the objectives of this work. In the retrodeformed sections, the stratigraphic thickness missing due to erosion was added on top of the section, mostly considering literature data.

2.1.2.2 Opposite vergence thrust plane

In the areas characterised by opposite vergence thrust plane (triangular zone), a simplified method was applied directly in the PetroMod software. This is because, to obtain a constraint reconstruction of the structural evolution of Alpine and Subalpine Nappes and of the formation of the triangular zone, a proper structural study must be carried out, integrating all the existing seismic, structural, stratigraphic, and regional geological data, which is beyond of the objectives of this study.

By the simplified method proposed herein, the present-day geometry of the basin was imported into the PetroMod software as it is now (section extracted from the GeoMol project). A dummy stratigraphic unit was added between the Molasse units below and above the triangular zone, with a paleo thickness of zero (Fig. 11, t2). At the time when the triangular zone started forming, the dummy unit was assigned a paleo thickness (Fig. 11, t1), which gradually increases, up to reach the present-day geometry (Fig. 11, t0). In this way, it is reproduced the formation of a structural wedge thrusted from southward into the middle of the Molasse deposits. Finally, the uppermost Molasse deposits were exhumed and eroded (Fig. 11, t0). The amount of erosion on the top of the triangular zone is in the order of magnitude necessary to establish an undeformed foreland geometry. This method was applied for sections 4, 5 and 6, where the triangular zone is present.

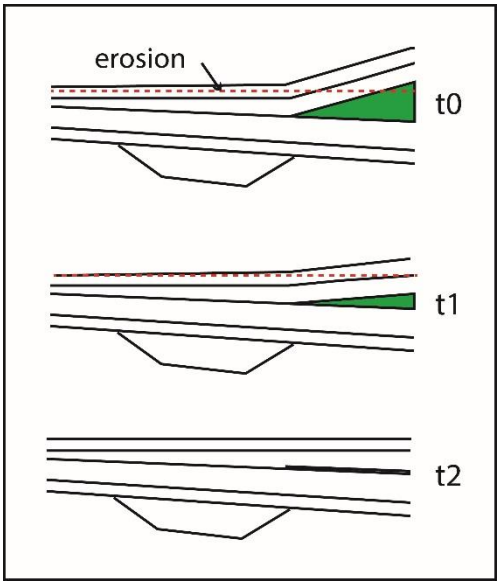


Fig. 11: Sketch explaining the simplified method to simulate the formation of the triangular zone directly in PetroMod.

2.1.3 Facies distribution

The facies assigned to the stratigraphic units composing the geological section control the petrophysical properties (porosity, permeability, thermal conductivity, etc.) simulated by the model. Facies along the section were assigned considering the lithological composition of each stratigraphic unit, expressed in the percentage of the main lithologies composing the related deposits. These data were extrapolated from the wells adjacent to the modelled section when the geological report was available. When lithological data were not available in the wells close to the section and/or no data were collected for the deepest units (case of shallow wells), facies were extrapolated from adjacent areas of the basin where data were available.

2.1.4 Source rock characterisation

To estimate the volume and type (oil or gas) of hydrocarbon generated by the source rocks, it is essential to define their hydrocarbon potential, based on the amount and type of organic matter (continental, lacustrine, marine) composing them. In the PetroMod software, it is defined the initial hydrocarbon potential of each source rock, expressed by the original TOC value (total organic carbon, %), indicating the amount of organic matter contained in the rock, the original HI (hydrogen index, mgHC/gTOC), indicating the potential of the rock to generate hydrocarbons, and the source rock kinetic, indicating the hydrocarbon transformation timing and temperature of the organic matter composing the source rock. The initial TOC and HI values cannot be measured today when the rocks have already been partially or completely thermally transformed, thus, they need to be indirectly estimated. To this purpose, the GeoChem module of the PetroMod suite was used, where the Peters' method is applied (Peters et al., 2005). By this method, the original TOC and HI values are calculated from the present-day TOC and HI values measured in the rock, through Rock-Eval analysis (Espitalié et al., 1986, 1985a, 1985b). Equations are applied to simulate the heating transformation process from their present thermal maturation state to the initial immature stage. The source rock kinetics of each source rock was defined by considering the type of kerogen resulting from the Rock-Eval data.

In the case that organic geochemical data are not available from the source rocks located in the modelled area, they are extrapolated from the closest area where the same stratigraphic levels have been analysed. This is the case for nearly all the Permian and Carboniferous source rocks, as their geochemistry was characterised only in the Weiach-1 well, in the north-eastern part of the basin (Ajuaba et al., 2023).

2.1.5 Boundary conditions

In thermal modelling, the boundary conditions define the heat transferred in the basin from the upper and lower basin boundaries. The upper boundary is the sediment-water interface temperature (SWIT), which defines the surface temperature variation over time, based on the evolution temperature at sea level, considering variations of the global mean surface temperature and the latitudinal variation of the study area through time (Wygrala, 1988) (Fig. 12). The paleo-temperature distribution in the area is automatically calculated by the software.

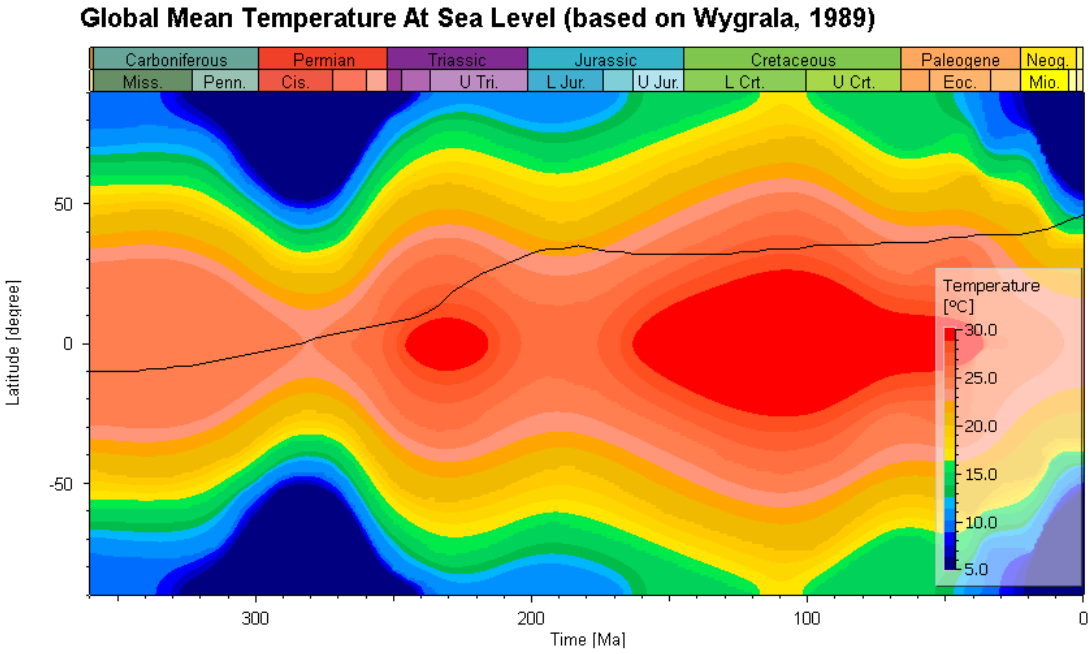


Fig. 12: Global mean temperature at sea level for a geographical area located at a latitude of 46°N (present Switzerland latitude), automatically calculated by the software and used as the upper thermal boundary condition (SWIT).

The lower boundaries are the paleo water depth and the basal heat flow. The paleo water depth is a correction of the burial depth calculated by decompaction of the sedimentary sequence, which takes into consideration the thickness of the water column on the top of the sedimentation surface during the basin evolution (Allen and Allen, 2013; Sclater and Christie, 1980). Its variation over time is reconstructed by considering the depositional environment of the main stratigraphic units forming the basin, which controls the water depth (platform, terrestrial, deep marine, etc.).

2.1.5.1 The basal heat flow

The basal heat flow represents the amount of heat transferred into the basin from the crust located beneath the basin. It is strictly related to the geodynamic setting where the basin forms and evolves, which controls, among other processes, the lithosphere thickness, the stretching forces, the magmatic activity, and the circulation of deep fluids (Allen and Allen, 2013; Poelchau et al., 1997; Royden and Keen, 1980; Tissot et al., 1987). In this study, to assess the variation of the heat flow over time they were considered the main geodynamic phases affecting the NAFB and its Mesozoic substratum. Literature data were mostly used to constrain this reconstruction (Dèzes et al., 2004; Loup and Wildi, 1994; Marchant et al., 2005; Mazurek et al., 2006; Pfiffner, 2014; Schegg and Leu, 1998; Stampfli et al., 2002). The subsidence curves of the basin were used to highlight the main tectonic events and to recognise the lithosphere stretching extensional phases, characterised by thermal surge, from thermal relaxation phases. A synthesis of the reconstruction of the basal heat flow evolution over time in the NAFB and its previous Mesozoic substratum is provided below (Fig. 13). More details can be found in (Omodeo-Salé et al., 2020).

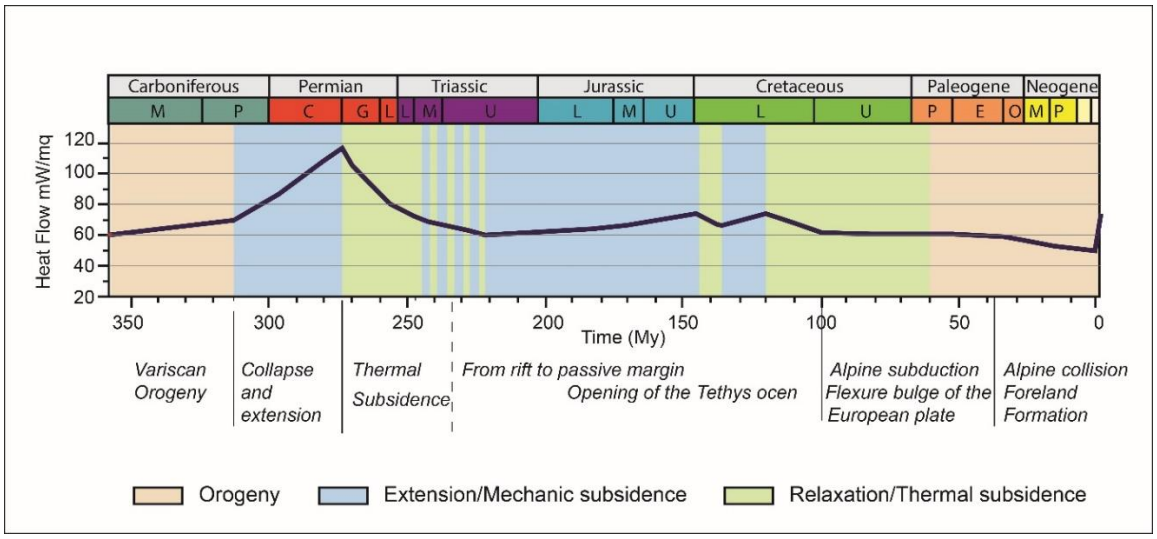


Fig. 13: Heat flow trend over time reconstructed from the geodynamic evolution of the NAFB and its Mesozoic substratum.

A first important thermal anomaly is hypothesised in the Stephanian-Early Permian period, because of magmatic activity and thinning and delamination of the lithosphere. A thermal surge up to 100-120 mW/m^2 is estimated, coherently with what is estimated for a strike-slip geodynamic setting with deep lithosphere involvement (Allen and Allen, 2013). Follows the Permian to Triassic thermal subsidence, interrupted by renewed subsidence acceleration phases in the Middle to Late Jurassic time. The latter is related to the lithosphere stretching affecting the European margin during the opening of the Tethys Ocean and preceding the opening of the North Atlantic, Bay of Biscay and the Valais Through (Handy et al., 2010; Pfiffner, 2014; Stampfli, 1993; Stampfli et al., 2002; Ziegler et al., 2004, 2002). Heat flow values of 75 mW/m^2 are assigned to these extensional pulses, under what is proposed in the literature for a rift to passive margin settings (Allen and Allen, 2013).

The lack of a Cretaceous record in the eastern sector of the NAFB makes the interpretation of the subsidence trend at that time uncertain. A recent study of the thermal evolution of the Northern sector of the NAFB (Omodeo-Salé et al., 2021) points out that the occurrence of another extensional phase of the lithosphere in the Early Cretaceous is associated with a new heat flow peak (70 mW/m^2). This hypothesis implies the deposition of Lower Cretaceous deposits, which were then uplifted and completely eroded between Late Cretaceous to Eocene time (see also discussion in the Geological Setting regarding the erosional unconformities in the basin).

A constant basal heat flow of 50-60 mW/m^2 is assigned in the Cenozoic, up to the Pliocene, when the Alpine foreland formed, as it is the range of values generally proposed in the literature for a foreland basin (Allen and Allen, 2013). At the present day, a geothermal gradient of 25-40 °C/km is measured throughout most of the NAFB (Fig. 14a), which corresponds to a heat flow of 65-105 mW/m^2, if an average thermal conductivity of 2.5-2.7 W/m/k is considered for the entire stratigraphic section (Chelle-Michou et al., 2017; Rybach, 1992; Rybach et al., 1987; Vollmayr, 1983). Recent heat flow data for the entire Switzerland are published at https://map.geo.admin.ch (Fig. 14b).

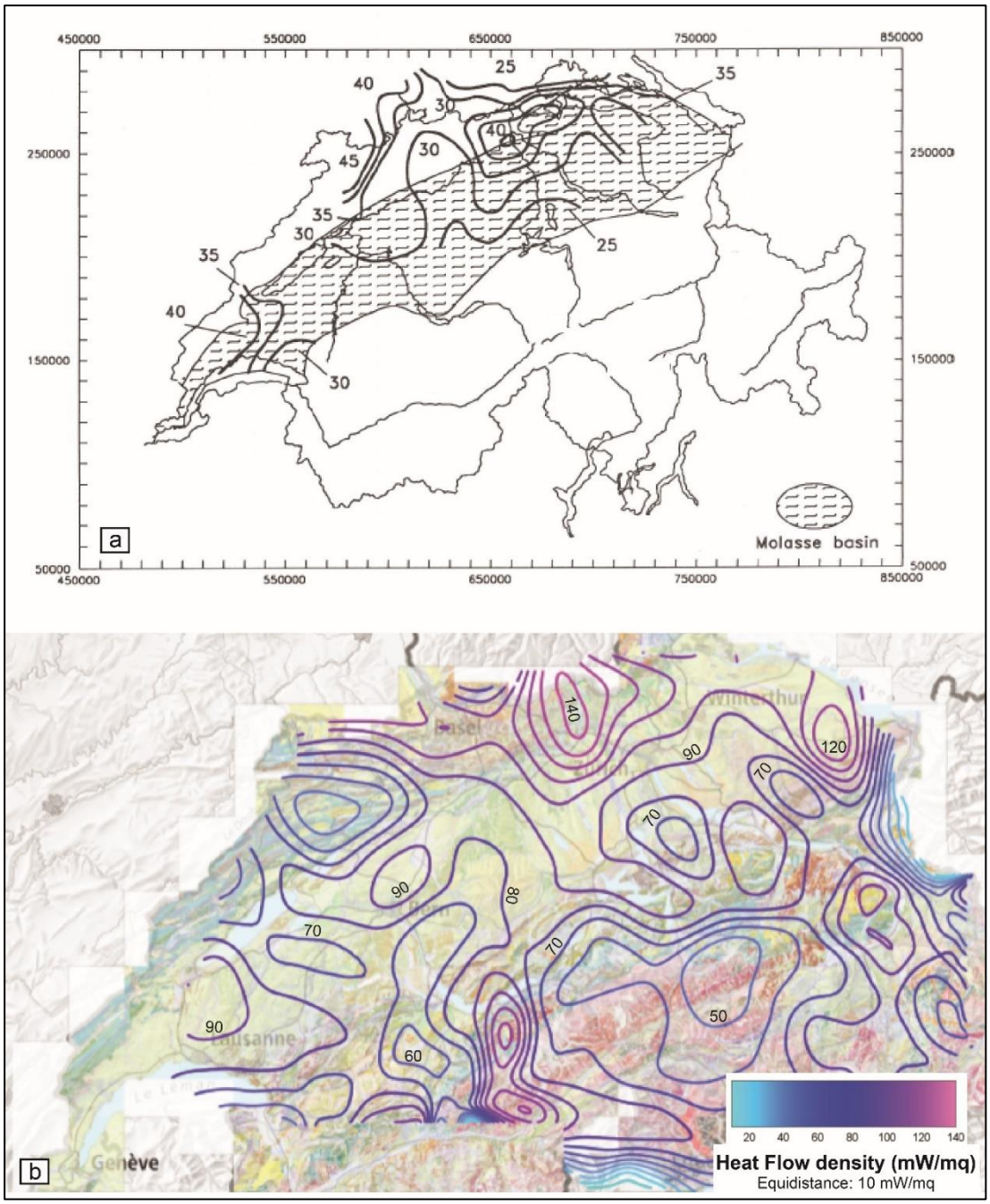


Fig. 14: (a) Present-day geothermal gradient throughout the NAFB (Modified from Rybach, 1992); (b) present-day heat flow density (mW/m^2) map (data source: https://map.geo.admin.ch)

In the model, the present-day heat flow values are in the range of 65-100 mW/m^2, depending on the location of the sections (Fig. 15). Because of that generally heat flow decreases from North to South, and a present-day heat flow trend was assigned along the sections.

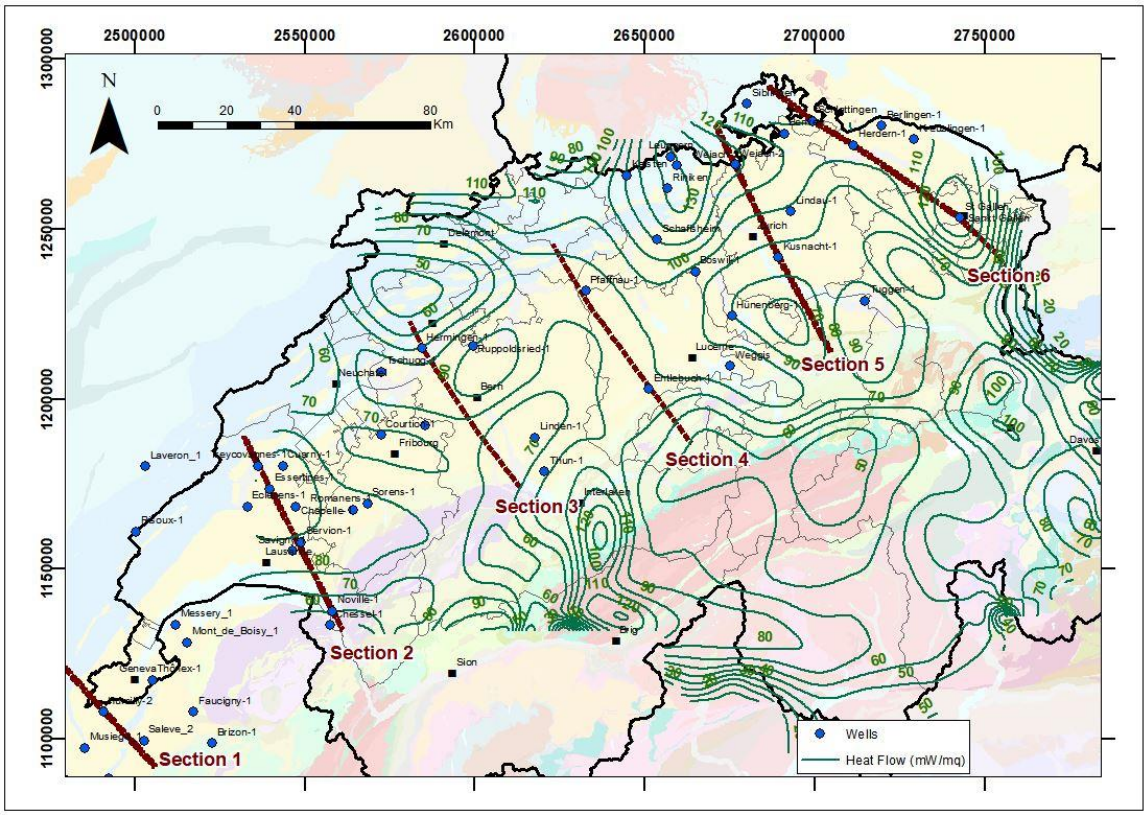


Fig. 15: Heat flow distribution throughout the NAFB (data source: https://map.geo.admin.ch). The location of wells and of the modelled section traces are shown.

2.1.6 Calibration of the model

To validate the results from the thermal models, the calculated basin properties must be calibrated to data directly measured in the rock (Welte et al., 1997; Welte and Yalcin, 1988). Calibration is performed at one or more points along the stratigraphic section, generally corresponding to the position of existing wells, where data were measured. The data mostly used for calibration are i) porosity, ii) present-day temperature and iii) paleotemperature, which are indicators of the maximum thermal conditions attained by the rock. To calibrate the model, an iterative approach is applied, consisting of modifying the input data to fit the theoretical results to the measured data, by modifying the input. Several runs were performed to simulate different scenarios.

2.1.6.1 Porosity

Porosity data are used to calibrate the mechanical compaction behaviour of the lithologies assigned to the stratigraphic units forming the basin infill. This is essential to correctly reconstruct the thermal conductivity of the basin infill and the permeability of the rocks composing the basin infill, thus properly simulating the hydrocarbon circulation. Porosity and permeability are controlled by the lithology of the basin infill, by the compaction process (burial) and by the diagenetic processes affecting the basin. If the first two factors can be easily reconstructed, considering the large variability of diagenetic processes that can occur in the basin during its entire evolution, it is hardly feasible, especially when diagenetic data are not available. However, for those wells where porosity data are available, an attempt to calibrate these data was carried out by changing the lithology mechanical compaction properties proposed by the software.

2.1.6.2 Temperature

The present-day temperature dataset contains direct temperature measurements taken from boreholes, along their entire length (borehole temperature data). It is generally available for recent or not-too-old wells as borehole logs. This data reflects the ability of the basin infill to transfer the

heat from the base to the top. This property is mostly controlled by the present-day basal heat flow (heat flow value at the base of the basin infill) and the thermal conductivity properties of the basin infill, in turn, are controlled by the lithologies of the latter. Lithologies a direct data, as they are defined by the stratigraphic description provided by the reports of the wells located close to the modelled section. However, because of that, the lithological data were extrapolated from the wells to the entire section, and uncertainties must be considered. Facies variation throughout the basin could hardly be represented, especially in the case that only a few wells, located in the vicinity of the modelled section, dispose of lithological data. The present basal heat flow is indirect data, as it cannot be measured the heat flow at the base of the basin, whereas it can only be estimated, because of the thinning of the lithosphere. Thus, this is the most uncertain variable, and it is the one mostly changed to calibrate the present-day temperature.

The present-day heat flow has been calculated for the entire NAFB, from the borehole temperature data (Fig. 14). However, it is observed throughout the entire basin that assigning to the model the heat flow value calculated today as the basal heat flow value at 0 Ma does not give good calibration results. This is because the present heat flow that is calculated today represents the surface heat flow, not the basal heat flow. Furthermore, an additional technical complication is that in the PetroMod software, the basal heat flow is placed at the base of the model, which usually does not correspond with the base of the basin but with the base of the basement. Thus, in the model, the effective heat flow reaching the basin is strictly related to the thickness of the basement drawn in the model. Furthermore, to calculate the amount of heat circulating in the basin, the model also takes into account the radiogenic heat produced by the basement and the basin infill. The radiogenic heat produced depends on the lithologies and is automatically calculated by the software. The effect of this factor is not easily controlled by the software user. Another important factor that can be responsible for the discrepancy between the basal heat flow and what is estimated at the surfaces is the rapid exhumation of the NAFB, in the Pliocene-Quaternary time. The uplift and erosion of the magnitude of 1-2 km in a short interval of time (see Cederbom et al., 2011) can avoid a thermal equilibration of the basin temperature to the steady-state conditions, causing anomalously high temperatures in the basin infill. These are the main arguments that explain why, throughout the entire basin, the present-day borehole temperatures can hardly be calibrated with the heat flow values measured at the surface today (Fig. 15). In most of cases, to achieve a satisfactory calibration result, it was assigned at the base of the model a heat flow value lower than the heat flow value measured today at the basin surface. See each modelled section chapter for details.

Fluid circulation is also crucial in the heat transfer process, controlled by facies permeability and faults. However, because of that, thermal modelling software is not able to simulate convective heat transfer, in this study, the effect of fluids is not properly considered.

2.1.6.3 Thermal maturity conditions

The reconstruction of the thermal conditions attained by the basin infill is one of the most relevant results performed by thermal modelling. This property defines the maximum temperature attained by the basin deposits during the entire evolution of the basin. It is essential to calculate it when the maturity state of the potential hydrocarbon source rock (immature, oil window, gas window, overmature) needs to be known. To validate these modelling results, paleothermometer data were used, which directly measure in the rocks the maximum temperature and/or thermal conditions attained by a rock at a specific depth.

The most common paleothermometer is the vitrinite reflectance (%Ro). Other paleotemperature indicators can be implemented if available, such as apatite fission tracks (AFT), clay mineralogy and other organic matter indicators (TAI, fluorescence, biomarkers, Rock-Eval, etc), although they are less reliable than the vitrinite reflectance. To calibrate the %Ro measured in the rocks, the main variables controlling the maximum temperature attained by the basin infill, the basal heat flow and the burial, are iteratively changed. The basal heat flow is controlled by the thickness of the lithosphere, thus, it is a consequence of the geodynamic setting of the basin (rift, passive margin, foreland, etc) and its evolution over time. The burial in a basin is the result of the subsidence mechanisms, which can be related to the geodynamic evolution of the basin (mechanical and thermal subsidence) and the sedimentation rate (subsidence for loading). To properly calculate the maximum burial of the basin, the timing and magnitude of the uplift and of the erosional processes

must also be considered. Thus, these variables are tested to fit the paleotemperature data measured in the rocks.

2.1.7 Simulation of the hydrocarbon generation, migration, and accumulation processes

The petroleum modelling software estimates the area on the modelled sections where hydrocarbon can form, based on the following parameters: i) geometry of the stratigraphic units, which determines the formation of potential stratigraphic traps; ii) fault location, which determines the formation of potential structural traps; iii) fault properties (open/not cemented or close/cemented), which determines the possibility for the hydrocarbons to flow along the faults; iv) permeability of the facies assigned to the stratigraphic units. The 2D model, compared to the 3D, has the great limitation that the trap efficiency cannot be properly determined, as lateral closure is not considered. Therefore, the reliability of the hydrocarbon accumulations simulated by the software on the 2D sections must be constrained by additional data able to improve the understanding of the 3D geometry of the areas where accumulations are supposed.

The software calculates the volume of hydrocarbons that can be accumulated in proper reservoirs (permeable units) as well as in low-permeable units (petroleum saturations). However, the estimates provided in this work must be considered only as indicative and qualitative, whereas they cannot be used as quantitative volumetric estimates. This is the result of various factors: i) 2D model cannot provide proper volume estimates because of that it does not take into consideration the volume of a potential reservoir; ii) the software considers optimal conditions (e.g. all pores are connected, regular intergranular space, etc.), which could not be representative of the reality; iii) the size of the grid-model used for a regional study is not optimal for calculating hydrocarbon volumes at a prospect level. If a quantitative estimate needs to be performed in a specific area, a 3D geological model at a greater scale resolution should be carried out and combined with software specifically conceived for volume estimation.

2.1.8 Evaluation of the uncertainties

Uncertainties in the petroleum system modelling results obtained for the five geological sections must be considered. That is mostly because there are several uncertainties in the modelling input data, which are based on several assumptions. To deal with that, in this work, for each section, a list of the uncertain parameters that could control the reliability of the modelling results is provided. Where possible, actions that could be carried out in the future to reduce uncertainties are proposed.

2.2 Common Risk Segment (CRS) maps

A Common Risk Segment (CRS) map illustrates the spatial distribution of geological risk associated with a "working petroleum system" within a wider active Petroleum Play, such as the Swiss Plateau. CRS maps are standard tools used in the hydrocarbon industry to assess and manage risks associated with exploration and production activities. These maps provide a visual representation of the potential hazards and vulnerabilities in a specific geographic area, helping decision-makers prioritise resources and plan mitigation strategies. Here's a general overview of how CRS maps are generated:

- Data Collection: The first step in creating a CRS map is to gather relevant data from various sources. This includes geological surveys, seismic data, well logs, production records, environmental assessments, and historical incident reports. Additionally, information about infrastructure, such as pipelines, platforms, and processing facilities, is collected.
- Risk Identification: Once the data is collected, a multidisciplinary team of experts, including geoscientists, engineers, environmental scientists, and risk analysts, works together to identify potential risks in the area of interest. These risks may include geological hazards (e.g., faults, subsidence), operational risks (e.g., equipment failure, human error), environmental risks (e.g., spills, habitat disruption), and socio-economic risks (e.g., impact on local communities, regulatory compliance).
- Risk Assessment: After identifying potential risks, the next step is to assess the likelihood and consequences of each risk. This involves analysing historical data, conducting simulations,

and using predictive models to estimate the probability of different events occurring and their potential impact on safety, environment, and business operations.

- Mapping: Once the risks are assessed, the data is synthesized into a visual format using Geographic Information System (GIS) software. GIS allows for the integration of various layers of information, such as topography, land use, infrastructure, and risk assessments, which will be used to create a comprehensive risk map. Different colours (usually consisting of red, yellow and green) or symbols may be used to represent different levels of risk, with areas of higher risk highlighted for closer attention.
- Validation and Review: Before finalizing the CRS maps, a validation process will be carried out where stakeholders, including regulators, industry partners, and local communities, review the map to ensure its accuracy and relevance. Feedback from stakeholders may lead to adjustments or refinements to the map.
- Updating and Maintenance: CRS maps are dynamic tools that require regular updates to reflect changes in the operating environment, such as new data and knowledge, technological advancements, regulatory requirements, and evolving risks. Therefore, it's essential to establish a process for maintaining and updating the CRS maps periodically.

By following these steps, the oil and gas industry developed Common Risk Segment maps used as valuable decision-support tools for identifying and managing risks associated with exploration and production activities. These maps help identification of new prospects while improving safety, environmental protection, and operational efficiency in the oil and gas sector.

In the context of the UNCONGEO project, the aim is to define the likeliness of encountering an accumulation of hydrocarbons in the Swiss Plateau where a future deep (> 0.5 km) geothermal well will be drilled and to represent this risk by using comprehensive and understandable graphic display, i.e. the CRS maps. The definition of risk about the outcomes of the CRS maps, explicitly refers to the risk of encountering hydrocarbons in the subsurface. In the past 80 years of subsurface exploration, in Switzerland, occurrences of hydrocarbon proved to be small.

The word “risk” in this report does not refer by any means to the overall risk that a geothermal project might have if located in a zone defined as “medium/high risk” in the CRS maps, but on the likelihood that hydrocarbons are found during the exploration and exploitation activities.

Hydrocarbon presence can be manageable if adapted technology such BOP and appropriate mud control at the rig side were implemented during the critical phases of drilling operations.

The maps produced are useful tools for planners and decision-makers, as they can be used to establish a first assessment of the risk of encountering hydrocarbon at depth. Therefore, if necessary, the maps can lead to proposing the necessary mitigation measures (i.e. further subsurface studies, reprocessing of existing seismic data, new data acquisition, etc) to de-risk the geothermal exploration activity, specifically in the region closely located to the foreseen drilling sites.

The workflow followed to build the CRS maps in this selection phase work is shown in Table 8. It is composed of six steps. The latter are described in the following paragraphs, together with a detailed description of the data considered. Once steps 1 to 5 have been completed, the results are then integrated in a GIS-based workflow to produce the CRS maps.

CRS Maps workflow

	Task	Data
1	**Plays definition**	
a	Definition of plays based on the stratigraphy of the basin and knowledge of the main hydrocarbon targets	Literature data
2	**Classes definition**	
a	Play elements data availability classes, based on the availability of data essential to define the properties of each petroleum system element (source rock, reservoir and seal)	Data available
b	Play elements assessment classes, based on the knowledge, extrapolation, and interpretation of the available data, which define the properties of each petroleum system element (source rock, reservoir and seal), throughout the entire Plateau.	Criteria to evaluate the properties of a petroleum system elements
3	**Source rocks occurrence and properties**	
a	Distribution of the Posidonia shale source rocks and definition of its hydrocarbon potential	Well report description, Rock-Eval data, Vitrinite reflectance, thermal modelling results
b	Distribution of the Permian and Carboniferous source rocks and definition of their hydrocarbon potential	Permo-Carboniferous graben geometry (Leu, 2008 and other local sources); Rock-Eval data; Vitrinite reflectance; thermal modelling result
c	Definition of data availability and Assessment classes for each area where data are available	Data collected in the previous points
c	To build the Source Rocks Assessment maps, the extrapolation of the classes previously assigned in the areas where data are not available	Data collected in the previous points
d	For each play, source rock maps, where the Data availability and assessment classes are assigned throughout the Plateau	Data collected in the previous points
4	**Reservoir occurrence and properties**	
a	Distribution and properties of the reservoir defining each play	GeoMol surfaces and faults; Stratigraphy and lithology from well reports; Porosity data
b	Definition of data availability and Assessment classes for each area where data are available	Data collected in the previous point
c	To build the Reservoir Assessment map, extrapolation of the classes previously assigned are extrapolated in the areas where data are not available	Data collected in the previous points
d	For each play, reservoir maps, where the Data availability and assessment classes are assigned throughout the Plateau	Data collected in the previous points
5	**Seal occurrence and properties**	
a	Distribution and properties of the seal defining each play	GeoMol surfaces and faults; Stratigraphy and lithology from well reports
b	Definition of data availability and Assessment classes for each area where data are available	Data collected in the previous point
c	To build the Seal Assessment maps, the extrapolation of the classes previously assigned in the areas where data are not available	Data collected in the previous points
d	For each play, seal maps, where the Data availability and assessment classes are assigned throughout the Plateau	Data collected in the previous points
6	**GIS Based CRS mapping**	
a	Multiply the Play assessment maps, obtaining a final map showing the risk of hydrocarbon occurrence throughout the Plateau, for each specific play	Maps previously obtained

Table 8: Workflow followed to reconstruct the CRS maps for the Swiss Plateau. For each step, the tasks and the data necessary to accomplish it are indicated.

The main data used to build the CRS maps are the following:

- the GeoMol 3D model[2] ;
- the lithologic data collected in the most relevant wells of the Swiss Plateau, and some of the analytical data available for these wells (Porosity, Rock-Eval, Vitrinite reflectance);
- thermal modelling results were obtained in the first modelling phase of this study.

The dataset used to build the CRS map was collected up to 2023. However, new data are available since the publication of this report. These new data were not included in this assessment.

To simplify the workflow proposed, the hydrocarbon potential accumulations shown in the CRS maps include both oil and gas. To differentiate them, it would necessitate implementing the thermal condition states (oil/gas windows) of the source rock/s in the different areas. However, the potential migration from deeper and farther source rocks would complicate this simple assumption. Further work could be done in the future to improve this aspect. In the CRS maps, only thermogenic gas is considered (gas generated because of the thermal transformation of organic matter, generally occurring at depth > 1.5 km) (Fig. 1). The risk associated with the presence of biogenic gas (gas generated by the decomposition of organic matter by anaerobic microorganisms, generally at depth < 1 km) is not considered. At present, in fact, there are no detailed data on the distribution of the organic matter-rich facies able to produce biogenic gas contained within the shallower stratigraphic units of the Swiss Plateau (Quaternary and Molasse units). Therefore, it is rather difficult to predict where biogenic gas could be present given the current state of knowledge. Further mapping of the Molasse organic facies and possibly deeply buried organic-rich interglacial Quaternary sediments would improve this aspect in the future.

2.2.1 Geothermal plays definition

For the CRS maps, six geothermal plays were considered and named concerning the main reservoir unit as indicated in Table 9. In this context, the Muschelkalk and Lower Triassic systems (Buntsandstein) were considered as a unique play because these units have not been differentiated in the GeoMol subsurface model. The Cenozoic play was not considered because of the complexity and heterogeneity of reservoir architecture and composition, whose understanding is currently scarce. The reservoir of this play is the Molasse, consisting of several stratigraphic units with variable distribution and proportion of sandstones and shales and marls, making the occurrence of intraformational seal and stratigraphic traps likely. As there is no detailed knowledge of the geometry and distribution of the reservoir and the seal horizons throughout the Plateau, it is currently difficult to produce reliable risk maps for the Cenozoic play.

Play	Reservoir unit	Seal unit	Source Rock/s unit
Cretaceous	Lower Cretaceous shallow carbonates	Molasse shales	Posidonia shale; Permo-Carboniferous
Malm	Upper Malm reefal carbonates	Lower Cretaceous marls or Molasse shales	Posidonia shale; Permo-Carboniferous
Dogger	Dogger shallow marine carbonates	Lower Malm marls	Posidonia shale; Permo-Carboniferous
Lias	Lias and/or Upper Trias shallow marine carbonates	Lias shales and marls and/or Dogger marls	Posidonia shale; Permo-Carboniferous
Muschelkalk	Muschelkalk dolomitic carbonates and Buntsandstein continental sandstone	Keuper and/or Muschelkalk evaporites	Permo-Carboniferous
Permo-Carboniferous	Permian and Carboniferous continental sandstone	Muschelkalk and/or Keuper evaporites	Permo-Carboniferous

[2] https://www.swisstopo.admin.ch/de/wissen-fakten/geologie/geologische-daten/3d-geologie/tief/geomol.htmlf

Table 9: Plays considered in this work to build the CRS maps of the Swiss Plateau. Details on the stratigraphic units composing each play are in the respective play sections. The Permian and Carboniferous source rocks are considered a unique source-rock unit for simplicity, because of the very few data available on those stratigraphic intervals.

2.2.2 Class definition

To define the risk associated with the presence of hydrocarbons in the subsurface, it is essential to assess the quality of the three elements composing a petroleum system (source rock, reservoir and seal). The quality assessment is based on the presence or absence of a series of properties specific to each play element. As a consequence, the knowledge of these properties is related to the availability of data. Based on the above, two types of important aspects were used to classify the data and information available:

1) Petroleum system elements data availability;

2) Petroleum system elements assessment.

The elements data availability classification defines for each petroleum system element the availability of data which are necessary to assess its quality and appropriateness to generate hydrocarbons in the case of the source rock, or to store hydrocarbons in the case of the reservoir, and to confine hydrocarbons in the case of the seal. Based on these data, the assessment of petroleum system elements is carried out. The elements assessment also considers our interpretation of the quality of these elements, particularly in cases when data are not available. Interpretation is based on both extrapolation of data from the areas where data are available, as well as from our geological knowledge and understanding of the Swiss Plateau petroleum system processes at the time of the project.

For each petroleum system element, nine classes were defined for the elements' data availability and five classes for the elements assessment. Details of these classifications are described in the following paragraphs. Initially, the classes were assigned to the main wells of the Plateau (Appendix 3), in the form of tables. Secondly, classes were assigned to the entire Swiss Plateau area in the form of maps.

2.2.3 Source rocks occurrence and properties.

For the CRS maps, only two source rocks were considered for all plays: the Posidonia shale and the Permo-Carboniferous. Because of the very scarce data available specifically for Permian and Carboniferous source rocks, the latter were considered as a unique unit and not separated. For each source rock, the Data availability and Assessment classes were then defined (Table 10).

The source rock data availability classes were defined based on the following parameters: i) occurrence, ii) TOC/Rock-Eval and iii) vitrinite reflectance (VR). Thermal modelling results were also considered to define the thermal maturity of the source rocks in the area where vitrinite reflectance data are not available.

The source rock assessment classes were defined on properties directly measured, when data are available, whereas, in the case there are no data for a specific area, data were extrapolated from the closest wells where data are available. The properties considered were presence (i.e. occurrence), maturity (%Ro > 0.5), and organic matter richness (TOC > 2%). As indicated before, oil and gas windows have not been differentiated.

SOURCE ROCK DATA availability

Class	Occurrence in well	TOC/Rock Eval	VR	Model calibration
A	Y	Y	Y	Y
B	Y	Y	Y	N
C	Y	N	Y	Y
D	Y	Y	N	N
E	Y	N	Y	N
F	Y	N	N	Y
G	Y	N	N	N
H	N	N	N	Y
I	N	N	N	N

SOURCE ROCK assessment

Class	SR Presence	SR Maturity	TOC > 2%
1	Y	Y	Y
2	Y	Y	N
3	Y	N	Y
4	Y	N	N
5	N	N	N

Table 10: Source rocks data availability and assessment classes

2.2.4 Reservoir occurrence and properties

For each reservoir, the Data availability and Assessment classes were defined (Table 11). The reservoir data availability classes were assigned considering the availability of data for the reservoir unit of each play. Data considered essential to define the properties of a reservoir are the following: i) the presence of the GeoMol surface for this reservoir unit, ii) the presence of GeoMol faults in this unit, iii) the occurrence of the reservoir unit in a specific well and the availability of porosity data.

The reservoir assessment is based on the following properties: the presence of the reservoir, the porosity (Phi) and the reservoir fracture. In this study, it was defined as an effective reservoir when the average matrix or fracture porosity of a unit is > 15%. For fractured reservoirs, as information on this property is very seldom available, it is assumed that the reservoir might present open fractures when nearby faults crossing this unit are oriented ± 45° to the maximum stress orientation sigma 1. The assignment of these properties throughout the maps was done considering the measured data when available. In the case of a complete absence of data, information was inferred and derived from the closest wells with available data.

RESERVOIR DATA availability

Class	GeoMol Surface	GeoMol Fault	Occurrence in well	Porosity data
A	Y	Y	Y	Y
B	Y	Y	Y	N
C	Y	N	Y	Y
D	Y	Y	N	N
E	Y	N	Y	N
F	N	N	Y	Y
G	Y	N	N	N
H	N	N	Y	N
I	N	N	N	N

RESERVOIR ROCK assessment

Class	R Presence	R Phi > 15%	R fractured
1	Y	Y	Y
2	Y	Y	N
3	Y	N	Y
4	Y	N	N
5	N	N	N

Table 11: Reservoir data availability and assessment classes

2.2.5 Seal occurrence and properties.

For each seal unit, the Data availability and Assessment classes were defined (Table 12). The seal data availability classes were assigned considering the availability of data for the seal unit of each play. The data considered essential to define the properties of a seal are the following: i) the presence of the GeoMol surface for this seal unit, ii) the presence of GeoMol faults in this unit, iii) the occurrence of the seal unit in a specific well and iv) the availability of lithologic data.

The seal assessment is based on the following properties: i) the presence of the seal, ii) the impermeability of the seal (based on the lithologies) and iii) the seal integrity. A lithology is considered impermeable when it is composed of >50% impermeable facies (shales, marls). Concerning the seal integrity, because of a lack of unambiguous data, it was assumed that the seal is not fractured when faults in this unit are oriented ± 45° to the minimum stress orientation sigma 3. The assignment of these properties throughout the maps was done considering the measured data when available. In the case where there are no data for a specific area, information was inferred and derived from the closest wells with available data.

SEAL DATA availability

Class	GeoMol Surface	GeoMol Fault	Occurrence in well	Lithology data
A	Y	Y	Y	Y
B	Y	Y	Y	N
C	Y	N	Y	Y
D	Y	Y	N	N
E	Y	N	Y	N
F	N	N	Y	Y
G	Y	N	N	N
H	N	N	Y	N
I	N	N	N	N

SEAL ROCK assessment

Class	S Presence	S integrity	S impermeable
1	Y	Y	Y
2	Y	N	Y
3	Y	Y	N
4	Y	N	N
5	N	N	N

Table 12: Seal data availability and assessment classes

2.2.6 GIS Based CRS mapping

To create the CRS maps using the GIS software, the following data were used:

- Borehole data. The UNCONGEO database contains an exhaustive list of boreholes in the Swiss Plateau, which reached a depth of at least 500 meters. This vectorised data contains the play assessment and data availability assessment in the attribute table. It is estimated that borehole data remains reliable 1,5 kilometres around the drilling site. The first buffer algorithm is used to create a buffer zone around the borehole with a radius of 1.5 kilometres. The list of boreholes includes only publicly and partly confidential data (Appendix 3)
- Faults data. Vectorised faults were provided by Swisstopo as fault cutoffs at the top of the main geological units in the Swiss Plateau. It was considered that the damage zone inherent to the fault represents a 200 m area on each side of the fault plane; therefore, a 200 m buffer was created.
- Top geological unit extent. The extension of geological units has been derived directly from the GeoMol geological model, which contains a selection of nine horizons across the study area corresponding to the Swiss Plateau. The source rock, reservoir and seal extensions have been considered and are represented as a classified vector file.

2.2.7 GIS CRS map production

Each play element (i.e. reservoir, seal, source rock occurrence and maturity) is represented by a vector map with values ranging from 1 to 5 corresponding to their assessment class (see Tables 70, 71, 72). When necessary (boreholes and faults), buffer zones were generated using the *native:buffer* QGIS algorithm with the following parameters:

- Distance: number of meters depending on the dataset.
- Segments: 5.
- End cap: round.
- Join style: round.

- Miter limit: 2.

For the Reservoir and Seal components of the play, the unit extent map and the fault map are aggregated in a single vector map. Vector data are then converted to raster format using the *gdal:rasterize* algorithm in QGIS using the following parameters:

- Raster size units: georeferenced units.
- Width/horizontal resolution: 100 m.
- Height/vertical resolution: 100 m.
- Output extent: 2620701.5625,2676826.7500,1221173.2838,1274775.0500.
- No data value: not set.
- Output CRS: EPSG:2056 - CH1903+ / LV95.
- Output format: Flot32 GTiff.

The CRS map is computed by a raster multiplication of the following rasters:

*Source Rock(s) * Reservoir * Seal*

The CRS map is then normalised mathematically on a scale from 1 to 5 to illustrate the classification used. Normalisation was done in the raster calculator algorithm using the mathematical formula for normalisation for the custom range:

$$Rnorm = (b - a) * \left(\frac{x - Rmin}{Rmax - Rmin}\right) + a$$

Where *a* and *b* are the lower and upper ranges, R_{min} and R_{max} are the minimum and maximum values of the raster.

The CRS maps are classified in terms of "Risks" of encountering hydrocarbons when drilling a given play. The categories of risks displayed on the CRS maps and their colour legends are shown in Table 13.

Risk	**Colour legend**
High	
Medium to high	
Medium	
Low to medium	
Low	

Table 13: Categories of risks displayed on the CRS maps and their colour legends.

3 Results

3.1 Petroleum System Modelling - Section 2

3.1.1 Data

3.1.1.1 Geological Model

Section 2 is extracted from the GeoMol project along a section line crossing the Canton of Vaud (Fig. 16). The trace of the section is NNW-SSE oriented, with the following extremity coordinates: NNW edge x, y: 2533773, 1185556; SSE edge x, y: 2566184, 1122231 (Reference coordinate System CH1903+ / LV95), and a total length of 71 km (Fig. 17a). The extracted section represents the present-day geological structure of the NAFB in the area, represented by a southern dipping foreland wedge, filled by the Cenozoic Molasse units and its Mesozoic substratum, which outcrops in the northernmost part of the section. In this area, the foreland basin is delimited to the north by the Jura Mountain Chain, where the Mesozoic strata outcrop, and to the South by the more external Subalpine thrusts, where the folded subalpine Molasse is exhumed. The erosional topographic surface cuts the uppermost Molasse units.

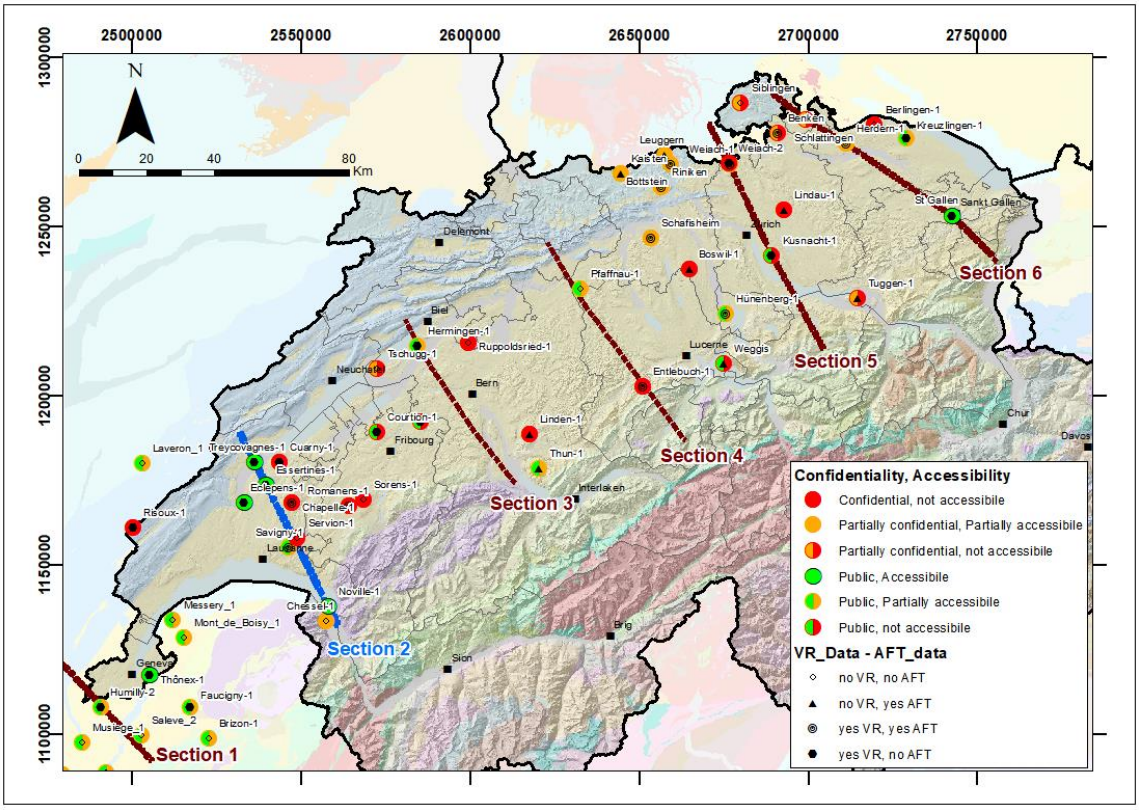


Fig. 16: Location of Section 2

To the southeast, the GeoMol project stops at the Leman Lake border, approximately. Thus, the geological surfaces of the southernmost 20-30 kilometres of the section are not available (Fig. 17a). Therefore, these parts of the section were drawn by considering other data and interpretations presented in (Marchant, 2016) (Fig. 17b) and (Leu, 2010) (Noville-1 well document, unpublished) (Fig. 17c). The location and geometry of the Permo-Carboniferous graben were deduced by Leu, (2008) along most of the section, and by Geoform 2010 (unpublished) for the southernmost part

(Fig. 17c) where the Noville-1 well is located. The final resulting section used for modelling is shown in Fig. 17d. In the latter, the type of faults, as classified in the GeoMol database, is indicated.

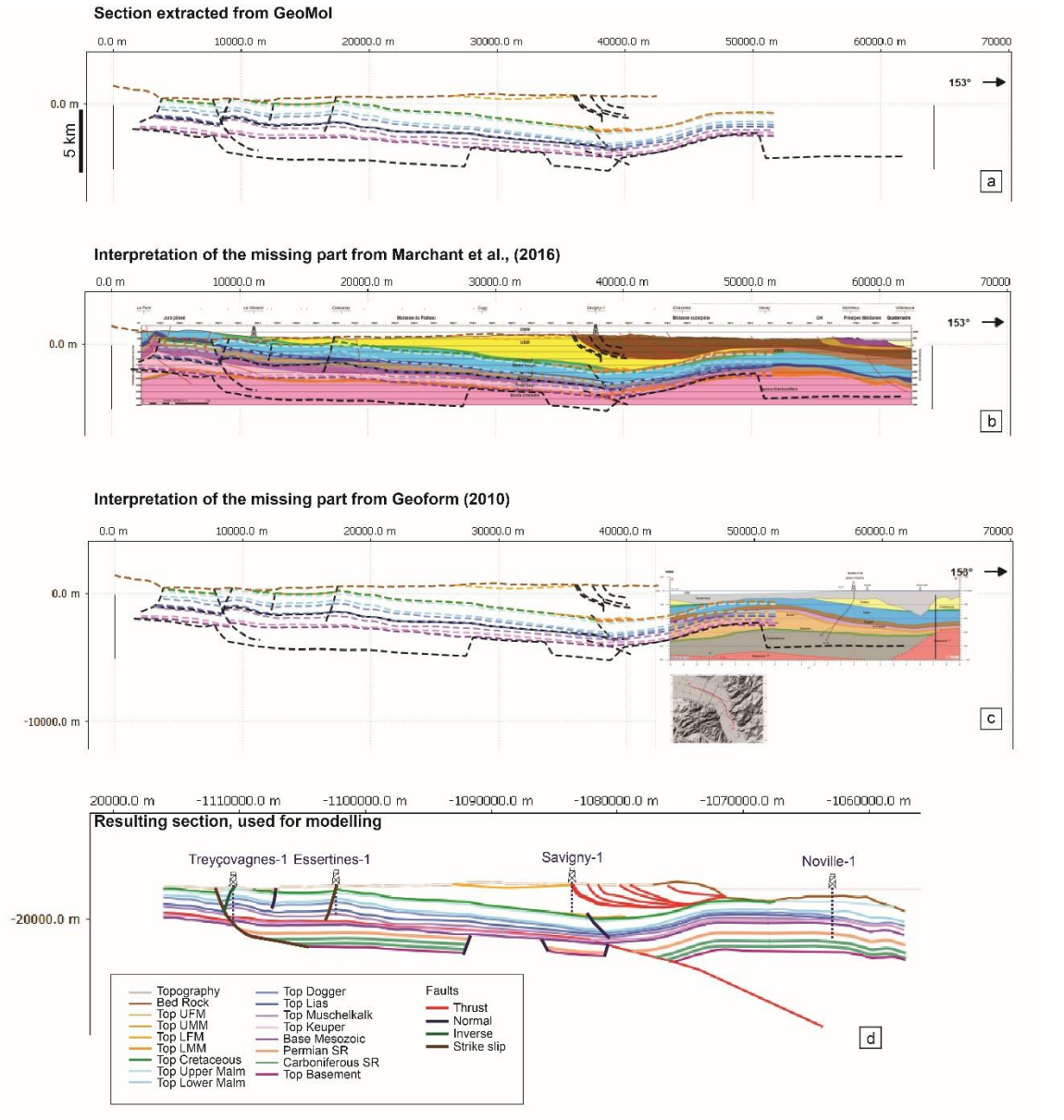


Fig. 17: (a) Horizons and faults extracted from Geomol at the Section 2 trace location. The reconstruction of the southward missing part of the section was based on literature data: in (b) from Marchant et al. (2016) and in (c) from Geoform (2010, unpublished). (d) Final resulting geological section used for modelling. The wells intersecting the section trace are shown. In the final section, the types of faults are differentiated as classified in the GeoMol database.

3.1.1.2 Wells

The section passes through the following wells: Treyçovagnes-1, Essertines-1, Savigny-1 and Noville-1. The nearby wells, Eclépens-1 (7 km from the section trace) and Chapelle-1 (20 km from the section trace) were also considered. For these wells, the availability of the most relevant data necessary for thermal modelling is summarised in Table 14. Further wells are located in the area (Cuarny-1, Romanens-1, Sorens-1, Servion-1 and Chessel-1 Table 14). However, in this work, they were not considered, as, at present, there are no data available for these wells. The stratigraphic logs of these wells are shown in Appendix 4.

Well	Distance from section (km)	Status	Well report	Stratigraphic log	Calibration data	Rock-Eval data
Treyçovagnes-1	0	Public, accessible	Yes	Yes	Phi, T, VR	Yes
Essertines-1	0	Public, accessible	Yes	Yes	Phi, T, VR	Yes
Savigny-1	0	Public, accessible	Yes	Yes	T, VR, AFT	No
Noville-1	0	Public, accessible	Yes	Yes	T, VR	No
Eclépens-1	7	Public, accessible	Yes	Yes	Phi, T, VR	Yes
Chapelle-1	30	Confidential, not accessible	No	Yes	T, VR, AFT	No
Cuarny-1	7	Confidential, not accessible	Yes	Yes	T	No
Romanens-1	17	Confidential, not accessible	No	No	No	No
Sorens-1	22	Confidential, not accessible	No	No	No	No
Servion-1	1	Confidential, not accessible	No	No	No	No
Chessel-1	2	Confidential, not accessible	No	No	No	No

Table 14: wells located closest to the Section 2 trace and availability of the most relevant data needed for thermal modelling. Calibration data: (Phi) Porosity; (T) temperature; (VR) vitrinite reflectance; (AFT) apatite fission tracks.

3.1.1.3 Deposition and erosional events

The burial history of the studied area is defined by a sequence of depositional and erosional events and their ages. Thus, in the model, an age for each stratigraphic unit and the main erosional event was assigned (Table 15).

Age top unit (Ma)	Unit	Event	Facies assigned
0	Quaternary	Deposition	Quaternary
4	Erosion Pliocene-Quaternary	Erosion	
7.24	UFM	Deposition	UFM
15.97	UMM	Deposition	UMM
20.44	LFM	Deposition	LFM-Noville; LFM-Savigny; LFM-Chapelle; LFM-Essertines
28	LMM	Deposition	LMM
33	Hiatus Cret/Eocene	Hiatus	
86	Erosion Cretaceous	Erosion	
113	Cretaceous	Deposition	Cretaceous-Savigny; Lower Cretaceous
145	Upper Malm	Deposition	Upper Malm
157.3	Lower Malm	Deposition	Lower Malm
163.5	Dogger	Deposition	Dogger-Treyçovagnes; Dogger-Essertines; Dogger-Noville
174.1	Lias	Deposition	Lias; Posidonia shale
201.3	Keuper	Deposition	Upper Keuper; Middle Keuper; Lower Keuper
237	Muschelkalk	Deposition	Muschelkalk
252	Hiatus Perm-Triassic	Hiatus	
259	Erosion Perm-Triassic	Erosion	
265	Permian	Deposition	Permian Verrucano; Permian Lower; Permian-Source rock (SR)

Age top unit (Ma)	Unit	Event	Facies assigned
284	Carboniferous	Deposition	Carboniferous; Carboniferous-Source rock (SR)
323	Hiatus/erosion pre-Carbon		
400	Basement	Deposition	Basement

Table 15: Depositional and erosional events defined in the thermal model. A facies is assigned to each layer.

The timing and magnitude of the erosional events were deduced by considering literature data (Table 16). In the case of the Permian-Triassic and Mesozoic-Eocene unconformities, no data are available to constrain the magnitude of the erosional events in the studied area. Thus, erosional trends, previously reconstructed at a regional scale and/or for other areas of the basin close to the Section 2 trace line, were considered for the entire section. An average of 200 meters was assigned at the Permian-Triassic unconformity and 500 meters at the Mesozoic-Eocene unconformity. For the Pliocene-Quaternary unconformity, more constraints are available. In Schegg et al. (1997) Erosion in the range of 2000-2600 meters has been estimated in the Vaud area. Lower values, in the range of 800-1400 meters, have been calculated by Omodeo-Salé and Moscariello (2019) and in the range of 1000-1100 meters by Cederbom et al. (2011). Therefore, in this work, it was considered a missing section ranging from 900-1000 meters in the north-central part of the section, 2500 meters in the external thrusting area, and more than 5000 meters in the internal thrusting area, in the southern extremity of the section.

Erosion unconformity	Amount of erosion estimated in previous studies (m)	Method	NAFB study area	Source
Quaternary-Pliocene	1000-1100	AFT	Chapelle-1 and Savigny-1 wells	(Cederbom et al., 2011)
	800-1400	VR, 1D and 2D thermal modelling	Canton of Vaud area	(Omodeo-Salé and Moscariello, 2019; Schegg et al., 1997)
	2000-2600	VR, 2D thermal modelling	Canton of Vaud area	Schegg et al., 1997
Mesozoic-Eocene	0	stratigraphy	Regional	(Burkhard and Sommaruga, 1998; Lemcke, 1988; Todorov et al., 1993; Wildi et al., 1989)
	500		NW sector	Omodeo-Salé and Moscariello 2019
	1000-1800	VR, clays, porosity, among others	Regional	(Schegg and Leu, 1998)
Permian-Triassic				
	200	VR, 1D thermal modelling	Weiach-1 well (NE sector	(Omodeo-Salé et al., 2021)
	1000	VR, stratigraphy	Weiach-1 well (NE sector)	(Diebold, 1988; Schegg and Leu, 1998)

Table 16: Erosion magnitude estimated in previous studies for the three main erosional unconformities at the regional scale and/or in areas close to the section 2 trace line.

3.1.1.4 Facies

Facies were assigned to the stratigraphic units composing the section by extrapolating the lithologic data described in the well reports of the following wells: Treyçovagnes-1, Essertines-1, Savigny-1, Chapelle-1 and Noville-1. For these wells, the lithologies for each unit, expressed in percentage, are listed in Appendix 5. For each unit, a unique or various facies were assigned along the section, depending first on the variability of the lithology and secondly on the availability of data (Table 17). Generally, for the shallower units (Molasse), more data are available than for the deeper units

(Triassic, Permo-Carboniferous), as only a few wells have been drilled deep enough to reach these deeper units.

Unit	Cgl	Sst	Silt	Shl	Lmt	Marls	Dlm	Anhyd	Halite	Reference Well
Quaternary										Various
UFM		20		20		60				Kusnacht-1
UMM		90				10				Chapelle-1
LFM Noville		25	5	65		5				Noville-1
LFM Ess-Sav-Chap		40		5	5	50				Essertines-1, Savigny-1, Chapelle-1
LMM		60				40				Savigny-1
Lower Cretaceous				10	80	10				Treyçovagnes-1; Essertines-1; Noville-1
Upper Malm				10	90					Treyçovagnes-1; Noville-1
Lower Malm				20	50	30				Treyçovagnes-1; Essertines-1; Noville-1
Dogger Trey-Essertines				15	40	45				Essertines-1; Treyçovagnes-1
Dogger Noville			20	20	20	40				Noville-1
Lias				75	25					Treyçovagnes-1; Essertines-1; Noville-1
Upper Keuper				25		25	25	25		Treyçovagnes-1; Essertines-1
Middle Keuper				10			40	50		Treyçovagnes-1; Essertines-1
Lower Keuper				30				30	40	Treyçovagnes-1
Muschelkalk		10		20	20		30	20		Treyçovagnes-1
Upper Muschelkalk Noville					50	10	40			Noville-1
Lower Muschelkalk Noville		70		24			5	1		Noville-1
Buntsandstein		90		10						Treyçovagnes-1; Noville-1
Permian Verrucano	8	72		20						Noville-1; Treyçovagnes-1
Permian Low		20	30	40	10					Noville-1
Autunian		20	40	40						Noville-1
Carboniferous		20	60	20						Noville-1
Basement	Gneiss									Various

Table 17: Facies, expressed as a percentage of lithological composition, assigned to the stratigraphic units forming the basin infill of section 2. The wells used as references are indicated. Cgl: conglomerate; Sdt: sandstone; Slst: siltstone; Shl: shale; Lmt: limestone; Mrl: marl; Dlm: dolomite; Anhd: anhydrite; Halt: halite; coal: coal.

3.1.1.5 Calibration data

Porosity data are available for the Essertines-1, Treyçovagnes-1 and Eclépens-1 wells, and they were used to calibrate the facies mechanical compaction properties along the section. Porosity data for those wells are listed in Appendix 6.

Borehole temperature data (BHT) are available for the Treyçovagnes-1, Essertines-1, Savigny-1, Noville-1 and Eclépens-1 wells, and they were used to calibrate the present-day temperature over depth in the basin infill. The temperature data for those wells are listed in Appendix 7.

The thermal maturity of the basin infill in the Canton of Vaud area is well documented, thanks to previous work (Schegg et al., 1997) and recent analyses performed for the Noville-1 exploration well (2010), now public (Geoform, 2010). %Ro data, necessary to calibrate the thermal modelling results, are available for the following wells: Treyçovagnes-1; Essertines-1; Savigny-1; Eclépens-1; Chapelle-1, Noville-1 (Appendix 8).



3.1.1.6 Source rocks parameters

According to the rest of the NAFB, three main source rocks are considered in the studied area: the marine Posidonia Black Shales (Toarcian in age), the lacustrine Autunian shales (Permian in age), and the Carboniferous coal and shales (Carboniferous in age) (Leu and Gautschi, 2014; Misch et al., 2017; Schegg and Leu, 1998). The presence of the Posidonia shale source rock is well-known in the northern part of the section (Dolivo, 2007). In this area, the geochemical data were directly measured through Rock-Eval Analysis on cutting and core samples of the Lias unit, which includes the Posidonia shale source rock, for the following wells: Essertines-1, Eclépens-1 and Treyçovagnes-1 (Appendix 1). An average TOC of 2% and HI index of 380 mgHC/gTOC indicates a Type II source rock with a good hydrocarbon potential, and the average T_{max} and %Ro data, respectively 432-438 °C and 0.5-0.8 %, indicate oil window thermal conditions. Thus, the Posidonia shale can be considered as a generating oil-prone source rock. These data are confirmed by oil-to-source biomarker analyses on the numerous oil seepages collected in the area (wells, quarry, etc), which indicate a marine origin of the organic matter generating the hydrocarbons (Dolivo, 2007). The presence of the Posidonia shale source rock in the central part of the section is unknown, as no wells penetrate the Lias unit in this area. In the southern part of the section (Noville-1 well), the Lias unit is not present. Thus, it was considered the extension of the Posidonia shale limited to the northern and central part of the section (up to the thrusted area), with an average thickness of 5 meters (maximum thickness measured in the Treyçovagnes-1, Essertines-1 and Eclépens-1 wells). By considering these data, the initial hydrocarbon potential of these source rocks is calculated and assigned in the model (Table 18).

In the Canton of Vaud area, where section 2 passes, the nature of the Permo-Carboniferous grabens infill is poorly known. However, the presence of a Permian and/or Carboniferous source rock/s in the area has been supposed, because of the geochemical signature of the gas seeps measured in the Cuarny quarry (Dolivo, 2007). The latter indicates a thermogenic origin from a mature gas-prone source rock such as the Carboniferous coals. The signature is quite similar to what is measured in the Hermrigen-1 well (see Section 3).

Because of the lack of direct data in the area, in the model, the internal subdivision of Permo-Carboniferous graben infill was extrapolated from the well-known Constance Frick Permo-Carboniferous graben (Northern Switzerland) (Madritsch et al., 2018). The source rocks geochemically parameters were considered similar to what was measured in the Weiach-1 well (Ajuaba et al., 2023) (Appendix 2). Therefore, in Section 2, the infill of the grabens was subdivided into two units, the Permian (33% of the total thickness) and the Carboniferous (67% of the total thickness). Secondly, in the Permian, for the Autunian lacustrine shales, an interbedded layer, with a thickness of 9% of the total Permian unit, was created (maximum thickness of 81 meters). For the two Carboniferous source rocks considered (coal and shales), two interbedded layers were created, with a total thickness of 9% of the total Carboniferous unit (maximum thickness of each unit, 80 meters). The initial organic geochemical data assigned into the model to the Permian and Carboniferous source rocks are shown in Table 18.

Source Rock	Lithology	Present average TOC (%)	Initial TOC (g rock)	Present average HI (mgHC/gTOC)	Initial HI (mgHC/g rock)	Kinetic
Posidonia shale	Black shales	2	4	380	500	TII(PB) (Behar et al., 1997)
Permian lacustrine shales	Shale organic rich	4.7	6.2	289	500	TI(C) (Pepper and Corvi, 1995)
Carboniferous coal	Coal	72	75	210	250	TIII-(Dogger) (Behar et al., 1997)
Carboniferous shales	Shale organic rich	8	8.5	95	150	TIIIH(DE) (Pepper and Corvi, 1995)

Table 18: Initial geochemical properties of the four source rocks assigned into the model.

3.1.2 Boundary Conditions

The upper boundary of the thermal model, the sediment-water interface temperature (SWIT), was automatically calculated by the software, for a geographical area located at a latitude of 46°N (present Switzerland latitude) (Fig. 12). The palaeowater depth was deduced by the depositional environment of the main stratigraphic units forming the basin and the basal heat flow trend was reconstructed considering the geodynamic evolution of the Molasse Foreland Basin (see Methods section) (Table 19).

Age to (Ma)	PWD (m)	Age from (Ma)	HF value (mW/m2)
0	0	0	50-80*
22	0	0.4	50
66	300	8	50
125	100	29	50
152	10	56	50
160	300	186	60
163.5	100	113	75
174.0	300	142	65
190	100	146	75
201.3	70	172	60
252	0	200	60
265	0	250	60
298	0	265	87
		273	110
		293	90
		318	64
		350	60
		500	60

Table 19: Paleowater depth (PWD) and basal heat flow variation over the time. (*) At the present day (0 My) a variation of the basal heat flow along the section was considered, based on the present heat flow distribution calculated throughout the NAFB (see Fig. 15).

At the present day (0 My), a variation of the basal heat flow along the section was considered (Fig. 18), based on the present heat flow distribution calculated throughout the NAFB (data source: https://map.geo.admin.ch, see Fig. 15).

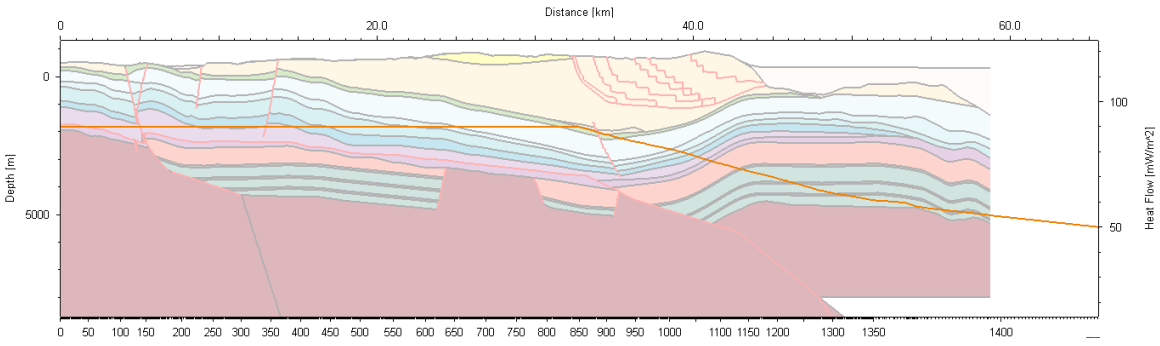


Fig. 18: Basal heat flow assigned along the Section 2 at the present-day (0 My)

3.1.3 Results

3.1.3.1 Restoration to the pre-Alpine thrusting phase

In the section used for modelling (Fig. 17d) inverted faults and thrust planes are present, in the southern part of the section mostly related to the subalpine Nappes thrusting and in the northern part of the section to the innermost Jura fold-and-thrust structures. Because of that, thermal models cannot handle multiple z-values generated by inverted faults and thrust planes, so the restoration of the present-day geometry to the geometry before the Alpine thrusting phase is necessary. To achieve this objective, the following restoration steps were performed:

- Step 1: Unfold and move back the Jura structures, located in the northern part of the section (Section t1 in Fig. 19), to obtain the basin geometry previous the deformation.
- Step 2: Unfold and move back the regional anticline located in the southern part of the section, which involves the subalpine nappes, part of the unthrusted foreland basin, the Mesozoic substratum and the Permo-carboniferous graben (Section t1 in Fig. 19), up to obtain the basin geometry previous the deformation. Because of that, the subalpine nappes thrust planes are folded, and it was considered that this anticline occurred after the thrusting of the subalpine nappes. From seismic, the Permo-Carboniferous graben is also folded, forming a regional antiform. Therefore, it is supposed that the Permo-Carboniferous graben has also been inverted, as a consequence of the reactivation of a deep basement fault. This fault could be part of a flat-and-ramp plane that extends northward, up to the end of the foreland basin, along the Triassic evaporite layer. This could be the plane along which the entire foreland basin was thrusted in the latest Alpine compression phase, with the formation of the Jura belt mountain (Burkhard, 1990; Burkhard and Sommaruga, 1998; Laubscher, 1965; Philippe et al., 1996). By restoration, the basin was shifted along the deep basement ramp, resulting in a foreland basin geometry in the southern part of the section. A greater shift is also possible, which would result in a greater burial in this area.
- Step 3: Move back the subalpine thrusts, located in the southern part of the section, up to obtain a foreland geometry (Section t2 in Fig. 19). At a regional scale, inside the thrusted area, no stratigraphic layers were found that could be used as references to calculate the amount of stretching of this deformation phase. Thus, the original length of the foreland basin before the deformation, shown here in Section t2, is only indicative.

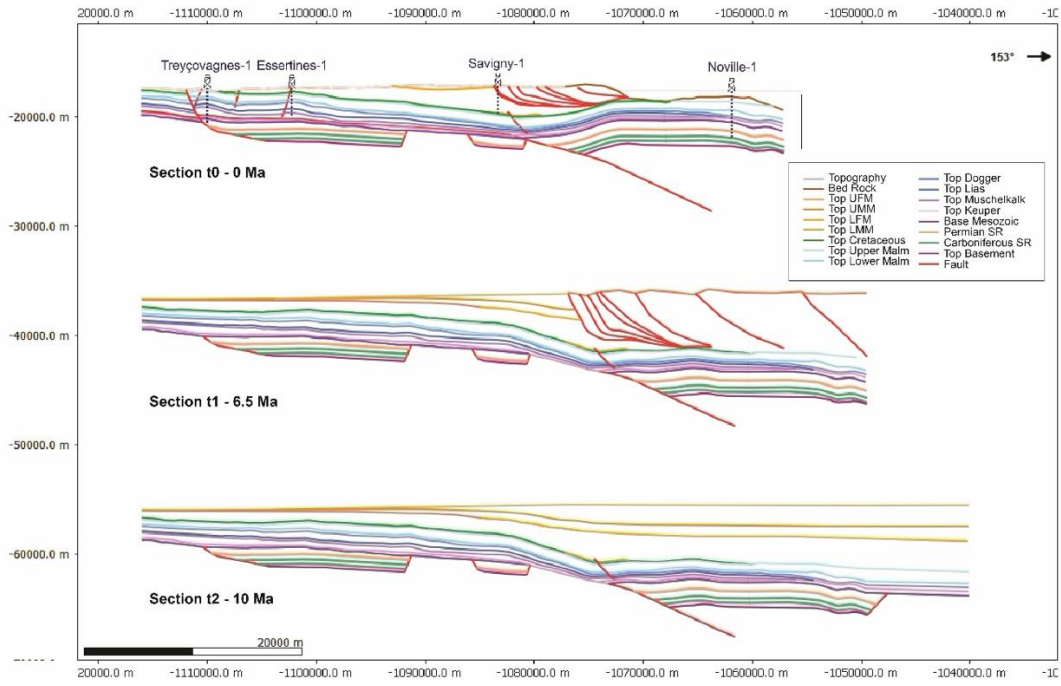


Fig. 19: Paleosections resulting from the Alpine thrusting restoration, representing the basin geometry evolution, from the present-day (section t0) to the pre-Alpine thrusting phase (section t2).

From the restoration process, three paleo-sections were obtained, representing the deformation evolution phases of the foreland basin up to the present-day geometry (Fig. 19). The section t2 is the oldest and it represents the geometry of the basin before the Alpine thrusting. Considering the subalpine thrust activity dating proposed by Von Hagke et al. (2012) (between 10 to 6-5 Ma) and the age of the UFM unit deposition (Kuhlemann and Kempf 2002) (Langhian to Tortonian, 15.97-7.24 Ma), an age of 10 Ma was assigned to this section. To simplify the model-building process, it was considered that all the Molasse units were deposited before the thrusting, despite of that there are no data to constrain this assumption. It could also be possible that the thrusting was already active in the area at that time and coeval to the deposition of the latest Molasse unit, the UFM, in the more external part of the basin. However, this uncertainty does not have a strong impact on the final modelling results. The thickness of the Molasse units before their uplift and erosion was estimated based on literature data (see previous Erosion section).

The section t1 represents the geometry of the basin after the Subalpine thrusting. The age of this section is assigned at 6.5 Ma. Uncertainties on the age and amount of thrusting (shortening) are large. The geometry proposed here is a simplified option.

The section t0 represents the present-day geometry of the basin. In this section the occurrence of several events are represented: i) the regional folding of the southern part of the section, along a deep basement ramp plane, which continues along a large flat up to the northern extremity of the basin; ii) the fold-and-thrust Jura Mountain formation, due to the shift of the foreland basin along the evaporite Triassic detachment, resulting in the formation of folding and inverted faults in the northern part of the section; iii) the uplift and erosion of the uppermost part of the basin.

3.1.3.2 Geological conceptual model evolution

The three paleo sections obtained in the previous step were imported in the PetroMod software, by applying the TecLink workflow (see Methods section above) (Fig. 20). For each section, each horizon was assigned to a stratigraphic unit and at a corresponding age (Table 17). The facies previously defined (Table 17) were assigned to the stratigraphic units composing the sections (Fig. 20). The paleo sections define the geometry of the basin from the present day to the phase previous to the Alpine thrusting.

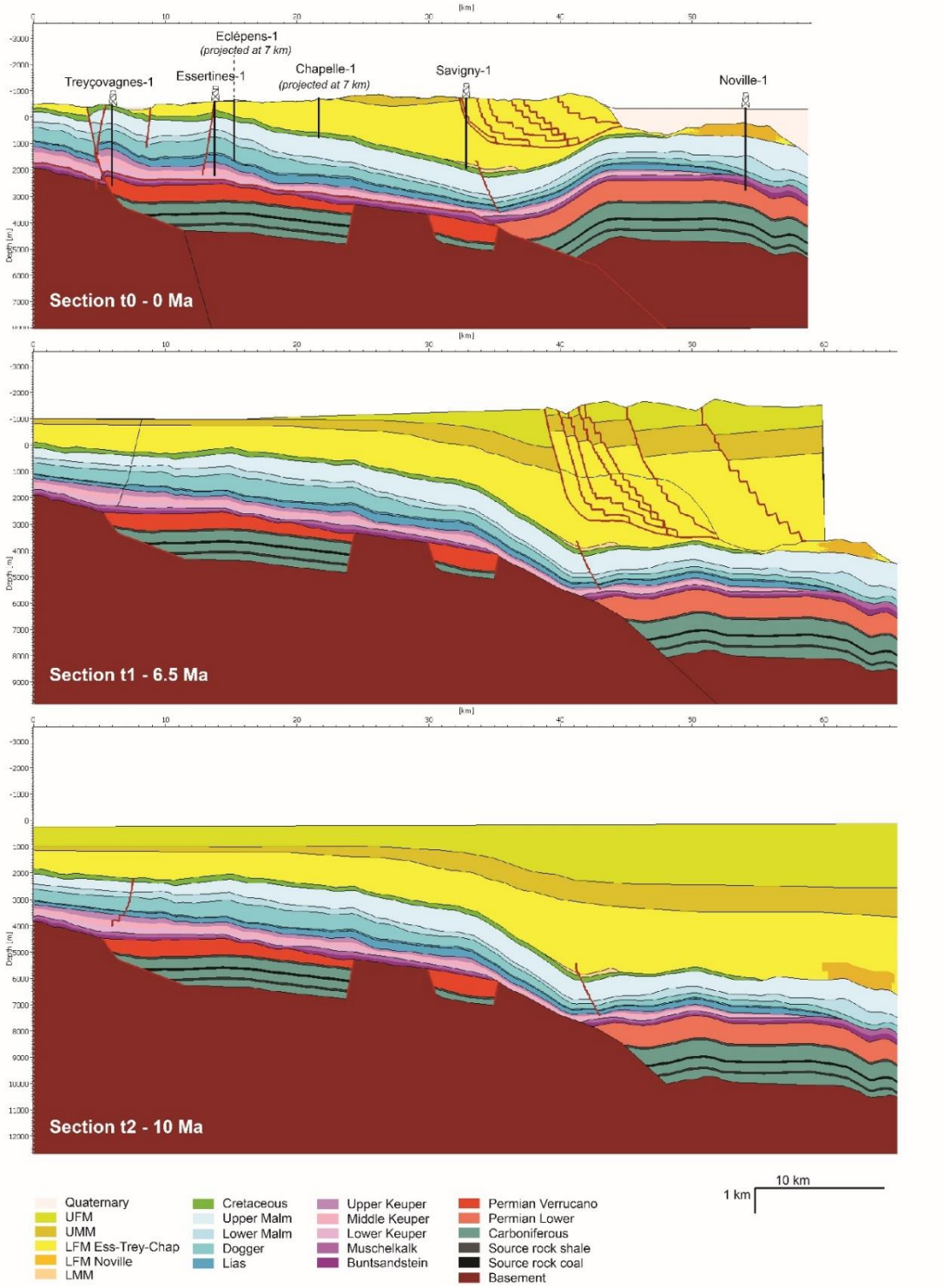


Fig. 20: Paleosections imported in Petromod and used as a geological model of the thrusting and erosion phases. Based on the stratigraphy described in the closest wells (see paleo section t0), facies were assigned to the present-day section and extrapolated to the other paleo sections. Sections vertical exaggeration 2:1.

The restoration to the geometry of the basin at the end of the deposition of each of the previous stratigraphic units was automatically performed by the modelling software, which also takes into consideration the decompaction factor (Fig. 21). The thickness eroded during the Permian-Triassic and Cretaceous-Eocene unconformities was added as paleo thickness of respectively 200 and 500 meters, assigned at the related periods (Table 15). The Pliocene-Quaternary erosion was estimated considering previous literature data (see Erosion section above), and it ranges from 900-

1000 meters in the north-central part of the section, 2500 meters in the more external thrusting area, and more than 5000 meters in the more internal thrusting area, in the southern extremity of the section.

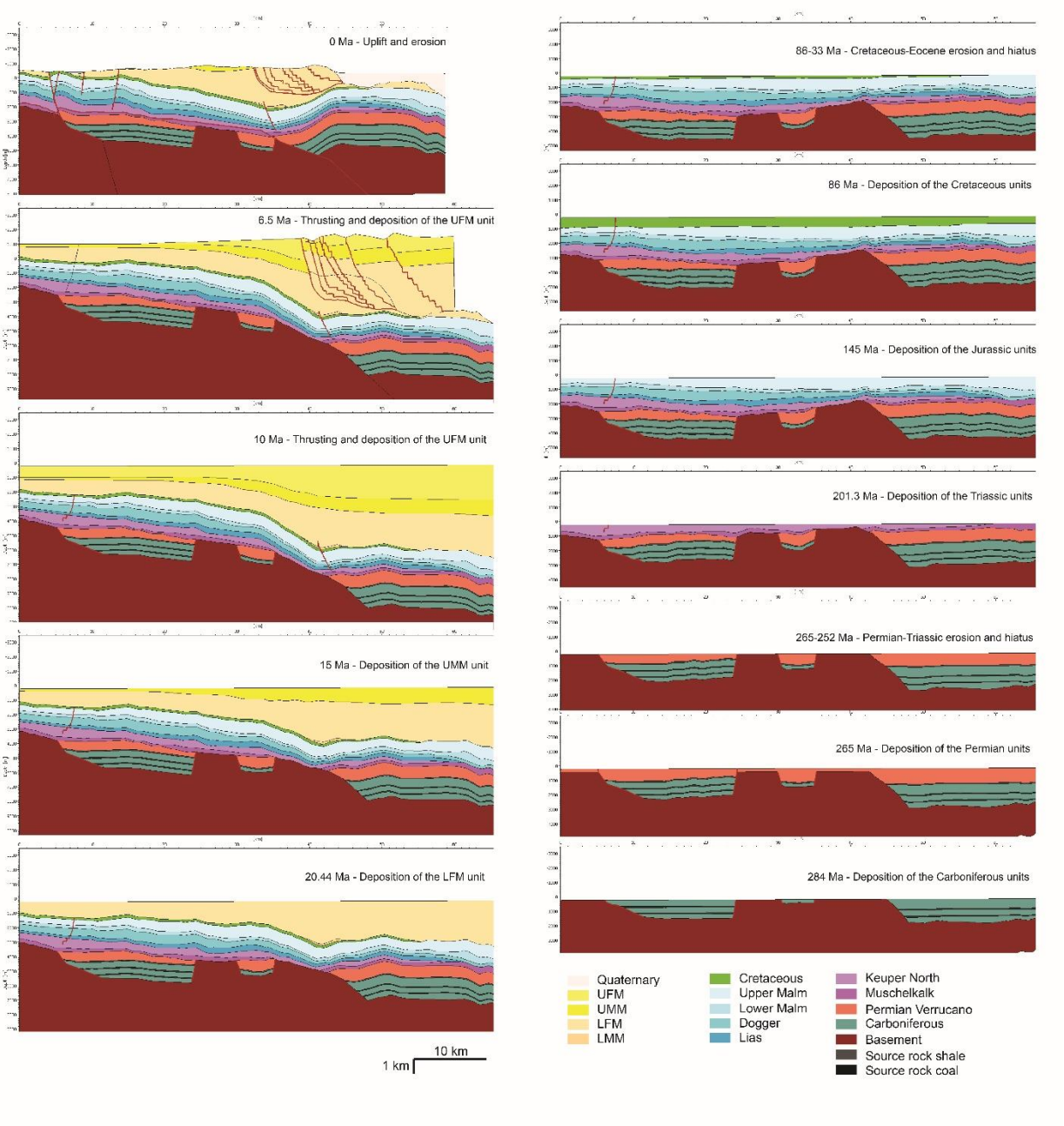


Fig. 21: Geological evolution of the studied area obtained in Petromod by retrodeformation and decompaction of the units forming the basin infill from the present day to the Carboniferous time. Sections vertical exaggeration 2:1.

3.1.3.3 Thermal model calibration

3.1.3.3.1 Porosity

The porosity was calibrated for the Treyçovagnes-1, Essertines-1 and Eclépens-1 wells (Fig. 22) and assigned along the entire section (Fig. 23). The mechanical compaction properties estimated by the software for the lithologies assigned to each stratigraphic unit, were iteratively changed up to fit the theoretical values calculated by the model with the porosity values measured along the wells. The porosity of the uppermost Molasse units (UFM and UMM) was extrapolated from the

values measured for the LFM in the Essertines-1 wells. The porosity data measured along the Eclépens-1 well are not correctly plotted on the stratigraphic section extracted from the modelled section at the location where the Eclépens-1 well is projected (Fig. 22). This is because the Eclépens-1 well is located on an anticline, which is not present along the modelled section. Data should be plotted at a lower stratigraphic position concerning what is shown in the graph extracted from the model.

The porosity extrapolation performed here along the section can be highly uncertain, especially, but not only, in the case of the dominantly limestone units (Mesozoic), where the porosity and permeability are strictly controlled by diagenetic processes and fracking, which can dramatically change from one point to another of the basin. To reduce this uncertainty, more porosity data should be available along the section.

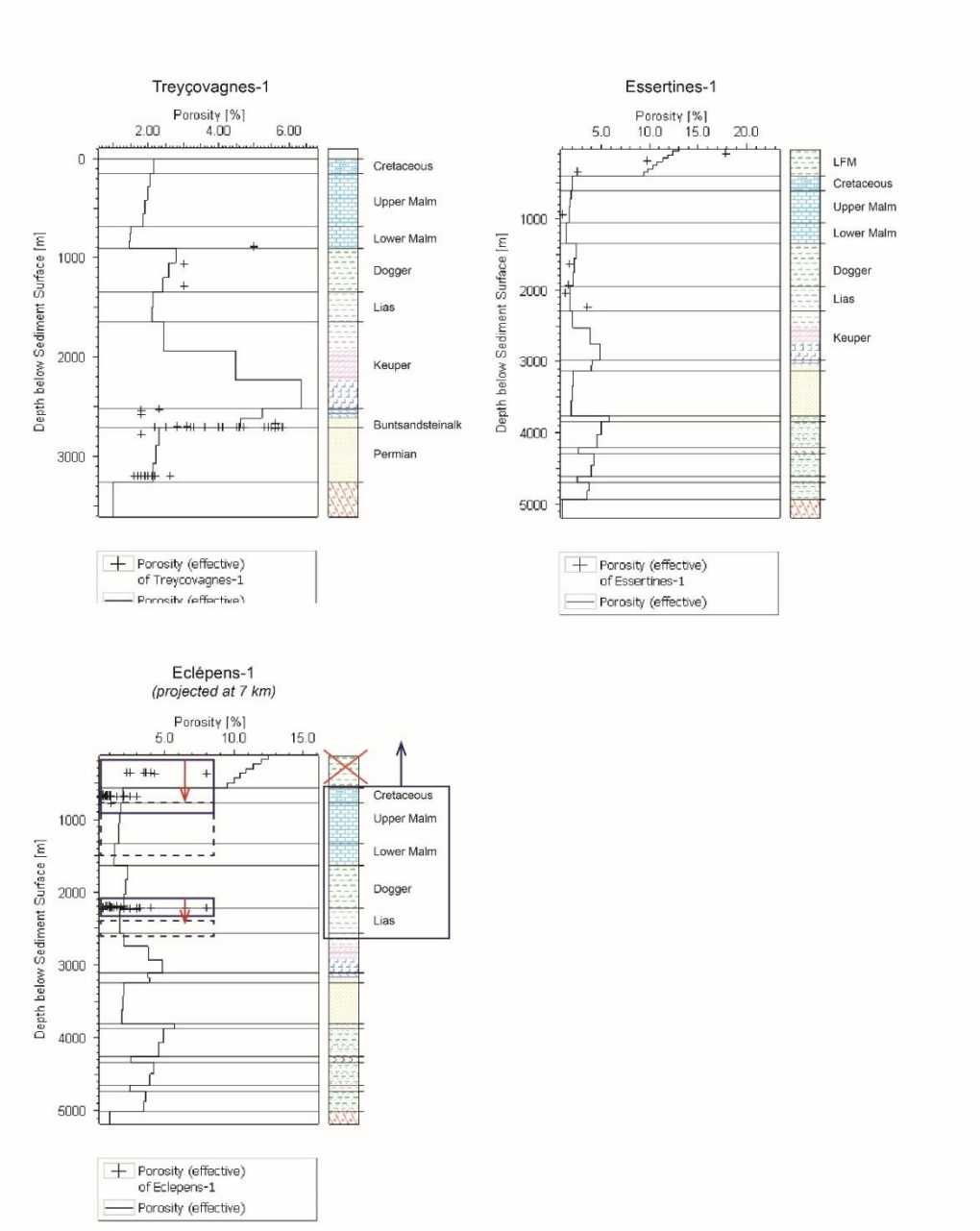


Fig. 22: Calibration of the porosity property with the data measured in the Treyçovagnes-1, Essertines-1 and Eclépens-1 wells. The porosity data measured along the Eclépens-1 well are not correctly plotted on the stratigraphic section extracted from the modelled section at the location where the Eclépens-1 well is projected. Data should be plotted at a lower stratigraphic position than what is shown in the graph (red arrows)

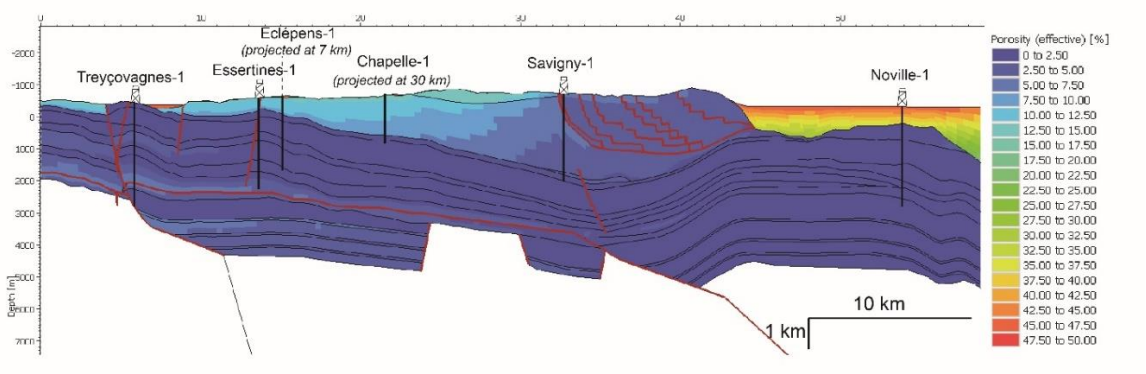


Fig. 23: Porosity along the section, modelled by the software, extrapolating the data calibrated in the Treyçovagnes-1, Essertines-1 and Eclépens-1 wells.

3.1.3.3.2 Present-day temperature

The present-day temperature calculated by the model was calibrated with the borehole temperature (BHT) measured in the wells Treyçovagnes-1, Essertines-1, Savigny-1 and Noville-1. Temperature data measured in the Eclépens-1 (projected 7 km) and Chapelle-1 (projected 30 km) wells were also considered, because of that they are considerably far from the section trace, the calibration of these data is less relevant.

To calibrate the modelling results, the variable that mostly changed was the present-day basal heat flow (see Method section). Firstly it was tested the heat flow values estimated in the entire basin from the borehole temperature data (Fig. 18 and Fig. 24, Scenario A). This scenario does not give satisfactory calibration results, as the temperature simulated by the model is higher than what is measured in the wells, especially in the case of the Savigny-1 and Noville-1 wells, located in the southern part of the section, in the thrusted area (Fig. 25). This is because of that the heat flow values measured at the present-day (Scenario A) represent the heat flow at the surface, whereas the heat flow that was assigned to the model refers to the amount of heat at the base of the model, basement included. Toward the basin surface, this heat is increased, mostly by the radiogenic heat produced by the basement and basin infill rocks. The effect of the rapid exhumation of the NAFB can also play a role in maintaining an anomalously high heat flow at the surface of the basin. Therefore, to reproduce the temperature measured in the wells, a lower heat flow needs to be assigned at the base of the model.

Another heat flow scenario is tested for 0 Ma (Fig. 24, scenario B), with values ranging from 70 to 25 mW/m^2 along the entire section. This scenario improves the calibration of the borehole temperature measured in most of the wells (Fig. 25). According to this scenario, the model calculates the temperature distribution along the section at the present day (Fig. 26).

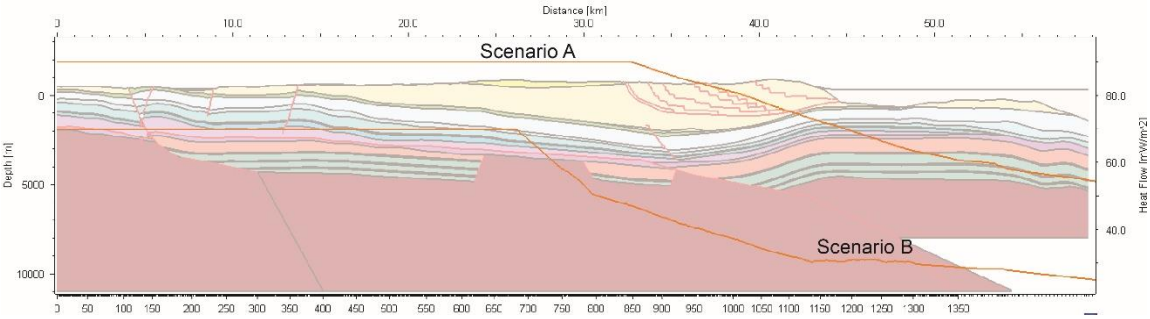


Fig. 24: Heat flow values assigned along the modelled section at 0 Ma. The two scenarios tested are shown

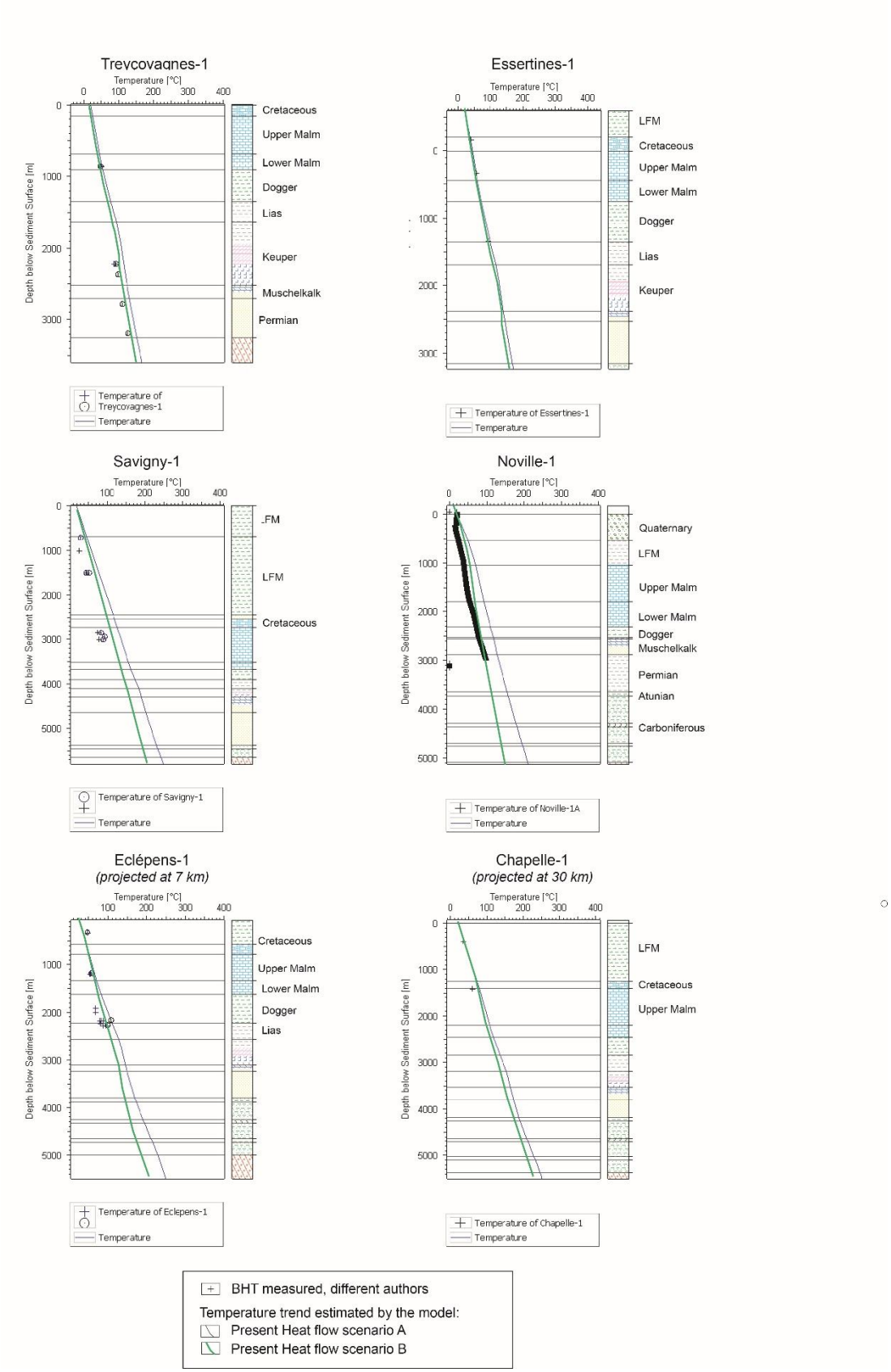


Fig. 25: Calibration of the present-day temperature modelling results with the BHT measured in the wells Treyçovagnes-1, Essertines-1, Savigny-1, Noville-1, Eclépens-1 and Chapelle-1.

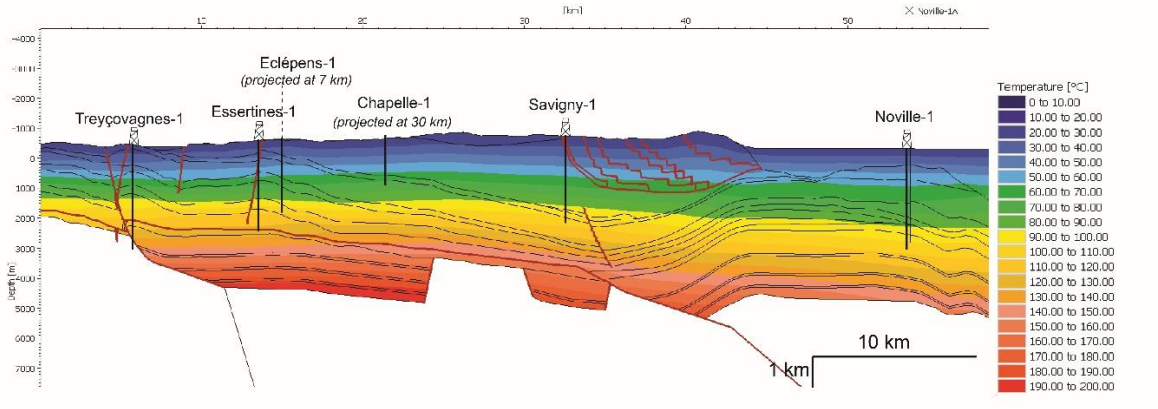


Fig. 26: Temperature variation with depth and along the section calculated by the model for the present day (0 My).

3.1.3.3.3 Thermal conditions / Source rocks maturity

The thermal conditions along the section were calibrated with the %Ro data of the following wells: Treyçovagnes-1, Essertines-1, Eclépens-1, Chapelle-1, Savigny-1 and Noville-1 (Fig. 27). The thermal conditions resulting along the entire section are shown in Fig. 28.

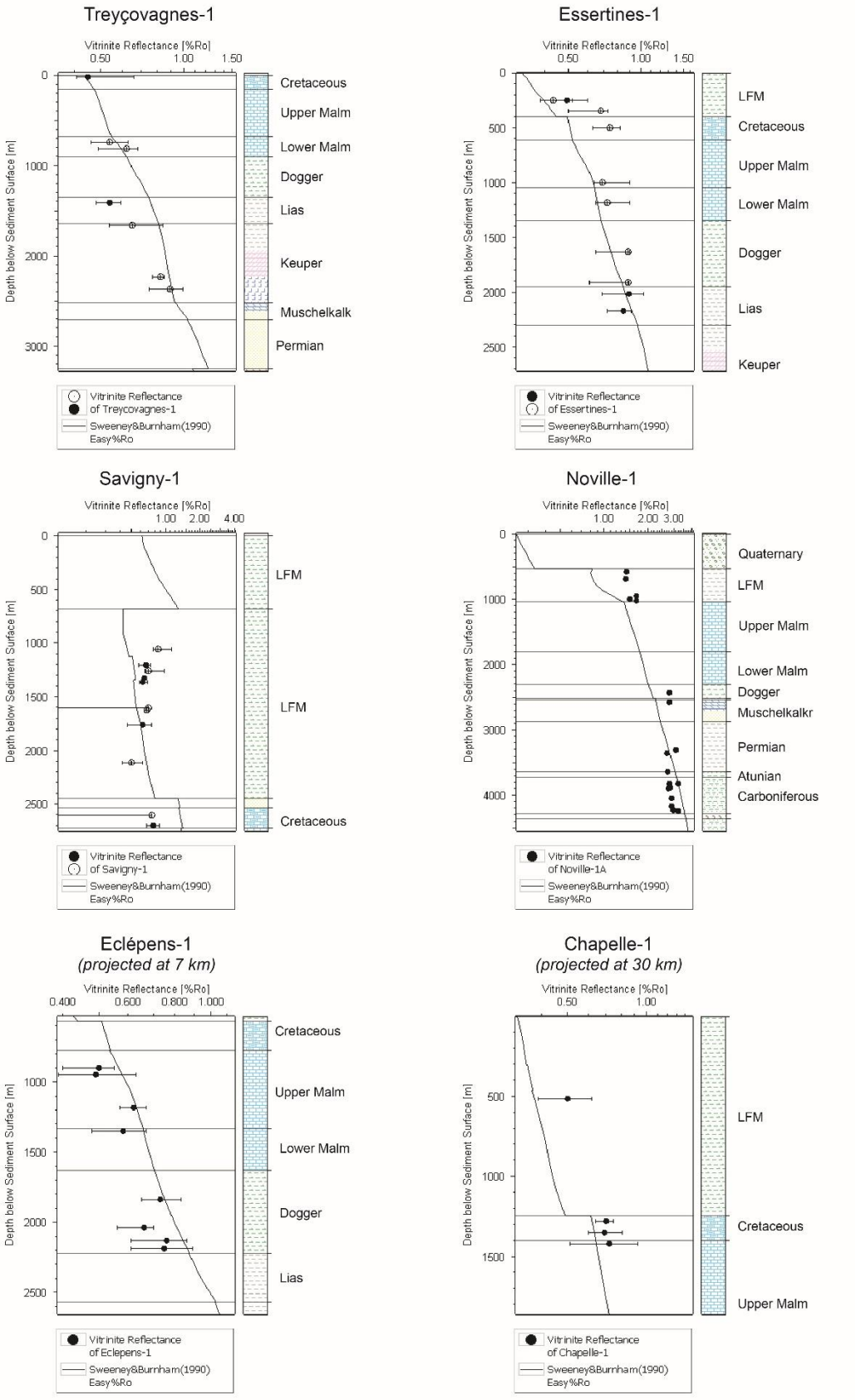


Fig. 27: Calibration of the thermal conditions calculated by the model with %Ro data measured for the Treyçovagnes-1, Essertines-1, Savigny-1, Noville-1, Eclépens-1 and Chapelle-1 wells.

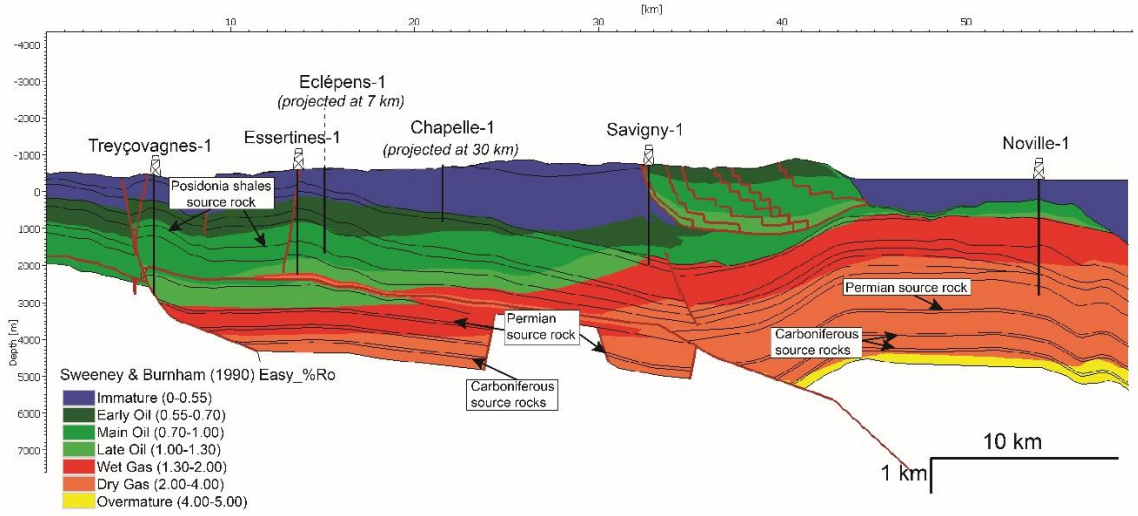


Fig. 28: Thermal conditions calculated by the model along the entire section

From the modelling results it is deduced that, in the south, all the source rocks are in the gas window conditions, whereas in the central and northern parts of the section, the Posidonia shale source rock is in the oil window thermal conditions, the Permian source rock is in the beginning of the wet gas window and the Carboniferous source rocks in the dry gas window.

The source rocks' maturation timing is deduced by the burial plot vs thermal conditions extracted at the Treyçovagnes-1 and Noville-1 wells position (Fig. 29). In the northern part of the section (Treyçovagnes-1 well area), the Lias unit (Posidonia shale source rock) enters the oil window in the Miocene time and the Permian source rock in the Cretaceous time. In the southern part of the section (Noville-1 well area), the Permian source rock enters the oil window in the Jurassic and Cretaceous and the gas window in the Miocene time. The Carboniferous source rock enters the oil window in the Permian time and the gas window in the Cretaceous time (deepest layers) to the Oligocene time.

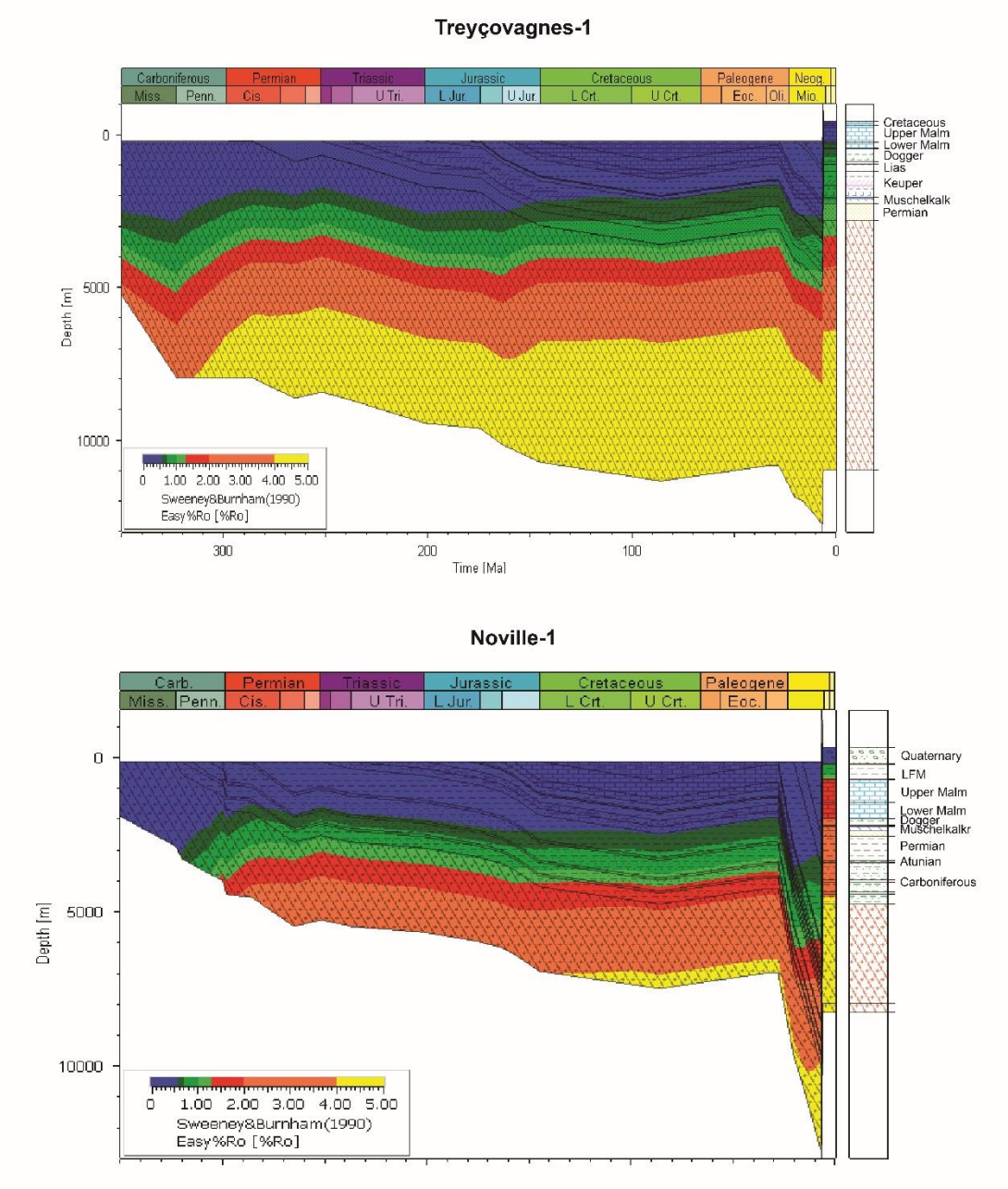


Fig. 29: Burial plot versus thermal maturity conditions, showing the time when the source rocks (Lias, Permian, Carboniferous) were matured.

3.1.3.4 Simulation of hydrocarbon generation, migration and accumulation processes

The model simulates the hydrocarbon generation, migration and accumulation processes for Section 2, as the effect of the source rock maturation and hydrocarbon expulsion. Migration paths and potential reservoirs are calculated based on the geometry of the basin and the permeability properties of its infill. Hydrocarbons were generated by the Permian, Carboniferous and Posidonia Shale source rocks, at different times. The first generation peak occurred in the late Jurassic to early Cretaceous time when the basin was affected by an important burial event and heat flow peak, and the second generation peak occurred in the Cenozoic time when the formation and infill of the foreland basin increased abruptly the burial depth of the basin (Fig. 30).

The rock that generates the greatest volume of hydrocarbons is the Carboniferous coal source rock, followed by the Carboniferous shale source rock, the Permian source rock, and finally, the Posidonia shale (Fig. 30). The Carboniferous source rocks generate hydrocarbons in both

generation peaks, whereas the Permian and Posidonia shale source rock mostly generate in the Miocene when the northern part of the basin was buried enough to mature these deposits.

Conventional high-permeable reservoirs formed in the Cretaceous and Paleogene times, mostly in the Muschelkalk unit, in the Buntsandstein facies, and only in smaller volumes in the Permian units. Accumulations in low permeable units (petroleum saturated) formed also in the Cretaceous and Paleogene times, mostly in the Carboniferous and Permian deposits and secondly, with very small volumes, in the LMM/LFM and Jurassic units.

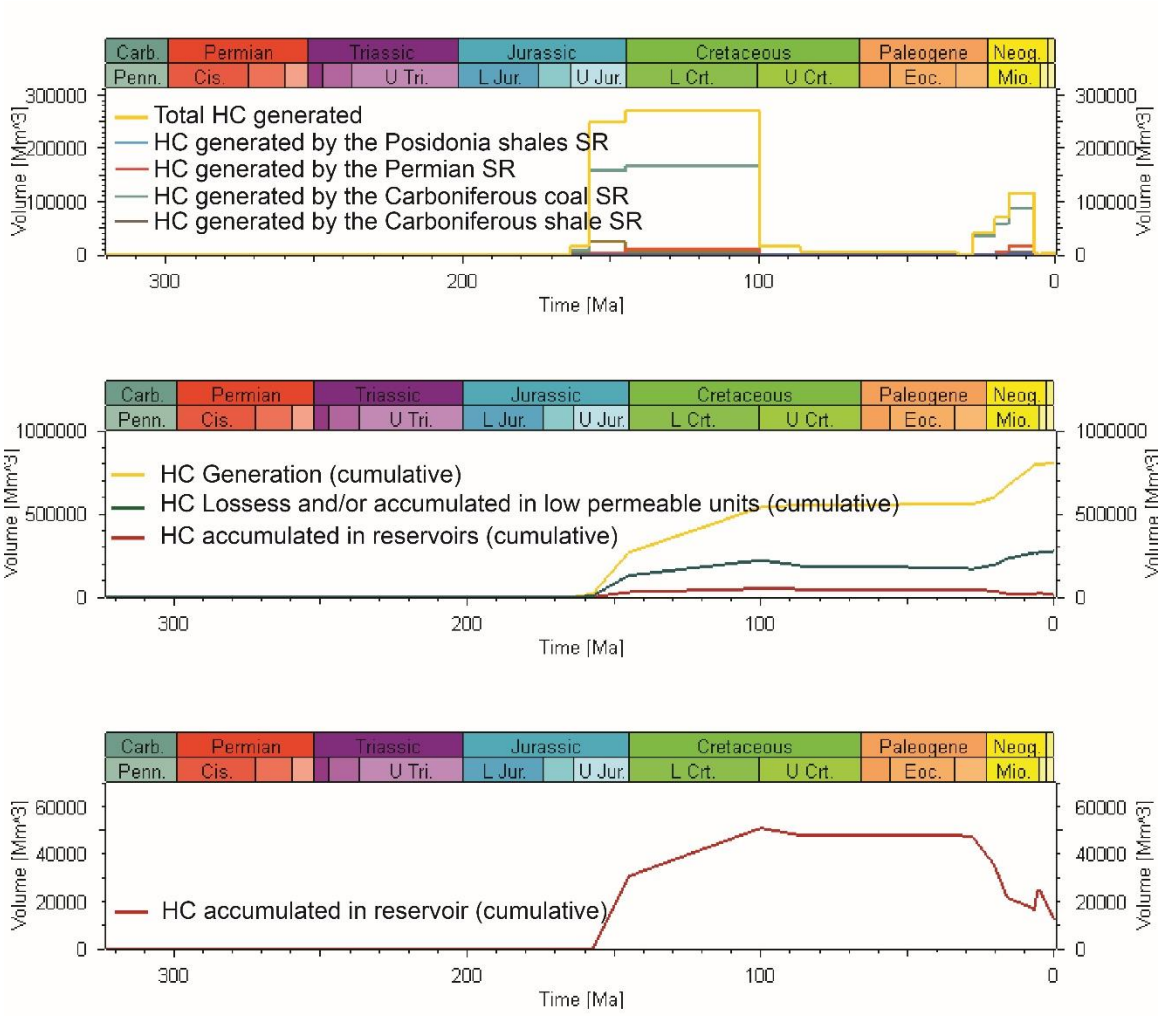


Fig. 30: Hydrocarbon generation and accumulation balances calculated by the software for the entire section

The model estimates the formation of gas hydrocarbon accumulations in the Muschelkalk deposits (Buntsandstein facies), in small anticlines located in the northern part of the section, in the Treyçovagnes-1 and Essertines-1 wells area, sealed by Triassic evaporite (Keuper unit) (Fig. 31). Another very large accumulation in the Buntsandstein/Muschelkalk is estimated in the regional anticline located in the southern part of the section, where the Noville-1 well is present. Minor gas accumulations are formed in the Muschelkalk unit along the entire section. These accumulations were generated most likely by the Permian and Carboniferous source rocks (Fig. 31).

In the northern part of the section (Treyçovagnes-1 and Essertines-1 wells area), the model estimates the formation of small oil and gas accumulations and/or migration paths along faults and in anticline structures (Fig. 31). These hydrocarbons were generated most likely by the Posidonia shale source rock, which in this area is in the oil window thermal conditions. Toward the central part of the section, small gas accumulations and migration paths formed along the entire stratigraphic section, generated by the Posidonia shale source rocks, which, toward the thrusted area, are in the gas window thermal conditions. However, because of that, it is unknown if the

Posidonia shale source rock is present in this part of the section, the hydrocarbon accumulations simulated by the model may not be reliable.

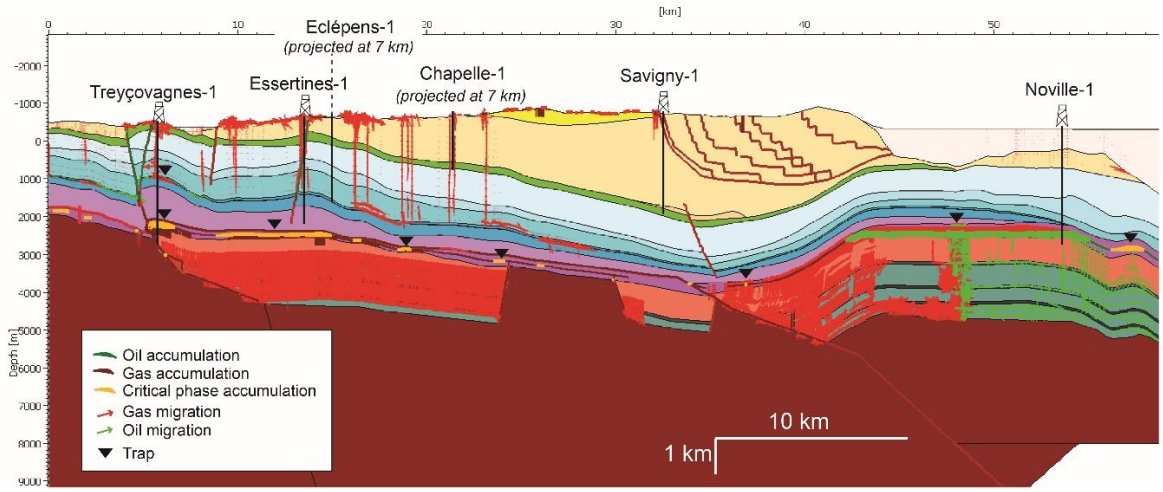


Fig. 31: Scenario Open Faults: Hydrocarbon accumulations and migration path calculated by the model along the section. Potential traps are indicated.

A second scenario was simulated, considering the “closed faults” option (Fig. 32), which means that faults can be cemented, thus hydrocarbons could hardly migrate along them. In this scenario largest accumulations formed in the Muschelkalk and Permian units. The leakage to the uppermost units observed in the previous scenario is less relevant because the hydrocarbons could escape to the top along the faults. The hydrocarbon accumulation and migration paths formed in the Jurassic and Cenozoic units are dominantly generated by the Posidonia shale source rock.

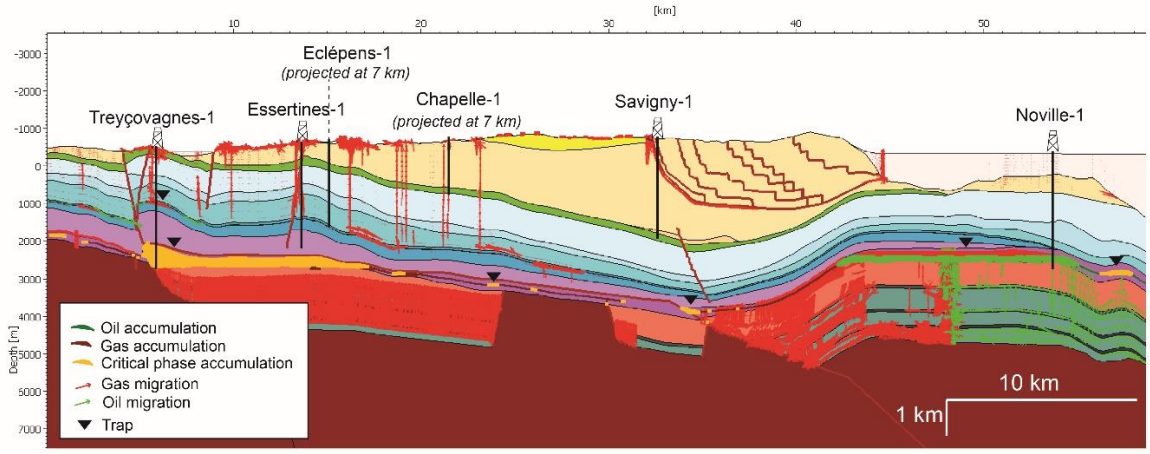


Fig. 32: Scenario Closed faults: Hydrocarbon accumulations calculated by the model along section 2. Potential traps are indicated.

In Fig. 33, the hydrocarbon accumulations over the basin evolution are shown. The thermal maturity is also represented. The hydrocarbon accumulations in the Permian and Muschelkalk (including Buntsandstein units) started forming since the Jurassic time, when the Permian and Carboniferous source rocks entered the oil window. These accumulations were filled over the entire evolution of the basin, as all the Permian and Carboniferous source rocks entered the oil and gas windows along the entire section and when a seal composed of anhydrite facies was deposited along the entire basin (Muschelkalk and Keuper units). They were partially preserved until the present day. Most of the hydrocarbons generated by the Posidonia shale source rock, as well as part of the hydrocarbons generated by deeper source rocks, migrated vertically to the top surface and were lost because of the lack of proper traps. Few small accumulations could form in the anticline structures formed in the northern part of the section, because of the Jura Mountain formation.

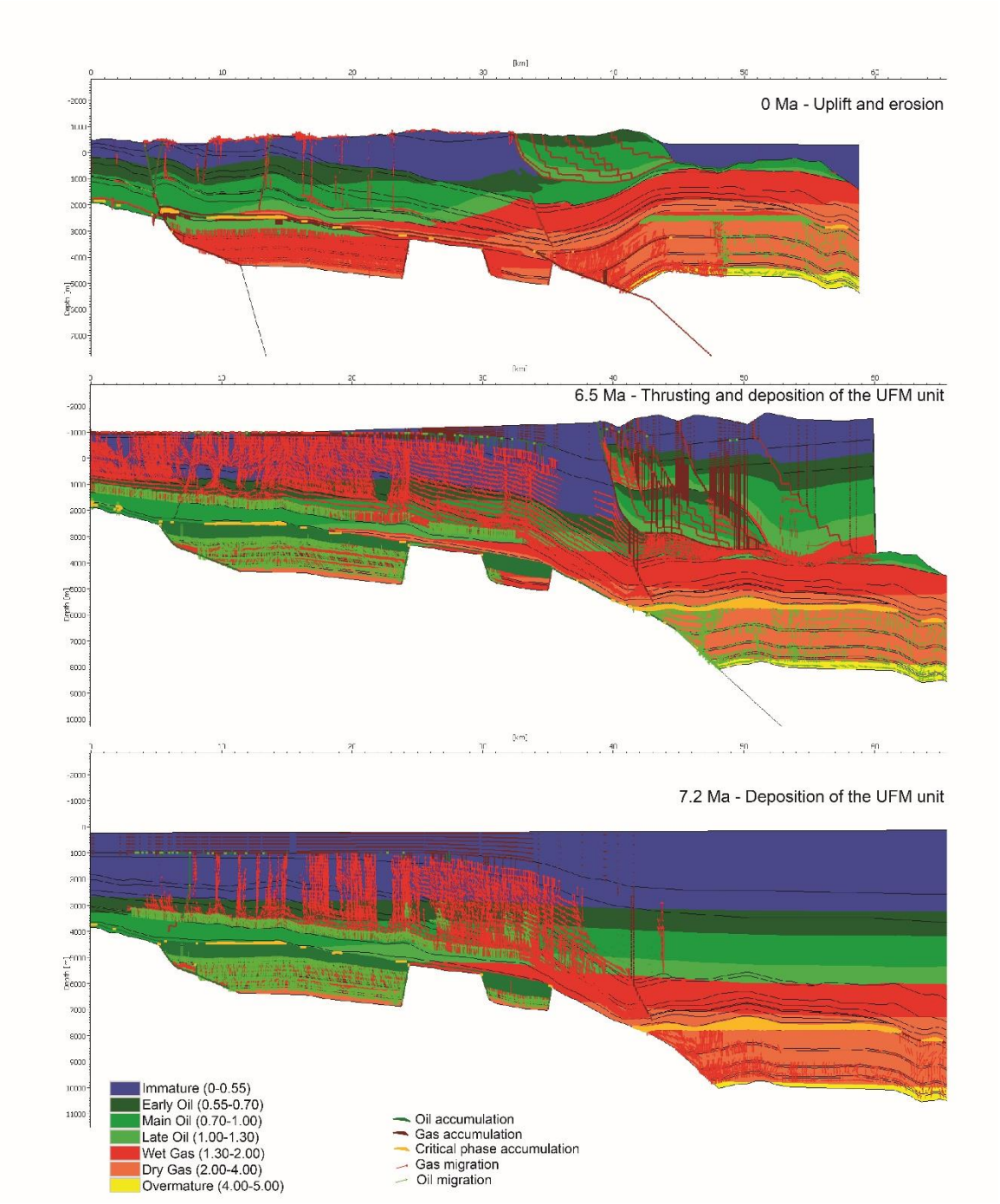


Fig. 33: Hydrocarbon accumulations and thermal maturity evolution over time (continues).

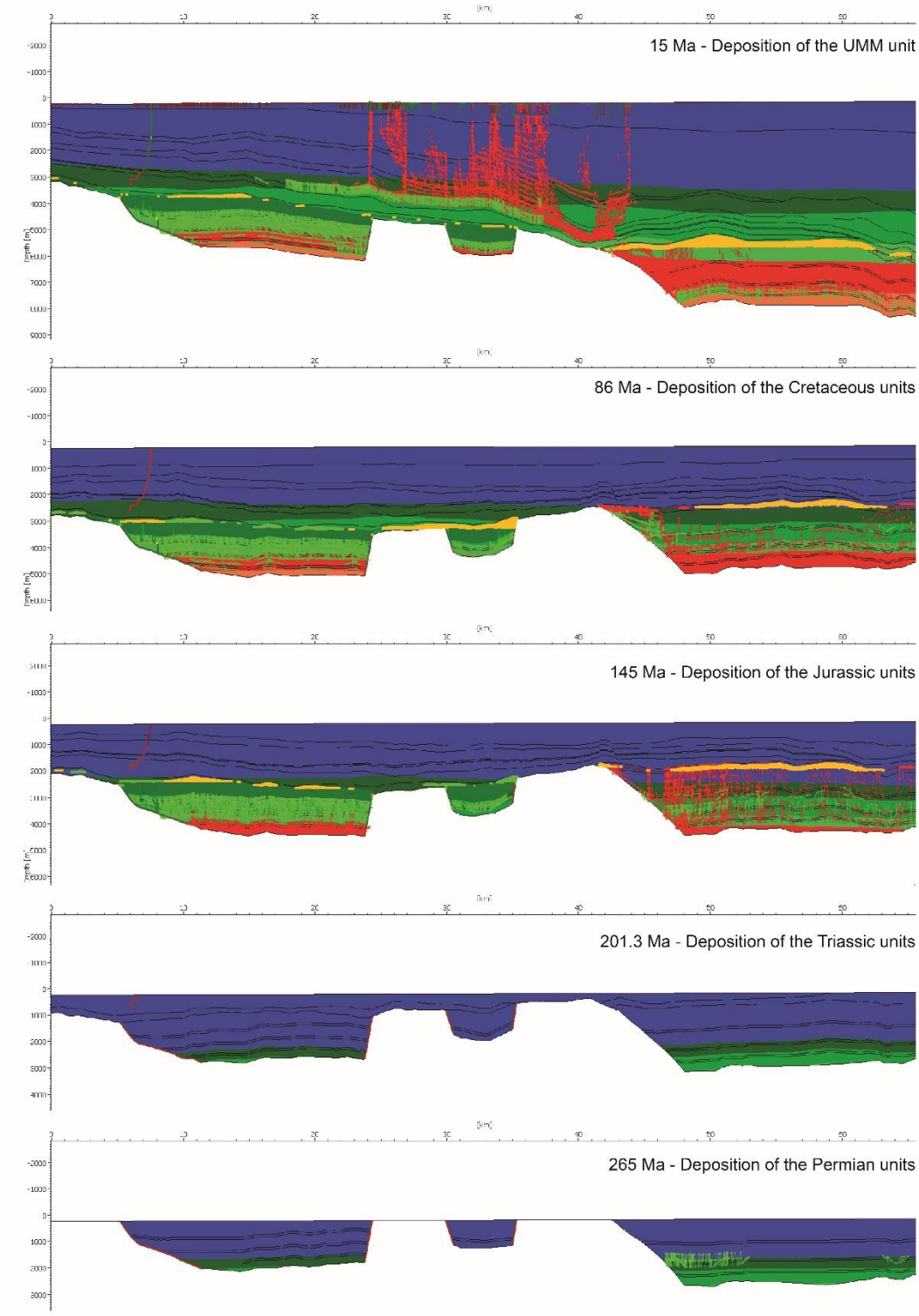


Fig. 33 (continues): Hydrocarbon accumulations and thermal maturity evolution over time.

Finally, the petroleum system evolution for the four source rocks considered was reconstructed in terms of a petroleum system chart (Magoon and Dow, 1994) (Fig. 34), where the source rocks, reservoir, seal, overburden rocks and trap elements are defined. The critical moment is defined

considering the fit among the formation of reservoirs, traps, the maturation timing of the source rocks and the hydrocarbon generation timing (Fig. 33).

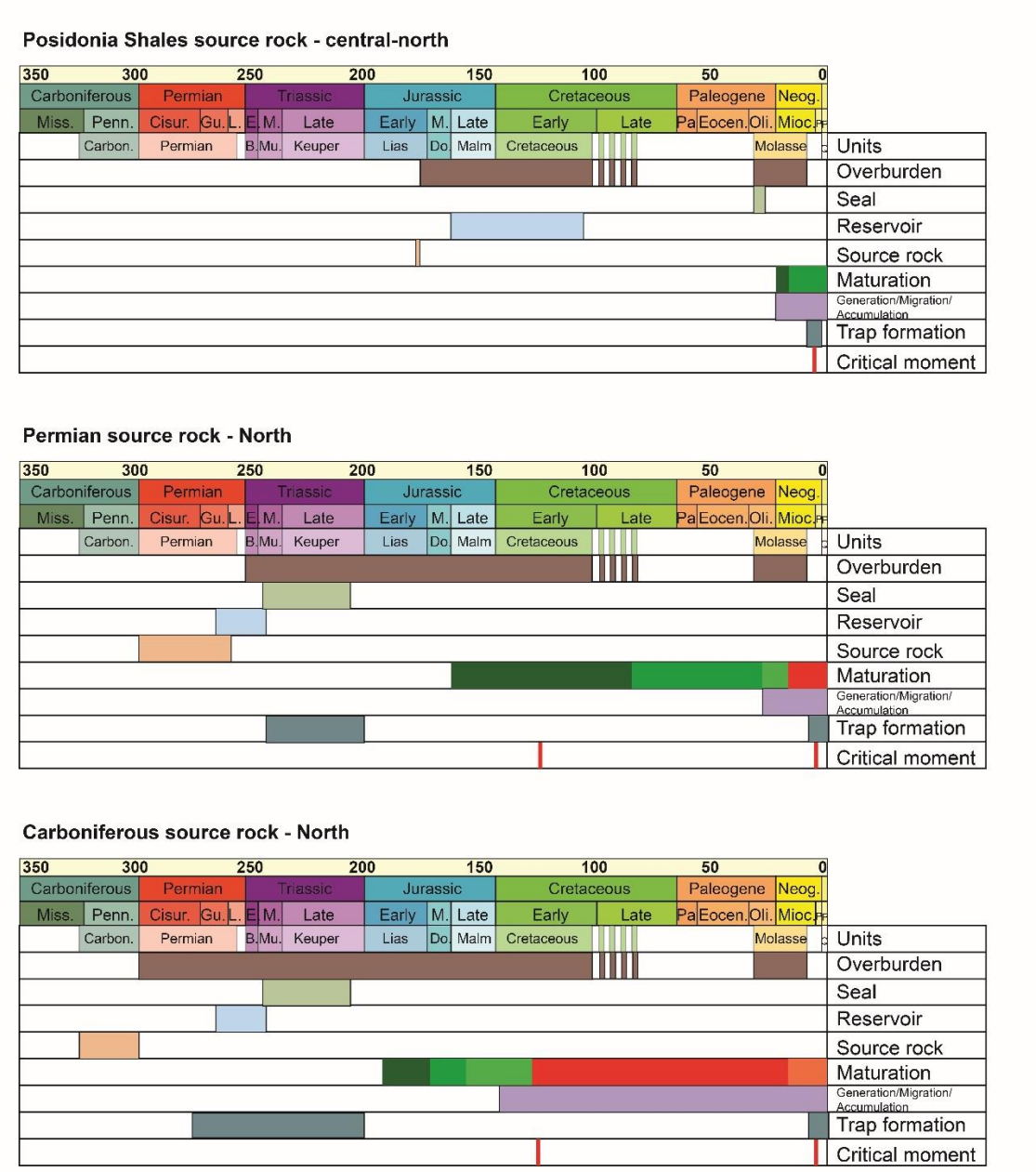


Fig. 34: Petroleum system charts reconstructed for the four source rocks defined in Section 2 (continues).

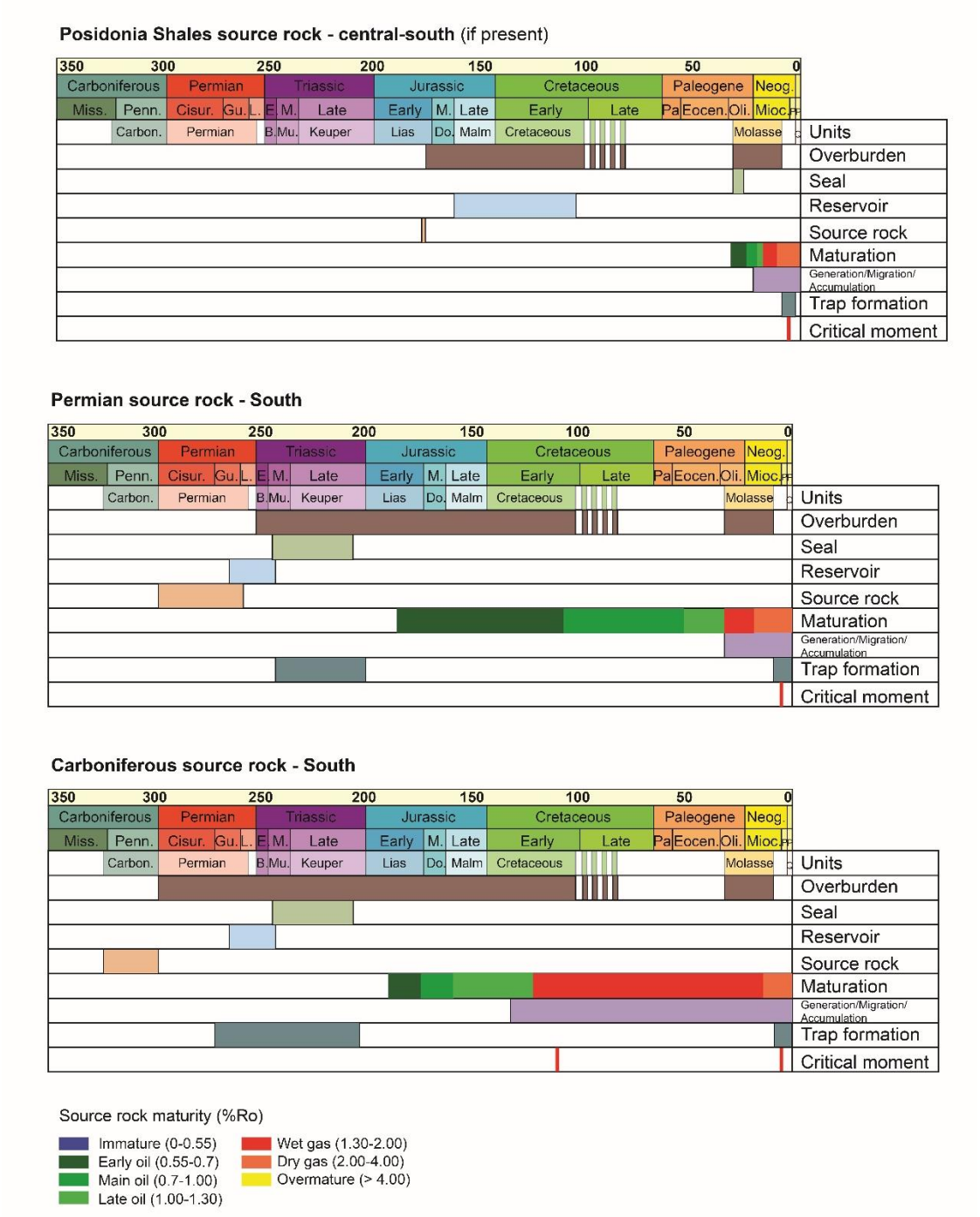


Fig. 34 (continues): Petroleum system charts reconstructed for the four source rocks defined in Section 2.

3.1.3.5 Comparison between the hydrocarbon findings and the modelling results

The modelling results are partially in agreement with what has been found in the drilling campaigns carried out over time in the study area (Table 20). In the Treyçovagnes-1 well (1978) oil was found in the uppermost Rhetian sandstone unit (20,8 m^3 oil) and minor methane flow in the Buntsandstein and Muschelkalk fractures. Therefore, there is effective evidence of gas accumulation in the unit below the anhydrite and salt forming the Keuper. However, a proper reservoir, as simulated by the model, was not found. In the Essertines-1 well, bitumen traces were found in the Cretaceous, oil in fractures in the Rhaetian and some gas shows in the Muschelkalk and Buntsandstein units. Similarly, in the near Eclépens-1 well, oil was found in the fractures of the Dogger and Lias units

and gas shows in the Lias and Keuper units. In the Chapelle-1 and Savigny-1 oil has been observed in the fractures of the Lower Cretaceous deposits (Barremian and Albian units). These findings agree with the modelling result. In the Noville-1 well, a tight gas accumulation was found in Paleozoic clastic rock. In this area, the model simulates a large hydrocarbon reservoir at the top of the Permo-Carboniferous graben, in the Permian and Muschelkalk units.

In most cases, the number and size of the reservoir calculated by the model, as well as the hydrocarbon flow paths, are larger than what has been found in the wells. The reasons for this discrepancy can be multiple:

- The Permian and Carboniferous source rocks' thickness and hydrocarbon potential could be overestimated. This can be particularly true in the case of the northern Permo-Carboniferous graben, where no wells penetrate deeply into these deposits. Therefore, their thickness and properties were extrapolated from the nearest wells penetrating these units (Northern Switzerland and Jura), which could not be representative of what is present in the area. In the case of the Noville-1 well, it is known that, in this area, the Permian source rock (Autunian shales) has been completely penetrated, whereas Carboniferous source rocks have been only partially attained.
- In the model, the basement faults bounding the P-C grabens were considered continuous into the Mesozoic sequence. This assumption favours in the model the migration of the hydrocarbons generated by the Permian and Carboniferous source rocks into the foreland basin, which could not be the case if these faults are not continuing. Thus, by this option, the formation of reservoirs in the Mesozoic and Cenozoic units would be less relevant.
- The seal (Keuper unit) is less efficient than what is calculated by the model. In the Treyçovagnes-1 area, the presence of a thrust plane makes it plausible that the entire stratigraphic section is pervasively fractured, including the Keuper unit, which has probably also an important brittle component. Indeed, anhydrites and evaporites are interlayered also with dolomite, shales and thin sandstone layers. In the Noville-1 area, the model simulates the formation of a large reservoir at the top of the basement anticline. The Noville-1 well is located at the edge of this anticline. The seal properties at the top of the entire anticline were extrapolated from what was described for the Keuper unit in the Noville-1 well. Therefore, the real composition and integrity of the entire structure is unknown. Leakage is possible, which could considerably reduce the size of this reservoir simulated by the model.
- More efficient lateral traps than what is crossed by the modelled section can be present. In this case, hydrocarbons could migrate and accumulate in the closest reservoirs, which would not be penetrated by the wells.

Well	Hydrocarbon finding	Modelling results	Discrepancy causes
Treyçovagnes-1	• Oil traces in the Rhetian unit (Upper Triassic); • Gas flow in the fractures of the Buntsandstein and Muschelkalk units.	• Large gas accumulation in the Buntsandstein and Muschelkalk units; • Vertical gas migration paths close to the well; • Oil traces along a fault close to the well, crossing the entire stratigraphy.	• Permo-Carboniferous source rocks thickness and properties overestimated • The deep Permo-Carboniferous faults do not continue into the Mesozoic sequence • Seal fractured • Lateral migration
Essertines-1	• Oil traces in the Lower Cretaceous and Rhetian (Upper Triassic) units; • Gas shows in the Muschelkalk and Buntsandstein units.	• Gas accumulation in the Buntsandstein and Muschelkalk units; • Oil traces along the fault crossed by the well in the Malm, Cretaceous and Molasse units; • Vertical gas migration paths close to the well.	• Permo-Carboniferous source rocks thickness and properties overestimated • Seal fractured

Well	Hydrocarbon finding	Modelling results	Discrepancy causes
Eclépens-1	• Oil traces in the Dogger and Lias units; • Gas shows in the Lias and Keuper units.	Out of the model area	Out of the model area
Chapelle-1	• Oil traces in fractures of the Lower Cretaceous unit.	• Vertical gas migration paths close to the well.	• Posidonia shale source rocks could be not present in the area
Savigny-1	• Oil traces in fractures of the Lower Cretaceous unit.	• No hydrocarbons accumulation	• Posidonia shale source rocks could be not present in the area
Noville-1	• Tight gas accumulation in the Permo-Carboniferous rocks.	• Very large gas and oil accumulation in the Permian and Muschelkalk units.	• Permo-Carboniferous source rocks thickness and properties overestimated • Seal fractured • Lateral migration

Table 20: Comparison between the hydrocarbon findings in the wells located close to the section trace and the modelling results. In case of discrepancy, the potential causes are indicated.

3.1.4 Uncertainties

The petroleum system model presented herein estimates the thermal maturity of the potential source rock, the type and amount of hydrocarbon generated and the potential areas where hydrocarbon can be accumulated and/or circulated. However, because of the several uncertain data and assumptions made in constructing the model, uncertainties in the results must be considered. The most uncertain parameters controlling the modelling results are listed in Table 21. A synthesis of the decision process carried out to handle the presented uncertainties is shown in Fig. 35.

Parameter	Uncertainty	Cause	Options/Scenarios	Effect on the Petroleum System Evolution	Impact	Potential improvements
Geometry of the basin	Horizons geometry, depth, and stratigraphic units' presence, especially in the southern part of the section (Noville-1 area)	Few deep wells to corroborate the seismic data. The southern part of the section (Noville-1 well area) is not included in the GeoMol project.	GeoMol 2021 Geoform, 2010 Marchant et al., 2016	Accumulation and migration areas under or over-estimated; Location and thickness of the source rocks can be different.	Medium/High	Acquisition of new 2D and 3D seismic and/or reprocessing of the existent geophysical data.
Faults	Faults location, extension, geometry	Low-resolution seismic data.	GeoMol 2021; Geoform, 2010 Marchant et al., 2016 Sommaruga et al. (2012) Greber et al. (2007)	The hydrocarbon migration can be different from what is simulated by the model.	Medium/High	Acquisition of new 2D and 3D seismic and/or reprocessing of the existent geophysical data.
	Faults connectivity and cementation state	Scarce direct measurements on faults and few description in the well reports.	Faults open (not cemented) Faults close (cemented)	The volume of hydrocarbon migrated and accumulated simulated by the model can be different.	Medium	Sampling fault cement; Monitoring fluids flow.
	Continuity of the basement faults bounding the P-C grabens into the Mesozoic and Cenozoic infill	Low seismic resolution.	Yes No	Hydrocarbon migration from the Permian and Carboniferous source rocks to the Mesozoic and Cenozoic deposits cannot be properly evaluated.	High	Acquisition of new 2D and 3D seismic and/or reprocessing of the existent geophysical data. Improving the understanding of the structural model of the basin.

Parameter	Uncertainty	Cause	Options/Scenarios	Effect on the Petroleum System Evolution	Impact	Potential improvements
Facies	Facies definition	Data are available only where deep wells are present. Facies were extrapolated along the section from these points; Facies are deduced from qualitative descriptions in the well report, there are no quantitative data.	Facies extrapolated only from the wells located along the transect.	Hydrocarbon migration paths and/or accumulations can be over or under-estimated.	Medium/High	Acquisition of new stratigraphic, petrographic and geochemical data of the basin infill.
			Facies extrapolated also from the wells located at an offset of nearly 7 km from the transect.			
	Facies distribution	Because of the complexity of the geological model used for modelling, it is hard to reproduce lateral facies variation in the same stratigraphic unit.	Lateral facies variation in the same stratigraphic unit is reproduced.	Lateral porosity and permeability variation can be hardly reproduced.	Medium/Low	Software improvements.
			Unique average facies are assigned for the same stratigraphic unit.			
Structural evolution	Restoration structural model	An accurate and detailed structural model strongly increases the complexity and difficulties of the thermal modelling reconstruction.	Simplified structural model	The timing of the structural trap formation and the maximum burial in the thrusted area can be unprecise.	Medium/Low	Reconstruction of a more accurate structural model; Improvement of the thermal modelling software.
			Complex and detailed structural model.			
	Magnitude of thrusting	Scarce stratigraphic reference in the thrusted area.	A representative shortening of 10 km is represented in the restored section.	The effect of thrusting on the thermal maturation process can be under or over-estimated in the southern part of the section.	Medium/Low	Reconstruction of a more accurate structural model; Acquisition of new %Ro and AFT data.
			Carry out a detailed study to calculate the shortening in the areas.			

Parameter	Uncertainty	Cause	Options/Scenarios	Effect on the Petroleum System Evolution	Impact	Potential improvements
Structural evolution	Timing of thrusting and erosion magnitude in this area	Scarce data dating the thrusting and able to calibrate the magnitude of the erosion in the thrusted area.	Thrusting starts at 10 Ma, after the deposition of the uppermost Molasse units.	Maturity and the timing of traps formation can be different in the southern part of the section.	Medium	Acquisition of new %Ro data; Reconstruction of a more accurate structural model.
			Thrusting starts coevally with the deposition of the uppermost Molasse units.			
Erosion	The magnitude of the erosion	The magnitude of the erosion cannot be measured directly, it can be only estimated by indirect data (%Ro, AFT, etc..).	Values estimated in the literature.	Burial, thus maturity, of the source rocks can be different.	Medium/High	Acquisition of more %Ro data along the section.
			Values estimated in the most recent literature, modified in order to calibrate the %Ro data.			
	Timing of the erosion	Difficulty in dating different erosion events.	Literature data.	The timing of the hydrocarbon generation can be different.	Medium	Acquisition of AFT data along the section.
Boundary conditions	Present-day heat flow	The heat flow values measured today do not calibrate correctly the present-day temperature data.	Assigning lower present-day heat flow values than what estimated in the literature.	None.	None	None
			Do not include in the simulation the radiogenic heat produced by the rock.			
	Paleo-heat flow	The paleo heat flow over the basin evolution cannot be measured directly, it can be only estimated.	Heat flow trend proposed in the literature.	The timing of the hydrocarbon generation can be different.	Medium/High	Reconstruction of the crustal model, in order to improve the estimates of the paleo-heat flow.
			Heat flow trend proposed in the literature, with peak values modified in order to calibrate the %Ro values.			

Parameter	Uncertainty	Cause	Options/Scenarios	Effect on the Petroleum System Evolution	Impact	Potential improvements
Permian and Carboniferous source rocks	Presence and geometry of the Permo-Carboniferous grabens along the entire section	Low seismic resolution.	Leu (2008) Geoform, 2010 Sommaruga et al. (2012) Greber et al., 2007	Potential presence of deep hydrocarbon source rocks.	High	Acquisition of new 2D and 3D seismic and/or reprocessing of the existent geophysical data.
	Presence, distribution and thickness of deposits rich in organic matter in the Permo-Carboniferous grabens	In the southern part of the section it is unknown the thickness of the Carboniferous source rock. In the northern-central part, it is unknown the presence of both Permian and Carboniferous source rocks.	Not present where they have not been identified Source rocks are present in all grabens with a thickness similar to what found in the Weiach-1 well.	Generation of a large/smaller volume of hydrocarbons from deep source rocks, which can migrate to the shallower units.	High	Acquisition of new geophysical data (seismic, deep wells); Penetrating these deposits along their entire thickness.
	The hydrocarbon potential of the source rocks	No direct data were measured along the section.	Source rocks geochemical data are extrapolated from the Weiach-1 well.	The volume of hydrocarbon generated can be different.	High	Geochemical and petrographic analyses of the Autunian (Permian) levels in the Noville-1 well; Penetrating the entire extension of these deposits along the section and direct measurement of the geochemical parameters.
Posidonia shale source rock	Presence of the Posidonia shale source rock	Data is available only in the northern part of the section, with no data in the central part.	Present only in the northern part of the section. Present in the northern and central parts (5 meters).	Generation, migration and accumulation of more hydrocarbon.	High/Medium	Acquisition of more data in the Liassic interval, especially in the central part of the section, where there are no data.

Parameter	Uncertainty	Cause	Options/Scenarios	Effect on the Petroleum System Evolution	Impact	Potential improvements
Posidonia shale source rock	The hydrocarbon potential of the source rock	Data available only for the Treyçovagnes-1, Eclépens-1 and Essertines-1 wells.	Extrapolated from the Northern Switzerland and the Canton of Vaud areas.	The volume of hydrocarbon generated can be different		
Calibration of the model	Porosity data	Data are available only for a few wells along the section.	Use of only the available data measured along the section	Along the section, getting far from the wells used for calibration, the porosity can be different from what is simulated, especially in the case of carbonate units. Thus, hydrocarbon migration and accumulations could be different.	Medium	Acquisition of more porosity data along the section.
			Use also of data measured in wells located at nearly 7 km from the section trace line.			
	Porosity calibration	The porosity reduction by the diagenetic process cannot be properly simulated by the software.	Modify the initial porosity of the facies in the lithology library of the software.	Reservoir properties can be different from what is simulated by the model.	Medium	Find a proper way to change in the software the porosity because of diagenetic processes and/or other process
	Present-day temperature data	Data are available only for a few wells along the section.	Use only the available data along the section.	The present-day temperature can be different from what is simulated, getting far from the wells where calibration data are available.	Low	Acquisition of more borehole temperature data along the section.
			Use also data measured in wells located at 30 km from the section trace line.			

Parameter	Uncertainty	Cause	Options/Scenarios	Effect on the Petroleum System Evolution	Impact	Potential improvements
Calibration of the model	Thermal maturity calibration	The exact calibration of the %Ro data along the entire stratigraphic section is hard to be achieved. Literature %Ro data have not been homogenously measured.	Achievement of a widely acceptable calibration along the entire section.	At some points in the section, the thermal maturity calculated can be slightly imprecise.	Low	Acquisition of new %Ro along the section. Improve the estimate of the erosion magnitude along the section, by implementing other paleotemperature data (AFT, etc…).
			Acquisition of more precise calibration data for all the wells located along the section.			
	Reconstruction of the thermal maturity along the section	Mistakes in the calculation of the thermal maturity in some cells of the model.	Acceptance of small mistakes in the model.	Thermal maturity is erroneously calculated at some specific point of the model.	Low	Software improvement.
			Looking for a different way to build the model up to solve the problematic.			

Table 21: List of the uncertainties parameters for the Section 2 model, their causes and their impact on the petroleum system modelling results. The options/scenarios available are indicated. In green is highlighted the option chosen in this study to build the petroleum system modelling. Potential improvements and actions to mitigate these uncertainties are suggested

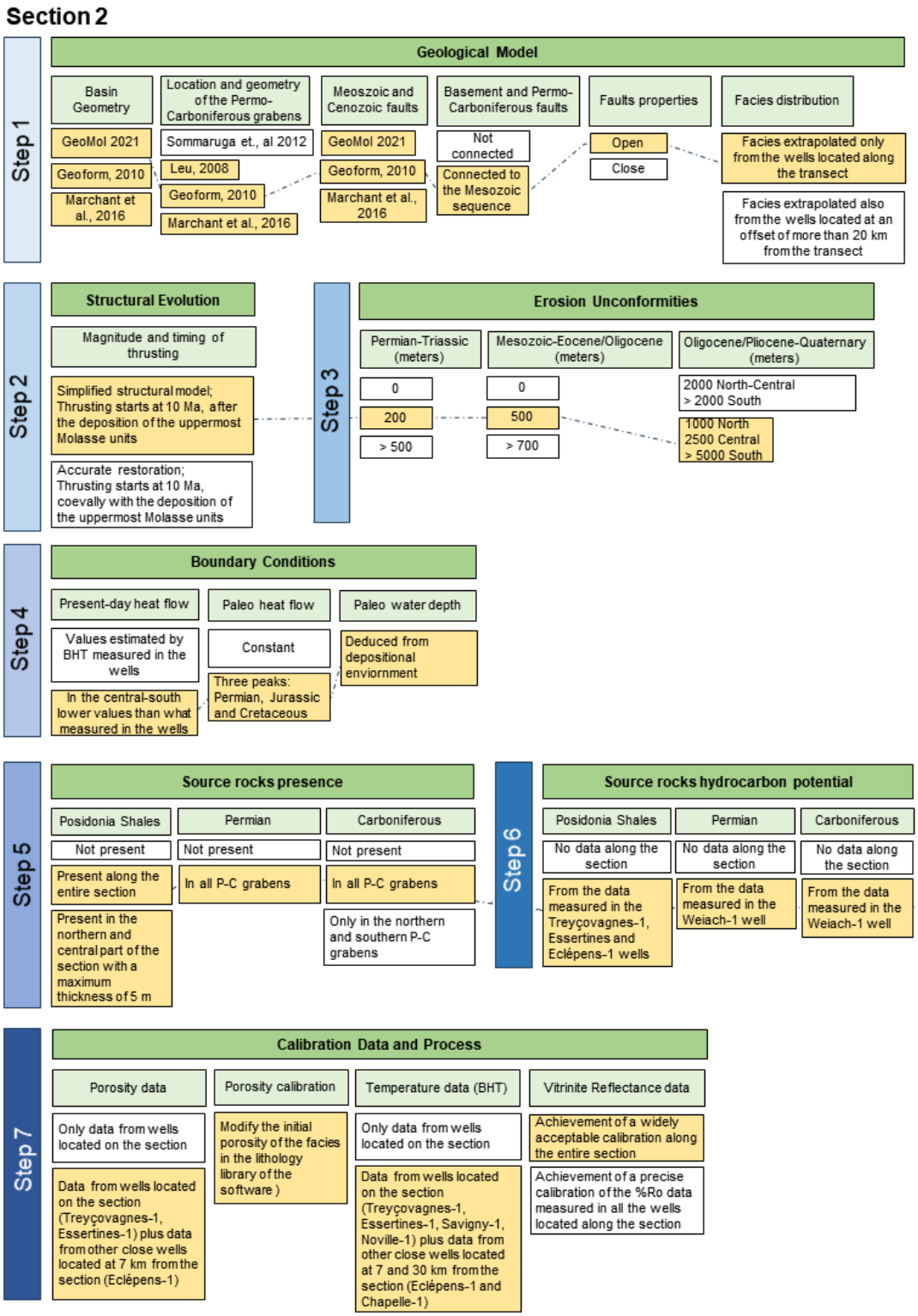


Fig. 35: Petroleum system modelling was built by selecting the specific combination of parameters, which are critical in controlling the thermal evolution of the basin and the hydrocarbon generation, migration and accumulation processes. In yellow are indicated the options chosen in this work

3.2 Petroleum System Modelling - Section 3

3.2.1 Data

3.2.1.1 Geological Model

Section 3 is extracted from the GeoMol project, along a section line passing through the Canton of Bern (Fig. 36). The trace of the section is NNW-SSE oriented, with the following extremity coordinates: NNW edge x, y: 2581340.5; 1221543.8 SSE edge x, y: 2613212.9; 1174253.1 (Reference coordinate System CH1903+ / LV95), and a total length of 56 km. The extracted section represents the present-day geological structure of the NAFB in the area, represented by a southern dipping foreland wedge, filled by the Cenozoic Molasse units, and its Mesozoic substratum (Fig. 37). The foreland basin is delimited to the north by the Jura Mountain Chain, where the Mesozoic strata outcrop, and to the South by the more external Subalpine thrusts, where the folded subalpine Molasse is exhumed. The erosional topographic surface cut the uppermost Molasse units. The location and geometry of the Permo-Carboniferous graben were deduced by Leu (2008) along most of the section (Fig. 37). In this section, the types of faults, as classified in the GeoMol database, are differentiated.

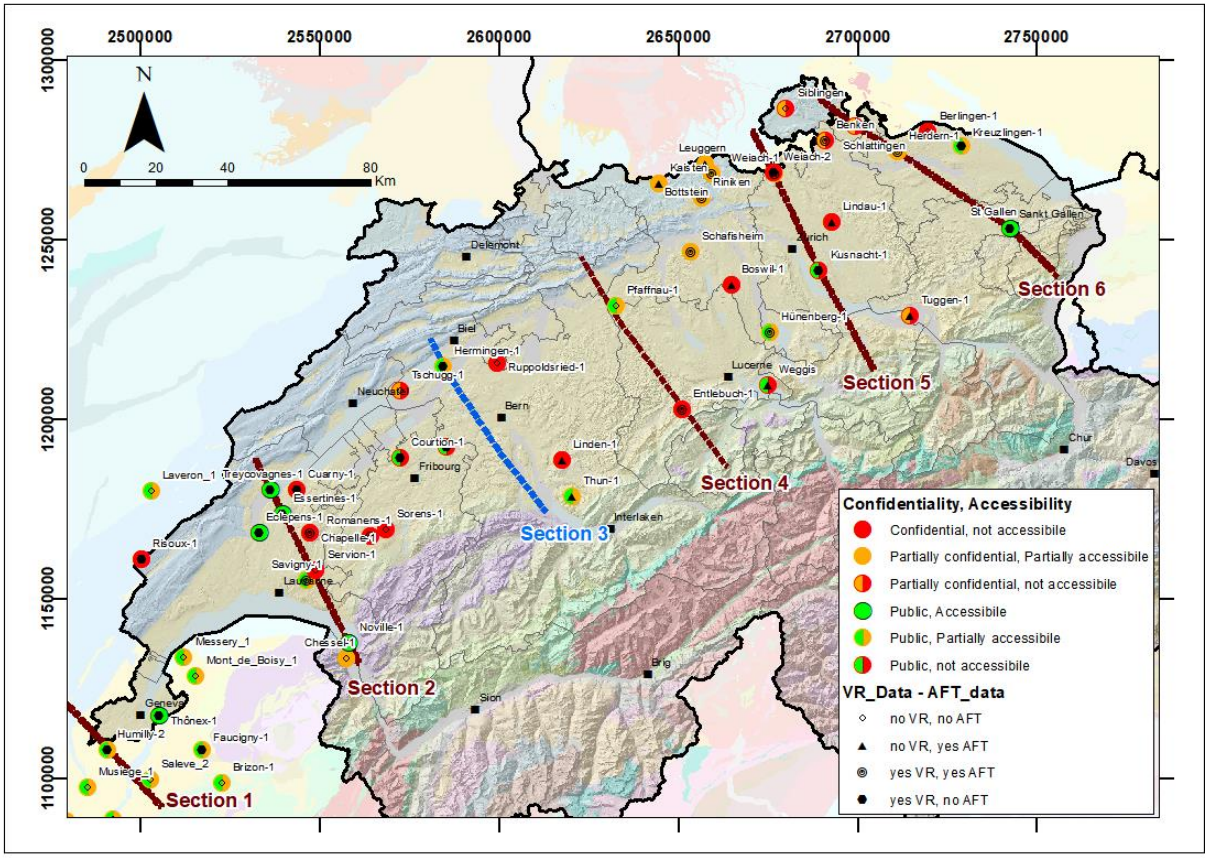


Fig. 36: Location of the Section 3. Confidentiality and accessibility status updated on June 2023

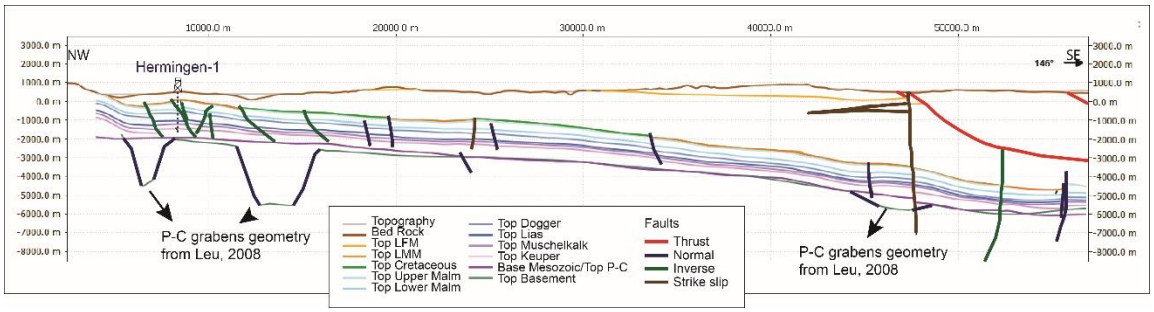


Fig. 37: Horizons and faults extracted from Geomol at the Section 3 trace location. The Permo-Carboniferou (P-C) graben geometry has been extrapolated from what was proposed by Leu (2008). The well intersecting the section trace is shown. In this section, the type of faults is differentiated, as classified in the GeoMol database.

3.2.1.2 Wells

Section 3 passes on the top of the Hermrigen-1 well and is relatively close to the following wells: Thun-1 (8 km ENE of the section trace), Linden-1 (12 km ENE of the section trace), Ruppoldsried-1 (13 km NW of the section trace) and Tschugg-1 (14 km SW of the section trace). For these wells, the availability of the most relevant data necessary for thermal modelling is summarized in Table 22. The stratigraphic logs of these wells are shown in Appendix 4. The wells Courtion-1 and Fendringen-1 (located respectively at 10 and 20 km from the section trace) were not considered, as no data are available for these wells.

Well	Distance from section (km)	Status	Well report	Stratigraphic log	Calibration data	Rock-Eval data
Hermrigen-1	0	Public; Partially accessible	No	Yes	Phi, T, VR, TAI	Yes
Thun-1	8	Public; Partially accessible	Yes	Yes	Phi, T, AFT, TAI	Yes
Courtion-1	10	Public, Not accessible	No	No	No	No
Linden-1	12	Confidential	No	Yes	T, AFT	No
Ruppoldsried-1	13	Confidential	No	Yes	T	No
Tschugg-1	14	Partially confidential, not accessible	No	Yes	T	No
Fendringen-1	20	Public, Not accessible	No	No	No	No

Table 22: wells closest to the Section 3 trace and availability of the most relevant data needed for thermal modelling. Thermal data: (T) temperature; (VR) vitrinite reflectance; (TAI) thermal alteration index; (AFT) apatite fission tracks.

3.2.1.3 Deposition and erosional events

The burial history of the studied area is defined by a sequence of depositional and erosional events and their ages. Thus, in the model, an age for each stratigraphic unit and the main erosional event was assigned (Table 23).

Age top unit (Ma)	Unit	Event	Facies
0	Quaternary	Deposition	Quaternary
4	Erosion Pliocene-Quaternary	Erosion	
7.24	UFM	Deposition	UFM
15.97	UMM	Deposition	UMM
20.44	LFM	Deposition	LFM-North; LFM-South; LFM-mix; LFM-Thrust

Age top unit (Ma)	Unit	Event	Facies
28	LMM	Deposition	LMM
33	Hiatus Cret/Eocene	Hiatus	
86	Erosion Cretaceous	Erosion	
113	Cretaceous	Deposition	Cretaceous
145	Upper Malm	Deposition	Upper Malm
157.3	Lower Malm	Deposition	Lower Malm
163.5	Dogger	Deposition	Dogger
174.1	Lias	Deposition	Lias-North; Lias-South; Posidonia shale
201.3	Keuper	Deposition	Keuper-North; Keuper-South; Gypskeuper-North; Gypskeuper-South
237	Muschelkalk	Deposition	Muschelkalk; Muschelkalk-Salt
252	Hiatus Perm-Triassic	Hiatus	
259	Erosion Perm-Triassic	Erosion	
265	Permian	Deposition	Permian Verrucano; Permian Lower; Permian-Source rock (SR)
284	Carboniferous	Deposition	Carboniferous; Carboniferous-Source rock (SR)
323	Hiatus/erosion pre-Carbon		
400	Basement	Deposition	Basement

Table 23: Depositional and erosional events defined in the thermal model. A facies is assigned to each layer. UFM upper freshwater Molasse; UMM upper marine Molasse; LFM lower freshwater Molasse; LMM lower marine Molasse

In the case of the Permian-Triassic and Mesozoic-Eocene unconformities, no data are available to constrain the magnitude of the erosional events in the studied area. Thus, erosional trends, previously reconstructed at a regional scale and/or for other areas of the basin close to the Section 3 trace line, were extrapolated for the entire section (Table 24). An average of 200 meters was assigned at the Permian-Triassic unconformity and 700 meters at the Mesozoic-Eocene unconformity. For the Pliocene-Quaternary unconformity, more constraints are available. In Cederbom et al. (2011), using AFT data, an erosion of 900 meters and 1300 meters, with a bar of error of ± 500 meters, was estimated in the Thun-1 and Linden-1 wells respectively. In the Canton of Vaud area, using 1D and 2D thermal modelling, it was estimated an erosion magnitude ranging from 800 to 1400 meters (Schegg et al., 1997; Omodeo-salé and Moscariello, 2019). Therefore, for this unconformity, an erosion thickness from 1200 in the north to 1800 meters in the south was initially considered in the model. These values were subsequently tested and constrained by the thermal modelling workflow proposed herein (see the Calibration result section).

Erosion unconformity	Amount of erosion estimated in previous studies (m)	Method	NAFB study area	Source
Quaternary-Pliocene	900 and 1300	AFT	Thun-1 and Linden-1 wells	Cederbom et al., 2011
	800-1400	VR, 1D and 2D thermal modelling	Canton of Vaud area	Schegg et al., 1997; Omodeo-Salé and Moscariello 2019
Mesozoic-Eocene	0	stratigraphy	Regional	Todorov et al., 1993; Burkhard and Sommaruga, 1998; Wildi et al., 1989; Lemcke, 1988
	500		NW sector	Omodeo-Salé and Moscariello 2019
	1000-1800	VR, clays, porosity, among others	Regional	Schegg and Leu, 1998

Erosion unconformity	Amount of erosion estimated in previous studies (m)	Method	NAFB study area	Source
Permian-Triassic				
	200	VR, 1D thermal modelling	Weiach-1 well (NE sector	Omdeo-Salé et al., 2021
	1000	VR, stratigraphy	Weiach-1 well (NE sector)	(Diebold, 1988; Schegg and Leu, 1998)

Table 24: Erosion magnitude estimated in previous studies for the three main erosional unconformities at a regional scale and/or in areas close to the section 3 trace line.

3.2.1.4 Facies

Facies were assigned to the stratigraphic units composing the section by extrapolating the lithologic data described in the well reports of the following wells: Hermrigen-1, Tschugg-1 Ruppoldsried-1, Linden-1 and Thun-1. For these wells, the lithologies for each unit, expressed in percentage, are listed in Appendix 5. For each unit a unique or various facies were assigned along the section, depending first on the variability of the facies and secondly on the availability of data (Table 25). Generally, for the shallower units (Molasse) more data are available than for the deeper units (Triassic, Permo-Carboniferous), as only a few wells have been drilled deep enough to reach them.

Unit	Cgl	Sdt	Slst	Shl	Lmt	Mrl	Dlm	Anhd	Halt	Coal	Reference Well
Quaternary		80		20							Various
UFM		20		20		60					Kusnacht-1
UMM	40	40		20							Linden-1 (modified)
LFM Thrust	40	40		20							Thun-1
LFM South		80		20							Hermrigen-1; Ruppoldsdried-1
LFM North		20		60		20					Thun-1; Linden-1
LFM mix		40		20		40					Mix
LMM		10		10		80					Tschugg-1
Cretaceous					80	20					Hermrigen-1; Tschugg-1
Upper Malm					100						Hermrigen-1; Ruppolsdried-1; Linden-1; Thun-1
Lower Malm					100						Hermrigen-1; Linden-1; Thun-1
Dogger				10	70	20					Hermrigen-1; Linden-1; Thun-1
Lias North		5		20	75						Hermrigen-1
Lias South		50		20	30						Linden-1; Thun-1
Posidonia Sh				100							Hermrigen-1
Keuper North				20			40	40			Hermrigen-1
GypsKeuper North				20				78	2		Hermrigen-1
Keuper South				35			5	60			Linden-1
GypsKeuper South				20			5	70	5		Linden-1
Muschelkalk		20			20		60				Hermrigen-1 (modified)
Muschelkalk Salt								5	95		Hermrigen-1
Permian Verrucano	8	72		20							Noville-1; Weiach-1

Unit	Cgl	Sdt	Slst	Shl	Lmt	Mrl	Dlm	Anhd	Halt	Coal	Reference Well
Permian Lower		20	40	40							Noville-1; Weiach-1
Permian SR											Noville-1; Weiach-1
Carboniferous		40	40	40							Weiach-1; Noville-1
Carbonif. SR1										100	Weiach-1
Carbonif. SR2				100							Weiach-1
Basement	Gneiss										Various

Table 25: Facies, expressed as a percentage of lithological composition, assigned into the model to the stratigraphic units forming the basin infill of section 3. The wells used as references are indicated. Cgl: conglomerate; Sdt: sandstone; Slst: siltstone; Shl: shale; Lmt: limestone; Mrl: marl; Dlm: dolomite; Anhd: anhydrite; Halt: halite; coal: coal.

3.2.1.5 Calibration data

Porosity data are available for the Hermrigen-1 and Thun-1 wells (Appendix 6) and they were used to calibrate the facies mechanical compaction properties along the section. Borehole temperature data (BHT) are available for the Hermrigen-1, Linden-1, Ruppolsried-1 and Thun-1 wells and they were used to calibrate the present-day temperature over depth in the basin infill (Appendix 7).
In the Section 3 area, very few paleothermal data are available to calibrate the thermal conditions attained during the evolution of the basin. These data consist of organic matter indices for the Hermrigen-1 and Thun-1 wells (Elf Aquitaine, 1989a, 1983; Leu, 2007) (Appendix 8).
The estimate of the Pliocene-Quaternary erosion deduced by AFT data for Linden-1 and Thun-1 wells (Cederbom et al., 2011, see Erosion section above) was used to constrain the erosion variable, despite of that these data cannot be directly used to calibrate the thermal model results. In Elf-Aquitaine studies, the thermal conditions of the rocks penetrated by these wells were determined by the TAI (thermal alteration index, colour of palynofacies in transmitted light). At that time, direct %Ro measurements were not carried out, most likely because of that the material was not enough and/or well preserved or because the laboratory did not dispose of the needed equipment and/or expertise to perform this analysis. In the present study the TAI values performed by Elf Aquitaine were converted in %Ro equivalent by applying the equivalence proposed in the literature (Taylor et al., 1998). In 2007, Stratochem provided a series of %Ro data for the Dogger unit (Leu, 2007) (Appendix 8).

3.2.1.6 Source rock parameters

According to the rest of the NAFB, three main source rocks are considered: the marine Posidonia Black Shales (Toarcian in age), the lacustrine Autunian shales (Permian in age), and the Carboniferous coal and shales (Carboniferous in age) (Leu and Gautschi, 2014; Misch et al., 2017; Schegg and Leu, 1998). In the Section 3 area there is very scarce direct data able to characterise these source rocks, as very few wells attained the Toarcian deposits (Hermrigen-1; Linden-1 and partially in Thun-1) and none of the Permo-Carboniferous units. In the Hermrigen-1 well, TOC has been measured for a set of samples representative of the entire Mesozoic units (from the Malm to the Muschelkalk) (Appendix 9) (Elf Aquitaine, 1983). Data indicate a low content of organic matter (TOC < 1%) for the entire sequence. By this geochemical study, only a few levels from the Lias and Triassic units have a certain hydrocarbon potential, however, neither stratigraphic unit can be considered a good source rock. Similarly, very low TOC (< 0.5%) has been measured for a set of Upper and Middle Jurassic samples in the Thun-1 well (Appendix 9) (Elf Aquitaine, 1989a). Unfortunately, in this well no measurements have been carried out for the Toarcian rocks. Furthermore, it is important to note that, in both wells, most of the samples measured were limestone, and lithology was generally poor in organic matter.

To assign the initial petroleum potential of the defined source rocks in the model for the Section 3 area, literature data throughout the entire NAFB were mostly used, due to the scarce and not fully representative acquired data. For the Posidonia shale geochemical data were extrapolated from what was measured in the Canton of Vaud area (Appendix 1). For the Permian and Carboniferous

source rocks, data were extrapolated from the Northern Switzerland area (Weiach-1 well) (Ajuaba et al., 2023). The thickness assigned to these source rocks was also extrapolated from other sectors of the basin where this data is well documented. For the Posidonia shale, by interpolating the data of the surrounding wells, an average thickness of 4 meters is considered along the studied section.

Along Section 3 there are no data about the nature of the Permo-Carboniferous grabens infill. Therefore, the internal subdivision of these deposits was extrapolated from the well-known Constance Frick Permo-Carboniferous graben (Northern Switzerland) (Madritsch et al., 2018), and regarding the source rocks geochemically properties, specifically from the Weiach-1 well (Ajuaba et al., 2023). Therefore, first, the infill of the grabens was subdivided into two units, the Permian (33% of the total thickness) and the Carboniferous (67% of the total thickness). Secondly, in the Permian, for the Autunian lacustrine shales an interbedded layer, with a thickness of 9% of the total Permian unit, was created (maximum thickness of 76 meters). For the two Carboniferous source rocks considered (coal and shales) two interbedded layers were created, with a total thickness of 9% of the total Carboniferous unit (maximum thickness of each unit, 100 meters). The initial organic geochemical data assigned in the model to the four source rocks are shown in Table 26.

Source Rock	Lithology	Present average TOC (%)	Initial TOC (g rock)	Present average HI (mgHC/TOC)	Initial HI (mgHC/g rock)	Kinetic
Posidonia shale	Black shales	2	4	380	500	TII(PB) (Behar et al., 1997)
Permian lacustrine shales	Shale organic rich	4.7	6.2	289	500	TI(C) (Pepper and Corvi, 1995)
Carboniferous coal	Coal	72	75	210	250	TIII-(Dogger) (Behar et al., 1997)
Carboniferous shales	Shale organic-rich	8	8.5	95	150	TIIIH(DE) (Pepper and Corvi, 1995)

Table 26: Initial geochemical properties of the four source rocks assigned to the model.

3.2.2 Boundary conditions

The upper boundary condition, the sediment-water interface temperature (SWIT), was automatically calculated by the software, for a geographical area located at a latitude of 46°N (present Switzerland latitude) (Fig. 12). The paleowater depth was deduced by the depositional environment of the main stratigraphic units forming the basin and the basal heat flow trend was reconstructed considering the geodynamic evolution of the Molasse Foreland Basin (see Methods section) (Table 27).

Age to (Ma)	PWD (m)	Age from (Ma)	HF value (mW/m2)
0	0	0	60-80*
22	0	0.4	50
66	300	8	50
125	100	29	50
152	10	56	50
160	300	186	60
163.5	100	113	75
174.0	300	142	65
190	100	146	75
201.3	70	172	60
252	0	200	60

Age to (Ma)	PWD (m)	Age from (Ma)	HF value (mW/m2)
265	0	250	60
298	0	265	87
		273	110
		293	90
		318	64
		350	60
		500	60

Table 27: Paleowater depth (PWD) and basal heat flow variation over the time. (*) At the present day (0 My) a variation of the basal heat flow along the section was considered, based on the present heat flow distribution calculated throughout the NAFB (see Fig. 15).

At the present day (0 My) a variation of the basal heat flow along the section was considered (Fig. 38), based on the present heat flow distribution calculated throughout the NAFB (data source: https://map.geo.admin.ch, see Fig. 15).

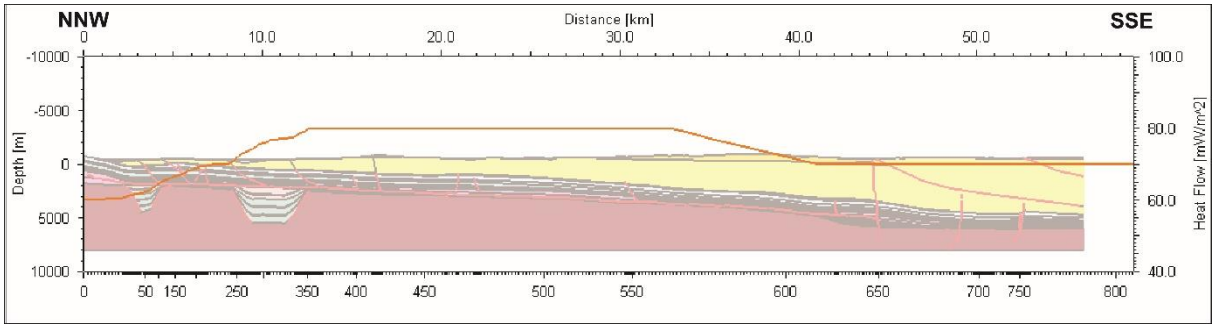


Fig. 38: Basal heat flow assigned along Section 3 at the present-day (0 My)

3.2.3 Results

3.2.3.1 Restoration to the pre-Alpine thrusting

Because of that, in Section 3 thrusts and inverted faults are present, it is essential to realize the structural restoration to the pre-Alpine thrusting. Thus, paleo sections representing the geometry of the basin during the thrusting, uplift and erosion processes were reconstructed, using the Move software. To simplify only four paleo-sections are presented below (Fig. 39). The magnitude of the Pliocene-Quaternary erosion was estimated considering previous literature data (see Erosion section above) and it ranges from 1200 in the north to 1800 meters in the south. The ages of these sections were defined by considering the structural and stratigraphic data of the area.

The paleosection t3 is the oldest and it represents the geometry of the NAFB, before the advance of the Alpine thrusts in the studied area. At this time the UMM was already deposited along the basin. An original average stratigraphic thickness of 1000 meters is considered for the UMM, coherently with what is observed in the rest of the basin (in the NAFB the maximum thickness of the UMM unit is nearly 1300 meters, 20-35 km from the studied section, just in front of the subalpine thrust, and it reaches 900 meters in the Linden-1 well). Because of that the depositional age of the UMM has been estimated as Burdigalian (20.44-15.97 Ma), this section is assigned to the age of 15 Ma.

In the paleosection t2, the most internal subalpine thrust was activated and the UFM was partially deposited along the northern and central part of the basin. It is excluded that the UFM unit was deposited on the top of the thrusted area, because it would result in a too-great thickness of the removed section concerning what was estimated by AFT data for this area: 900 meters of erosion

for the Thun-1 well and 1300 meters for the Linden-1 well, with a bar of error of ± 500 meters (Cederbom et al., 2011). Considering the subalpine thrust activity dating proposed by Von Hagke et al., (2012) (between 10 to 6-5 Ma) and the age of the UFM unit deposition (Langhian to Tortonian, 15.97-7.24 Ma) (Kuhlemann and Kempf, 2002), an age of 10 Ma was assigned to this section.
In the paleosection t1 also the most external Subalpine thrust is activated and the UFM is completely deposited in the central and northern parts of the basin. Considering the subalpine thrust activity dating proposed by Von Hagke et al., (2012) and the UFM unit deposition, the age of 6,5 Ma was assigned to this paleosection. The shortening in the Jura is estimated around 5-7 Ma (Burkhard, 1990; Philippe et al., 1996), thus the Jura deformation is considered contemporaneously or subsequently after this stage.
The uplift and erosion of the entire NAFB have been estimated around 4 to 5 Ma (Cederbom et al., 2011). The paleosection t0 represents the present-day geometry, where occurred both the Jura and Alpine deformation and the uplift and erosion of the basin.

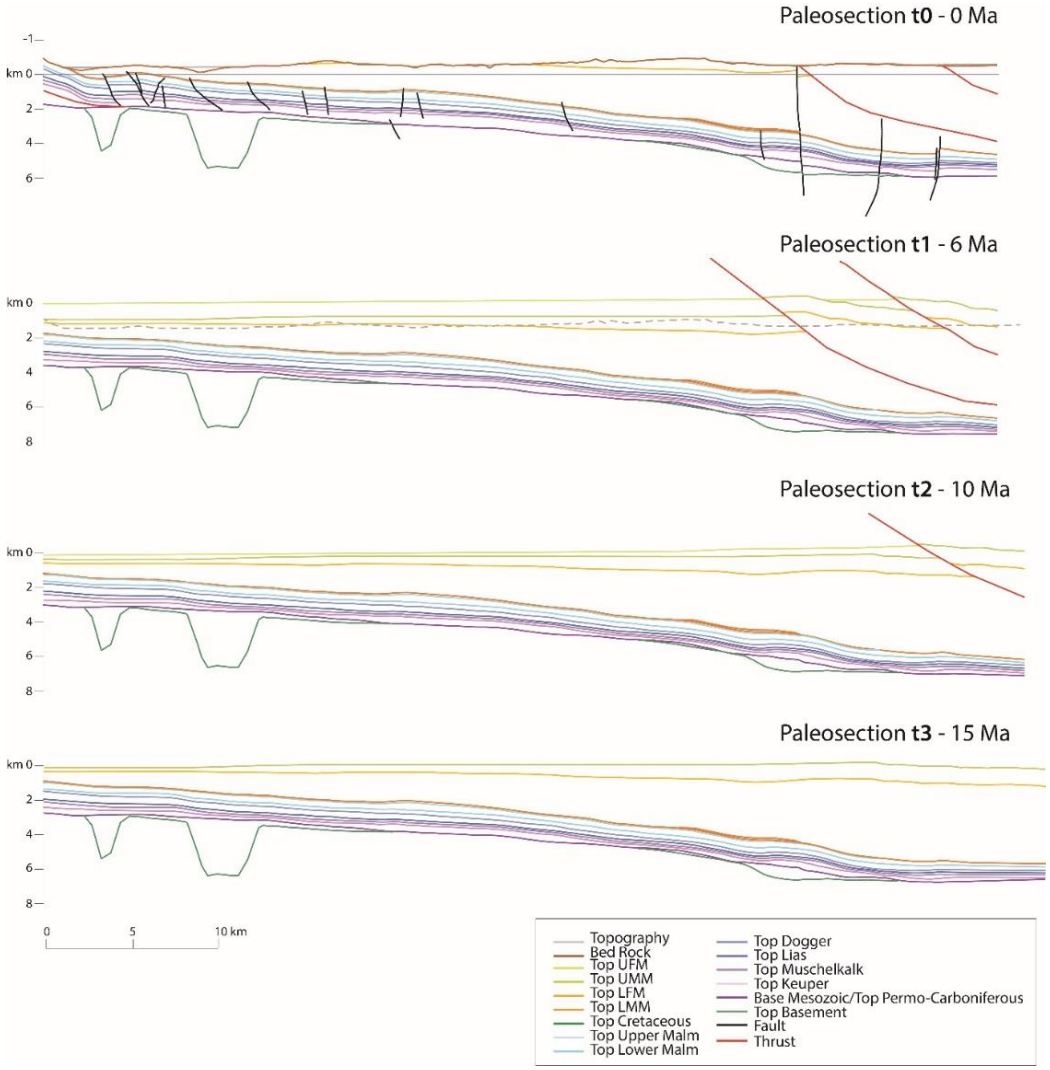


Fig. 39: Paleosections showing the structural and stratigraphic evolution of the area from the foreland infill phase before the thrusting (paleosection t3) to the following advance of the Alpine frontal thrusts in the area (paleosection t1 and t2) to the final present-day geometry, with the Jura Mountain formation and uplift and the erosion of the basin (paleosection t0).

3.2.3.2 Geological conceptual model evolution

The four paleosections, obtained as described above, were imported in the PetroMod software, by applying the TecLink workflow (see Methods section above) (Fig. 40). For each section, each

horizon was assigned to a stratigraphic unit and at a corresponding age (Table 23). The facies previously defined (Table 25) were assigned to the stratigraphic units composing the sections (Fig. 40). The paleosections define the geometry of the basin from the present-day to the phase previous to the Alpine thrusting.

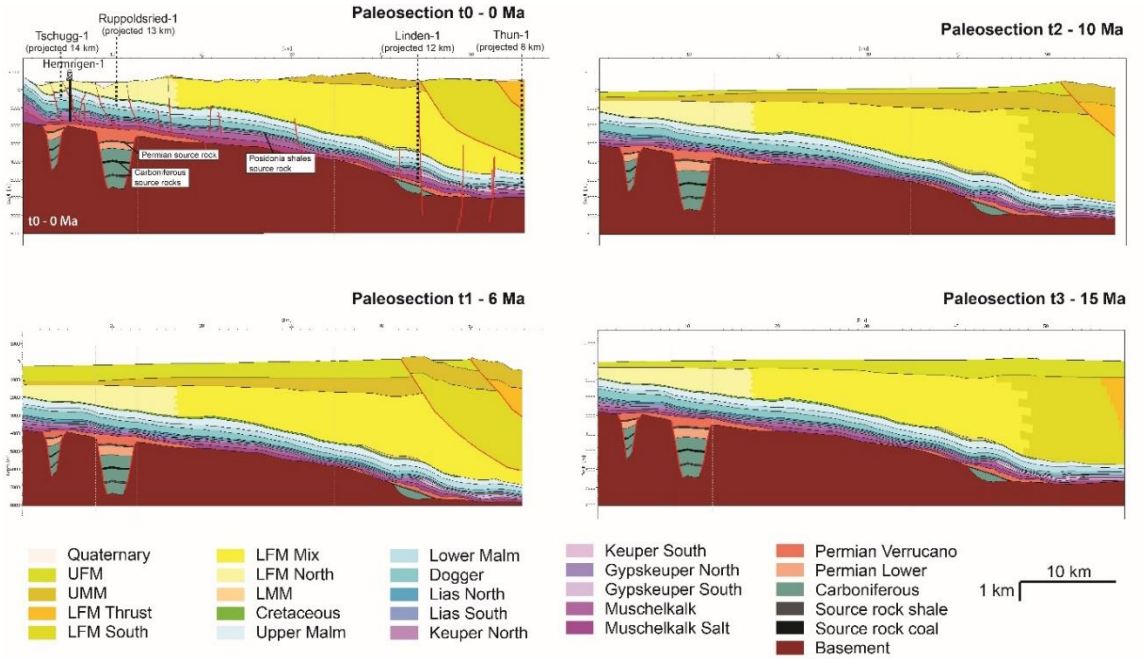


Fig. 40: Paleosections imported in Petromod and used as a geological model of the thrusting and erosion phases. Based on the stratigraphy described in the closest wells, facies were assigned to the present-day section and extrapolated to the other paleosections. Sections vertical exaggeration 2:1.

The restoration of the geometry at the end of the deposition of each of the previous stratigraphic units was automatically performed by the modelling software, which also takes into consideration the decompaction factor (Fig. 41). The thickness eroded during the Permian-Triassic and Cretaceous-Eocene unconformities was added as paleothickness of respectively 200 and 700 meters, assigned at the related periods (Table 23). The Pliocene-Quaternary erosion was estimated considering previous literature data (see Erosion section above) and it ranges from 1200 in the north to 1800 meters in the south.

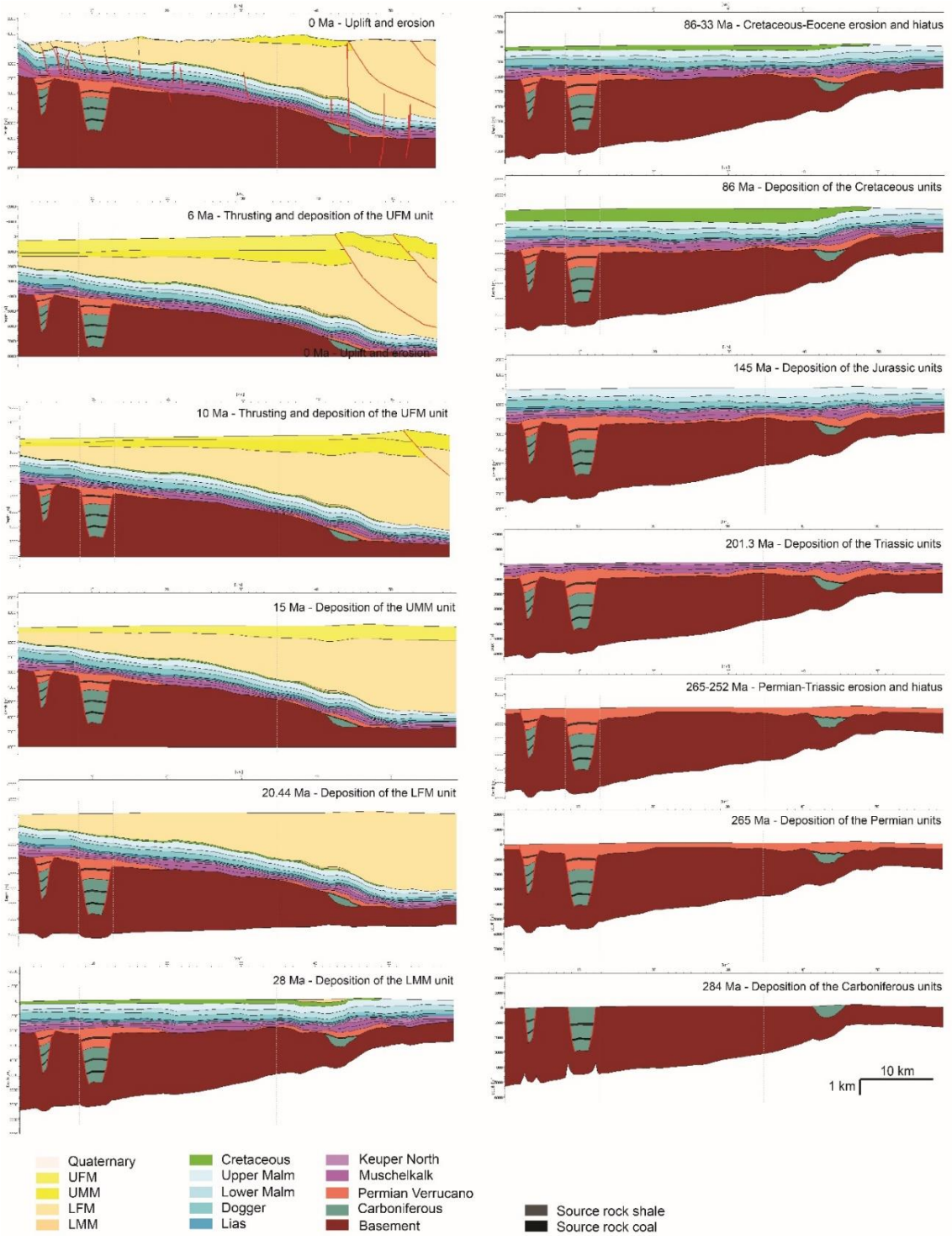


Fig. 41: Geological evolution of the studied area obtained in Petromod by retrodeformation and decompaction of the units forming the basin infill, from the present-day to the Carboniferous time. Sections vertical exaggeration 2:1.

3.2.3.3 Thermal Model Calibration

3.2.3.3.1 Porosity

The porosity was calibrated for the Hermrigen-1, and Thun-1 wells (Fig. 42) and the calibrated values were assigned along the entire section (Fig. 43). The mechanical compaction properties estimated by the software for the lithologies assigned to each stratigraphic unit, were iteratively changed up to fit the theoretical values calculated by the model with the porosity values measured

along the wells. The porosity of the uppermost Molasse units (UFM and UMM) was extrapolated from the values measured for the LFM in the Hermrigen-1 and Thun-1 wells.

The porosity extrapolation performed here along the section can be highly uncertain, especially, but not only, in the case of the dominant limestone units (Mesozoic), where the porosity and permeability are strictly controlled by diagenetic processes and fracking, which can dramatically change from one point to the other of the basin. To reduce this uncertainty, more porosity data with depth should be available along the section.

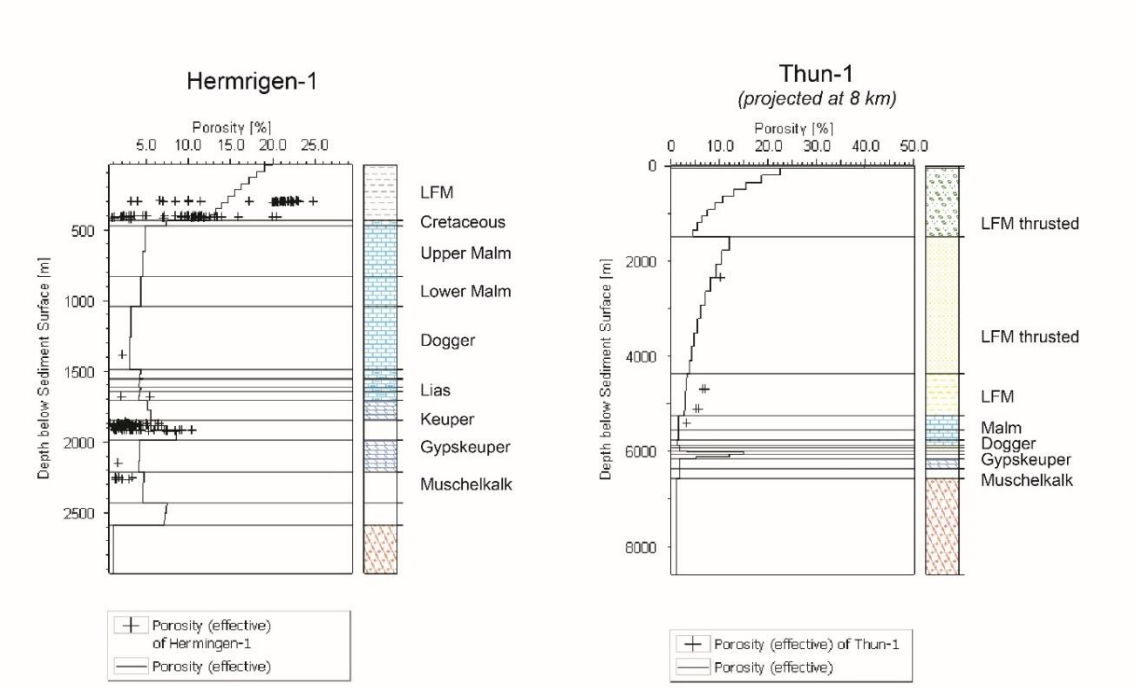


Fig. 42: Calibration of the porosity property with the data measured in the Hermrigen-1 and Thun-1 wells.

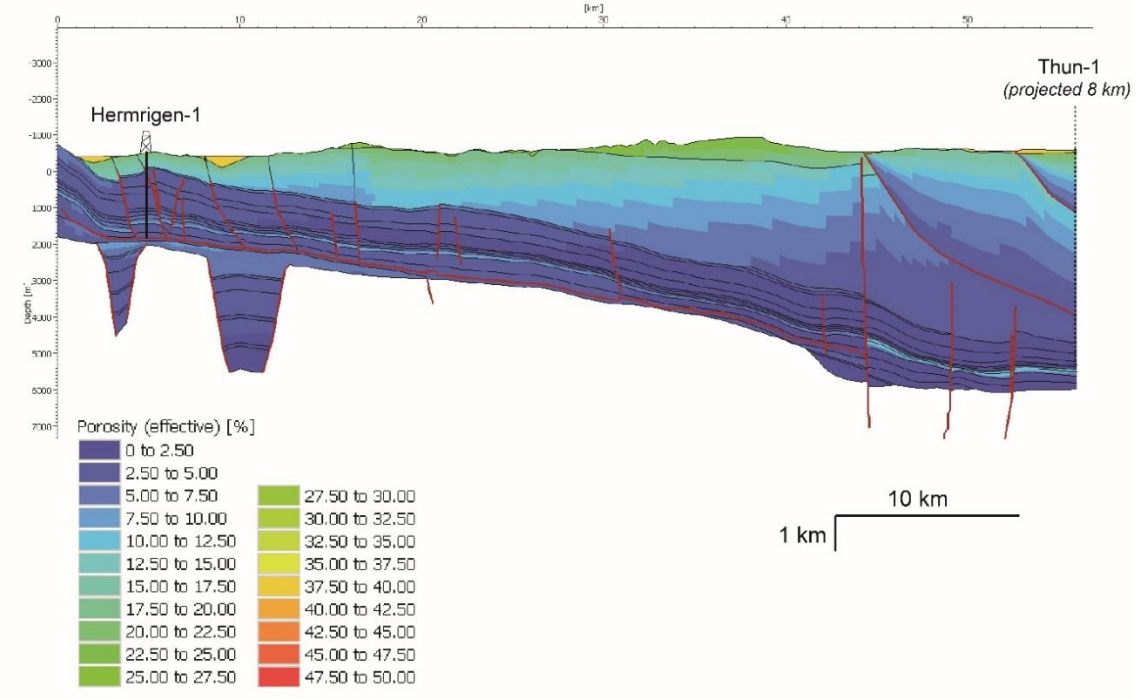


Fig. 43: Porosity simulated by the software along the section, extrapolating the data calibrated in the Hermrigen-1 and Thun-1 wells.

3.2.3.3.2 Present-day temperature

The present-day temperature calculated by the model was calibrated with the borehole temperature (BHT) measured in the well Hermrigen-1. Temperature data measured in the Thun-1 (projected 8 km), Linden-1 (projected 12 km), Ruppolsdried-1 (projected 13 km) and Tschugg-1 (projected 14 km) wells were also considered. To calibrate the modelling results, the variable that mostly changed was the present-day basal heat flow (see Method section). The heat flow values estimated in the entire basin from borehole temperature data give satisfactory calibration results, shown in Fig. 44. According to this calibration, the model calculates the temperature distribution along the section at the present day (Fig. 45).

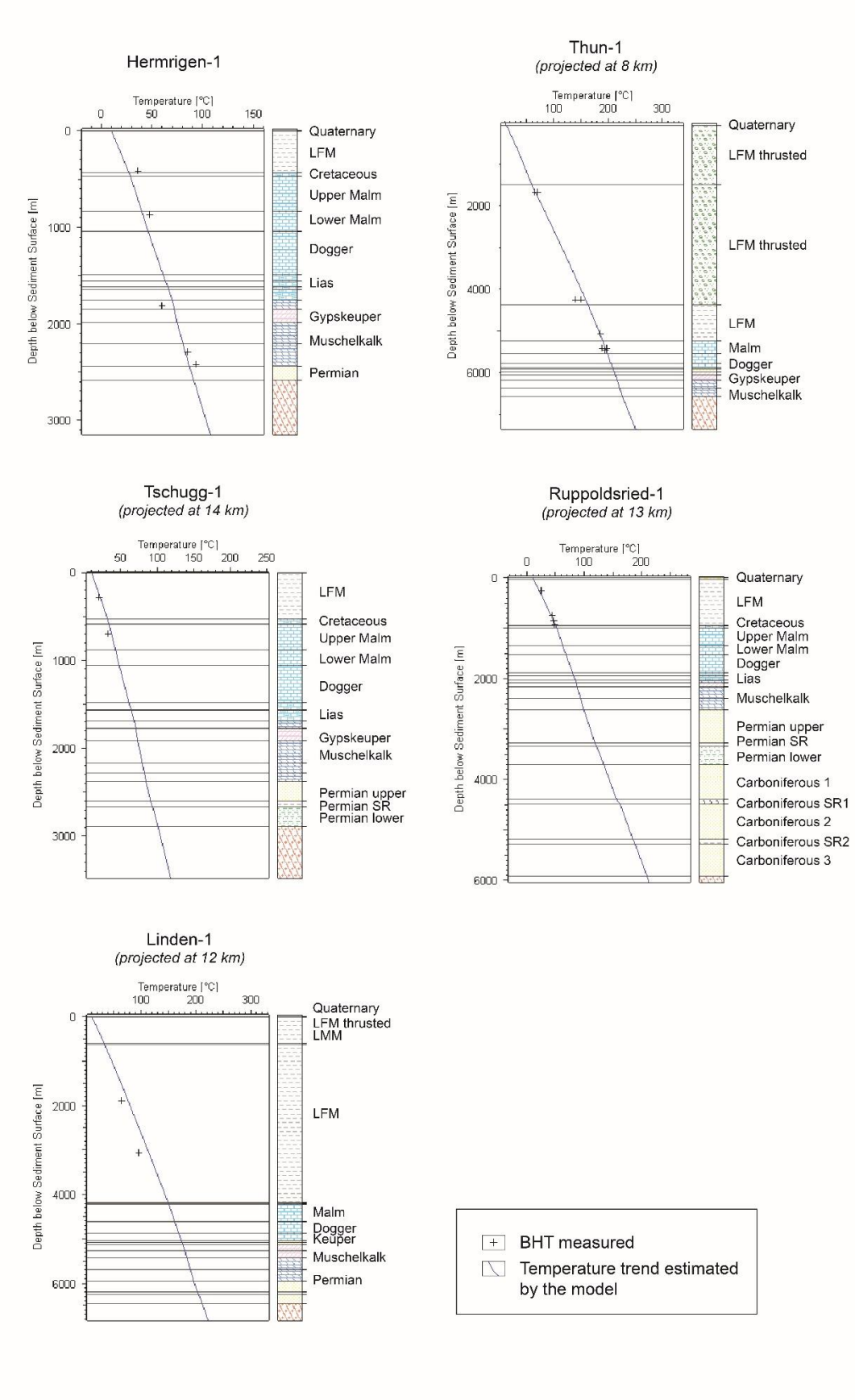


Fig. 44: Calibration of the present-day temperature modelling results with the BHT measured in the wells closest to Section 3.

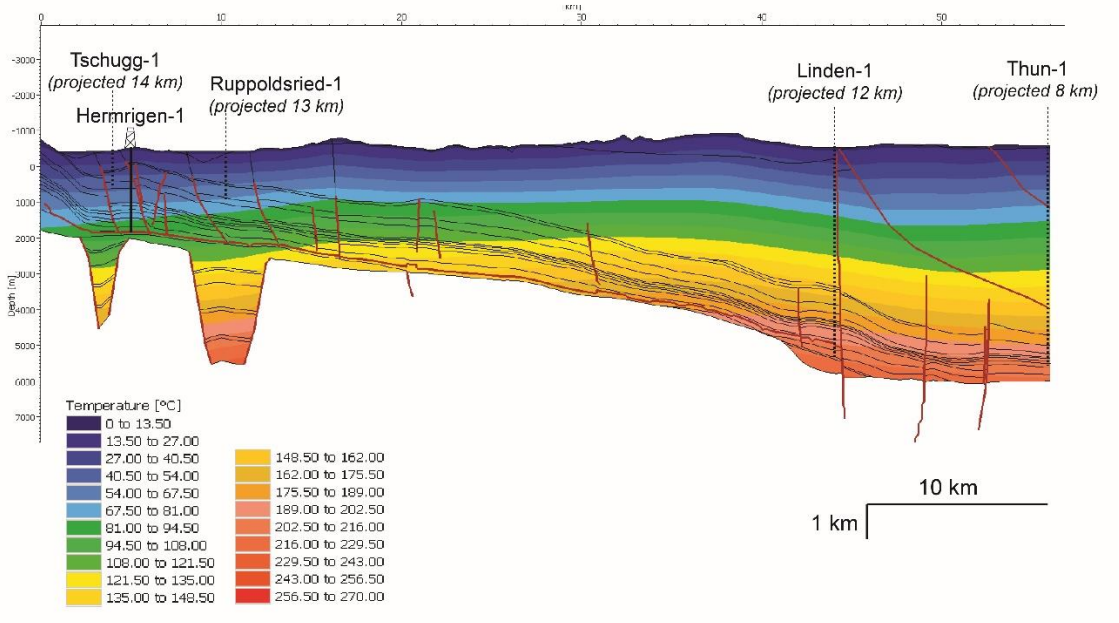


Fig. 45: Temperature variation with depth and along the section calculated by the model for the present day (0 My).

3.2.3.3.3 Thermal conditions / Source rocks maturity

The thermal conditions were calibrated with the Hermrigen-1 and Thun-1 data (Fig. 46). In the Hermrigen-1 well, the model was validated by most of the %Ro equivalent from TAI data (Elf Aquitaine, 1983), by considering the erosion in the northern edge of the section of 1500 meters. On the other hand, the %Ro measured data (Leu, 2007) are considerably higher than what is simulated by the model. To calibrate the latter data, a very elevated erosion magnitude should be considered (> 2-3 km), which is not likely in this part of the basin, with respect to what is estimated by literature previous works. In the Thun-1 well, most of the %Ro equivalent form TAI are higher than what is estimated by the model, considering an erosion of a maximum of 1800 meters. If these data are correct, a greater erosion should be considered in the southern edge of the section, in the Subalpine area, in contrast with the low ranges estimated by AFT data (900-1300 meters) (Cederbom et al., 2011). To properly reconstruct the erosion in this area, new %Ro data must be acquired in the future. The thermal conditions resulting along the entire section are shown in Fig. 47.

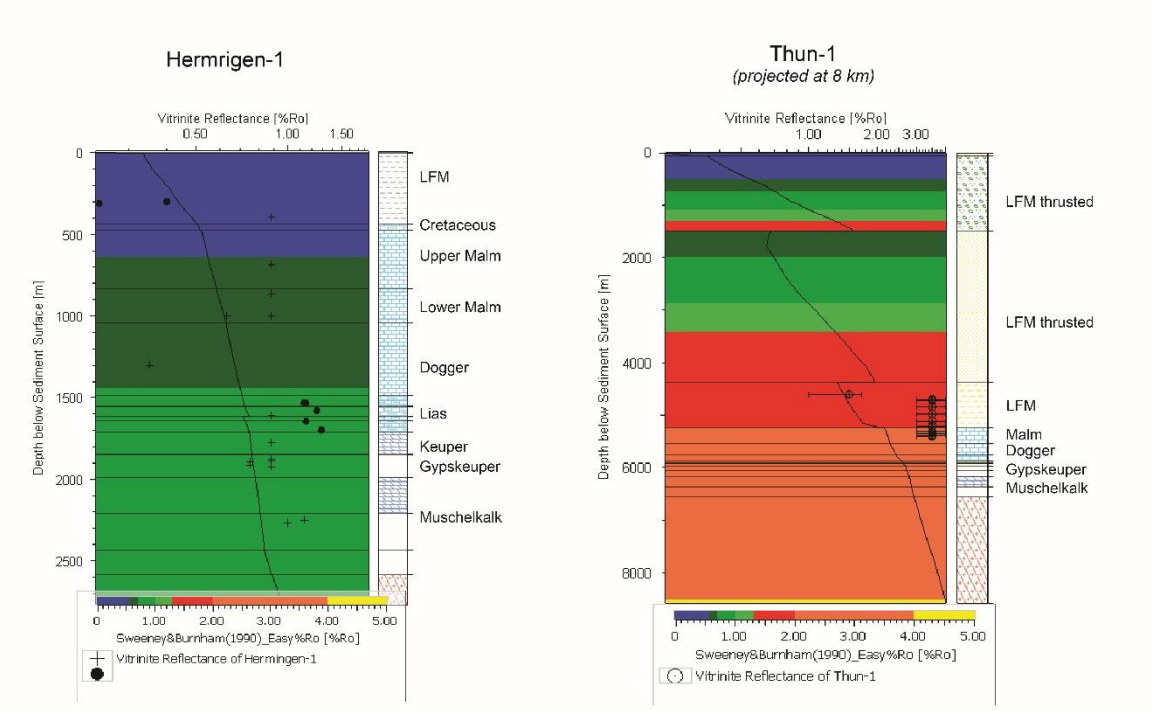


Fig. 46: Calibration of the thermal conditions calculated by the model with %Ro data measured in the Hermrigen-1 and Thun-1 wells.

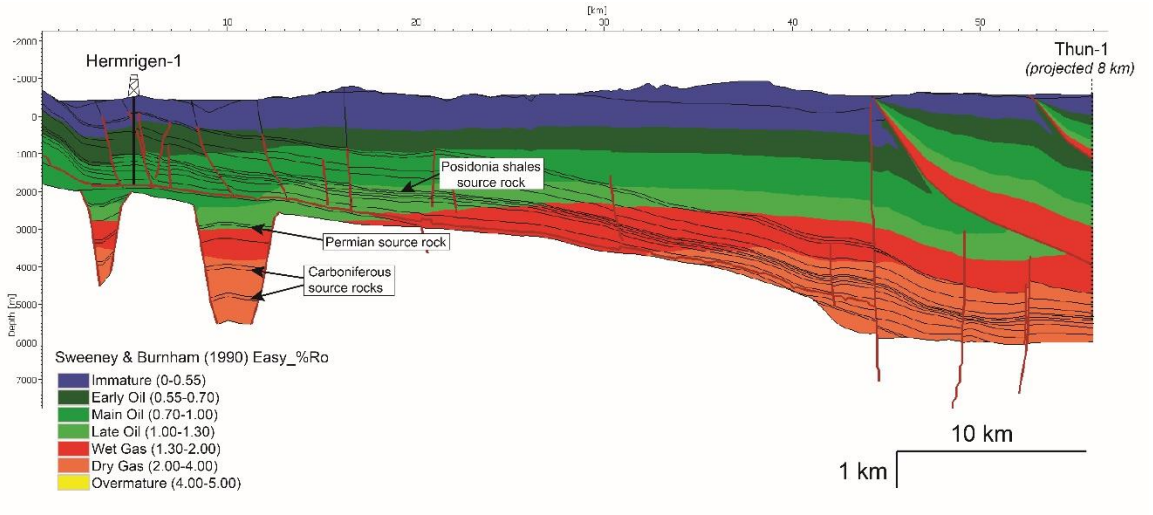


Fig. 47: Thermal conditions calculated by the model along the entire section

From the modelling results it is deduced that, in the south, all the source rocks are in the gas window conditions, whereas northward, the Permian source rock is in the late oil window and the Toarcian source rock in the middle oil window, and the Carboniferous source rocks are in the gas window. A burial plot vs thermal conditions could not be extracted from the model of Section 3. This is because of the software limitation in the case of the application of the TecLink workflow. In these cases, burial plot diagrams with no geological sense are generated.

3.2.3.4 Simulation of the hydrocarbon generation, migration and accumulation processes

The model simulates the hydrocarbon generation, migration and accumulation processes for Section 3, as an effect of the source rock maturation and hydrocarbon expulsion. Migration paths and potential reservoirs are calculated based on the geometry of the basin and the permeability

properties of its infill. In the first scenario, it was tested the “open faults” option, thus the faults are not cemented. Hydrocarbons were generated by the Permian, Carboniferous and Posidonia shale source rocks, at different times. A first very small generation peak occurred in the Permian, because of the burial of the Permian and Carboniferous source rocks in the grabens. A second larger generation peak, the most relevant, occurred in the late Jurassic to early Cretaceous time, when the basin was affected by another burial event and heat flow peak, and the third generation peak occurred in the Cenozoic time (Fig. 48) when the formation and infill of the foreland basin increase abruptly the burial depth of the basin.

The rocks that generate the greatest volume of hydrocarbons are the Carboniferous source rock, followed by the Permian source rock, and finally the Posidonia shale (Fig. 48). The Carboniferous source rock generates hydrocarbons mostly in the late Jurassic to early Cretaceous time, whereas the Permian and Posidonia shale source rock mostly generate in the Miocene, when the northern part of the basin was buried enough to mature these deposits.

Conventional high permeable reservoir form in the Cretaceous and Paleogene times, mostly in the Muschelkalk unit with a smaller amount in the Cretaceous units. Accumulations in low permeable units (petroleum saturated) form in the Oligocene and Miocene times, mostly in the Carboniferous and Permian deposits and secondly in the Lias and, in very small amounts, also in the LFM/LMM Molasse unit.

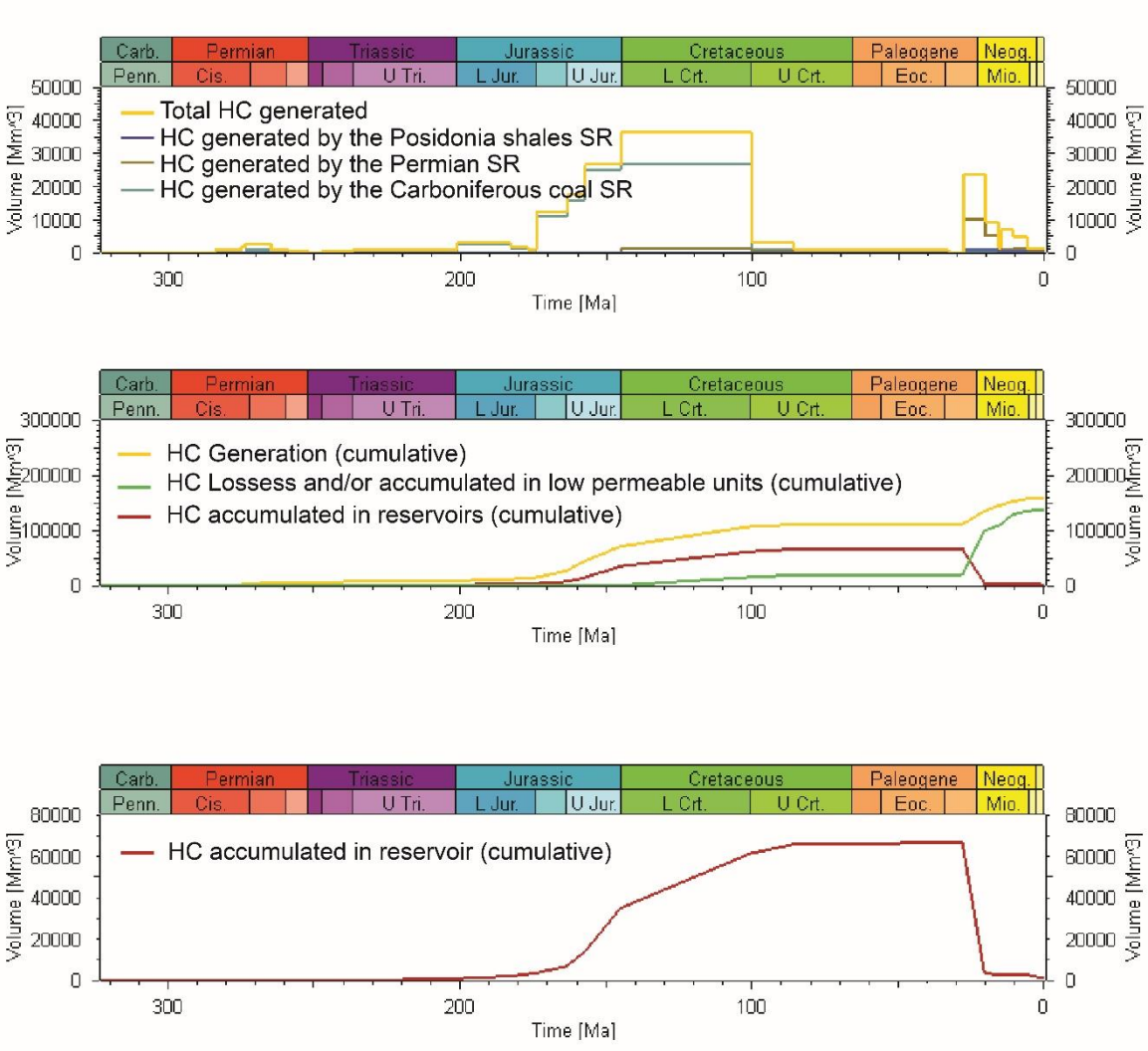


Fig. 48: Hydrocarbon generation and accumulation balances calculated by the software for the entire section

Accumulations in the Muschelkalk deposits form along the entire section (Fig. 49a), composed of gas and sealed by the Keuper evaporite units. In the northern part of the section, gas and oil accumulations form also in the Cretaceous and/or Upper Malm units, in the anticline structure drilled by the Hermrigen-1 well and/or in structural traps sealed by faults. Several of these latter accumulations are leaking from underneath reservoirs located in the Muschelkalk. In the southern part of the section, a gas accumulation forms also in the LMM unit. In the entire basin, important hydrocarbon migration paths form along most of the main faults (Fig. 49b). Gas migration and/or small gas pockets, can be found in the entire Molasse, especially in the south of the basin and along the faults.

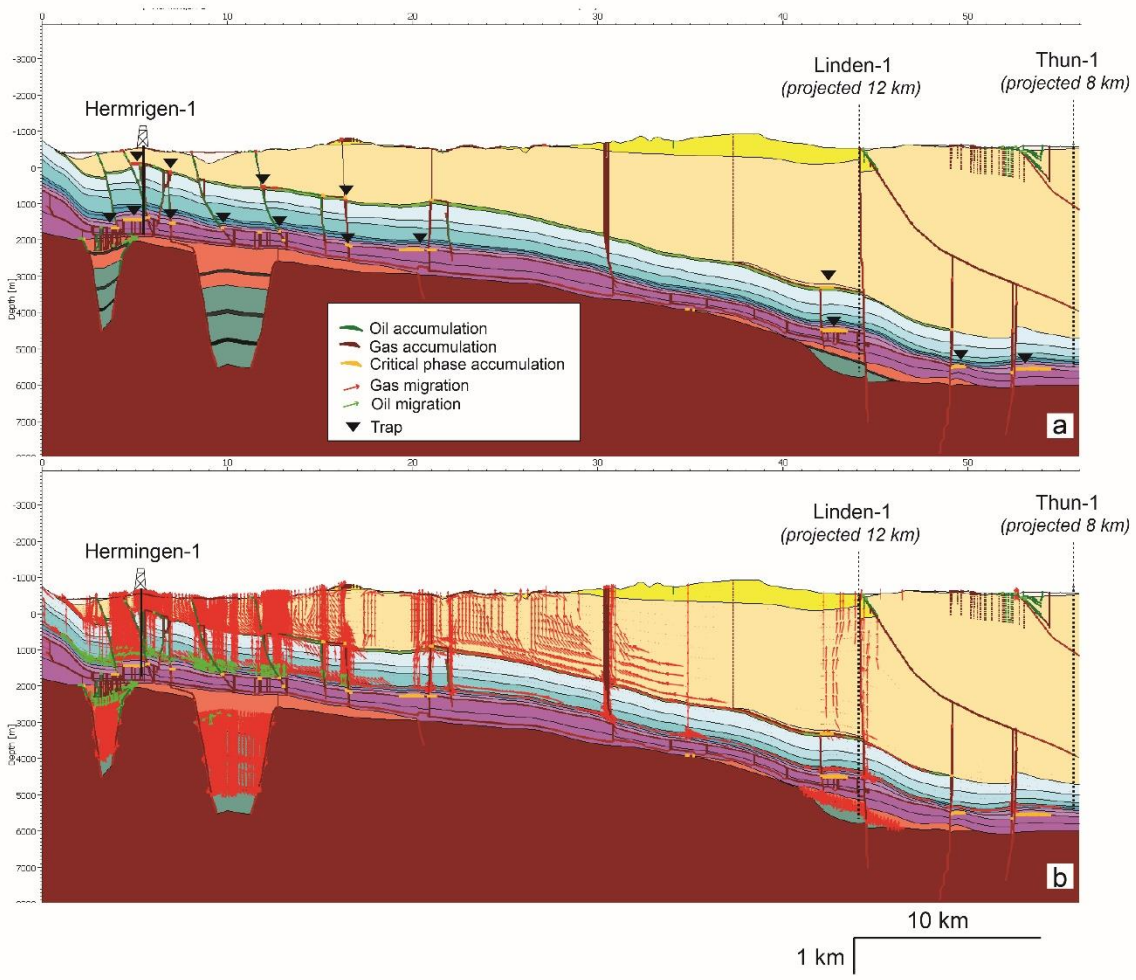


Fig. 49: Scenario Open Faults: (a) Hydrocarbon accumulations calculated by the model along section 3. Potential traps are indicated (b) Hydrocarbon migration path calculated by the model along the section.

A second scenario was simulated, considering the “closed faults” option, thus that faults are cemented. The main difference is related to the units where hydrocarbon simulations are simulated (Fig. 50). Considering the faults as close, most of the hydrocarbon accumulations formed in the Muschelkalk and Permian units. The leakage to the uppermost units observed in the previous scenario does not occur if the faults are considered closed. The volume of hydrocarbons accumulated in the reservoirs is slightly higher than what was simulated in the previous model, where hydrocarbons could easily escape to the top along the faults.

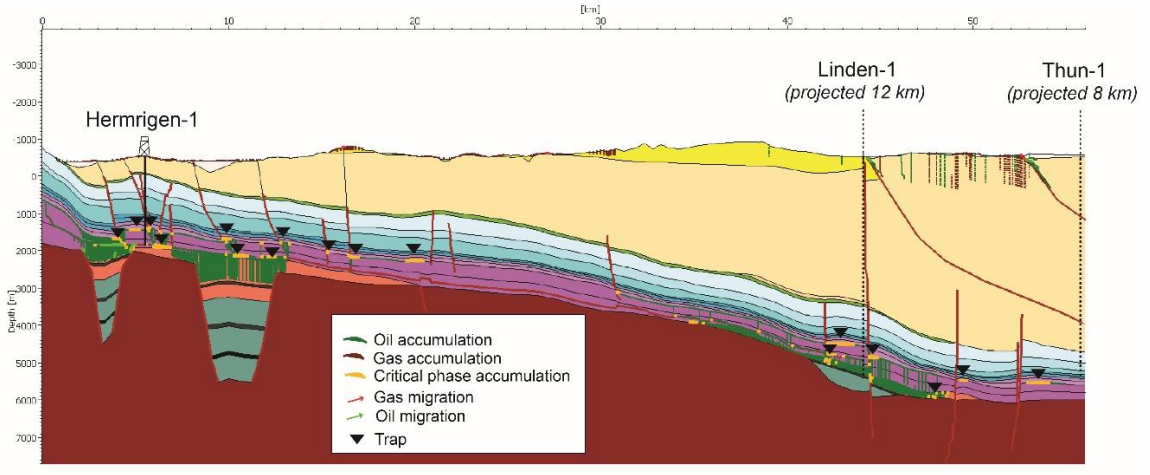


Fig. 50: Scenario Closed faults: Hydrocarbon accumulations calculated by the model along section 3. Potential traps are indicated

In Fig. 51 the hydrocarbon accumulations over the basin evolution are shown. The thermal maturity is also represented. In the northern part of the section, the Permian and Carboniferous units have entered the oil window since the Permian-Triassic times, as in this part of the section the grabens are very deep. The hydrocarbon accumulations in the Permian and Muschelkalk (including Buntsandstein units) have started forming since the Jurassic time when the Permian and Carboniferous source rocks in the northern part of the section entered the gas window and when a seal composed of anhydrite facies was deposited along the entire basin (Muschelkalk and Keuper units). In the southern part of the section, hydrocarbon accumulations started forming since the deposition of the Molasse units, when the Permian and Carboniferous source rocks entered the oil and gas windows because of the rapid burial of the basin. The accumulations formed in the Permian and Muschelkalk units were filled over the entire evolution of the basin and they were partially preserved until the present day. Most of the hydrocarbon generated by the Posidonia shale source rock, as well as part of the hydrocarbons generated by deeper source rocks, migrated vertically to the top surface and were lost, because of the lack of proper traps. Few small accumulations could form in the anticline structures formed in the northern part of the section, as a consequence of the Jura Mountain formation.

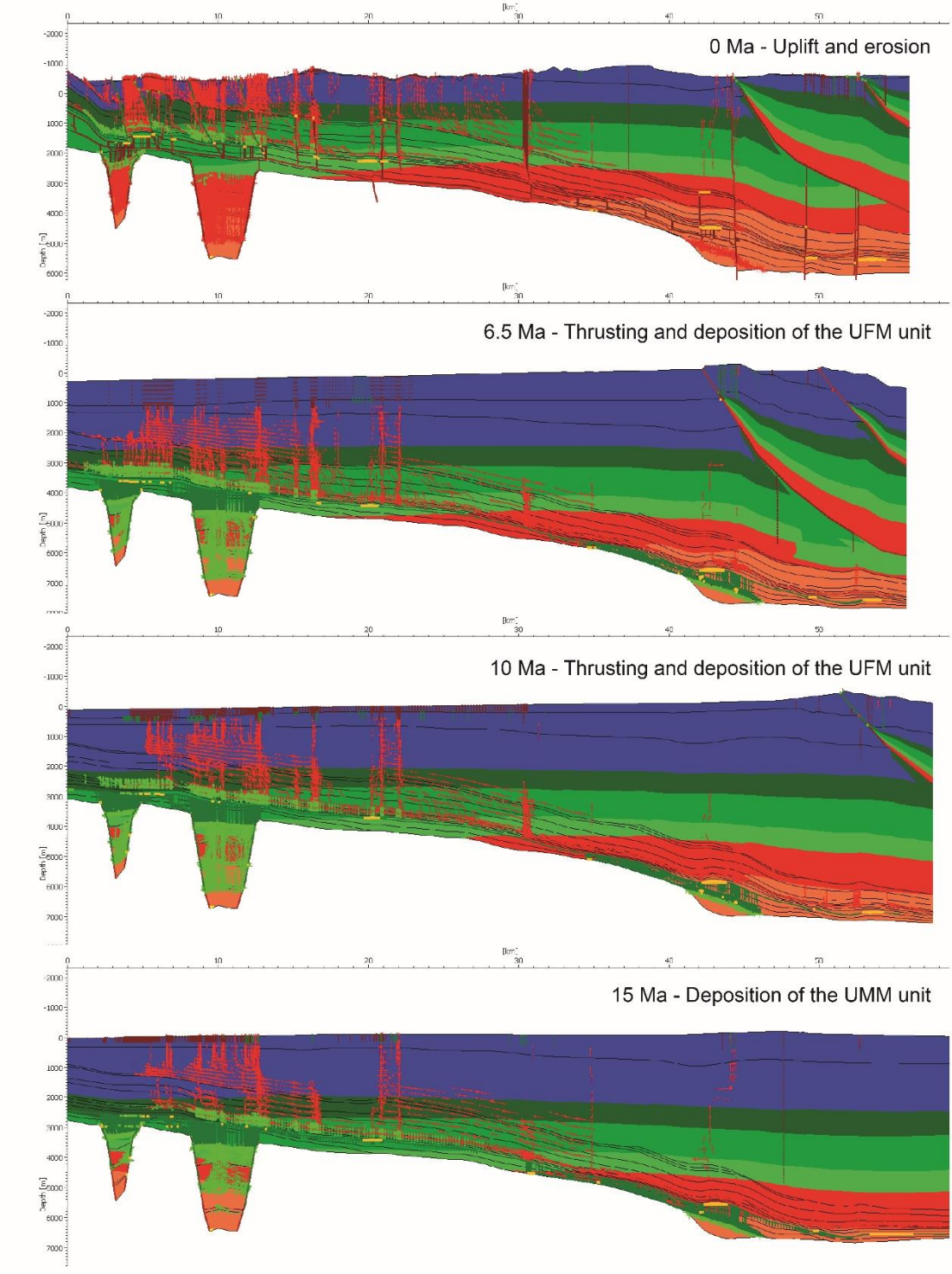


Fig. 51: Hydrocarbon accumulations over the evolution of the basin (continues).

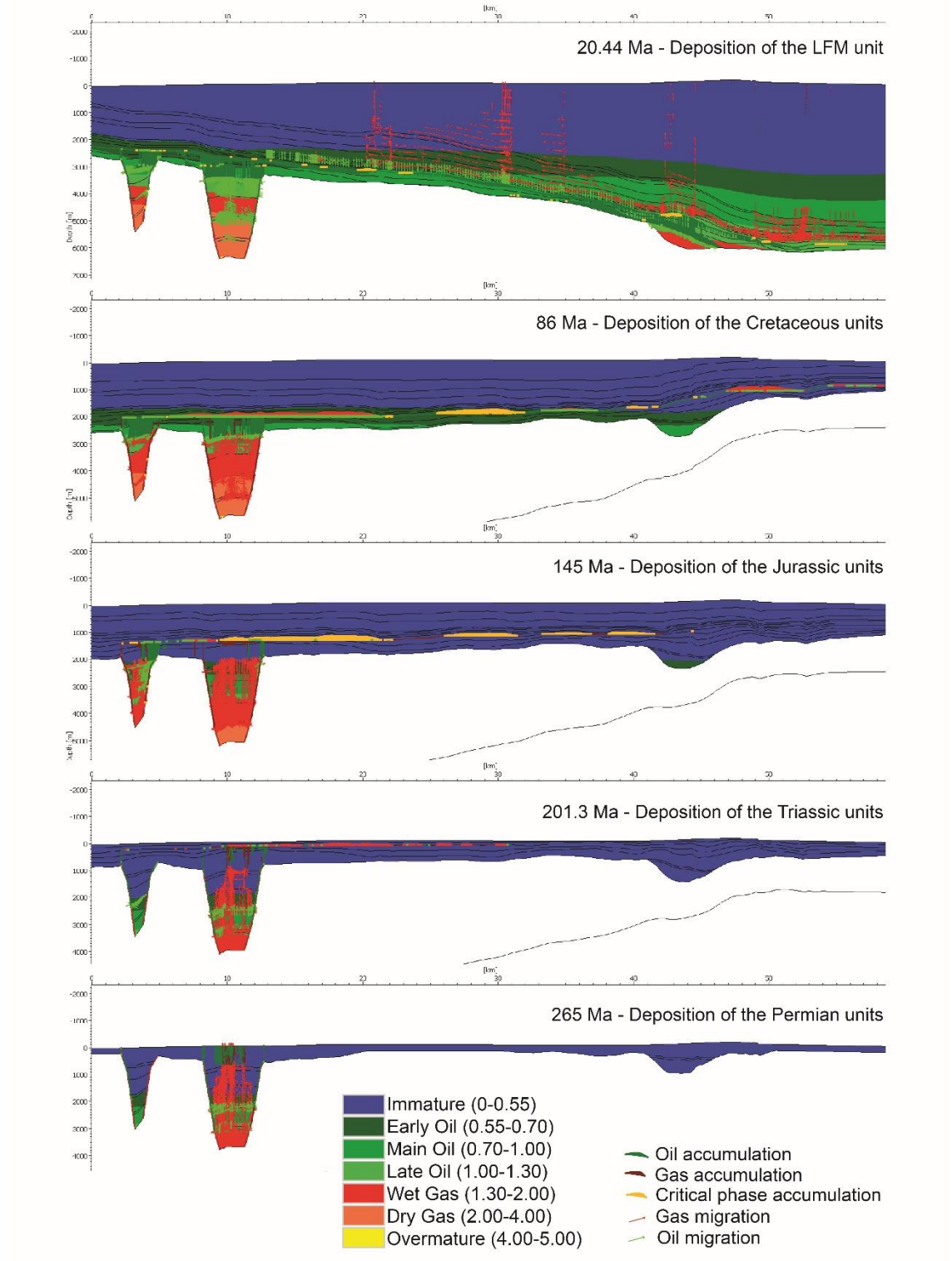


Fig. 51 (continues): Hydrocarbon accumulations over the evolution of the basin.

Finally, the petroleum system evolution for the four source rocks considered is shown in terms of a petroleum system chart (Magoon and Dow, 1994) (Fig. 52), where the source rocks, reservoir, seal, overburden rocks and trap elements are defined. The critical moment is defined considering the fit

among the formation of reservoirs, traps, the maturation timing of the source rocks and the hydrocarbon generation timing (Fig. 51).

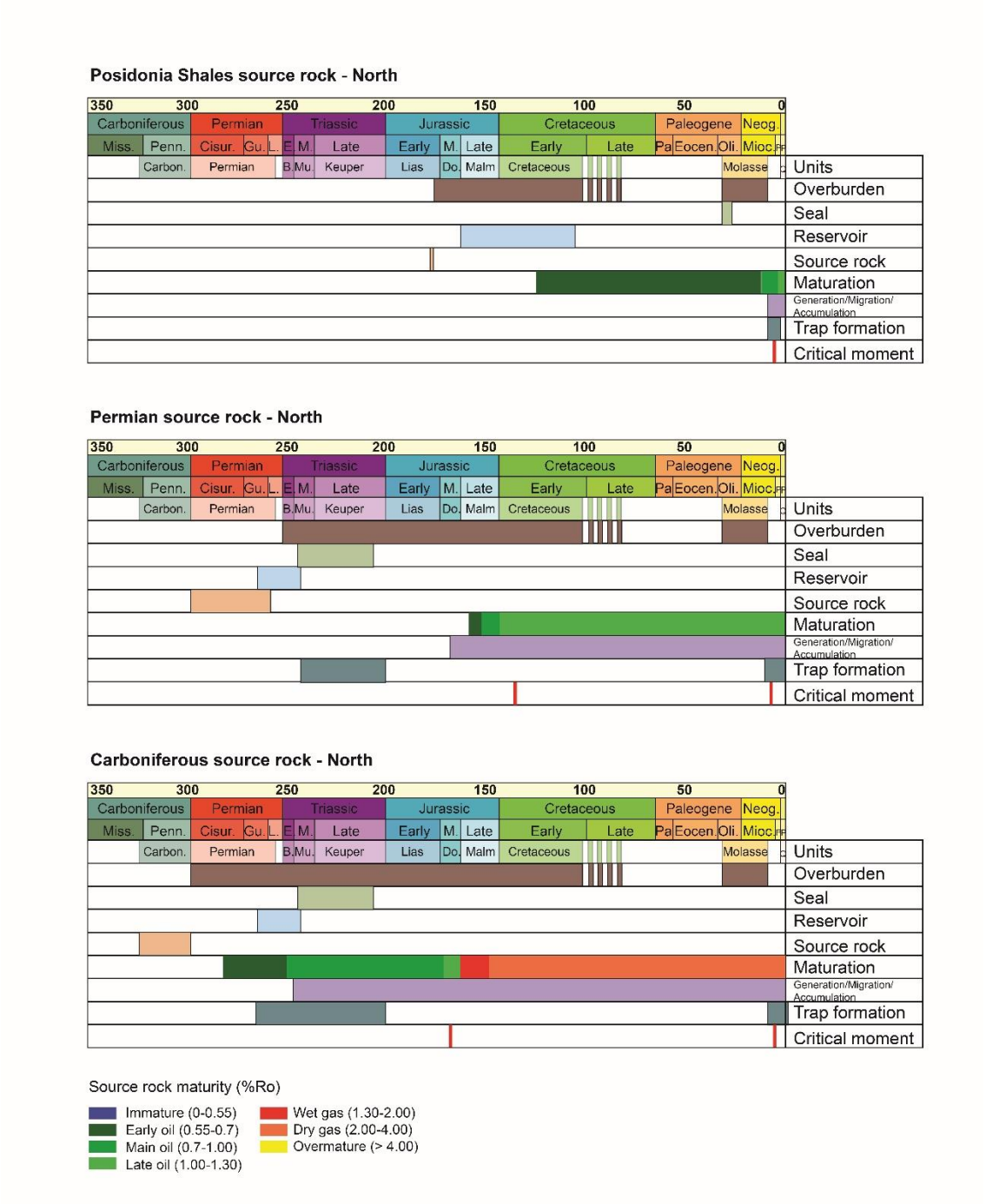


Fig. 52: Petroleum system charts reconstructed for the four source rocks defined in Section 3 (continues).

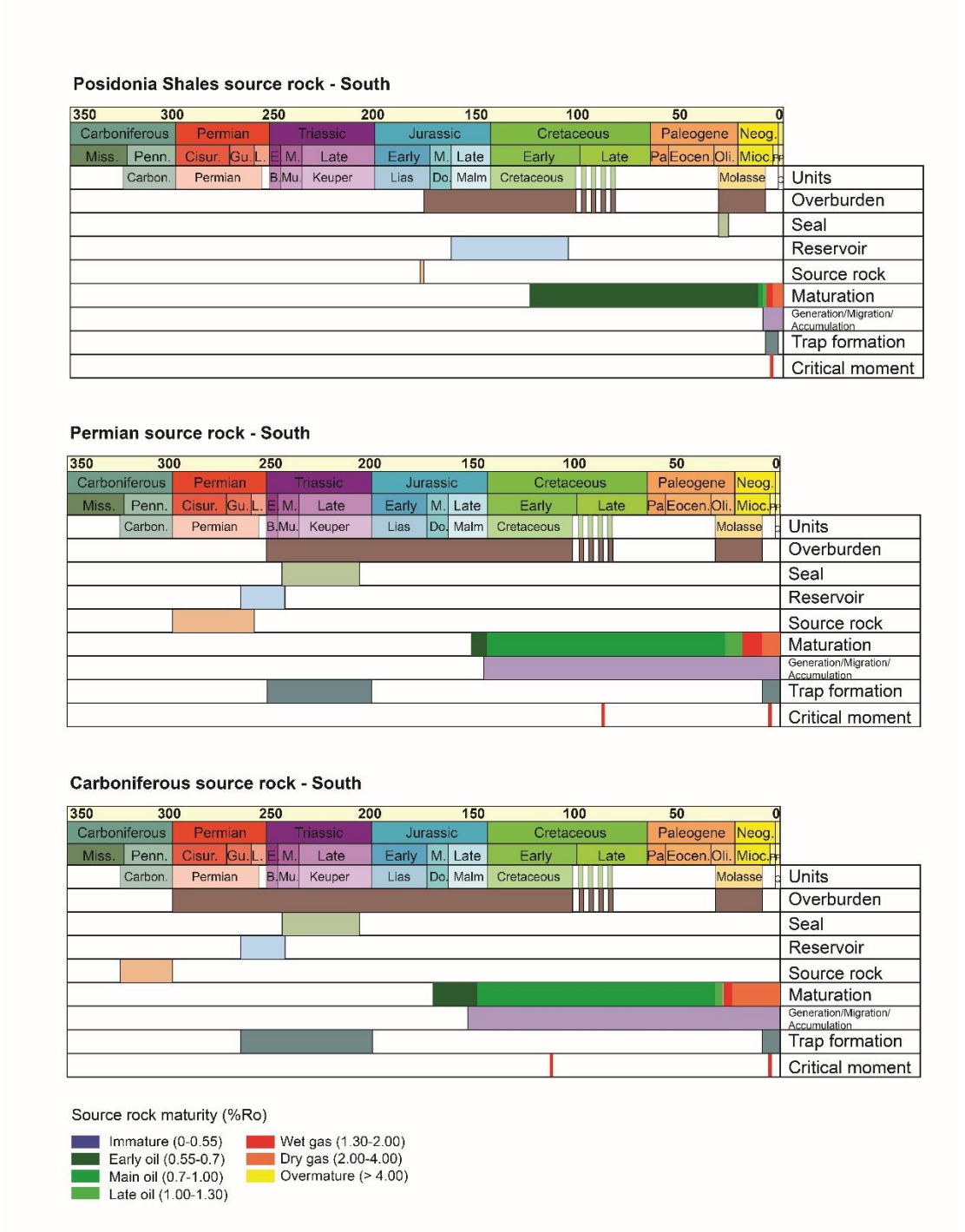


Fig. 52 (continues): Petroleum system charts reconstructed for the four source rocks defined in Section 3.

3.2.3.5 Hydrocarbons findings and modelling results comparison

The modelling results are partially in agreement with what has been found in the drilling campaigns carried out over time in the study area. In the Hermrigen-1 well, oil impregnations were found along the Mesozoic sequence, especially in the upper part, similar to what was reconstructed by the model (Elf Aquitaine, 1989a, 1989b, 1983). Gas seeps were found in the Muschelkalk unit, where the model simulates the formation of a reservoir (Fig. 49). Gas shows were found also in the Dogger unit (Leu, 2012). However, in the Hermrigen-1 wells, a commercial amount of gas was not found at that time. The origin of the oil and gas rests found in this well could not be determined, because of the biodegraded state of these hydrocarbons. In the Linden-1 well, drilled in 1971, gas shows were found in the Lias and Malm units (Leu, 2012). In the Thun-1 well gas rests were found in the Malm

unit, however even in this case, not in commercial quantity (Elf Aquitaine, 1989a, 1989b). From geochemical analysis, this gas could be generated from a mature terrestrial source rock, which could be the Permo-Carboniferous. The gas appears more evolved than the gas found in Linden-1 and Entlebuch-1 wells. In the model, in the Thun-1 well area, the Permo-Carboniferous unit is in the dry gas window, thus it can be the source rock of the hydrocarbons accumulated in the area, by the model mostly in the Muschelkalk unit (Fig. 47). Gas migration paths form along the faults crossing the Mesozoic sequence and the thrust planes in the Molasse sequence. In 2012-2013, potential new hydrocarbon exploration was planned in the Linden and Thun area by SEAG (Berner Zeitung journal, 1st February 2013; https://www.bernerzeitung.ch/das-erdgas-fieber-flammt-wieder-auf-810970743699), which could not be carried out mostly because of the new the Swiss Federal «2050 energy strategy».

In most cases, the size and number of the reservoirs calculated by the model, as well as the hydrocarbon flow paths, are larger than what has been found in the wells (Table 28). The reasons for this discrepancy can be multiple:

- The Permian and Carboniferous source rocks' thickness and hydrocarbon potential could be overestimated. In the area of the modelled section, no wells penetrate these deposits. Therefore, their thickness and properties were extrapolated from the nearest wells penetrating these units (Northern Switzerland), which could not be representative.
- In the model, the basement faults bounding the P-C grabens are considered continuous into the Mesozoic sequence. This option facilitates the migration of the hydrocarbons generated by the Permian and Carboniferous source rocks into the basin, which could not be the case if these faults do not continue. Thus, by this option, the formation of reservoirs in the Mesozoic and Cenozoic units would be less relevant.
- The seal of the Muschelkalk reservoir (Keuper unit) is less efficient than what is calculated by the model. Pervasive fracturation can be present in the faulted areas. Indeed, anhydrites and evaporites can be interlayered also with dolomite, shales and thin sandstone layers. Thus, this seal might have also an important brittle component.

  More efficient lateral traps than what is crossed by the modelled section can be present. In this case, hydrocarbons could migrate and accumulate in the closest reservoirs, not penetrated by wells. The Thun-1 well is not exactly located on the top of the section trace, thus lateral variation of the trap's geometry is possible.

Well	Hydrocarbon finding	Modelling results	Discrepancy causes
Hermrigen-1	• Oil traces in the lower Cretaceous, Malm and Lias units • Gas flow in the fractures of the Buntsandstein and Muschelkalk units; • Gas shows in the Dogger.	• Gas accumulation in the Muschelkalk unit; • Gas and/or oil accumulation in the Cretaceous unit; • Oil and gas vertical migration along the well area, associated with the presence of a fault.	• Permo-Carboniferous source rocks thickness and properties overestimated • The deep Permo-Carboniferous faults do not continue into the Mesozoic sequence • Seal fractured • Lateral migration
Thun-1	• Gas shows in the Malm units	• Gas accumulation in the Muschelkalk unit; • Gas migration paths along a fault crossing the Mesozoic units; • Oil and gas migration paths along thrust planes, in the Molasse units.	• Permo-Carboniferous source rocks thickness and properties overestimated • The deep Permo-Carboniferous faults do not continue into the Mesozoic sequence • Seal fractured • The well is not exactly located on the top of the section trace.

Well	Hydrocarbon finding	Modelling results	Discrepancy causes
Linden-1	• Gas shows in the Malm and Lias units	• Gas reservoir in the Muschelkalk unit, which leakage from another reservoir in the uppermost Mesozoic units (Cretaceous)	• Permo-Carboniferous source rocks thickness and properties overestimated • Seal fractured • The well is not exactly located on the top of the section trace. Lateral variation of the trap geometry.

Table 28: Comparison between the hydrocarbon findings in the wells located close to the section trace and the modelling results. In case of discrepancy, the potential causes are indicated.

3.2.4 Uncertainties

The petroleum system model presented herein estimates the thermal maturity of the potential source rock, the type and amount of hydrocarbon generated and the potential areas where hydrocarbon can be accumulated and/or flow model. However, because of the several assumptions made by constructing the model, a number of key uncertainties in the results must be considered. The most uncertain variables controlling the modelling results presented are listed in Table 29. A synthesis of the decision process carried out to handle the presented uncertainties is shown in Fig. 53.

Parameter	Uncertainty	Cause	Options	Effect on the Petroleum System Evolution	Impact	Potential improvements
Geometry of the basin	Horizons geometry, depth, stratigraphic units' presence.	Interpolation of a few 2D seismic lines across the Plateau. Few deep wells to corroborate the seismic data.	GeoMol 2021. Sommaruga et al. (2012).	Accumulation and migration areas could not be properly evaluated	Medium	Acquisition of new 2D and 3D seismic and/or reprocessing of the existent geophysical data
Faults	Faults location, extension, geometry.	Low-resolution seismic data.	GeoMol 2021 Sommaruga et al. (2012). Greber et al. (2007).	The hydrocarbon migration can be different from what is simulated by the model	Medium/High	Acquisition of new 2D and 3D seismic and/or reprocessing of the existent geophysical data
	Faults connectivity and cementation state	Very scarce direct measurement and few description in well reports.	Faults open (not cemented). Faults close (cemented).	The volume of hydrocarbon accumulations simulated by the model can be different.	Medium	Sampling fault cement; Monitoring fluids flow.
	Continuity of the basement faults bounding the P-C grabens into Mesozoic and Cenozoic.	Low seismic resolution .	Yes. No.	Potential hydrocarbon migration from the Permian and Carboniferous source rocks to the Mesozoic and Cenozoic deposits can be different.	High	Acquisition of new 2D and 3D seismic and/or reprocessing of the existent geophysical data.
Facies	Facies distribution	Data are available only where deep wells are present.	Facies extrapolated only from the wells located along the transect.	Hydrocarbon migration and accumulation can be different.	Medium/High	Acquisition of new stratigraphic, petrographic and geochemical data of the basin infill.

Parameter	Uncertainty	Cause	Options	Effect on the Petroleum System Evolution	Impact	Potential improvements
Facies	Facies distribution	Facies are deduced from qualitative descriptions in the well report, there are no quantitative data.	Facies extrapolated also from the wells located at an offset of nearly 14 km from the transect.	Hydrocarbon migration and accumulation can be different.	Medium/High	Acquisition of new stratigraphic, petrographic and geochemical data of the basin infill.
Structural evolution	Timing and magnitude of thrusting	Scarce data dating the thrusting and able to calibrate the magnitude of the erosion in the South	Thrusting starts at 10 Ma, during the deposition of the uppermost Molasse units.	The maturity of the southern part of the section and the timing of trap formation can be different.	Medium	Acquisition of new %Ro data; Reconstruction of a more accurate structural model.
			Thrusting starts after 7 Ma			
Erosion	The magnitude of the erosion	The magnitude of the erosion is estimated by indirect data (%Ro, AFT, etc.)	Values estimated in the literature.	Burial, thus maturity, of the source rocks can be different.	Medium/High	Acquisition of more %Ro data along the section.
			Values estimated in the most recent literature, modified to calibrate the %Ro data.			
	Timing of the erosion	Difficulty in dating different erosion events	Literature data	The timing of the hydrocarbon generation can be different.	Medium	Acquisition of AFT data along the section.
Boundary conditions	Present-day heat flow	The heat flow values measured today calibrate correctly the present-day temperature data.	Assigning the present-day heat flow values.	None	None	None
			Do not calculate the radiogenic heat produced by the rock.			
	Paleo-heat flow	The paleo heat flow over the basin evolution cannot be measured directly, it can be only estimated.	Heat flow from literature.	Timing of the hydrocarbon generation.	Medium/High	Reconstruction of the crustal model to improve the estimates of the paleo-heat flow.
			Heat flow from literature modified to calibrate the %Ro values.			

Parameter	Uncertainty	Cause	Options	Effect on the Petroleum System Evolution	Impact	Potential improvements
Permian and Carboniferous source rocks	Presence and geometry of the Permo-Carboniferous grabens along the entire section.	Low seismic resolution.	Leu (2008) Sommaruga et al. (2012) Greber et al., 2007	Potential presence of more deep hydrocarbon source rocks.	High	Acquisition of new 2D and 3D seismic and/or reprocessing of the existent geophysical data.
	Presence, distribution and thickness of deposits rich in organic matter in the Permo-Carboniferous grabens	No data along the section.	No present Permian and Carboniferous source rocks present in both grabens	Generation of deep hydrocarbon accumulations, which can migrate to the shallower units.	High	Acquisition of new geophysical data (seismic, deep wells).
	Hydrocarbon potential.	No data along the section	Geochemical data extrapolated from the Weiach-1 well	The volume of hydrocarbon generated can be different.	High	Penetrating these deposits in other locations and direct measurement of the geochemical parameters.
Posidonia shale source rock	Presence of the Posidonia shale source rock.	No data	No present Present along the entire section (4 meters)	Generation, migration and accumulation of more hydrocarbon in the Mesozoic and Cenozoic sequence can be different.	High	Acquisition of more data in the Liassic interval, especially in the central-southern part of the section.
	Hydrocarbon potential	None, based on what was measured in a set of Jurassic samples for the Hermrigen-1 and Thun-1 wells.	Extrapolated from Northern Switzerland and Canton of Vaud area.	The volume of hydrocarbon generated can be different.		

Parameter	Uncertainty	Cause	Options	Effect on the Petroleum System Evolution	Impact	Potential improvements
Calibration of the model	Porosity data	Data are available only in a few wells. Getting far from the wells used for calibration, the porosity can be different from what is simulated.	Use only the available data along the section.	Hydrocarbon migration and accumulations could be different.	Medium	Acquisition of more porosity data along the section.
			Use of data measured in wells located at nearly 10 km from the section trace line.			
	Porosity calibration	The porosity reduction by the diagenetic process cannot be properly simulated by the software.	Modify the initial porosity of the facies in the lithology library of the software.	Reservoir properties can be different from what is simulated by the model.	Medium	Find a proper way to change the software the porosity because of diagenetic processes and/or other processes.
	Present-day temperature data	Data are available only in a few wells.	Use only the available data along the section	The present-day temperature can be different from what is simulated, getting far from the wells where calibration data are available.	Low	Acquisition of more borehole temperature data along the section.
			Use also data measured in wells located at 15 km from the section trace line.			
	Thermal maturity calibration	Few and uncertain %Ro data measured along the section.	Calibration with the %Ro data measured in the Hermrigen-1 wells and the data converted from TAI to %Ro in the Hermrigen-1 and Thun-1 wells.	Erroneous calculation of the thermal maturity of the source rocks along the section, thus of the volume of hydrocarbons potentially generated.	High	Acquisition of new %Ro along the section.

Table 29: List of the uncertainties parameters for the Section 3 model, their causes and their impact on the petroleum system modelling results. The options/scenarios available are indicated. In green is highlighted the option chosen in this study to build the petroleum system modelling. Potential improvements and actions to mitigate these uncertainties are suggested.

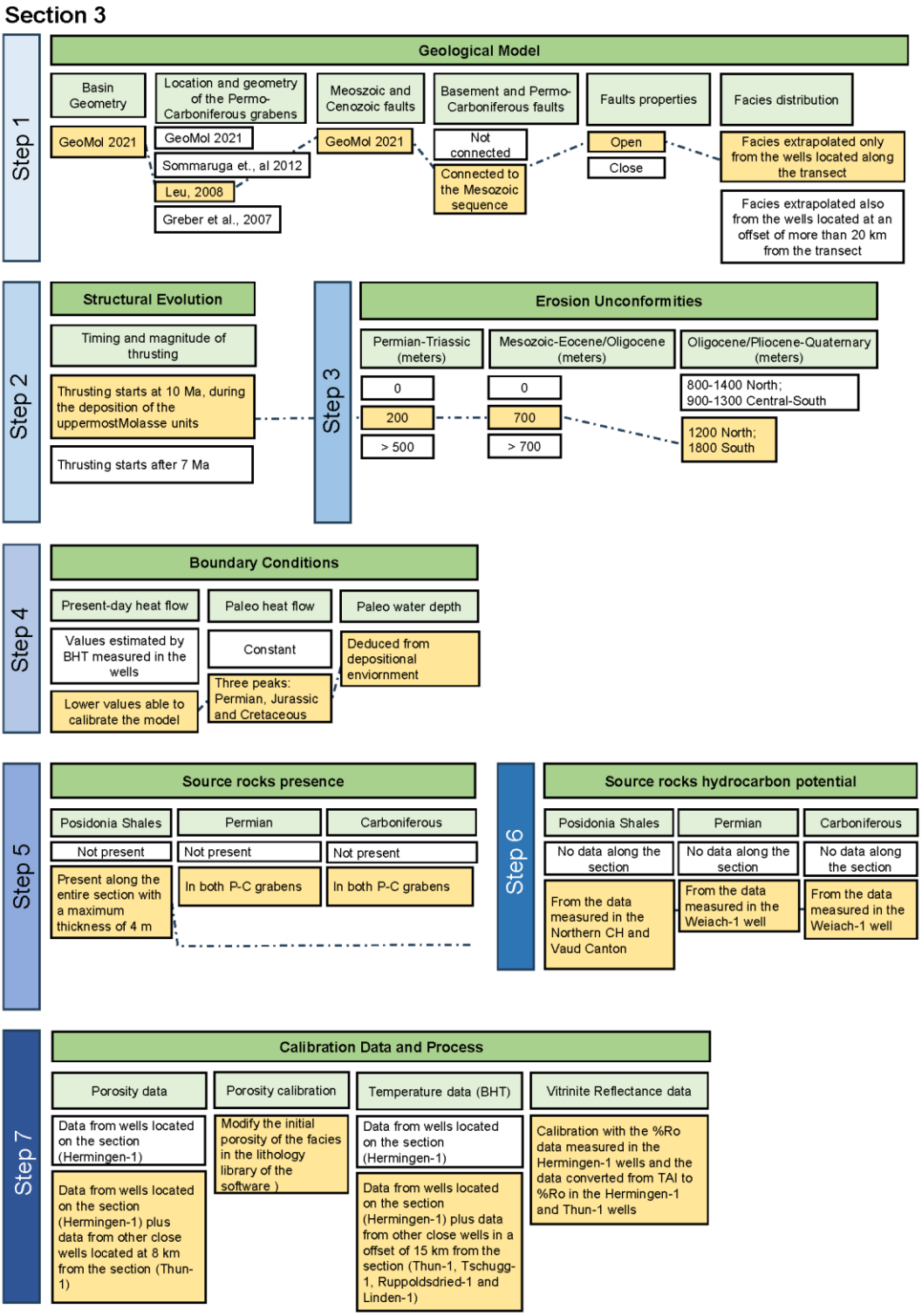


Fig. 53: Petroleum system modelling was built by selecting the specific combination of parameters, which are critical in controlling the thermal evolution of the basin and the hydrocarbon generation, migration and accumulation processes. In yellow are indicated the option chosen in this work.

3.3 Petroleum System Modelling - Section 4

3.3.1 Data

3.3.1.1 Geological Model

Section 4 is extracted from the GeoMol project, along a section line passing from the Cantons of Solothurn, Aargau, Luzern and Obwalden (Fig. 54). The trace of the section is NNW-SSE oriented, with the following extremity coordinates: NNW edge x, y: 2622273.0; 1245687.5 SSE edge x, y: 2663235.9; 1187895.0 (Reference coordinate System CH1903+ / LV95), and a total length of 49 km (Fig. 55). The extracted section represents the present-day geological structure of the NAFB in the area, represented by a southern dipping foreland wedge, filled by the Cenozoic Molasse units, and its Mesozoic substratum. The foreland basin is delimited to the north by the tabular Jura Mountain Chain, where the Mesozoic strata outcrop, and to the South by the more external Subalpine thrusts. The erosional topographic surface cut the Mesozoic substratum units in the northern part of the section and the uppermost Molasse units in the southern part (Fig. 55). The location and geometry of the Permo-Carboniferous graben were deduced by Leu (2008) along the entire section. In this section, the types of faults are differentiated, as classified in the GeoMol database (Fig. 55).

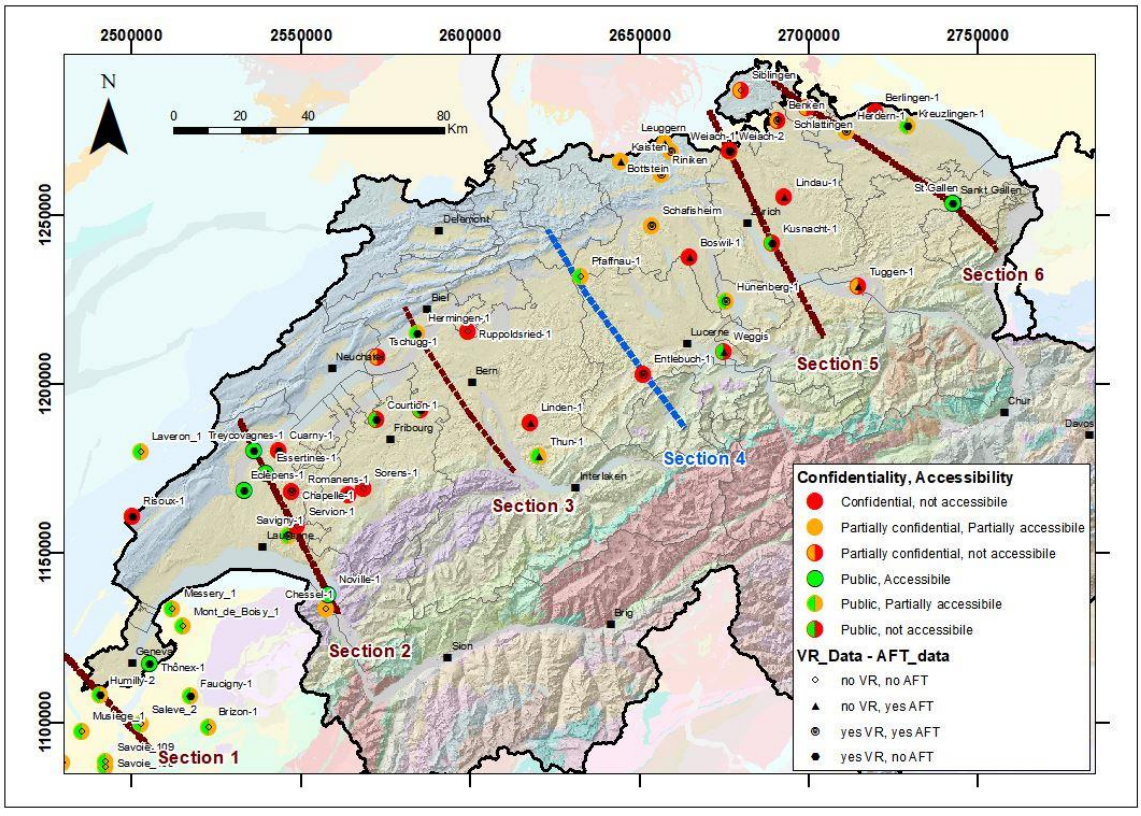


Fig. 54: Location of the section 4.

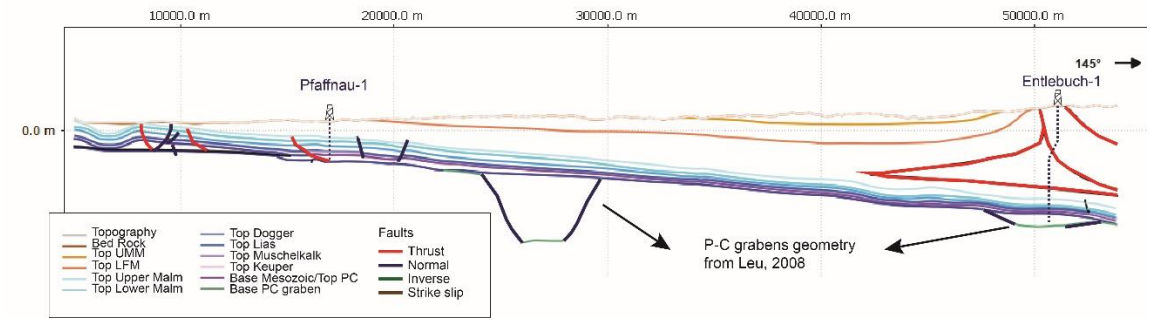


Fig. 55: Horizons and faults extracted from Geomol at the Section 4 trace location. The Permo-Carboniferou (P-C) graben geometry was extrapolated from what was proposed by Leu (2008). The wells intersecting the section trace are shown. In this section, the type of faults is differentiated, as classified in the GeoMol database.

3.3.1.2 Wells

Section 4 intersects only the Pfaffnau-1 and Entlebuch-1 wells, (Fig. 55). Because of the lack of input data along the section, the closest wells where data are available were also considered (Weggis-1, Schafisheim-1 and Hünemberg-1, 21, 27 and 32 km respectively, from the section line). For these wells, the availability of the most relevant data necessary for thermal modelling is summarized in Table 30. The stratigraphic logs of these wells are shown in Appendix 4. The well Boswil-1 (located 29 km from the section trace) was not considered, as no data are available for this well.

Well	Distance from section (km)	Status	Well report	Stratigraphic log	Calibration data	Rock-Eval data
Pfaffnau-1	0	Public, Partially accessible	Yes	Yes	Phi, T, AFT	No
Entlebuch-1	0	Confidential, Not accessible	No	Yes	T, AFT	No
Weggis-1	21	Public, Not accessible	No	Yes	T, AFT	No
Schafisheim-1	27	Partially confidential, Partially accessible	Yes	Yes	Phi, T, VR, AFT	Yes
Hünenberg-1	32	Public, Partially accessible	Yes	Yes	Phi, T, AFT	No
Boswil-1	29	Confidential, Not accessible	No	No	No	No

Table 30: wells closest to the Section 4 trace and availability of the most relevant data needed for thermal modelling. Calibration data: (T) temperature; (VR) vitrinite reflectance; (AFT) apatite fission tracks, (Phi) porosity.

3.3.1.3 Deposition and erosional events

The burial history of the studied area is defined by a sequence of depositional and erosional events and their ages. Thus, in the model, an age for each stratigraphic unit and the main erosional event was assigned (Table 31).

Age top unit (Ma)	Unit	Event	Facies
0	Quaternary	Deposition	Quaternary
4	Erosion Pliocene-Quaternary	Erosion	
7.24	UFM	Deposition	UFM
15.97	UMM	Deposition	UMM
20.44	LFM	Deposition	LFM Thrust; LFM Authocht above; LFM Autocht below; LFM Central

Age top unit (Ma)	Unit	Event	Facies
33	Hiatus Cret/Eocene	Hiatus	
86	Erosion Cretaceous	Erosion	
113	Cretaceous	Deposition	
145	Upper Malm	Deposition	Upper Malm
157.3	Lower Malm	Deposition	Lower Malm
163.5	Dogger	Deposition	Dogger lower South; Dogger lower Central; Dogger Callovian
174.1	Lias	Deposition	Lias. Posidonia shale SR
201.3	Keuper	Deposition	Keuper
237	Muschelkalk	Deposition	Upper Muschelkalk; Muschelkalk Salt; Lower Muschelkalk
252	Hiatus Perm-Triassic	Hiatus	
259	Erosion Perm-Triassic	Erosion	
265	Permian	Deposition	Permian; Permian-Source rock (SR)
284	Carboniferous	Deposition	Carboniferous; Carboniferous-Source rock (SR)
323	Hiatus/erosion pre-Carbon		
400	Basement	Deposition	Basement

Table 31: Depositional and erosional events defined in the thermal model for section 4. A facies is assigned to each layer. UFM upper freshwater Molasse; UMM upper marine Molasse; LFM lower freshwater Molasse; LMM lower marine Molasse

Throughout the Section 4 area, there is very little data on the magnitude of the main erosion events that occurred during the evolution of the basin (Table 32). Along the section, only erosion estimates from AFT data are available for the Pliocene-Quaternary unconformity (Cederbom et al., 2011). Other erosion estimates at the regional scale by older studies were summarized in Schegg and Leu (1998) for most of the unconformities.

Therefore, based on the literature data, it is considered an erosion of 500 meters for the Permian-Triassic unconformity. For the Mesozoic-Eocene unconformity, it is considered an erosion of 700 meters along the entire section. For the Quaternary-Pliocene unconformity, is considered an erosion of 1700 meters in the northern edge of the section (Pfaffnau-1 well), increasing to 4000 meters toward the southern edge (Entelbuch-1 well). These values were subsequently tested and constrained by the thermal modelling workflow proposed herein (see the Calibration result section). In the southern extremity of the section, these great erosion values were necessary to geometrically reconstruct the undeformed geometry of the foreland previous to the triangular zone formation. To present there are no calibration data to constrain this data.

Erosion unconformity	Amount of erosion estimated in previous studies (m)	Method	NAFB study area	Source
Quaternary-Pliocene	500	AFT, VR, 1D thermal modelling	Schafisheim-1 well	(Omodeo-Salé et al., 2021; Villagomez et al., 2021)
	1600	AFT	Entlebuch-1 well	Cederbom et al., 2011
	1700	Clays, subsidence analysis	Pfaffnau-1 well;	Monnier, 1982 ; Lemcke, 1974 ; Schegg and Leu
	1800	AFT	Hünemberg-1 well	Cederbom et al., 2011
	2700	AFT	Weggis-1 well	Cederbom et al., 2011
Mesozoic-Eocene	0	Stratigraphy	Regional	Todorov et al., 1993; Burkhard and Sommaruga, 1998; Wildi et al., 1989; Lemcke, 1988

Erosion unconformity	Amount of erosion estimated in previous studies (m)	Method	NAFB study area	Source
Mesozoic-Eocene	700	AFT, VR, 1D thermal modelling	Schafisheim-1 well	Omodeo-Salé et al., 2021
	600-900	VR, clays, porosity, subsidence analysis	W-central sector	Schegg and Leu, 1998
Permian-Triassic				
	200	VR, 1D thermal modelling	Weiach-1 well	Omdeo-Salé et al., 2021
	200-600	VR	Weiach-1 well	(Mazurek et al., 2006)
	1000	VR, stratigraphy	Weiach-1 well	Diebold, 1988; Schegg and Leu, 1998

Table 32: Erosion magnitude estimated in previous studies for the three main erosional unconformities at the regional scale and/or in areas close to the section 4 trace line.

3.3.1.4 Facies

Facies were assigned to the stratigraphic units composing the section by extrapolating the lithologic data described in the well reports of the Entlebuch-1 and Pfaffnau-1 wells. Because of that, these wells do not cross the uppermost unit (UFM), the lithological description of these units was taken by the Hünemberg-1 well (32 km from the section trace line). For these wells, the lithologies for each unit, expressed in percentage, are listed in Appendix 5. For each unit a unique or various facies were assigned along the section (Table 33), depending first on the variability of the facies and secondly on the availability of data.

Unit	Cgl	Sst	Silt	Shl	Lmt	Marls	Dlm	Anhyd	Halite	Reference Well
Quaternary	50		20	30						Entlebuch-1
UFM		15		5	5	75				Hunenberg-1 (mod)
UMM	10	50		10		30				Hunenberg-2 (mod)
LFM Thrust		40	30	30						Entlebuch-1
LFM Autocht above		20	50	30						Entlebuch-1
LFM Autocht below		40	30	30						Entlebuch-1
LFM central		20		10		70				Pffnau-1
Upper Malm		5			90	5				Pffnau-1
Lower Malm					70	30				Pffanau-1; Entlebuch-1
Dogger (Callovian)				30	30	40				Pffanau-1; Entlebuch-1
Dogger lower central					80	20				Pffnau-1
Dogger lower South				50	50					Entlebuch-1
Lias		45		5	50					Pffanau-1; Entlebuch-1
Keuper		10		10		45	20	15		Pffanau-1; Entlebuch-1
Upper Muschelkalk					10	60	20	10		Pffnau-1
Muschelkalk Salt						80			20	Pffnau-1
Lower Muschelkalk				30	10	40	5	15		Pffnau-1
Permian		60		40						Pffanau-1
Carboniferous		50		45					5 coal	Entlebuch-1
Basement	Gneiss									Pfaffnau-1

Table 33: Facies, expressed as a percentage of lithological composition, assigned to the stratigraphic units forming the basin infill of section 4. The wells used as references are indicated. Cgl: conglomerate; Sdt: sandstone; Slst: siltstone; Shl: shale; Lmt: limestone; Mrl: marl; Dlm: dolomite; Anhd: anhydrite; Halt: halite.

3.3.1.5 Calibration data

Porosity data are available for the Pfaffnau-1 well (Appendix 6). The porosity data for the Shafisheim-1 and Hünenberg-1 wells were also considered (Appendix 6). However, because of that they are located 27 and 32 km from the section trace line, the calibration of these data was not straightforward. To calibrate the present-day temperature over depth in the basin infill, they used the borehole temperature data (BHT) of the Entlebuch-1 and Pfaffnau-1 wells (Appendix 7). BHT data for the Shafisheim-1 and Hünenberg-1 wells were also considered (Appendix 7). However, because they are located 27 and 32 km from the section trace line, the calibration of these data was not straightforward.

For the wells located close to the Section 4 area, there are no vitrinite reflectance data, which could be used to calibrate the thermal conditions simulated by the model during the evolution of the basin. The closest well where %Ro data are available is Shafisheim-1 (Appendix 8). However, as this well is located 27 km away from the trace line, the calibration was not straightforward. The Cretaceous and Pliocene-Quaternary erosions estimate, obtained using AFT data (Table 32), were also used to constrain the erosion variable, despite that these data cannot be directly used to calibrate the thermal model results.

3.3.1.5 Source rock parameters

According to the rest of the NAFB, three main source rocks are considered: the marine Posidonia Black Shales (Toarcian in age), the lacustrine Autunian shales (Permian in age), and the Carboniferous coal and shales (Carboniferous in age) (Leu and Gautschi, 2014; Misch et al., 2017; Schegg and Leu, 1998). There is no evidence that the Posidonia shale source rock is present along Section 4, as it has not been found in the Pfaffnau-1 and Entlebuch-1 wells. However, a scenario where the Posidonia shale source rock is present along the entire section, with an average of 3 meters thick, was simulated. In the model, they were assigned the geochemical properties defined in Section 5, which are based on the geochemical analyses performed for these rocks in the Weiach-1, Riniken-1 and Shafisheim-1 wells (Appendix 1). A summary of the data used in the model is presented in Table 34.

The presence of the Permian and Carboniferous source rocks is uncertain along the entire section. The Permian unit was penetrated in the Pfaffnau-1 wells (around 10 meters) and the Carboniferous unit in the Entlebuch-1 well (around 200 meters). In the latter well, the Carboniferous unit was directly below the Mesozoic layers. Therefore, Permo-Carboniferous grabens were considered in these areas. The shape and depths of the grabens were drawn coherently with what was proposed by Leu (2008). It is considered that these grabens contain Permian and Carboniferous deposits rich in organic matter, which could be hydrocarbon source rocks, despite that there is no data to confirm this hypothesis. Therefore, the internal subdivision of these deposits was extrapolated from the well-known Constance Frick Permo-Carboniferous graben (Northern Switzerland) (Madritsch et al., 2018), and regarding the source rocks geochemically properties, specifically from the Weiach-1 well (Ajuaba et al., 2023) (Appendix 2). Therefore, first, the infill of the grabens was subdivided into two units, the Permian (33% of the total thickness) and the Carboniferous (67% of the total thickness). Secondly, in the Permian, for the Autunian lacustrine shales an interbedded layer, with a thickness of 9% of the total Permian unit, was created (maximum thickness of 55 meters). The Permian unit is represented only in the northern graben, because of that in the Entlebuch-1 wells it has not been found. For the Carboniferous source rocks considered (coal and shales) two interbedded layers were created, with a total thickness of 9% of the total Carboniferous unit (maximum thickness of each unit, 28-48 meters). In Table 34 a synthesis of the geochemical properties assigned into the Section 4 model is presented.

Source Rock	Lithology	Present average TOC (%)	Initial TOC (g rock)	Present average HI (mgHC/TOC)	Initial HI (mgHC/TOC)	Kinetic
Posidonia shale	Black shales	5	6.5	565	680	TII(PB) (Behar et al., 1997) _
Permian lacustrine shales	Shale organic rich	4.7	6.2	289	500	TI(C) (Pepper and Corvi, 1995)
Carboniferous coal	Coal	72	75	210	250	TIII-(Dogger) (Behar et al., 1997)
Carboniferous shales	Shale organic-rich	8	8.5	95	150	TIIIH(DE) (Pepper and Corvi, 1995)

Table 34: Present-day and initial geochemical properties assigned into the model for the four source rocks.

Along the section, the internal subdivision of the Permo-Carboniferous grabens in the stratigraphic unit was done following what was proposed by Madritsch et al. (2018) and what was observed in the Weiach-1 well. The total thicknesses of the Permian and Carboniferous source rocks concerning the entire Permian and Carboniferous deposits are 8% and 9% respectively, as observed in the Weiach-1 well. In the southern graben, below the Entlebuch-1 well, it is considered that only the Carboniferous unit is present, as the Permian has not been found in this well.

3.3.2 Boundary conditions

The upper boundary, the sediment-water interface temperature (SWIT), was automatically calculated by the software, for a geographical area located at a latitude of 46°N (present Switzerland latitude) (Fig. 12). The paleowater depth was deduced by the depositional environment of the main stratigraphic units forming the basin and the basal heat flow trend was reconstructed considering the geodynamic evolution of the Molasse Foreland Basin (see Methods section) (Table 35).

Age to (Ma)	PWD (m)	Age from (Ma)	HF value (mW/m2) initially assigned	HF value (mW/m2) calibrating the model
0	0	0	variable*	variable*
22	0	0.4	50	variable*
66	300	5	40	40
		8	50	50
125	100	29	50	50
152	10	80	50	50
160	300	118	60	60
		127	72	72
163.5	100	142	70	70
174.0	300	146	75	75
190	100	172	60	60
201.3	70	200	60	60
252	0	250	60	60
265	0	260	87	87
		270	100	100
		290	120	120
		300	80	80
		400	60	60

Table 35: Paleowater depth (PWD) and basal heat flow variation over time. To calibrate the present-day temperature and the vitrinite reflectance data, the heat flow trend was iteratively changed to obtain a satisfactory result. To fit the calibration data, a variation of the heat flow trend along the section was necessary.

At the present day (0 My) a variation of the basal heat flow along the section was considered (Fig. 56), based on the present heat flow distribution calculated throughout the NAFB (data source: https://map.geo.admin.ch, see Fig. 15).

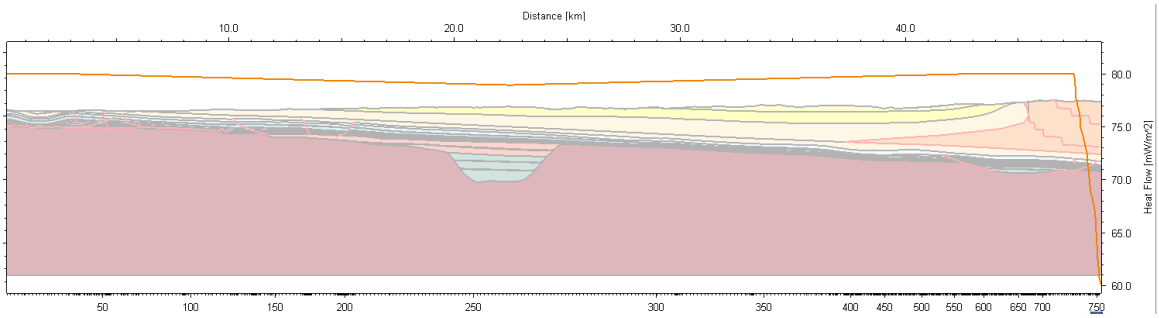


Fig. 56: Basal heat flow assigned along Section 4 at the present-day (0 My).

3.3.3 Results

3.3.3.1 Restoration to the pre-Alpine deformation phases

Because of that, in Section 4 thrusts and inverted faults are present, previous to the thermal modelling workflow, it is essential to realize the structural restoration to the pre-Alpine deformation phase. However, because of that the southern part of the sections passes throughout the triangular zone, a simplified method is applied, which simulates the formation of this complex structure directly in the PetroMod software (see Method section). Therefore, for this section, the TecLink workflow was not applied, which tremendously simplified the modelling workflow.

3.3.3.2 Geological conceptual model evolution

The section extracted from Geomol (Fig. 55) was imported into the PetroMod software and each horizon was assigned to a stratigraphic unit and at a corresponding age (Table 31). The facies previously defined (see Facies in the Data section) were assigned to the stratigraphic units composing the sections (Fig. 57).

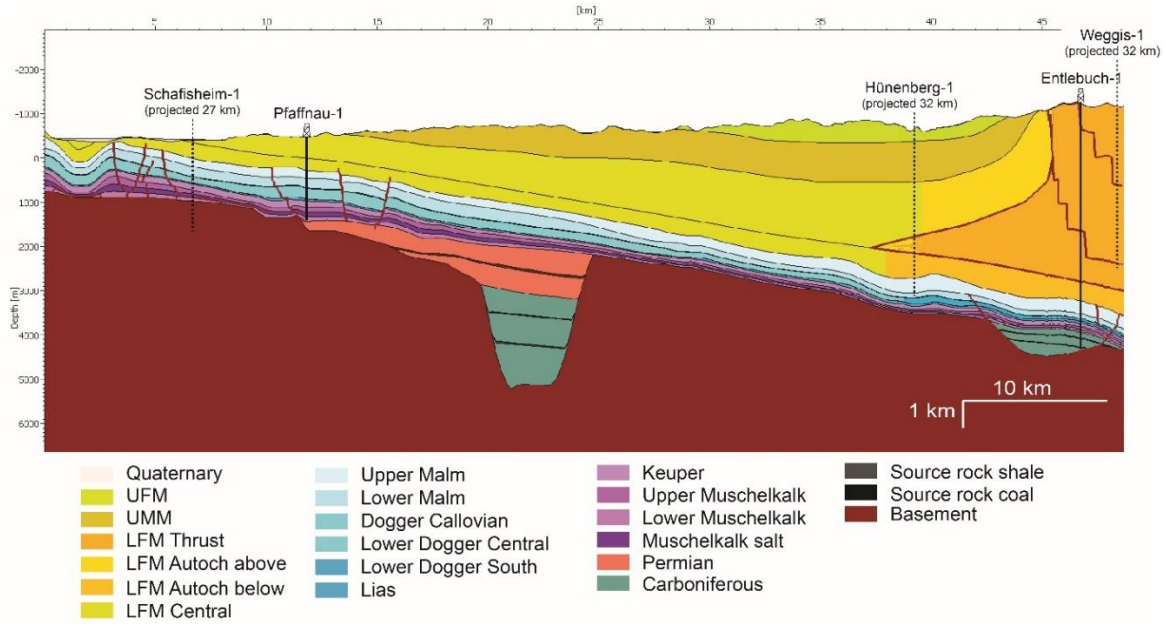


Fig. 57: Section imported in Petromod and used as the geological model. Based on the stratigraphy described in the closest wells, facies were assigned to the present-day section. Sections vertical exaggeration 2:1.

The geological evolution of the basin along this section is shown in Fig. 58. The formation of the triangular zone was simulated in the PetroMod software, through the introduction of an additional layer with paleo-thickness increasing from 7 to 0 Ma. Because of the thrusting and formation of the triangular zone, the Molasse units, located in the southern part of the basin, were uplifted and eroded. In the same period, the Jura structures started forming northward, while the entire basin was exhumed and eroded.

The magnitude of the Pliocene-Quaternary erosion was estimated considering previous literature data (Table 32) and calibrated with vitrinite reflectance data of the Schafischeim-1 well (see Calibration section below). Erosion data estimated along the section from AFT were also considered but modified to harmonize the reconstruction of the geometry of the foreland basin. Therefore, in our model, the Pliocene-Quaternary erosion estimated along the section ranges from 500 meters in the north (projected Sschafischeim-1 well area) to 1000 meters in the central part (Pfaffnau-1 well area) to over 4000 meters toward the southern edge. In the southern extremity of the section, these great erosion values were necessary to geometrically reconstruct the undeformed geometry of the foreland previous to the triangular zone formation. To present there are no calibration data to constrain this data.

To simulate the deposition and the erosion of the Cretaceous, because the Cretaceous layer is not represented along the section, it was assigned an additional paleothickness at the Malm unit, from 145 to 90 Ma, which was removed from 90 Ma to 56 Ma as the effect of the erosion. The thickness of the eroded Cretaceous deposits is 700 meters along the entire section. For the Permo-Triassic unconformity, it was considered an erosion of 500 meters of Permian deposits, located on the top of the Permo-Carboniferous grabens.

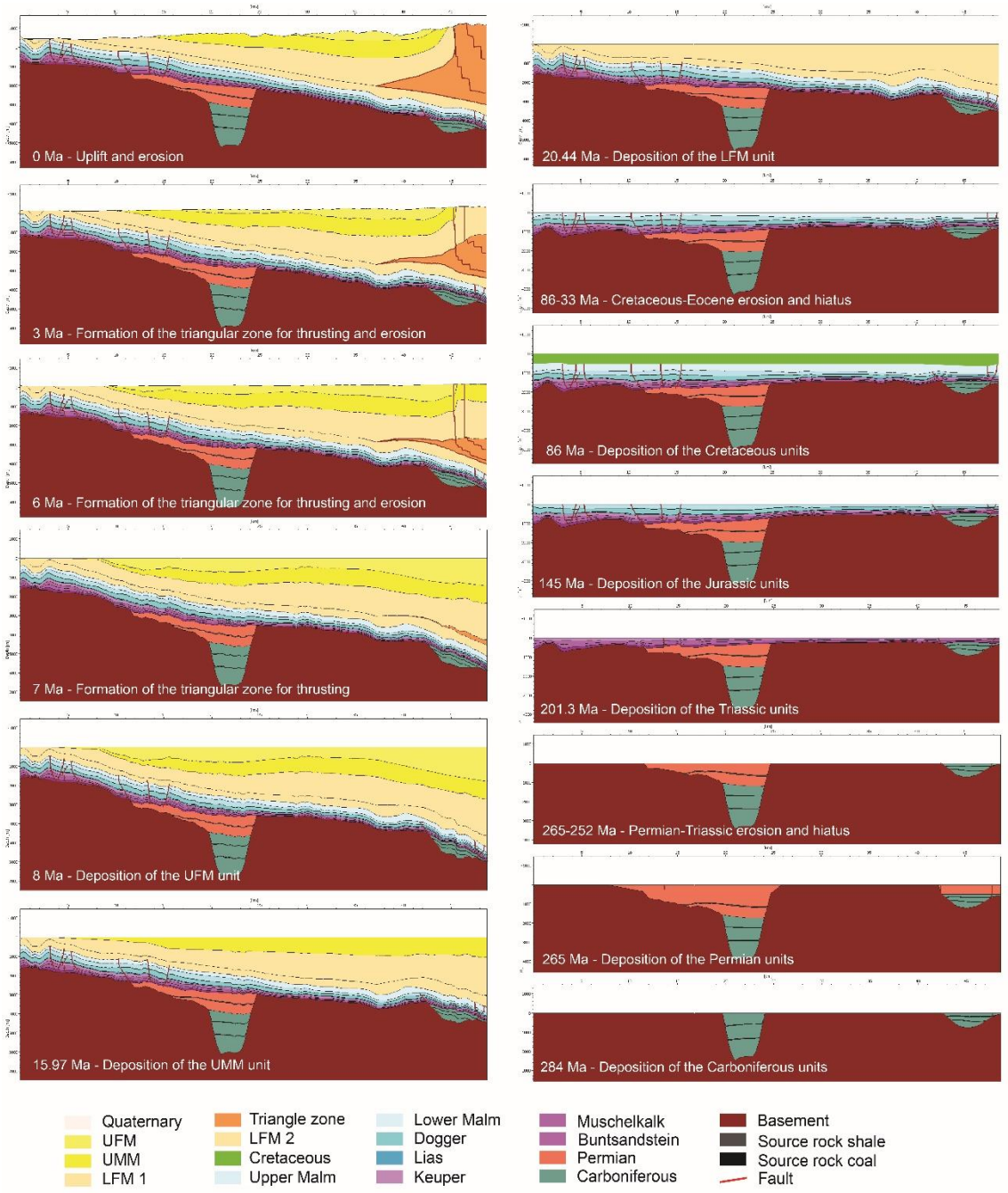


Fig. 58: Geological evolution of the studied area obtained in Petromod by retrodeformation and decompaction of the units forming the basin infill, from the present-day to the Carboniferous time. Sections vertical exaggeration 2:1.

3.3.3.3 Thermal model calibration

3.3.3.3.1 Porosity

The porosity was calibrated for the Pfaffnau-1 well (Fig. 59) and the calibrated values were assigned along the entire section (Fig. 60). Porosity values measured along the Schafisheim-1 (projected 27 km) and Hünenberg-1 (projected 32 km) wells were also considered and used to calibrate the model. The mechanical compaction properties estimated by the software for the lithologies assigned to each stratigraphic unit were iteratively changed to fit the theoretical values calculated by the model with the porosity values measured along the wells. The porosity of the

uppermost Molasse units (UFM and UMM) was extrapolated from the values measured for the LFM in the Pfaffnau-1 well.

The porosity extrapolation performed here along the section can be highly uncertain, especially, but not only, in the case of the predominantly limestone units (Mesozoic), where the porosity and permeability are strictly controlled by diagenetic processes and fracking, which can dramatically change from one point to the other of the basin. To reduce this uncertainty, more porosity data with depth should be available along the section.

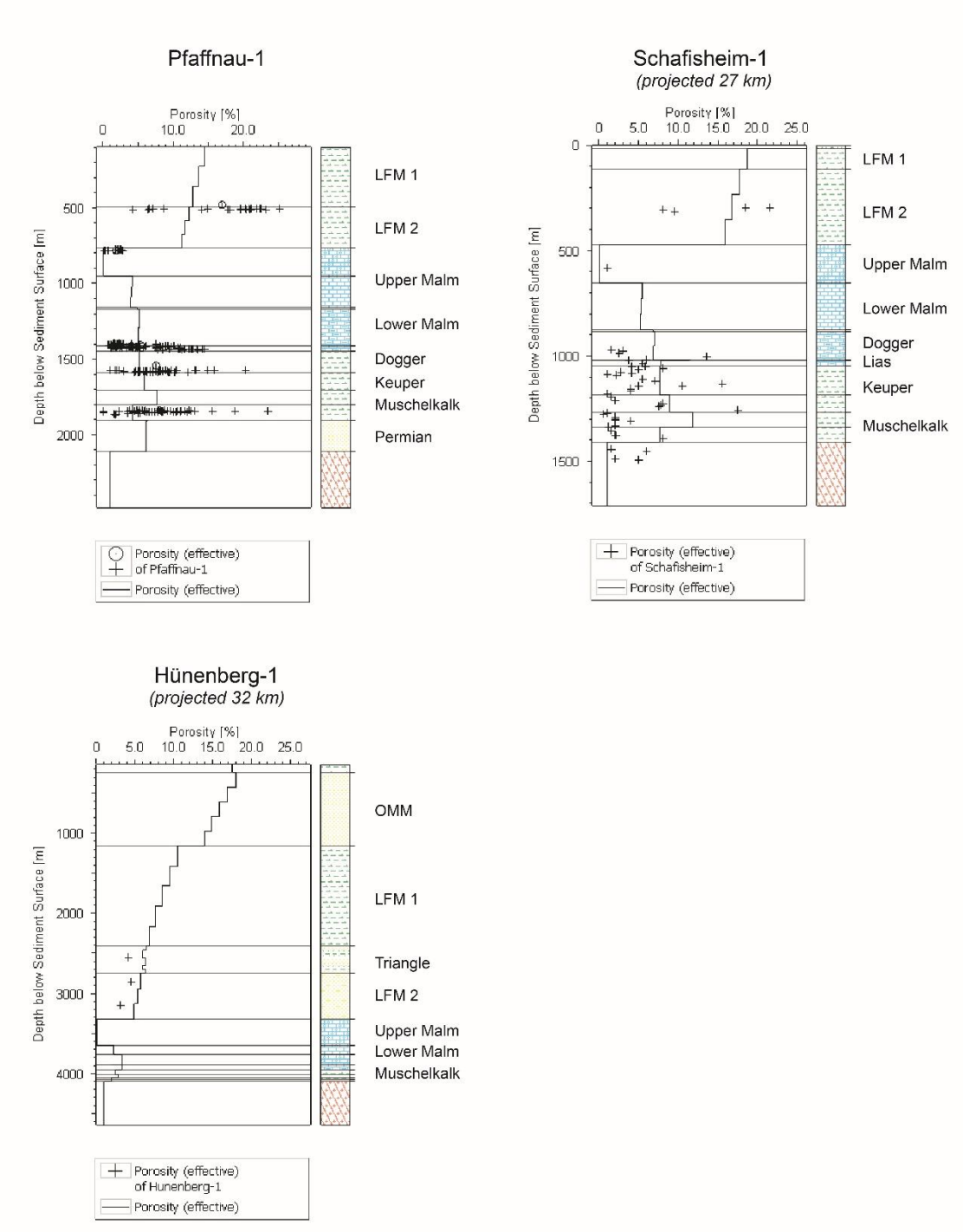


Fig. 59: Calibration of the porosity property with the data measured in the Pfaffau-1, Schafisheim-1 and Hünenberg-1 wells.

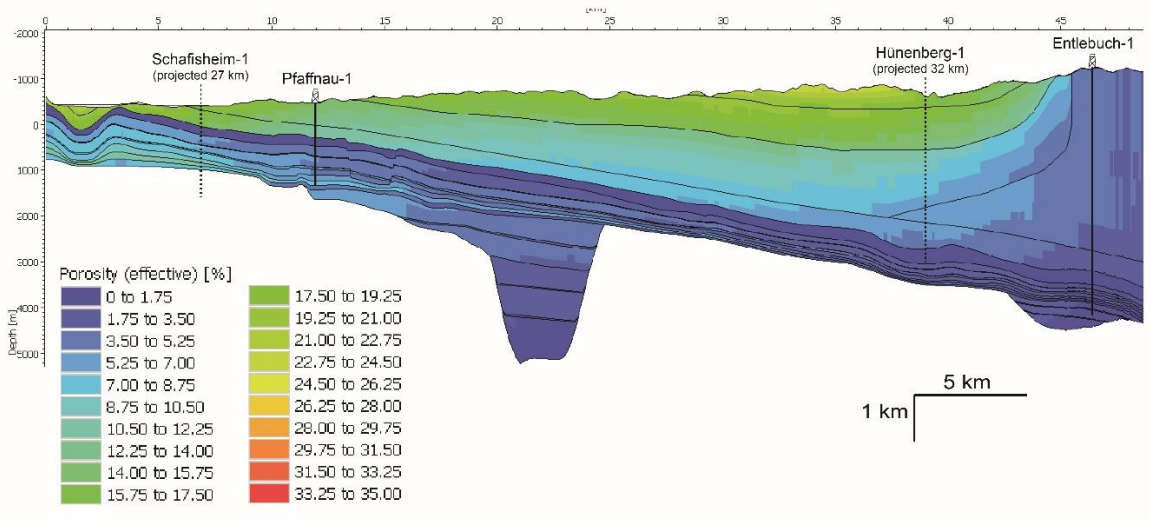


Fig. 60: Porosity modelled by the software along the section, extrapolating the data calibrated in the Pfaffnau-1, Schafisheim-1 and Hünenberg-1 wells.

3.3.3.3.2 Present-day temperature

The present-day temperature calculated by the model was calibrated with the borehole temperature (BHT) measured in the wells Pfaffnau-1, and Entlebuch-1. Temperature data measured in the Weggis-1 (projected 21 km), Hünenberg-1 (projected 32 km) and Shafisheim-1 (projected 27 km) wells were also considered, despite that, because of that they are considerably far from the section trace, the calibration of these data is less relevant. To calibrate the modelling results, the variable that mostly changed was the present-day basal heat flow (see Method section). Firstly, it was tested the heat flow values estimated in the entire basin from borehole temperature data (Fig. 61, scenario A). This scenario does not give satisfactory calibration results, as the temperature simulated by the model is considerably higher than what is measured in the wells (Fig. 62). This is because the heat flow values of Scenario A represent the heat flow at the surface, whereas the heat flow that was assigned into the model refers to the amount of heat at the base of the model, basement included. Toward the basin surface, this heat is increased, mostly by the radiogenic heat produced by the basement and basin infill rocks. The effect of the rapid exhumation of the NAFB can also play a role in maintaining an anomalously high heat flow at the surface of the basin.

Another heat flow scenario is tested for 0 Ma (Fig. 61, scenario B), with values in the range of 30 mW/m2 along the entire section. In the Pfaffnau-1 well area, to calibrate the temperature data measured in this well, the heat flow was lowered to 6 mW/m2. This scenario considerably improves the calibration of borehole temperatures measured in the Pfaffnau-1, Entlebuch-1, Hünenberg-1 and Weggis-1wells (Fig. 62). The temperature measured in the Schafisheim-1 well is partially calibrated. However, as the well is located 30 km away from the trace, this discrepancy is considered as not relevant. According to the calibration results with Scenario B, the model calculated the temperature distribution along the section in the present day (Fig. 63).

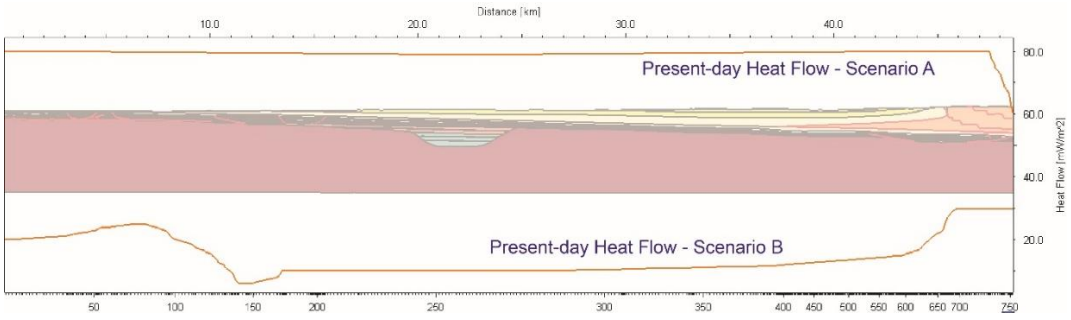


Fig. 61: Heat flow values assigned along the modelled section at 0 Ma. The two scenarios tested are shown.

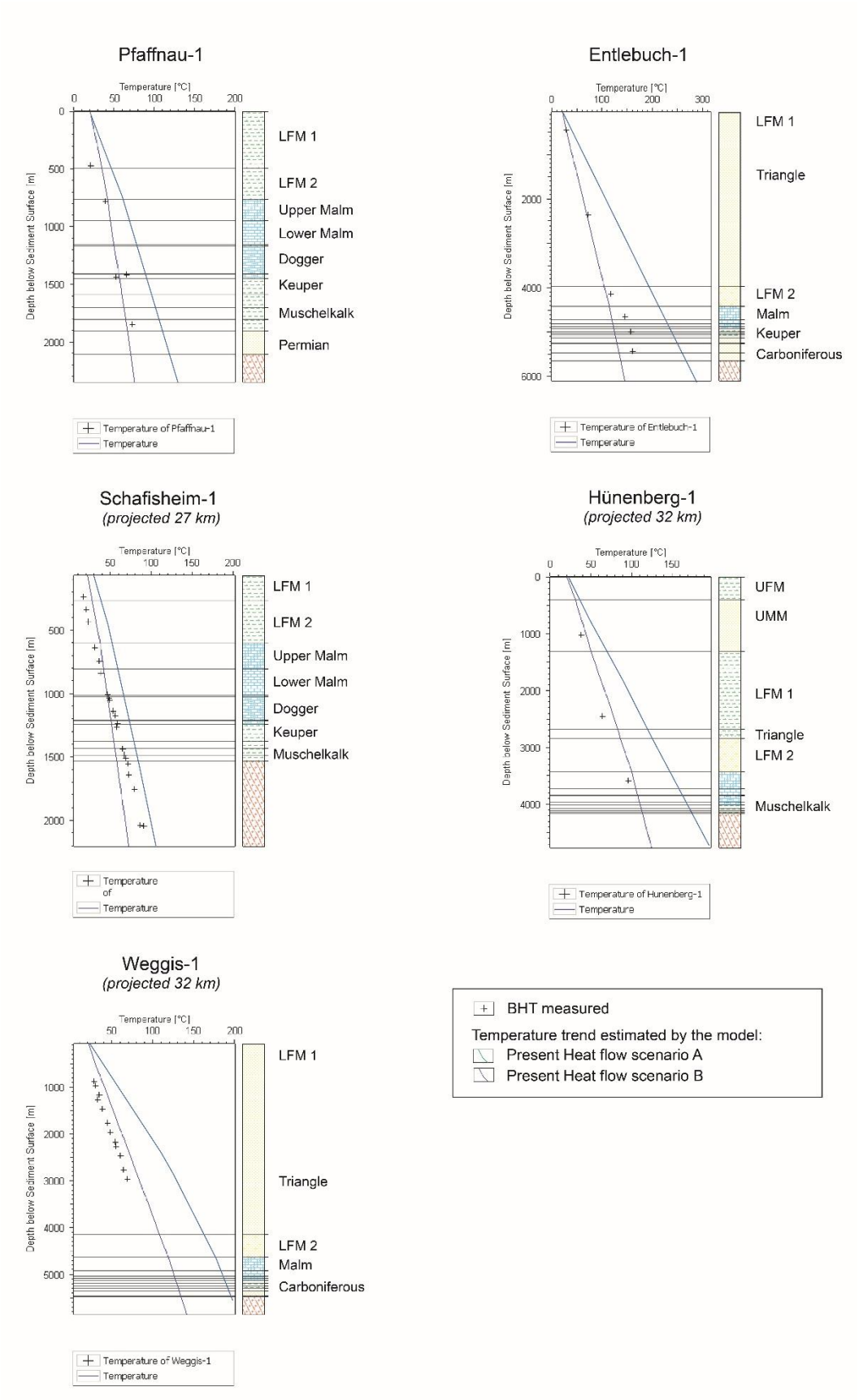


Fig. 62: Calibration of the present-day temperature modelling results with the BHT measured in the wells closest to Section 4.

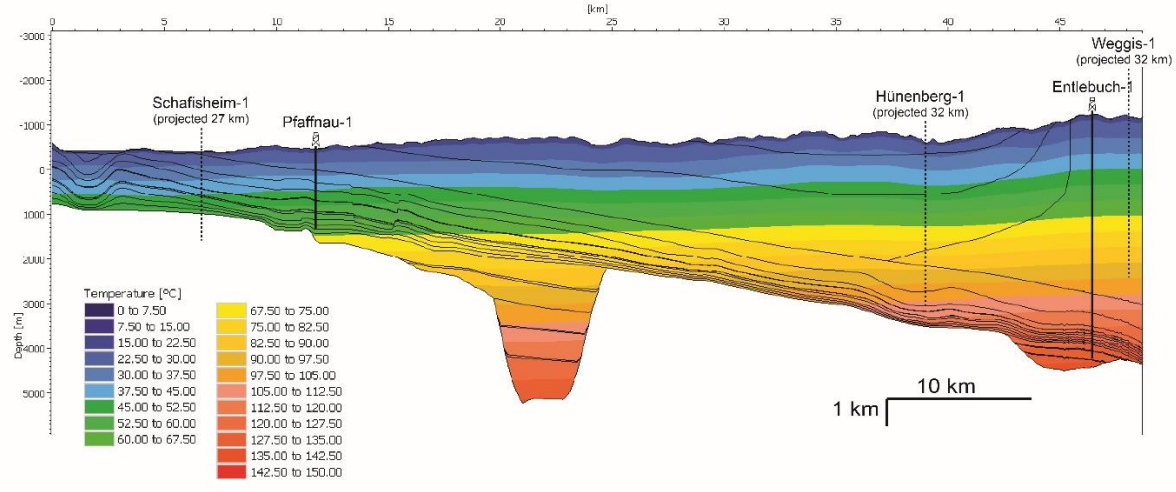


Fig. 63: Temperature variation with depth and along the section calculated by the model for the present day (0 My), calibrated with the present-day heat flow scenario B.

3.3.3.3.3 Thermal conditions / Source rocks maturity

Because of that there are no VR data measured in the wells located along the Section 4 trace, so validating the thermal conditions calculated by the model along the section is not straightforward. The northern part of the model was calibrated with respect to the %Ro data measured along the Schafisheim-1 well. Because it is located nearly 30 km from the section trace, uncertainties in the results must be considered. The southern part of the section is not calibrated. The %Ro values measured in Schafisheim-1 well were satisfactorily calibrated with nearly 1000 meters of Plio-Quaternary erosion (Fig. 64). The thermal conditions resulting along the entire section are shown in Fig. 65.

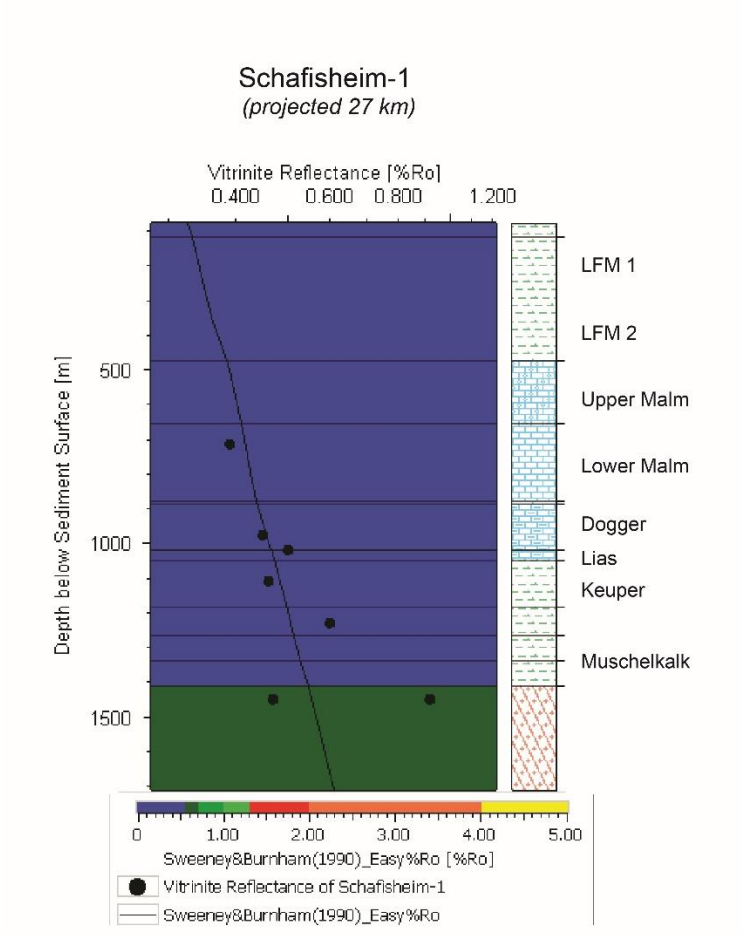


Fig. 64: Calibration of the thermal conditions calculated by the model with %Ro data measured for the Shafisheim-1 well.

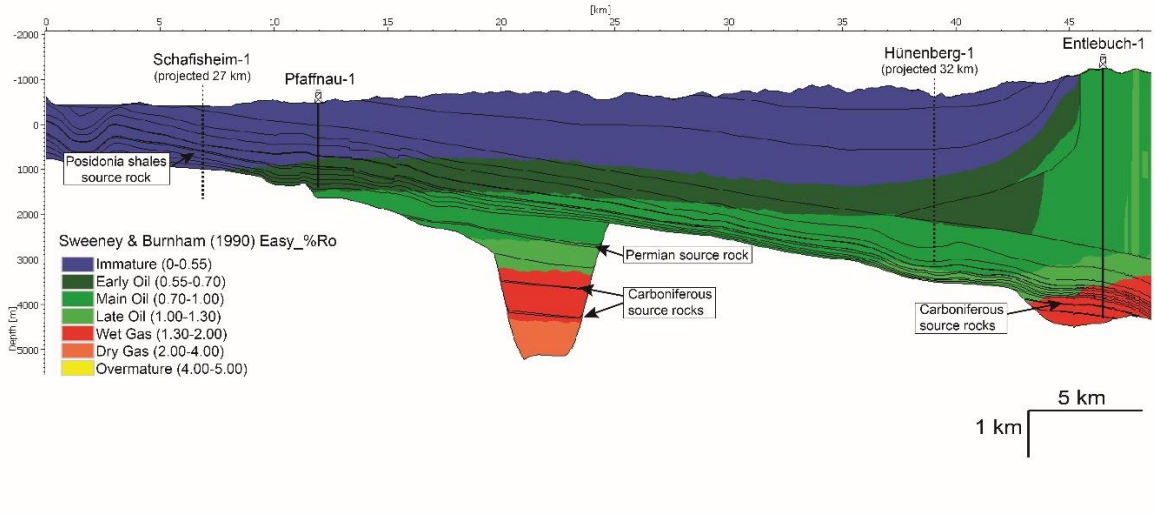


Fig. 65: Thermal conditions calculated by the model along the entire section

From the modelling results it is deduced that the Posidonia shale source rock, if present, is in the immature thermal stage on the northern edge of the section (Schafisehim-1 well area) and the oil window thermal stage and the central to the southern part. The Permian source rock is in the late oil window thermal conditions in the Permo-Carboniferous graben located in the central part of the

section. The Carboniferous source rocks are in the wet gas thermal conditions in both central and southern grabens.

The source rocks maturation timing is deduced by the burial plot vs thermal conditions extracted at the Pfaffnau-1 and Entlebuch-1 wells position (Fig. 66). In the northern part of the section (Pfaffnau-1 well area), the Lias unit (Posidonia shale source rock) enters in the oil window in the Miocene and the Permian source rock in the Cretaceous (deepest layers) and in the Oligocen-Miocene time. In the southern part of the section (Entlebuch-1 well area), the Carboniferous source rock enters the oil window in the Oligocene.

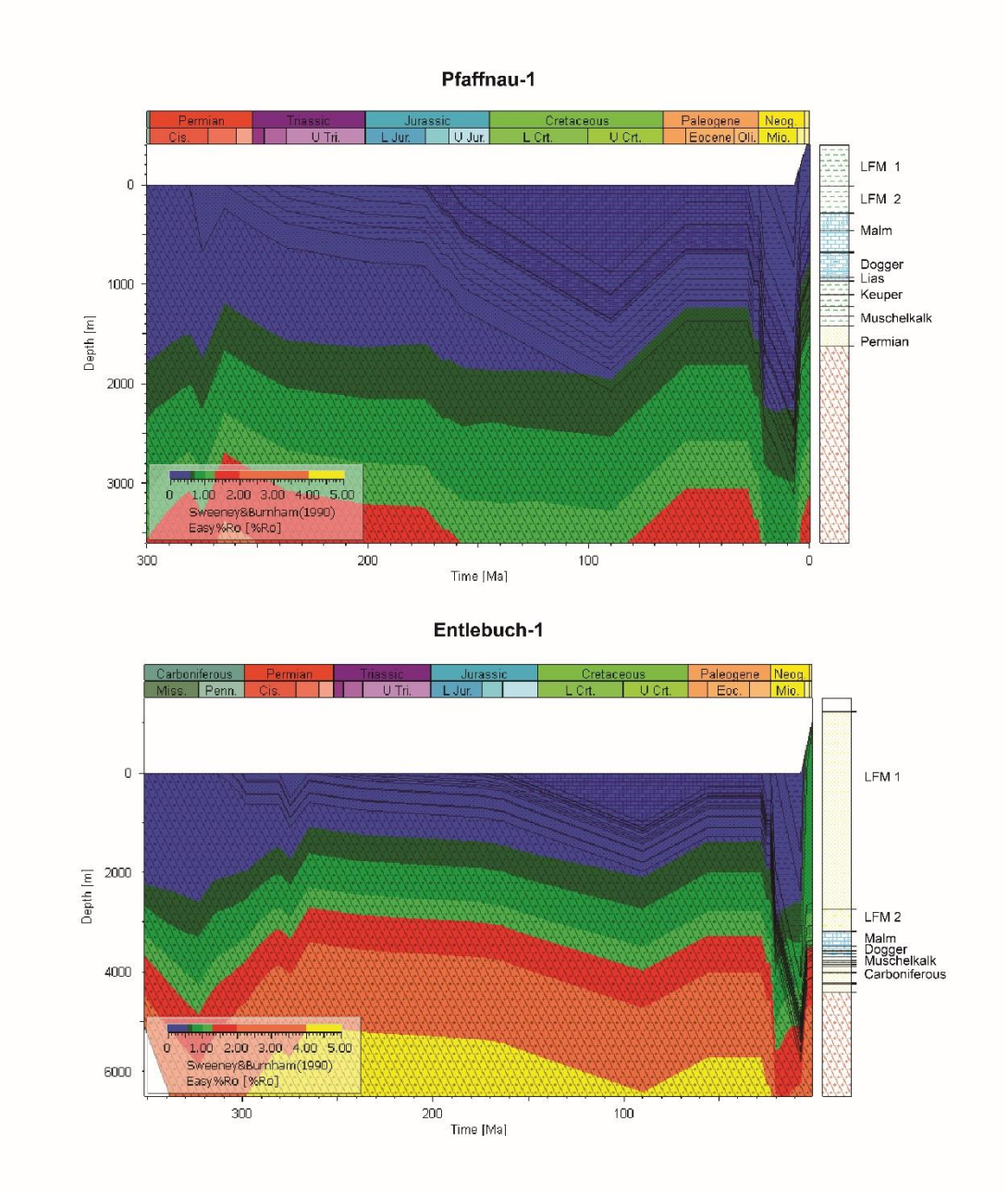


Fig. 66: Burial plot versus thermal maturity conditions, showing the time when the source rocks (Lias, Permian, Carboniferous) were matured.

3.3.3.4 Simulation of the hydrocarbon generation, migration and accumulation processes

The model simulates the hydrocarbon generation, migration and accumulation processes for Section 4, as an effect of the source rock maturation and hydrocarbon expulsion. Migration paths and potential reservoirs are calculated based on the geometry of the basin and the permeability

properties of its infill. Hydrocarbons were generated by the Permian, Carboniferous and Posidonia shale source rocks, at different times. A first-generation peak occurred in the Permian, because of the burial of the Permian and Carboniferous source rocks in the grabens. A second larger generation peak occurred in the Cretaceous when the basin was affected by another burial event and heat flow peak, and thirdly, the most relevant, in the Cenozoic (Fig. 67), when the formation and infill of the foreland basin increased abruptly the burial depth of the basin.

The rocks that generate the greatest volume of hydrocarbons are the Carboniferous source rock, followed by the Permian source rock, and finally the Posidonia shale (Fig. 67). The Carboniferous source rocks start to generate in the Permian time, whereas the Posidonia shale source rock starts to generate in the Miocene when the northern part of the basin was buried enough to mature these deposits.

Conventional high permeable reservoir form in the Jurassic-Cretaceous and Cenozoic times, mostly in the Malm (Entlebuch-1 area) and secondly in the Molasse units. Accumulations in low permeable units (petroleum saturated) are volumetrically higher than accumulations in proper reservoirs and they mostly form in the Permian, Carboniferous and Lias deposits, and in smaller amounts, also in the Dogger unit.

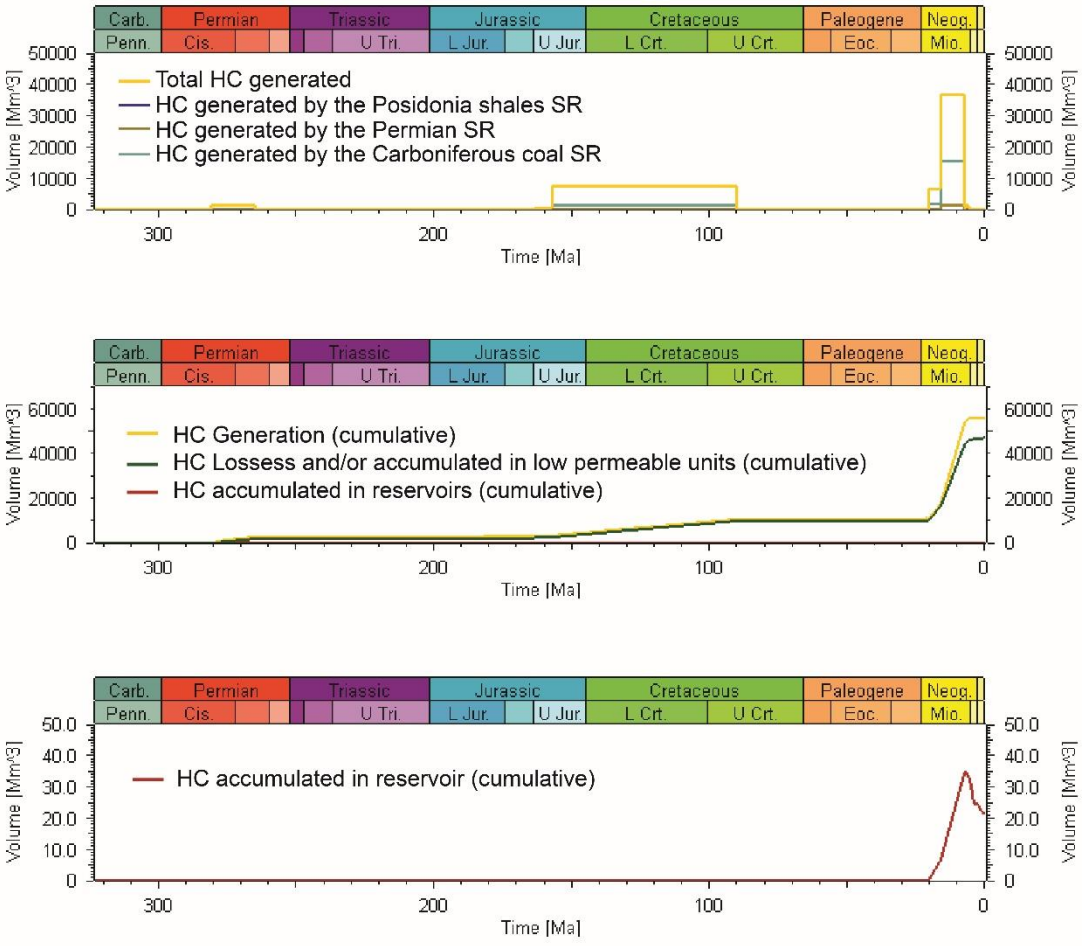


Fig. 67: Hydrocarbon generation and accumulation balances calculated by the software for the entire section

In the “open faults” scenario, where the faults were considered as not cemented, the model simulates the formation of hydrocarbon accumulations mostly in the proximity of the Permo-Carboniferous grabens, where deep faults connect the Permian and Carboniferous deposits to the Mesozoic sequence (Fig. 68). Gas accumulations were simulated in the southern area of the section, in the Malm unit, where hydrocarbons were effectively found in the Entlebuch-1 well, the

only economically gas field of Switzerland discovered and exploited (Lahusen and Wyss, 1995). Hydrocarbon accumulations, mostly formed by oil and secondly by gas, are simulated in the Pfaffnau-1 well area, in the Malm unit. They can be generated by the Posidonia shale, Permian and Carboniferous source rocks, located stratigraphically below and migrating to the uppermost units along Mesozoic faults. In the model, in the Pfaffnau-1 area, gas is also migrating from the southernmost part of the basin, along the northward dipping foreland basin monocline, and vertically raising the subsurface through the Molasse unit. In this area, gas has been recently found during the drilling of shallow geothermal wells (https://www.20min.ch/fr/story/du-gaz-naturel-sechappe-lors-dun-forage-geothermique-270308636433). Differently from the other sections, in this section hydrocarbon accumulations do not form in the Permian and Triassic units, whereas mostly in the Jurassic (Malm) unit. This is because along this section the Muschelkalk is not composed of proper reservoir facies. Further studies need to be carried out to constrain this data.

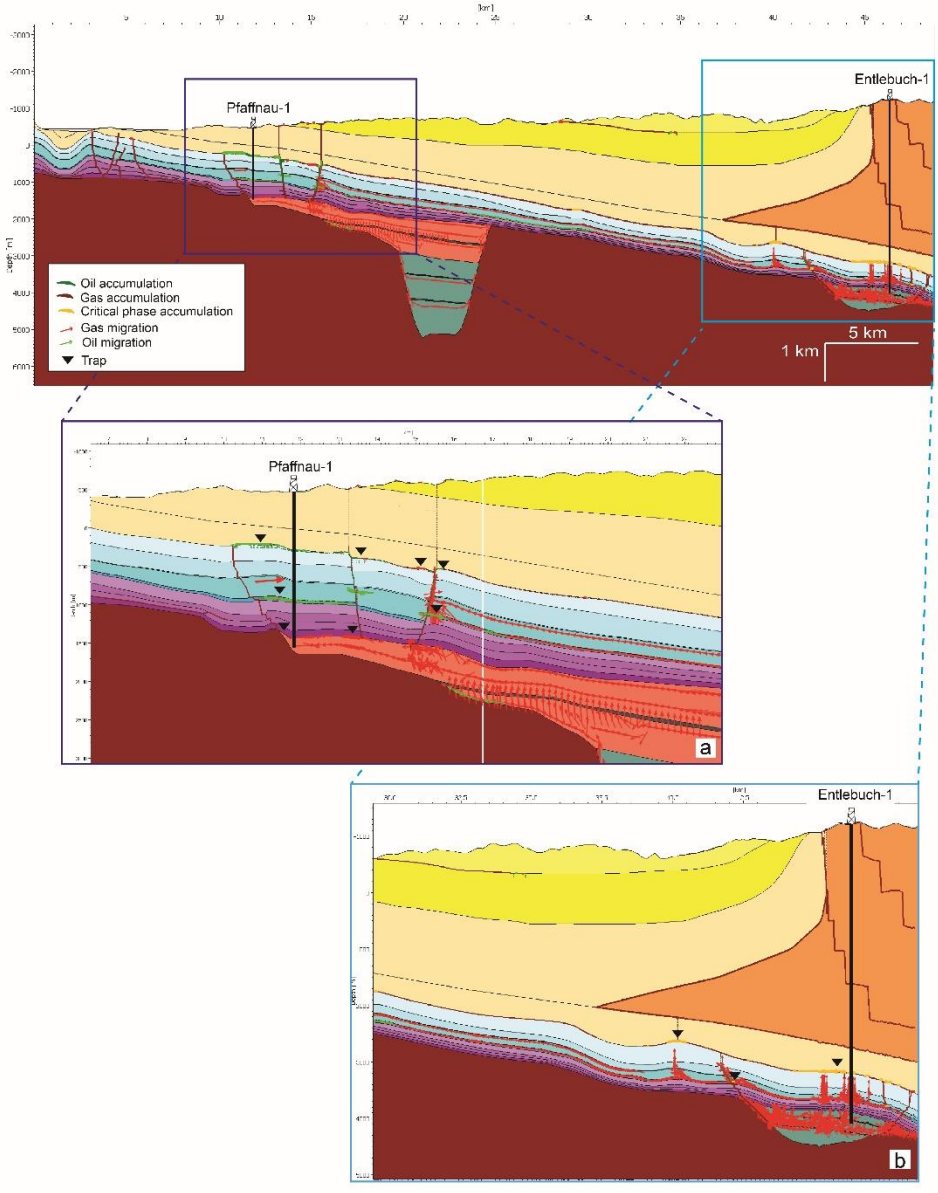


Fig. 68: Hydrocarbon accumulations and migration paths calculated by the model along section 4, in the “open faults” scenario. In (a) zoom on the central area of the section (Pfaffnau-1 well), and in (b) zoom on the southern area of the section (Entlebuch-1 well). Potential traps are indicated.

A second scenario was simulated, considering the “closed faults” option (Fig. 69), where the faults were considered as cemented. The main differences with the “open faults” scenario are in the

northern part of the section, whereas the results in the southern parts are very similar. By this option, fewer reservoirs are formed in Jurassic units, as the hydrocarbon leakage and migration from the Permian and Carboniferous source rocks to the uppermost stratigraphic units is less efficient.

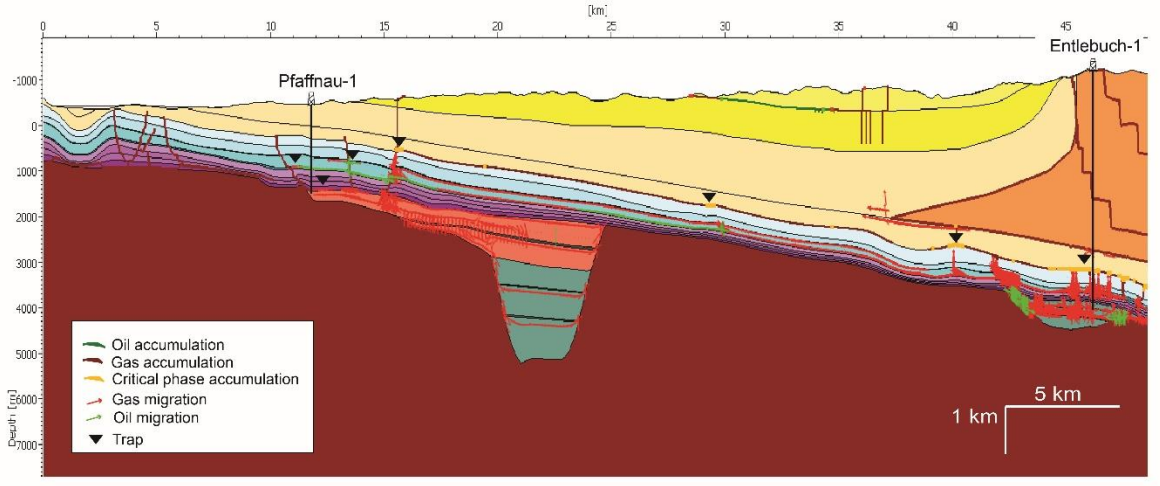


Fig. 69: Hydrocarbon accumulations and migration paths calculated by the model along section 4, in the “closed faults” scenario. Potential traps are indicated.

In Fig. 70 the hydrocarbon accumulations over the basin evolution are shown. The thermal maturity is also represented. In the northern part of the section, the Permian and Carboniferous units have entered the oil window since the Permian-Triassic times, as in this part of the section the grabens are very deep. The hydrocarbon accumulations in the Permian unit have started forming since the Triassic and Jurassic times when the entire Permian and Carboniferous source rocks in the northern part of the section entered the oil and gas windows. In the southern part of the section, hydrocarbon accumulations started forming since the deposition of the Molasse units, when the Permian and Carboniferous source rocks entered the oil and gas windows because of the rapid burial of the basin. The accumulations formed in the Permian unit were poorly preserved, as most of the hydrocarbon migrated to the uppermost units through faults. Most of the hydrocarbon generated by the Posidonia shale source rock, as well as part of the hydrocarbons generated by deeper source rocks, migrated vertically to the top surface and were lost, because of the lack of proper traps. Accumulations preserved until today mostly form, along the entire section, in the Jurassic units, in the Cenozoic time, when small stratigraphic and structural traps were formed.

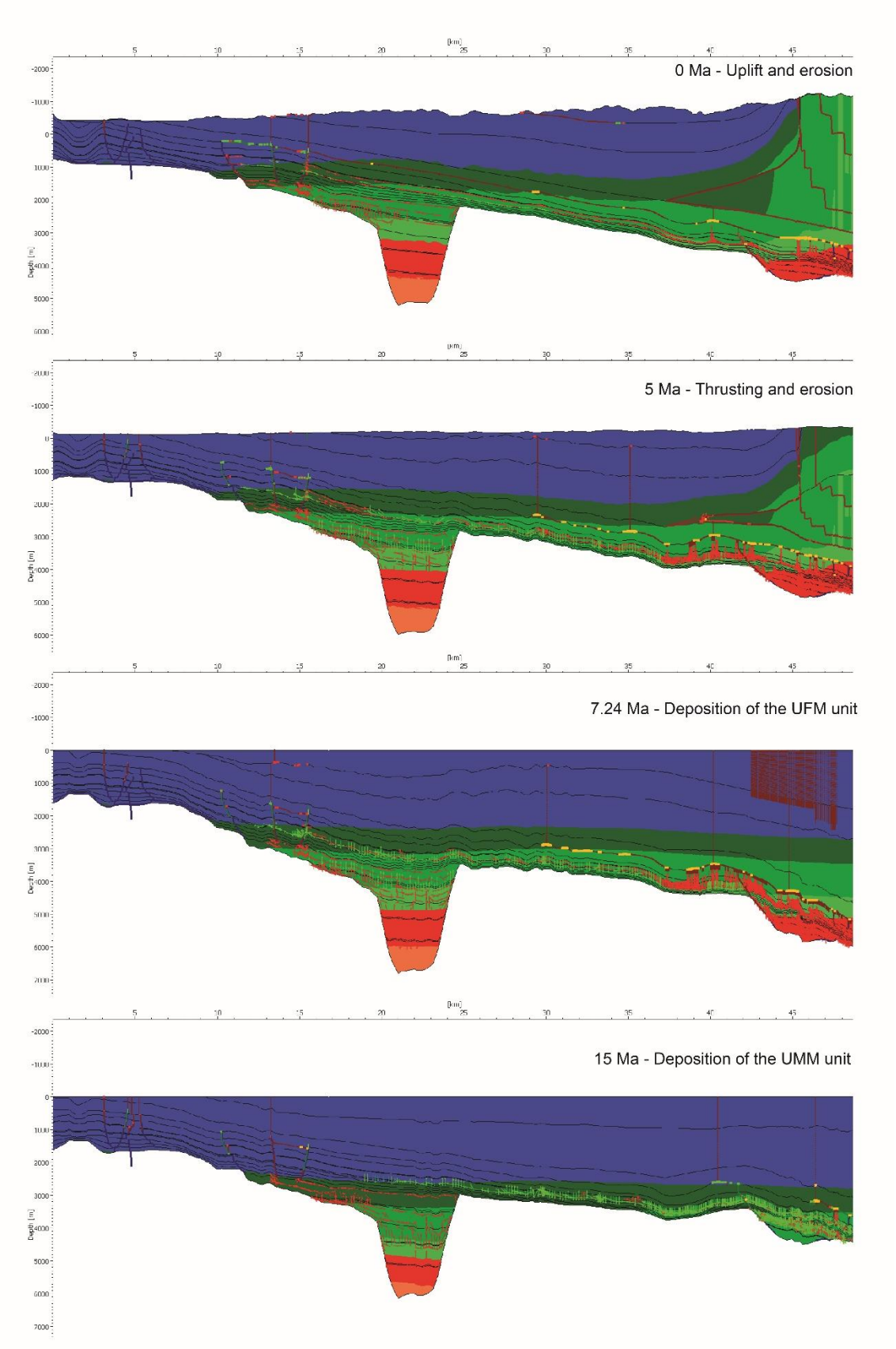


Fig. 70: Hydrocarbon accumulations over the evolution of the basin (continues).

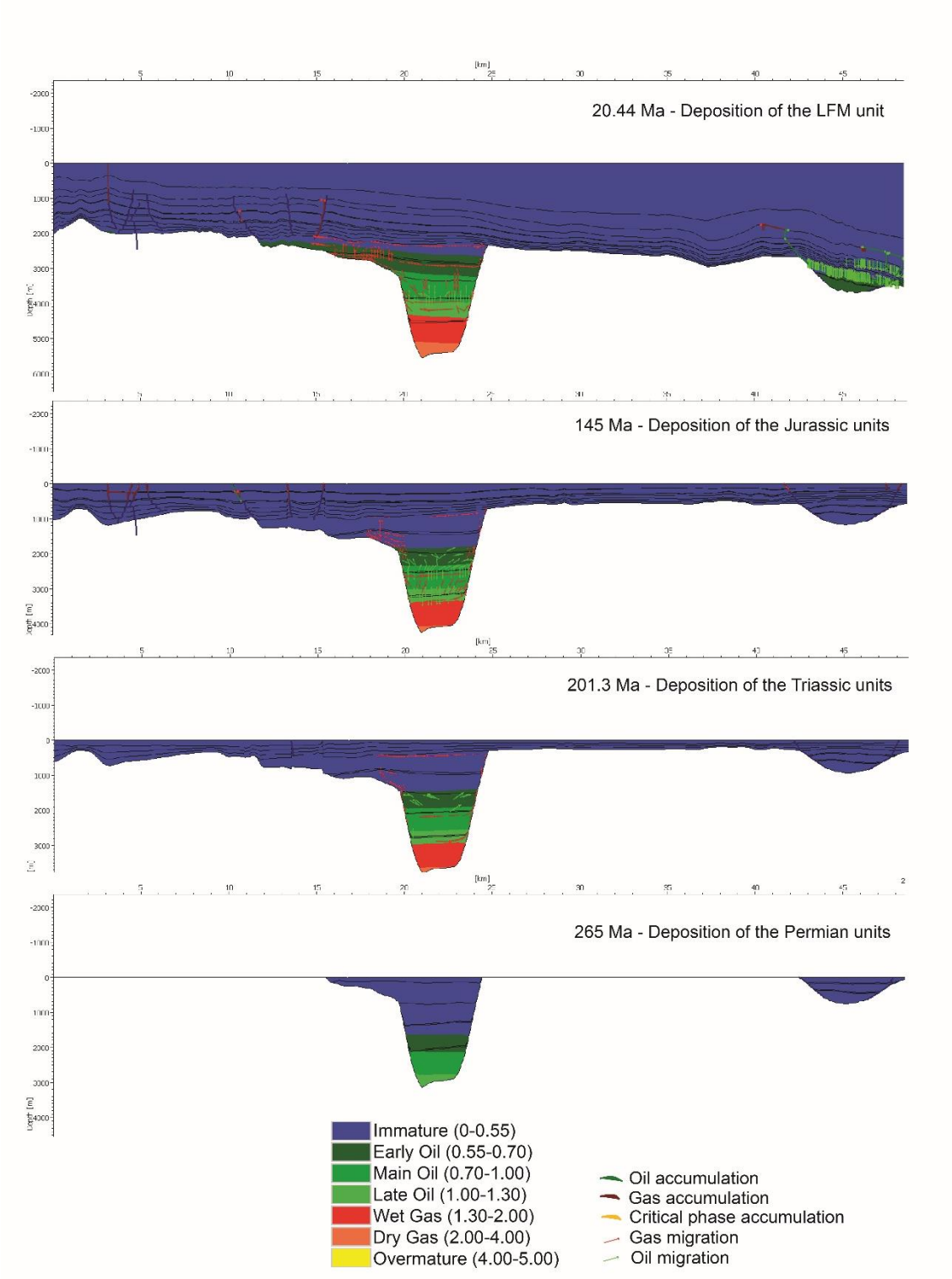


Fig.70 (continues): Hydrocarbon accumulations over the evolution of the basin

The petroleum system evolution for the four source rocks considered is shown in terms of the petroleum system chart (Magoon and Dow, 1994) (Fig. 71), where the source rocks, reservoir, seal, overburden rocks and trap elements are defined. The critical moment is defined considering the fit among the formation of reservoirs, traps, the maturation timing of the source rocks and the hydrocarbon generation timing (Fig. 71).

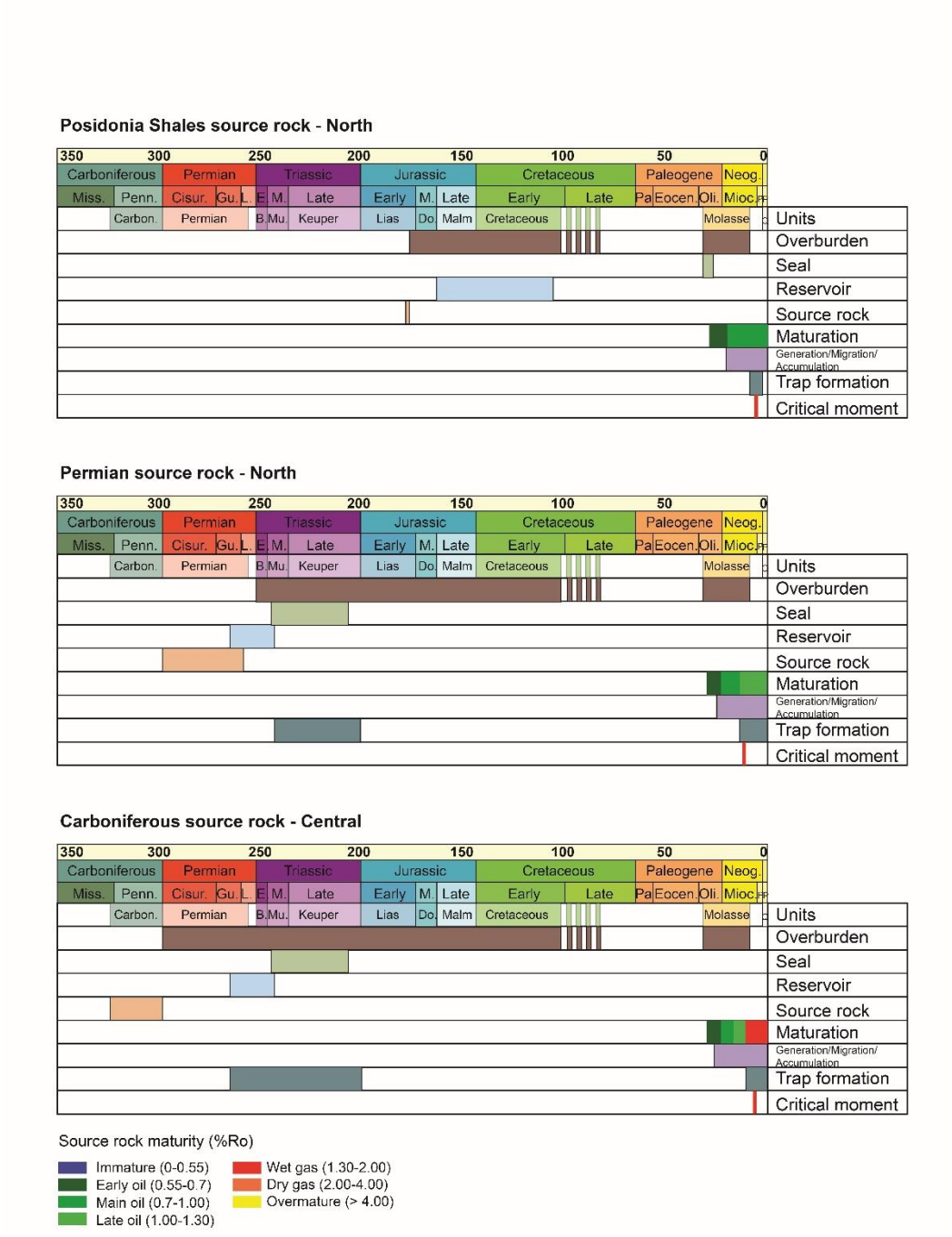


Fig. 71: Petroleum system charts reconstructed for the four source rocks defined in Section 4 (continues).

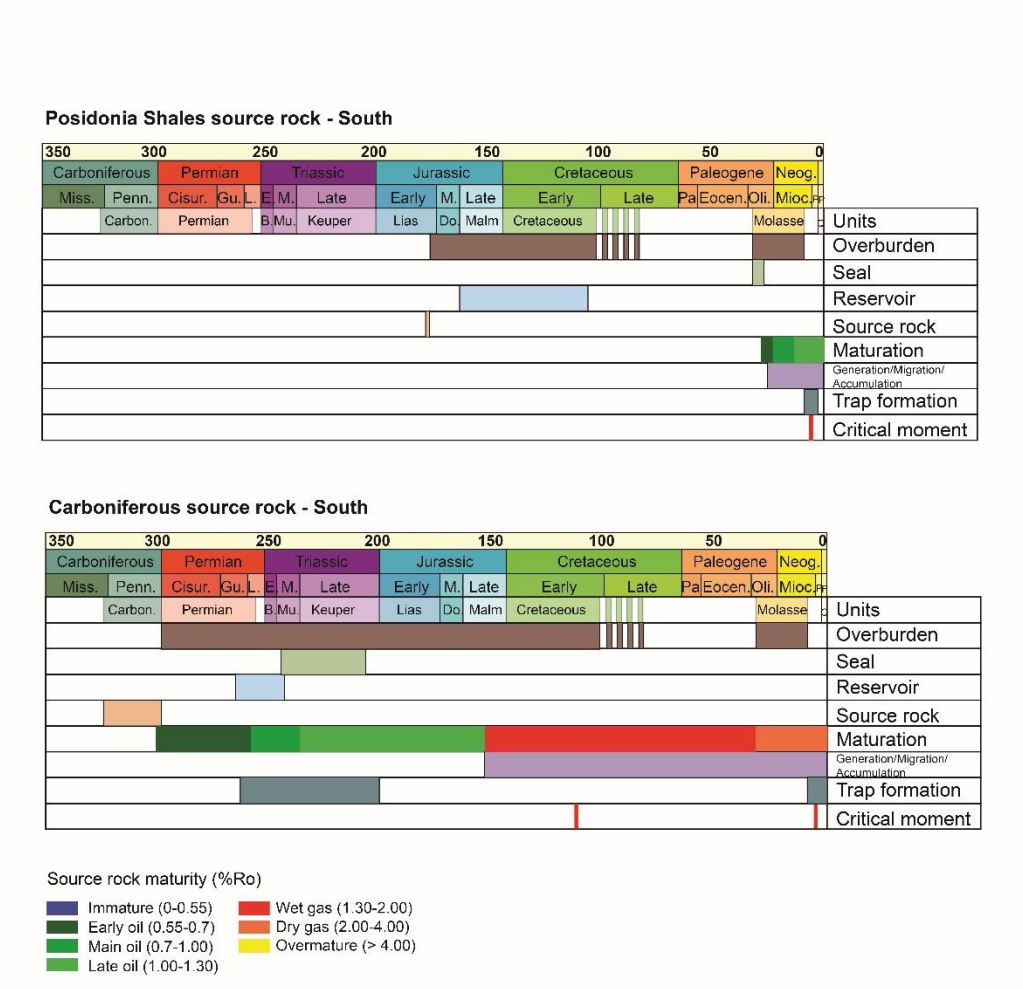


Fig. 71 (continues): Petroleum system charts reconstructed for the four source rocks defined in Section 4.

3.3.3.5 Comparison between the hydrocarbon findings and the modelling results

Despite that the modelling results are in general good agreement with what was found in the wells, some discrepancies exist (Table 36), which reasons could be the following:

- The Permian and Carboniferous source rocks' thickness and hydrocarbon potential could be overestimated. In the Pfaffnau-1 well area, a Permo-Carboniferous graben has been estimated based on seismic data, with low resolution making uncertain the extension and depth of the graben. In the Pfaffnau-1 well only a few meters of Permian deposits were penetrated. Therefore, it is unknown the presence, thickness and geochemical properties of the potential Permian and Carboniferous source rocks. In the model, they extrapolated the properties measured in the Weaich-1 well, which could be not representative of what is effectively present in the area. In the Entlebuch-1 well, the Carboniferous deposits were penetrated. However, geochemical data for this unit to properly characterise it as source rock are not available. Therefore, also in this case the Carboniferous source rock properties were extrapolated from the Weiach-1 well, which could not be representative.
- In the model the basement faults bounding the P-C grabens are considered as continuous into the Mesozoic sequence. This facilitates the migration of the hydrocarbons generated by the Permian and Carboniferous source rocks into the basin, which could not be the case if these faults do not continue. Thus, by this option, the formation of reservoirs in the Mesozoic and Cenozoic units would be less relevant.
- The seal of the Muschelkalk reservoir (Keuper unit) is less efficient than what is calculated by the model. Pervasive fracturation can be present in the faulted areas. Indeed, anhydrites and

evaporites can be interlayered also with dolomite, shales and thin sandstone layers. Thus, this seal might have also an important brittle component, reducing its efficiency.

- More efficient lateral traps than what is crossed by the modelled section can be present. In this case, hydrocarbons could migrate and accumulate in the closest reservoirs. The Thun-1 well is not exactly located at the top of the section trace, thus lateral variation of the trap's geometry is possible.

Well	Hydrocarbon finding	Modelling results	Discrepancy causes
Pfaffnau-1	• Oil traces in the LFM Molasse unit; • Gas shows during the drilling of a shallower geothermal well	• Oil and gas accumulations in the Malm unit; • Oil and gas migration paths along the Lias and Dogger units, migrating from the Posidonia shale and Permo-Carboniferous source rocks; • Gas vertically migrating to the subsurface through the Molasse unit.	• Permo-Carboniferous source rocks thickness and properties overestimated • The deep Permo-Carboniferous faults do not continue into the Mesozoic sequence • Seal not efficient • Lateral migration
Entlebuch-1	• Gas reservoir in the Malm unit	• Large gas reservoir in the Malm unit	• Permo-Carboniferous source rocks thickness and properties overestimated • The deep Permo-Carboniferous faults do not continue into the Mesozoic sequence • Seal not efficient • Lateral migration from traps

Table 36: Comparison between the hydrocarbon findings in the wells located close to the section trace and the modelling results. In case of discrepancy, the potential causes are indicated.

3.3.4 Uncertainties

The petroleum system model presented herein estimates the thermal maturity of the potential source rock, the type and amount of hydrocarbon generated and the potential areas where hydrocarbon can be accumulated and/or flow. However, because of the several assumptions made in constructing the model, several key uncertainties in the results must be considered. The most uncertain variables controlling the modelling results presented are listed in Table 37. A synthesis of the decision process carried out to handle the presented uncertainties is shown in Fig. 70.

Parameter	Uncertainty	Cause	Options	Effect on the Petroleum System Evolution	Impact	Potential improvements
Geometry of the basin	Horizons geometry, depth, presence of stratigraphic unit.	Interpolation of a few 2D seismic lines across the Plateau. Few deep wells to corroborate the seismic data.	GeoMol 2021 Sommaruga et al. (2012)	Accumulation and migration areas can be different.	Medium	Acquisition of new 2D and 3D seismic and/or reprocessing of the existent geophysical data.
Faults	Faults location, extension, geometry.	Low-resolution seismic data.	GeoMol 2021 Sommaruga et al. (2012) Greber et al. (2007)	The hydrocarbon migration can be different from what is simulated by the model.	Medium/High	Acquisition of new 2D and 3D seismic and/or reprocessing of the existent geophysical data.
	Faults connectivity and cementation state.	Very scarce direct measurement and description in well reports.	Faults open (not cemented) Faults close (cemented)	The volume of hydrocarbon accumulations simulated by the model can be different.	Medium	Sampling fault cement; Monitoring fluids flow.
	Continuity of the basement faults bounding the P-C grabens into Mesozoic and Cenozoic.	Low seismic resolution.	Yes. By this option, the model can simulate the hydrocarbon migration from the P-C graben to the uppermost basin infill No. By this option, the model is not able to simulate the hydrocarbon migration from the P-C graben to the uppermost basin infill	Hydrocarbons migration from the Permian and Carboniferous source rocks to the Mesozoic and Cenozoic deposits can be different.	High	Acquisition of new 2D and 3D seismic and/or reprocessing of the existent geophysical data.

Parameter	Uncertainty	Cause	Options	Effect on the Petroleum System Evolution	Impact	Potential improvements
Facies	Facies distribution.	Data are available only where deep wells are present. Facies are deduced from qualitative descriptions in the well report, there are no quantitative data.	Facies extrapolated only from the wells located along the transect.	Hydrocarbon migration paths and/or accumulations can be different.	Medium/High	Acquisition of new stratigraphic, petrographic and geochemical data of the basin infill.
			Facies extrapolated also from the wells located at an offset of nearly 20 km from the transect.			
Structural evolution	Timing and magnitude of thrusting	Scarce data dating the thrusting and able to calibrate the magnitude of the erosion in the South.	Thrusting starts at 7 Ma, after the deposition of the Molasse units.	The maturity of the southern part of the section and the timing of traps formation can be different.	Medium	Acquisition of new %Ro data; Reconstruction of a more accurate structural model.
			Thrusting starts before 7 Ma.			
	Triangular zone formation mechanisms	The triangular zone formation mechanisms in the NAFB are poorly understood. The reconstruction of a proper structural model is highly time-consuming.	Simple model simulating the formation of the triangular zone just after the deposition of the Molasse units.	Formation and timing of structural traps in the southern part of the section can be unprecise.	Medium-Low	Reconstruction of a proper structural restoration.
			Reconstruction of the triangular zone formation and Molasse deposition using a proper structural restoration.			
Erosion	The magnitude of the erosion	The magnitude of the erosion can be only estimated by indirect data (%Ro, AFT, etc..).	Values estimated in the literature.	Burial, thus maturity, of the source rocks can be different.	Medium/High	Acquisition of more %Ro data along the section.
			Values estimated in literature, modified to calibrate the %Ro data.			

Parameter	Uncertainty	Cause	Options	Effect on the Petroleum System Evolution	Impact	Potential improvements
Erosion	Timing of the erosion.	Difficulty in dating different erosion events.	Literature data.	Timing of the hydrocarbon generation.	Medium	Acquisition of AFT data along the section.
Boundary conditions	Present-day heat flow.	The heat flow values measured today in the wells are higher than what is necessary to calibrate the present-day temperature data.	Assigning lower heat flow values than what is measured today.	None, because it is a technical issue related to the software.	None	
			Do not calculate the radiogenic heat produced by the rock.			
	Paleo-heat flow.	The paleo heat flow over the basin evolution cannot be measured directly, it can be only estimated.	Heat flow trend reflecting the geodynamic evolution of the basin proposed in the literature.	The timing of the hydrocarbon generation can be different.	Medium/High	Reconstruction of the crustal model to improve the estimates of the paleo-heat flow.
			Heat flow trend reflecting the geodynamic evolution of the basin proposed in the literature, with peak values modified to calibrate the %Ro values.			
Permian and Carboniferous source rocks	Presence and geometry of the Permo-Carboniferous grabens in the southern part of the section.	Low seismic resolution; The Permian and Carboniferous deposits have been partially penetrated in the Pfaffnau-1 and Entlebuch-1 wells respectively.	Leu (2008).	The potential presence of deep hydrocarbon source rocks also in the South.	Medium	Acquisition of new 2D and 3D seismic and/or reprocessing of the existent geophysical data.
			Sommaruga et al. (2012).			
			Greber et al., 2007.			

Parameter	Uncertainty	Cause	Options	Effect on the Petroleum System Evolution	Impact	Potential improvements
Permian and Carboniferous source rocks	Presence, distribution and thickness of deposits rich in organic matter in the Permo-Carboniferous grabens in both grabens.	Scarce data because in the Pfaffnau-1 and the Entlebuch-1 well these deposits were only partially penetrated; No data on the total thickness of the source rocks.	Present only in the Entlebuch-1 area, where the Carboniferous has been partially documented.	Generation of deep hydrocarbon accumulations, which can migrate to the shallower units.	High, especially in the northern sector.	Acquisition of new geophysical data (seismic, deep wells).
			Carboniferous source rock is present in both P-C grabens and the Permian source rock is only in the southern graben.			
	Hydrocarbon potential.	No data.	Geochemical data extrapolated from the Weiach-1 well.	The volume of hydrocarbon generated can be different.	High	Penetrating these deposits in other locations and direct measurement of the geochemical parameters.
Posidonia shale source rock	Presence of the Posidonia shale source rock.	No data in the Pfaffnau-1 and Entlebuch-1 wells.	No present.	Generation, migration and accumulation of hydrocarbon in the Mesozoic and Cenozoic sequence can be different.	High	Acquisition of more data in the Liassic interval, especially in the central-southern part of the section.
			Present along the entire section (3 meters).			
	Hydrocarbon potential.	No data along the section.	Extrapolated from the Weiach-1, Shafisheim-1 and Riniken-1 wells.	The volume of hydrocarbon generated can be different.		
Calibration of the model	Porosity data.	Data are available only in a few wells. Far from these wells, the porosity can be different from what is simulated.	Use only the available data along the section.	Hydrocarbon migration and accumulations can be different.	Medium	Acquisition of more porosity data along the section.
			Use of data measured in wells located at nearly 30 km from the section trace line.			

Parameter	Uncertainty	Cause	Options	Effect on the Petroleum System Evolution	Impact	Potential improvements
Calibration of the model	Porosity calibration.	The porosity reduction by the diagenetic process cannot be properly simulated by the software.	Modify the initial porosity of the facies in the lithology library of the software.	Reservoir properties can be different from what is simulated by the model.	Medium	Find a proper way to change the software the porosity because of diagenetic processes and/or other processes.
	Present-day temperature data.	Data are available only in a few wells.	Use only the available data along the section.	The present-day temperature can be different from what is simulated, getting far from the wells where calibration data are available.	Low	Acquisition of more borehole temperature data along the section.
			Use also data measured in wells located at 30 km from the section trace line.			
	Thermal maturity calibration.	No %Ro data along the section.	Calibration with the %Ro data measured in the Shaficheim-1 well (27 km).	Erroneous calculation of the thermal maturity of the source rocks along the section, thus of the amount of hydrocarbons potentially generated.	High	Acquisition of %Ro along the section.

Table 37: List of the uncertainties parameters for the Section 4 model, their causes and their impact on the petroleum system modelling results. The options/scenarios available are indicated. In green is highlighted the option chosen in this study to build the petroleum system modelling. Potential improvements and actions to mitigate these uncertainties are suggested.

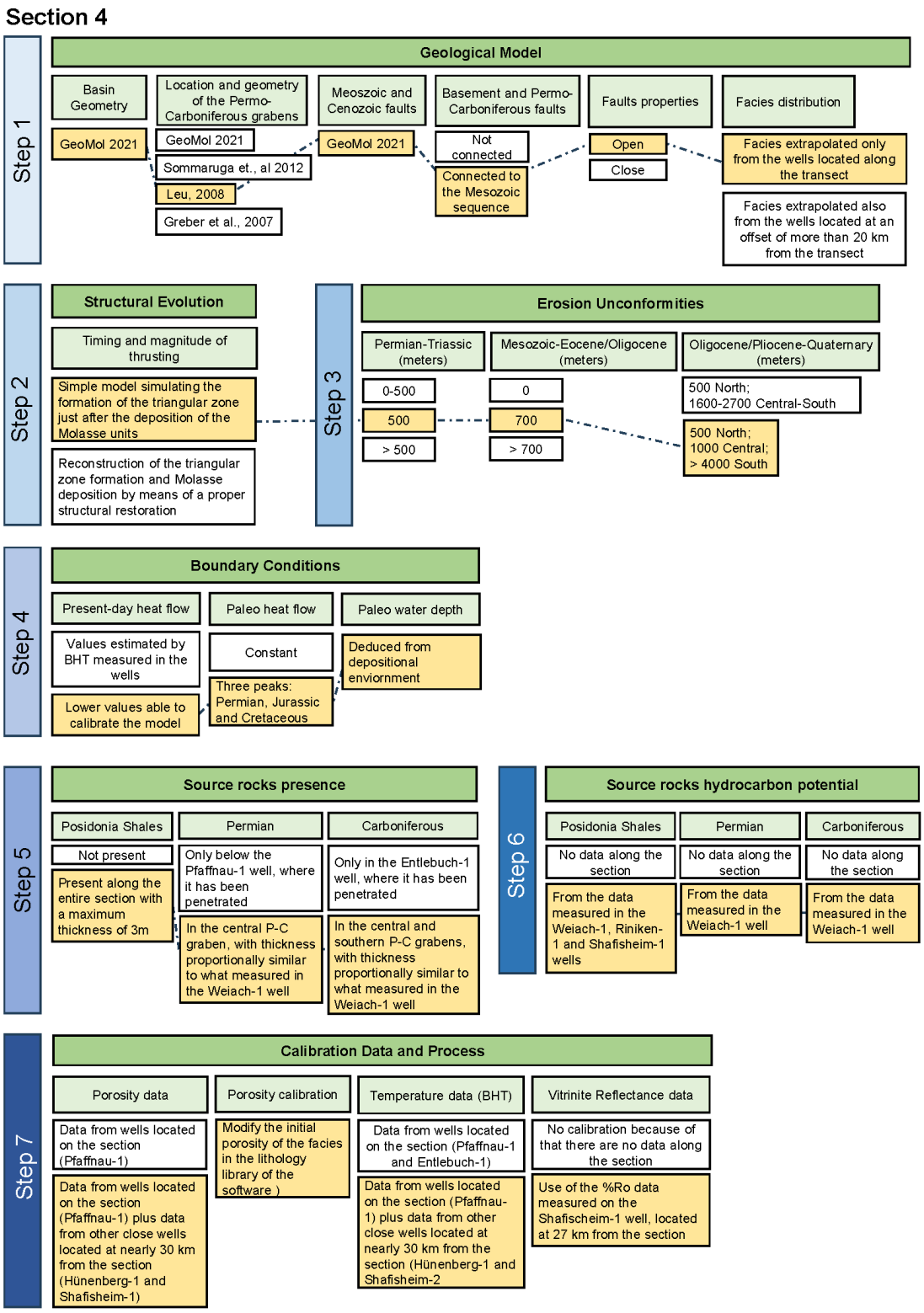


Fig. 72: Petroleum system modelling was built by selecting the specific combination of parameters, which are critical in controlling the thermal evolution of the basin and the hydrocarbon generation, migration and accumulation processes. In yellow are indicated the option chosen in this work.

3.4 Petroleum System Modelling - Section 5

3.4.1 Data

3.4.1.1 Geological Model

Section 5 is extracted from the GeoMol project, along a section line passing from the Cantons of Zurich and Canton of Schwyz (Fig. 73). The trace of the section is NNW-SSE oriented, with the following extremity coordinates: NNW edge x, y: 2670377.9; 128221.8 SSE edge x, y: 2703587.7; 1214802.1 (Reference coordinate System CH1903+ / LV95), and a total length of 75 km (Fig. 74). The extracted section represents the present-day geological structure of the NAFB in the area, represented by a southern dipping foreland wedge, filled by the Cenozoic Molasse units, and its Mesozoic substratum. The foreland basin is delimited to the north by the Jura Mountain Chain, where the Mesozoic strata outcrop, and to the South by the more external Subalpine thrusts. The erosional topographic surface cut the Mesozoic substratum units in the northern part of the section and the uppermost Molasse units in the southern part (Fig. 74).

The northern part of the section crosses the area of the NAFB where the distribution of the Permo-Carboniferous grabens is well known, thanks to the availability of a large geophysical dataset, (Madritsch et al., 2018 and references herein). Thanks to these data, the Permo-Carboniferous grabens geometry has been reconstructed with good detail and integrated into the GeoMol project. On the other hand, in the southern part of the section, the presence of Permo-Carboniferous grabens is uncertain, as in the rest of the NAFB. Their location and geometry were deduced by Leu (2008). In this section, the types of faults are differentiated, as classified in the GeoMol database (Fig. 74).

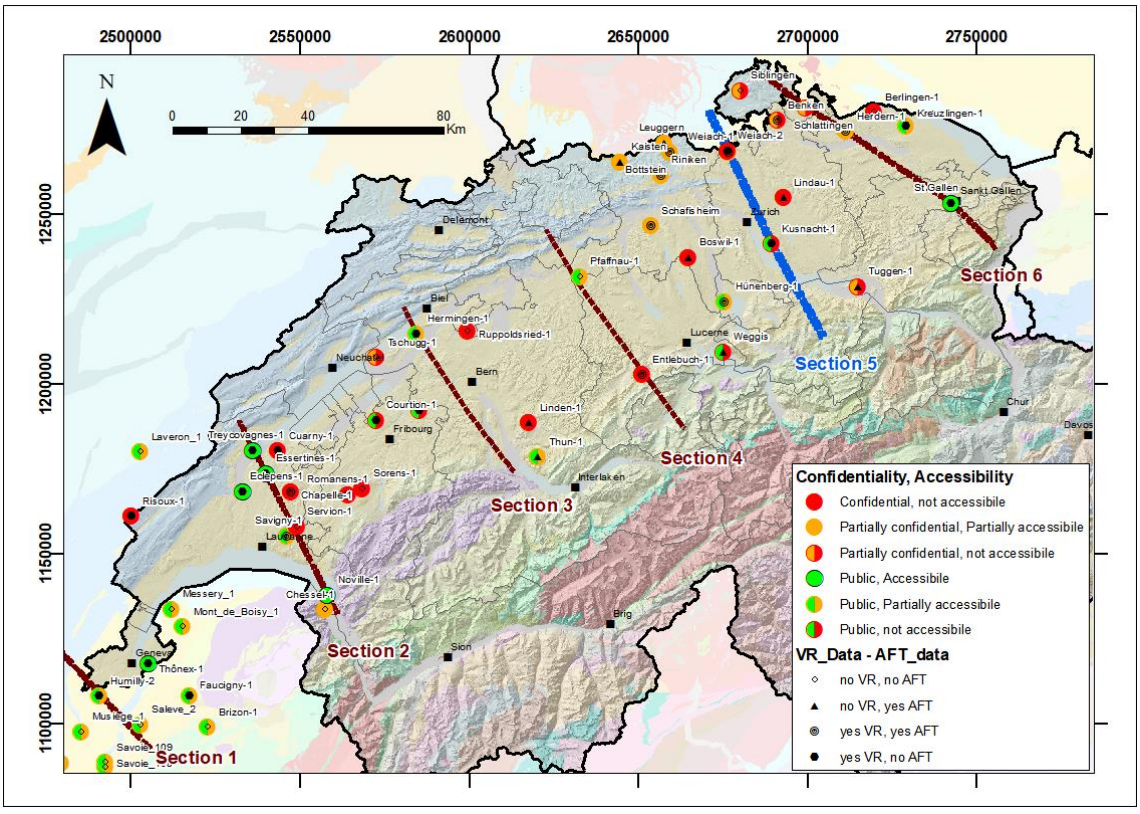


Fig. 73: Location of the section 5.

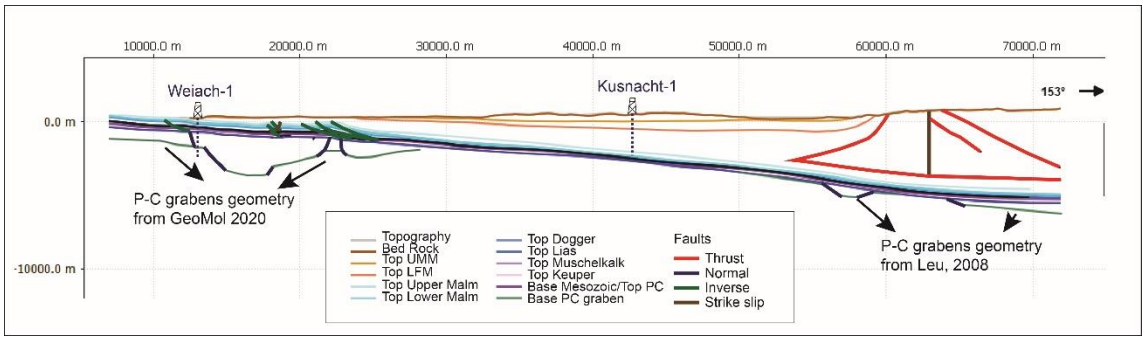


Fig. 74: Horizons and faults extracted from Geomol at the Section 5 trace location. The Permo-Carboniferou (P-C) graben geometry in the southern section was extrapolated from what was proposed in Leu (2008). The wells intersecting the section trace are shown. In this section, the types of faults are differentiated, as classified in the GeoMol database.

3.4.1.2 Wells

Section 5 passes on the top of the Weiach-1 and Kusnacht-1 wells, and is relatively close to the wells Lindau-1 (9 km E of the section trace) and Tuggen-1 (16 km E of the section trace) (Fig. 73 and Fig. 74). For these wells, the availability of the most relevant data necessary for thermal modelling is summarized in Table 38. The stratigraphic logs of these wells are shown in Appendix 4. The well Weiach-2 was not considered as no data are available for this well.

Well	Distance from section (km)	Status	Well report	Stratigraphic log	Calibration data	Rock-Eval data
Weiach-1	0	Partially confidential; Partially accessible	Yes	Yes	Phi, T, VR, AFT	Yes
Kusnacht-1	0	Public, Not accessible	Yes	Yes	VR	No
Lindau-1	9	Confidential, not accessible	No	Yes	T, AFT	No
Tuggen-1	16	Partially confidential; Not accessible	Yes	Yes	No	No
Hünenberger-1	20	Public, Partially accessible	Yes	Yes	Phi, T, AFT	No
Weggis-1	27	Public, Not accessible	No	Yes	T, AFT	No
Riniken-1	22	Partially confidential; Partially accessible	Yes	Yes	Phi, VR, AFT	Yes
Weiach-2	0	Confidential	No	No	No	No

Table 38: wells closest to the Section 5 trace and availability of the most relevant data needed for thermal modelling. Calibration data: (T) temperature; (VR) vitrinite reflectance; (AFT) apatite fission tracks, (Phi) porosity.

3.4.1.3 Deposition and erosional events

The burial history of the studied area is defined by a sequence of depositional and erosional events and their ages. Thus, in the model, an age for each stratigraphic unit and the main erosional event was assigned (Table 39).

Age top unit (Ma)	Unit	Event	Facies
0	Quaternary	Deposition	Quaternary
4	Erosion Pliocene-Quaternary	Erosion	
7.24	UFM	Deposition	UFM
15.97	UMM	Deposition	UMM
20.44	LFM	Deposition	LFM-North; LFM-Central; LFM-Thrust

Age top unit (Ma)	Unit	Event	Facies
28	LMM	Deposition	LMM
33	Hiatus Cret/Eocene	Hiatus	
86	Erosion Cretaceous	Erosion	
113	Cretaceous	Deposition	Cretaceous
145	Upper Malm	Deposition	Upper Malm
157.3	Lower Malm	Deposition	Lower Malm
163.5	Dogger	Deposition	Dogger
174.1	Lias	Deposition	Lias-North; central; Posidonia shale
201.3	Keuper	Deposition	Keuper
237	Muschelkalk	Deposition	Upper Muschelkalk; Middle Muschelkalk; Lower Muschelkalk
252	Hiatus Perm-Triassic	Hiatus	
259	Erosion Perm-Triassic	Erosion	
265	Permian	Deposition	Permian Lower; Permian-Source rock (SR)
284	Carboniferous	Deposition	Carboniferous; Carboniferous-Source rock (SR)
323	Hiatus/erosion pre-Carbon		
400	Basement	Deposition	Basement

Table 39: Depositional and erosional events defined in the thermal model for section 5. A facies is assigned to each layer. UFM upper freshwater Molasse; UMM upper marine Molasse; LFM lower freshwater Molasse; LMM lower marine Molasse

In the northern sector of the NAFB, where the northern part of the section passes, several studies have been carried out to estimate the magnitude of the main erosion events that occurred during the evolution of the basin (Table 40). That is because in this area a large data set of the basin infill of the NAFB, its substratum and its crystalline basement is available (see paragraph 1.4.2 and Table 40). On the other hand, in the central-southern part of the section, data are available mostly for the Quaternary-Pliocene unconformity (Schegg and Leu, 1998; Cederbom et al., 2011) (Table 40). Therefore, based on the literature data, it is considered an erosion of 400 meters for the Permian-Triassic unconformity, 1000 meters in the northern part, decreasing to 500 meters toward the south, for the Mesozoic-Eocene unconformity, and 300 meters in the northern edge of the section, increasing to 3000 meters toward the southern edge, for the Quaternary-Pliocene unconformity. These values were subsequently tested and constrained by the thermal modelling workflow proposed herein (see the Calibration result section).

Erosion unconformity	Amount of erosion estimated in previous studies (m)	Method	NAFB study area	Source
Quaternary-Pliocene	350 600	VR, clays, porosity, subsidence analysis	Zurich area, Kusnacht-1	Schegg and Leu, 1998; Lemcke, 1974 ; Monnier, 1982 ; Brink, 1992
	300-500	AFT, VR, 1D thermal modelling	Weiach-1 well	Villagomez et al., 2021 Omodeo-Salé et al., 2021
	1050	AFT, VR, 1D thermal modelling	NE sector	Mazurek et al., 2006
	800	AFT	Tuggen-1 well	Cederbom et al., 2011
	1600	AFT	Lindau-1 well	Cederbom et al., 2011
	1800	AFT	Hünenberg-1 well	Cederbom et al., 2011
	2700	AFT	Weggis-1 well	Cederbom et al., 2011
Mesozoic-Eocene	0	stratigraphy	Regional	Todorov et al., 1993; Burkhard and Sommaruga, 1998; Wildi et al., 1989; Lemcke, 1988

Erosion unconformity	Amount of erosion estimated in previous studies (m)	Method	NAFB study area	Source
Mesozoic-Eocene	600	AFT, VR, 1D thermal modelling	Weiach-1 well	Mazurek et al., 2006
	800-1300	AFT, VR, 1D thermal modelling VR, clays, porosity, subsidence analysis	NE sector, Weiach-1 well ENE sector	Villagomez et al., 2021 ; Omodeo-Salé et al., 2021 Schegg and Leu, 1998
Permian-Triassic				
	200	VR, 1D thermal modelling	Weiach-1 well	Omdeo-Salé et al., 2021
	200-600	VR	Weiach-1 well	Mazurek et al., 2006
	1000	VR, stratigraphy	Weiach-1 well	Diebold, 1988; Schegg and Leu, 1998

Table 40: Erosion magnitude estimated in previous studies for the three main erosional unconformities at the regional scale and/or in areas close to the section 5 trace line.

3.4.1.4 Facies

Facies were assigned to the stratigraphic units composing the section by extrapolating the lithologic data described in the well reports of the following wells: Weiach-1, Kusnacht-1, Lindau-1, and Tuggen-1. The facies described in the Riniken-1 well were not used, as it is located more than 20 km from the section trace and has a similar stratigraphy to the Weiach-1 well, located on the section trace. For the wells considered, the lithologies for each unit, expressed in percentage, are listed in Appendix 5. For each unit a unique or various facies were assigned along the section, depending first on the variability of the facies and secondly on the availability of data (Table 41). Generally, for the shallower units (Molasse) more data are available than for the deeper units (Triassic, Permo-Carboniferous), as only a few wells have been drilled deep enough to reach them.

Unit	Cgl	Sst	Silt	Shl	Lmt	Marls	Dlm	Anhd	Halt	Coal	Reference Well
Quaternary	25	50		25							All
UFM		20		5		75					Kusnacht-1; Lindau-1
UMM		65		10		25					Kusnacht-1; Lindau-1
LFM Thrust		15				85					Tuggen-1
LFM central		20		25	5	50					Kusnacht-1; (Lindau-1)
LFM North		70	20	10							Weiach-1
Upper Malm					80	20					Tuggen-1; Kusnacht-1; Lindau-1; Weiach-1
Lower Malm					20	80					Lindau-1; Weiach-1
Dogger				30	30	40					Weiach-1; Lindau-1
Lias central		30		40	30						Lindau-1
Lias North				30	10	60					Weiach-1
Keuper				15		40	45				Weiach-1; Lindau-1
Gypskeuper				20		30	20	30			Weiach-1
Upper Muschelkalk					10	10	70	10			Weiach-1; Lindau-1
Middle Muschelkalk				20			40	40			Weiach-1; Lindau-1
Lower Muschelkalk				30		30	30	10			Weiach-1; Lindau-1
Buntsandstein North		80		20							Weiach-1

Unit	Cgl	Sst	Silt	Shl	Lmt	Marls	Dlm	Anhd	Halt	Coal	Reference Well
Buntsandstein central		20				80					Lindau-1
Permian	15	10	40	35							Weiach-1
Carboniferous		40	25	33				I	2		Weiach-1
Basement	Gneiss									Various	

Table 41: Facies, expressed as a percentage of lithological composition, assigned to the stratigraphic units forming the basin infill of section 5. The wells used as references are indicated. Cgl: conglomerate; Sdt: sandstone; Slst: siltstone; Shl: shale; Lmt: limestone; Mrl: marl; Dlm: dolomite; Anhd: anhydrite; Halt: halite.

3.4.1.5 Calibration data

Porosity data are available for the Hünenberg-1 and Weiach-1 wells (Appendix 6). The latter is the only well that disposes of a porosity data set for the entire stratigraphic section. In the Hünenberg-1 well, located 20 km from the section trace, few porosity data were measured for the Molasse unit. To calibrate the present-day temperature over depth in the basin infill the borehole temperature data (BHT) of the Weiach-1 and Lindau-1 wells were used (Appendix 7). Because of that, there are no wells located along the southern part of the section trace, for this part, they were projected the temperature data measured in the wells Hünenberg-1 (located 20 km from the section trace) and Weggis-1 (located 27 km from the section trace).

In the Section 5 area, the data necessary to calibrate the thermal conditions attained during the evolution of the basin are mostly available in the northern part of the section (Table 40). Only the vitrinite reflectance data measured in the Weiach-1 and Riniken-1 wells were considered (Appendix 8), as they are the wells closest to the section 5 trace. In the southern part of the section, few vitrinite reflectance data are available for the Kusnacht-1 well. The estimate of the Cretaceous and Pliocene-Quaternary erosions using AFT data, in the northern area of the section (Villagomez et al., 2021; Mazurek et al., 2006) and for the Hünenberg-1, Lindau-1, Weggis-1 and Tuggen-1 wells (Cederbom et al., 2011, see Erosion section above), was used to constrain the erosion variable, despite of that these data cannot be directly used to calibrate the thermal model results.

3.4.1.6 Source rock parameters

According to the rest of the NAFB, three main source rocks are considered: the marine Posidonia Black Shales (Toarcian in age), the lacustrine Autunian shales (Permian in age), and the Carboniferous coal and shales (Carboniferous in age) (Leu and Gautschi, 2014; Misch et al., 2017; Schegg and Leu, 1998). Because of that, section 5 crosses the northeastern area of the NAFB, where there is the largest amount of data on the three mentioned source rocks, the latter can be well characterised. By mean of the Rock-Eval 6 analysis, the Posidonia shale were characterised in the Weiach-1, Riniken-1 and Shafisheim-1 wells (Appendix 1), and the Permian and Carboniferous source rocks in the Weiach-1 well (Appendix 2), the only well where these deposits have been entirely penetrated. A more detailed characterization of the Permian and Carboniferous source rocks in the Weiach-1 well is presented in Ajuaba et al. (2023), where Rock-Eval analysis has been integrated into organic petrography and palynology studies.

The lower Jurassic rocks, which include the Posidonia shale, the Toarcian, and the Lias units, were analysed in the Weiach-1, Riniken-1 and Shsfisheim-1 wells. They have a very variable content of organic matter, ranging from 0 to 10% of TOC, with an average of 3.5%. Similarly, the HI index, measured for the samples with a TOC > 1, ranges from 173 to 673 mg HC/g TOC, indicating the presence of both Type III and Type II kerogen (terrestrial and marine). The samples composed of marine kerogen with, an HI index is > 400 mgHC/g TOC, have an average TOC of 5% and an average HI of 565 mgHC/g TOC. T_{max} is 420-430 °C, indicating that these rocks are thermally immature. Coherently, the %Ro data measured for the Lias unit, show values of 0.43-0.46% in the Schaffischeim-1 well (Nagra, 1992; Matter et al., 1988) and Riniken-1 well (Matter, 1987; Matter et al., 1987), indicating immature thermal conditions. In the Weiach-1 well, the %Ro measured at the top of the Lias is 0.57%, indicating early oil window thermal conditions (Matter, 1987; Nagra, 2002) (see %Ro values measured for the Dogger unit in Appendix 8). The Posidonia shale have been

recognized only in the wells located in the northern part of the section, whereas there is no evidence of the presence of this organic-rich unit in the central part (Lindau-1 well). From the central toward the southern edge of the section, there is no data about the presence of this source rock, as the wells located in this area (Kusnacht, Tuggen-1, Hünenberg-1, Weggis-1) did not penetrate the Lias unit. Therefore, in the model, the Posidonia shale source rock has been assigned only from the northern edge of the section to the Lindau-1 well, with an average thickness of 4 meters.

In northeastern Switzerland, the Permian and Carboniferous source rocks were analysed only in the Weiach-1 well. The Permian fine-grained deposits have been analysed in detail by Ajuaba et al. (2023). The TOC of these rocks ranges from 1 to 9.89%, with an average of 4.7%. The HI of the samples with a TOC >1 ranges from 24 to 488 mgHC/gTOC, with an average of 289 mgHC/gTOC. By integrating these data with organic petrography and biomarkers, it has been interpreted that these deposits are composed of Type II, Type III and a mix of Type-I-III kerogens, with terrestrial and lacustrine origin. The average Tmax is 440 °C, indicating middle oil window conditions. %Ro measured in the Permian deposits is 0.64-0.7%, confirming the oil window thermal conditions (Appendix 8). The interval between 1310.08 and 1358.9 meters (Autunian Shales) exhibits the highest hydrocarbon potential, and it is classified as a good to very good oil-prone source rock (Ajuaba et al., 2023).

In the Weiach-1 well the Carboniferous source rocks are composed of several intervals of organic-rich shales and coal seams, 1 to 10-15 meters thick. To characterise these rocks, shales and coal deposits have been differentiated. The TOC of the coal samples ranges from 1.5 to 77 %, with an average of 67%, whereas the TOC of shaly coal, coaly shale and shale ranges from 28.8 to 2 %, with an average of 8%. An average HI of 216 mgHC/gTOC is measured for the coal group and o2 mgHC/g TOC for the shales group, indicating a Type III kerogen, terrestrial in origin. Tmax is around 450-455 for the entire interval, indicating middle to late oil window thermal conditions. %Ro measured in the Carboniferous interval ranges from 0.78 to 1.28% (Appendix 8), confirming the middle to late oil thermal window conditions and the beginning of the gas window. The type of kerogen defined for the Carboniferous deposits (Type III) suggests that these source rocks are mainly gas-prone but may also generate minor amounts of oil. However, a low percentage of liptinite macerals and a relatively high percentage of inertinite macerals indicate that the oil potential is limited.

The internal subdivision of the Permo-Carboniferous grabens was determined considering the interepretations provided by (Madritsch et al., 2018). Therefore, first, the infill of the grabens was subdivided into two units, the Permian (33% of the total thickness) and the Carboniferous (67% of the total thickness). Secondly, in the Permian, for the Autunian lacustrine shales an interbedded layer, with a thickness 8% of the total Permian unit, was created (maximum thickness of 200 meters in the central part of the graben, where the Permian unit is thicker than in the Weiach-1 well position). The Permian unit is represented only in the northern graben, as in the southern part, in the closest well, similarly located in the internal part of the basin and where these deposits have been penetrated (Entlebuch-1), the Permian unit was not found. For the two Carboniferous source rocks considered (coal and shales) two interbedded layers were created, with a total thickness of 9% of the total Carboniferous unit (maximum thickness of each unit, 50 meters).

From the data described above, the petroleum potential was assigned to the four source rocks considered, defined by the initial TO and C, HI indices of the deposits before their thermal transformation. The kinetic was assigned by considering the type of organic matter composing each source rock. To calculate the initial petroleum potential, the GeoChem module of the PetroMod suite was used, where the Peters' method is applied (Peters et al., 2005). The four source rocks considered and the related initial organic geochemical data assigned in the model are shown in Table 42.

Source Rock	Lithology	Present average TOC (%)	Initial TOC (g rock)	Present average HI (mgHC/gTOC)	Initial HI (mgHC/gTOC)	Kinetic
Posidonia shale	Black shales	5	**6.5**	565	**680**	TII(PB) (Behar et al., 1997)_
Permian lacustrine shales	Shale organic rich	4.7	**6.2**	289	**500**	TI(C) (Pepper and Corvi, 1995)
Carboniferous coal	Coal	72	**75**	210	**250**	TIII-(Dogger) (Behar et al., 1997)
Carboniferous shales	Shale organic rich	8	**8.5**	95	**150**	TIIIH(DE) (Pepper and Corvi, 1995)

Table 42: Initial geochemical properties of the four source rocks assigned to the model.

3.4.2 Boundary conditions

The upper boundary, the sediment-water interface temperature (SWIT), was automatically calculated by the software, for a geographical area located at a latitude of 46°N (present Switzerland latitude) (Fig. 12). The paleowater depth was deduced by the depositional environment of the main stratigraphic units forming the basin and the basal heat flow trend was reconstructed considering the geodynamic evolution of the Molasse Foreland Basin (Table 43).

Age to (Ma)	PWD (m)	Age from (Ma)	HF value (mW/m2) initially assigned	HF value (mW/m2) calibrating the model
0	0	0	variable*	variable*
22	0	0.4	50	variable*
66	300	5	50	50
		7	50	60
		8	50	60
125	100	29	50	70
152	10	80	50	90
160	300	118	75	90
163.5	100	142	65	90
174.0	300	146	75	110
190	100	172	60	110
201.3	70	200	60	100
252	0	250	60	90
265	0	260	87	100
		270	100	120
		290	120	160
		300	80	170
		320	60	80
		318	60	100
		350	60	100
		400	60	60

Table 43: Paleowater depth (PWD) and basal heat flow variation over time. (*) At the present day (0 My) a variation of the basal heat flow along the section was considered, based on the present heat flow distribution calculated throughout the NAFB. The heat flow trend has been changed to calibrate the temperature and paleotemperature data (see calibration section).

At the present day (0 My) a variation of the basal heat flow along the section was considered (Fig. 75), based on the present heat flow distribution calculated throughout the NAFB (data source: https://map.geo.admin.ch, see Fig. 15).

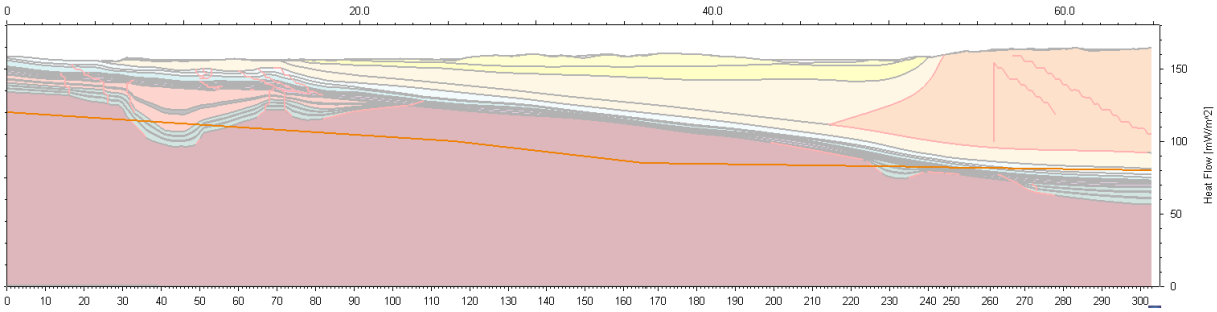


Fig. 75: Basal heat flow assigned along the Section 5 at the present-day (0 My)

3.4.3 Results

3.4.3.1 Restoration to the pre-Alpine deformation phases

Because of that, in section 5 thrusts and inverted faults are present, previous to the thermal modelling workflow, it is essential to restore the geometry of the basin before the pre-Alpine deformation phase. However, because of that the southern part of the sections passes throughout the triangular zone, a simplified method is applied, which simulates the formation of this complex structure directly in the PetroMod software (see paragraph 2.1.2). Therefore, for this section, the TecLink workflow was not applied, which tremendously simplified the modelling work.

3.4.3.2 Geological conceptual model evolution

The section extracted from Geomol (Fig. 74) was imported into the PetroMod software and each horizon was assigned to a stratigraphic unit and at a corresponding age (Table 39). The facies previously defined (see Facies in the Data section) were assigned to the stratigraphic units composing the sections (Fig. 76).

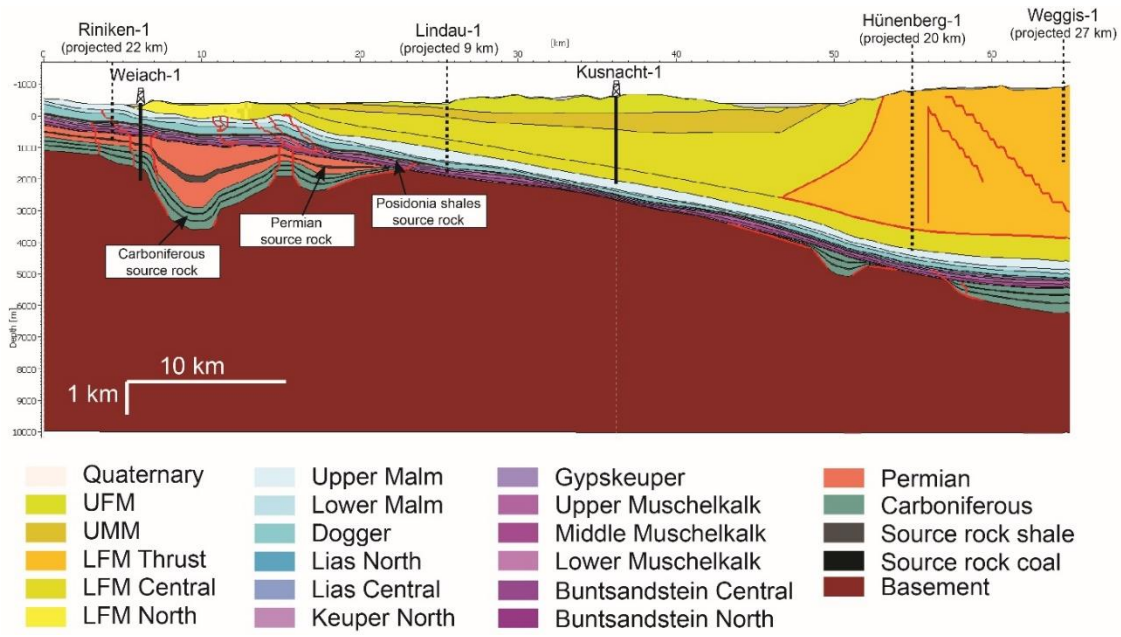


Fig. 76: Section imported in Petromod and used as a geological model. Based on the stratigraphy described in the well reports, facies were assigned to the present-day section. Sections vertical exaggeration 2:1.

The geological evolution of the basin along Section 5 is shown in Fig. 77. The formation of the triangular zone was simulated in the PetroMod software, using the introduction of an additional layer with paleo-thickness increasing from 7 to 0 Ma. Because of the thrusting and formation of the

triangular zone, the Molasse units, located in the southern part of the basin, were uplifted and eroded. In the same period, the Jura structures started forming northward, while the entire basin was exhumed and eroded.

The magnitude of the Pliocene-Quaternary erosion was estimated considering previous literature data (Table 40) and calibrated with vitrinite reflectance data (see Calibration section below). It ranges from 350 in the north (Weiach-1 well area) to 600 meters in the central part (kusnacht-1 well area), to over 4000 meters to the south. In the southern extremity of the section, the erosion is deduced by geometrical reconstruction, to obtain the undeformed geometry of the foreland previous to the triangular zone formation. For the latter part of the section, at present, there is no data to corroborate this interpretation.

To simulate the deposition and the erosion of the Cretaceous, because the Cretaceous layer is not represented along the section, it was assigned an additional paleothickness at the Malm unit, from 145 to 90 Ma, which was removed from 90 Ma to 56 Ma as the effect of the erosion. The thickness of the eroded Cretaceous deposits ranges from 1000 meters in the northern part of the section to 500 meters in the southern part. For the Permo-Triassic unconformity, it was considered an erosion of 400 meters of Permian deposits, located on the top of the Permo-Carboniferous grabens.

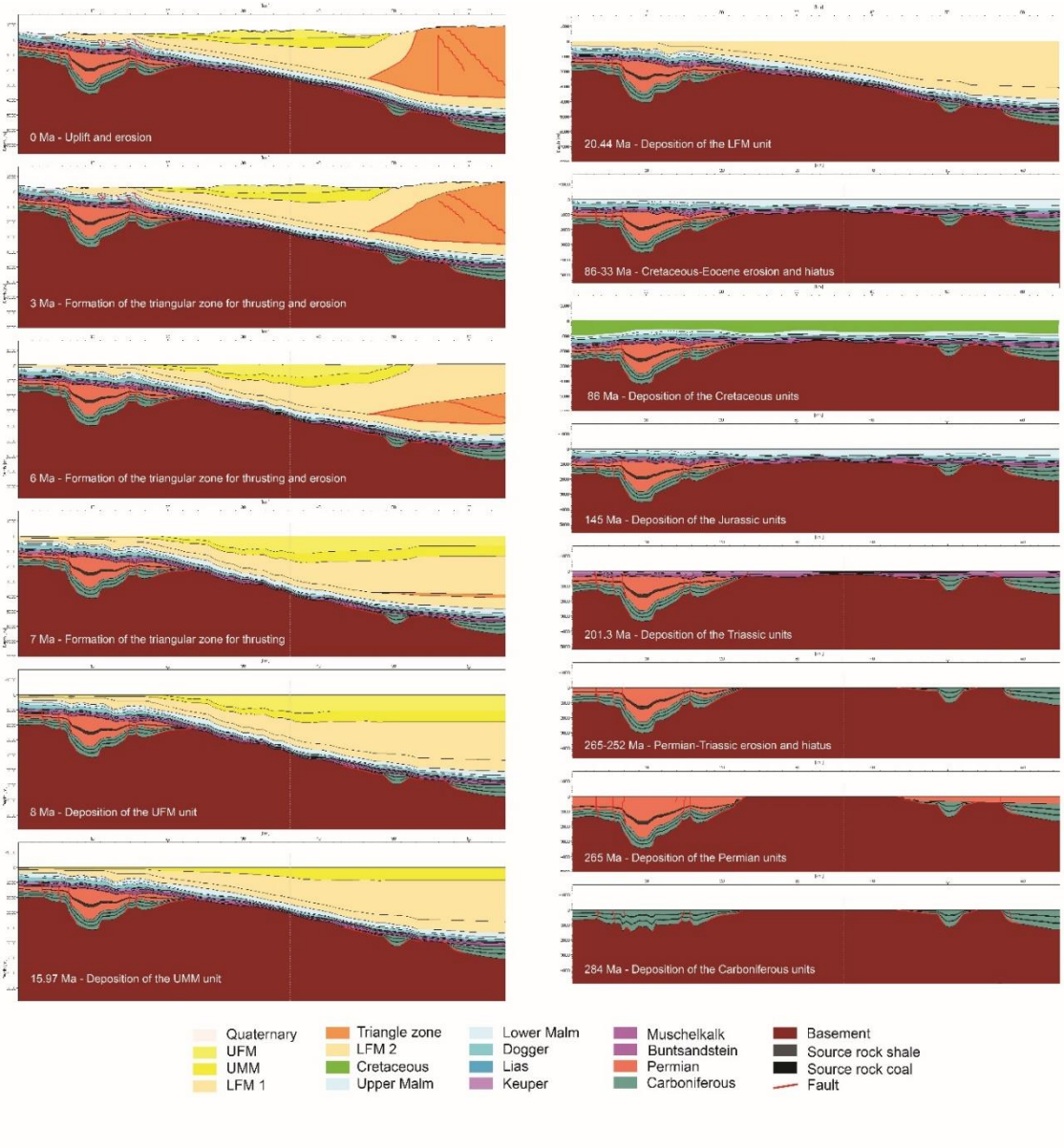


Fig. 77: Geological evolution of the studied area obtained in Petromod by retrodeformation and decompaction of the units forming the basin infill, from the present-day to the Carboniferous time. Sections vertical exaggeration 2:1.

3.4.3.3 Thermal Model Calibration

3.4.3.3.1 Porosity

The porosity was calibrated for the Weiach-1, Riniken-1 and Hünenberg-1 wells. The mechanical compaction properties estimated by the software for the lithologies assigned to each stratigraphic unit were iteratively changed to fit the theoretical values calculated by the model with the porosity values measured along the wells. The calibration results are shown in Fig. 78. The porosity values calibrated in these wells were assigned along the entire section (Fig. 79). This extrapolation could be erroneous, especially in the case of the dominant limestone units (Mesozoic), where the porosity and permeability are strictly controlled by diagenetic processes and fracking, which can dramatically change from one point to the other of the basin. To reduce this uncertainty, more porosity data with depth should be available.

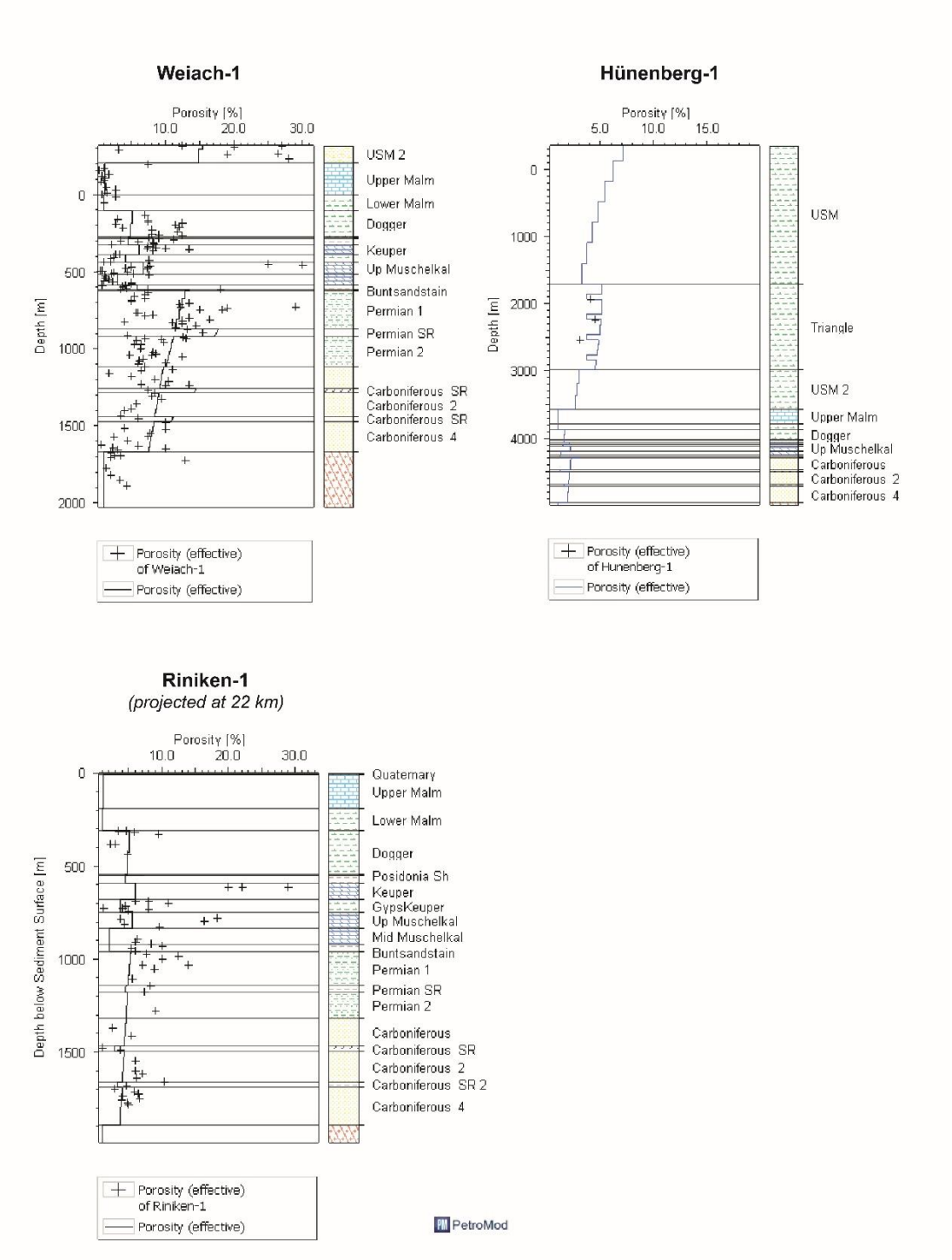


Fig. 78: Calibration of the porosity property with the data measured in the Weiach-1 and Hünenberg-1 wells.

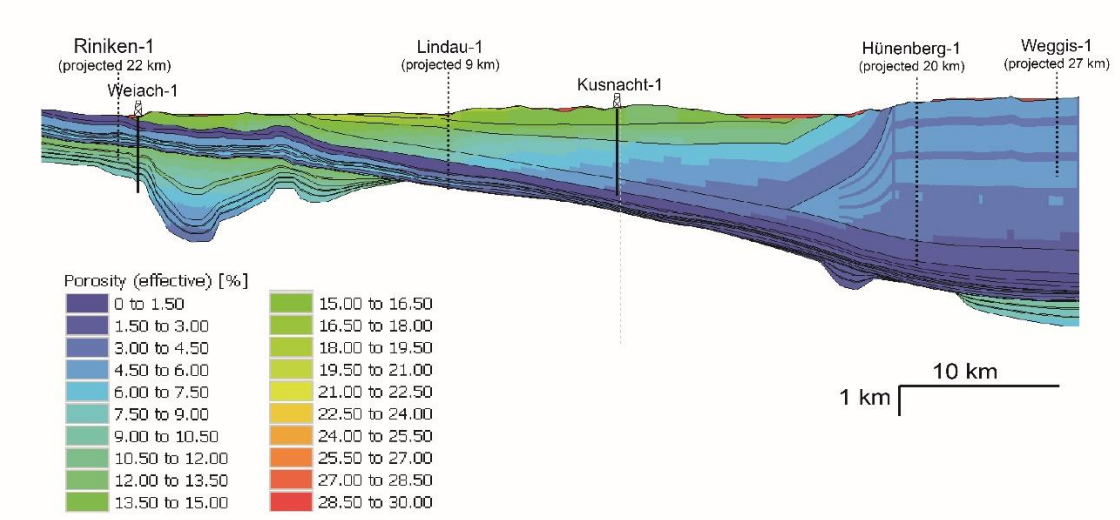


Fig.: Porosity estimated along the section by the software, extrapolating the data calibrated in the Weiach-1, Riniken-1 and Hünenberg-1 wells.

3.4.3.3.2 Present-day temperature

The present-day temperature calculated by the model was calibrated with the borehole temperature (BHT) measured in the wells close to the section. To calibrate the modelling results, the variable that mostly changed was the present-day basal heat flow (see Method section). Firstly, it was tested the heat flow values estimated in the entire basin from borehole temperature data (Fig. 80, scenario A). This scenario does not give satisfactory calibration results, as the temperature simulated by the misl is considerably higher than what is measured in the wells (Fig. 81). This is because the heat flow values of Scenario A represent the heat flow at the surface, whereas the heat flow that was assigned into the model refers to the amount of heat at the base of the model, basement included. Toward the basin surface, this heat is increased, mostly by the radiogenic heat produced by the basement and basin infill rocks. The effect of the rapid exhumation of the NAFB can also play a role in maintaining an anomalously high heat flow at the surface of the basin. For more details, see the explanation in the Method section, Calibration subsection.

A second basal heat flow scenario is tested for 0 Ma (Fig. 80, scenario B), with values at least 80 mW/m^2 lower than Scenario A. Assigning in model scenario B as heat flow boundary condition, the borehole temperature measured in the wells are considerably better calibrated (Fig. 81). According to this scenario, the model calculates the temperature distribution along the section at the present day (Fig. 82).

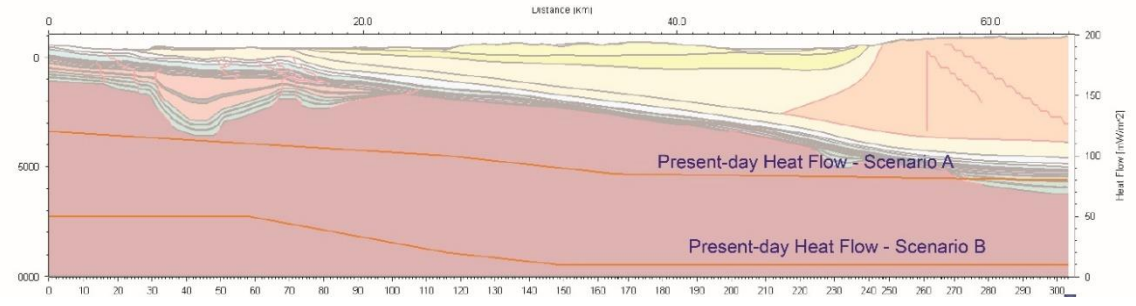


Fig. 80: Heat flow values assigned along the modelled section at 0 Ma. The two scenarios tested are shown.

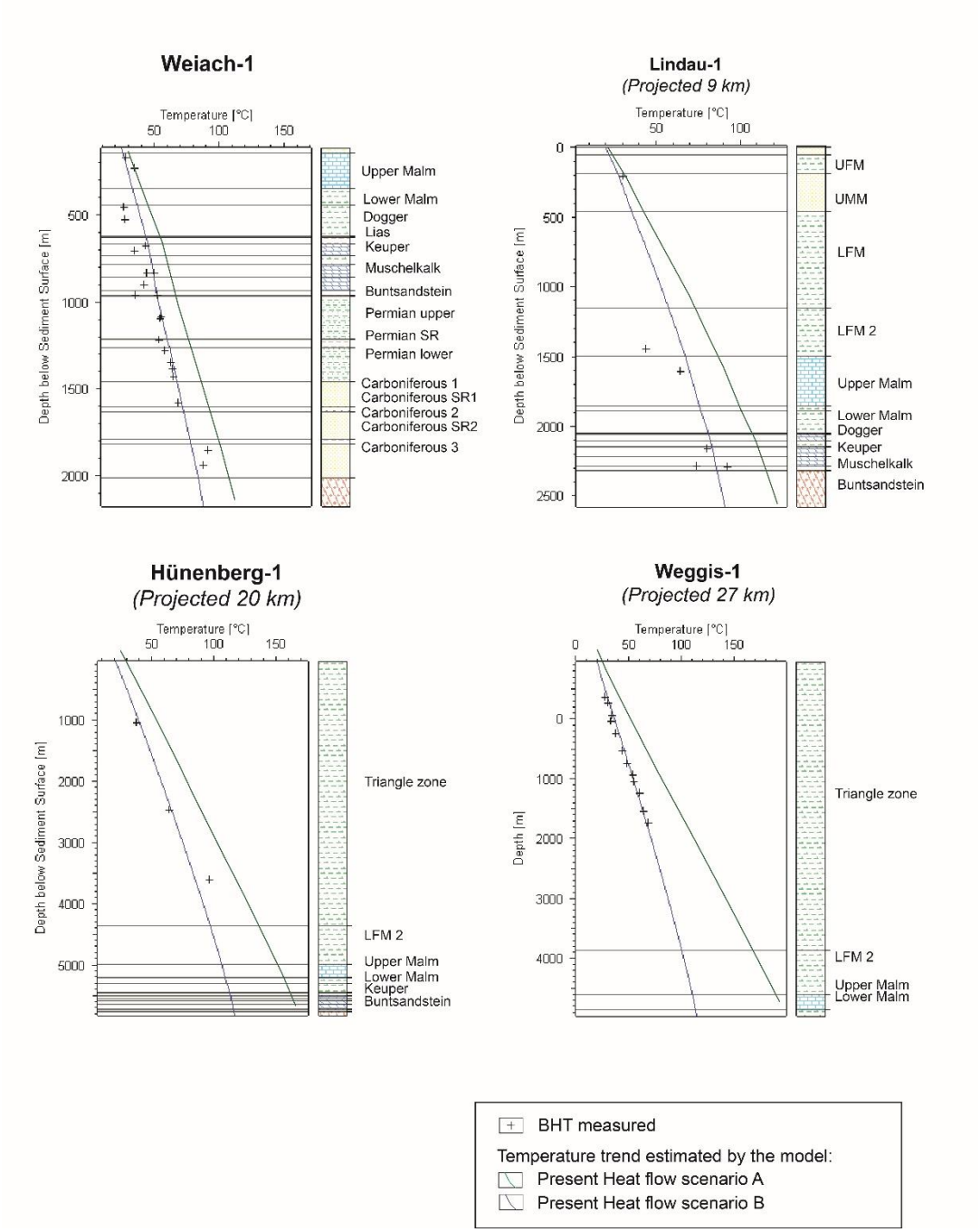


Fig. 81: Calibration of the present-day temperature modelling results with the BHT measured in the wells closest to Section 5.

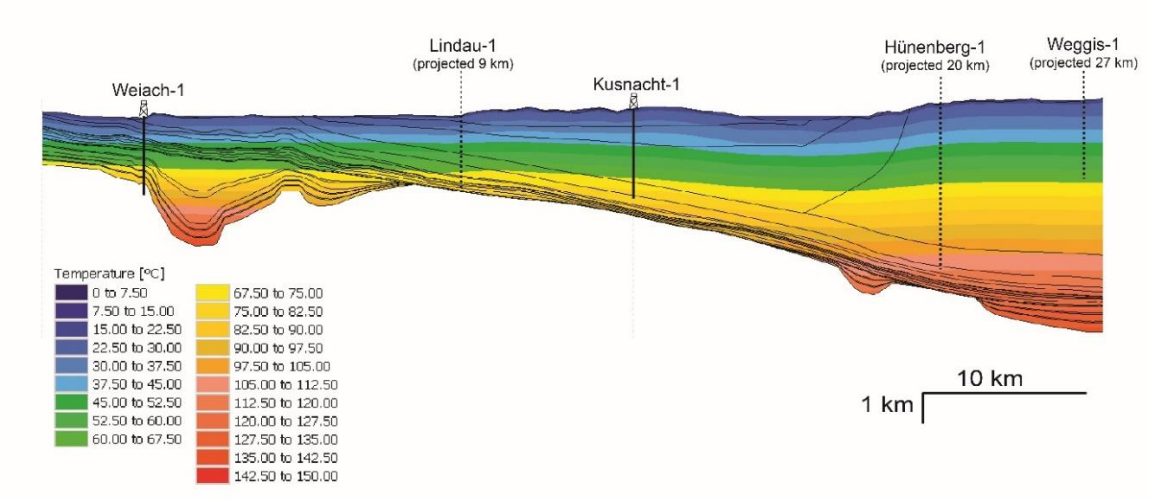


Fig. 82: Temperature variation with depth and along the section calculated by the model for the present day (0 My), calibrated with the present-day heat flow scenario B.

3.4.3.3.3 Thermal conditions / Source rocks maturity

The thermal conditions calculated by the model can be validated only in the northern and central parts of the section, as paleothermal data useful for calibration (%Ro) are available only for the Weiach-1 and Kusnacht-1 wells. The %Ro data measured in the Riniken-1, located 22 km westward of the section trace, were also projected into the section. The calibration results are shown in Fig. 83.

The %Ro values measured along the Weiach-1 and Kusnacht-1 wells are satisfactorily calibrated with the following erosion values: for the Weiach-1 area, 400 meters for the Permo-Triassic unconformity; 900 meters for the Jurassic-Eocene unconformity and 350 meters for the Miocene-Quaternary unconformity; for the Kusnacht-1 area, 600 meters for the Permo-Triassic unconformity; 500 meters for the Jurassic-Eocene unconformity and 600 meters for the Miocene-Quaternary unconformity. In the southern part of the section, for the Pliocene-Quaternary unconformity, the erosion was assigned in agreement with geometrical reconstruction (over 4000 meters, triangular zone area). To improve the calibration, the paleo-heat flow trend was slightly modified concerning the trend initially assigned, as shown in Table 43. In the Weiach-1 well, the thermal conditions of the Posidonia shale are not exactly calibrated, as %Ro data indicate early oil window conditions whereas the model calculates immature thermal conditions. At present the calibration cannot be improved because of software limitations (if the maturity of the uppermost Mesozoic layers the Permian and Carboniferous unit was increased it would result in excessively mature). The %Ro data measured in the Riniken-1 well do not calibrate the thermal conditions calculated by the model in the corresponding area. Because of that the %Ro values with depth trend are nearly constant, it is considered that they do not properly represent the thermal maturity trend in this area. Furthermore, because the Riniken-1 well is far from the modelled section (22 km), the %Ro data measured in this well could not be representative of the maturity trend along section 5.

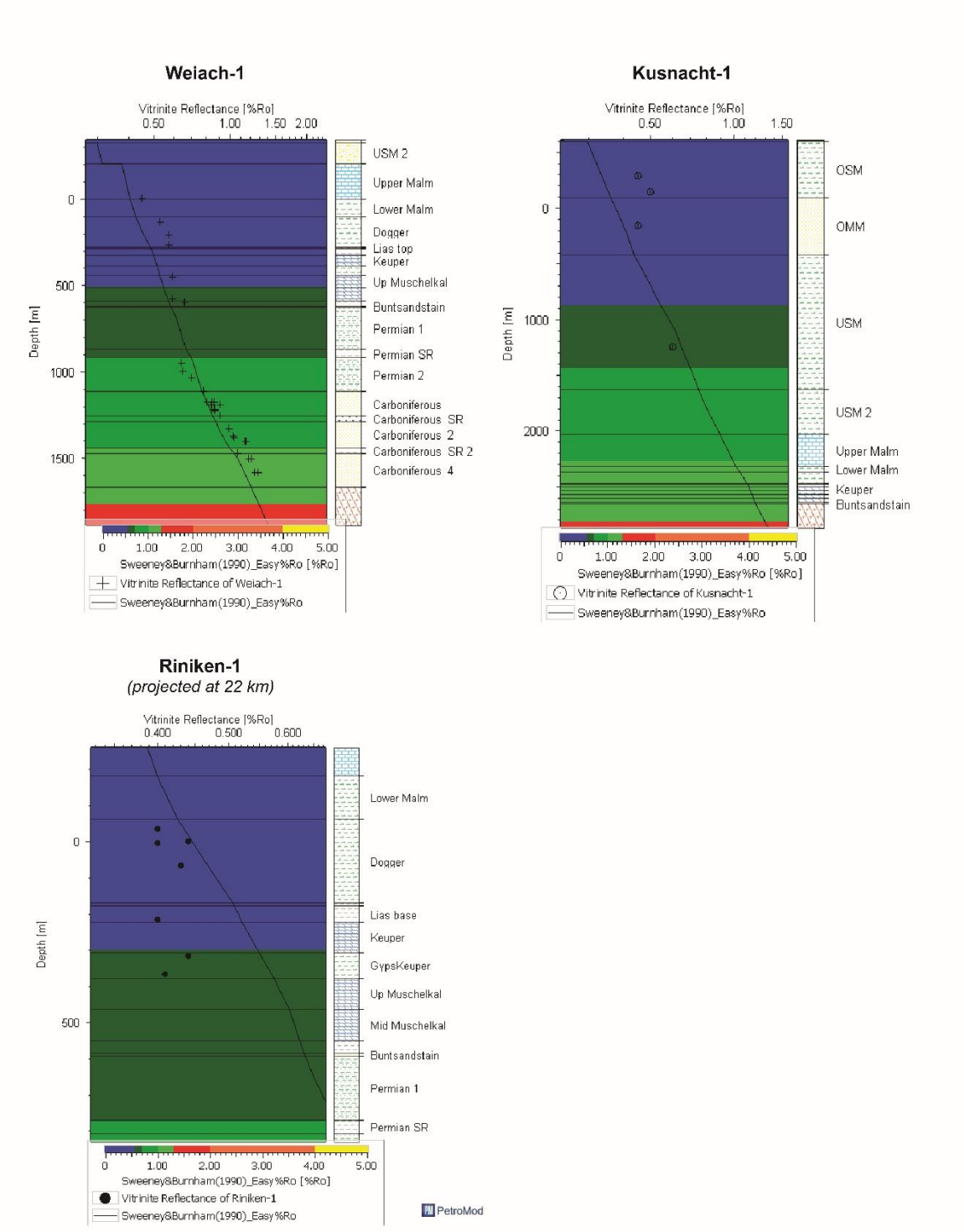


Fig. 83: Calibration of the thermal conditions calculated by the model with %Ro data measured in the Weiach-1, Kusnacht-1 and Riniken-1 wells.

The thermal conditions resulting along the entire section are shown in Fig. 84. From this output it is deduced that, in the northern part of the section, the Posidonia shale source rock is in the immature to early oil window thermal stage, the Permian source rock is in the oil window thermal conditions and the Carboniferous source rock is in the oil window thermal conditions, along the shoulders of the grabens, and in the gas window in the central and deeper part of the graben. In the southern part of the section, the Carboniferous source rock is in the dry gas thermal conditions,

whereas in this part of the section, the Posidonia shale and Permian source rocks are considered absent.

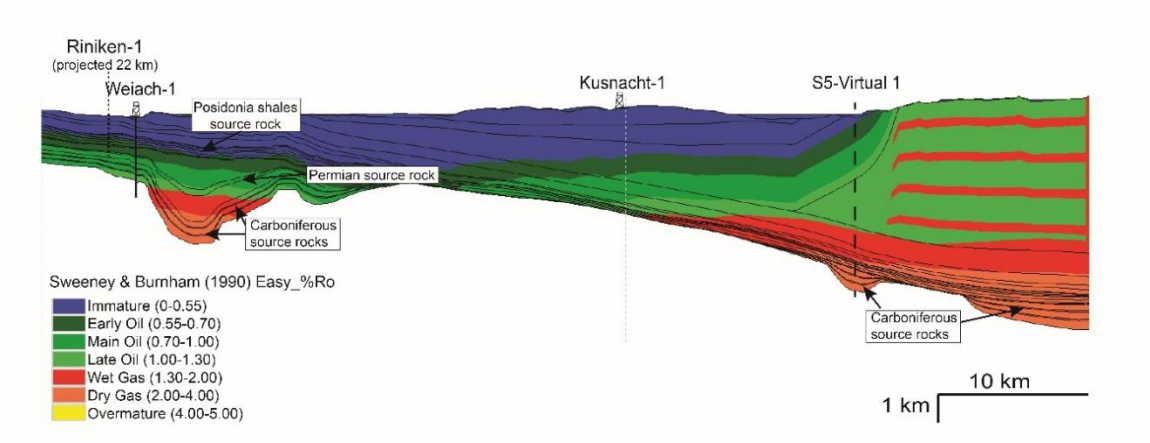


Fig. 84: Thermal conditions calculated by the model and calibrated with the %Ro data in the Weiach-1 area

The source rocks maturation timing is deduced by the burial plot vs thermal conditions extracted at the Weiach-1 and well position and in the southern part of the section (Virtual well 1, see Fig. 84) (Fig. 85). In the northern part of the section (Weiach-1 well area), the Lias unit (Posidonia shale source rock) enters in the oil window in the Miocene and the Permian source rock in the Cretaceous. In the southern part of the section (virtual well), the Permian and Carboniferous source rocks enter the oil window in the Cretaceous and the gas window in the Miocene.

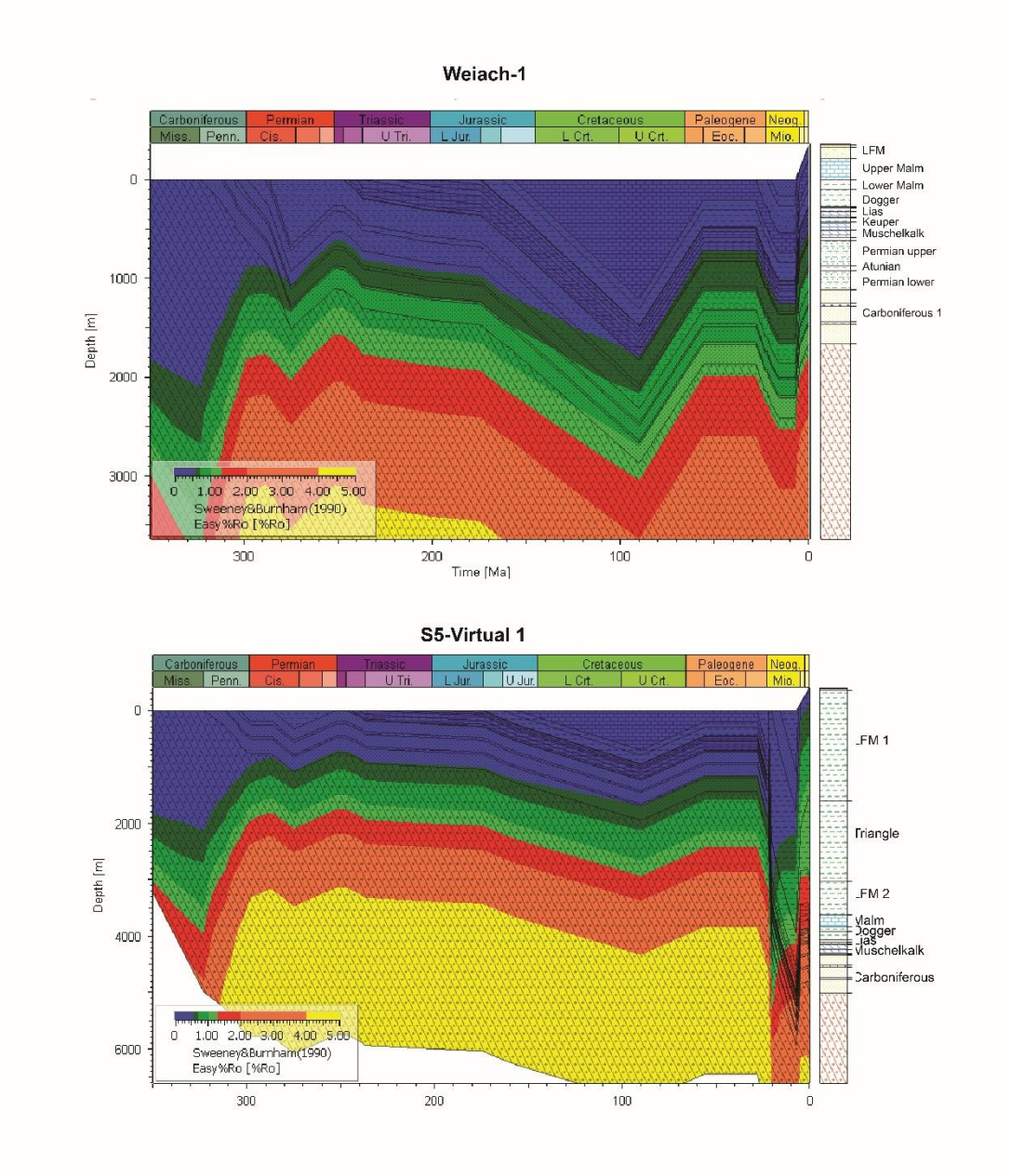


Fig. 85: Burial plot versus thermal maturity conditions, showing the time when the source rocks (Lias, Permian, Carboniferous) were matured.

3.4.3.4 Simulation of the hydrocarbon generation, migration and accumulation processes

The model simulates the hydrocarbon generation, migration and accumulation processes for Section 5, as the effect of the source rock maturation and hydrocarbon expulsion. Migration paths and potential reservoirs are calculated based on the geometry of the basin and the permeability properties of its infill. Hydrocarbons were generated by the Permian, Carboniferous and Posidonia shale source rocks, at different times. A first-generation peak occurred in the Permian (Fig. 86), because of the burial of the Permian and Carboniferous source rocks in the grabens and the presence of a high heat flow in this period (Fig. 13 and Table 43). A second-generation peak, less relevant, occurred in the Cretaceous, when the basin was affected by another heat flow peak and burial, and the third-generation peak was in the Cenozoic (Fig. 86) when the formation and infill of the foreland basin increased abruptly the burial depth of the basin. The rocks that generate the greatest volume of hydrocarbons are the Carboniferous coal deposits, followed by the Permian shales and finally the Carboniferous shales (Fig. 86). The Posidonia shale source rock does not

generate a relevant amount of hydrocarbon, as it is mostly immature to the northern part of the section, whereas to the south, where the basin is deeply buried, it is absent. Hydrocarbon accumulations in proper reservoirs form in the Cretaceous and in the Cenozoic times, and they are volumetrically lower than accumulations in low permeable units (petroleum saturated). The latter formed mostly in the Cenozoic, then in the Cretaceous and lessly in the Permian time.

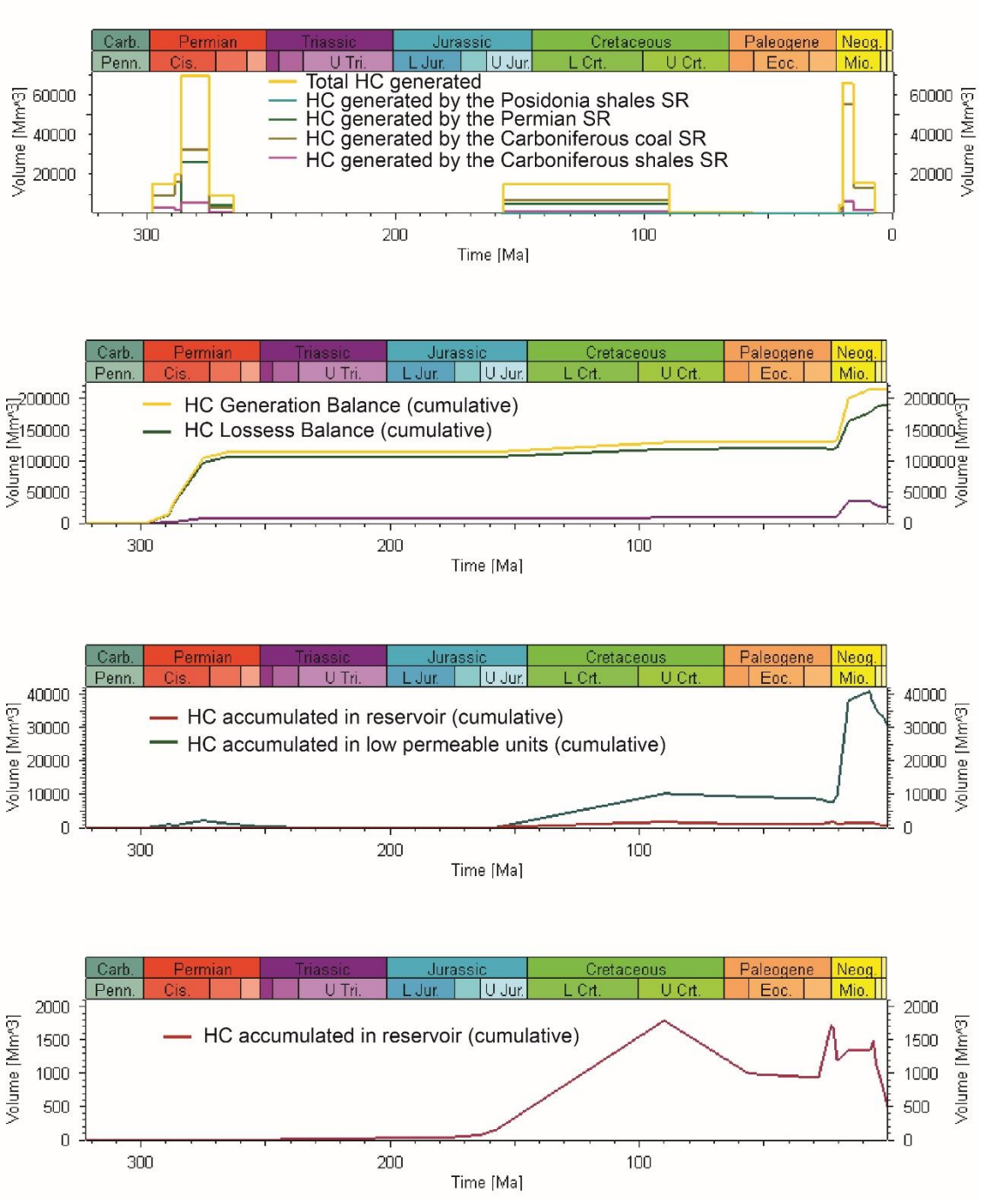


Fig. 86: Hydrocarbon generation and accumulation balances calculated by the software for the entire section

Firstly, the “open faults” scenario was tested, which means that the faults are considered as not cemented. The model simulates the formation of hydrocarbon accumulations mostly in the northern part of the section, in the Buntsandestein and Permian sandstone deposits along the entire Constance-frick graben (Fig. 87). In this area, small traps are also formed in the Jurassic units, in

correspondence of anticlines bounded by faults. Leakage from these reservoirs forms hydrocarbon migration flow to the top surface of the uppermost units. Migration occurred mostly along faults.

To the south, petroleum saturations are simulated in the Permian and Carboniferous sandstone deposits. There are no relevant migrations from the Permian and Carboniferous source rocks to the uppermost units. Hydrocarbon paths remain mostly confined in the Mesozoic units, especially in the lowermost ones (Triassic). Few hydrocarbon flows can be expected in the Molasse units (Fig. 87).

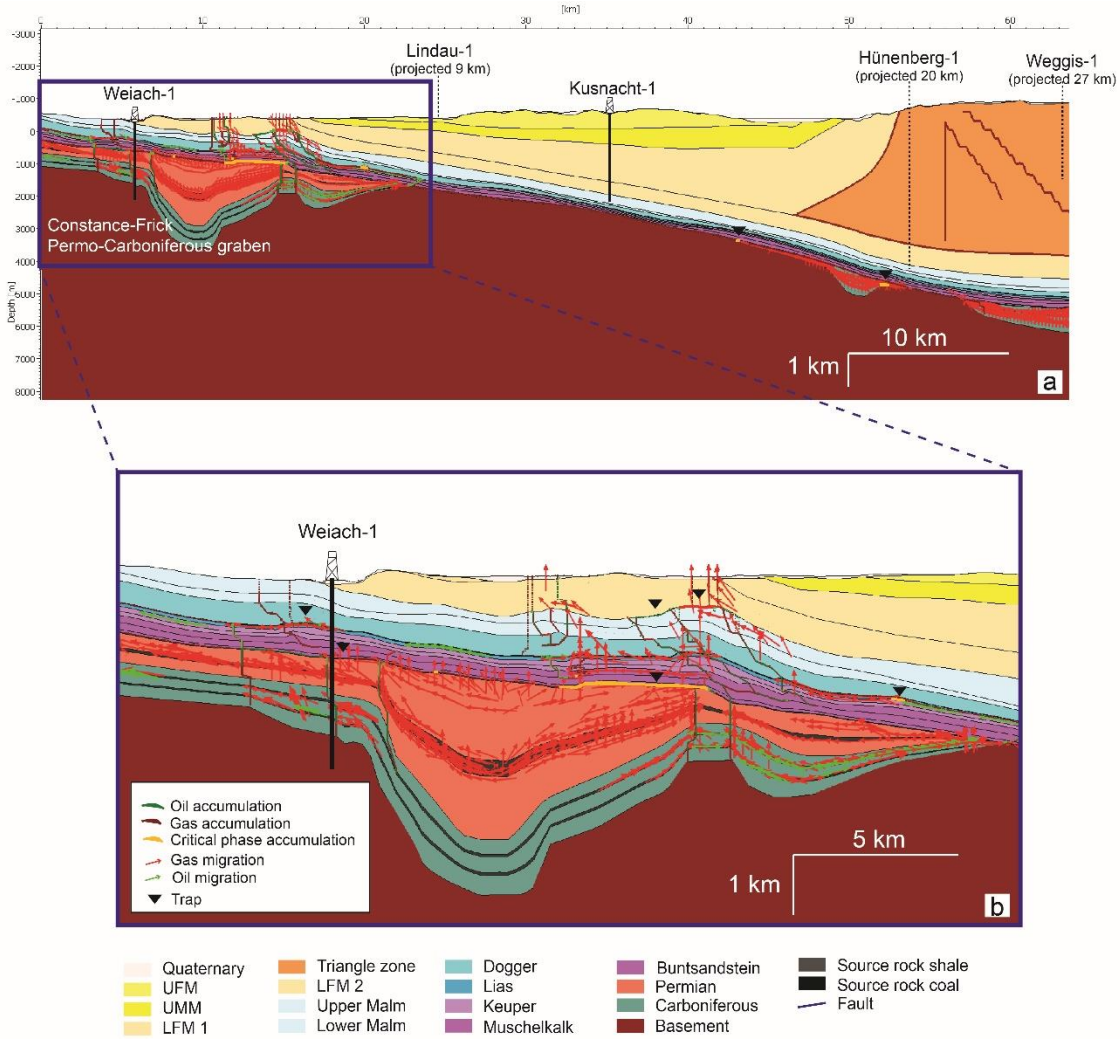


Fig. 87: Open fault scenario: (a) Hydrocarbon accumulations and migration paths calculated by the model along section 5. In (b) zoom in on the northern area of the section, where the Weiach-1 well is located. Potential traps are indicated.

A second scenario was simulated, considering the “closed faults” option, which means that the faults are considered as cemented (Fig. 88). The main different results with the “open faults” scenario are in the northern part of the section, whereas the results in the central and southern parts are very similar. By this option, in the north, larger reservoirs formed in the Permian and Buntsandstein units at the top of the Constance-Frick graben, whereas reservoirs in the Jurassic units are not present. The leakage and migration to the uppermost stratigraphic units are also strongly reduced.

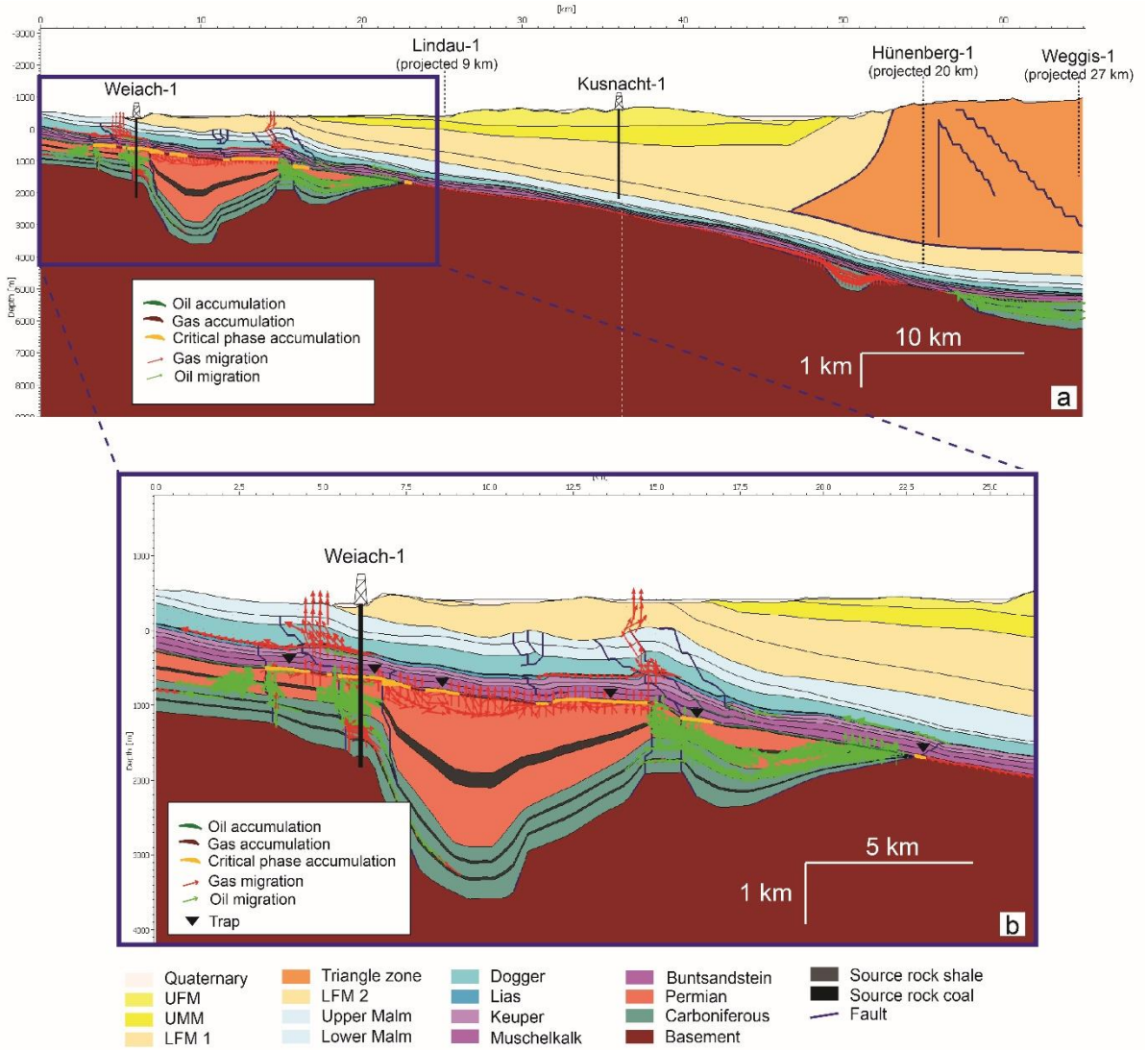


Fig. 88: Closed fault scenario: (a) Hydrocarbon accumulation and migration paths calculated by the model along section 5. In (b) zoom in on the northern area of the section, where the Weiach-1 well is located. Potential traps are indicated.

In Fig. 89 the hydrocarbon accumulations over the basin evolution are shown. The thermal maturity is also represented. In the northern part of the section, the Permian and Carboniferous units have entered the oil and gas windows since the Permian-Triassic times, as in this part of the section the grabens are very deep. The hydrocarbon accumulations in the Permian and Muschelkalk (including Buntsandstein units) have started forming since the Triassic time when a seal composed of anhydrite facies was deposited along the entire basin (Muschelkalk and Keuper units). These accumulations were filled over the entire evolution of the basin and they were partially preserved until the present day. In the southern part of the section, hydrocarbon accumulations started forming since the deposition of the Molasse units, when the Permian and Carboniferous source rocks entered the oil and gas windows because of the rapid burial of the basin. Accumulations formed in this sector were not preserved because of the intense structural deformation of the areas. Most of the hydrocarbon generated by the Posidonia shale source rock, as well as part of the hydrocarbons generated by deeper source rocks, migrated vertically to the top surface and were lost, because of the lack of proper traps. Few small accumulations could form in the anticline structures formed in the northern part of the section, as a consequence of the Jura Mountain formation.

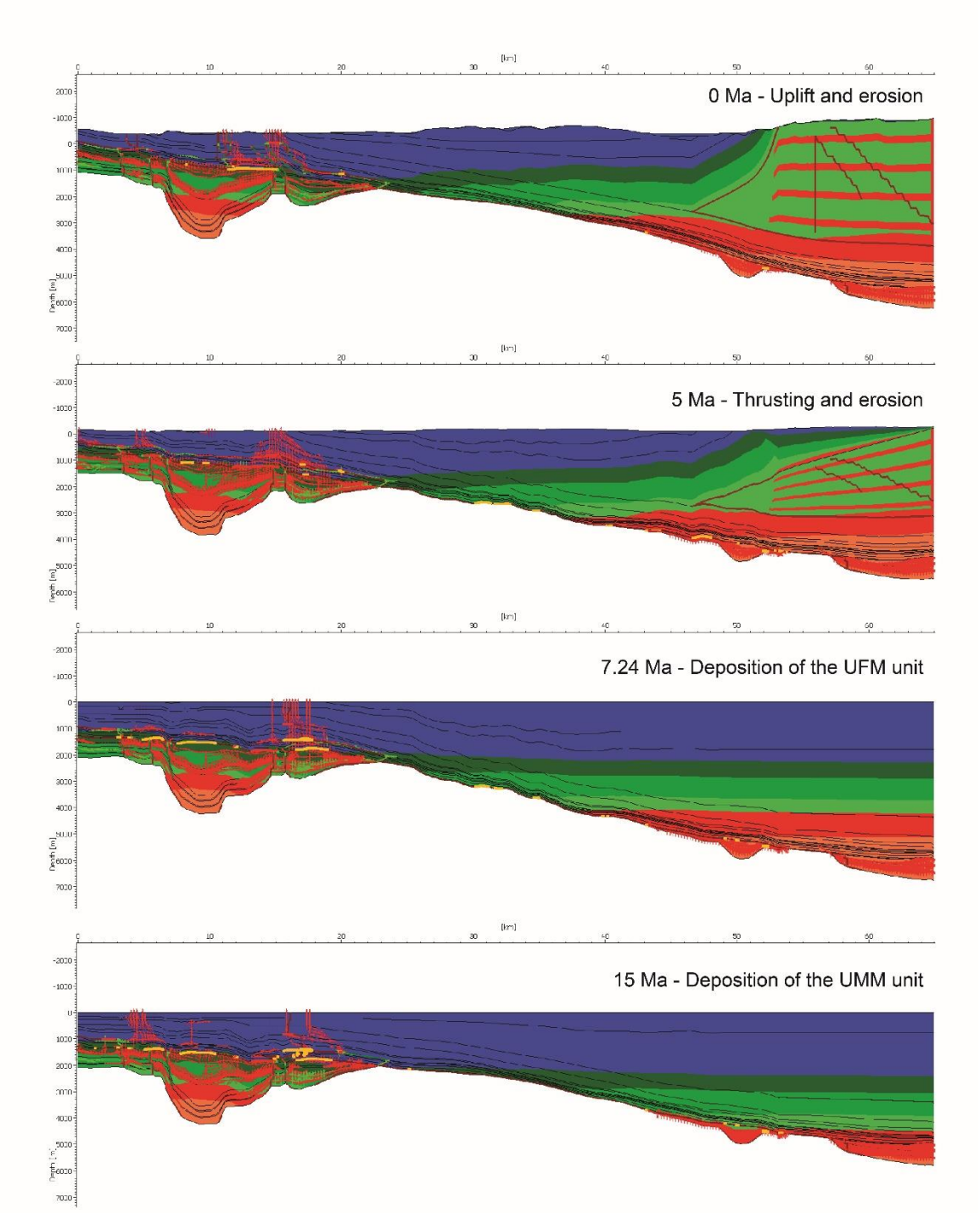


Fig. 89: Hydrocarbon accumulations over the evolution of the basin (continues)

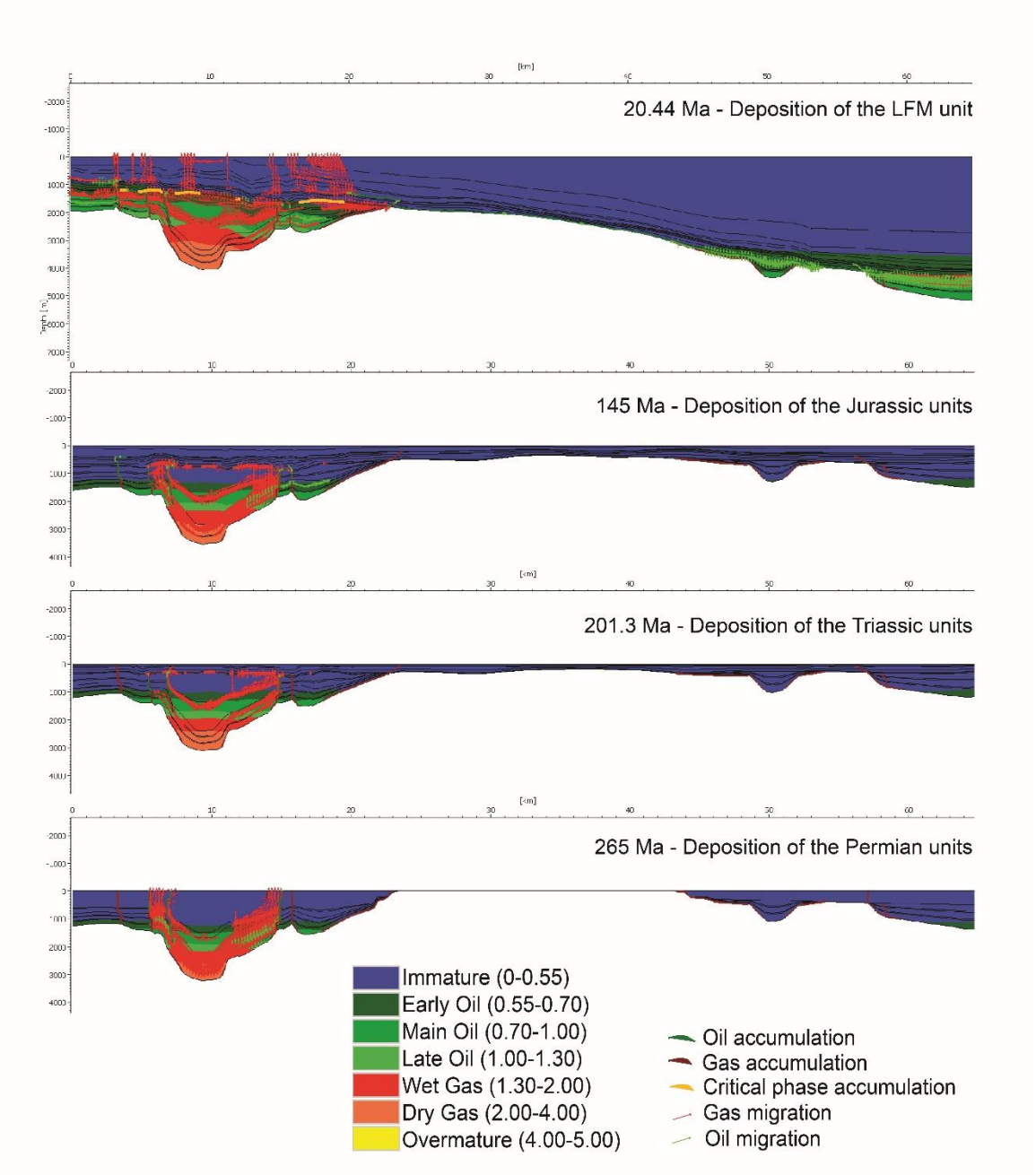


Fig. 89 (continues): Hydrocarbon accumulations over the evolution of the basin

The petroleum system evolution for the four source rocks considered is shown in terms of the petroleum system chart (Magoon and Dow, 1994) (Fig. 90), where the source rocks, reservoir, seal, overburden rocks and trap elements are defined. The critical moment is defined considering the fit among the formation of reservoirs, traps, the maturation timing of the source rocks and the hydrocarbon generation timing (Fig. 90)

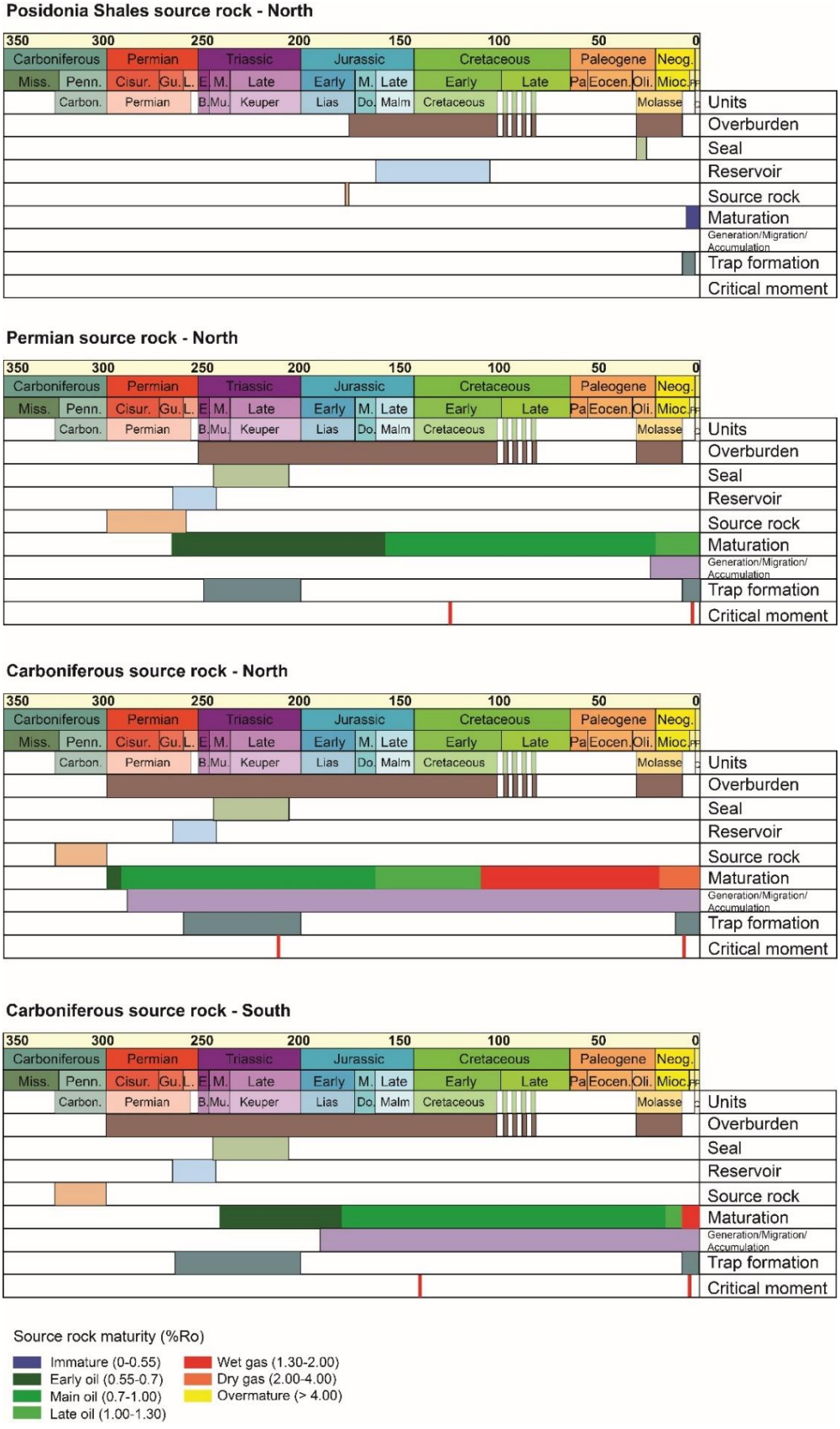


Fig. 90: Petroleum system charts reconstructed for the four source rocks defined in the Section 5

3.4.4 Comparison between the hydrocarbon findings and the modelling results

The most relevant hydrocarbon findings in the area are located in the northern part of the section (Weiach-1 and Weiach-2 wells area), in the Permian and Carboniferous deposits, which is in agreement with the modelling results, which simulates large hydrocarbon reservoirs in the Buntsandestein and Permian sandstones deposits (Table 44). In the Weiach-1 well, drilled by NAGRA in 1983, to explore the crystalline basement as potential nuclear waste storage, gas shows were found in the Permo-Carboniferous deposits. Therefore, in 2000, the SEAG consortium drilled the Weiach-2 well, located 350 meters from Weiach-1, to explore the tight reservoirs' natural gas potential. In this well gas was found at around 2000 meters, most likely in the Permian and Carboniferous tight reservoirs. Several tests of the gas-bearing strata were carried out. However, because of that the porosity and permeability of the rock were poor, despite breaking up the rock with a small explosive charge, there was no commercial gas flow to the well (SEAG, 2012).

In the Kusnacht-1 well, hydrocarbon traces were found in the Molasse unit, which is not simulated by the model, as the latter does not simulate relevant hydrocarbon migration into the uppermost Mesozoic and Molasse units in the central and southern part of the section (Table 36). Similarly, in the Tuggen-1 and Weggis-1 wells (located respectively at 16 and 27 km from the Section 5 trace line) several oil and gas shows were found in the Molasse section, which were not simulated in the model. However, it is relevant to underline that none in this area, real hydrocarbon reservoirs were not discovered.

The reasons for the discrepancies between the hydrocarbon findings and the modelling results can be multiple (Table 44):

- To the northern part of the section, the Permian and Carboniferous reservoir properties can be overestimated. Despite of that the porosity measured in the Weiach-1 well is satisfactorily calibrated in the model, the effective permeability can be not properly represented.
- In the model, the Permian and Carboniferous source rocks thickness and hydrocarbon potential defined in the Weiach-1 well were homogeneously extended to the entire Constance-Frick Permo-Carboniferous graben. However, it is unknown if these source rocks exist and if they maintain the same properties far away from the Weiach-1 well. In the case they are not, the amount of hydrocarbon generated by these source rocks in the area would be considerably different from what is simulated by the model.
- The seal of the Muschelkalk reservoir (Keuper unit) can be less efficient than what is calculated by the model. Pervasive fracturation can be present in the faulted areas. Indeed, anhydrites and evaporites can be interlayered also with dolomite, shales and thin sandstone layers. Thus, this seal might have also an important brittle component, reducing its efficiency.
- In the model, it is considered that only the Carboniferous source rock is present in the Permo-Carboniferous graben located in the southern part of the section, with thickness and geochemical properties similar to what is characterised in the Weiach-1 well. However, because of that, there are very poor data to constrain the presence, extension and filling of this graben, the volume of hydrocarbon generated by the Permian and Carboniferous source rocks in the southern area of the section, and migrated to the uppermost units, can be over or underestimated.
- Faulting in the lowermost Mesozoic units can be more extended than what is represented in the model, permitting the hydrocarbons generated by the Permian and Carboniferous source rock to migrate to the uppermost Mesozoic and Cenozoic units.
- The presence of the Posidonia shale in the southern part of the section is unknown, as none wells in this area penetrate the Lias unit. From paleogeographic reconstruction and data collected in other deeper wells, in the model, it is considered that this source rock is absent in the area. However, if present, more hydrocarbon migration paths could be present in the uppermost Mesozoic units and the Molasse sequence.
- More efficient lateral traps than what is crossed by the modelled section can be present. In this case, hydrocarbons could migrate and accumulate close to the reservoirs, which have not been penetrated by wells.

Well	Hydrocarbon finding	Modelling results	Discrepancy causes
Weiach-1 Weiach-2	• Gas shows in the Permian and Carboniferous units	• Gas reservoir in the Buntsandstein and Permian unit • Oil and gas migration paths in the uppermost Mesozoic units, generated by the Posidonia shale	• Permo-Carboniferous source rocks thickness and properties overstimated • Reservoir efficiency overestimated; • Seal not efficient • Lateral migration
Kusnacht-1	• Gas shows in the Molasse unit	• None	• Permo-Carboniferous source rocks thickness and properties underestimated • Faulting more extended • Lateral migration from traps
Lindau-1	• Gas shows in the Molasse unit	• None	• Permo-Carboniferous source rocks thickness and properties underestimated • Faulting more extended • Lateral migration from traps
Tuggen-1	• Oil and gas shows in the Molasse unit	• None	• Permo-Carboniferous source rocks thickness and properties underestimated • Faulting more extended • Lateral migration from traps • Well located too far from the modelled section trace to be representative
Weggis-1	• Oil and gas shows in the Molasse unit	• None	• Permo-Carboniferous source rocks thickness and properties underestimated • Faulting more extended • Lateral migration from traps • Well located too far from the modelled section trace to be representative

Table 44: Comparison between the hydrocarbon findings in the wells located close to the section trace and the modelling results. In case of discrepancy, the potential causes are indicated.

3.4.5 Uncertainties

The petroleum system model presented herein estimates the thermal maturity of the potential source rock, the type and amount of hydrocarbon generated and the potential areas where hydrocarbon can be accumulated and/or flow. However, because of the several assumptions made in constructing the model, several key uncertainties in the results must be considered. The most uncertain variables controlling the modelling results presented are listed in Table 45. A synthesis of the decision process carried out to handle the presented uncertainties is shown in Fig. 91.

Parameter	Uncertainty	Cause	Options	Effect on the petroleum system evolution	Impact	Potential improvements
Geometry of the basin	Horizons geometry, depth, stratigraphic units presence.	Interpolation of few 2D seismic lines across the Plateau. Few deep wells to corroborate the seismic data.	GeoMol 2021. Sommaruga et al. (2012).	Accumulation and migration areas can be different.	Medium	Acquisition of new 2D and 3D seismic and/or reprocessing of the existent geophysical data.
Faults	Faults location, extension, geometry.	Low resolution seismic data.	GeoMol 2021 Sommaruga et al. (2012). Greber et al. (2007).	The hydrocarbon migration can be different from what simulated by the model.	Medium/High	Acquisition of new 2D and 3D seismic and/or reprocessing of the existent geophysical data.
	Faults connectivity and cementation state.	Very scarce direct measurement and few description in well reports.	Faults open (not cemented). Faults close (cemented).	The volume of hydrocarbon accumulations can be different from what simulated by the model.	Medium	Sampling fault cement; Monitoring fluids flow.
	Continuity of the basement faults bounding the P-C grabens into Mesozoic and Cenozoic.	Low seismic resolution.	Yes. By this option, the hydrocarbon migration from the P-C grabens to the uppermost basin infill is facilitated No. By this option, the hydrocarbon migration from the P-C graben to the uppermost basin infill is not facilitated	Hydrocarbons migration from the Permian and Carboniferous source rocks to the Mesozoic and Cenozoic deposits can vary.	High	Acquisition of new 2D and 3D seismic and/or reprocessing of the existent geophysical data.
Facies	Facies distribution.	Data are available only where deep wells are present.	Facies extrapolated only from the wells located along the transect.	Hydrocarbon migration and/or accumulations.	Medium/High	Acquisition of new data.

Parameter	Uncertainty	Cause	Options	Effect on the petroleum system evolution	Impact	Potential improvements
Facies	Facies distribution.	Facies are deduced from qualitative description in the well report, there are no quantitative data.	Facies extrapolated also from the wells located at an offset of nearly 20 km from the transect.	Hydrocarbon migration and/or accumulations.	Medium/High	Acquisition of new data.
Structural evolution	Timing and magnitude of thrusting.	Scarce data dating the thrusting and able to calibrate the magnitude of the erosion in the South.	Thrusting starts at 7 Ma, after the deposition of the Molasse units.	The maturity of the southern part of the section and the timing of traps formation can be different.	Medium	Acquisition of new %Ro data; Reconstruction of a more accurate structural model.
			Thrusting starts before 7 Ma.			
	Triangular zone formation mechanisms.	The triangular zone formation mechanisms in the NAFB are poorly understood. The reconstruction of a proper structural model is highly time-cosuming.	Adoption of a simple model simulating the formation of the triangular zone just after the deposition of the Molasse units	Formation timing of the structural traps in the southern part of the section can be different.	Medium-Low	Reconstruction of a proper structural restoration.
			Reconstruction of the triangular zone formation and Molasse deposition by means of a proper structural restoration.			
Erosion	Magnitude of the erosion	The magnitude of the erosion cannot be measured directly, it can be only estimated by indirect data (%Ro, AFT, etc..).	Values estimated in the literature.	Burial, thus maturity, of the source rocks can be different.	Medium/High	Acquisition of more %Ro data along the section.
			Values estimatated in the most recent literature, modified in order to calibrate the %Ro data.			
	Timing of the erosion	Difficulty to date different erosion events.	Literature data.	Timing of the hydrocarbon generation.	Medium	Acquisition of AFT data along the section.

Parameter	Uncertainty	Cause	Options	Effect on the petroleum system evolution	Impact	Potential improvements
Boundary conditions	Present-day heat flow.	The heat flow values measured today in the wells are higher than what necessary to calibrate the present-day temperature data.	Assigning lower heat flow values than what measured today. Do not calculate the ragiogenic heat produced by the rock.	None, because it is a technical issue related to the software.	None	Acquisition of AFT data along the section.
	Paleo-heat flow.	The paleo heat flow over the basin evolution cannot be measured directly, it can be only estimated.	Heat flow trend in the literature. Heat flow trend in the literature, modified in order to calibrate the %Ro values.	Timing of the hydrocarbon generation can be different.	Medium/High	Reconstruction of crustal model to improve the estimates of the paleo-heat flow.
Permian and Carboniferous source rocks	Presence and geometry of the Permo-Carboniferous grabens in the Southern part of the section.	Low seismic resolution.	Leu (2008). Sommaruga et al. (2012). Greber et al. (2007).	Potential presence of deep hydrocarbon source rocks also in the South, thus hydrocarbons generation and migration also in this area.	Medium	Acquisition of new 2D and 3D seismic and/or reprocessing of the existent geophysical data.
	Presence, distribution and thickness of source rocks.	In the northern graben, source rocks have been identified only in the Weiach-1 well. It is not known if they are present in the others graben. In the southern graben there are no data.	Source rocks are present in the entire Northern graben and not in the Southern one. Source rocks are present in both northern and southern grabens, with a thickness based on the Weiach-1 well data.	Generation of different amount of hydrocarbons along the section.	High, especially in the southern sector.	To the North, improve the accuracy of velocity model, seismic contrast, filters, etc, in order to improve the identification of source rocks seismic facies .

Parameter	Uncertainty	Cause	Options	Effect on the petroleum system evolution	Impact	Potential improvements
Permian and Carboniferous source rocks	Presence, distribution and thickness of source rocks.	In the northern graben, source rocks have been identified only in the Weiach-1 well. It is not known if they are present in the others graben. In the southern graben there are no data.	The Permian source rock presents only in the northern graben, whereas the Carboniferous source rock present in both northern and southern grabens. Thickness based on the Weiach-1 well data.	Generation of different amount of hydrocarbons along the section.	High, especially in the southern sector.	Reconstruction of detailed stratigraphic model along the graben; To the South, acquisition of new geophysical data (seismic, deep wells).
	Hydrocarbon potential.	Data available only for the deposits sampled in the Weiach-1 well. No data throughout the rest of the grabens.	Geochemical data extrapolated from the Weiach-1 well along the entire section.	Volume of hydrocarbon generated can be different.	High	Penetrating these deposits in other location and direct measurement of the geochemical parameters.
Posidonia shale source rock	Presence of the Posidonia shale source rock.	It has been identified only in the northern part of the section. In the central and southern parts there are no data.	Present only in the northern sector, up to the Lindau-1 well	Generation, migration and accumulation of different amount of hydrocarbon.	High, especially in the southern part of the section.	Acquisition of more data in the Liassic interval, especially in the central-southern part of the section.
			Present along the entire section .			
	Hydrocarbon potential.	Data available only in the northern part of the section.	Extrapolated from the Weiach-1, Shafisheim-1 and Riniken-1 wells for the entire section	Volume of hydrocarbon generated		
Calibration of the model	Porosity data	Data are available only for few wells. Getting far from the wells used for calibration, the porosity can be different from what simulated	Use only of the available data along the section.	Hydrocarbons migration and accumulations could be different.	Medium	Acquisition of more porosity data along the section.
			Use of data measured in wells along the section plus from wells located at nearly 20 km from the section trace line.			

Parameter	Uncertainty	Cause	Options	Effect on the petroleum system evolution	Impact	Potential improvements
Calibration of the model	Porosity calibration.	The porosity reduction by diagenetic process cannot be properly simulated by the software.	Modify the initial porosity of the facies in the lithology library of the software.	Reservoir properties can be different from what simulated by the model.	Medium	Find a proper way to change in the software the porosity as a consequence of diagenetic processes and/or other processes.
	Present-day temperature data.	Data are available only for few wells.	Use only the data of the wells located along the section.	The present-day temperature can be different from what simulated, getting far from the wells where calibration data are available. There are no main consequence on the PS evolution.	Low	Acquisition of more borehole temperature data along the section.
			Use the data of the wells along the section and also the data measured in wells located at 30 km from the section trace line			
	Thermal maturity calibration.	For the Weiach-1 well, difficultly to perfectly calibrate the uppermost Mesozoic layers and the lowermost Permian and Carboniferous units.	Good calibration of the upper Mesozoic units; Less good calibration of the Permian and Carboniferous units.	The thermal maturity of the Posidonia shale is slightly higher (early oil window conditions) than what calculated by the model (immature).	Medium-Low	Improvement of the understanding of the thermal evolution of the basin and of the calibration processes provided by the software.
			Good calibration of the Permian and Carboniferous units; Less good calibration of the upper Mesozoic units.			

Table 45: List of the uncertainties parameters for the Section 5 model, their causes and their impact on the petroleum system modelling results. The options/scenarios available are indicated. In green is highlighted the option chosen in this study to build the petroleum system modelling. Potential improvements and actions to mitigate these uncertainties are suggested.

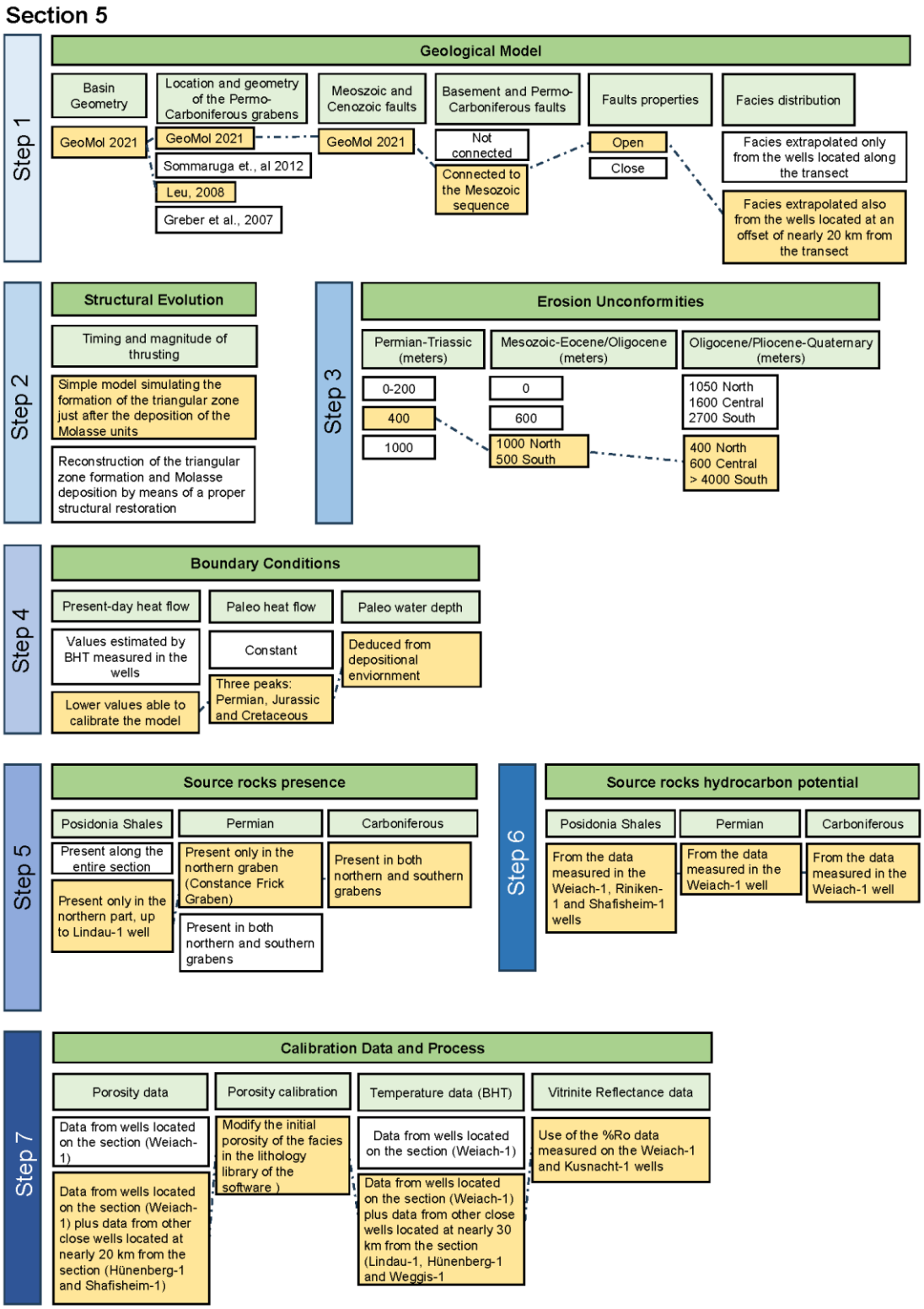


Fig. 91: Petroleum system modelling was built by selecting a specific combination of parameters, which are critical in controlling the thermal evolution of the basin and the hydrocarbon generation, migration and accumulation processes. In yellow are indicated the options chosen in this work.

3.5 Petroleum System Modelling - Section 6

3.5.1 Data

3.5.1.1 Geological Model

Section 6 is extracted from the GeoMol project, along a section line passing from the Cantons of Schaffhausen, Thurgau, St. Gallen, Appenzell Ausserrhoden and Appenzell Innerrhoden (Fig. 92). The trace of the section is NW-SE oriented, with the following extremity coordinates: NW edge x, y: 2686275.1; 1291998.8 SSE edge x, y: 2755323.8; 1239769.8 (Reference coordinate System CH1903+ / LV95), and a total length of 80 km (Fig. 92). The extracted section represents the present-day geological structure of the NAFB in the area, represented by a southern dipping foreland wedge, filled by the Cenozoic Molasse units, and its Mesozoic substratum (Fig. 93). The foreland basin is delimited to the north by the tabular Jura Mountain Chain, where the Mesozoic strata outcrop, and to the South by the more external Subalpine thrusts. The erosional topographic surface cut the Mesozoic substratum units in the northern part of the section and the uppermost Molasse units in the southern part.

In the southern part of the section, crossing the St. Gallen canton, the distribution of the Permo-Carboniferous grabens is better known, thanks to the availability of a 3D geophysical dataset (Naef and Schlanke, 2014; Heuberger et al., 2016; Omodeo-Salé et al., 2020). By these data, their geometry has been reconstructed with good detail and integrated into the GeoMol project so that the section trace passes exactly on the top of the St. Gallen-GT1 well, in the modelled section the deepest part of the graben located in the area is not represented. The faults delimiting the triangular zone were also adjusted to what was interpreted in the 3D seismic. On the other hand, in the northern part of the section, the presence of Permo-Carboniferous grabens is uncertain, as in the rest of the NAFB. Their location and geometry were deduced by Leu (2008). In this section, the types of faults are differentiated, as classified in the GeoMol database (Fig. 93).

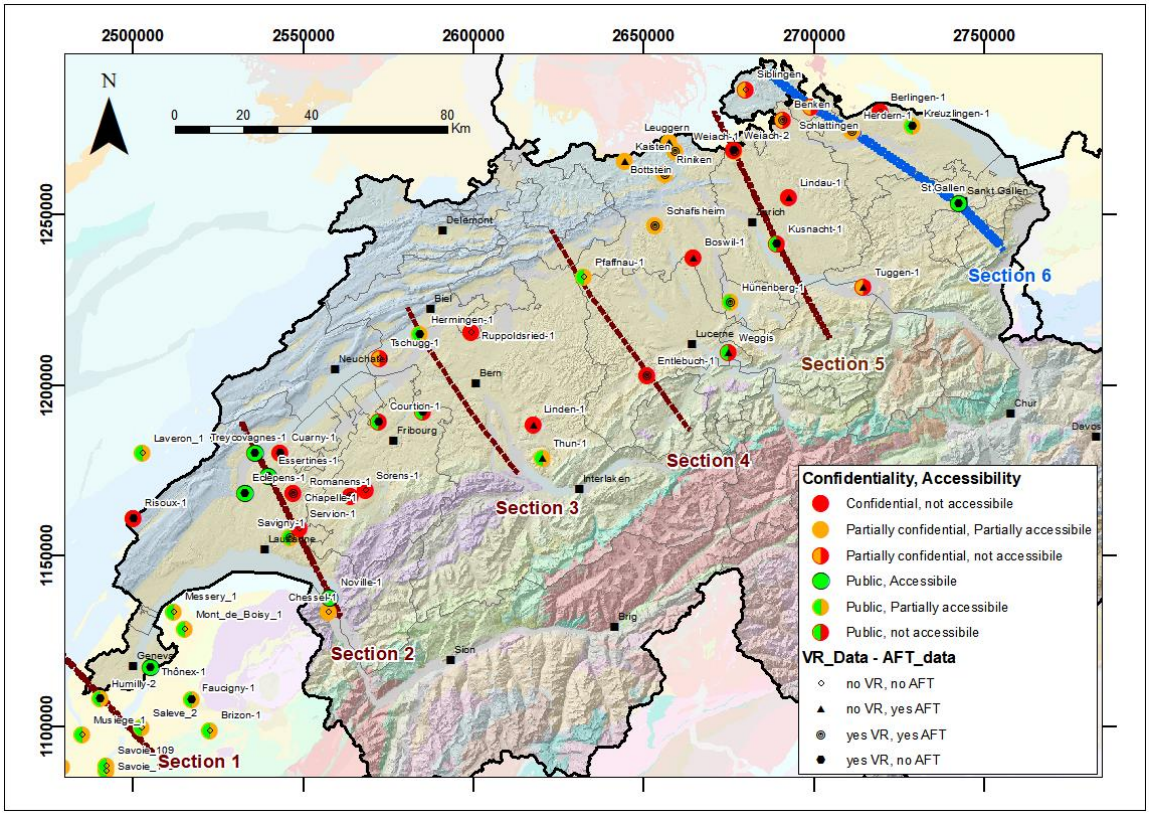


Fig. 92: Location of section 6.

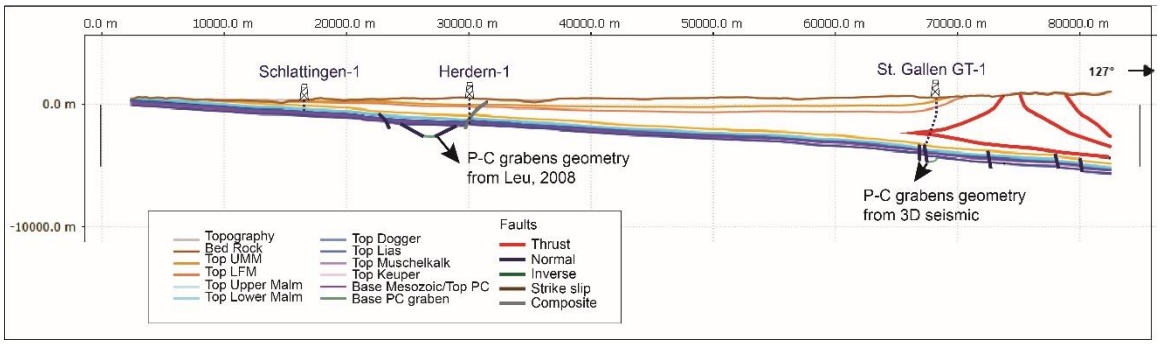


Fig. 93: Horizons and faults extracted from Geomol at the Section 6 trace location. The Permo-Carboniferou (P-C) graben geometry in the southern part of the section was extrapolated from the St. Gallen 3D seismic and in the southern part from what was proposed in Leu (2008). The wells intersecting the section trace are shown. In this section, the type of faults is differentiated, as classified in the GeoMol database.

3.5.1.2 Wells

Section 6 intersects the St. Gallen GT-1, Herdern-1 and Schlattingen-1wells, and it is relatively close to the wells Benken-1 (8 km E of the section trace), Berlingen-1 (9 km NE of the section trace) and Kreuzlingen-1 (11.5 km NE of the section trace) (Fig. 92). For these wells, the availability of the most relevant data necessary for thermal modelling is summarized in Table 46. The stratigraphic logs of these wells are shown in Appendix 4.

Well	Distance from section (km)	Status	Well report	Stratigraphic log	Calibration data	Rock-Eval data
St. Gallen GT-1	0	Public, Accessible	Yes	Yes	Phi, T, VR	Yes
Herdern-1	0	Partially confidential, Partially accessible	Yes	Yes	T, VR, AFT	
Schlattingen-1	0	Public, Not accessible	Yes	Yes	Phi, VR from T_{max}	Yes
Benken-1	8	Partially confidential; Not accessible	Yes	Yes	Phi, T, VR, AFT	No
Berlingen-1	9	Confidential, Not accessible	Yes	Yes	No	No
Kreuzlingen-1	11.5	Public, Partially accessible	Yes	Yes	Phi, T	No

Table 46: wells closest to the Section 6 trace and availability of the most relevant data needed for thermal modelling. Calibration data: (T) temperature; (VR) vitrinite reflectance; (AFT) apatite fission tracks, (P) porosity.

3.5.1.3 Deposition and erosional events

The burial history of the studied area is defined by a sequence of depositional and erosional events and their ages. Thus, in the model, an age for each stratigraphic unit and the main erosional event was assigned (Table 47).

Age top unit (Ma)	Unit	Event	Facies
0	Quaternary	Deposition	Quaternary
4	Erosion Pliocene-Quaternary	Erosion	
7.24	UFM	Deposition	UFM South; UFM Kreuz; UFM Central
15.97	UMM	Deposition	UMM South; UMM Central; UMM Kreuz
20.44	LFM	Deposition	LFM South upper; LFM South Triangle; LFM South Lower; LFM central; LFM North
33	Hiatus Cret/Eocene	Hiatus	

Age top unit (Ma)	Unit	Event	Facies
86	Erosion Cretaceous	Erosion	
113	Cretaceous	Deposition	
145	Upper Malm	Deposition	Upper Malm Central; Upper Malm North; Malm South
157.3	Lower Malm	Deposition	Lower Malm Central; Lower Malm North; Malm South
163.5	Dogger	Deposition	Dogger South; Dogger Central; Dogger North
174.1	Lias	Deposition	Lias Central; Lias North; Posidonia shale
201.3	Keuper	Deposition	Keuper Central; Keuper North; Gypskeuper Central; Gypskeuper North
237	Muschelkalk	Deposition	Upper Muschelkalk Central; Middle Muschelkalk Central; Lower Muschelkalk central; Upper Muschelkalk North; Middle Muschelkalk North; Lower Muschelkalk North
252	Hiatus Perm-Triassic	Hiatus	
259	Erosion Perm-Triassic	Erosion	
265	Permian	Deposition	Permian; Permian-Source rock (SR)
284	Carboniferous	Deposition	Carboniferous; Carboniferous-Source rock (SR)
323	Hiatus/erosion pre-Carbon		
400	Basement	Deposition	Basement

Table 47: Depositional and erosional events defined in the thermal model for section 6. A facies is assigned to each layer (see facies properties in the table in the facies section). UFM upper freshwater Molasse; UMM upper marine Molasse; LFM lower freshwater Molasse; LMM lower marine Molasse

In the northern sector of the NAFB, where the northern part of the section passes, several studies have been carried out to estimate the magnitude of the main erosion events that occurred during the evolution of the basin (Table 48). That is because it is available a large data set of the entire stratigraphic section of the NAFB, its substratum and crystalline basement (see Erosion subsection in the Method section). For the central-southern part of the section, data are available mostly for the Quaternary-Pliocene unconformity (Schegg and Leu, 1998; Cederbom et al., 2011) (Table 48). Therefore, based on the literature data, it is considered an erosion of 500 meters for the Permian-Triassic unconformity. For theMesozoic-Eocene unconformity, is considered an erosion of 1200 meters in the northern extremity of the section part (Benken-1 well), decreasing to 700 meters in the central part (Herdern-1 well) and to 500 m toward the south (St. Gallen GT-1 well). The Quaternary-Pliocene unconformity considered an erosion of 500 meters in the northern edge of the section (Benken-1 well), increasing to 1500 meters in the central part (Herdern-1 well) and to 2000 meters toward the southern edge (St. Gallen GT-1 well). For the Permian-Triassic unconformity, a uniform erosion value of 500 meters was assigned along the entire section. These values were subsequently tested and constrained by the thermal modelling workflow proposed herein (see the Calibration result section).

Erosion unconformity	Amount of erosion estimated in previous studies (m)	Method	NAFB study area	Source
Quaternary-Pliocene	0-500	Clays	E sector (Berlingen-1, Kreuzlingen-1)	Monnier, 1982 ; Lemcke, 1974
	500-600	subsidence analysis	E sector	Lemcke, 1974
	450	AFT, VR, 1D thermal modelling	Benken-1 well	Villagomez et al., 2021 Omodeo-Salé et al., 2021
	700	AFT	Herdern-1	Cederbom et al., 2011

Erosion unconformity	Amount of erosion estimated in previous studies (m)	Method	NAFB study area	Source
	1050	AFT, VR, 1D thermal modelling	NE sector (Herdern-1; Benken-1; Weiach-1 wells)	Mazurek et al., 2006
	1700	AFT, VR, 1D thermal modelling	Herdern-1 well	Villagomez et al., 2021; Omodeo-Salé et al., 2021
	1800	VR, 3D thermal modelling	St.Gallen GT-1	Omodeo-Salé et al., 2020
Mesozoic-Eocene	0	stratigraphy	Regional	Todorov et al., 1993; Burkhard and Sommaruga, 1998; Wildi et al., 1989; Lemcke, 1988
	600	AFT, VR, 1D thermal modelling	Benken-1 well	Mazurek et al., 2006
	700	AFT, VR, 1D thermal modelling	Herdern-1 well	Mazurek et al., 2006 and Omodeo-Salé et al., 2021
	700	VR, 3D Thermal modelling	St.Gallen GT1	Omodeo-Salé et al., 2020
	1200	AFT, VR, 1D thermal modelling	Benken-1 well	Villagomez et al., 2021; Omodeo-Salé et al., 2021
	1300	VR, clays, porosity, subsidence analysis	ENE sector	Schegg and Leu, 1998
Permian-Triassic				
	200	VR, 1D thermal modelling	Weiach-1 well	Omdeo-Salé et al., 2021
	200-600	VR	Weiach-1 well	Mazurek et al., 2006
	1000	VR, stratigraphy	Weiach-1 well	Diebold, 1988; Schegg and Leu, 1998

Table 48: Erosion magnitude estimated in previous studies for the three main erosional unconformities at the regional scale and/or in areas close to the section 6 trace line.

3.5.1.4 Facies

Facies were assigned to the stratigraphic units composing the section by extrapolating the lithologic data described in the well reports of the following wells: St. Gallen GT-1, Herdern-1, Benken-1, Kreuzlingen-1 and Berlingen-1. For these wells, the lithologies for each unit, expressed in percentage, are listed in Appendix 5. For each unit a unique or various facies were assigned along the section (Table 49), depending first on the variability of the facies and secondly on the availability of data. Because of that, no wells penetrate the Permo-Carboniferous grabens, the facies of these units were extrapolated from the Weiach-1 well.

Unit	Cgl	Sst	Silt	Shl	Lmt	Marls	Dlm	Anhyd	Halite	Reference Well
Quaternary	25	50		25						All
UFM South		10				90				St.Gallen
UFM central		10		20		70				Herdern-1; Berlingen-1
UFM Kreuzlingen		30				70				Kreuzlingen-1
UMM South	10	30	30			30				St.Gallen
UMM central	10	40	10			40				Herdern-1; Berlingen-1
UMM Kreuzling		80				20				Kreuzlingen-1
LFM South upper		20			5	75				St.Gallen

Unit	Cgl	Sst	Silt	Shl	Lmt	Marls	Dlm	Anhyd	Halite	Reference Well
LFM South Triangle		30			15	55				St.Gallen
LFM South lower		13			2	85				St.Gallen
LFM central 2		20		10		70				Herdern-1, Berlingen-1; Kreuzlingen-1
LFM North 2		30		10		60				Benken-1
Malm South					100					St.Gallen
Upper Malm central				15	85					Herdern-1; Berlingen-1; kreuzlingen-1
Upper Malm North					80	20				Benken-1
Lower Malm central				10	70	20				Herdern-1; Berlingen-1, Kreuzlingen-1
Lower Malm North				55	45					Benken-1
Dogger South		20		50	30					St.Gallen
Dogger Central		5		15	20	65				Herdern-1; Berlingen-1- Kreuzlingen-1
Dogger North		5		80	15					Benken-1
Lias central		10		50	20	20				Herdern-1; Berlingen-1, Kreuzlingen-1
Lias North				30	20	50				Benken-1
Keuper Central		5		55		20	15	5		Herdern-1; Berlingen-1- Kreuzlingen-1
Keuper North				40		30	20	10		Benken-1
Gypskeuper central		5		25		10	40	20		Herdern-1; Berlingen-1; Kreuzlingen-1
Gypskeuper North				50		30		20		Benken-1
Upper Muschelkalk central		10		20	20		30	20		Herdern-1; Berlingen-1; Kreuzlingen-1
Upper Muschelkalk North					50		50			Benken-1
Muschelkalk middle central				40	10		20	25	5	Herdern-1; Berlingen-1; Kreuzlingen-1
Muschelkalk middle North				25			30	30	15	Benken-1
Lower Muschelkalk central		5		45		20	25	5		Herdern-1; Berlingen-1; kreuzlingen-1
Lower Muschelkalk North						60	40			Benken-1
Buntsandstein central		100								all
Permian	15	25	25	35						Weiach-1, Kreuzlingen-1
Carboniferous		40	25	33					2 coal	Weiach-1
Basement										Herdern-1

Table 49: Facies, expressed as a percentage of lithological composition, assigned to the stratigraphic units forming the basin infill of section 6. The wells used as references are indicated. Cgl: conglomerate; Sdt: sandstone; Slst: siltstone; Shl: shale; Lmt: limestone; Mrl: marl; Dlm: dolomite; Anhd: anhydrite; Halt: halite.

3.5.1.5 Calibration data

Porosity data are available for the Schlattingen-1, Benken-1, Kreuzlingen-1 and St. Gallen GT-1 wells (Appendix 6). Along these wells, the porosity was measured only for the supposed potential reservoirs, mostly located in the Mesozoic units, which were the exploration targets at the time

when the wells had been drilled. Therefore, in the Section 6 area, there are no porosity data measured directly in the Molasse units.

Using the St. Gallen GT-1 well logging data, the porosity along the Molasse units could be estimated from the density and sonic logs. Firstly, an estimated density log was calculated from the sonic log by applying Gardner's equation (Gardner and Gardner, 1974). Then porosity was calculated by the estimated density log, considering an average matrix density of 2.7 g/cc and an average fluid, salt water, density of 1.15 g/cc. A continuous porosity log was obtained. To simplify in Petromod representative's values of this log, every 100 meters, were considered. In Appendix 6, it is reported only the average of the porosity estimated for each Molasse stratigraphic unit. For the rest of the section, it was considered the Molasse porosity measured for this unit throughout the NAFB and reported by Greber et al. (2007), which ranges from 8-15 % in the northern sector (wells Pfaffnau-1, Essertines-1, Hermrigen-1, Schafisheim-1 and Weiach-1) and 2-10 in the southern sector (Thun-1 and Savigny-1).

To calibrate the present-day temperature over depth in the basin infill, they used the borehole temperature data (BHT) of the Benken-1, Herdern-1 and St. Gallen GT1 wells (Appendix 7).

To calibrate the thermal conditions attained during the evolution of the basin, they were used the vitrinite reflectance data measured along the Benken-1, Herdern-1 and St. Gallen GT-1 wells (Appendix 8). In the Schlattingen-1 well, %Ro data were estimated from T_{max} values measured by Rock-Eval analysis, by applying the empirical relationship between Tmax and vitrinite reflectance developed (Jarvie et al., 2001) for type II and type III kerogens (Wersin et al., 2013). The estimate of the Cretaceous and Pliocene-Quaternary erosions using AFT data, in the northern area of the section (Villagomez et al., 2021; Mazurek et al., 2006; Cederbom et al., 2011, see Erosion section above), was used to constrain the erosion variable, despite of that these data cannot be directly used to calibrate the thermal model results

3.5.1.5 Source rock parameters

According to the rest of the NAFB, three main source rocks are considered: the marine Posidonia Black Shales (Toarcian in age), the lacustrine Autunian shales (Permian in age), and the Carboniferous coal and shales (Carboniferous in age) (Leu and Gautschi, 2014; Misch et al., 2017; Schegg and Leu, 1998). In the modelled section, the Posidonia shale source rock is most likely present in the northern and central part, as it has been found in the Schlattingen-1 well, Benken-1 well (10 meters of thickness) and in the Kreuzlingen-1 well (8 meters of thickness). However, there is no evidence of the presence of the Posidonia shale source rock in the Herdern-1 well. To the south, its presence is unknown as the St. Gallen GT-1 well did not penetrate the Lias unit. Therefore, this source rock was assigned from the northern edge to the central part, at around 40 km from the northern edge (after the position of the projection of the Kreuzlingen-1 well), with an average thickness of 5 meters. In the Schlattingen-1 well, the petroleum potential of the Posidonia shale was measured on one sample using Rock-Eval (Wersin et al., 2013). The analysis results in a TOC of 742%, an HI of 668 mg/g TOC and a T_{max} of 428 °C for this rock, indicating an immature source rock with good hydrocarbon potential. In the Section 6 model, the source rock properties of the Posidonia shale source rock were assigned by considering the Schlattingen-1 data together with the larger data measured in the northern Switzerland (Weiach-1, Riniken-1 and Schafisheim-1 wells) (Table 50).

The presence of the Permian and Carboniferous source rocks is uncertain along the entire section. To the south, in the St. Gallen GT-1 well area, Permo-Carboniferous grabens were recognized, thanks to the availability of high-resolution 3D seismic (Heuberger et al., 2016). Because of that, thermogenic gas was found during the St. Gallen GT-1 well exploration activities (Diehl et al., 2017; Moeck et al., 2015; Wolfgramm et al., 2015) it has been deduced that Permian and/or Carboniferous organic matter-rich layers are present in these grabens (Eichinger, 2014; Jurisch, 2013; Omodeo-Salé et al., 2020; Wolfgramm et al., 2015). In the modelled section, only the more external and shallower part of the Permo-Carboniferous graben below the St. Gallen GT-1 well is represented. Permian and Carboniferous source rocks were assigned to these deposits, with geochemical properties similar to those determined for the corresponding source rocks analysed in the Weiach-1 well. To the north, the presence of the Permian and Carboniferous source rocks is more uncertain. A graben has been recognized by Leu (2008), which is most likely the same

Constance Frick graben described in Madritsch et al., (2018). Therefore, it is considered that the infill of this graben can be similar to what is described in the Weiach-1 well (see Section 5). The synthesis of the geochemical properties of the Permian and Carboniferous source rocks is presented in Table 50.

Source Rock	Lithology	Present average TOC (%)	Initial TOC (g rock)	Present average HI (mgHC/gTOC)	Initial HI (mgHC/gTOC)	Kinetic
Posidonia shale	Black shales	7	**8**	667	**700**	TII(PB) (Behar et al., 1997)_
Permian lacustrine shales	Shale organic rich	4.7	**6.2**	289	**500**	TI(C) (Pepper and Corvi, 1995)
Carboniferous coal	Coal	72	**75**	210	**250**	TIII-(Dogger) (Behar et al., 1997)
Carboniferous shales	Shale organic rich	8	**8.5**	95	**150**	TIIIH(DE) (Pepper and Corvi, 1995)

Table 50: Present-day and initial geochemical properties assigned into the model for the four source rocks.

Along the section, the internal subdivision of the Permo-Carboniferous grabens in the stratigraphic unit was done following what was proposed by Madritsch et al., (2018) and what was observed in the Weiach-1 well. The total thicknesses of the Permian and Carboniferous source rocks concerning the entire Permian and Carboniferous deposits are 8% and 9% respectively, with a maximum thickness of 56 and 40 meters.

3.5.2 Boundary conditions

The upper boundary condition, the sediment-water interface temperature (SWIT), was automatically calculated by the software, for a geographical area located at a latitude of 46°N (present Switzerland latitude) (Fig. 12). The paleowater depth was deduced by the depositional environment of the main stratigraphic units forming the basin and the basal heat flow trend was reconstructed considering the geodynamic evolution of the Molasse Foreland Basin (see Methods section) (Table 51).

Age to (Ma)	PWD (m)	Age from (Ma)	HF value (mW/m2) initially assigned	HF value (mW/m2) calibrating the model	
				North-Central	Central-south
0	0	0	variable*	30	30
22	0	0.4	50	35*	35
66	300	5	50	40	40
125	100	29	50	60	50
152	10	80	50	90	90
160	300	118	75	95	95
		127	75	80	80
163.5	100	142	75	75	65
174.0	300	146	75	80	85
190	100	172	60	75	75
201.3	70	200	60	70	70
252	0	250	60	70	70
265	0	260	87	90	90
		270	100	110	110
		290	120	130	130
		300	80	120	120
		400	60	60	60

Table 51: Paleowater depth (PWD) and basal heat flow variation over time. To calibrate the present-day temperature and the vitrinite reflectance data, the heat flow trend was iteratively changed to obtain a satisfactory result. To fit the calibration data, a variation of the heat flow trend along the section was necessary.

At the present day (0 My) a variation of the basal heat flow along the section was considered (Fig. 94), based on the present heat flow distribution calculated throughout the NAFB (data source: https://map.geo.admin.ch, see Fig. 15).

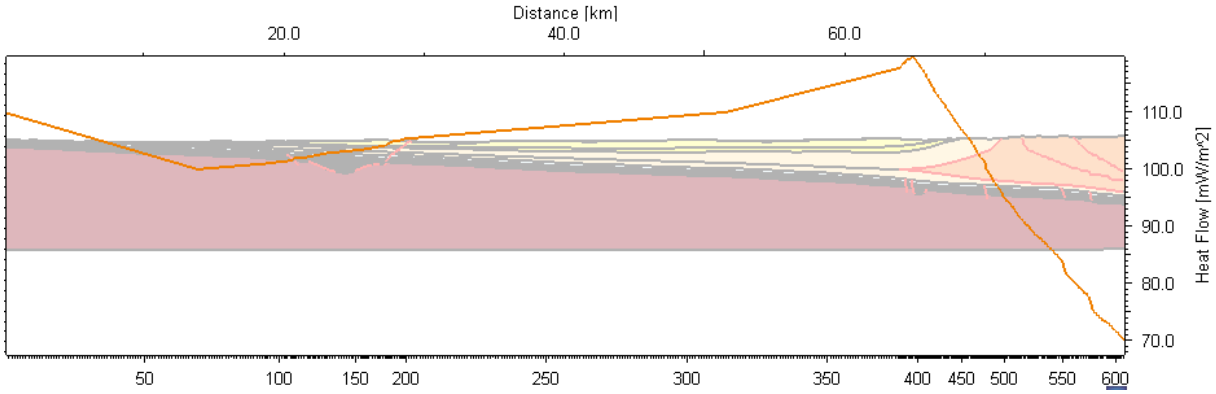


Fig. 94: Basal heat flow assigned along the Section 6 at the present-day (0 My)

3.5.3 Results

3.5.3.1 Restoration to the pre-Alpine deformation phases

Because of that, in Section 6 thrusts and inverted faults are present, and it is essential to restore the geometry of the basin to the pre-Alpine deformation phase. Because of that the southern part of the sections passes throughout the triangular zone, a simplified method is applied, which simulates the formation of this complex structure directly in the PetroMod software (see Method section). Therefore, for this section, the TecLink workflow was not applied, which tremendously simplified the modelling work.

3.5.3.2 Geological conceptual model evolution

The section extracted from Geomol (Fig. 93) was imported into the PetroMod software and each horizon was assigned to a stratigraphic unit and at a corresponding age (Table 47). The facies previously defined (Table 49) were assigned to the stratigraphic units composing the sections (Fig. 95).

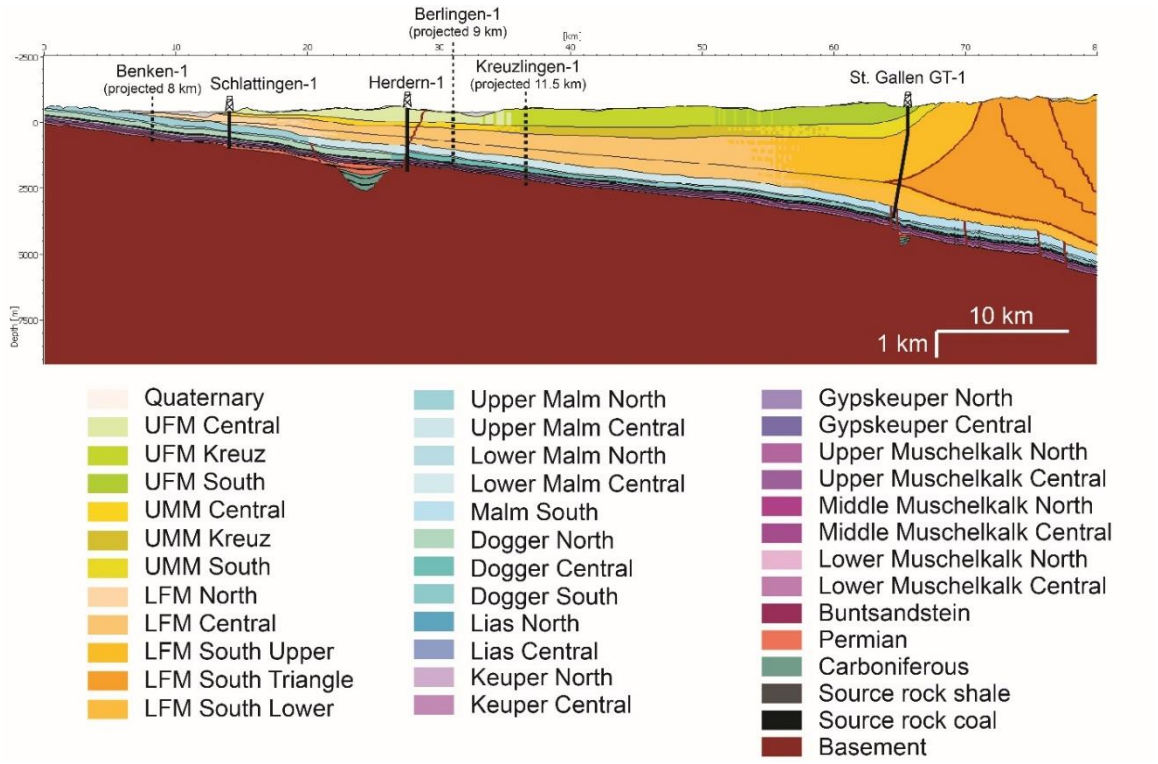


Fig. 95: Section imported in Petromod and used as a geological model. Based on the stratigraphy described in the closest wells, facies were assigned to the present-day section. Sections vertical exaggeration 2:1.

The geological evolution of the basin along Section 6 is shown in Fig. 96. The formation of the triangular zone was simulated in the PetroMod software, using the introduction of an additional layer with paleo-thickness increasing from 7 to 0 Ma. Because of the thrusting and the formation of the triangular zone, the Molasse units, located in the southern part of the basin, were uplifted and eroded. In the same period, northward the Jura structures started forming, while the entire basin was exhumed and eroded.

The magnitude of the Pliocene-Quaternary erosion was estimated considering previous literature data (Table 48) and calibrated with vitrinite reflectance data (see Calibration section below). It ranges from 450-600 in the north (projected Benken-1 well area) to 900 meters in the central part (Herdern-1 well area) to 1800 meters southward (St. Gallen GT-1 well) and over 5000 meters toward the southern edge. In the southern extremity of the section, these great erosion values were necessary to geometrically reconstruct the undeformed geometry of the foreland previous to the triangular zone formation. To present there are no calibration data to constrain this data.

To simulate the deposition and the erosion of the Cretaceous, because the Cretaceous layer is not represented along the section, it was assigned an additional paleothickness at the Malm unit, from 145 to 90 Ma, which was removed from 90 Ma to 56 Ma as the effect of the erosion. The thickness of the eroded Cretaceous deposits was based on literature data (Table 48), and it ranges from 1300 meters in the northern part of the section (Benken-1 well) to 1000 meters in the central and southern parts. For the Permo-Triassic unconformity, it was considered an erosion of 500 meters of Permian deposits, located on the top of the Permo-Carboniferous grabens.

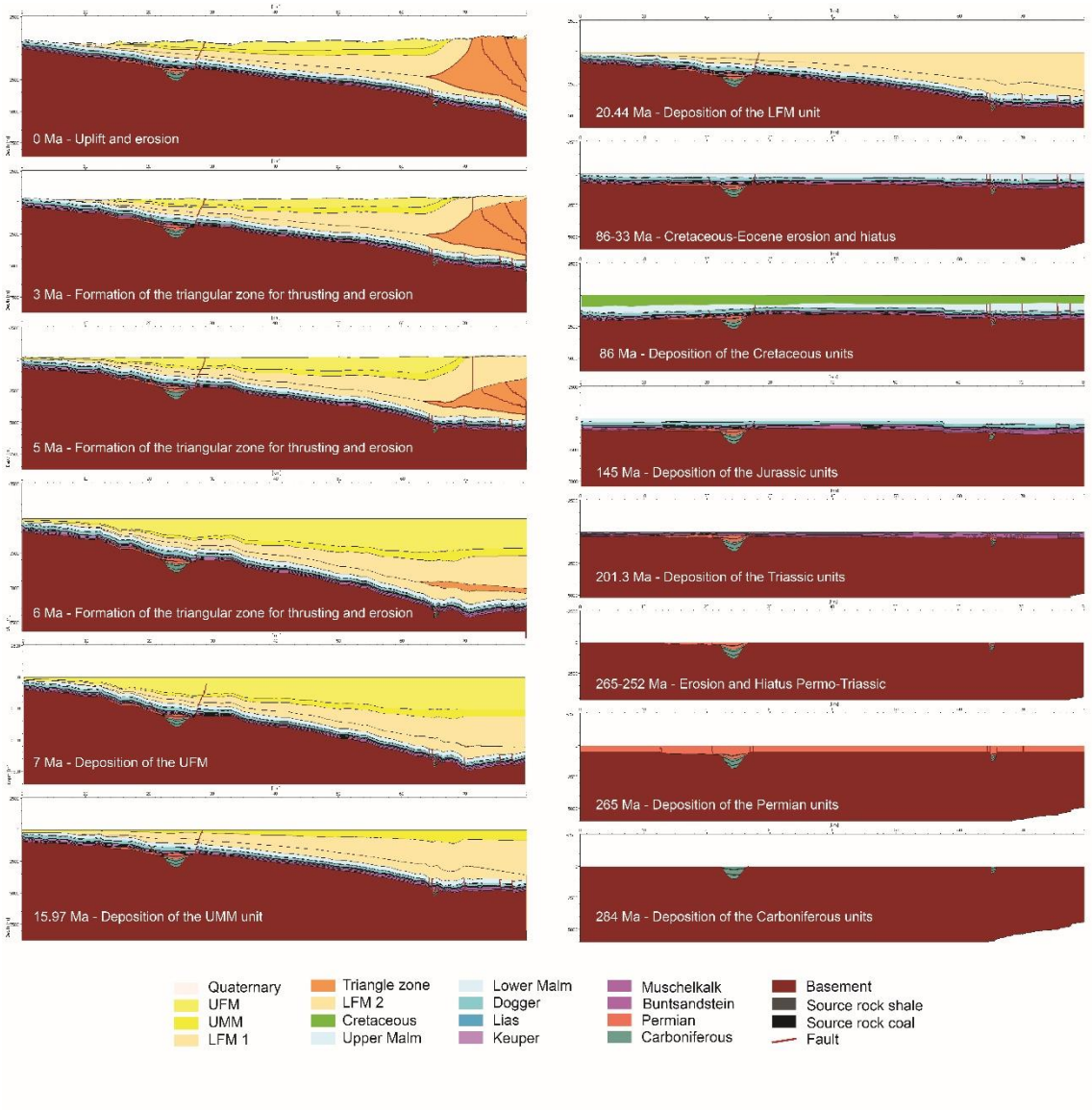


Fig. 96: Geological evolution of the studied area obtained in Petromod by retrodeformation and decompaction of the units forming the basin infill, from the present-day to the Carboniferous time. Sections vertical exaggeration 2:1.

3.5.3.3 Thermal Model Calibration

3.5.3.3.1 Porosity

The porosity was calibrated for the Schlattingen-1, Benken-1 (projected 8 km), Kreuzlingen-1 (projected 11.5 km) and St. Gallen GT-1 wells. The mechanical compaction properties estimated by the software for the lithologies assigned to each stratigraphic unit were iteratively changed to fit the theoretical values calculated by the model with the porosity values measured along the wells. The calibration results are shown in Fig. 97. The porosity values calibrated in these wells were assigned along the entire section (Fig. 98). For the St. Gallen GT-1 well, the Molasse unit porosity was calibrated with the values estimated from the sonic and velocity logs (see data paragraph) and extrapolated along the entire southern sector of the modelled section. Along the rest of the section, in the central and northern sector, the Molasse unit porosity was extrapolated from the few values available for these units in other wells throughout the Plateau (wells Pfaffnau-1, Essertines-1, Hermrigen-1, Schafisheim-1 and Weiach-1, data from Greber et al., 2007), which are in the range of 8-15 %.

The porosity extrapolation performed here along the section can be highly uncertain, especially, but not only, in the case of the dominant limestone units (Mesozoic), where the porosity and permeability are strictly controlled by diagenetic processes and fracking, which can dramatically change from one point to the other of the basin. To reduce this uncertainty, more porosity data with depth should be available along the section.

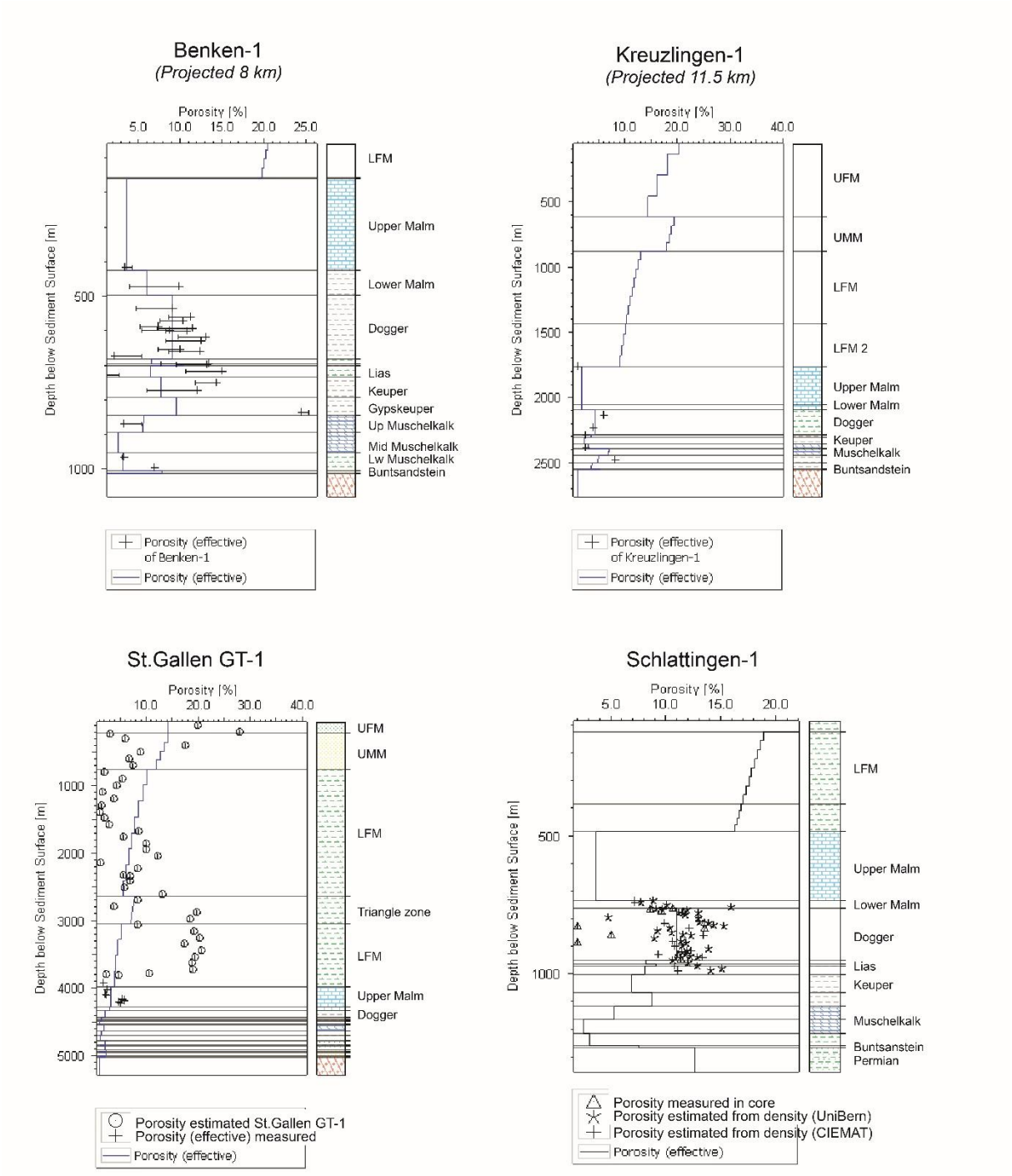


Fig. 97: Calibration of the porosity property with the data measured in the Benken-1, Kreuzlingen-1, St.Gallen GT-1, and Schlattingen-1 wells. In the latter wells porosity data were also estimated from logs.

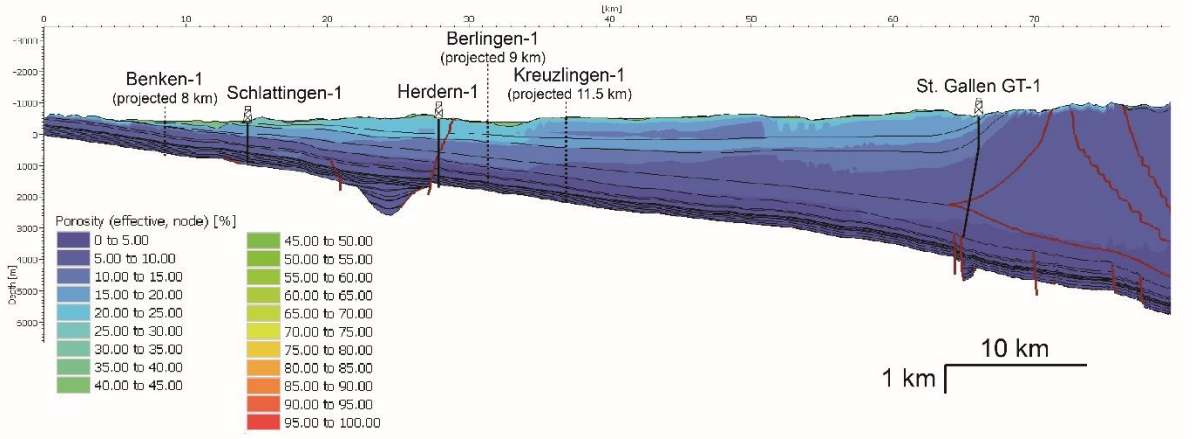


Fig. 98: Porosity simulated along the section by the software, extrapolating the data calibrated in the Schlattingen-1, Benken-1, Kreuzlingen-1 and St. Gallen GT-1 wells.

3.5.3.3.2 Present-day temperature

The present-day temperature calculated by the model was calibrated with the borehole temperature (BHT) measured in the wells Benken-1, Herdern-1, Kreuzlingen-1 and St. Gallen-GT-1. To calibrate the modelling results, the variable that mostly changed was the present-day basal heat flow (see Method section). Firstly, it was tested the heat flow values estimated in the entire basin from borehole temperature data (Fig. 99, scenario A). This scenario does not give satisfactory calibration results, as the temperature simulated by the model is considerably higher than what is measured in the wells (Fig. 100). This is because the heat flow values of Scenario A represent the heat flow at the surface, whereas the heat flow that was assigned into the model refers to the amount of heat at the base of the model, basement included. Toward the basin surface, this heat is increased, mostly by the radiogenic heat produced by the basement and basin infill rocks. The effect of the rapid exhumation of the NAFB can also play a role in maintaining an anomalously high heat flow at the surface of the basin. For more details, see the explanation in the Method section, Calibration subsection.

Another heat flow scenario is tested for 0 Ma (Fig. 99, scenario B), with a unique value of 30 mW/m2 along the entire section. This scenario considerably improves the calibration of the borehole temperature measured in the wells (Fig. 100). According to this scenario, the model calculates the temperature distribution along the section at the present day (Fig. 101).

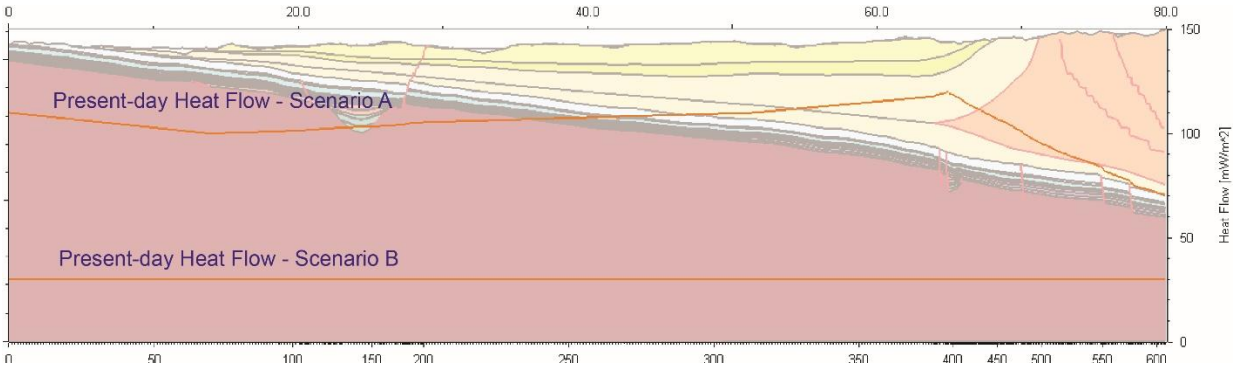


Fig. 99: Heat flow values assigned along the modelled section at 0 Ma. The two scenarios tested are shown.

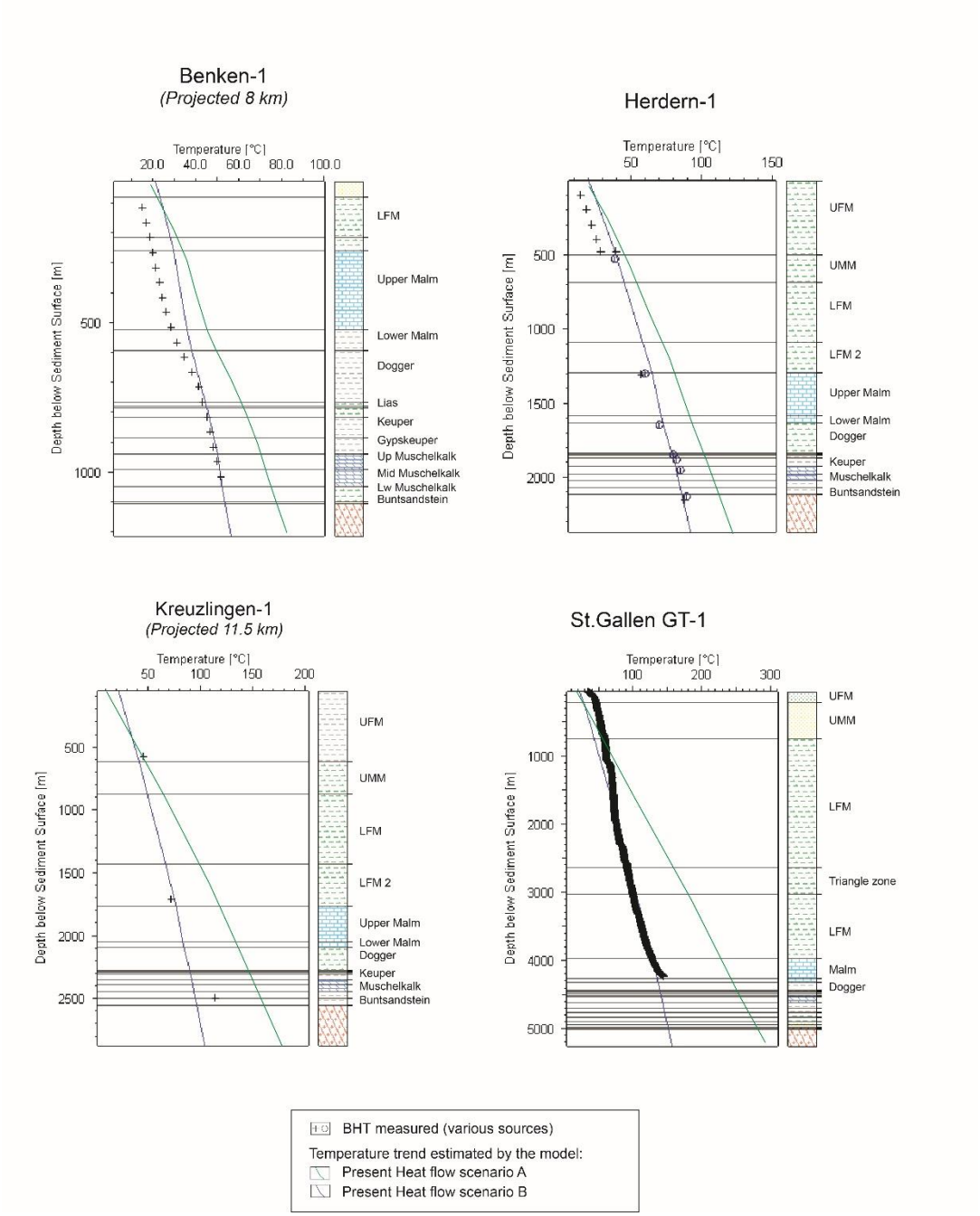


Fig. 100: Calibration of the present-day temperature modelling results with the BHT measured in the wells closest to Section 6.

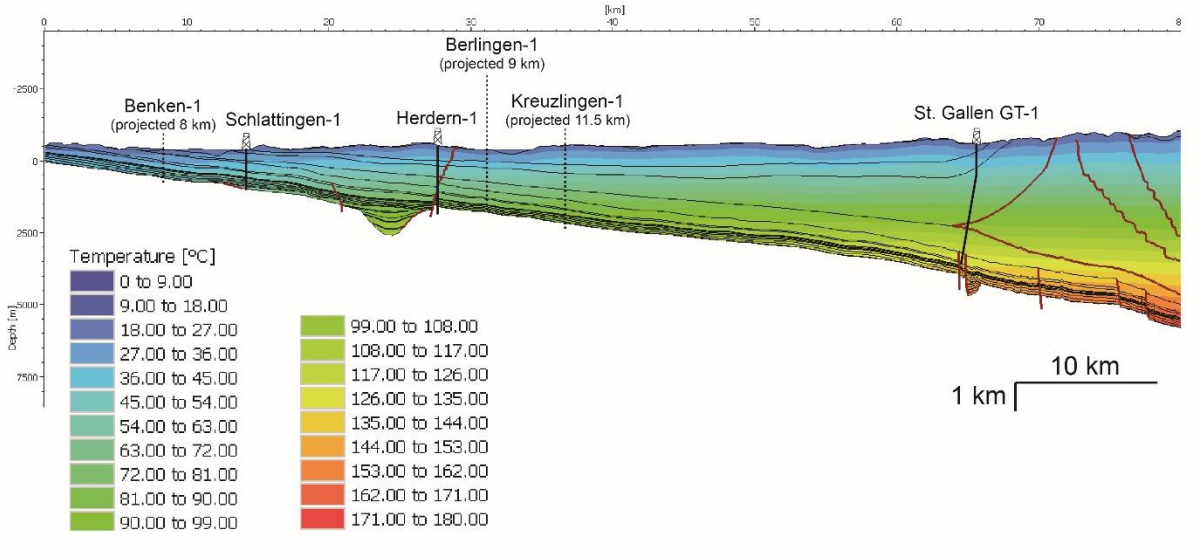


Fig. 101: Temperature variation with depth calculated by the model along the section for the present day (0 My), calibrated with the present-day heat flow scenario B.

3.5.3.3.3 Thermal conditions / Source rocks maturity

The %Ro values measured in the Schlattingen-1, Benken-1, Herdern-1 and St. Gallen-GT-1 wells were satisfactorily calibrated with the erosion values described in the geological model result section (Fig. 102). The thermal conditions resulting along the entire section are shown in Fig. 103. To obtain a satisfactory calibration, the paleo heat flow was changed to fit the %Ro data in the three wells. A variation of the heat flow trend along the section was necessary, with higher heat flow values in the northern part of the section (Benken-1 and Herdern-1 wells area) than in the south, during the Jurassic-Cretaceous extensional phase.

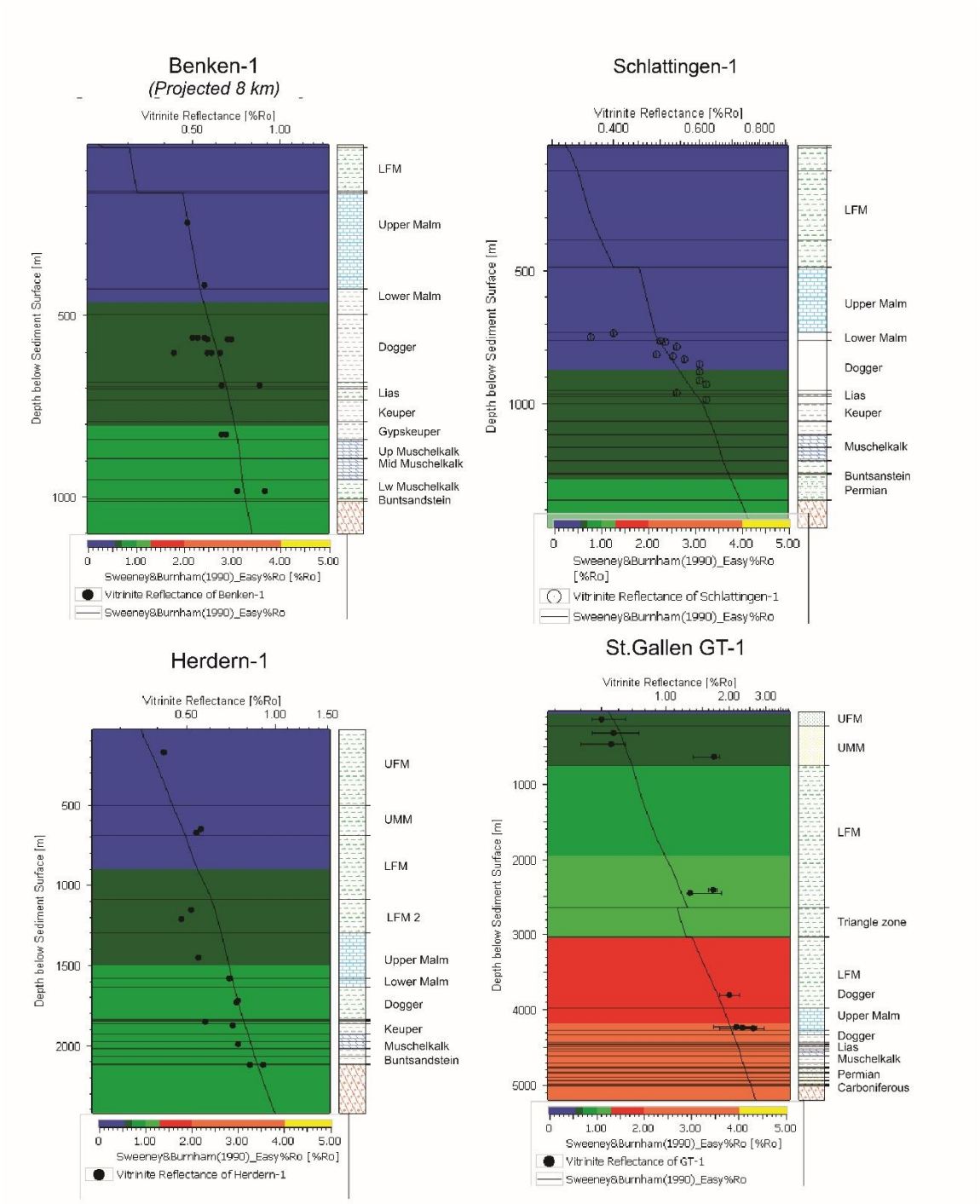


Fig. 102: Calibration of the thermal conditions calculated by the model with %Ro data measured for the Benken-1, Herdern-1 and St. Gallen GT-1 wells.

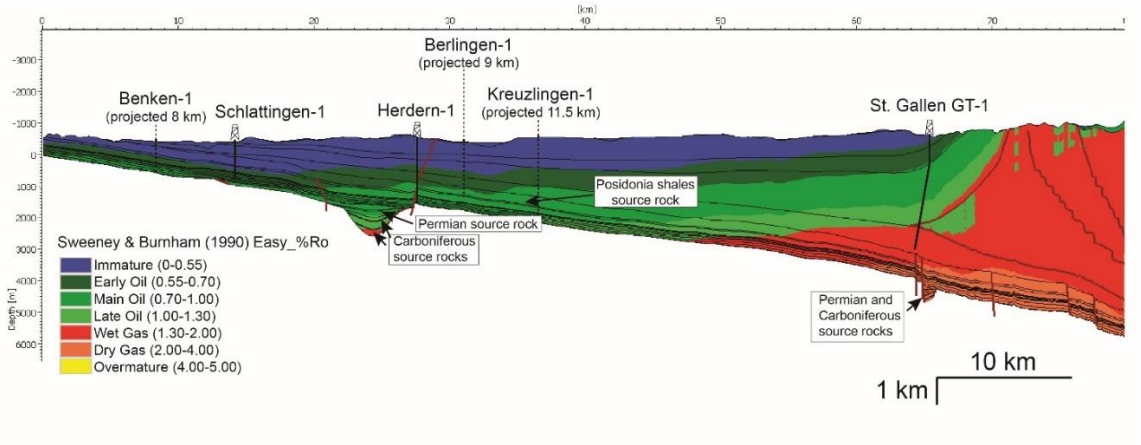


Fig. 103: Thermal conditions calculated by the model along the entire section

From the modelling results it is deduced that, in the northern part of the section (Benken-1 and Shclattingen-1 wells area), the Posidonia shale source rock is in the early oil window thermal stage and the northern-central part (Herdern-1 and Kreuzlingen-1 wells area), in the main oil window thermal stage. To the south, this source rock is most likely absent. The Permian source rock is in the late oil window thermal stage in the northern graben and the gas conditions in the southern graben. Finally, the Carboniferous source rocks are in the late oil window to the wet gas thermal stage in the northern graben and the dray gas window thermal stage in the southern graben.

The source rocks maturation timing is deduced by the burial plot vs thermal conditions extracted at the Benken-1 and St. Gallen GT-1 wells position (Fig. 104). In the northern part of the section (Benken-1 well area), the Posidonia shale, Permian and Carboniferous source rocks enter the oil window during the Cretaceous. In the southern part of the section (St. Gallen GT-1 well area), the Permian and Carboniferous source rocks enter the oil window in the Cretaceous and the gas window in the Oligocene and Miocene.

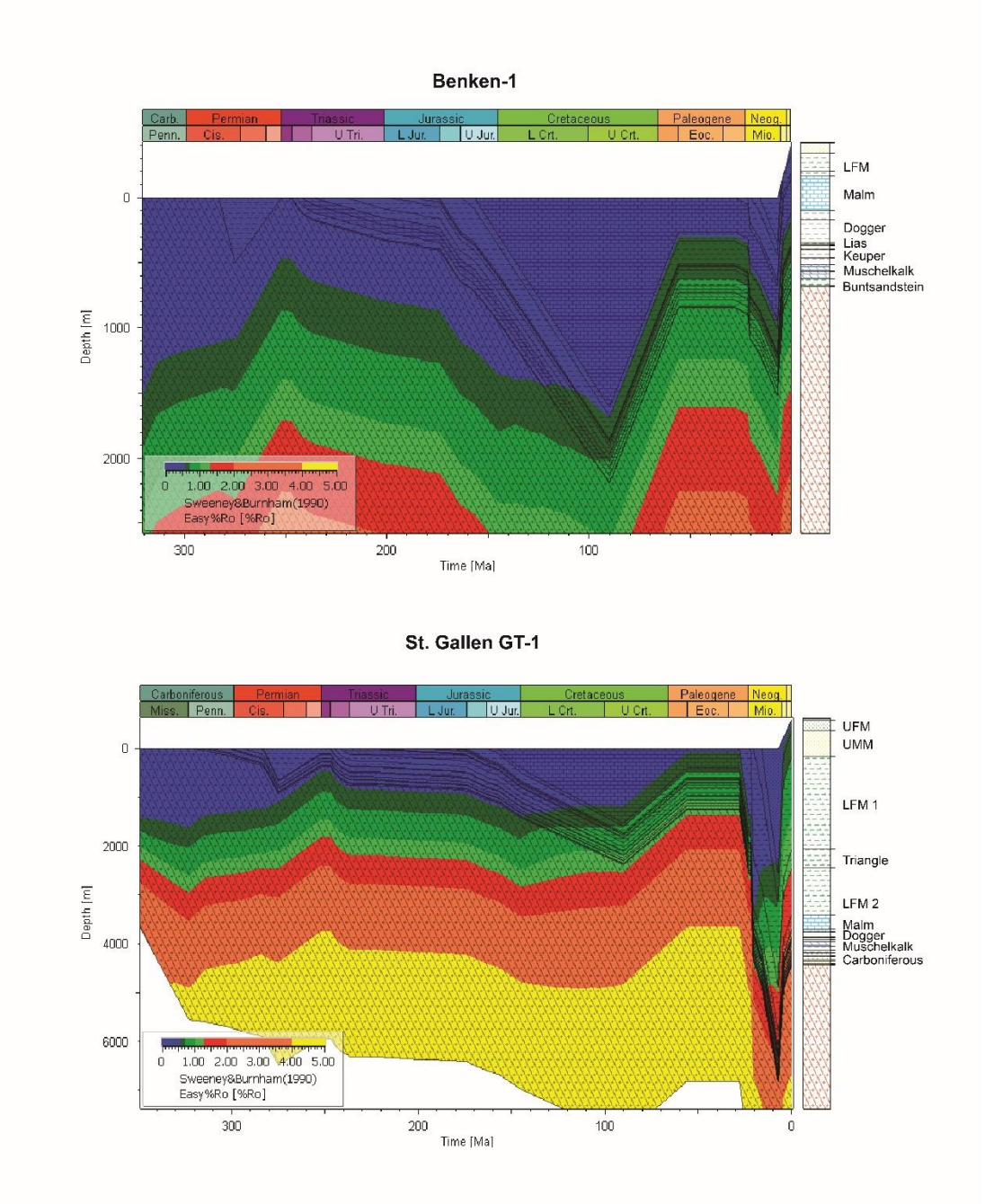


Fig. 104: Burial plot versus thermal maturity conditions, showing the time when the source rocks (Lias, Permian, Carboniferous) were matured.

3.5.3.4 Simulation of hydrocarbon generation, migration and accumulation processes

The model simulates the hydrocarbon generation, migration and accumulation processes for Section 6, as the effect of the source rock maturation and hydrocarbon expulsion. Migration paths and potential reservoirs are calculated based on the geometry of the basin and the permeability properties of its infill. Hydrocarbons were generated by the Permian, Carboniferous and Posidonia shale source rocks, at different times. A first-generation peak occurred in the Permian, because of the burial of the Permian and Carboniferous source rocks in the grabens. However, the hydrocarbon generation peak at that time is lower than what was observed in Section 5 (Fig. 86). Hydrocarbon generation peaks occurred firstly in the Cretaceous, when the basin was affected by another burial event and heat flow peak, and secondly, the most relevant, in the Cenozoic (Fig. 105), when the formation and infill of the foreland basin increases abruptly the burial depth of the

basin. Differently from Section 5, there is not a generation peak in the Permian time, most likely because the grabens along Section 6 are less deep, thus they were not buried enough at that time.

The rocks that generate the greatest volume of hydrocarbons are the Permian shales, followed by the Carboniferous coal and shale deposits, and finally the Posidonia shale (Fig. 105). Permian and Carboniferous source rocks start to generate in the Cretaceous. A second generation peak occurred in the Miocene when the Molasse foreland basin was formed and these source rocks were deeply buried. The Posidonia shale source rock started to generate only in the Miocene when the basin was buried enough to mature these deposits.

Hydrocarbon accumulations form in the Cretaceous and in the Cenozoic time. Conventional high permeable reservoir form in the Permian and Buntsandstein sandstones unit and secondly in the Muschelkalk and Malm units. Accumulations in low permeable units (petroleum saturated) are volumetrically higher than accumulations in proper reservoirs and they mostly form in the Permian, Carboniferous, Keuper and Muschelkalk deposits, and in smaller amounts, also in the Lias, Dogger and Molasse units.

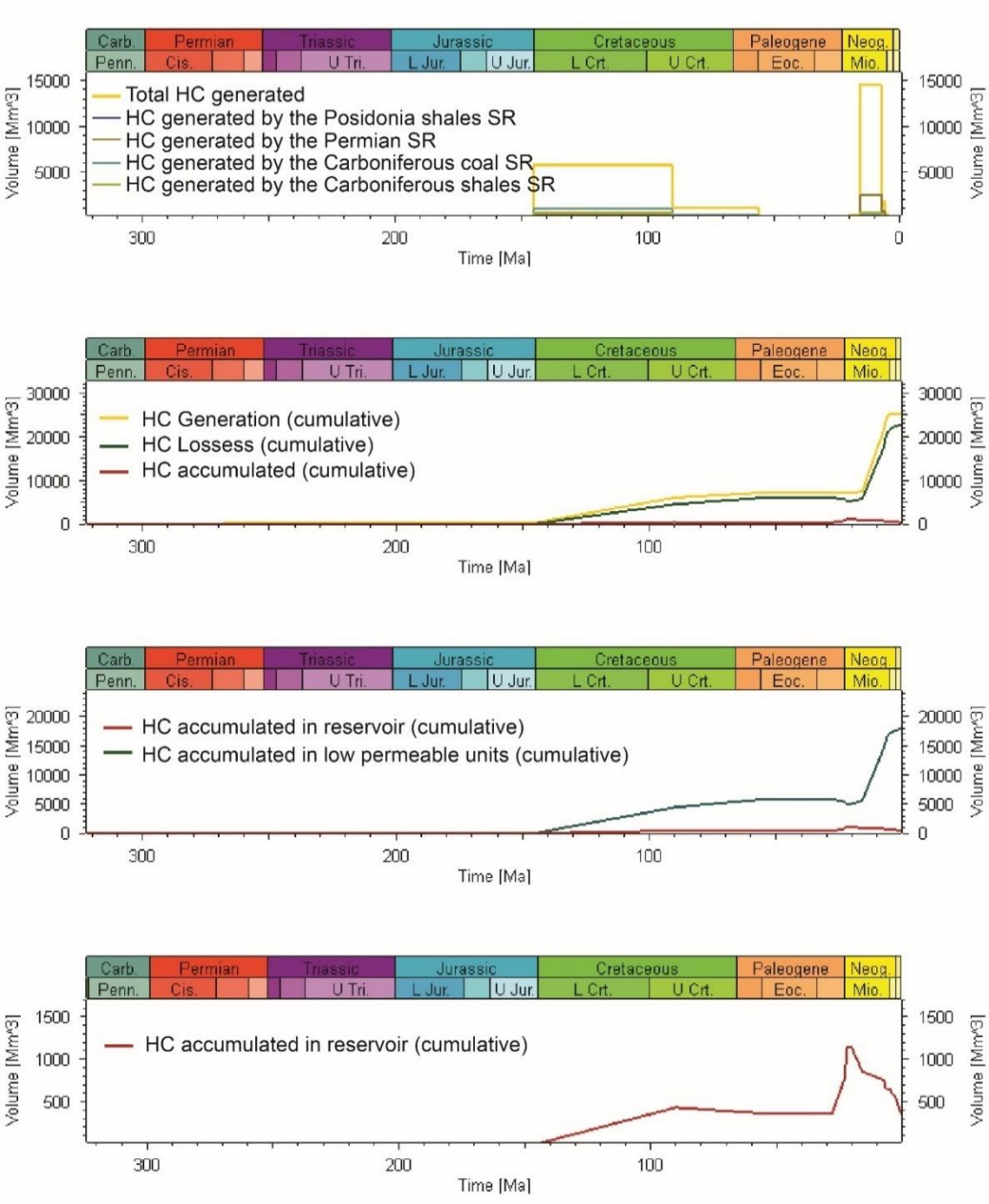


Fig. 105: Hydrocarbon generation and accumulation balances calculated by the software for the entire section

First, an “open faults” scenario was tested, which considers the faults as not cemented. In this scenario, the model simulates the formation of hydrocarbon accumulations mostly in the proximity of the Permo-Carboniferous grabens, in the Buntsandstein and/or Permian and Carboniferous units (Fig. 106). In the northern part of the section, small oil and gas accumulations form also in the Mesozoic sequence, mostly in the Malm units. Oil and gas northward migration paths formed along the Mesozoic unit, due dipping basin toward the south. In the southern part of the section, gas accumulation is simulated on the top of the Permo-Carboniferous graben just beneath the St. Gallen GT-1 well. Hydrocarbon migration mostly occurred in the Mesozoic units, along faults and the unconformity with the Cenozoic unit. Relevant migration paths are simulated toward the uppermost Molasse units, especially in the triangular zone area and in the northern part of the section, where faults are crossing the entire basin infill (Fig. 106).

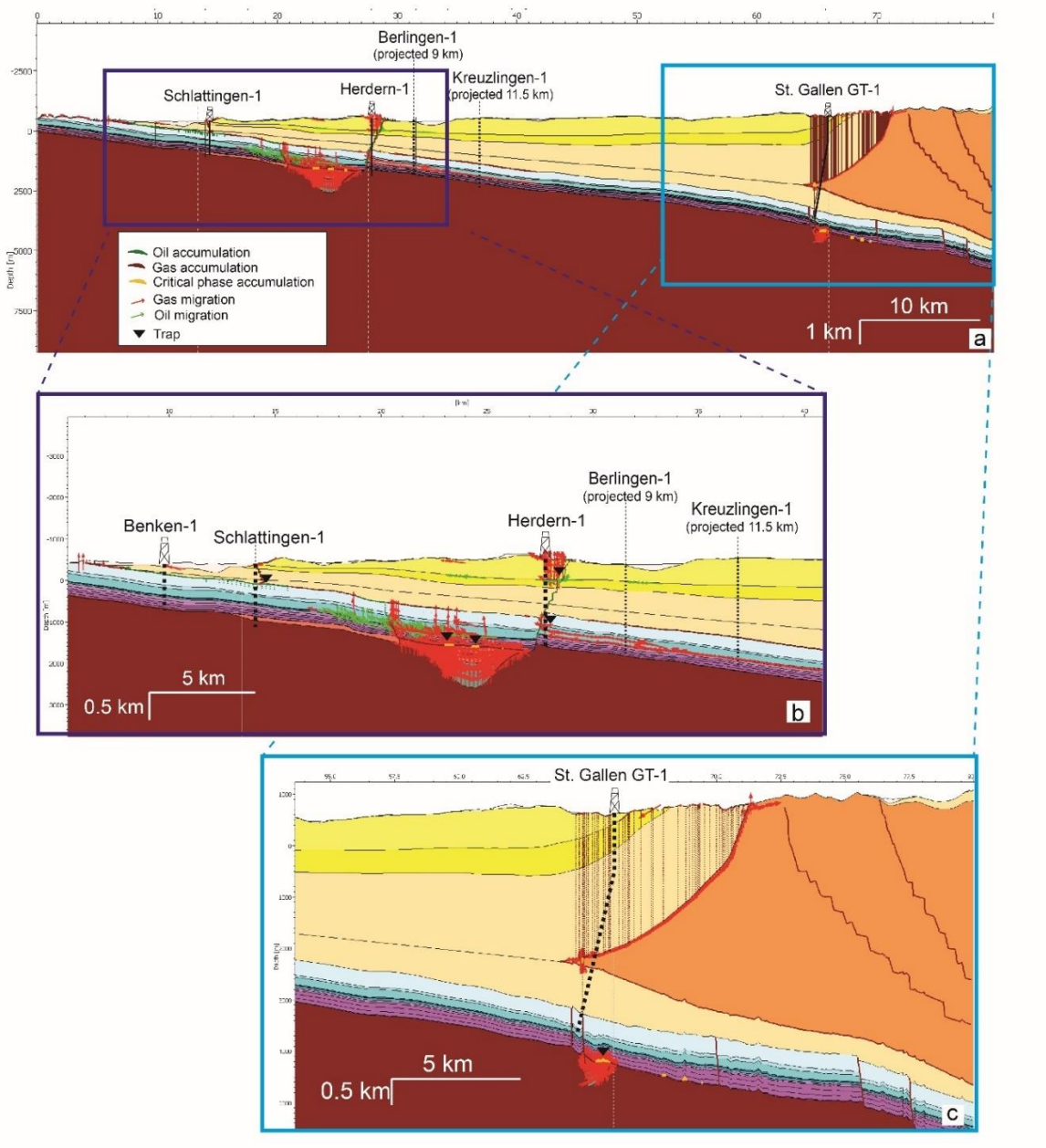


Fig. 106: Open faults scenario: (a) Hydrocarbon accumulations and migration paths calculated by the model along section 6. In (b) zoom in on the northern area of the section, and in (c) zoom in on the southern area of the section. Potential traps are indicated.

A “closed faults” scenario was also simulated, where the faults are considered as cemented. The main difference with the “open faults” scenarios is the less efficient migration of the hydrocarbons

generated by the Permian and Carboniferous source rocks to the uppermost Mesozoic and Cenozoic sequence (Fig. 107).

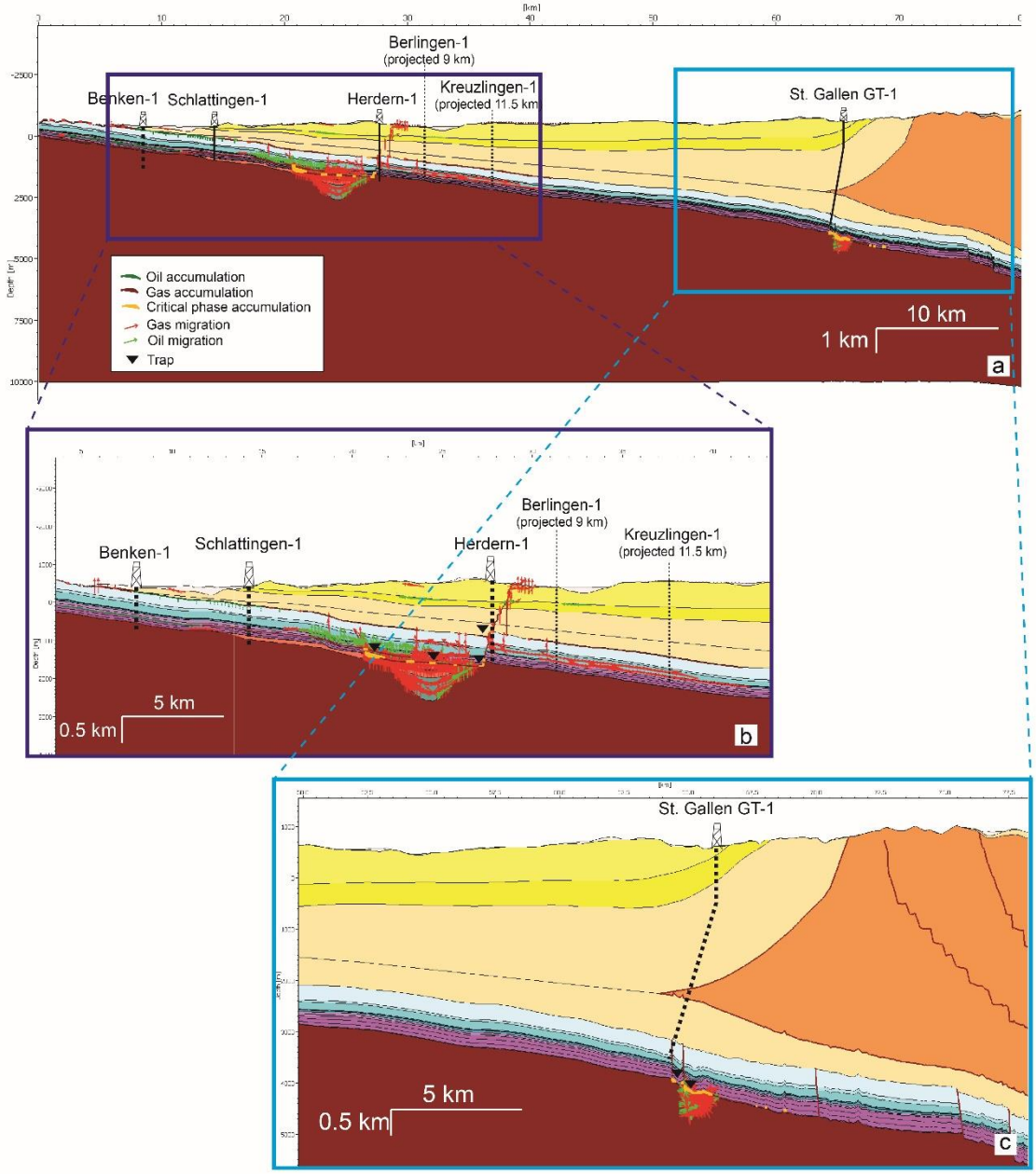


Fig. 107: Closed faults scenario: (a) Hydrocarbon accumulations and migration paths calculated by the model along section 6. In (b) zoom in on the northern area of the section, and in (c) zoom in on the southern area of the section. Potential traps are indicated.

In Fig. 108 the hydrocarbon accumulations over the basin evolution are shown. The thermal maturity is also represented. In the northern part of the section, the Permian and Carboniferous units enter the oil window since the Triassic and Jurassic times, as in this part of the section the grabens are deeper than in the south, where hydrocarbons started to be generated later, in the Oligocene time. Because of the strong burial, the Permian and Carboniferous source rocks in the southern part of the section enter also in the gas window. The hydrocarbon accumulations in the Permian and Muschelkalk (including Buntsandstein units) have started forming since the Triassic when a seal composed of anhydrite facies was deposited along the entire basin (Muschelkalk and Keuper units). These accumulations were filled over the entire evolution of the basin and they were partially preserved until the present day. In the southern part of the section, hydrocarbon accumulations started forming since the deposition of the Molasse units, when the Permian and

Carboniferous source rocks entered the oil and gas windows because of the rapid burial of the basin. Most of the hydrocarbon generated by the Posidonia shale source rock, as well as part of the hydrocarbons generated by deeper source rocks, migrated vertically to the top surface and were lost, because of the lack of proper traps. Few small accumulations could form in the Jurassic units, trapped in the anticline structures formed in the northern part of the section, because of the Jura mountain formation.

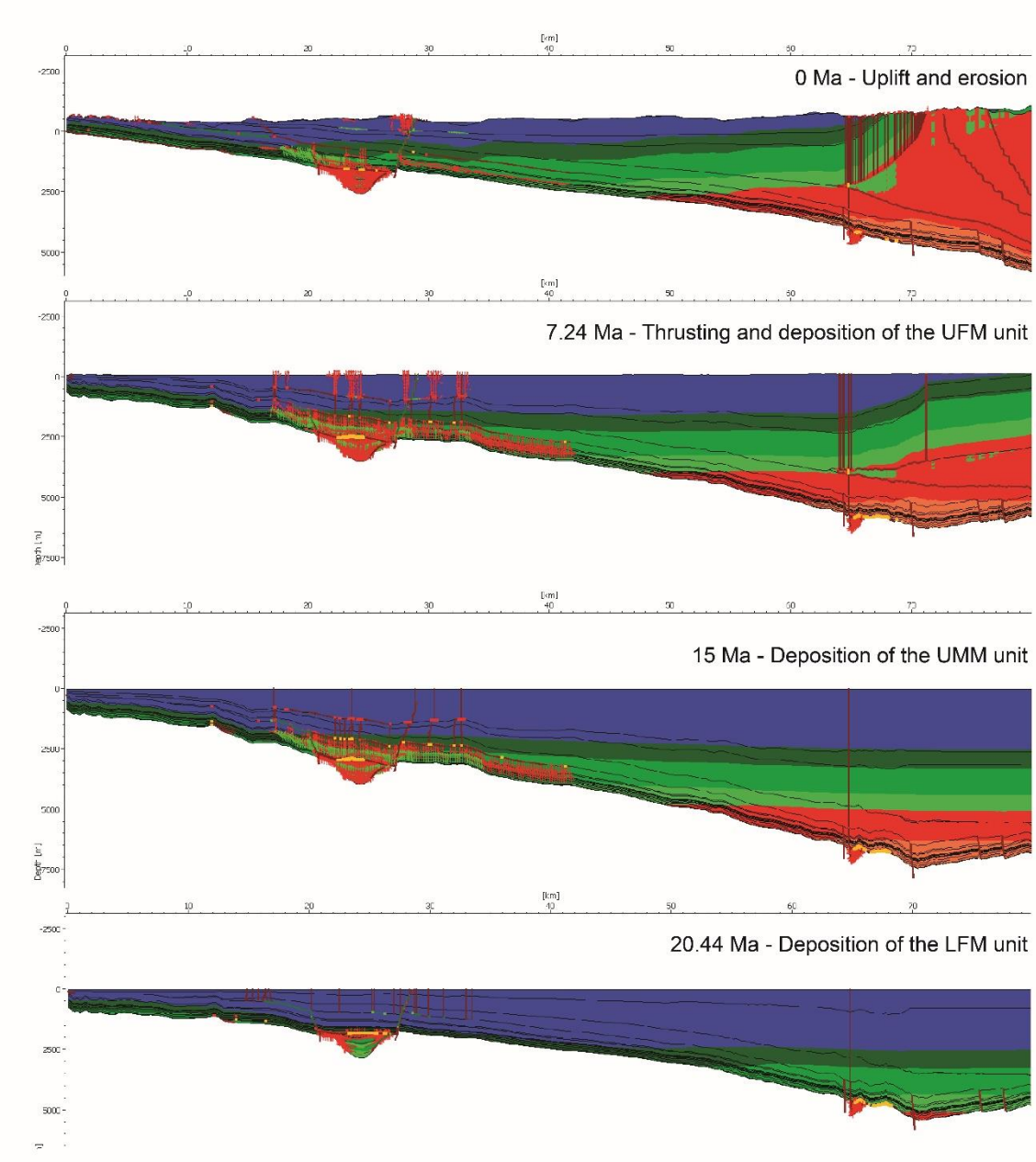


Fig. 108: Hydrocarbon accumulations over the evolution of the basin (continues)

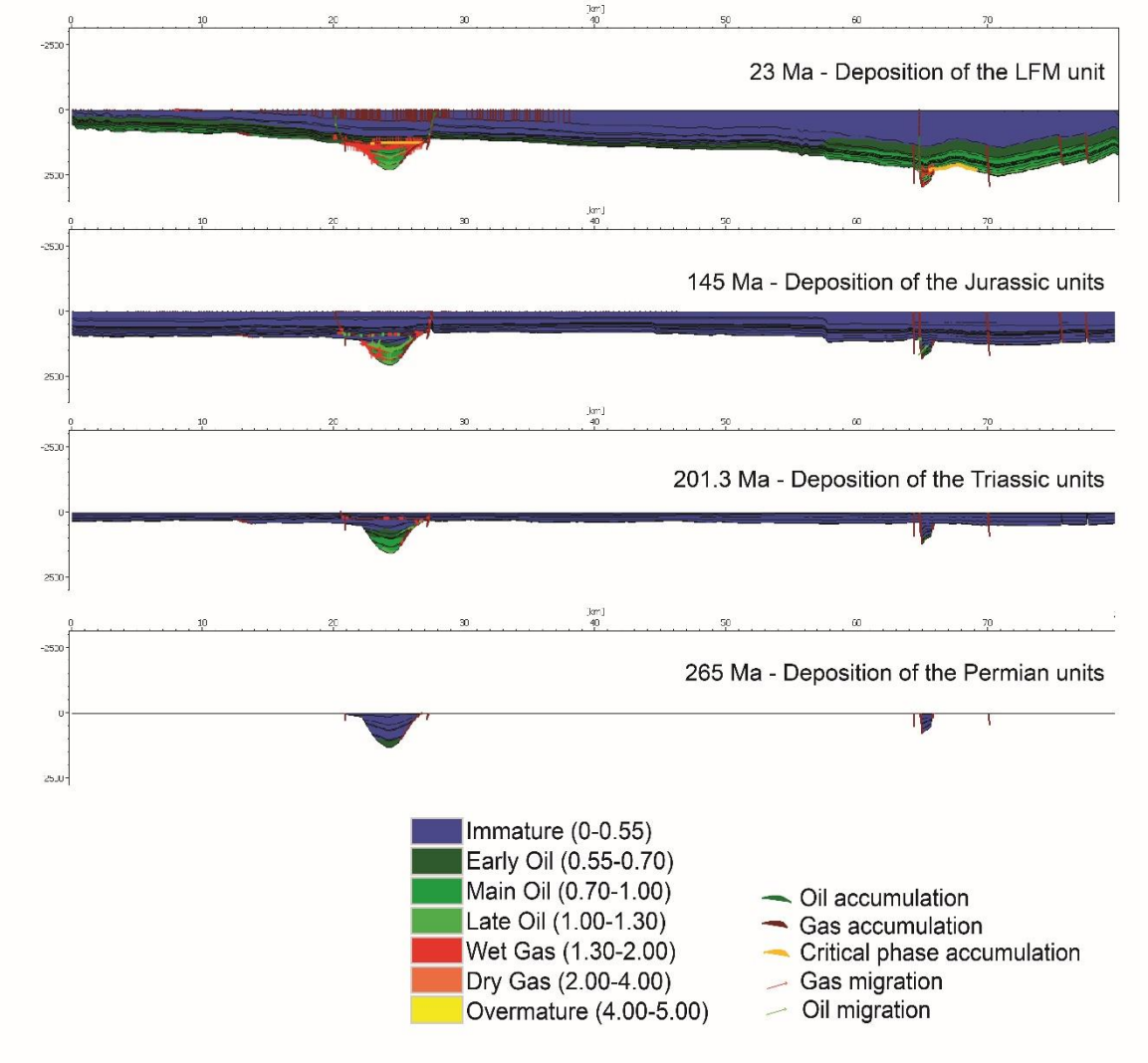


Fig. 108 (continues): Hydrocarbon accumulations over the evolution of the basin

The petroleum system evolution for the four source rocks considered is shown in terms of a petroleum system chart (Magoon and Dow, 1994) (Fig. 109) where the source rocks, reservoir, seal, overburden rocks and trap elements are defined. The critical moment is defined considering the fit among the formation of reservoirs, traps, the maturation timing of the source rocks and the hydrocarbon generation timing.

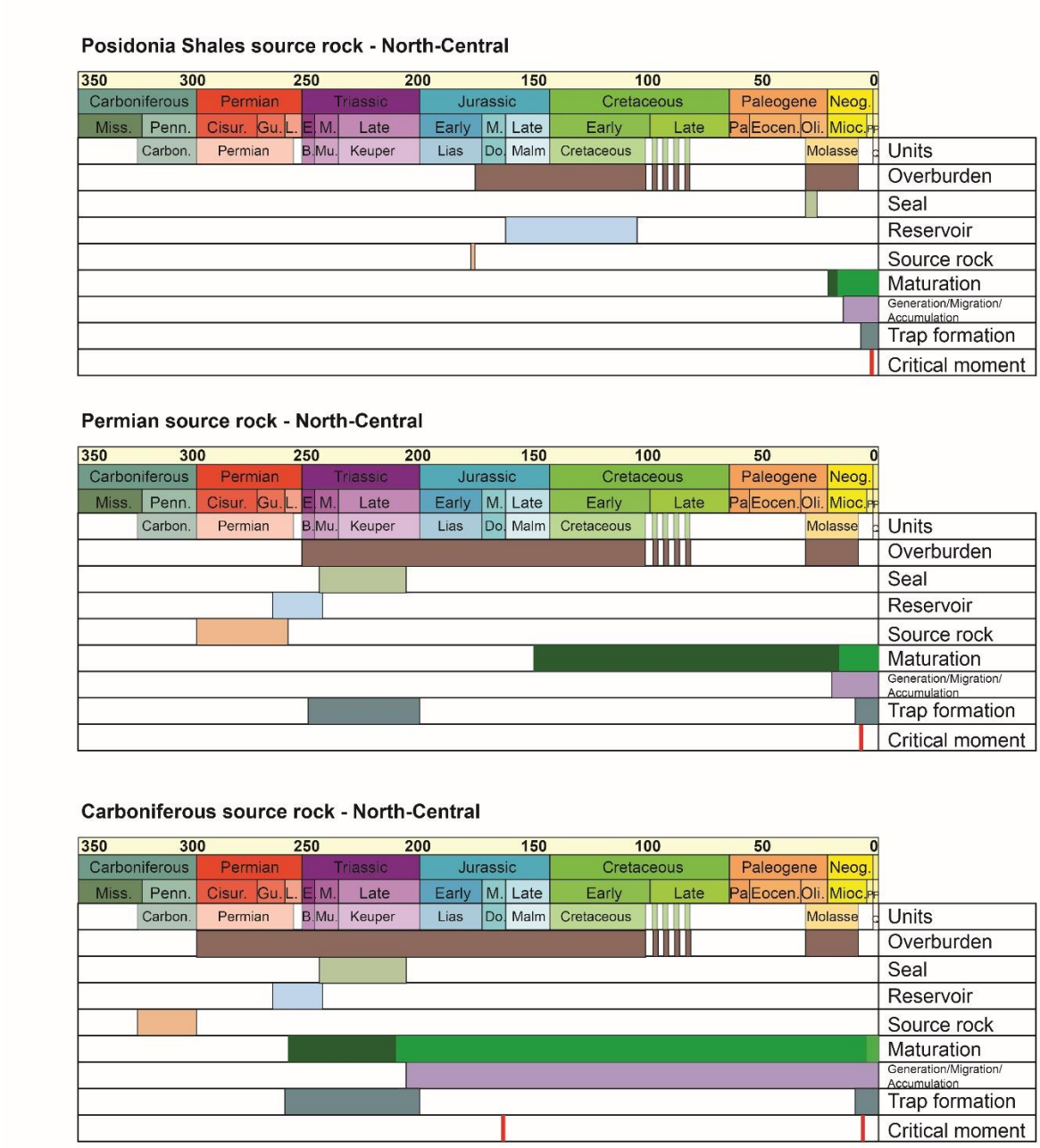


Fig. 109: Petroleum system charts reconstructed for the four source rocks defined in Section 6 (continues).

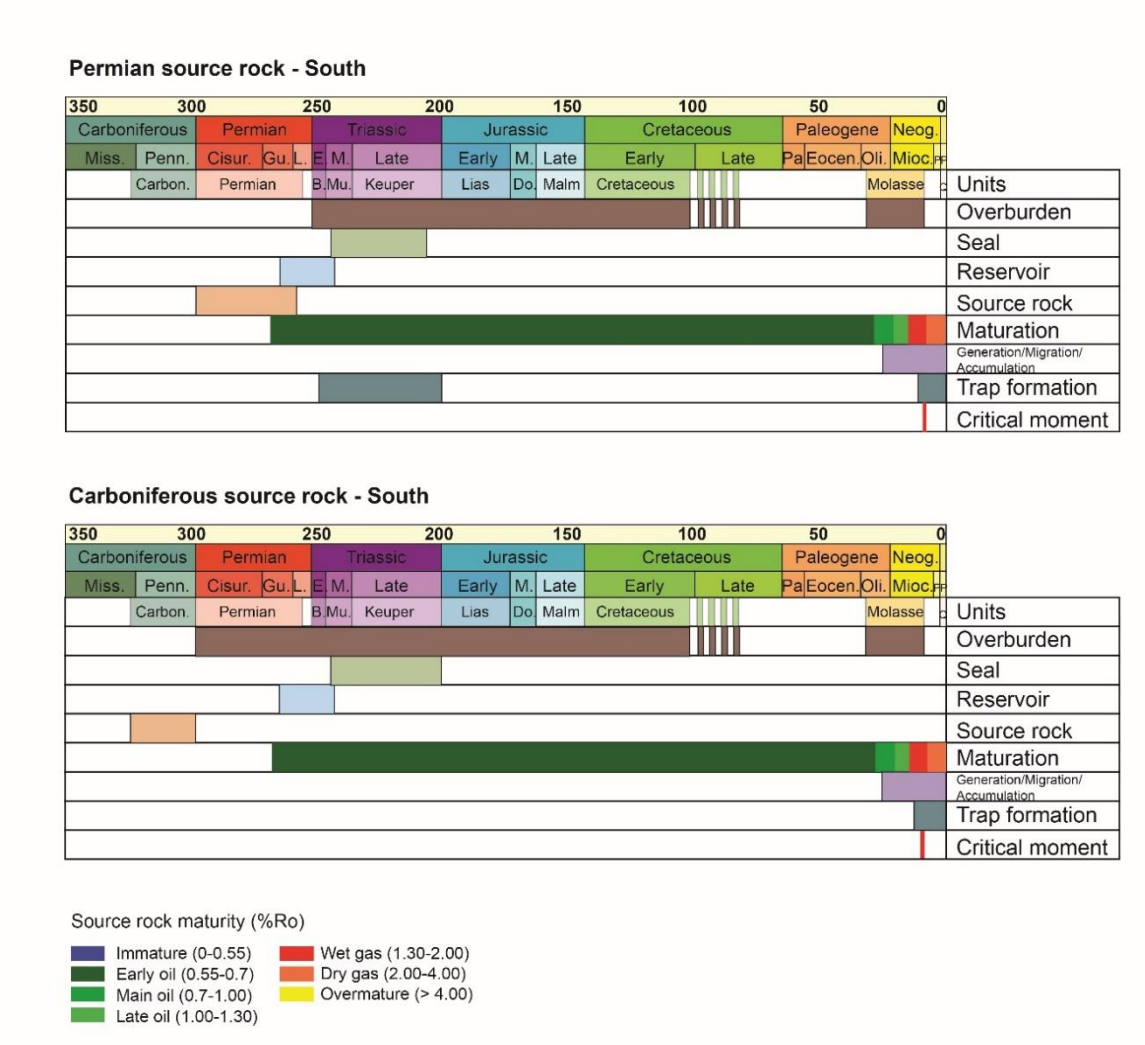


Fig. 109 (continues): Petroleum system charts reconstructed for the four source rocks defined in Section 6.

3.5.3.5 Comparison between the Hydrocarbons findings and the modelling results

The most relevant hydrocarbon findings in section 6 are the gas flows encountered during the drilling of the St. Gallen GT-1 geothermal well (2012). The gas started to enter into the borehole producing a gas kick. To control the sudden increase of gas inflow, heavy drill mud, freshwater and lost-circulation materials were pumped into the well. This operation triggered microseismicity around the area mainly below target depth, resulting in a series of earthquakes ML 3.5, widely felt by the population in northeastern Switzerland (intensity IV on the European Macroseismic Scale EMS-98, Diehl et al., 2015, 2017; Edwards et al., 2015). The natural gas in the St. Gallen GT-1 well consists mostly of thermogenic methane (Eichinger, 2014; Jurisch, 2013). The isotopic data indicate the gas was generated by a mature source rock, composed of Type II and Type III kerogens (Eichinger, 2014; Jurisch, 2013; Wolfgramm et al., 2015), which could be located in the Permo-Carboniferous graben located just below the St. Gallen GT-1 well. In the 2D modelled section, a gas reservoir formed at the top of the Permo-Carboniferous graben located in this area, a few hundred meters below the St. Gallen GT-1 well. In Omodeo-Salé et al. (2020), a higher resolution 3D petroleum system model was reconstructed in the entire St. Gallen area, which could include the entire extension of the Permo-Carboniferous grabens recognized in the 3D seismic, only partially represented in the 2D section reconstructed in the present work. The 3D modelling results indicate the formation of gas reservoirs in the Permian and Mesozoic units.

In the case of the Schlattingen-1 geothermal well, oil traces were found during drilling. The hot water discharged into the Rhine River while testing was found to contain some amounts of oil (Frieg et al., 2015). This discharge generated water contamination concerns (Hilzinger, 2018). In our

model, gas and oil migration paths are simulated in the area along the entire stratigraphic section. By the model, these hydrocarbons are generated by the Permo-Carboniferous source rocks contained in a close graben, and migrating upward to the north along the basin monocline. An oil accumulation is simulated in the Malm unit and gas accumulation in the UMM unit. Hydrocarbons could be also generated by the Posidonia shale source rocks, which are most likely present in the area.

In the Herdern-1 well, hydrocarbon traces were found in the Dogger unit. According to the model, in this area, several small oil and gas accumulations and migration paths formed in the Malm and UMM units. Hydrocarbons migrate from the Permo-Carboniferous graben, located close by the area, along a fault crossing the entire stratigraphic section, from the basement to the top surface. In the Berlingen-1 and Kreuzlingen-1 wells area, the model simulates the formation of gas accumulation in the Malm unit. Gas was generated by the Posidonia shale source rocks and vertically migrated to the uppermost Jurassic units. At the time of the uppermost Molasse unit deposition, oil and gas leaked from these reservoirs to the top and accumulated in local anticlines structures in the LMM unit. By the model, at present these accumulations are preserved only in the Berlingen-1 well area. During drilling, hydrocarbon traces were found in the LFM in the Berlingen-1 well and in the UFM in the Kreuzlingen-1 well. The latter were not encountered in the well, whereas only hydrocarbon traces were found in the Molasse units. Finally, in the Benken-1 area, oil accumulations are simulated by the model at the top of the Malm unit, most likely generated by the Posidonia shale source rock. However, no hydrocarbon traces were found during the drilling of this well.

Despite that, there is a good fit between the hydrocarbon findings and the modelling results, there are several discrepancies, which can be multiples (Table 52):

- To the northern part of the section, the Permian and Carboniferous source rocks' presence, thickness and geochemical properties could be overestimated. This is because the nature of the rocks filling the Permo-Carboniferous graben in this area is unknown. In the model, they were assigned the same properties observed in the Weiach-1 well. In the case this well is not representative of this area, the amount of hydrocarbon generated by these source rocks could be considerably different from what is simulated by the model.
- In the model, the basement faults bounding the P-C grabens were considered continuous into the Mesozoic sequence. This facilitates the migration of the hydrocarbons generated by the Permian and Carboniferous source rocks into the basin, which could not be the case if these faults do not continue. Thus, by this option, the formation of reservoirs in the Mesozoic and Cenozoic units would be less relevant.
- The seal topping the Permian and Buntsandstein units, the Muschelkalk and/or Keuper units, can be less efficient than what is calculated by the model. Pervasive fracturation can be present in the faulted areas. Indeed, anhydrites and evaporites can be interlayered also with dolomite, shales and thin sandstone layers. Thus, this seal might have also an important brittle component, reducing its efficiency.
- The seal topping the Malm unit, where the model simulates several small hydrocarbon accumulations, is the Molasse sequence, which could be less efficient than what is considered by the model. The faulting of this unit cannot be properly represented in the model.
- In the Kreuzlingen-1, Berlingen-1 and Herdern-1 wells area, the model simulates the formation of small traps in the Malm and Molasse units in local anticline structures, which were not encountered in these wells. This could be because the geometry of the basin used in the model is based on the interpolation of seismic interpretation (GeoMol), thus, it can be not exactly representative of the real geometry.
- More efficient lateral traps than what is crossed by the modelled section can be present. In this case, hydrocarbons could migrate and accumulate in the closest reservoirs, which have not been penetrated by wells.
- It is considered that the Posidonia shale are present throughout the entire northern area of the modelled section. From the Herdern-1 well up to the southern extremity of the section, the Posidonia shale source rock is considered as not present. However, the presence of the

Posidonia shale along the section is certainly known only in the Benken-1 and Kreuzlingen-1 wells area. Because of that, there is no geochemical data available in the area for this unit, they were assigned the geochemical properties measured in the northern part of Switzerland (Weiach-1, Riniken-1 and Shafisheim). A different extension, thickness and properties of this source rock along the section can result in the generation of different hydrocarbon volumes.

Well	Hydrocarbon finding	Modelling results	Discrepancy causes
St. Gallen GT-1	• Gas kick during drilling at the Dogger unit depth	• Gas reservoir in the Buntsandstein and Permian unit • Oil and gas migration paths in the entire Molasse section.	• Permo-Carboniferous source rocks thickness and properties overstimated • The deep Permo-Carboniferous faults do not continue into the Mesozoic sequence • Seal not efficient • Lateral migration
Kreuzlingen-1	• Hydrocarbon traces in the UFM unit	• Gas accumulation in the Malm unit	• Posidonia shale source rock presence, thickness and properties overestimated • Presence of faults and/or high permeability zone, not taken into account by the model, along which hydrocarbons could migrate to the uppermost units • The geometry used in the model can be not representative at the scale of small traps • Seal not efficient • Lateral migration from traps
Berlingen-1	• Hydrocarbon traces in the LFM unit	• Gas accumulation in the Malm unit • Oil accumulation in the UMM unit	• Posidonia shale source rock presence, thickness and properties overestimated • The geometry used in the model can be not representative at the scale of small traps • Seal not efficient • Lateral migration from traps
Herdern-1	• Hydrocarbons traces in the Dogger	• Oil and gas accumulation in the Malm and UMM units • Oil and gas migration paths along a fault crossing the entire stratigraphic section	• Posidonia shale, Permian and Carboniferous source rocks thickness and properties overestimated • The geometry used in the model can be not representative at the scale of small traps • Seal not efficient • Lateral migration from traps
Schlattingen-1	• Oil traces during drilling	• Oil accumulation in the Malm unit • Gas accumulation in the Molasse unit • Oil and gas migration pahts along the entire section	• Posidonia shale, Permian and Carboniferous source rocks thickness and properties overestimated • The deep Permo-Carboniferous faults do not continue into the Mesozoic sequence • Lateral migration from traps
Benken-1	• None	• Oil accumulation in the Malm unit	• Posidonia shale source rock thickness and properties overestimated • Seal not efficient • Lateral migration from traps

Table 52: Comparison between the hydrocarbon findings in the wells located close to the section trace and the modelling results. In case of discrepancy, the potential causes are indicated.

3.5.4 Uncertainties

The petroleum system model presented herein estimates the thermal maturity of the potential source rock, the type and amount of hydrocarbon generated and the potential areas where hydrocarbon can be accumulated and/or flow. However, because of the several assumptions made in constructing the model, several key uncertainties in the results must be considered. The most uncertain variables controlling the modelling results presented are listed in Table 53. A synthesis of the decision process carried out to handle the presented uncertainties is shown in Fig. 110.

Parameter	Uncertainty	Cause	Options	Effect on the petroleum system evolution	Impact	Potential improvements
Geometry of the basin	Horizons geometry, depth, stratigraphic units presence	Interpolation of few 2D seismic line across the Plateau. Few deep wells	GeoMol 2021 Sommaruga et al. (2012).	Accumulation and migration areas can be different.	Medium	Acquisition of new 2D and 3D seismic and/or reprocessing of the existent geophysical data.
Faults	Faults location, extension, geometry	Low resolution seismic data.	GeoMol 2021. 3D Seismic St. Gallen. Sommaruga et al. (2012). Greber et al. (2007).	The hydrocarbon migration can be different from what simulated by the model.	Medium/High	Acquisition of new 2D and 3D seismic and/or reprocessing of the existent geophysical data.
	Faults connectivity and cementation state	Very scarce direct measurement and description in well reports.	Faults open (not cemented). Faults close (cemented).	The volume of hydrocarbon accumulations simulated by the model can be different.	Medium	Sampling fault cement; Monitoring fluids flow.
	Continuity of the basement faults bounding the P-C grabens into Mesozoic and Cenozoic.	Low seismic resolution.	Yes. Hydrocarbon can migrate from the P-C graben to the uppermost basin infill . No. Hydrocarbon can hardly migrate from the P-C graben to the uppermost basin infill.	Migration from the deepest source rocks.	High	Acquisition of new 2D and 3D seismic and/or reprocessing of the existent geophysical data.
Facies	Facies distribution.	Data are available only where deep wells are present. Facies are deduced from qualitative description in the well report, there are no quantitative data.	Facies extrapolated only from the wells located along the transect. Facies extrapolated also from the wells located at an offset of nearly 12 km from the transect.	Hydrocarbon migration paths and/or accumulations can be different.	Medium/High	Acquisition of new stratigraphic, petrographic and geochemical data of the basin infill.

Parameter	Uncertainty	Cause	Options	Effect on the petroleum system evolution	Impact	Potential improvements
Structural evolution	Timing and magnitude of thrusting.	Scarce data dating the thrusting and able to calibrate the magnitude of the erosion in the South.	Thrusting starts at 7 Ma, after the deposition of the Molasse units.	The maturity of the southern part of the section and the timing of trap formation can be different.	Medium	Acquisition of new %Ro data; Reconstruction of a more accurate structural model.
			Thrusting starts before 7 Ma.			
	Triangular zone formation mechanisms.	The triangular zone formation mechanisms in the NAFB are poorly understood. The reconstruction of a proper structural model is highly time-cosuming.	Simple model simulating the formation of the triangular zone just after the deposition of the Molasse units.	The formation timing of the structural traps in the southern part of the section can be different.	Medium-Low	Reconstruction of a proper structural restoration.
			Reconstruction of the triangular zone formation and Molasse deposition by means of a proper structural restoration.			
Erosion	Magnitude of the erosion	The magnitude of the erosion cannot be measured directly, it can be only estimated by indirect data (%Ro, AFT, etc..).	Values estimated in the literature.	Burial, thus maturity, of the source rocks can be different.	Medium/High	Acquisition of more %Ro data along the section.
			Values estimatated in the most recent literature, modified in order to calibrate the %Ro data.			
	Timing of the erosion	Difficulty to date different erosion events.	Literature data.	Timing of the hydrocarbon generation can be different	Medium	Acquisition of AFT data along the section..

Parameter	Uncertainty	Cause	Options	Effect on the petroleum system evolution	Impact	Potential improvements
Boundary conditions	Present-day heat flow	The heat flow values measured today in the wells are higher than what necessary to calibrate the present-day temperature data.	Assigning lower heat flow values than what measured today.	None, because it is a technical issue related to the software.	None	
			Do not calculate the ragiogenic heat produced by the rock.			
	Paleo-heat flow	The paleo heat flow over the basin evolution cannot be measured directly, it can be only estimated	Heat flow trend reflecting the geodynamic evolution of the basin proposed in the literature.	Timing of the hydrocarbon generation can be different.	Medium/High	Reconstruction of crustal model to improve the estimates of the paleo-heat flow.
			Heat flow trend , with peak values modified to calibrate the %Ro values.			
Permian and Carboniferous source rocks	Presence and geometry of the grabens along the section.	Low seismic resolution, especially in the northern sector.	Leu (2008).	Potential presence of deep hydrocarbon source rocks also in the South, generating more hydrocarbons	Medium/High to the North Low to the South.	Acquisition of new 2D and 3D seismic and/or reprocessing of the existent geophysical data, especially in the northern sector.
			3D seismic St. Gallen.			
			Sommaruga et al. (2012).			
			Greber et al. (2007).			
	Source rock presence.	The Permo-Carboniferous grabens have not been penetrated by wells.	No source rocks.	Volume of the hydrocarbon generated can be different	High	To the North, acquisition of new geophysical data. To the South, improve the accuracy of velocity model, seismic contrast, filters, etc,.

Parameter	Uncertainty	Cause	Options	Effect on the petroleum system evolution	Impact	Potential improvements
Permian and Carboniferous source rocks	Source rock presence.	The Permo-Carboniferous grabens have not been penetrated by wells.	Permian and Carboniferous source rocks are present in both grabens.	Volume of the hydrocarbon generated can be different.	High	To the North, acquisition of new geophysical data. To the South, improve the accuracy of velocity model, seismic contrast, filters, etc,.
	Hydrocarbon potential.	No data.	Geochemical data extrapolated from the Weiach-1 well.	Volume of the hydrocarbon generated can be different	High	Penetrating the Permian and Carboniferous deposits in and direct measurement of the geochemical parameters.
Posidonia shale source rock	Presence of the Posidonia shale source rock.	It has been identified only in the northern and central part of the section. In the southern parts there are no data.	Present only in the northern and central sector, up to the Kreuzlingen-1 well.	Generation, migration and accumulation of more hydrocarbon in the Mesozoic and Cenozoic sequence.	High, especially in the southern part of the section	Acquisition of more data in the Liassic interval, especially in the central-southern part of the section.
			Present along the entire section.			
	Hydrocarbon potential	No data along the section.	Extrapolated from the Weiach-1, Shafisheim-1 and Riniken-1 wells	Volume of hydrocarbon generated can be different.		
Calibration of the model	Porosity data	Data are available only for few wells. From these points, porosity data were extrapolated along the section.	Use only of the available data along the section .	Hydrocarbons migration and accumulations can be different.	Medium	Acquisition of more porosity data along the section
			Use of data measured in wells located at nearly 12 km from the section trace line.			
	Porosity calibration	The porosity reduction by diagenetic process cannot be properly simulated by the software.	Modify the initial porosity of the facies in the lithology library of the software.	Reservoir properties can be different from what simulated by the model.	Medium	Improve the software porosity editing.

Parameter	Uncertainty	Cause	Options	Effect on the petroleum system evolution	Impact	Potential improvements
Calibration of the model	Present-day temperature data.	Data are available only for few wells.	Use only of the available data along the section.	The present-day temperature can be different from what simulated, getting far from the wells where calibration data are available. There are no main consequence on the PS evolution.	Low	Acquisition of more borehole temperature data along the section.
			Use also data measured in wells located at 12 km from the section trace line.			
	Thermal maturity calibration.	%Ro data are available for the St. Gallen-GT-1 and Herdern-1 wells. No data in the southern part o the section. No data in the northern and southern extremity of the section.	Calibration with the data of only the wells located along the section.	To the North, thermal condition of the Posidonia shale source rock can be more or less mature; To the South, uncertainty of the thermal conditions of the triangular zone area.	Medium	Acquisition of more %Ro data in the northern part of the section.
			To the North, projection also of data from wells located at nearly 10 km from the section trace.			

Table 53: List of the uncertainties parameters for the Section 6 model, their causes and their impact on the petroleum system modelling results. The options/scenarios available are indicated. In green is highlighted the option chosen in this study to build the petroleum system modelling. Potential improvements and actions to mitigate these uncertainties are suggested.

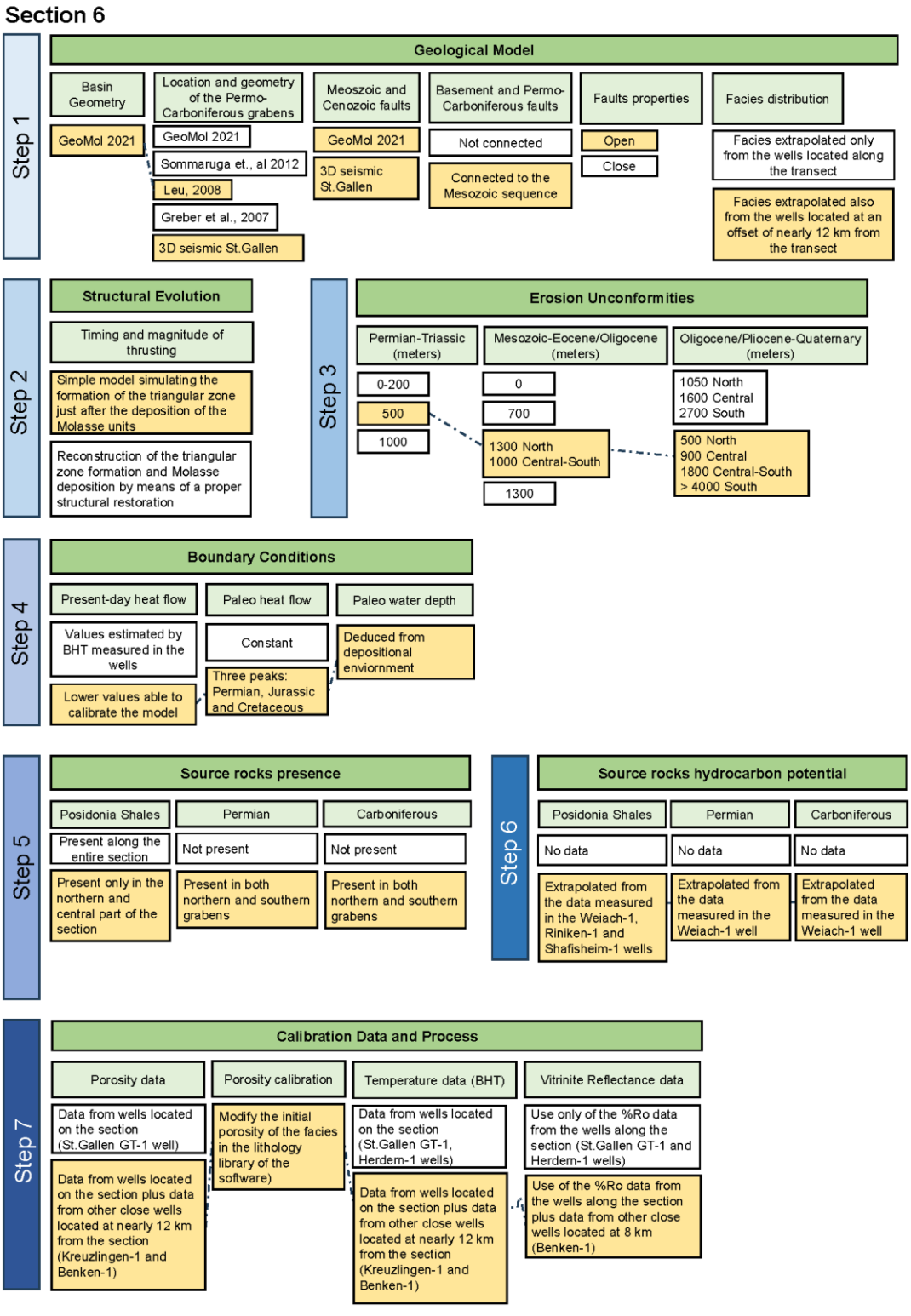


Fig. 110: Petroleum system modelling was built by selecting a specific combination of parameters, which are critical in controlling the thermal evolution of the basin and the hydrocarbon generation, migration and accumulation processes. In yellow are indicated the option chosen in this work.

3.6 CRS maps

CRS maps were built for each potential geothermal play, by integrating all the data collected in this study about the source rocks, reservoirs and seals. Firstly, data availability and quality assessment classes were defined for each petroleum system element. Classes were defined for the most relevant wells of the Swiss Plateau and extrapolated to the closest areas. A synthetic reminder of the meaning of the Data availability and Assessment classes defined for the source rocks, reservoirs and seals is presented in Fig. 111, Fig. 112 and Fig. 113.

SOURCE ROCK DATA availability					
Class	Occurrence in well	TOC/Rock Eval	VR	Model calibration	Pattern Legend
A	Y	Y	Y	Y	
B	Y	Y	Y	N	
C	Y	N	Y	Y	
D	Y	Y	N	N	
E	Y	N	Y	N	
F	Y	N	N	Y	
G	Y	N	N	N	
H	N	N	N	Y	
I	N	N	N	N	

SOURCE ROCK assessment				
Class	Presence	Maturity	TOC > 2%	Color Legend
1	Y	Y	Y	
2	Y	Y	N	
3	Y	N	Y	
4	Y	N	N	
5	N	N	N	

Fig. 111: Synthesis of the classes assigned to the source rocks

RESERVOIR DATA availability					
Class	GeoMol Surface	GeoMol Fault	Occurrence in well	Porosity data	Pattern Legend
A	Y	Y	Y	Y	
B	Y	Y	Y	N	
C	Y	N	Y	Y	
D	Y	Y	N	N	
E	Y	N	Y	N	
F	N	N	Y	Y	
G	Y	N	N	N	
H	N	N	Y	N	
I	N	N	N	N	

RESERVOIR assessment				
Class	Presence	Phi > 15%	Fractured	Color Legend
1	Y	Y	Y	
2	Y	Y	N	
3	Y	N	Y	
4	Y	N	N	
5	N	N	N	

Fig. 112: Synthesis of the classes assigned to the reservoirs

SEAL DATA availability					
Class	GeoMol Surface	GeoMol Fault	Occurrence in well	Lithology data	Pattern Legend
A	Y	Y	Y	Y	
B	Y	Y	Y	N	
C	Y	N	Y	Y	
D	Y	Y	N	N	
E	Y	N	Y	N	
F	N	N	Y	Y	
G	Y	N	N	N	
H	N	N	Y	N	
I	N	N	N	N	

SEAL assessment				
Class	Presence	Integrity	Impermeable	Color Legend
1	Y	Y	Y	
2	Y	N	Y	
3	Y	Y	N	
4	Y	N	N	
5	N	N	N	

Fig. 113: Synthesis of the classes assigned to the seal

3.6.1 Source rocks maps

In this study, it is assumed that all the plays defined for the Swiss Plateau share the same source rocks: the Posidonia shale and the Permo-Carboniferous deposits. Thus, the same source rock maps were generated for all the plays. In the Muschelkalk and Permo-Carboniferous plays the Posidonia shale source rock was not considered, as it is at a higher stratigraphic level.

The Posidonia shale source rock properties were reconstructed mostly considering the occurrence of this source rock in the wells and the geochemical analysis performed for these rocks. The presence of this source rock is certain only when the well has been drilled deep enough to reach the Lias unit and when a detailed description of the lithologies crossed by the well is available. When this is not the case, its presence is unknown, thus it can be only extrapolated from near wells where data are available.

The thermal maturity of the Posidonia shale source rocks was determined from the thermal modelling results, obtained along the five sections considered in the petroleum system modelling part of this work (Fig. 114). From these results, the maturity was extrapolated throughout the entire Plateau.

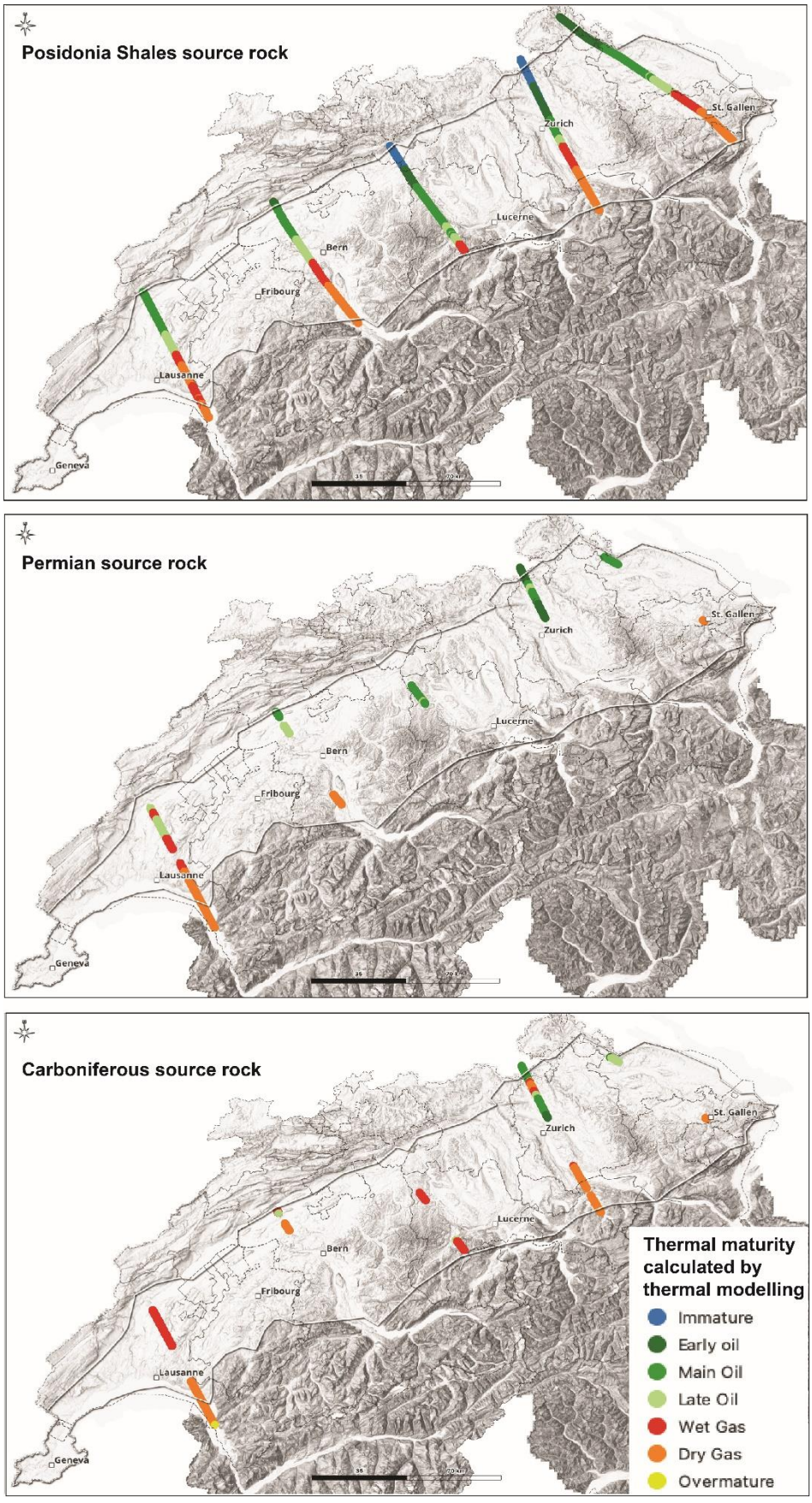


Fig. 114: Thermal maturity calculated by thermal modelling along the five sections considered in the petroleum system modelling.

The availability of the geochemical data for the Posidonia shale deposits is scarce, mostly present in the Vaud area and north-eastern Switzerland (respectively in the Treyçovagnes-1, Essertines-1, Eclépens-1 wells and Weiach-1, Riniken-1, Schafisheim-1 wells). Thus, for the rest of the Plateau, the properties of the Posidonia shale source rock were extrapolated from these few available data. Based on these data, the data availability and assessment classes were assigned to most of the relevant deep wells of the Plateau (Table 54). From this output, the data availability distribution and the source rock assessment maps were generated and shown respectively in Fig. 115 and Fig. 116.

Posidonia shale source rock	**Data availability**					**Assessement**			
Well	Occurrence	VR	TOC/ Rock Eval	Model calibration	Class	Presence	Maturity (%Ro >0.5%)	TOC >2%	Class
Altishofen-1	Yes	No	No	No	G	Yes	Yes*	No*	2
Benken	Yes	Yes	No	Yes	C	Yes	Yes	Yes*	1
Berlingen-1	No	No	No	No	I	Yes*	Yes*	Yes*	1
Boswil-1	No	No	No	No	I	No	No	No	5
Bottstein	No	No	No	No	I	No	No	No	5
Bozberg-1	Yes	No	No	No	G	Yes	Yes*	Yes*	1
Bulach-1	Yes	No	No	No	G	Yes	Yes*	Yes*	1
Chapelle-1	No	No	No	Yes	H	Yes	Yes*	Yes*	1
Chessel-1	No	No	No	No	I	No	No	No	5
Courtion-1	Yes	No	No	No	G	Yes	Yes*	Yes*	1
Cuarny-1	No	No	No	No	I	Yes	Yes*	Yes*	1
Eclepens-1	Yes	Yes	Yes	Yes	A	Yes	Yes	Yes	1
Entlebuch-1	No	No	No	Yes	H	No	No	No	5
Essertines-1	Yes	Yes	Yes	Yes	A	Yes	Yes	Yes	1
Fendringen-1	No	No	No	No	I	Yes*	Yes*	No*	2
Herdern-1	Yes	Yes	No	Yes	C	Yes	Yes	Yes*	1
Hermingen-1	Yes	Yes	Yes	Yes	A	Yes	Yes	No	2
Humilly-2	Yes	Yes	Yes	Yes	A	Yes	Yes	Yes	1
Hünenberg-1	No	No	No	Yes	H	No	No	No	5
Kaisten	No	No	No	No	I	No	No	No	5
Kreuzlingen-1	Yes	No	No	No	G	Yes	Yes*	Yes*	1
Kusnacht-1	No	No	No	Yes	H	No	No	No	5
Leuggern	No	No	No	No	I	No	No	No	5
Lindau-1	No	No	No	No	I	No	No	No	5
Linden-1	Yes	No	No	No	G	Yes	Yes*	No*	2
Marthalen-1	Yes	No	No	No	G	Yes	Yes*	Yes*	1
Noville-1	No	No	No	Yes	H	No	No	No	5
Pfaffnau-1	No	No	No	Yes	H	Yes*	Yes*	No*	2
Riniken-1	Yes	Yes	Yes	Yes	A	Yes	Yes	Yes	1
Romanens-1	Yes	No	No	No	G	Yes	Yes*	Yes*	1
Ruppoldsried-1	No	No	No	No	I	Yes*	Yes*	No*	2
Savigny-1	No	No	No	Yes	H	Yes*	Yes*	Yes*	1
Schafisheim-1	Yes	Yes	Yes	Yes	A	Yes	Yes	No	2
Schlattingen-1	Yes	Yes	No	Yes	C	Yes	Yes	Yes*	1
Servion-1	No	No	No	No	E	Yes*	Yes*	Yes*	1
Siblingen-1	Yes	No	No	No	G	Yes	Yes	Yes*	1

Posidonia shale source rock	Data availability					Assessement			
Well	Occurrence	VR	TOC/ Rock Eval	Model calibration	Class	Presence	Maturity (%Ro >0.5%)	TOC >2%	Class
Sorens-1	No	No	No	No	I	Yes*	Yes*	Yes*	1
St Gallen GT-1	No	No	No	Yes	H	No	No	No	5
Thônex-1	No	No	No	No	I	Yes*	Yes*	Yes*	1
Thun-1	No	No	No	Yes	H	No	No	No	5
Treycovagnes-1	Yes	Yes	Yes	Yes	A	Yes	Yes	Yes	1
Truellikon-1	Yes	No	No	No	G	Yes	Yes*	Yes*	1
Tschugg-1	No	No	No	Yes	H	Yes*	Yes	No*	2
Tuggen-1	No	No	No	No	I	No	No	No	5
Weggis	No	No	No	No	I	No	No	No	5
Weiach-1	Yes	Yes	Yes	Yes	A	Yes	Yes	Yes	1
Weiach-2	No	No	No	No	I	Yes*	Yes*	Yes*	1

Table 54: Data availability and assessment classes assigned to the Posidonia shale source rock in the most relevant wells of the Plateau. In the Data Availability: Occurrence is “Yes” if the Lias unit has been penetrated. It is not discussed if it exists or not a real hydrocarbon source rock. This is defined in the assessment. (VR) vitrinite reflectance, is “Yes” when VR has been measured specifically for the Lias unit, “No” when it is not, independently of VR data availability for uppermost units. Model calibration is “Yes” if the well coincides with one of the 2D models or the well is not far and has been used to calibrate a 2D model; “No” if the well is not on a 2D modelling section and has not been used for calibration. In the Assessment * means that there are no data to define this property, thus Yes/No is deduced extrapolating what has been defined in the closest wells where data are available and/or thermal modelling results. To simplify, when the presence of the source rock is assessed as “no”, all the other properties are defined as “no”.

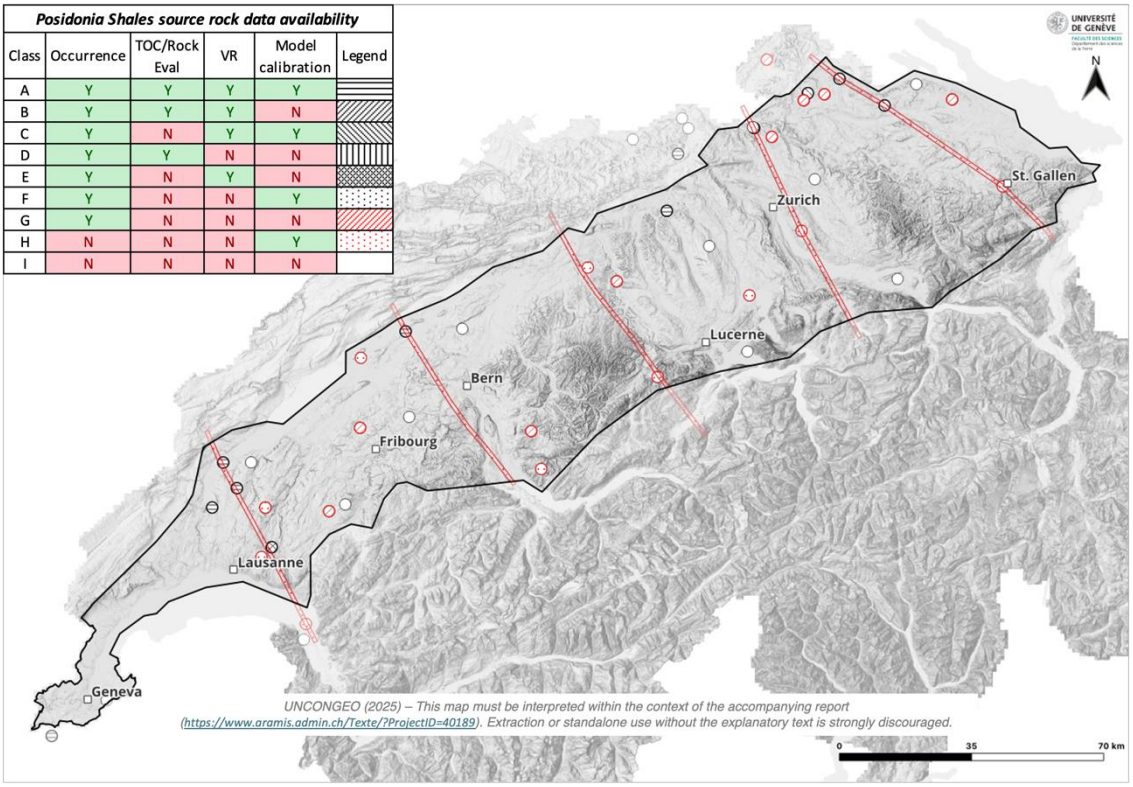


Fig. 115: Posidonia shale source rock data availability.

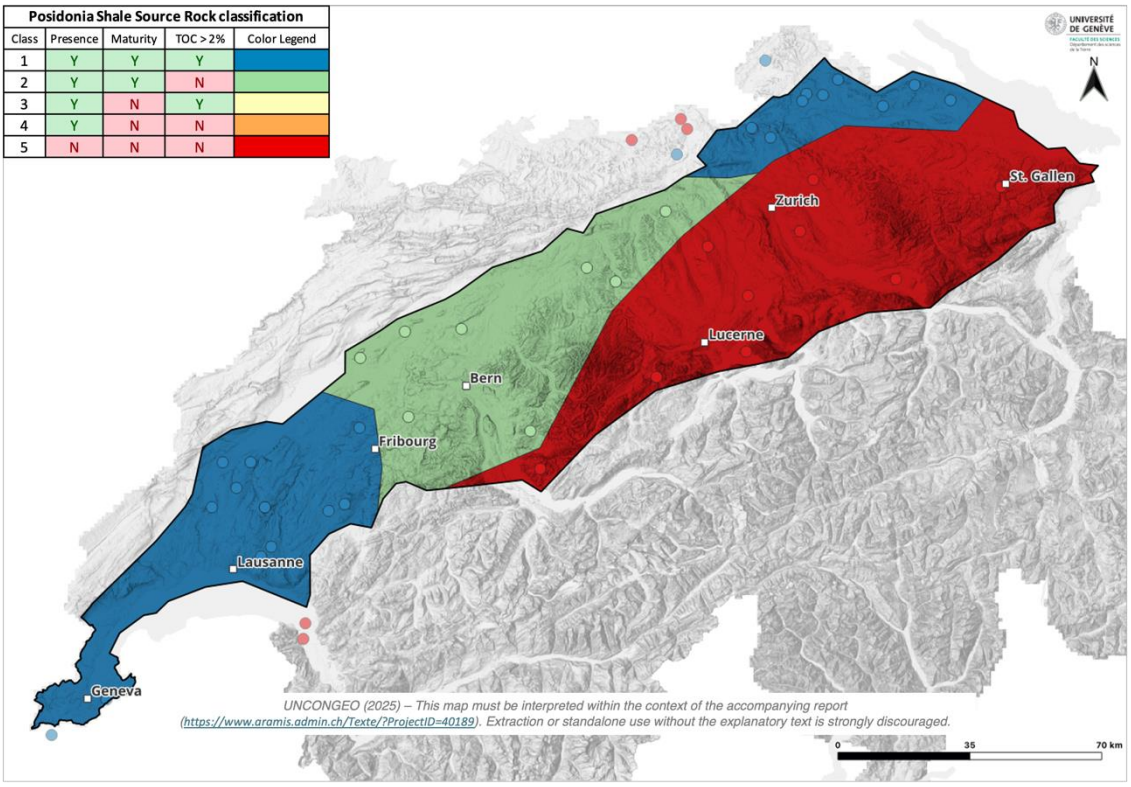


Fig. 116: Posidonia shale source rock assessment and classification

The assessment map shows that the Posidonia shale source rock is most likely present in the western and northern sectors of the Plateau, but absent in the south-eastern sector. Based on available data it is deduced that this rock has a good hydrocarbon potential mostly in the western and eastern areas, while the potential is poorer in the central part.

The Permo-Carboniferous source rock properties were mostly reconstructed considering the occurrence of these source rocks in wells and the geochemical analysis performed for these rocks. Because the Permian and Carboniferous deposits have been penetrated in very few wells; very scarce data are available. Furthermore, at present geochemical data able to confirm the presence of effective hydrocarbon source rocks are available only for the Weiach-1 well. Therefore, to assess the presence and properties of the Permo-Carboniferous source rock, an extrapolation was made from the few available data for the rest of the Plateau. In the assessment, when no data are available, it was considered that a Permo-Carboniferous source rock is present whenever a Permo-Carboniferous graben has been recognized in the area. The maturity is assessed mostly from the thermal modelling results and the TOC content is deduced from the presence or absence of thermogenic gas in the considered area. This is the case of the Vaud area, where there are no Rock-Eval data available for the Permo-Carboniferous source rocks. However, it is known that thermogenic gas was generated from a deep source rock in this area (Cuarny surface seepage, Noville-1 well). Therefore, it is considered that the grabens recognized in this area, present a Permian and/or a Carboniferous source rock with a good hydrocarbon potential (mature and with TOC >2%). In a similar case, the grabens are in the central and eastern internal sector of the Plateau, close to the subalpine front. In this sector, the Permo-Carboniferous units were not penetrated due to their depth, thus no data were measured on these deposits. The Entlebuch-1 well is an exception as the Carboniferous rocks were drilled. This well is confidential, meaning that data are not available. However, as thermogenic gas has been found in several wells close to the subalpine front (Entlebuch-1, St. Gallen-GT-1 well, Tuggen-1 and Weggis-1 wells) it is supposed that organic matter-rich deposits filled the P-C grabens recognized in these areas.

Based on these data and assumptions, the data availability and assessment classes were assigned to most of the relevant deep wells of the Plateau (Table 55). From this output, the data availability distribution and the source rock assessment maps were generated and shown respectively in Fig. 118.

P-C source rock	**Data availability**					**Assessement**			
Well	Occurrence	VR	TOC/ Rock Eval	Model calibration	Class	Presence	Maturity (%Ro >0.5%)	TOC >2%	Class
Altishofen-1	No	No	No	No	I	No	No	No	5
Benken	No	No	No	Yes	H	No	No	No	5
Berlingen-1	No	No	No	No	I	Yes*	Yes*	Yes*	1
Boswil-1	No	No	No	No	I	No	No	No	5
Bottstein	No	No	No	No	I	No	No	No	5
Bozberg-1	Yes	No	No	No	G	Yes	Yes*	Yes*	1
Bulach-1	Yes	No	No	No	G	Yes	Yes*	Yes*	1
Chapelle-1	No	No	No	Yes	H	Yes*	Yes*	Yes*	1
Chessel-1	No	No	No	No	I	Yes*	Yes*	Yes*	1
Courtion-1	No	No	No	No	I	No	No	No	5
Cuarny-1	No	No	No	No	I	Yes*	Yes*	Yes*	1
Eclepens-1	No	No	No	Yes	H	No	No	No	5
Entlebuch-1	Yes	No	No	Yes	F	Yes	Yes*	Yes*	1
Essertines-1	No	No	No	Yes	H	Yes*	Yes*	Yes*	1
Fendringen-1	No	No	No	No	I	No	No	No	5
Herdern-1	No	No	No	Yes	H	No	No	No	5
Hermingen-1	No	No	No	Yes	H	No	No	No	5

P-C source rock	Data availability					Assessement			
Well	Occurrence	VR	TOC/ Rock Eval	Model calibration	Class	Presence	Maturity (%Ro >0.5%)	TOC >2%	Class
Humilly-2	Yes	Yes	Yes	No	B	Yes	Yes	Yes	1
Hünenberg-1	No	No	No	Yes	H	Yes*	Yes*	Yes*	1
Kaisten	Yes	No	No	No	G	Yes	Yes*	No*	2
Kreuzlingen-1	Yes	No	No	No	G	Yes	Yes*	No*	2
Kusnacht-1	No	No	No	Yes	H	No	No	No	5
Leuggern	No	No	No	No	I	No	No	No	5
Lindau-1	No	No	No	No	I	No	No	No	5
Linden-1	No	No	No	No	I	Yes*	Yes*	Yes*	1
Marthalen-1	Yes	No	No	No	G	Yes	Yes*	Yes*	1
Noville-1	Yes	Yes	No	Yes	C	Yes	Yes	Yes*	1
Pfaffnau-1	Yes	No	No	Yes	F	Yes	Yes*	No	2
Riniken-1	Yes	No	No	Yes	F	Yes	Yes*	Yes*	1
Romanens-1	No	No	No	No	I	Yes*	Yes*	Yes*	1
Ruppoldsried-1	No	No	No	No	I	No	No	No	5
Savigny-1	No	No	No	Yes	H	Yes*	Yes*	Yes*	1
Servion-1	No	No	No	No	I	Yes*	Yes*	Yes*	1
Schafisheim-1	No	No	No	Yes	H	No	No	No	5
Schlattingen-1	Yes	No	No	Yes	F	Yes	Yes*	No	2
Siblingen-1	No	No	No	No	I	No	No	No	5
Sorens-1	No	No	No	No	I	Yes*	Yes*	Yes*	1
St Gallen GT-1	No	No	No	Yes	H	Yes*	Yes*	Yes*	1
Thônex-1	No	No	No	No	I	No	No	No	5
Thun-1	No	No	No	Yes	H	No	No	No	1
Treycovagnes-1	Yes	No	No	Yes	F	Yes	Yes*	Yes*	1
Truellikon-1	Yes	No	No	No	G	Yes	Yes*	Yes*	1
Tschugg-1	No	No	No	No	I	Yes*	Yes*	No	2
Tuggen-1	No	No	No	No	I	Yes*	Yes*	Yes*	1
Weggis	No	No	No	No	I	Yes*	Yes*	Yes*	1
Weiach-1	Yes	Yes	Yes	Yes	A	Yes	Yes	Yes	1
Weiach-2	Yes	No	No	No	G	Yes	Yes*	Yes*	1

Table 55: Data availability and assessment classes assigned at the Permo-Carboniferous source rock in the most relevant wells of the Plateau. In the **Data Availability**: Occurrence is “Yes” if the P-C unit has been penetrated. It is not discussed if it exists or not a real hydrocarbon source rock. This is defined in the assessment. (VR) vitrinite reflectance is “Yes” when VR has been measured specifically for the Permian and/or Carboniferous units, and “No” when is not, independent from VR available for uppermost units. Model calibration is “Yes” if the well is on the top of a 2D modelling section or the well is not far, and it has been used to calibrate a 2D model; “No” if the well is not on a 2D modelling section and it has not been used for calibration. The **Assessment** (*) means that for this well there is no data to define this property, thus Yes/No is deduced extrapolating what has been defined in the closest wells where data are available and/or thermal modelling results. Presence is “Yes” when it has been recognized as a P-C graben in the well area. To simplify, when the presence of the source rock is assessed as “no”, all the other properties are defined as “no”. TOC>2% is “Yes” when it is known that thermogenic gas, most likely generated by a Permiand and/or Carboniferous source rock, is circulating in the area.

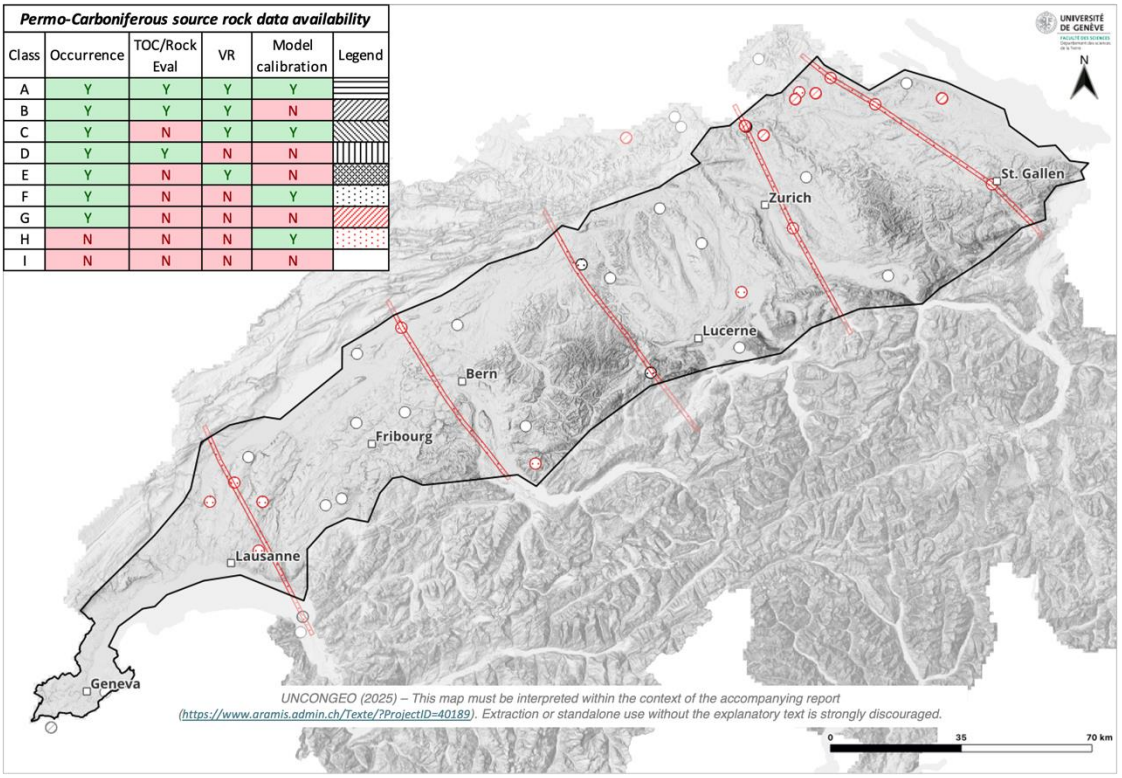


Fig. 117: Permo-Carboniferous source rock data availability.

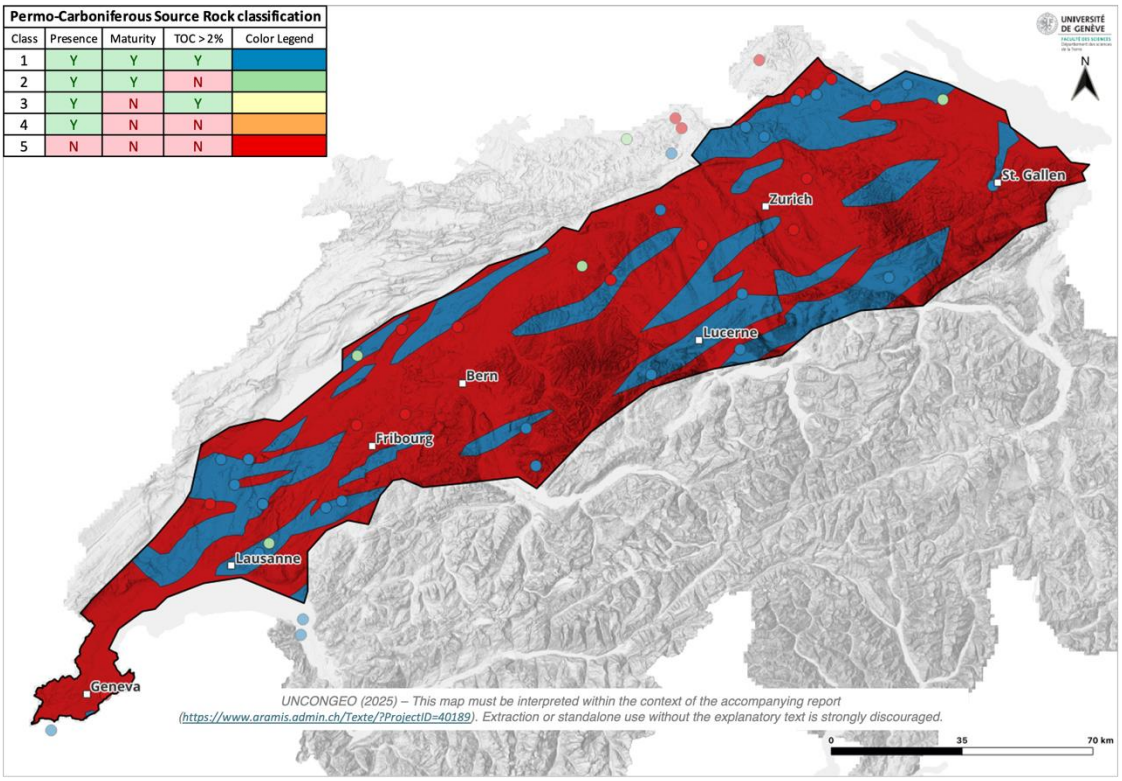


Fig. 118: Permo-Carboniferous source rock assessment and classification.

The assessment map shows that the Permo-Carboniferous source rock is present only in the areas where a Permo-Carboniferous trough has been identified. In these areas, a good hydrocarbon

potential is supposed, taking into consideration that data needed to confirm this hypothesis are very scarce (Fig. 117).

3.6.2 Lower Cretaceous Play

The Cretaceous play is present only in the western sector of the Swiss Plateau. The source rocks of this play are both the Posidonia shale and the Permo-Carboniferous units, whose properties are defined in section 3.6.1. The reservoir is represented by the karstified and/or fractured limestones and marls composing the Lower Cretaceous unit (Early Cretaceous in age) and the seal is represented by the shales and marls composing the Molasse units (Cenozoic in age).

The Reservoir data availability and assessment and the related classes assigned for the most relevant wells of the Plateau are listed in (Table 56). Porosity data (Phi) are available for very few wells and in all the cases the average is < 15% (Appendix 6). This is why in the Assessment, it is assigned “No” to the *Phi>15%* properties for all the wells. The resulting Data availability and Assessment maps for the Cretaceous reservoir are shown in Fig. 119 and Fig. 120.

Reservoir Cretaceous	**Data availability**					**Assessement**			
Well	GeoMol surface	GeoMol fault	Occurrence in well	Porosity data	Class	Presence	Phi>15%	Fractured	Class
Altishofen-1	No	No	No	No	I	No	No	No	5
Benken-1	No	No	No	No	I	No	No	No	5
Berlingen-1	No	No	No	No	I	No	No	No	5
Boswil-1	No	No	No	No	I	No	No	No	5
Bottstein-1	No	No	No	No	I	No	No	No	5
Bozberg-1	No	No	No	No	I	No	No	No	5
Bulach-1	No	No	No	No	I	No	No	No	5
Chapelle-1	Yes	No	Yes	No	E	Yes	No	No	4
Chessel-1	No	No	No	No	I	No	No	No	5
Courtion-1	Yes	No	Yes	No	I	Yes	No	No	4
Cuarny-1	Yes	Yes	Yes	No	B	Yes	No	Yes	3
Eclepens-1	Yes	Yes	Yes	No	B	Yes	No	Yes	3
Entlebuch-1	No	No	No	No	I	No	No	No	5
Essertines-1	Yes	No	Yes	Yes	C	Yes	No	No	4
Fendringen-1	Yes	No	Yes	No	E	Yes	No	No	4
Herdern-1	No	No	No	No	I	No	No	No	5
Hermingen-1	Yes	No	Yes	No	E	Yes	No	No	4
Humilly-2	Yes	No	Yes	No	E	Yes	No	No	4
Hünenberg-1	No	No	No	No	I	No	No	No	5
Kaisten	No	No	No	No	I	No	No	No	5
Kreuzlingen-1	No	No	No	No	I	No	No	No	5
Kusnacht-1	No	No	No	No	I	No	No	No	5
Leuggern-1	No	No	No	No	I	No	No	No	5
Lindau-1	No	No	No	No	I	No	No	No	5
Linden-1	No	No	No	No	I	No	No	No	5
Marthalen-1	No	No	No	No	I	No	No	No	5
Noville-1	No	No	No	No	I	No	No	No	5
Pfaffnau-1	No	No	No	No	I	No	No	No	5
Riniken-1	No	No	No	No	I	No	No	No	5
Romanens-1	Yes	No	Yes	No	E	Yes	No	No	4
Ruppoldsried-1	No	No	No	No	I	No	No	No	5

Reservoir Cretaceous	Data availability					Assessement			
Well	GeoMol surface	GeoMol fault	Occurrence in well	Porosity data	Class	Presence	Phi>15%	Fractured	Class
Savigny-1	Yes	No	Yes	No	E	Yes	No	No	4
Schafisheim-1	No	No	No	No	I	No	No	No	5
Schlattingen-1	No	No	No	No	I	No	No	No	5
Servion-1	Yes	No	Yes	No	E	Yes	No	No	4
Siblingen	No	No	No	No	I	No	No	No	5
Sorens-1	Yes	No	Yes	No	E	Yes	No	No	4
St Gallen GT-1	No	No	No	No	I	No	No	No	5
Thônex-1	No	No	Yes	No	H	Yes	No	No	4
Thun-1	No	No	No	No	I	No	No	No	5
Treycovagnes-1	No	No	Yes	No	H	Yes	No	No	4
Truellikon-1	No	No	No	No	I	No	No	No	5
Tschugg-1	Yes	No	Yes	No	E	Yes	No	No	4
Tuggen-1	No	No	No	No	I	No	No	No	5
Weggis-1	No	No	No	No	I	No	No	No	5
Weiach-1	No	No	No	No	I	No	No	No	5
Weiach-2	No	No	No	No	I	No	No	No	5

Table 56: Data availability and assessment classes assigned at the Cretaceous Play reservoir (Lower Cretaceous unit) in the most relevant wells of the Plateau. In the **Data availability**, Porosity is “Yes” when porosity data are available in this well, specifically for the Cretaceous unit.

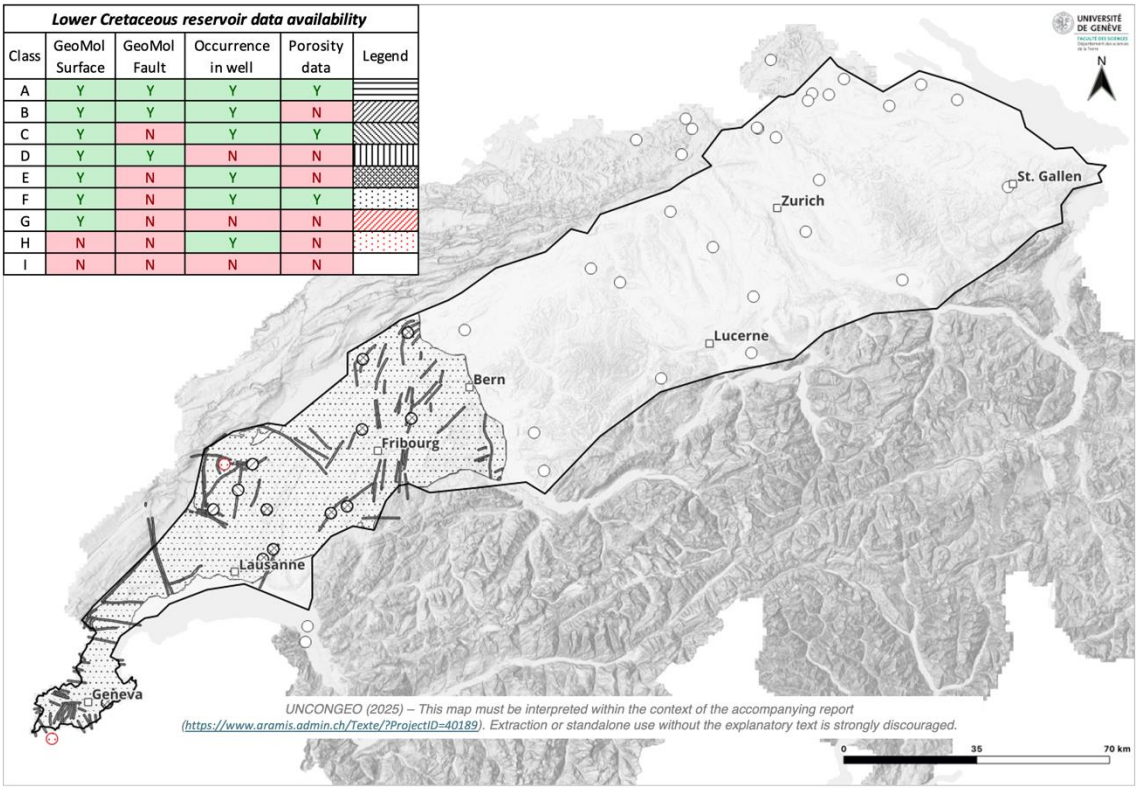


Fig. 119: Lower Cretaceous reservoir data availability.

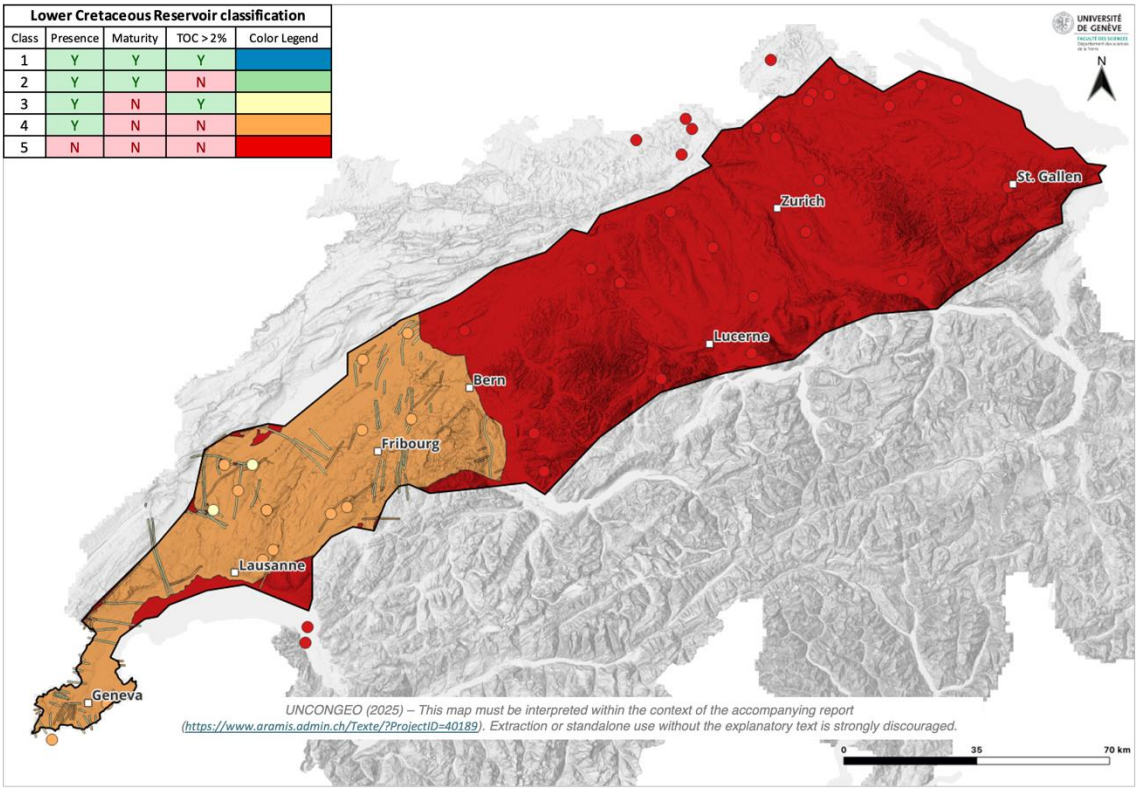


Fig. 120: Lower Cretaceous reservoir assessment and classification.

The Molasse seal data availability and assessment for the most relevant wells of the Plateau and the related class assignments are listed in Table 57. In the Assessment, the *Impermeable* property is defined on the general facies of the Molasse units described in the well reports, expressed as a percentage of lithologies (Table 58). When lithological data are not available for a well, the *Impermeable* property is extrapolated from the lithological data of the closest wells. The resulting Data availability and Assessment maps for the Cretaceous seal are shown in Fig. 121 and Fig. 122.

Seal Molasse	**Data availability**						**Assessement**			
Well	Unit	GeoMol surface	GeoMol fault	Occurrence in well	Lithologic data	Class	Presence	Integrity	Impermeable	Class
Altishofen-1	LFM	Yes	No	Yes	Yes	C	Yes	Yes	Yes	1
Benken-1	LFM	Yes	No	Yes	Yes	C	Yes	Yes	Yes	1
Berlingen-1	LFM	Yes	No	Yes	Yes	C	Yes	Yes	Yes	1
Boswil-1	LFM	Yes	No	Yes	Yes	C	Yes	Yes	No	3
Bottstein-1	No	No	No	No	No	I	No	No	No	5
Bozberg-1	LFM	Yes	No	Yes	Yes	C	Yes	Yes	No	3
Bulach-1	LFM	Yes	No	Yes	Yes	C	Yes	Yes	No	3
Chapelle-1	LFM	Yes	No	Yes	Yes	C	Yes	Yes	Yes	1
Chessel-1	LFM	Yes	No	No	No	G	Yes	Yes	No	3
Courtion-1	LFM	Yes	No	Yes	No	E	Yes	Yes	No*	3
Cuarny-1	LFM	Yes	No	Yes	No	E	Yes	Yes	No*	3
Eclepens-1	None	No	No	No	No	I	No	No	No	5
Entlebuch-1	LFM	Yes	No	Yes	Yes	C	Yes	Yes	No	3
Essertines-1	None	No	No	Yes	Yes	F	Yes	Yes	No	3
Fendringen-1	None	No	No	Yes	No	H	Yes	Yes	No*	3
Herdern-1	LFM	Yes	Yes	Yes	Yes	A	Yes	No	Yes	2
Hermingen-1	None	No	No	Yes	Yes	F	Yes	Yes	Yes	1
Humilly-2	None	No	No	Yes	Yes	F	Yes	Yes	Yes	1
Hünenberg-1	LFM	Yes	No	Yes	Yes	C	Yes	Yes	Yes	1
Kaisten	None	No	No	No	No	I	No	No	No	5
Kreuzlingen-1	LFM	Yes	No	Yes	Yes	C	Yes	Yes	Yes	1
Kusnacht-1	LFM	Yes	No	Yes	Yes	C	Yes	Yes	Yes	1
Leuggern-1	None	No	No	No	No	I	No	No	No	5
Lindau-1	LFM	Yes	No	Yes	Yes	C	Yes	Yes	Yes	1
Linden-1	LMM	Yes	Yes	Yes	Yes	A	Yes	No	No	4
Marthalen-1	LFM	Yes	No	Yes	Yes	C	Yes	Yes	No	3
Noville-1	LFM	Yes	No	Yes	Yes	C	Yes	Yes	Yes	1
Pfaffnau-1	LFM	Yes	No	Yes	Yes	C	Yes	Yes	Yes	1
Riniken	None	No	No	No	No	I	No	No	No	5
Romanens-1	LMM	Yes	Yes	Yes	Yes	A	Yes	No	No	5
Ruppoldsried-1	LMM	Yes	No	Yes	Yes	C	Yes	Yes	Yes	1
Savigny-1	LMM	Yes	No	Yes	Yes	C	Yes	Yes	No	3
Schafisheim-1	LFM	Yes	No	Yes	Yes	C	Yes	Yes	Yes	1
Schlattingen-1	LFM	Yes	No	Yes	Yes	C	Yes	Yes	No	3
Servion-1	LFM	Yes	Yes	Yes	No	B	Yes	No	Yes*	2
Siblingen	None	No	No	No	No	I	No	No	No	5
Sorens-1	LMM	Yes	Yes	Yes	No	B	Yes	Yes	No	3
St Gallen GT-1	LMM	Yes	No	Yes	Yes	C	Yes	Yes	Yes	1
Thônex-1	None	No	No	Yes	Yes	F	Yes	Yes	No	3

Seal Molasse	Data availability						Assessement			
Well	Unit	GeoMol surface	GeoMol fault	Occurrence in well	Lithologic data	Class	Presence	Integrity	Impermeable	Class
Thun-1	LFM	Yes	No	Yes	Yes	C	Yes	Yes	No	3
Treycovagnes-1	None	No	No	No	No	I	No	No	No	5
Truellikon-1	LFM	Yes	Yes	Yes	Yes	A	Yes	No	No	4
Tschugg-1	None	No	No	Yes	Yes	F	Yes	Yes	Yes	1
Tuggen-1	LFM	Yes	No	Yes	Yes	C	Yes	Yes	Yes	1
Weggis	LFM	Yes	No	Yes	No	E	Yes	Yes	Yes*	1
Weiach-1	LFM	Yes	No	Yes	Yes	C	Yes	Yes	Yes	1
Weiach-2	LFM	Yes	No	Yes	No	E	Yes	Yes	Yes*	1

Table 57: Data availability and assessment classes assigned at the Cretaceous Play Seal (Molasse units) in the most relevant wells of the Plateau. In the **Data availability**, Lithologic data is "Yes" when lithologic data are available in this well specifically for the Molasse unit considered as a seal. In the **Assessment**, in the Impermeable property, (*) means that for this well there are no lithological data to define the permeability, thus Yes/No is deduced extrapolating what has been defined in the closest wells where data are available.

Seal	Molasse
Well	**Lithology**
Altishofen-1	20%shales; 30% marls; 50% kalk sandstones
Benken	30% sandstones; 40% shales; 30% marls
Berlingen-1	50% marls; 30% shales; 20% sandstones
Boswil-1	sandstones
Bozberg-1	sandstones
Bulach-1	sandstones and marls
Chapelle-1	5% limestones; 60% marls; 35% sandstones
Eclepens-1	Eroded
Entlebuch-1	40% carbonatic sandstones; 30% siltstones; 30% shales
Essertines-1	50% marls; 50% sandstones
Herdern-1	80% shales and marls
Hermingen-1	50% sandstones; 30% limestones; 20% shales
Humilly-2	70% marls; 30% sandstones
Hünenberg-1	50% marls; 30% sandstones; 20% shales
Kreuzlingen-1	60% marls; 25% sandstones; 3% shales; 2% limestones
Kusnacht-1	50% marls; 20% sandstones; 25% shales; 5% limestones
Lindau-1	70% marls; 30% sandstones
Linden-1	50% shales; 40% sandstones; 10% limestones
Marthaleen-1	sandstones and shales
Noville-1	65% shales; 25% sandstones; 5% marls; 5% silstones
Pfaffnau-1	70% marls; 20% sandstones; 10% shales
Riniken-1	Eroded
Romanens-1	40% sandstone 35% marls 20% shales 5% conglomerate
Ruppoldsried-1	80% marls; 20% silt
Savigny-1	50% sandstone; 50% marls
Schafisheim-1	77% marls; 23% shales
Schlattingen-1	Mostly sandstones-marls
Sibilingen-1	Eroded

Seal	Molasse
Well	**Lithology**
St Gallen	40% sandstones; 10% shales; 50% marls
Thonex-1	75% sandstones; 25%marls
Thun-1	80% sandstones; 20% shales
Treycovagnes-1	Eroded
Truillikon-1	Mostly sandstones
Tschugg-1	70% marls; 10% sandstones; 17% shales; 3% gypsum
Tuggen-1	85% marls; 15% sandstones
Weggis	Unknown
Weiach-1	70% sandstones; 20% silt; 10% shales

Table 58: General facies of the seal of the Cretaceous Play in the main wells of the Plateau, represented by the Molasse unit.

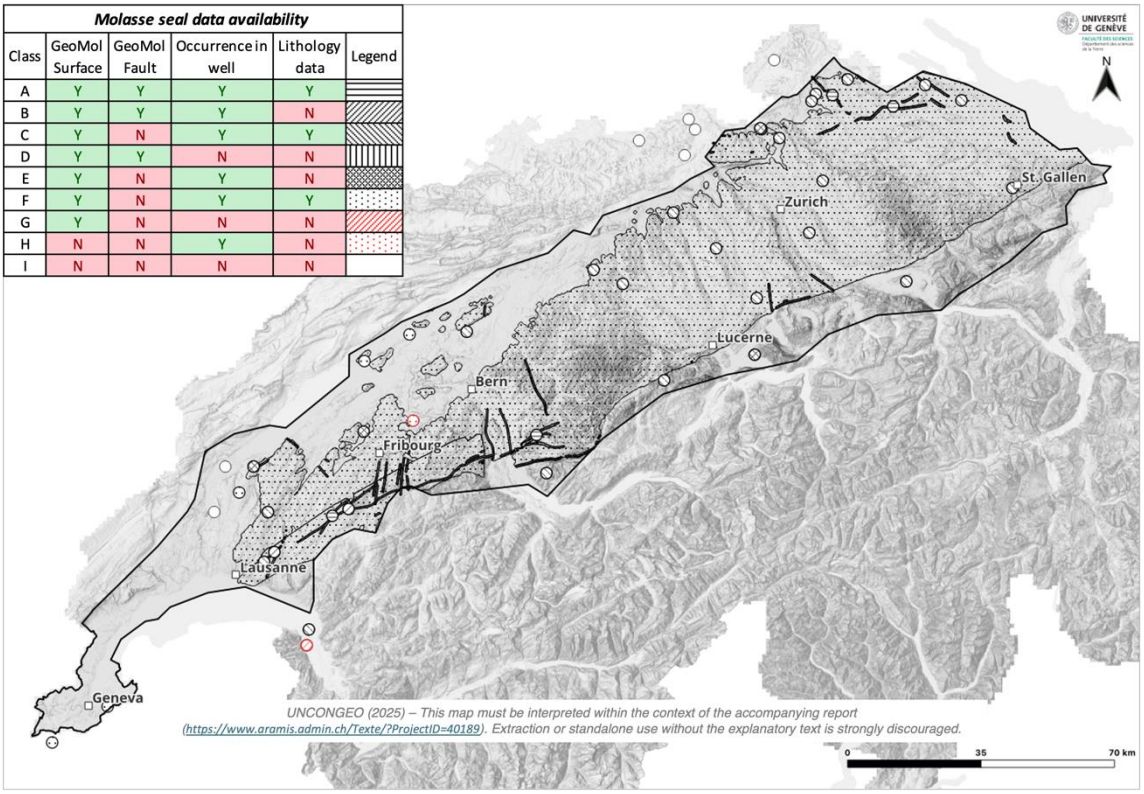


Fig. 121: Cretaceous seal (Molasse units) data availability.

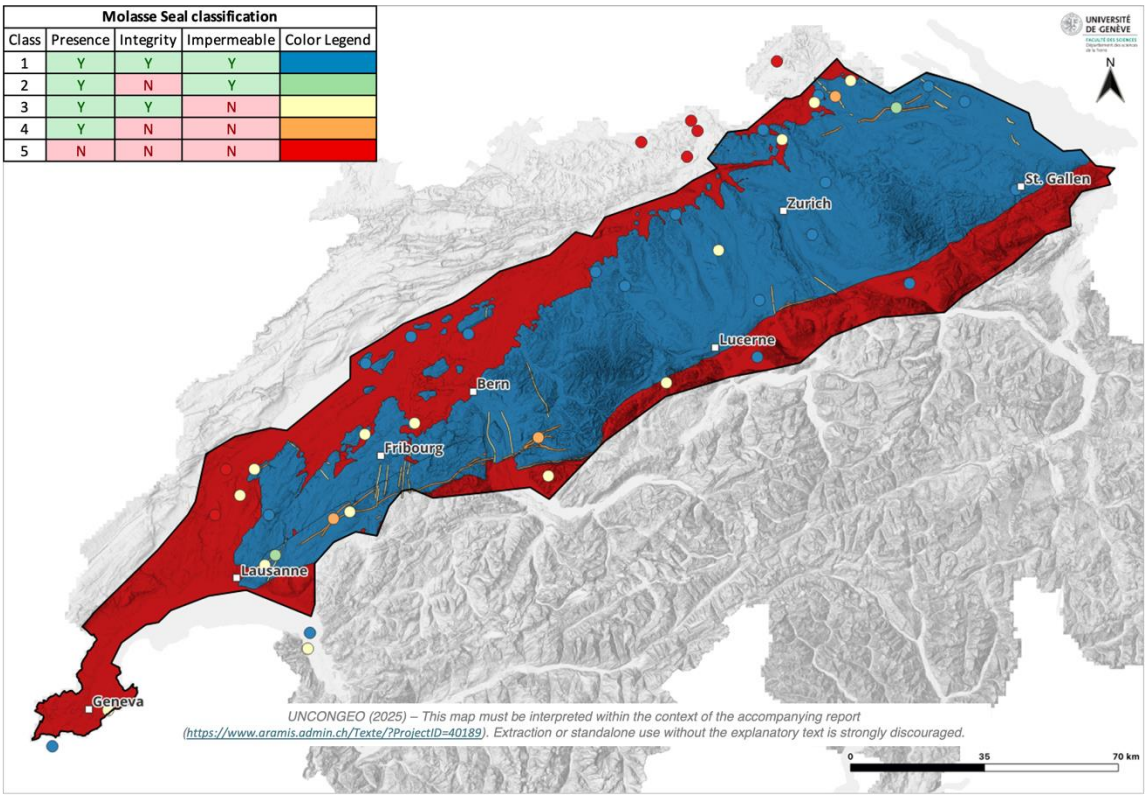


Fig. 122: Cretaceous seal (Molasse units) assessment and classification.

The results for the CRS map for the Cretaceous play are presented in Fig. 123. The western area of the Plateau, where the Lower Cretaceous unit is present, displays medium-low risk. This risk increases to “medium to high” on top of the Permo-Carboniferous troughs.

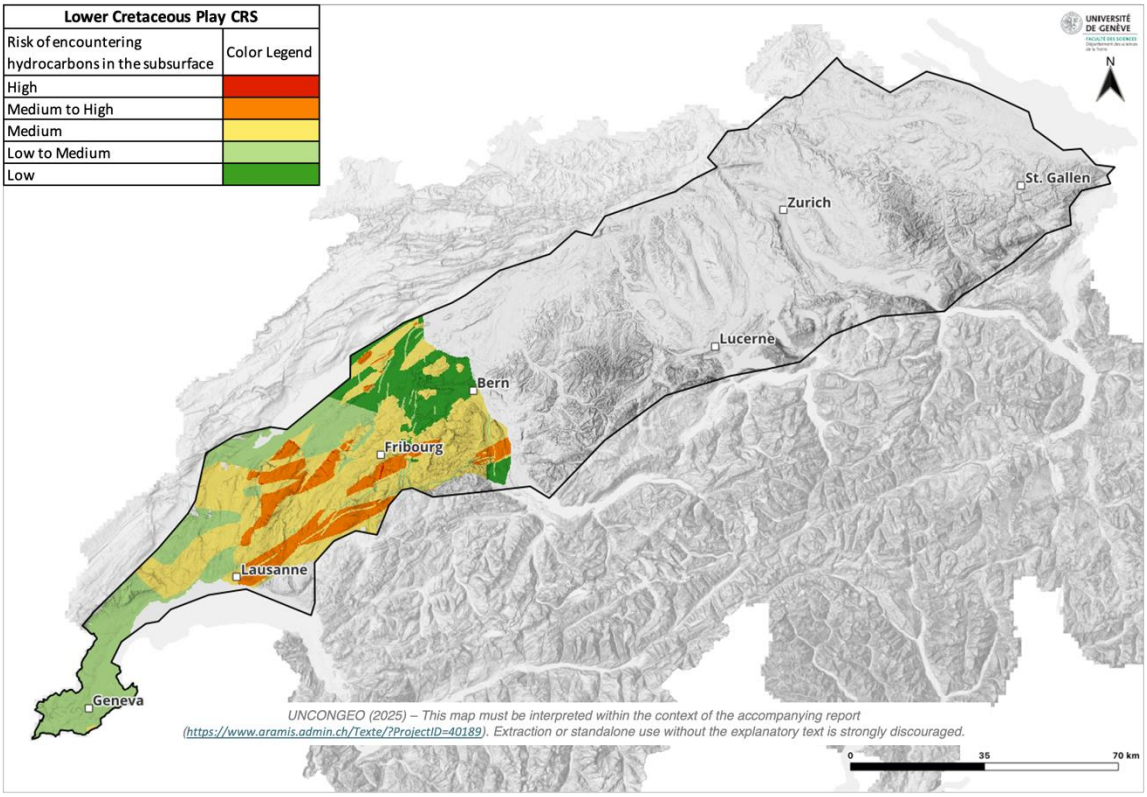


Fig. 123: CRS map for the Lower Cretaceous play.

3.6.3 Malm Play

The Malm play is present in the entire Plateau. The source rocks of this play are both the Posidonia shale and the Permo-Carboniferous units, whose properties are defined in the 3.6.1 section. The reservoir is represented by Karstified and/or fractured micritic limestones and reef composing the Upper Malm unit (Late Jurassic in age) and the seal is represented by the argillaceous limestones intercalated in the Malm (not representable at a regional scale), the Cretaceous marls, or the shales and marls composing the Molasse units when the Cretaceous is not present.

The Reservoir data availability for the most relevant wells of the Plateau and the related class assignments are listed in Table 59. Porosity data (Phi) are available for very few wells, and in most cases, it is < 15% (Appendix 6). This is why in the Assessment, it is assigned “No” to the *Phi>15%* properties for all the wells. In the Assessment, in the cases when the Malm unit has not been penetrated, its *Presence* is deduced from the closest wells. The resulting Data availability and Assessment maps for the Malm reservoir are shown in Fig. 124 and Fig. 125.

Reservoir Malm	**Data availability**					**Assessement**			
Well	GeoMol surface	GeoMol fault	Occurrence in well	Porosity data	Class	Presence	Phi>15 %	Fractured	Class
Altishofen-1	Yes	No	Yes	No	E	Yes	No*	No	4
Benken-1	Yes	No	Yes	Yes	C	Yes	No	No	4
Berlingen-1	Yes	No	Yes	No	E	Yes	No*	No	4
Boswil-1	Yes	No	Yes	No	E	Yes	No*	No	4
Böttstein	No	No	No	No	I	No	No	No	5
Bozberg-1	No	No	Yes	Yes	F	Yes	No	No	4

Reservoir Malm	Data availability					Assessement			
Well	GeoMol surface	GeoMol fault	Occurrence in well	Porosity data	Class	Presence	Phi>15 %	Fractured	Class
Bulach-1	Yes	No	Yes	Yes	C	Yes	No	No	4
Chapelle-1	Yes	No	No	No	G	Yes*	No*	No	4
Chessel-1	No	No	Yes	No	H	Yes	No*	No	4
Courtion-1	Yes	No	Yes	No	E	Yes	No*	No	4
Cuarny-1	Yes	Yes	Yes	No	B	Yes	No*	Yes	3
Eclepens-1	Yes	Yes	Yes	Yes	A	Yes	No	Yes	3
Entlebuch-1	Yes	No	Yes	No	E	Yes	No*	No	4
Essertines-1	Yes	Yes	Yes	Yes	A	Yes	No	Yes	3
Fendringen-1	Yes	Yes	No	No	D	Yes*	No*	Yes	3
Herdern-1	Yes	Yes	Yes	No	B	Yes	No*	No	4
Hermingen-1	Yes	Yes	Yes	Yes	A	Yes	No	Yes	3
Humilly-2	No	No	Yes	Yes	F	Yes	No	No	4
Hünenberg-1	Yes	No	Yes	No	E	Yes	No*	No	4
Kaisten-1	No	No	No	No	I	No	No	No	5
Kreuzlingen-1	Yes	Yes	Yes	Yes	A	Yes	No	No	4
Kusnacht-1	Yes	No	Yes	No	E	Yes	No*	No	4
Leuggern-1	No	No	No	No	I	No	No	No	5
Lindau-1	Yes	No	Yes	No	E	Yes	No*	No	4
Linden-1	Yes	No	Yes	No	E	Yes	No*	No	4
Marthalen-1	Yes	No	Yes	Yes	C	Yes	No	No	4
Noville-1	No	No	Yes	No	H	Yes	No*	No	4
Pfaffnau-1	Yes	Yes	Yes	Yes	A	Yes	No	No	4
Riniken-1	No	No	Yes	No	H	Yes	No*	No	4
Romanens-1	Yes	Yes	Yes	Yes	A	Yes	No	Yes	3
Ruppoldsried-1	Yes	Yes	No	No	D	Yes*	No*	No	4
Savigny-1	Yes	No	No	No	G	Yes*	No*	No	4
Servion-1	Yes	No	Yes	No	E	Yes*	No*	No	4
Schafisheim-1	Yes	No	Yes	Yes	C	Yes	No	No	4
Schlattingen-1	Yes	No	Yes	Yes	C	Yes	No	No	4
Siblingen	No	No	No	No	I	No	No	No	5
Sorens-1	Yes	No	No	No	G	Yes*	No*	No	4
St Gallen-GT-1	Yes	Yes	Yes	Yes	A	Yes	No	Yes	3
Thônex-1	Yes	No	Yes	No	E	Yes	No*	No	4
Thun-1	Yes	No	Yes	Yes	C	Yes	No	No	4
Treycovagnes-1	Yes	No	Yes	No	E	Yes	No*	No	4
Truellikon-1	Yes	Yes	Yes	Yes	A	Yes	No	Yes	3
Tschugg-1	Yes	Yes	No	No	D	Yes*	No	Yes	3
Tuggen-1	Yes	No	No	No	G	Yes*	No	No	4
Weggis-1	Yes	No	No	No	G	Yes*	No	No	4
Weiach-1	Yes	No	Yes	Yes	C	Yes	No	No	4
Weiach-2	Yes	No	Yes	No	E	Yes	No*	No	4

Table 59: Data availability and assessment classes assigned at the Malm Play reservoir (Upper Malm unit) in the most relevant wells of the Plateau. In the **Data availability**, Porosity is "Yes" when porosity data are available in this well specifically for the Upper Malm unit. In the **Assessment**, (*) means that for this well there are not data to define this property, thus Yes*/No* is deduced extrapolating what it has been defined in in the closest wells where data are available. Specifically, Presence "Yes*" means that in

this well the Upper Malm has not been penetrated, thus its presence has been deduced from the closest wells and/or seismic interpolation (GeoMol). Similarly for the Phi >15%, "No*" means that porosity data are not available for the Upper Malm in this well, thus it has been deduced from the closest wells where data are available.

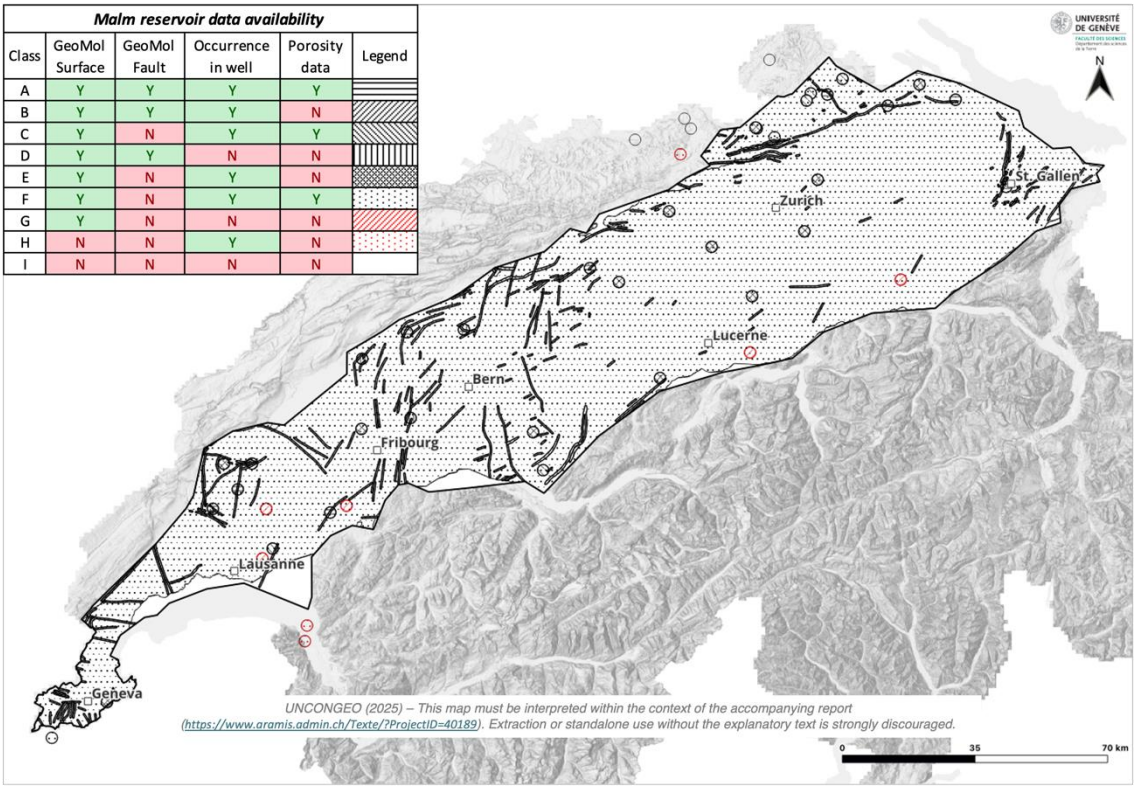


Fig. 124: Malm reservoir data availability.

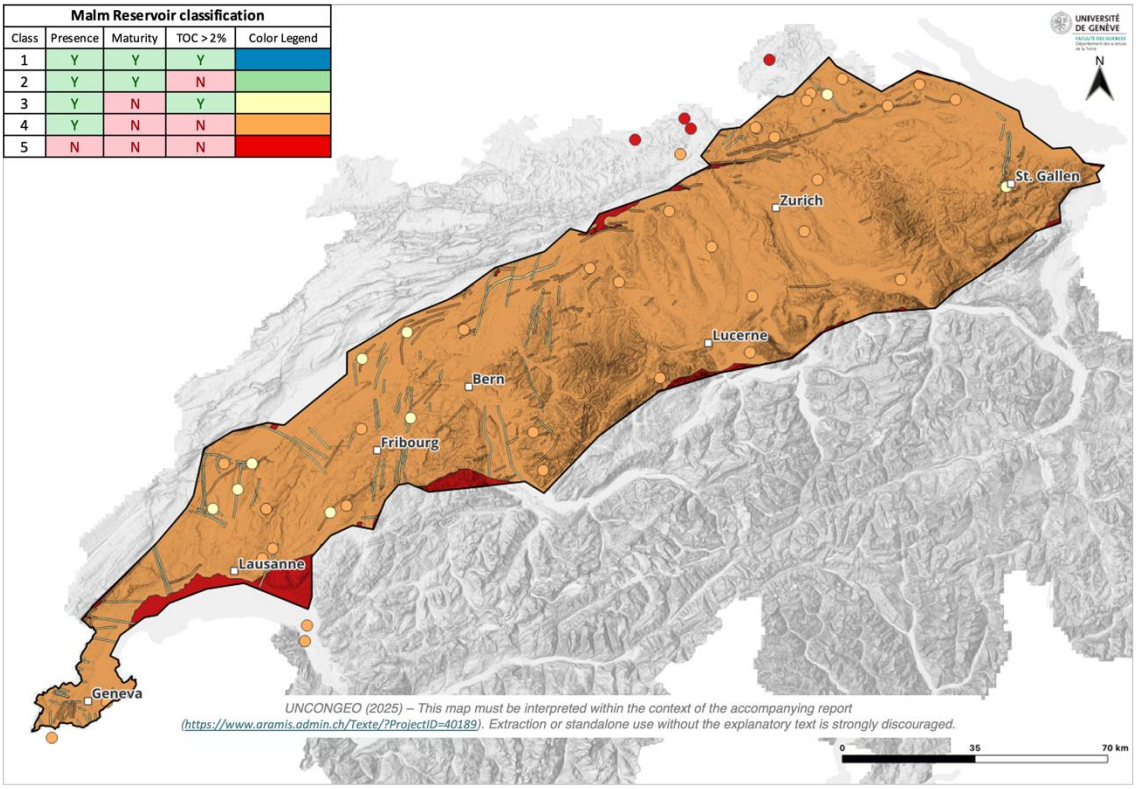


Fig. 125: Malm reservoir assessment and classification.

The Lower Cretaceous or Molasse seal data availability and assessment for the most relevant wells of the Plateau and the related classes assignment are listed in Table 60. In the Assessment, the *Impermeable* property is defined on the general facies of the Cretaceous or Molasse unit described in the well reports, expressed as a percentage of lithologies (Table 61). When lithological data are not available for a well, the *Impermeable* property is extrapolated from the lithological data of the closest wells. The resulting Data availability and Assessment maps for the Malm seal are shown in Fig. 126 and Fig. 127.

Seal Molasse/ Cretaceous	**Data availability**						**Assessement**			
Well	Unit	Geo Mol surface	GeoMol fault	Occurrence in a well	Lithologic data	Class	Presence	Integrity	Impermeable	Class
Altishofen-1	LFM	Yes	No	Yes	Yes	C	Yes	Yes	Yes	1
Benken-1	LFM	Yes	No	Yes	Yes	C	Yes	Yes	Yes	1
Berlingen-1	LFM	Yes	No	Yes	Yes	C	Yes	Yes	Yes	1
Boswil-1	LFM	Yes	No	Yes	Yes	C	Yes	Yes	No	3
Bottstein	None	No	No	No	No	I	No	No	No	5
Bozberg-1	LFM	No	No	Yes	Yes	F	Yes	Yes	No	3
Bulach-1	LFM	Yes	No	Yes	Yes	C	Yes	Yes	No	3
Chapelle-1	Cretaceous	Yes	No	Yes	Yes	C	Yes	Yes	Yes	1
Chessel-1	None	No	No	No	No	I	No	No	No	5
Courtion-1	LFM	Yes	No	Yes	No	E	Yes	Yes	Yes*	1
Cuarny-1	LFM	Yes	Yes	Yes	No	B	Yes	No	Yes*	2
Eclepens-1	Cretaceous	Yes	Yes	Yes	Yes	A	Yes	Yes	Yes	1
Entlebuch-1	LFM	Yes	No	Yes	Yes	C	Yes	Yes	No	3
Essertines-1	Cretaceous	Yes	Yes	Yes	Yes	A	Yes	No	Yes	2
Fendringen-1	?	Yes	Yes	Yes	No	B	Yes	Yes	Yes*	1
Herdern-1	LFM	Yes	Yes	Yes	Yes	A	Yes	No	Yes	2
Hermingen-1	Cretaceous	Yes	No	Yes	Yes	C	Yes	Yes	Yes	1
Humilly-2	Cretaceous	No	No	Yes	Yes	F	Yes	Yes	Yes	1
Hünenberg-1	LFM	Yes	No	Yes	Yes	C	Yes	Yes	Yes	1
Kaisten-1	None	No	No	No	No	I	No	No	No	5
Kreuzlingen-1	LFM	Yes	Yes	Yes	Yes	A	Yes	No	Yes	2
Kusnacht-1	LFM	Yes	No	Yes	Yes	C	Yes	Yes	Yes	1
Leuggern-1	None	No	No	No	No	I	No	No	No	5
Lindau-1	LFM	Yes	No	Yes	Yes	C	Yes	Yes	Yes	1
Linden-1	LMM	Yes	No	Yes	Yes	C	Yes	Yes	No	3
Marthalen-1	LFM	Yes	No	Yes	Yes	C	Yes	Yes	No	3
Noville-1	LFM	No	No	Yes	Yes	F	Yes	Yes	Yes	1
Pfaffnau-1	LFM	Yes	Yes	Yes	Yes	A	Yes	No	Yes	2
Riniken-1	None	No	No	No	No	I	No	No	No	5
Romanens-1	Cretaceous	Yes	Yes	Yes	Yes	A	Yes	Yes	Yes	1
Ruppoldsried-1	LMM	Yes	Yes	Yes	Yes	A	Yes	No	Yes	2
Savigny-1	Cretaceous	Yes	No	Yes	Yes	C	Yes	Yes	Yes	1
Servion-1	LFM	Yes	No	Yes	Yes	C	Yes	Yes	Yes	1
Schafisheim-1	LFM	Yes	No	Yes	Yes	C	Yes	Yes	No	3
Schlattingen-1	Molasse	Yes	No	Yes	No	E	Yes	Yes	Yes*	1
Siblingen	None	No	No	No	No	I	No	No	No	5
Sorens-1	Cretaceous	Yes	No	Yes	Yes	C	Yes	Yes	Yes	1

Seal Molasse/ Cretaceous	Data availability						Assessement			
Well	Unit	Geo Mol surface	GeoMol fault	Occurrence in a well	Lithologic data	Class	Presence	Integrity	Impermeable	Class
St Gallen-GT-1	LMM	Yes	No	Yes	Yes	C	Yes	Yes	Yes	1
Thônex-1	Cretaceous /LFM	Yes	No	Yes	Yes	C	Yes	Yes	No	3
Thun-1	LFM	Yes	No	Yes	Yes	C	Yes	Yes	No	3
Treycovagnes-1	Cretaceous	No	No	Yes	Yes	F	Yes	Yes	Yes	1
Truellikon-1	LFM	Yes	Yes	Yes	Yes	A	Yes	No	No	4
Tschugg-1	Cretaceous	Yes	Yes	Yes	Yes	A	Yes	No	Yes	2
Tuggen-1	LFM	Yes	No	Yes	Yes	C	Yes	Yes	Yes	1
Weggis-1	LFM	Yes	No	Yes	No	E	Yes	Yes	Yes*	1
Weiach-1	LFM	Yes	No	Yes	Yes	C	Yes	Yes	Yes	1
Weiach-2	LFM	Yes	No	Yes	No	E	Yes	Yes	Yes*	1

Table 60: Data availability and assessment classes assigned at the Malm Play seal (Lower Cretaceous or Molasse units) in the most relevant wells of the Plateau. In the **Data availability**, Lithologic data is "Yes" when lithologic data are available in this well, specifically for the Cretaceous or Molasse units considered as a seal. In the **Assessment**, in the Impermeable property, (*) means that for this well, there are no lithological data to define the permeability; thus, Yes*/No* is assigned based on what is extrapolated from the closest wells where data are available.

Seal	Molasse or Cretaceous	
Well	**Unit**	**Lithology**
Altishofen-1	LFM	20%shales; 30% marls; 50% kalk sandstones
Benken	LFM	30% sandstones; 40% shales; 30% marls
Berlingen-1	LFM	50% marls; 30% shales; 20% sandstones
Boswil-1	LFM	sandstones
Bulach	LFM	sandstones
Bozberg-1	LFM	sandstones and marls
Chapelle-1	Cretaceous	90% limestones; 10% shales
Eclepens-1	Cretaceous	100% limestone
Entlebuch-1	LFM	40% carbonatic sandstones; 30% siltstones; 30% shales
Essertines-1	Cretaceous	100% Marl limestone
Herdern-1	LFM	80% shales and marls
Hermingen-1	Cretaceous	50% marls; 50% limestone
Hünenberg-1	LFM	50% marls; 30% sandstones; 20% shales
Kreuzlingen-1	LFM	60% marls; 25% sandstones; 3% shales; 2% limestones
Kusnacht-1	LFM	50% marls; 20% sandstones; 25% shales; 5% limestones
Lindau-1	LFM	70% marls; 30% sandstones
Linden-1	LMM	50% shales; 40% sandstones; 10% limestones
Marthaleen	LFM	sandstones and shales
Noville-1	LFM	65% shales; 25% sandstones; 5% marls; 5% silstones
Pfaffnau-1	LFM	70% marls; 20% sandstones; 10% shales
Riniken-1	None	Eroded
Romanens-1	Cretaceous	100% limestone
Ruppoldsried-1	LMM	80% marls; 20% silt
Schafisheim	LFM	77% marls; 23% shales
Schlattingen-1	LFM	sandstones-marls

Seal	Molasse or Cretaceous	
Well	**Unit**	**Lithology**
Savigny-1	Cretaceous	50% sandstone; 50% marls
Sorens-1	Unknown	Unknown
St Gallen-GT-1	LMM	40% sandstones; 10% shales; 50% marls
Thonex-1	Cretaceous/LFM	70% sandstones; 20% marls; 2% coal; 8% siltstone
Thun-1	LFM	80% sandstones; 20% shales
Treycovagnes-1	Cretaceous	30% limestone; 40% marls; 30% shales
Truillikon-1	LFM	sandstones
Tschugg-1	Cretaceous	100% limestone
Tuggen-1	LFM	85% marls; 15% sandstones
Weggis	LFM	Unknown
Weiach-1	LFM	70% sandstones; 20% silt; 10% shales

Table 61: General facies of the seal of the Malm Play in the main wells of the Plateau, represented by the Cretaceous or Molasse unit

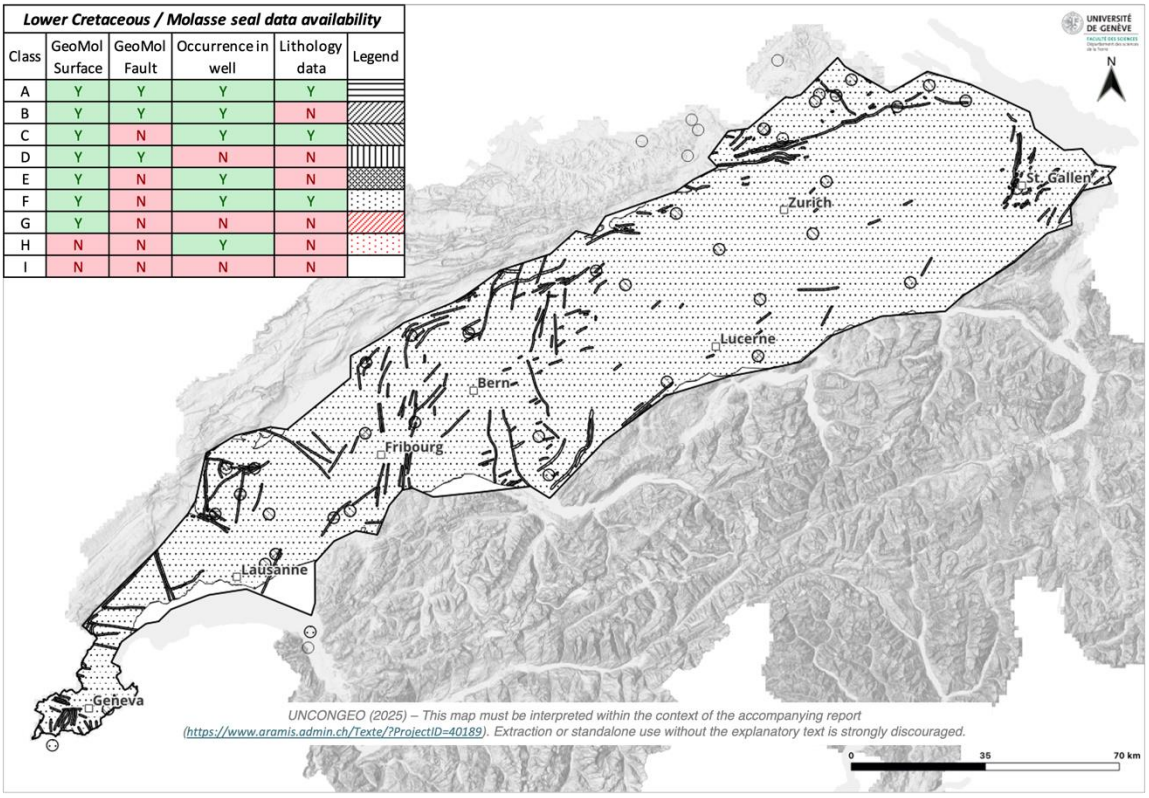


Fig. 126: Malm seal (Molasse or Lower Cretaceous units) data availability.

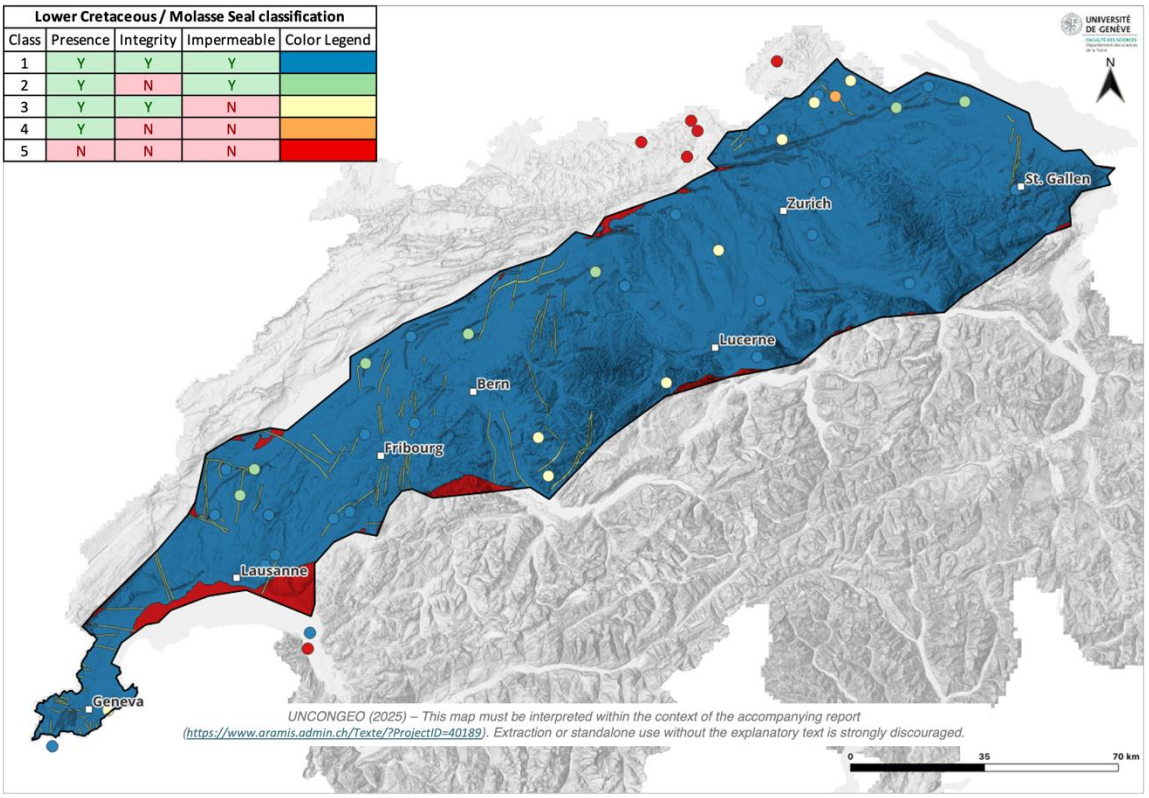


Fig. 127: Malm seal (Molasse or Lower Cretaceous units) assessment and classification

The results for the CRS map for the Malm play is shown in Fig. 128. Most of the western and central sector of the Plateau, displays a medium risk. This risk increases to medium-high on top of the Permo-Carboniferous troughs. The south-eastern part of the Swiss Plateau exhibits the lowest risk associated with the absence (non -deposition) of the Posidonia shale and poor reservoir properties.

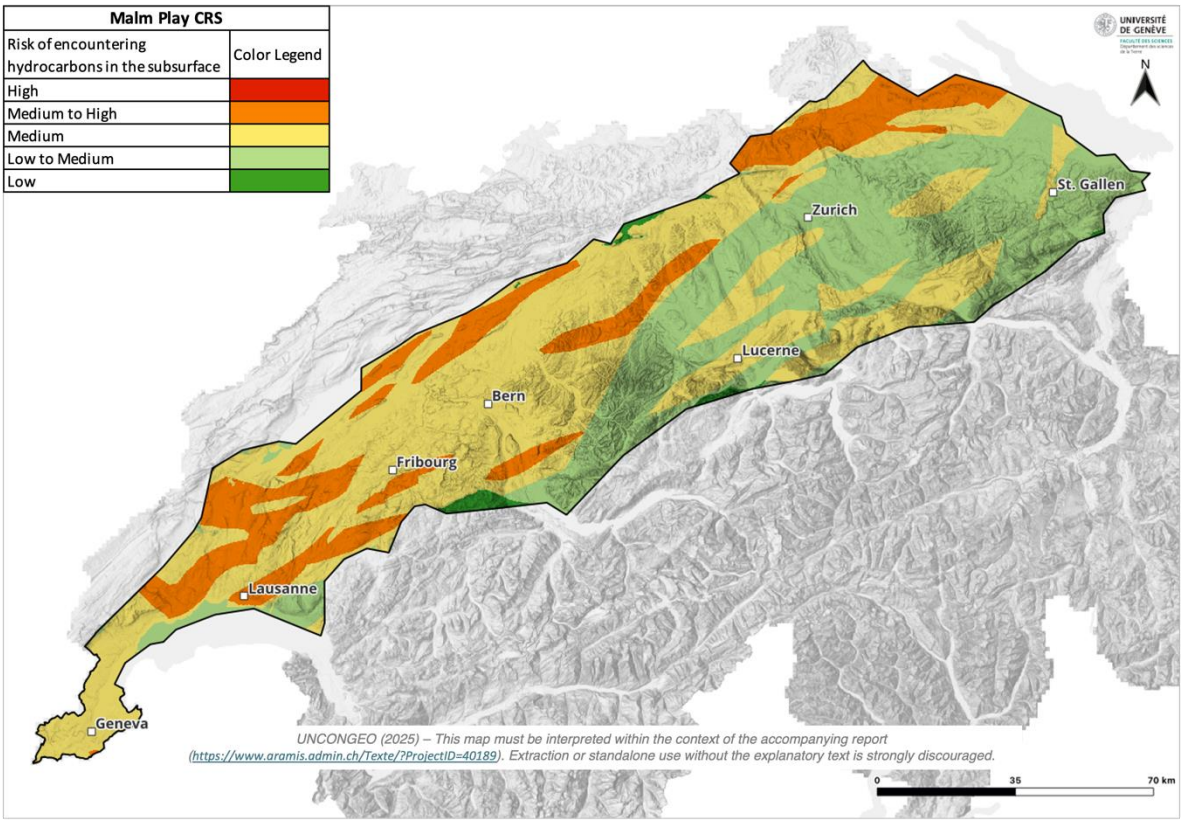


Fig. 128: CRS map for the Malm play.

3.6.4 Dogger Play

The Dogger play is present in mostly the entire Plataeau. The source rocks of this play are both the Posidonia shale and the Permo-Carboniferous units, whose properties are defined in the 3.6.1 section. The reservoir is represented by oolitic limestones composing the Dogger unit (Middle Jurassic in age) and the seal is represented by marly and shaly limestones composing Lower Malm unit (Late Jurassic in age).

The Reservoir data availability for the most relevant wells of the Plateau and the related classes assignment are listed in Table 62. Porosity data (Phi) are available for very few wells and in most of the cases it is < 15% (Appendix 6). This is why in the Assessment, it is assigned “No” to the *Phi>15%* properties for all the wells. In the Assessment, in the cases when the Dogger unit has not been penetrated, its *Presence* is deduced from the closest wells. The resulting Data availability and Assessment maps for the Dogger reservoir are shown in Fig. 129 and Fig. 130.

Reservoir Dogger	Data availability					Assessment			
Well	GeoMol surface	GeoMol fault	Occurrence in well	Porosity data	Class	Presence	Phi>15%	Fractured	Class
Altishofen-1	Yes	No	No	No	G	Yes*	No*	No	4
Benken-1	Yes	No	Yes	Yes	C	Yes	No	No	4
Berlingen-1	Yes	No	Yes	No	E	Yes	No*	No	4
Boswil-1	Yes	No	No	No	G	Yes*	No*	No	4
Bottstein-1	No	No	No	No	I	No	No	No	5
Bozberg-1	No	No	Yes	Yes	F	Yes	No	No	4
Bulach-1	Yes	No	Yes	Yes	C	Yes	No	No	4
Chapelle-1	Yes	No	No	No	G	Yes*	No*	No	4
Chessel-1	No	No	Yes	No	H	Yes	No*	No	4
Courtion-1	Yes	Yes	Yes	No	B	Yes	No*	Yes	3
Cuarny-1	Yes	Yes	Yes	No	B	Yes	No*	No	4
Eclepens-1	Yes	Yes	Yes	No	B	Yes	No*	Yes	3
Entlebuch-1	Yes	No	Yes	No	E	Yes	No*	No	4
Essertines-1	Yes	Yes	Yes	Yes	A	Yes	No	Yes	3
Fendringen-1	Yes	Yes	No	No	E	Yes*	No*	Yes	3
Herdern-1	Yes	Yes	Yes	No	B	Yes	No*	No	4
Hermingen-1	Yes	Yes	Yes	Yes	A	Yes	Yes	No	2
Humilly-2	No	No	Yes	Yes	F	Yes	No	No	4
Hünenberg-1	Yes	No	No	No	G	Yes*	No*	No	4
Kaisten-1	No	No	No	No	I	No	No	No	5
Kreuzlingen-1	Yes	Yes	Yes	Yes	A	Yes	No	No	4
Kusnacht-1	Yes	No	No	No	G	Yes*	No*	No	4
Leuggern-1	No	No	No	No	I	No	No	No	5
Lindau-1	Yes	No	Yes	No	E	Yes	No*	No	4
Linden-1	Yes	No	Yes	No	E	Yes	No*	No	4
Marthalen-1	Yes	No	Yes	Yes	C	Yes	No	No	4
Noville-1	No	No	Yes	No	H	Yes	No*	No	4
Pfaffnau-1	Yes	Yes	Yes	No	B	Yes	No*	No	4
Riniken-1	No	No	Yes	Yes	F	Yes	No	No	4
Romanens-1	Yes	Yes	Yes	No	B	Yes	No*	No	4
Ruppoldsried-1	Yes	No	No	No	G	Yes*	Yes*	No	2
Savigny-1	Yes	No	No	No	G	Yes*	No*	No	4
Schafisheim-1	Yes	No	Yes	Yes	C	Yes	No	No	4
Schlattingen	Yes	No	Yes	Yes	C	Yes	No	No	4
Servion-1	Yes	No	No	No	G	Yes*	No*	No	4
Siblingen-1	No	No	No	No	I	No	No	No	5
Sorens-1	Yes	No	No	No	G	Yes*	No*	No	4
St Gallen-GT-1	Yes	No	Yes	Yes	C	Yes	No	No	4
Thônex-1	Yes	No	No	No	G	Yes*	No*	No	4
Thun-1	Yes	No	Yes	No	E	Yes	No*	No	4
Treycovagnes-1	Yes	Yes	Yes	Yes	A	Yes	No*	Yes	3
Truellikon-1	Yes	No	Yes	Yes	C	Yes	No*	No	4
Tschugg-1	Yes	Yes	No	No	D	Yes*	Yes*	No	2
Tuggen-1	Yes	No	No	No	G	Yes*	No*	No	4

Reservoir Dogger	Data availability					Assessment			
Well	GeoMol surface	GeoMol fault	Occurrence in well	Porosity data	Class	Presence	Phi>15%	Fractured	Class
Weggis-1	Yes	No	No	No	G	Yes*	No*	No	4
Weiach-1	Yes	No	Yes	Yes	C	Yes	No	No	4
Weiach-2	Yes	No	Yes	No	E	Yes	No*	No	4

Table 62: Data availability and assessment classes assigned at the Dogger Play reservoir (Dogger unit) in the most relevant wells of the Plateau. In the **Data availability**, Porosity is "Yes" when porosity data are available in this well, specifically for the Dogger unit. In the **Assessment**, (*) means that for this well, there are no data to define this property; thus, Yes*/No* is deduced by extrapolating what has been defined in the closest wells where data are available. Specifically, Presence "Yes*" means that in this well, the Dogger unit has not been penetrated, thus its presence has been deduced from closest wells and/or seismic interpolation (GeoMol). Similarly, for the Phi >15%, "No*" means that porosity data are not available for the Dogger unit in this well; thus, it has been deduced from the closest wells where data are available.

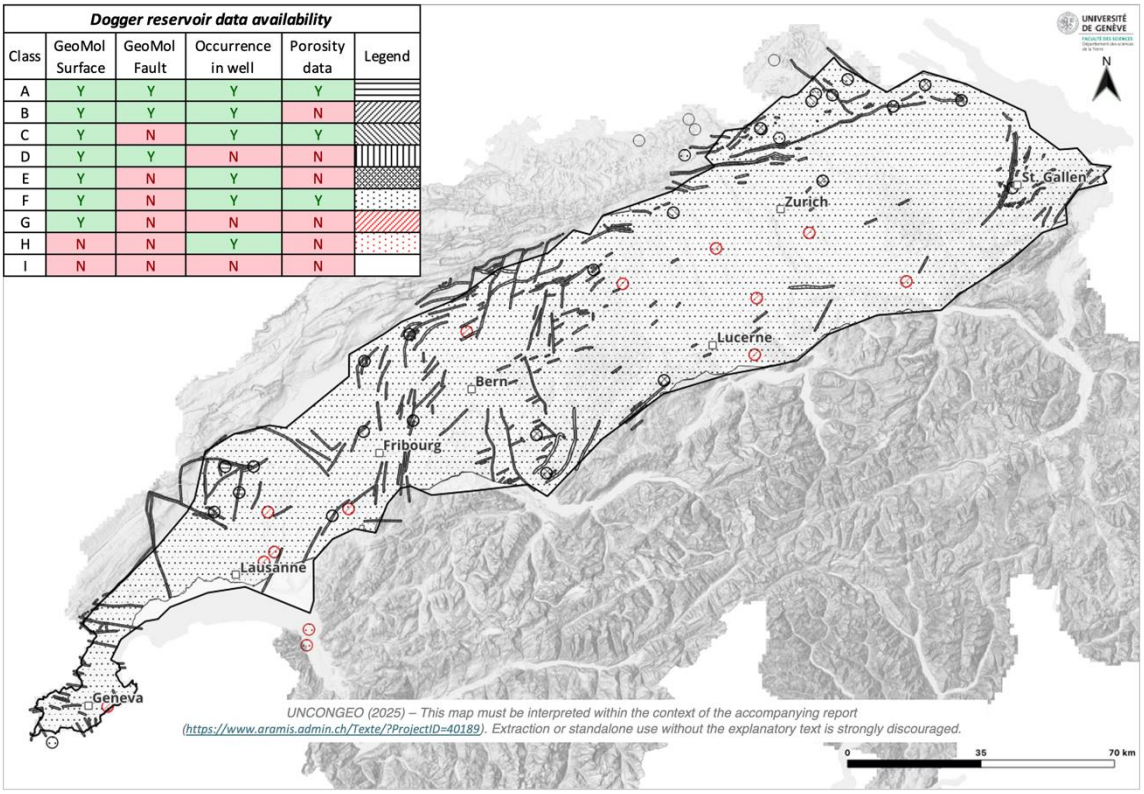


Fig. 129: Dogger reservoir data availability.

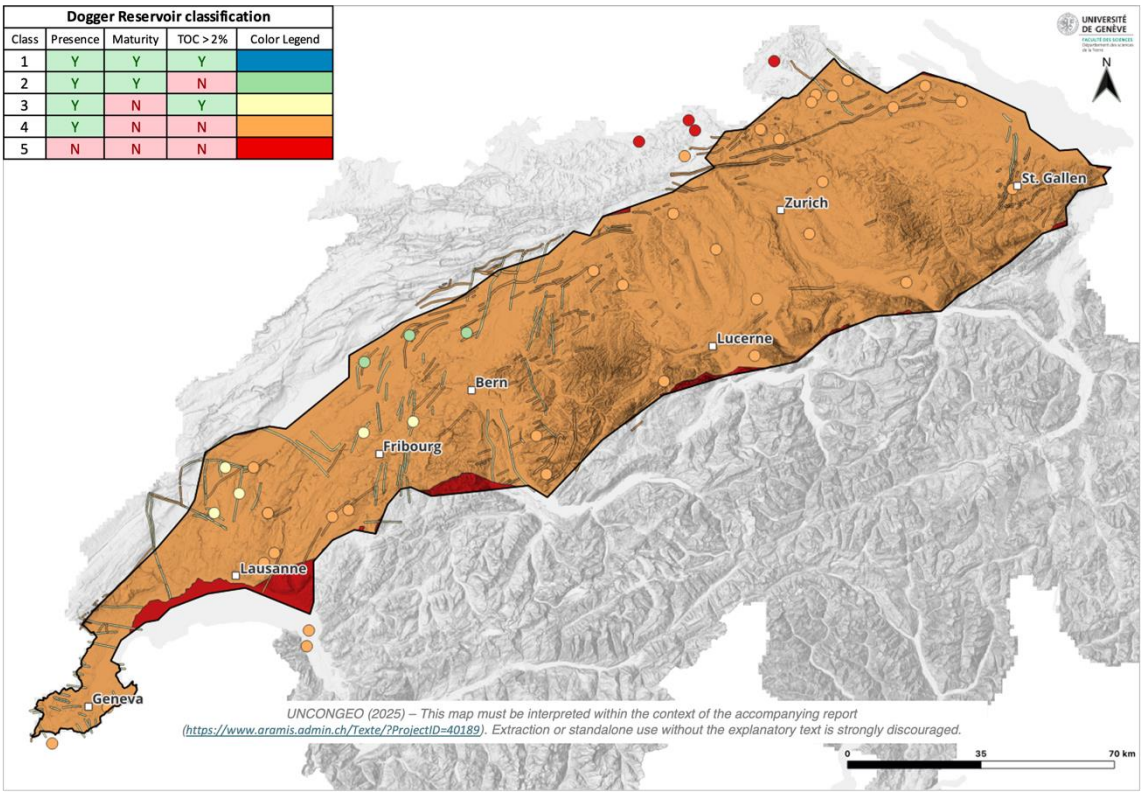


Fig. 130: Dogger reservoir assessment and classification

The Lower Malm seal data availability and assessment for the most relevant wells of the Plateau and the related classes assignment are listed in Table 63. In the Assessment, the *Impermeable* property is defined on the general facies of the Lower Malm unit described in the well report, expressed as a percentage of lithologies (Table 64). When lithological data are not available for a well, the *Impermeable* property is extrapolated from the lithological data of the closest wells. The resulting Data availability and Assessment maps for the Dogger play seal (Lower Malm unit) are shown in Fig. 131 and Fig. 132.

Seal Lower Malm	**Data availability**					**Assessment**			
Well	GeoMol surface	GeoMol fault	Occurrence in a well	Lithologic data	Class	Presence	Integrity	Impermeable	Class
Altishofen-1	Yes	No	No	No	G	Yes*	Yes	Yes*	1
Benken-1	Yes	No	Yes	Yes	C	Yes*	Yes	Yes	1
Berlingen-1	Yes	No	Yes	Yes	C	Yes*	Yes	Yes	1
Boswil-1	Yes	No	No	No	G	Yes*	Yes	Yes*	1
Bottstein-1	No	No	No	No	I	No	No	No	5
Bozberg-1	No	No	Yes	Yes	F	Yes	Yes	Yes	1
Bulach-1	Yes	No	Yes	Yes	C	Yes	Yes	Yes	1
Chapelle-1	Yes	No	No	No	G	Yes*	Yes	Yes*	1
Chessel-1	No	No	Yes	No	H	Yes	Yes	Yes*	1
Courtion-1	Yes	No	Yes	No	E	Yes	Yes	Yes*	1
Cuarny-1	Yes	Yes	Yes	No	B	Yes	Yes	Yes*	1
Eclepens-1	Yes	Yes	Yes	Yes	A	Yes	No	Yes	2
Entlebuch-1	Yes	No	Yes	Yes	C	Yes	Yes	Yes	1
Essertines-1	Yes	Yes	Yes	Yes	A	Yes	No	Yes	2
Fendringen-1	Yes	Yes	No	No	D	Yes*	No	Yes*	2
Herdern-1	Yes	Yes	Yes	Yes	A	Yes	Yes	Yes	1
Hermingen-1	Yes	Yes	Yes	Yes	A	Yes	Yes	Yes	1
Humilly-2	No	No	Yes	Yes	F	Yes	Yes	Yes	1
Hünenberg-1	Yes	No	No	No	G	Yes*	Yes	Yes*	1
Kaisten-1	No	No	No	No	I	No	No	No	5
Kreuzlingen-1	Yes	Yes	Yes	Yes	A	Yes	Yes	Yes	1
Kusnacht-1	Yes	No	No	No	G	Yes*	Yes	Yes*	1
Leuggern-1	No	No	No	No	I	No	No	No	5
Lindau-1	Yes	No	Yes	Yes	C	Yes	Yes	Yes	1
Linden-1	Yes	No	Yes	Yes	C	Yes	Yes	Yes	1
Marthalen-1	Yes	No	Yes	Yes	C	Yes	Yes	yes	1
Noville-1	No	No	Yes	Yes	F	Yes	Yes	Yes	1
Pfaffnau-1	Yes	Yes	Yes	Yes	A	Yes	Yes	Yes	1
Riniken-1	No	No	Yes	Yes	F	Yes	Yes	Yes	1
Romanens-1	Yes	Yes	Yes	Yes	A	Yes	Yes	Yes	1
Ruppoldsried-1	Yes	No	No	No	G	Yes*	Yes	Yes*	1
Savigny-1	Yes	No	No	No	G	Yes*	Yes	Yes*	1
Schafisheim-1	Yes	No	Yes	Yes	C	Yes	Yes	Yes	1
Schlattingen	Yes	No	Yes	Yes	C	Yes	Yes	Yes	1
Servion-1	Yes	No	No	No	G	Yes*	Yes	Yes*	1
Siblingen-1	No	No	No	No	I	No	No	No	5
Sorens-1	Yes	No	No	No	G	Yes*	Yes	Yes*	1

Seal Lower Malm	Data availability					Assessment			
Well	GeoMol surface	GeoMol fault	Occurrence in a well	Lithologic data	Class	Presence	Integrity	Impermeable	Class
St Gallen-GT-1	Yes	No	Yes	Yes	C	Yes	Yes	Yes	1
Thônex-1	Yes	No	No	No	G	Yes*	Yes	Yes*	1
Thun-1	Yes	No	Yes	Yes	C	Yes	Yes	Yes	1
Treycovagnes-1	Yes	Yes	Yes	Yes	A	Yes	No	Yes	2
Truellikon-1	Yes	No	Yes	Yes	C	Yes	Yes	Yes	1
Tschugg-1	Yes	Yes	No	No	D	Yes*	No	Yes*	2
Tuggen-1	Yes	No	No	No	G	Yes*	Yes	Yes*	1
Weggis-1	Yes	No	No	No	G	Yes*	Yes	Yes*	1
Weiach-1	Yes	No	Yes	Yes	C	Yes	Yes	Yes	1
Weiach-2	Yes	No	Yes	No	E	Yes	Yes	Yes*	1

Table 63: Data availability and assessment classes assigned at the Dogger Play seal (Lower Malm unit) in the most relevant wells of the Plateau. In the **Data availability**, Lithologic data is "Yes" when lithologic data are available in this well, specifically for the Lower Malm unit. In the **Assessment**, in the presence property, "Yes*" means that in this well, the Lower Malm has not been penetrated, thus its presence has been deduced from the closest wells where data are available and/or seismic (GeoMol). In the Impermeable property, (*) means that for this well, there are no lithological data to define the permeability; thus, Yes*/No* is assigned based on what is extrapolated from the closest wells where data are available.

Seal Lower Malm

Well	Lithology
Altishofen-1	Not penetrated
Benken-1	55% shales, 45% marls
Berlingen-1	80% marls; 20% limestones
Boswil-1	Not penetrated
Bozberg-1	Calcareous marls
Bulach-1	Calcareous marls and shales
Chapelle-1	Not penetrated
Eclepens-1	90% marlstone 10% marls
Entlebuch-1	70% limestones; 30% marls
Essertines-1	100% Marl limestone
Herdern-1	35% shales; 65% limestones
Hermingen-1	50% marls; 50% limestone
Humilly-2	marls
Hünenberg-1	Not penetrated
Kreuzlingen-1	90% limestones; 10% marls
Kusnacht-1	Not penetrated
Lindau-1	90% marls; 10% limestones
Linden-1	100% limestones (micrite)
Marthaleen	Limestones and marls
Noville-1	70% marls; 20% limestones; 10% shales
Pfaffnau-1	70% marls; 30% limestones
Romanens-1	100% micrite
Ruppoldsried-1	Not penetrated
Riniken-1	86% shales; 14% limestones

Seal Lower Malm

Well	Lithology
Schafisheim-1	60% shales; 40% limestones
Schlattingen-1	argillaceous limestones
Savigny-1	Not penetrated
St Gallen-GT-1	100% limestone
Thun-1	80% limestones; 20% dolomestones
Treycovagnes-1	70% marls; 30% limestone
Truillikon-1	Limestones and marls
Tuggen-1	Not penetrated
Tschugg-1	Not penetrated
Weiach-1	70% marls; 30% limestones
Weggis	Not penetrated

Table 64: General facies of the seal of the Dogger Play in the main wells of the Plateau, represented by the Lower Malm unit

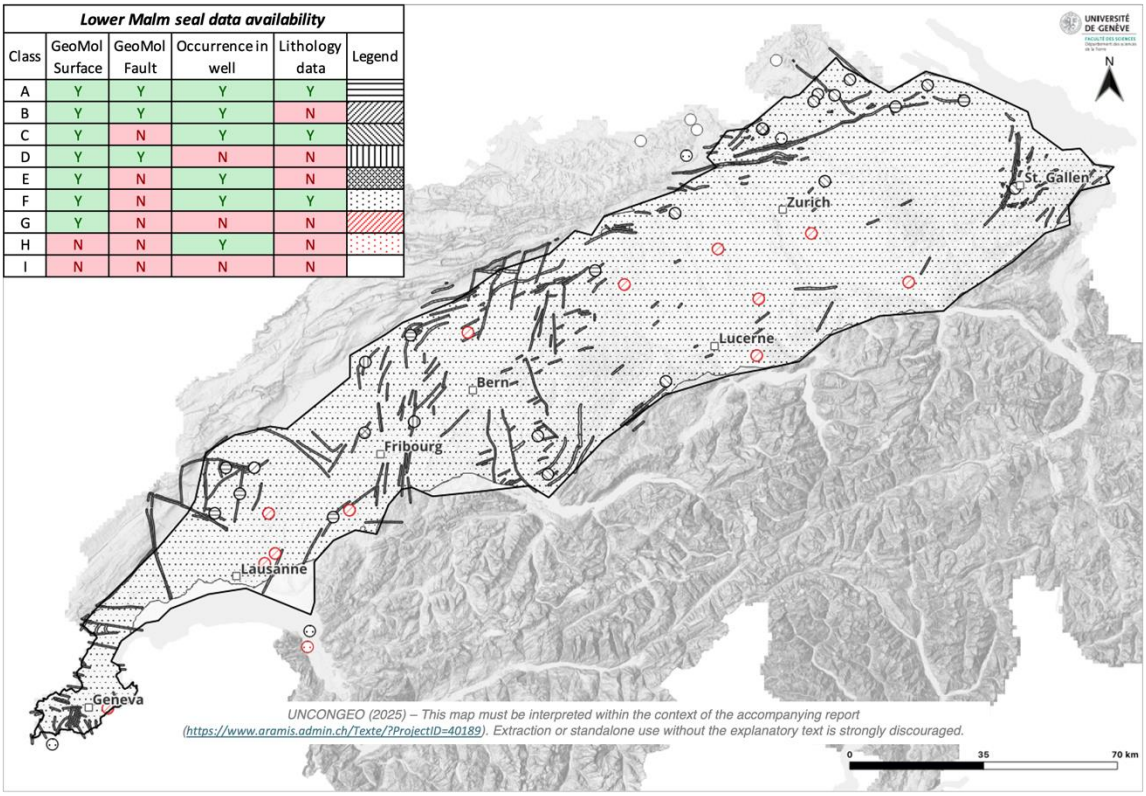


Fig. 131: Dogger seal (Lower Malm unit) data availability

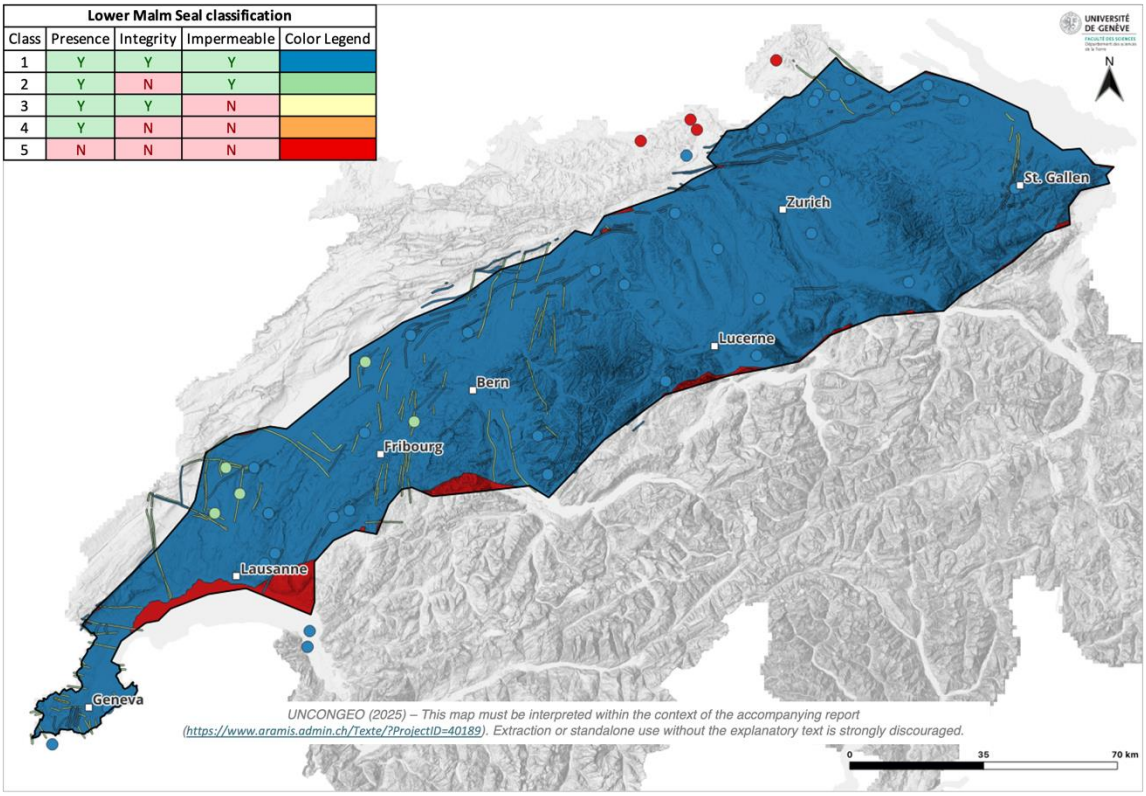


Fig. 132: Dogger seal (Lower Malm) assessement and classification

The results for the CRS map for the Dogger play is shown in Fig. 133. In the western sector of the Plateau, an extended area results in the medium risk class. This risk increases to medium-high on top of the Permo-Carboniferous troughs. In the areas located in the south-eastern part of the Swiss Plateau, result as low risk, due to the non-deposition of the Posidonia shale and an overall poor reservoir property.

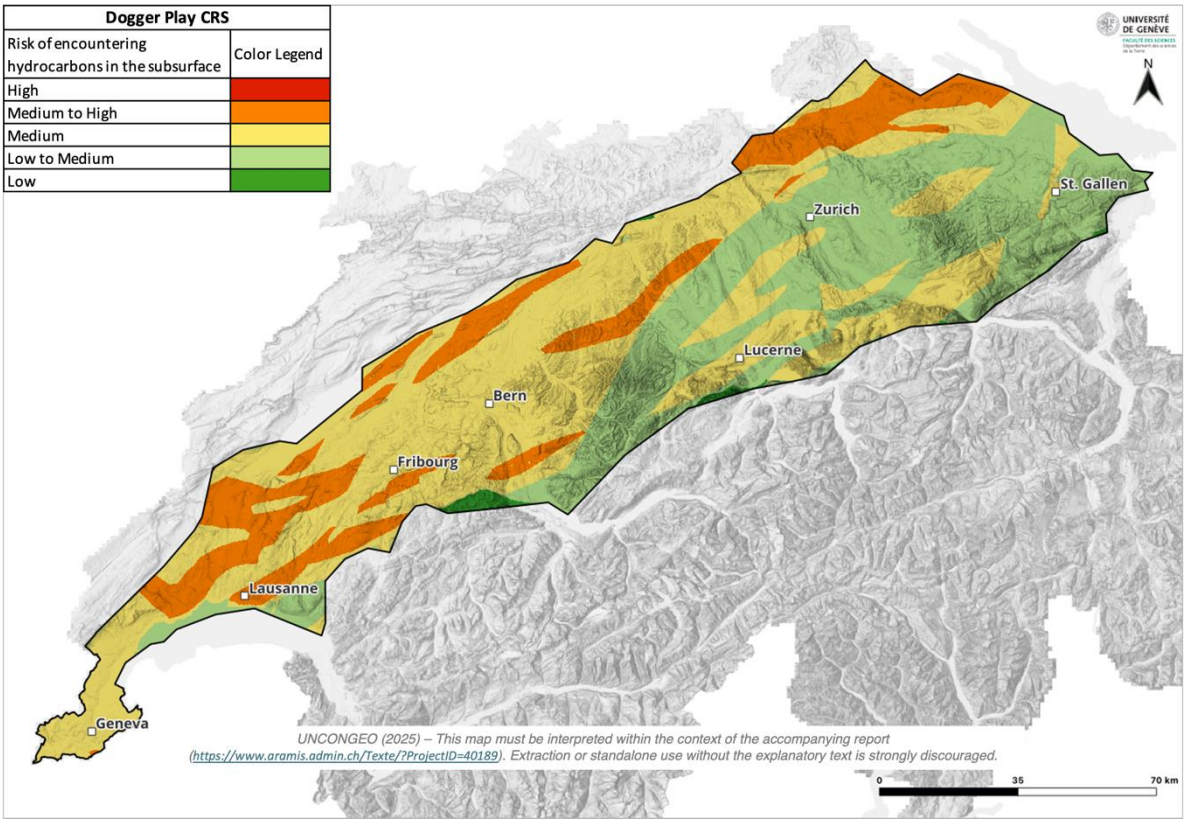


Fig. 133: CRS map for the Dogger play.

3.6.5 Lias Play

The Lias play is present in mostly the entire Plataeau. The source rocks of this play are both the Posidonia shale and the Permo-Carboniferous units, which properties are defined in the 3.6.1 section. The reservoir is represented by sanstones bodies, forming the Rhaetian and/or Lias units (Late Triassic, Early Jurassic in age) and the seal is represented by superimposed shales deposits, included in the same Lias unit and/or in the Dogger unit (Opalinus Clays).

The Reservoir data availability for the most relevant wells of the Plateau and the related classes assignement are listed in Table 65. In this table it is specified at which unit refers the reservoir (Lias or Rhetian). When sandstone facies are not described in none of these two units, the Lias is not considered a proper reservoir. In this case, in the Assessment, the *Presence* is marked as “No”. Porosity data (Phi) are available for very few wells, and in most cases, it is < 15% (Appendix 6). This is why in the Assessment, it is assigned “No” to the *Phi>15%* properties for all the wells. In the Assessment, in the cases when the Lias unit has not been penetrated, its *Presence* is deduced from the closest wells. The resulting Data availability and Assessment maps for the Lias reservoir are shown in Fig. 134 and Fig. 135.

Reservoir Lias+Rhetian		Data availability					Assessement			
Well	Reservoir Unit*	GeoMol surface	GeoMol fault	Occurrence in a well	Porosity data	Class	Presence	Phi>15%	Fractured	Class
Altishofen-1	Unknown	Yes	No	No	No	G	Yes*	No*	No	4
Benken	None	Yes	No	Yes	Yes	C	No*	No	No	5
Berlingen-1	Lias	Yes	No	Yes	No	E	Yes	No*	No	4
Boswil-1	Unknown	Yes	No	No	No	G	Yes*	No*	No	4
Bottstein-1	Not penetrated	No	No	No	No	I	No	No*	No	5
Bozberg-1	None	No	No	Yes	No	H	No*	No*	No	5
Bulach-1	None	Yes	No	Yes	No	E	No*	No*	No	5
Chapelle-1	Unknown	Yes	No	No	No	G	Yes*	No*	No	4
Chessel-1	Unknown	No	No	No	No	I	No	No*	No	5
Courtion-1	Unknown	Yes	No	Yes	No	E	Yes*	No*	No	4
Cuarny-1	Unknown	Yes	Yes	Yes	No	B	Yes*	No*	No	4
Eclepens-1	Rheatian	Yes	Yes	Yes	Yes	A	Yes	No	Yes	3
Entlebuch-1	Lias	Yes	No	Yes	No	E	Yes	No*	No	4
Essertines-1	Rheatian	Yes	Yes	Yes	Yes	A	Yes	No	Yes	3
Fendringen-1	Unknown	Yes	Yes	No	No	D	Yes*	No*	Yes	3
Herdern-1	None	Yes	Yes	Yes	No	B	No*	No*	No*	5
Hermingen-1	Lias	Yes	Yes	Yes	Yes	A	Yes	No	Yes	3
Humilly-2	None	No	No	Yes	Yes	F	No*	No*	No	5
Hünenberg-1	Unknown	Yes	No	No	No	G	Yes*	No*	No	4
Kaisten	Not penetrated	No	No	No	No	I	No	No*	No	5
Kreuzlingen-1	None	Yes	Yes	Yes	Yes	A	No*	No	No*	5
Kusnacht-1	Unknown	Yes	No	No	No	G	Yes*	No*	No	4
Leuggern-1	Not penetrated	No	No	No	No	I	No	No*	No	5
Lindau-1	Lias	Yes	No	Yes	No	E	Yes	No*	No	4
Linden-1	Lias	Yes	No	Yes	No	E	Yes	No*	No	4
Marthalen-1	None	Yes	No	Yes	No	E	No*	No*	No	5
Noville-1	Not present	No	No	No	No	I	No	No	No	5
Pfaffnau-1	Lias	Yes	Yes	Yes	Yes	A	Yes	No	Yes	3
Riniken-1	None	No	No	Yes	Yes	F	No*	No	No	5
Romanens-1	None	Yes	Yes	Yes	Yes	A	No*	No	No	5
Ruppoldsried-1	Unknown	Yes	No	No	No	G	Yes*	No*	No	4
Savigny-1	Unknown	Yes	No	No	No	G	No*	No*	No	5
Schafisheim-1	None	Yes	Yes	Yes	No	B	No*	No*	No*	5
Schlattingen-1	None	Yes	No	Yes	Yes	C	No*	No*	No	5
Servion-1	Unknown	Yes	No	No	No	G	No*	No*	No	5
Siblingen	None	No	No	Yes	No	H	No*	No*	No	5
Sorens-1	Unknown	Yes	No	No	No	G	No*	No*	No	5
St Gallen	Unknown	Yes	No	No	No	G	No*	No*	No	5
Thônex-1	Unknown	Yes	No	No	No	G	No*	No*	No	5
Thun-1	Lias	Yes	No	Yes	No	E	Yes	No*	No	4

Reservoir Lias+Rhetian		**Data availability**					**Assessement**			
Well	Reservoir Unit*	GeoMol surface	GeoMol fault	Occurrence in a well	Porosity data	Class	Presence	Phi>15%	Fractured	Class
Treycovagnes-1	Rheatian	Yes	No	Yes	Yes	C	Yes	No*	No	4
Truellikon-1	None	Yes	No	Yes	No	E	No*	No*	No	5
Tschugg-1	Unknown	Yes	Yes	No	No	D	Yes*	No*	Yes	3
Tuggen-1	Unknown	Yes	No	No	No	G	Yes*	No*	No	4
Weggis-1	Unknown	Yes	No	No	No	G	Yes*	No*	No	4
Weiach-1	None	Yes	No	Yes	Yes	C	No*	No	No	5
Weiach-2	Unknown	Yes	No	Yes	No	E	No*	No*	No	5

Table 65: Data availability and assessment classes assigned at the Lias Play reservoir (Lias or Rhetian units) in the most relevant wells of the Plateau. In the Reservoir Unit column, it is indicated which unit can be a reservoir, based on the facies. In this column, “none” means that in both units, there are no coarse-grained facies that can represent a reservoir. In the **Data availability**, Porosity is “Yes” when porosity data are available in this well, specifically for the Lias/Rhetian unit. In the **Assessment**, (*) means that for this well, there are no data to define this property; thus, Yes*/No* is deduced by extrapolating what has been defined in the closest wells where data are available. Specifically, Presence “Yes*” means that in this well the Lias unit has not been penetrated, thus its presence has been deduced from the closest wells where data are available and/or seismic interpolation (GeoMol). “No*” means that even if the Lias and/or Rhetian unit is present, there are no coarse-grained facies that can be a reservoir. In Phi >15%, “No*” means that porosity data are not available for the Lias/Rhetian unit in this well; thus, it has been deduced from the closest wells where data are available.

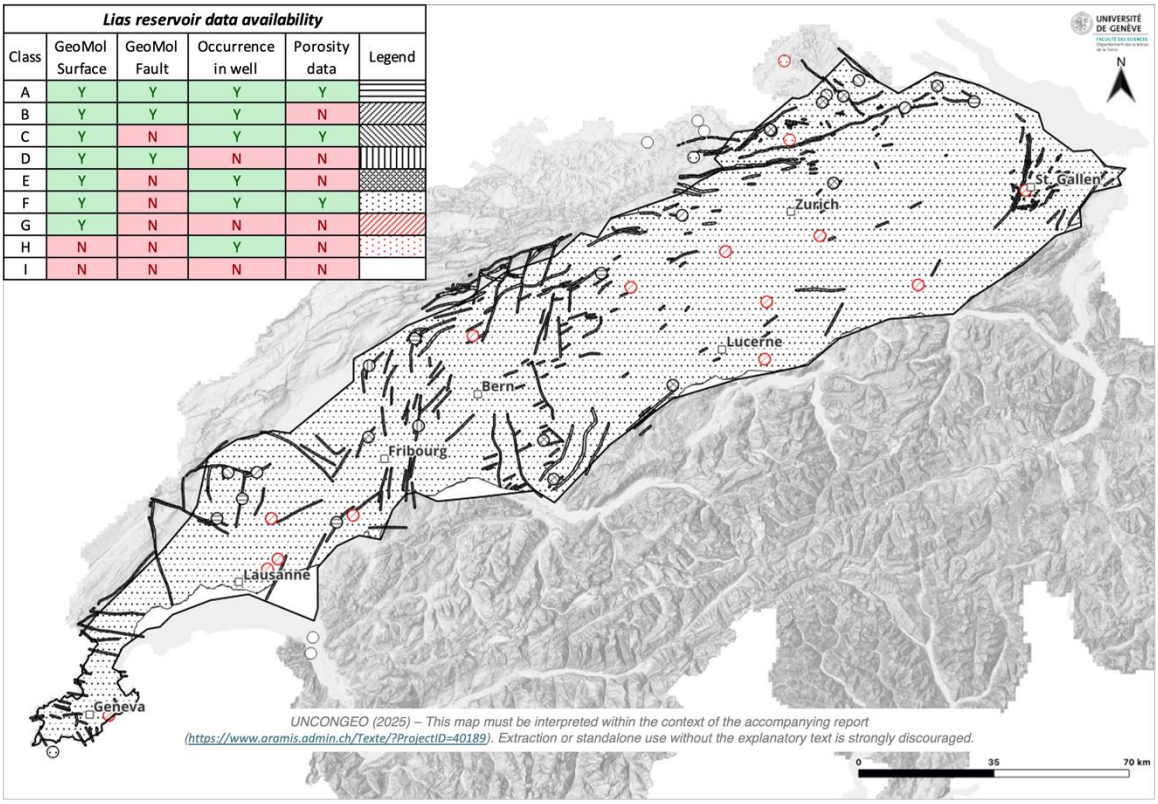


Fig. 134: Lias reservoir data availability.

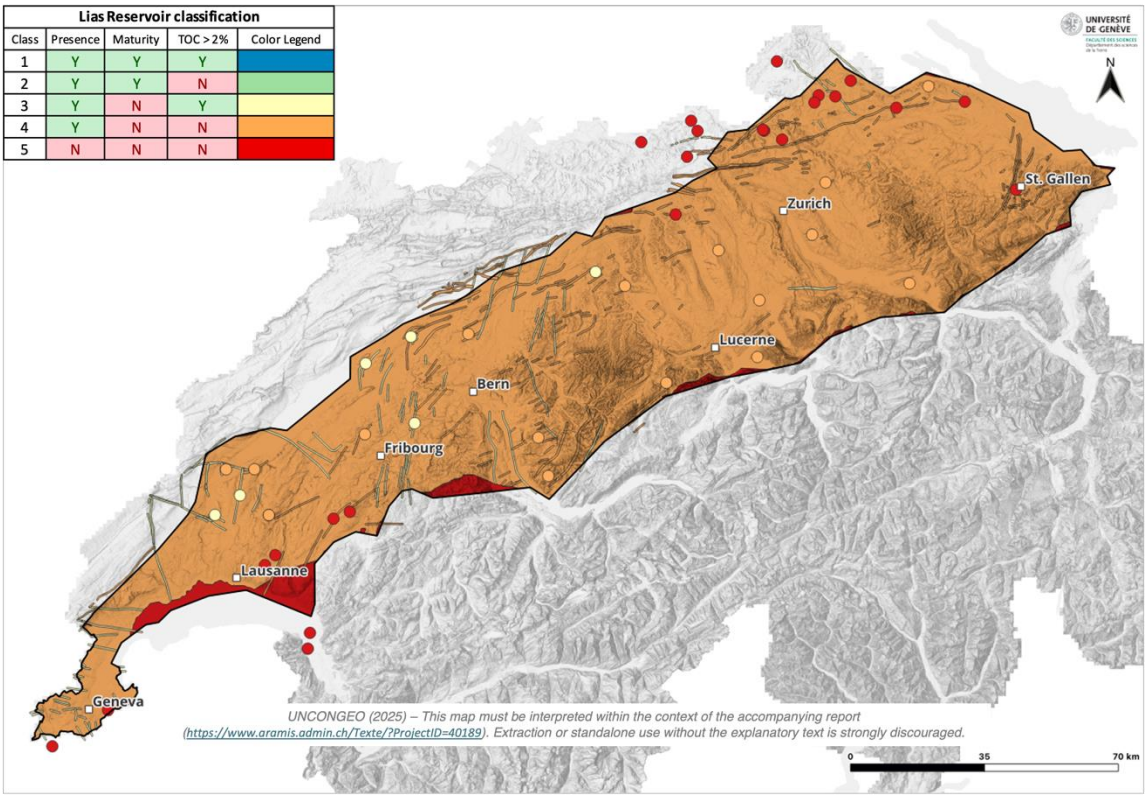


Fig. 135: Lias reservoir assessement and classification

The Lias seal (Lias and/or Dogger shaly units) data availability and assessment for the most relevant wells of the Plateau and the related classes assignment are listed in Table 66. In the Assessment, the Impermeable property is defined on the general facies of the Dogger and/or Lias units described in the well reports, expressed as a percentage of lithologies (Table 67). When lithological data are not available for a well, the Impermeable property is extrapolated from the lithological data of the closest wells. The resulting Data availability and Assessment maps for the Dogger seal (Lias and/or Dogger) are shown in Fig. 136 and Fig. 137.

Seal Lias and/or Dogger		**Data availability**					**Assessement**			
Well	Unit	GeoMol surface	GeoMol fault	Occurrence in a well	Lithologic data	Class	Presence	Integrity	Impermeable	Class
Altishofen-1	Not penetrated	Yes	No	No	No	G	Yes*	Yes	Yes*	1
Benken-1	Dogger	Yes	No	Yes	Yes	C	Yes	Yes	Yes	1
Berlingen-1	Lias and Dogger	Yes	No	Yes	Yes	C	Yes	Yes	Yes	1
Boswil-1	Not penetrated	Yes	No	No	No	G	Yes*	Yes	Yes*	1
Bottstein-1	Not penetrated	No	No	No	No	I	No	No	No	5
Bozberg-1	Lias and Dogger	No	No	Yes	Yes	F	Yes	Yes	Yes	1
Bulach-1	Lias and Dogger	Yes	No	Yes	Yes	C	Yes	Yes	Yes	1
Chapelle-1	Not penetrated	Yes	No	No	No	G	Yes*	Yes	Yes*	1
Chessel-1	Not present	No	No	No	No	I	No	No	No	5
Courtion-1	Lias	Yes	No	Yes	No	E	Yes	Yes	Yes*	1
Cuarny-1	Lias	Yes	Yes	Yes	No	B	Yes	No	Yes*	2
Eclepens-1	Lias	Yes	Yes	Yes	Yes	A	Yes	Yes	Yes	1
Entlebuch-1	Dogger	Yes	No	Yes	Yes	C	Yes	Yes	Yes	1
Essertines-1	Lias	Yes	Yes	Yes	Yes	A	Yes	Yes	Yes	1
Fendringen-1	Not penetrated	Yes	Yes	No	No	D	Yes*	No	Yes*	2
Herdern-1	Lias	Yes	Yes	Yes	Yes	A	Yes	No	Yes	2
Hermingen-1	Lias	Yes	Yes	Yes	Yes	A	Yes	No	Yes	2
Humilly-2	Lias	No	No	Yes	Yes	F	Yes	Yes	Yes	1
Hünenberg-1	Not penetrated	Yes	No	No	No	G	Yes*	Yes	Yes*	1
Kaisten-1	Not present	No	No	No	No	I	No	No	No	5
Kreuzlingen-1	Lias	Yes	Yes	Yes	Yes	A	Yes	No	Yes	2
Kusnacht-1	Not penetrated	Yes	No	No	No	G	Yes*	Yes	Yes*	1
Leuggern-1	Not present	No	No	No	No	I	No	No	No	5
Lindau-1	Lias and Dogger	Yes	Yes	Yes	Yes	A	Yes	No	Yes	2
Linden-1	Opalinus	Yes	No	Yes	Yes	C	Yes	Yes	No	3
Marthalen-1	Lias and Dogger	Yes	No	Yes	Yes	C	Yes	Yes	Yes	1
Noville-1	Dogger	No	No	Yes	No	H	No	No	No	5
Pfaffnau-1	Opalinus and Lias	Yes	Yes	Yes	Yes	A	Yes	No	Yes	2
Riniken-1	Lias	No	No	Yes	Yes	F	Yes	Yes	Yes	1
Romanens-1	Lias	Yes	Yes	Yes	Yes	A	Yes	No	Yes	2
Ruppoldsried-1	Not penetrated	Yes	No	No	No	G	Yes*	Yes	Yes*	1
Savigny-1	Not penetrated	Yes	No	No	No	G	Yes*	Yes	Yes*	1

Seal Lias and/or Dogger		Data availability					Assessement			
Well	Unit	GeoMol surface	GeoMol fault	Occurrence in a well	Lithologic data	Class	Presence	Integrity	Impermeable	Class
Schafisheim-1	Lias	Yes	Yes	Yes	Yes	A	Yes	No	Yes	2
Schlattingen-1	Lias and Dogger	Yes	No	Yes	Yes	C	Yes	Yes	Yes	1
Servion-1	Not penetrated	Yes	No	No	No	G	Yes*	Yes	Yes*	1
Siblingen-1	Lias	No	No	Yes	Yes	F	Yes	Yes	Yes	1
Sorens-1	Not penetrated	Yes	No	No	No	G	Yes*	Yes	Yes*	1
St Gallen-GT-1	Not penetrated	Yes	Yes	No	No	D	Yes*	No	Yes*	2
Thônex-1	Not penetrated	Yes	No	No	No	G	No	No	No	5
Thun-1	Opalinus and Lias	Yes	No	Yes	Yes	C	Yes	Yes	Yes	1
Treycovagnes-1	Lias	Yes	No	Yes	Yes	C	Yes	Yes	Yes	1
Truellikon-1	Lias and Dogger	Yes	No	Yes	Yes	C	Yes	Yes	Yes	1
Tschugg-1	Not penetrated	Yes	Yes	No	No	D	Yes*	Yes*	Yes*	1
Tuggen-1	Not penetrated	Yes	No	No	No	G	Yes*	Yes	Yes*	1
Weggis-1	Not penetrated	Yes	No	No	No	G	Yes*	Yes	Yes*	1
Weiach-1	Lias	Yes	No	Yes	Yes	C	Yes	Yes	Yes	1
Weiach-2	Lias	Yes	No	Yes	No	E	Yes	Yes	Yes*	1

Table 66: Data availability and assessment classes assigned at the Lias Play seal (Lias and/or Dogger units) in the most relevant wells of the Plateau. In the Unit column, it is indicated if the seal is most likely the Lias or the Dogger or both units, based on the facies description. In the **Data availability**, Lithologic data is "Yes" when lithologic data are available in this well, specifically for the Lias/Dogger units. In the **Assessment**, in the Presence property, "Yes*" means that in this well the Lias/Dogger has not been penetrated, thus its presence has been deduced from the closest wells where data are available and/or seismic (GeoMol). In the Impermeable property, (*) means that for this well, there are no lithological data to define the permeability; thus, Yes*/No* is assigned based on what is extrapolated from the closest wells where data are available.

Seal Lias shales and/or Dogger Opalinus clays

Well	Unit	Lithology
Altishofen-1	Not penetrated	
Benken-1	Dogger	80% shales; 15% limestones; 5% sandstones
Berlingen-1	Lias and Dogger	Lias: 60% shales; 20% limestones; 20% sandstones; Dogger: 70% marls; 20% limestones; 10% sandstones
Boswil-1	Not penetrated	
Bozberg-1	Lias and Dogger	80% Shales; 10% marls; 10% limestones
Bulach-1	Lias and Dogger	80% Shales; 10% marls; 10% limestones
Chapelle-1	Not penetrated	
Eclepens-1	Lias	50% marls 50% shales
Entlebuch-1	Dogger	70% shales; 30% limestones
Essertines-1	Lias	80% Shales 20% Limestones
Herdern-1	Lias	95% shales; 5% limestone
Hermingen-1	Lias	80% limestones; 20% black shales
Humilly-2	Lias	40% shales; 60% limestones
Hünenberg-1	Not penetrated	
Kreuzlingen-1	Lias	85% shales; 10% marl% 5% limestones

Seal Lias shales and/or Dogger Opalinus clays

Well	Unit	Lithology
Kusnacht-1	Not penetrated	
Lindau-1	Lias and Dogger	Lias: 30% limestones; 40% shales; 30% sandstones; Dogger:70% marls; 30% limestones
Linden-1	Opalinus	100% sandstones
Marthaleen-1	Lias and Dogger	60% shales; 40% marls
Noville-1	Dogger	40% marls; 20% limestones; 20% siltstones; 20% shales
Pfaffnau-1	Opalinus+Lias	100% marly limestones
Riniken-1	Lias	50% shale, 40% Marly-shale, 10 % Limestone
Romanens-1	Lias	100% shales
Ruppoldsried-1	Not penetrated	
Savigny-1	Not penetrated	
Schafisheim-1	Lias	94% Shales, 5% limestone, 1% marls
Schlattingen-1	Lias and Dogger	60% shales; 40% marls
Sibilingen-1	Lias	74% shales; 16% marls; 10% limestones
St Gallen-GT-1	Not penetrated	
Thun-1	Opalinus+Lias	100% shale
Treycovagnes-1	Lias	65% shales; 35% limestones
Truillikon-1	Lias and Dogger	60% shales; 40% marls
Tschugg-1	Not penetrated	
Tuggen-1	Not penetrated	
Weiach-1	Lias	60% marls; 30% shales; 10% limestones
Weggis-1	Not penetrated	

Table 67: General facies of the seal of the Lias Play in the main wells of the Plateau, represented by the Lias and/or Dogger units, define the permeability; thus, Yes*/No* is assigned based on what is extrapolated from the closest wells.

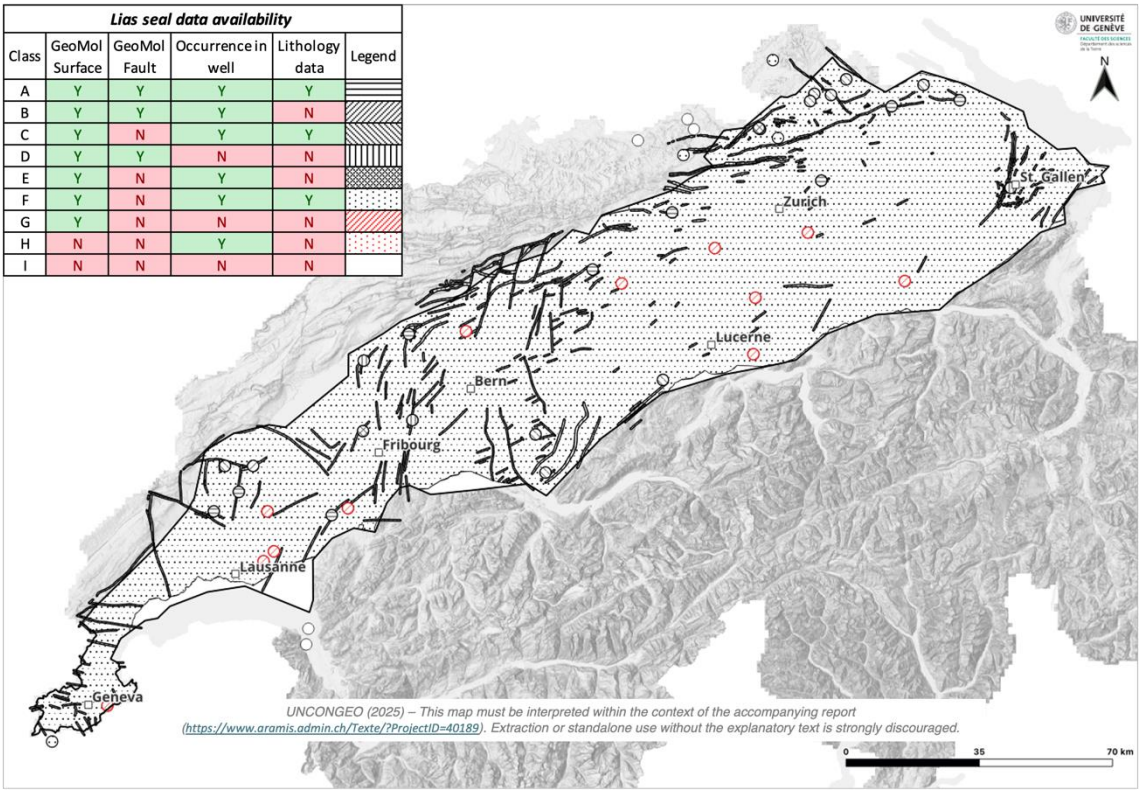


Fig. 136: Lias seal data availability.

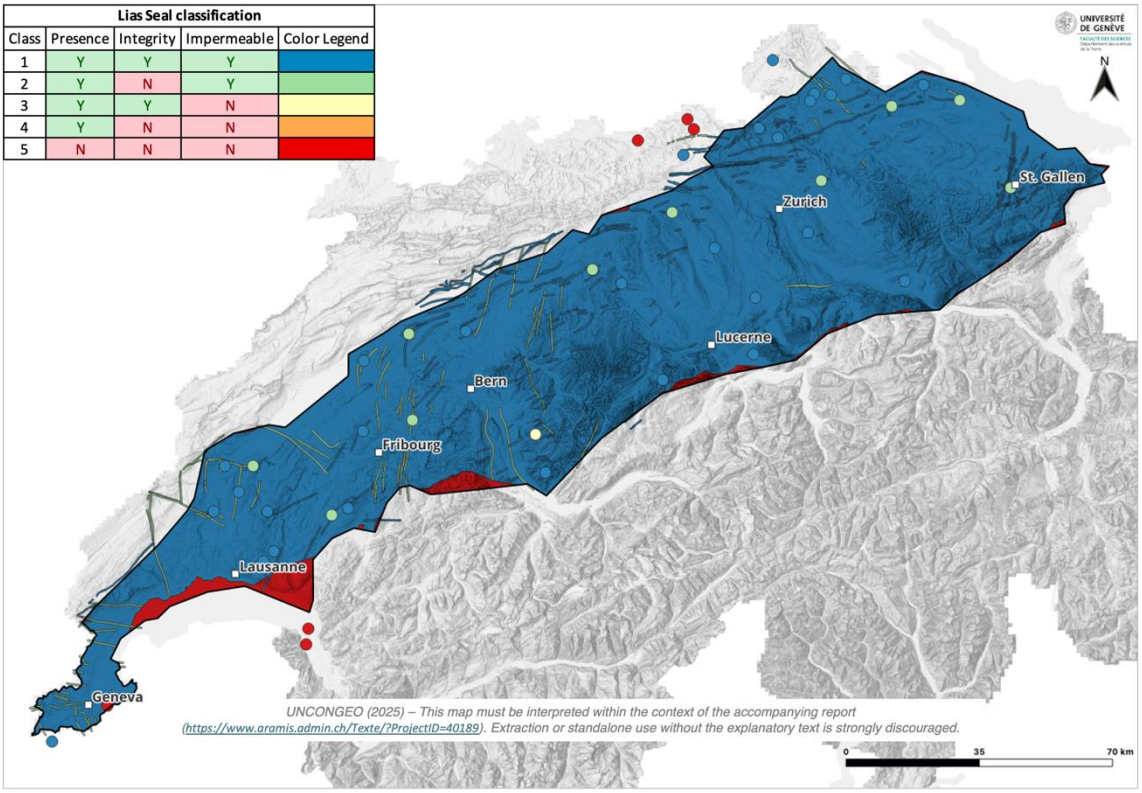


Fig. 137: Lias seal assessement and classification.

The CRS map for the Lias play is shown in Fig. 138. In the west-central part of the Plateau, an extended area displays medium risk, which increases to medium-high on top of the Permo-Carboniferous troughs. The south-eastern part of the Swiss Plateau exhibits low risk associated with a non-deposition of the Posidonia shale and overall poor reservoir properties. Make and exception the areas on the top of the Permo-Carboniferous trough, where the risk is medium. In the north-eastern sector the risk is medium to high, because of that both Posidonia shale and Permo-Carboniferous source rocks are present.

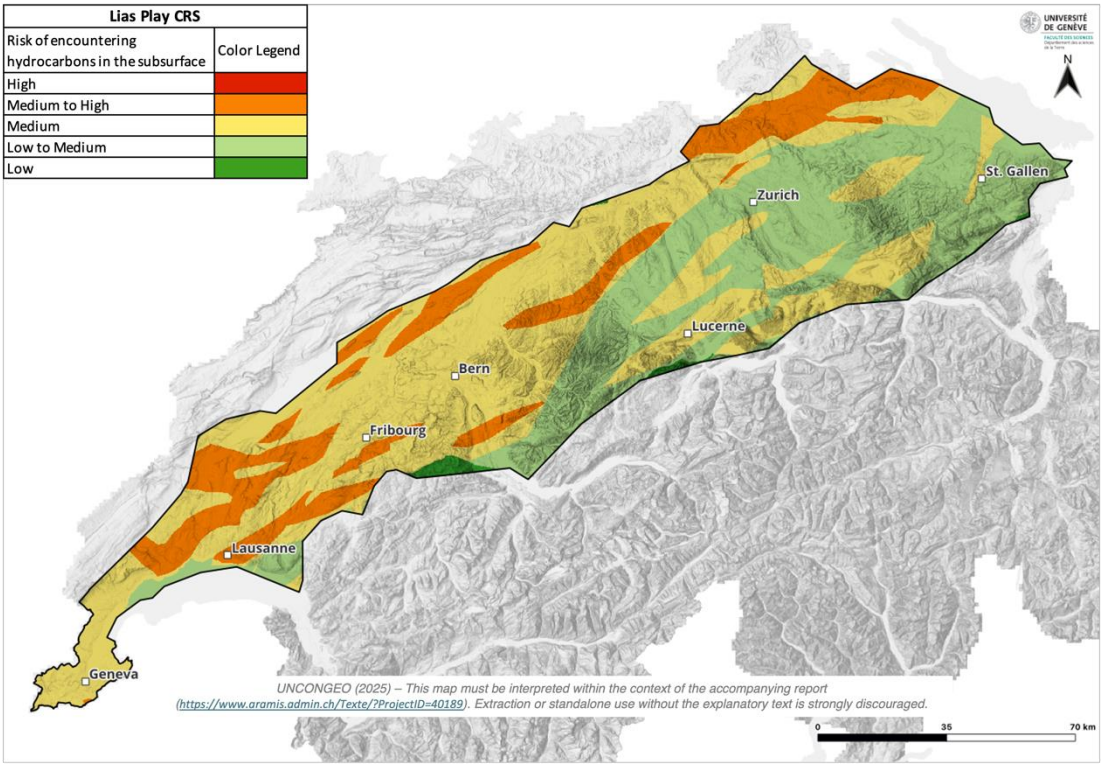


Fig. 138: CRS map for the Lias play.

3.6.6 Muschelkalk Play

The Muschelkalk play is present in the entire Plataeau. The source rock of this play is only the Permo-Carboniferous unit, which properties are defined in the 3.6.1 section. The reservoir is represented by the Trigonodus dolomite and the Melser sandstones deposits, composing the Muschelkalk unit (Middle Triassic in age), as well as the Buntsandstein sandstones (Early Triassic in age). The seal is represented by anhydrite and sault, alternated with shales and marls, composing the Middle Muschelkalk and Keuper units (middle to late Triassic in age).

The Reservoir data availability for the most relevant wells of the Plateau and the related classes assignement are listed in Table 68. Porosity data (Phi) are available for very few wells and in most of the cases the average is < 15% (Appendix 6). This is why in the Assessment, it is assigned “No” to the *Phi>15%* properties for most of the wells. In the Assessment, in the cases when the Muschelkalk unit has not been penetrated, its *Presence* is deduced from the closest wells. The resulting Data availability and Assessment maps for the Muschelkalk reservoir are shown in Fig. 139 and Fig. 140.

Reservoir Muschelkalk	Data availability					Assessement			
Well	GeoMol surface	GeoMol fault	Occurrence in well	Porosity data	Class	Presence	Phi>15%	Fractured	Class
Altishofen-1	Yes	No	No	No	G	Yes*	No*	No	4
Benken-1	Yes	No	Yes	Yes	C	Yes	No	No	4
Berlingen-1	Yes	No	Yes	No	E	Yes	No*	No	4
Boswil-1	Yes	No	No	No	G	Yes*	No*	No	4
Bottstein-1	No	No	Yes	Yes	F	Yes	No	No	4
Bozberg-1	No	No	Yes	Yes	F	Yes	Yes	No	2
Bulach-1	Yes	No	Yes	Yes	C	Yes	No	No	4
Chapelle-1	Yes	No	No	No	G	Yes*	No*	No	4
Chessel-1	No	No	No	No	I	Yes*	No*	No	4
Courtion-1	Yes	Yes	Yes	No	B	Yes	No*	No	4
Cuarny-1	Yes	No	No	No	G	Yes*	No*	No	4
Eclepens-1	Yes	No	No	No	G	Yes*	No*	No	4
Entlebuch-1	Yes	No	Yes	No	E	Yes	No*	No	4
Essertines-1	Yes	No	No	No	G	Yes*	No*	No	4
Fendringen-1	Yes	Yes	No	No	D	Yes*	No*	No	4
Herdern-1	Yes	Yes	Yes	No	B	Yes	No*	Yes	3
Hermingen-1	Yes	Yes	Yes	No	B	Yes	No*	Yes	3
Humilly-2	No	No	Yes	Yes	F	Yes	No	No	4
Hünenberg-1	Yes	No	No	No	G	Yes*	No*	No	4
Kaisten-1	No	No	Yes	No	H	Yes	No*	No	4
Kreuzlingen-1	Yes	Yes	Yes	Yes	A	Yes	No	Yes	3
Kusnacht-1	Yes	No	No	No	G	Yes*	No*	No	4
Leuggern-1	No	No	Yes	No	H	Yes	No*	No	4
Lindau-1	Yes	No	Yes	No	E	Yes	No*	No	4
Linden-1	Yes	No	No	No	G	Yes*	No*	No	4
Marthalen-1	Yes	No	Yes	Yes	C	Yes	Yes	No	2
Noville-1	No	No	Yes	No	H	Yes	No*	No	4
Pfaffnau-1	Yes	Yes	Yes	Yes	A	Yes	No	Yes	3
Riniken	No	No	Yes	Yes	F	Yes	No	No	4
Romanens-1	Yes	Yes	No	No	D	Yes*	No*	Yes	3
Ruppoldsried-1	Yes	No	No	No	G	Yes*	No*	No	4
Savigny-1	Yes	No	No	No	G	Yes*	No*	No	4
Schafisheim	Yes	Yes	Yes	Yes	A	Yes	No	Yes	3
Schlattingen	Yes	No	Yes	No	E	Yes	No*	No	4
Servion-1	Yes	No	No	No	G	Yes*	No*	No	4
Siblingen-1	No	No	Yes	No	H	Yes	No*	No	4
Sorens-1	Yes	No	No	No	G	Yes*	No*	No	4
St Gallen-GT-1	Yes	No	No	No	G	Yes*	No*	No	4
Thônex-1	Yes	No	No	No	G	Yes*	No*	No	4
Thun-1	Yes	No	No	No	G	Yes*	No*	No	4
Treycovagnes-1	No	No	Yes	Yes	F	Yes	No	No	4
Truellikon-1	Yes	No	Yes	No	E	Yes	No*	No	4
Tschugg-1	Yes	Yes	No	No	D	Yes*	No*	No	4
Tuggen-1	Yes	No	No	No	G	Yes*	No*	No	4

Reservoir Muschelkalk	Data availability					Assessement			
Well	GeoMol surface	GeoMol fault	Occurrence in well	Porosity data	Class	Presence	Phi>15%	Fractured	Class
Weggis-1	Yes	No	No	No	G	Yes*	No*	No	4
Weiach-1	Yes	No	Yes	Yes	C	Yes	No	No	4
Weiach-2	Yes	No	Yes	No	E	Yes*	No*	No	4

Table 68: Data availability and assessment classes assigned at the Muschelkalk Play reservoir (Muschelkalk unit) in the most relevant wells of the Plateau. In the **Data availability**, Porosity is "Yes" when porosity data are available in this well specifically for the Muschelkalk and Buntsandstain units. In the **Assessment**, (*) means that for this well there are not data to define this property, thus Yes*/No* is deduced extrapolating what it has been defined in the closest wells where data are available. Specifically, Presence "Yes*" means that in this well the Muschelkalk unit has not been penetrated, thus its presence has been deduced from the closest wells where data are available and/or seismic interpolation (GeoMol). Similarly for the Phi >15%, "No*" means that porosity data are not available for the Muschelkalk unit in this well, thus it has been deduced from the closest wells where data are available.

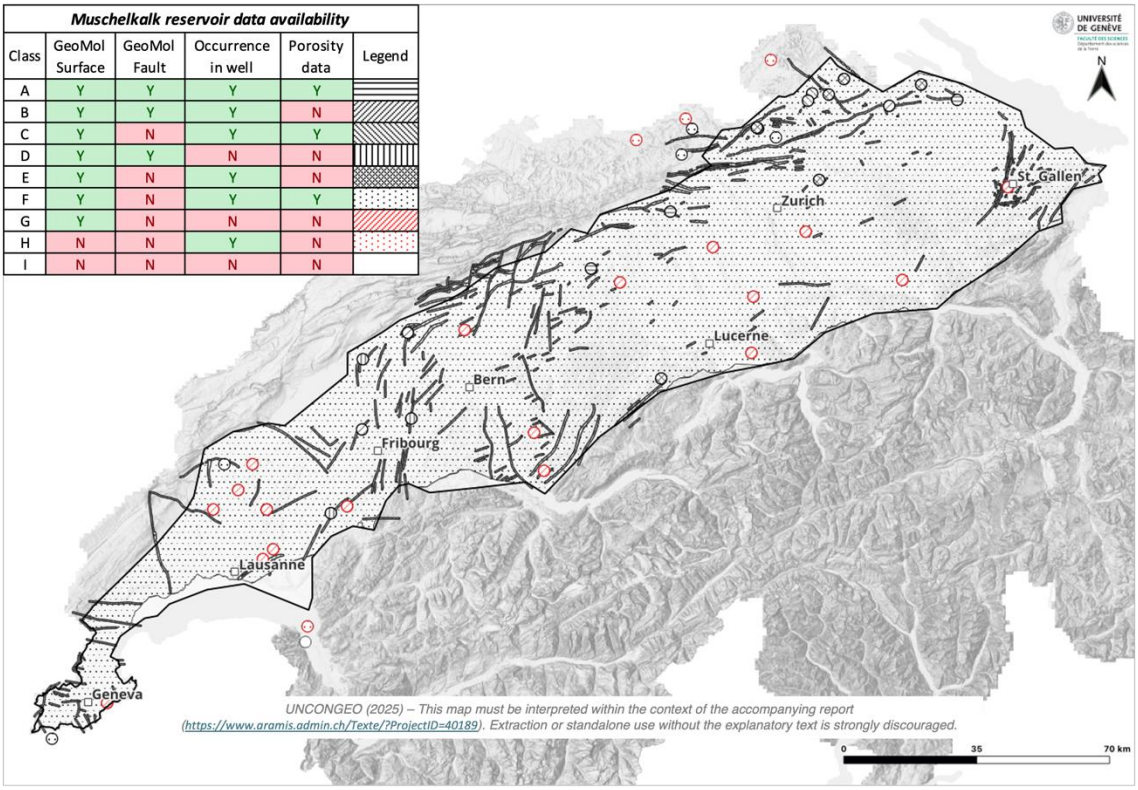


Fig. 139: Trigonodus dolomite and the Melser sandstones deposits (Muschelkalk unit) reservoir data availability.

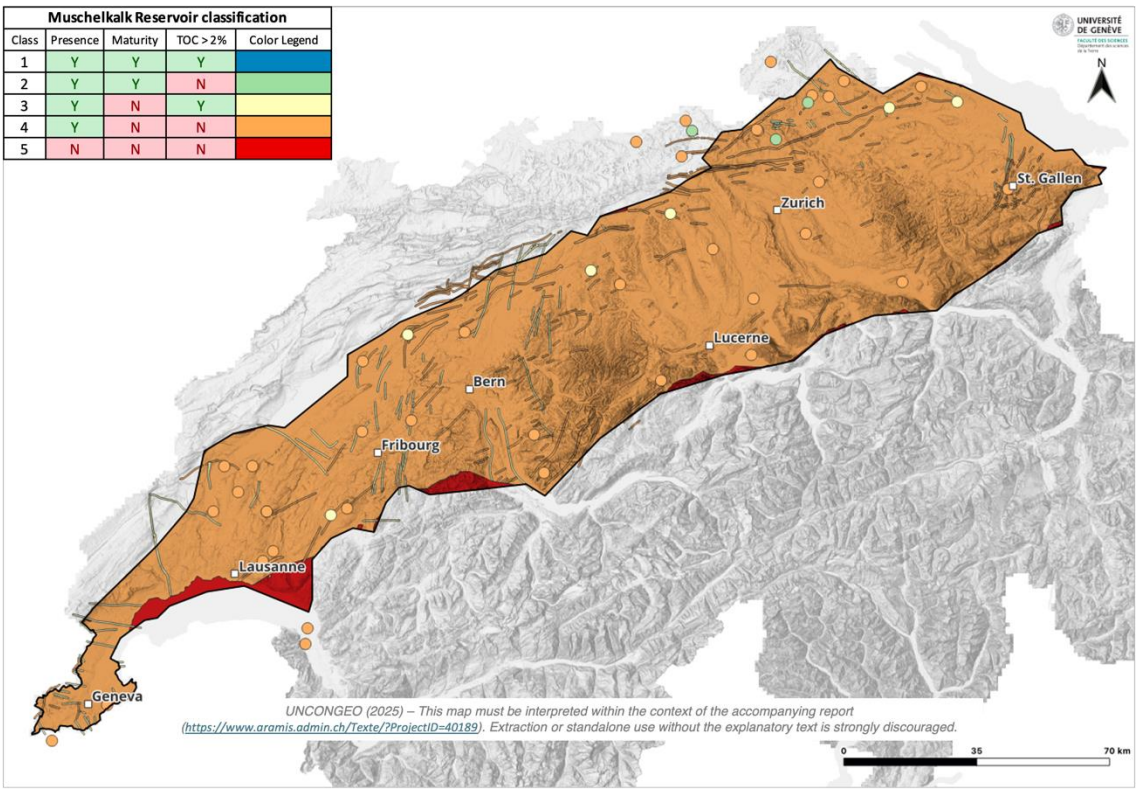


Fig. 140: Trigonodus dolomite and the Melser sandstones deposits (Muschelkalk unit) reservoir assessement and classification.

The Muschelkalk seal (Keuper unit) data availability and assessment for the most relevant wells of the Plateau and the related classes assignment are listed in Table 69. In the Assessment, the *Impermeable* property is defined on the general facies of the Keuper unit described in the well report, expressed as a percentage of lithologies (Table 70). When lithological data are not available for a well, the *Impermeable* property is extrapolated from the lithological data of the closest wells. The resulting Data availability and Assessment maps for the Muschelkalk seal (Keuper unit) are shown in Fig. 141 and Fig. 142.

Seal Keuper	**Data availability**					**Assessement**			
Well	GeoMol surface	GeoMol fault	Occurrence in a well	Lithologic data	Class	Presence	Integrity	Impermeable	Class
Altishofen-1	Yes	No	No	No	G	Yes*	Yes	Yes*	1
Benken-1	Yes	No	Yes	Yes	C	Yes	Yes	Yes	1
Berlingen-1	Yes	No	Yes	Yes	C	Yes	Yes	Yes	1
Boswil-1	Yes	No	No	No	G	Yes*	Yes	Yes*	1
Bottstein-1	No	No	Yes	Yes	F	Yes	Yes	No	3
Bozberg-1	No	No	Yes	Yes	F	Yes	Yes	Yes	1
Bulach-1	Yes	No	Yes	Yes	C	Yes	Yes	Yes	1
Chapelle-1	Yes	No	No	No	G	Yes*	Yes	Yes*	1
Chessel-1	No	No	Yes	No	H	Yes	Yes	Yes*	1
Courtion-1	Yes	Yes	Yes	No	B	Yes	No	Yes*	2
Cuarny-1	Yes	No	No	No	G	Yes*	Yes	Yes*	1
Eclepens-1	Yes	Yes	Yes	Yes	A	Yes	Yes	Yes	1
Entlebuch-1	Yes	No	Yes	Yes	C	Yes	Yes	Yes	1
Essertines-1	Yes	Yes	Yes	Yes	A	Yes	Yes	Yes	1
Fendringen-1	Yes	Yes	No	No	D	Yes*	Yes	Yes*	1
Herdern-1	Yes	Yes	Yes	Yes	A	Yes	No	Yes	2
Hermingen-1	Yes	Yes	Yes	Yes	A	Yes	No	Yes	2
Humilly-2	No	No	Yes	Yes	F	Yes	Yes	Yes	1
Hünenberg-1	Yes	No	No	No	G	Yes*	Yes	Yes*	1
Kaisten-1	No	No	No	No	I	No	No	No	5
Kreuzlingen-1	Yes	Yes	Yes	Yes	A	Yes	No	Yes	2
Kusnacht-1	Yes	No	No	No	G	Yes*	Yes	Yes*	1
Leuggern-1	No	No	No	No	I	No	No	No	5
Lindau-1	Yes	No	Yes	Yes	C	Yes	Yes	Yes	1
Linden-1	Yes	No	Yes	Yes	C	Yes	Yes	Yes	1
Marthalen-1	Yes	No	Yes	Yes	C	Yes	Yes	Yes	1
Noville-1	No	No	No	No	I	No	No	No	5
Pfaffnau-1	Yes	Yes	Yes	Yes	A	Yes	No	Yes	2
Riniken	No	No	Yes	Yes	F	Yes	Yes	Yes	1
Romanens-1	Yes	Yes	Yes	Yes	A	Yes	No	Yes	2
Ruppoldsried-1	Yes	No	No	No	G	Yes*	Yes	Yes*	1
Savigny-1	Yes	No	No	No	G	Yes*	Yes	Yes*	1
Schafisheim	Yes	Yes	Yes	Yes	A	Yes	No	Yes	2
Schlattingen	Yes	No	Yes	No	E	Yes	Yes	Yes*	1
Servion-1	Yes	No	No	No	G	Yes*	Yes	Yes*	1
Siblingen-1	No	No	Yes	Yes	F	Yes	Yes	No	3
Sorens-1	Yes	No	No	No	G	Yes*	Yes	Yes*	1

Seal Keuper	Data availability					Assessement			
Well	GeoMol surface	GeoMol fault	Occurrence in a well	Lithologic data	Class	Presence	Integrity	Impermeable	Class
St Gallen-GT-1	Yes	Yes	No	No	D	Yes*	No	Yes*	2
Thônex-1	Yes	No	No	No	G	Yes*	Yes	Yes*	1
Thun-1	Yes	Yes	No	No	D	Yes*	No	Yes*	2
Treycovagnes-1	No	No	Yes	Yes	F	Yes	Yes	Yes	1
Truellikon-1	Yes	No	Yes	Yes	C	Yes	Yes	Yes	1
Tschugg-1	Yes	Yes	No	No	D	Yes*	Yes	Yes*	1
Tuggen-1	Yes	No	No	No	G	Yes*	Yes	Yes*	1
Weggis-1	Yes	No	No	No	G	Yes*	Yes	Yes*	1
Weiach-1	Yes	No	Yes	Yes	C	Yes	Yes	Yes	1
Weiach-2	Yes	No	Yes	No	E	Yes*	Yes	Yes*	1

Table 69: Data availability and assessment classes assigned at the Muschelkalk Play seal (Keuper unit) in the most relevant wells of the Plateau. In the **Data availability**, Lithologic data is "Yes" when lithologic data are available in this well, specifically for the Keuper unit. In the **Assessment**, in the Presence property, "Yes*" means that in this well the Keuper has not been penetrated, thus its presence has been deduced from the closest wells where data are available and/or seismic (GeoMol). In the Impermeable property, (*) means that for this well, there are no lithological data to define the permeability; thus, Yes*/No* is assigned based on what is extrapolated from the closest wells where data are available.

Seal	Keuper/Gypskeuper
Well	**Lithology**
Benken-1	20% anhydrite; 50% shales; 30% marls
Berlingen-1	20% shales; 30% marls; 30% anhydrite; 20% dolomite
Boswil-1	Not penetrated
Bottstein-1	Very thin
Bozberg-1	Anhydrite
Bulach-1	Anhydrite
Chapelle-1	Not penetrated
Eclepens-1	50% marls 30% shales 20% dolomie
Entlebuch-1	45% anhydrit; 40% dolomite; 10% shales; 5% sandstones
Essertines-1	30% Shales; 30% Anhydrites; 40% Salt
Herdern-1	40% shales; 30% sandstones; 30% dolomite
Hermingen-1	78% anhydrite; 20% shales; 2% halite
Hünenberg-1	Not penetrated
Kaisten-1	Eroded
Kreuzlingen-1	50% dolomite; 10% sanstone; 10% marls; 30% shales
Kusnacht-1	Not penetrated
Leuggern-1	Very thin
Lindau-1	50% anhydrite; 20% shales; 30% marls
Linden-1	70% anhydrite; 20% shales; 5% dolomestones; 5% halite
Marthaleen-1	Anhydrite
Noville-1	50% limestones; 40% dolomite; 10% marls
Pfaffnau-1	10% dolomestones; 40% marls; 50% anydrite
Riniken-1	40% shales; 40% limestones; 20% evaporite
Romanens-1	40% anhydrite; 60% shales

Seal	Keuper/Gypskeuper
Well	**Lithology**
Ruppoldsried-1	Not penetrated
Savigny-1	Not penetrated
Schafisheim-1	50% limestones; 35% shales; evaporite
Schlattingen-1	Not found
Sibilingen-1	Very thin
St Gallen-GT-1	Not penetrated
Thun-1	Not penetrated
Treycovagnes-1	40% salt; 30% shales; 30% anhydrite
Truillikon-1	Anhydrite
Tuggen-1	Not penetrated
Tschugg-1	Not penetrated
Weggis-1	Not penetrated
Weiach-1	30% Anhydrite; 20% dolomite; 30% mergel; 20% shales

Table 70: General facies of the seal of the Muschelkalk Play in the main wells of the Plateau, represented by the Keuper and Gypskeuper units.

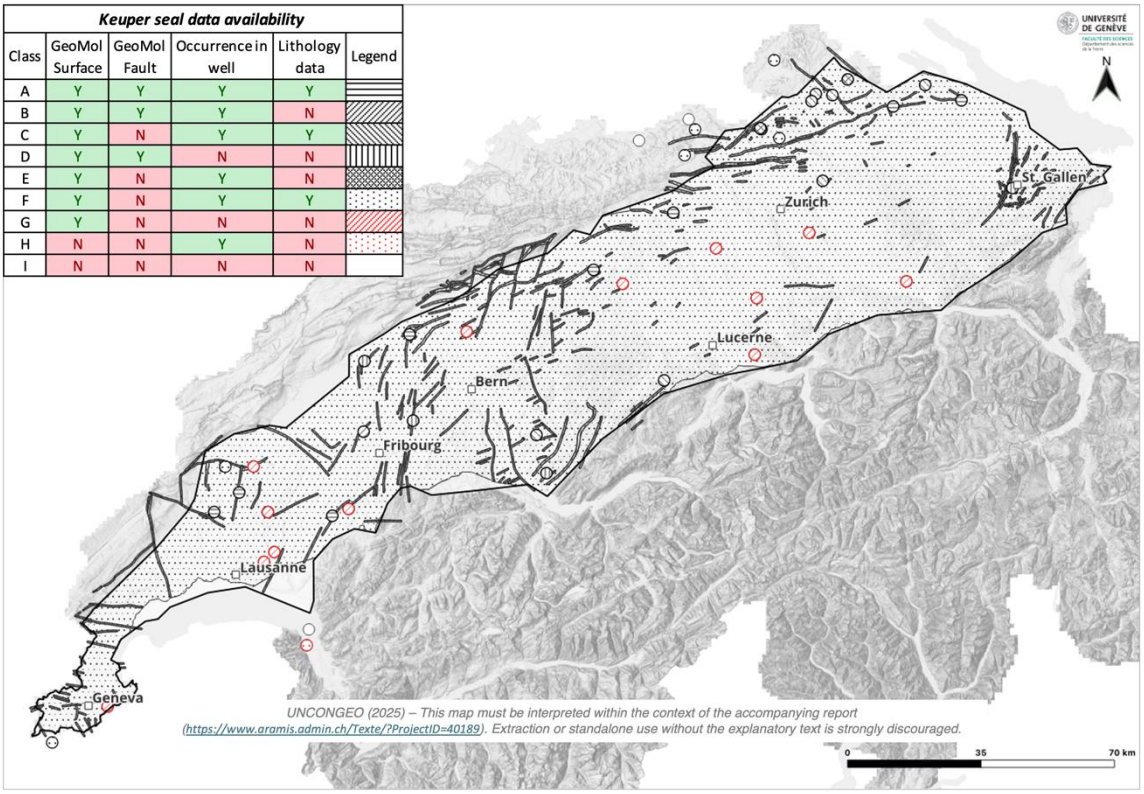


Fig. 141: Muschelkalk seal (Keuper unit) data availability.

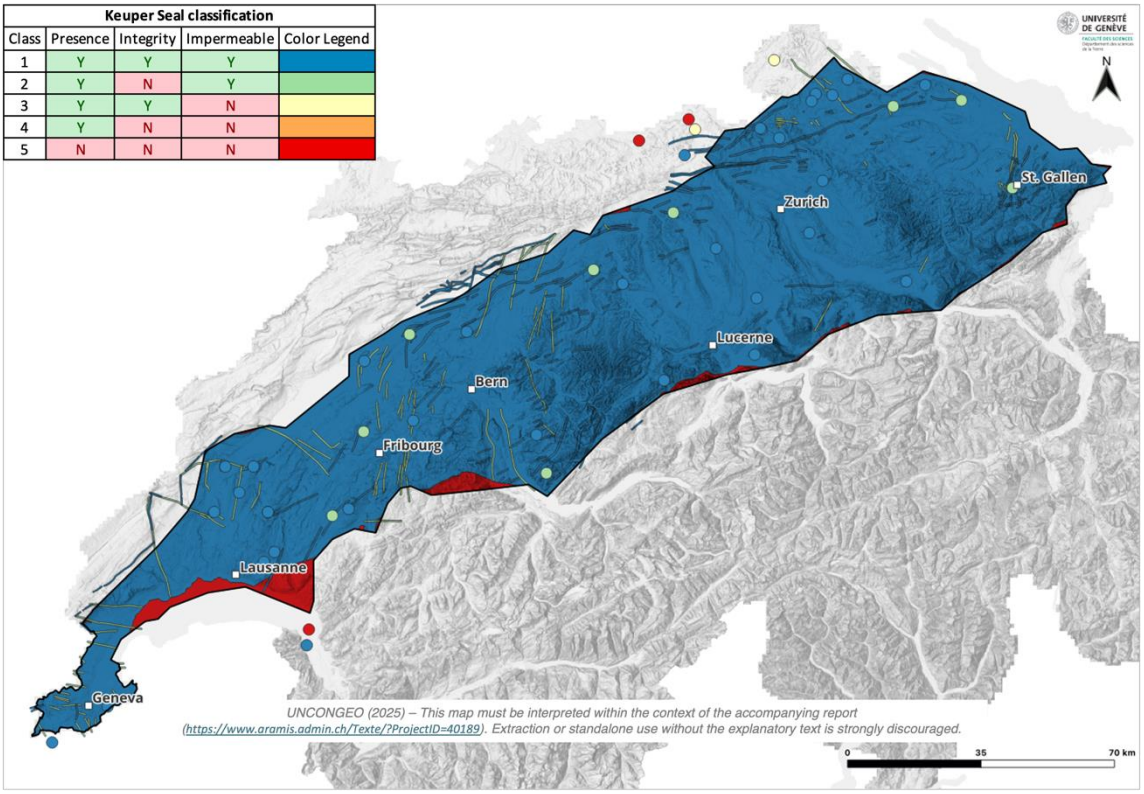


Fig. 142:Muschelkalk seal (Keuper unit) assessement and classification.

The CRS map for the Muschelkalk play is shown in Fig. 143. The Muschelkalk play exhibits low to medium risk throughout the entire Swiss Plateau. Medium to high risk areas are located on the top of the Permo-Carboniferous troughs and in the proximity of certain faults where the risk is medium to medium-high.

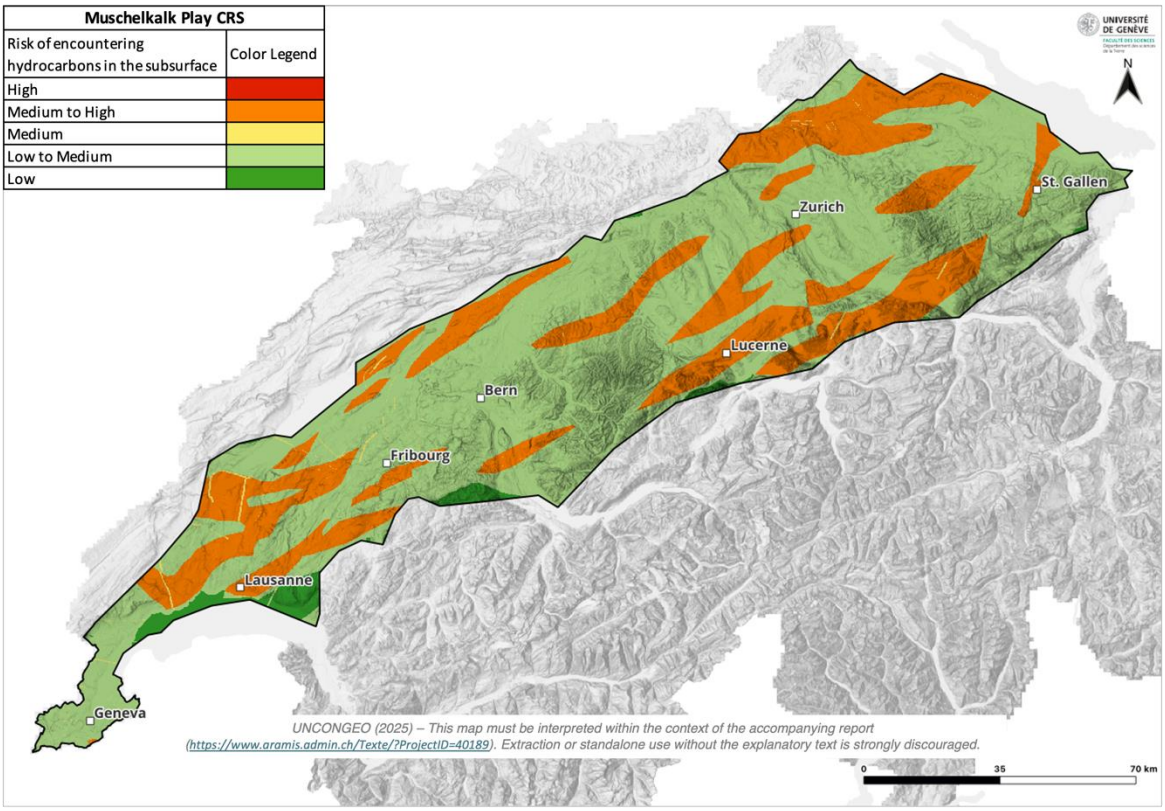


Fig. 143: CRS map for the Muschelkalk play.

3.6.7 Permo-Carboniferous Play

The Permo-Carboniferous play is present only in the areas where Permo-Carboniferous troughs are present. The source rock of this play is only the Permo-Carboniferous unit, which properties are defined in section 3.6.1. The reservoir is represented by the Permian and Carboniferous units, composed by sandstones and the seal is represented by anhydrite and shales composing the Mushelkalk and Keuper units, middle to late Triassic in age.

The Reservoir data availability for the most relevant wells of the Plateau and the related classes assignment are listed in Table 71. Porosity data (Phi) are available for very few wells, and in most of the cases it is < 15% (Appendix 6). This is why in the Assessment, *Phi>15%* is assigned “No” at all the wells. When the Permian and Carboniferous units have not been penetrated, their *Presence* is deduced from the closest wells, and/or seismic data. The resulting Data availability and Assessment maps for the Permo-Carboniferous reservoir are shown in Fig. 144 and Fig. 145.

Reservoir P-C	Data availability					Assessement			
Well	GeoMol surface	GeoMol fault	Occurrence in a well	Porosity data	Class	Presence	Phi>15 %	Fractured	Class
Altishofen-1	Yes	No	No	No	G	No	No*	No	5
Benken-1	No	No	No	No	I	No	No*	No	5
Berlingen-1	Yes	No	No	No	G	Yes*	No*	No	4
Boswil-1	No	No	No	No	I	No	No*	No	5
Bottstein-1	No	No	No	No	I	No	No*	No	5
Bozberg-1	No	No	Yes	Yes	F	Yes	No	No	4
Bulach-1	Yes	No	Yes	Yes	C	Yes	No	No	4
Chapelle-1	No	No	No	No	I	Yes*	No*	No	4
Chessel-1	No	No	No	No	I	Yes*	No*	No	4
Courtion-1	No	No	No	No	I	No	No*	No	5
Cuarny-1	No	No	No	No	I	Yes*	No*	No	4
Eclepens-1	No	No	No	No	I	No	No*	No	5
Entlebuch-1	Yes	No	Yes	No	E	Yes	No*	No	4
Essertines-1	Yes	No	No	No	G	Yes*	No*	No	4
Fendringen-1	No	No	No	No	I	No	No*	No	5
Herdern-1	No	No	No	No	I	No	No*	No	5
Hermingen-1	No	No	No	No	I	No	No*	No	5
Humilly-2	No	No	Yes	Yes	F	Yes	No	No	4
Hünenberg-1	No	No	No	No	I	Yes*	No*	No	4
Kaisten-1	No	No	Yes	No	H	Yes	No*	No	4
Kreuzlingen-1	No	No	Yes	No	H	Yes	No*	No	4
Kusnacht-1	No	No	No	No	I	No	No*	No	5
Leuggern-1	No	No	No	No	I	No	No*	No	5
Lindau-1	No	No	No	No	I	No	No*	No	5
Linden-1	Yes	No	No	No	G	Yes*	No*	No	4
Marthalen-1	Yes	No	Yes	Yes	C	Yes	No	No	4
Noville-1	No	No	Yes	No	H	Yes	No*	No	4
Pfaffnau-1	No	No	Yes	No	H	Yes	No*	No	4
Riniken-1	No	No	Yes	Yes	F	Yes	No	No	4
Romanens-1	Yes	No	No	No	G	Yes*	No*	No	4
Ruppoldsried-1	No	No	No	No	I	No	No*	No	5
Savigny-1	Yes	No	No	No	G	Yes*	No*	No	4
Servion-1	Yes	No	No	No	G	Yes*	No*	No	4
Schafisheim-1	No	No	No	No	I	No	No*	No	5
Schlattingen-1	Yes	No	Yes	No	E	Yes	No*	No	4
Siblingen	No	No	No	No	I	No	No*	No	5
Sorens-1	Yes	No	No	No	G	Yes*	No*	No	4
St Gallen-GT-1	No	No	No	No	I	Yes*	No*	No	4
Thônex-1	No	No	No	No	I	No	No*	No	5
Thun-1	No	No	No	No	I	No	No*	No	5
Treycovagnes-1	Yes	No	Yes	Yes	C	Yes	No	No	4
Truellikon-1	Yes	No	Yes	Yes	C	Yes	No	No	4
Tschugg-1	Yes	No	No	No	G	Yes*	No*	No	4
Tuggen-1	Yes	No	No	No	G	Yes*	No*	No	4

Reservoir P-C	Data availability					Assessement			
Well	GeoMol surface	GeoMol fault	Occurrence in a well	Porosity data	Class	Presence	Phi>15 %	Fractured	Class
Weggis-1	Yes	No	No	No	G	Yes*	No*	No	4
Weiach-1	Yes	No	Yes	Yes	C	Yes	No	No	4
Weiach-2	Yes	No	Yes	No	E	Yes*	No*	No	4

Table 71: Data availability and assessment classes assigned at the Permo-Carboniferous Play reservoir (Permian and Carboniferous units) in the most relevant wells of the Plateau. In the **Data availability**, Porosity is "Yes" when porosity data are available in this well specifically for the Permian and Carboniferous units. In the **Assessment**, (*) means that for this well there are no data to define this property; thus, Yes*/No* is deduced by extrapolating what has been defined in the closest wells where data are available. Specifically, Presence "Yes*" means that in this well, the Permian and Carboniferous units have not been penetrated, thus their presence has been deduced from the closest wells where data are available and/or seismic. Similarly, for the Phi >15%, "No*" means that porosity data are not available for the Permian and Carboniferous units in this well; thus, it has been deduced from the closest wells where data are available.

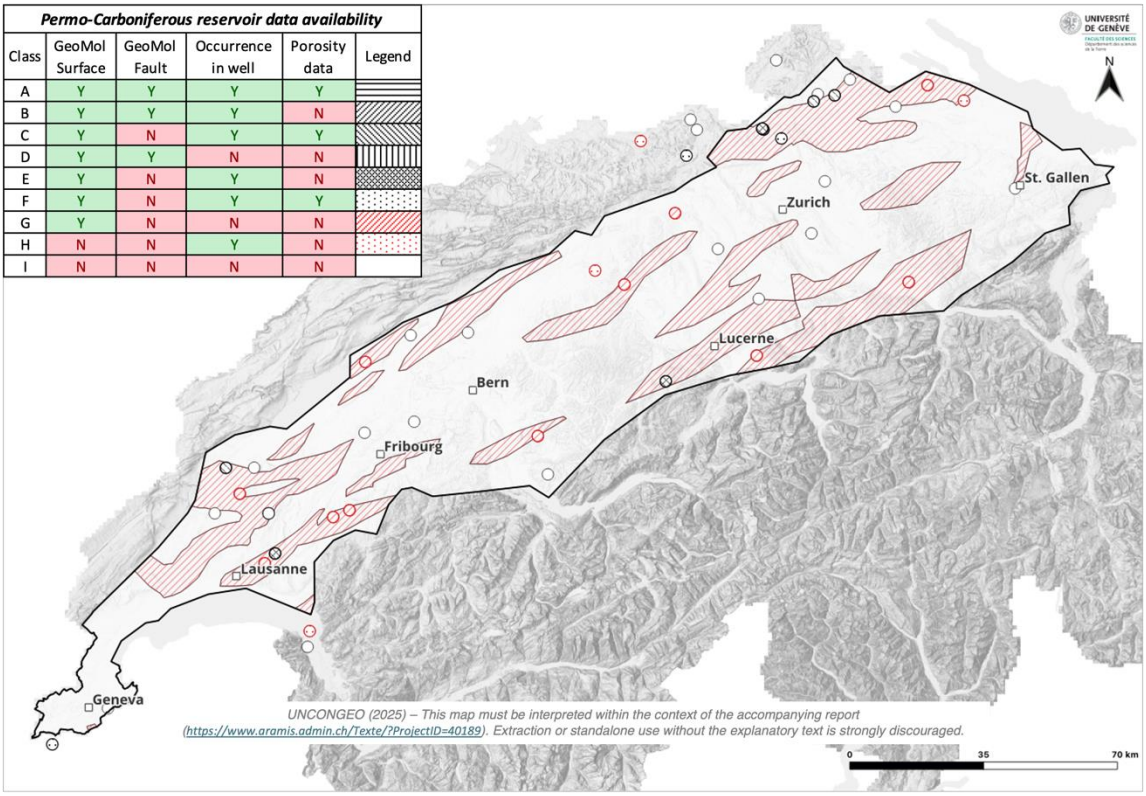


Fig. 144: Permo-Carboniferous reservoir data availability.

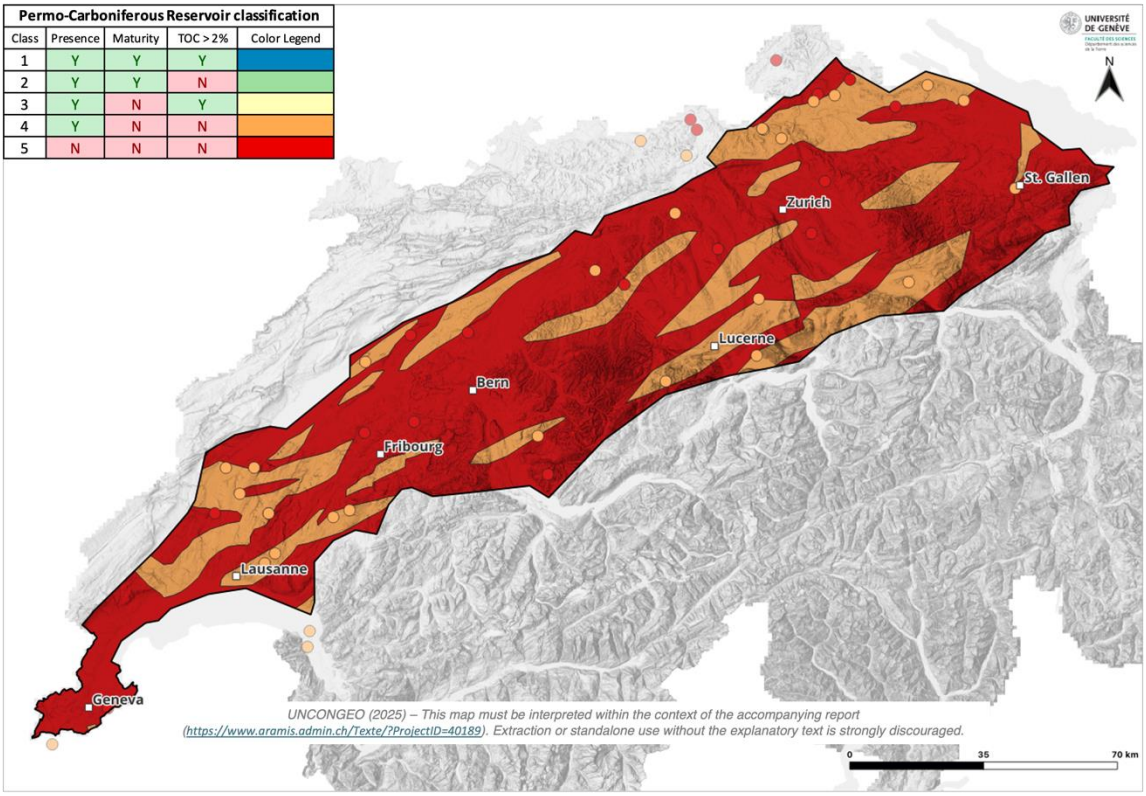


Fig. 145: Permo-Carboniferous reservoir assessement and classification

The Permo-Carboniferous seal (Muschelkalk unit) data availability and assessment for the most relevant wells of the Plateau and the related classes assignment are listed in Table 72. In the Assessment, the *Impermeable* property is defined on the general facies of the lower and middle Muschelkalk unit described in the well reports, expressed as a percentage of lithologies (Table 73). When lithological data are not available for a well, the *Impermeable* property is extrapolated from the lithological data of the closest wells. The resulting Data availability and Assessment maps for the Permo-Carboniferous seal (Muschelkalk unit) are shown in Fig. 146 and Fig. 147.

Seal Lower and Middle Muschelkalk	**Data availability**					**Assessement**			
Well	GeoMol surface	GeoMol fault	Occurrence in a well	Lithologic data	Class	Presence	Integrity	Imperm eable	Class
Altishofen-1	Yes	No	No	No	G	Yes*	Yes	Yes*	1
Benken-1	Yes	No	Yes	Yes	C	Yes	Yes	Yes	1
Berlingen-1	Yes	No	Yes	Yes	C	Yes	Yes	Yes	1
Boswil-1	Yes	No	No	No	G	Yes*	Yes	Yes*	1
Bottstein-1	No	No	Yes	Yes	F	Yes	Yes	Yes	1
Bozberg-1	No	No	Yes	Yes	F	Yes	Yes	Yes	1
Bulach-1	Yes	No	Yes	Yes	C	Yes	Yes	Yes	1
Chapelle-1	Yes	No	No	No	G	Yes*	Yes	Yes*	1
Chessel-1	No	No	No	No	I	Yes*	Yes	Yes*	1
Courtion-1	Yes	Yes	Yes	No	B	Yes	No	Yes*	2
Cuarny-1	Yes	No	No	No	G	Yes*	Yes	Yes*	1
Eclepens-1	Yes	No	No	No	G	Yes*	Yes	Yes*	1
Entlebuch-1	Yes	No	Yes	Yes	C	Yes	Yes	Yes	1
Essertines-1	Yes	No	No	No	G	Yes*	Yes	Yes*	1
Fendringen-1	Yes	Yes	No	No	D	Yes*	Yes	Yes*	1
Herdern-1	Yes	Yes	Yes	Yes	A	Yes	No	Yes	2
Hermingen-1	Yes	Yes	Yes	Yes	A	Yes	No	Yes	2
Humilly-2	No	No	Yes	Yes	F	Yes	Yes	Yes	1
Hünenberg-1	Yes	No	No	No	G	Yes*	Yes	Yes*	1
Kaisten-1	No	No	Yes	Yes	F	Yes	Yes	No	3
Kreuzlingen-1	Yes	Yes	Yes	Yes	A	Yes	No	Yes	2
Kusnacht-1	Yes	No	No	No	G	Yes*	Yes	Yes*	1
Leuggern-1	No	No	Yes	Yes	F	Yes	Yes	Yes	1
Lindau-1	Yes	No	Yes	Yes	C	Yes	Yes	Yes	1
Linden-1	Yes	No	No	Yes		Yes*	Yes	Yes*	1
Marthalen-1	Yes	No	Yes	Yes	C	Yes	Yes	Yes	1
Noville-1	No	No	Yes	Yes	F	Yes	Yes	Yes	1
Pfaffnau-1	Yes	Yes	Yes	Yes	A	Yes	No	Yes	2
Riniken-1	No	No	Yes	Yes	F	Yes	Yes	Yes	1
Romanens-1	Yes	Yes	No	No	D	Yes*	No	Yes*	2
Ruppoldsried-1	Yes	No	No	No	G	Yes*	Yes	Yes*	1
Savigny-1	Yes	No	No	No	G	Yes*	Yes	Yes*	1
Schafisheim-1	Yes	Yes	Yes	Yes	A	Yes	No	Yes	2
Schlattingen-1	Yes	No	Yes	Yes	C	Yes	Yes	Yes*	1
Servion-1	Yes	No	No	No	G	Yes*	Yes	Yes*	1
Siblingen-1	No	No	Yes	Yes	F	Yes	Yes	Yes*	1

Seal Lower and Middle Muschelkalk	Data availability					Assessement			
Well	GeoMol surface	GeoMol fault	Occurrence in a well	Lithologic data	Class	Presence	Integrity	Imperm eable	Class
Sorens-1	Yes	No	No	No	G	Yes*	Yes	Yes*	1
St Gallen-GT-1	Yes	No	No	No	G	Yes*	Yes	Yes*	1
Thônex-1	Yes	No	No	No	G	Yes*	Yes	Yes*	1
Thun-1	Yes	Yes	No	No	D	Yes*	No	Yes*	2
Treycovagnes-1	No	No	Yes	Yes	F	Yes	Yes	Yes	1
Truellikon-1	Yes	No	Yes	Yes	C	Yes	Yes	Yes	1
Tschugg-1	Yes	Yes	No	No	D	Yes*	Yes	Yes*	1
Tuggen-1	Yes	No	No	No	G	Yes*	Yes	Yes*	1
Weggis-1	Yes	No	No	No	G	Yes*	Yes	Yes*	1
Weiach-1	Yes	No	Yes	Yes	C	Yes	Yes	Yes	1
Weiach-2	Yes	No	Yes	No	E	Yes*	Yes	Yes*	1

Table 72: Data availability and assessment classes assigned at the Permo-Carboniferous Play seal (Muschelkalk unit) in the most relevant wells of the Plateau. In the **Data availability**, Lithologic data is "Yes" when lithologic data are available in this well, specifically for the Muschelkalk unit. In the **Assessment**, in the Presence property, "Yes*" means that in this well the Muschelkalk has not been penetrated, thus its presence has been deduced from the closest wells where data are available and/or seismic (GeoMol). In the Impermeable property, (*) means that for this well, there are no lithological data to define the permeability; thus, Yes*/No* is assigned based on what is extrapolated from the closest wells where data are available.

Seal	Muschelkalk (lower and middle)
Well	**Lithology**
Benken	Lower-60% marls; 40% dolomite; Middle-15% salt; 30% anhydrite; 30% dolomite; 25% shales
Berlingen-1	Lower-20% marls; 10% dolomite; 40% shales; 30% sandstones; Middle-95% anhydrite; 5% shales
Boswil-1	Not penetrated
Bottstein-1	40% limestones; 30% shales; 30% anhydrite
Bozberg-1	lower-marls; middle-anhydrite
Bulach-1	Marls, shales, halite
Chapelle-1	Not penetrated
Eclepens-1	Not penetrated
Entlebuch-1	5% anhydrite; 35% shales; 60% dolomite
Essertines-1	Not penetrated
Herdern-1	15% salt; 30% anhydrite; 30% dolomite; 25% shales
Hermingen-1	95% Halite 5% anhydrite
Hünenberg-1	Not penetrated
Kaisten-1	100% dolomite, only 45 m
Kreuzlingen-1	20% marls; 5% anhydrite; 75% shales
Kusnacht-1	Not penetrated
Leuggern-1	40% marly limestones; 30% anhydrite; 30% dolomite
Lindau-1	70% marls; 10% anhydrite; 20% marls
Linden-1	Not penetrated
Marthaleen-1	lower-sandy shales; middle-anhydrite
Noville-1	lower-70% sandstones; 24% shales; 5% dolomite; 1% gypsum; middle-50% limestones; 40% dolomite; 10% marls

Seal	Muschelkalk (lower and middle)
Well	**Lithology**
Pfaffnau-1	70% anydrite; 20% marls; 5% limestones; 5% dolomestones
Ruppoldsried-1	Not penetrated
Riniken-1	10% sandstones; 20% shales; 45% limestones; 25% anhydrite
Savigny-1	Not penetrated
Schafisheim-1	5% sandstones; 10% shales; 55% limestones; 30% anhydrite
Schlattingen-1	40% limestones; 30% anhydrite; 30% dolomite
Sibilingen-1	35% Dolomit, 35% shale, 15% limestone, 15% anhydrite
St Gallen-GT-1	Not penetrated
Thun-1	Not penetrated
Treycovagnes-1	10% sandstones; 30% dolomite; 20% limestone; 20% anhydrite; 20% shales
Truillikon-1	Lower-silty marls; Middle-Anhydrite
Tuggen-1	Not penetrated
Tschugg-1	Not penetrated
Weggis-1	Not penetrated
Weiach-1	60% shales; 30% dolomite; 10% marls

Table 73: General facies of the seal of the Muschelkalk Play in the main wells of the Plateau, represented by the Muschelkalk unit.

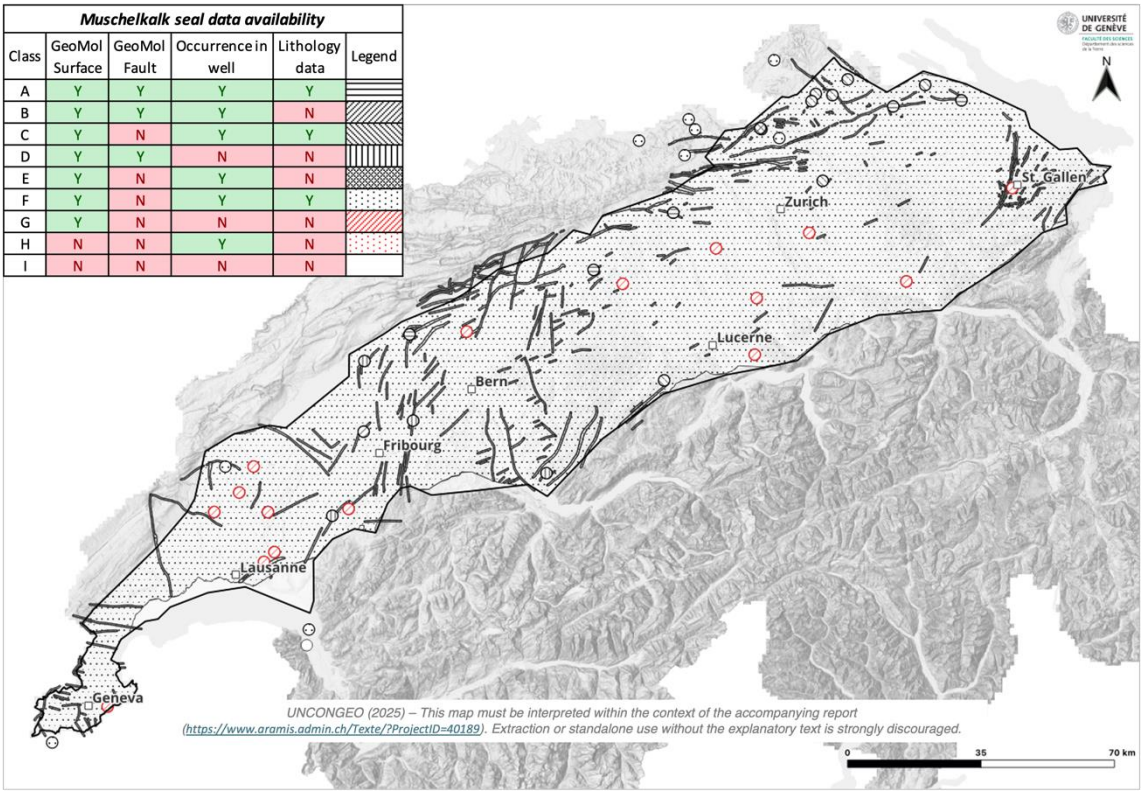


Fig. 146: Permo-Carboniferous seal (Muschelkalk unit) data availability.

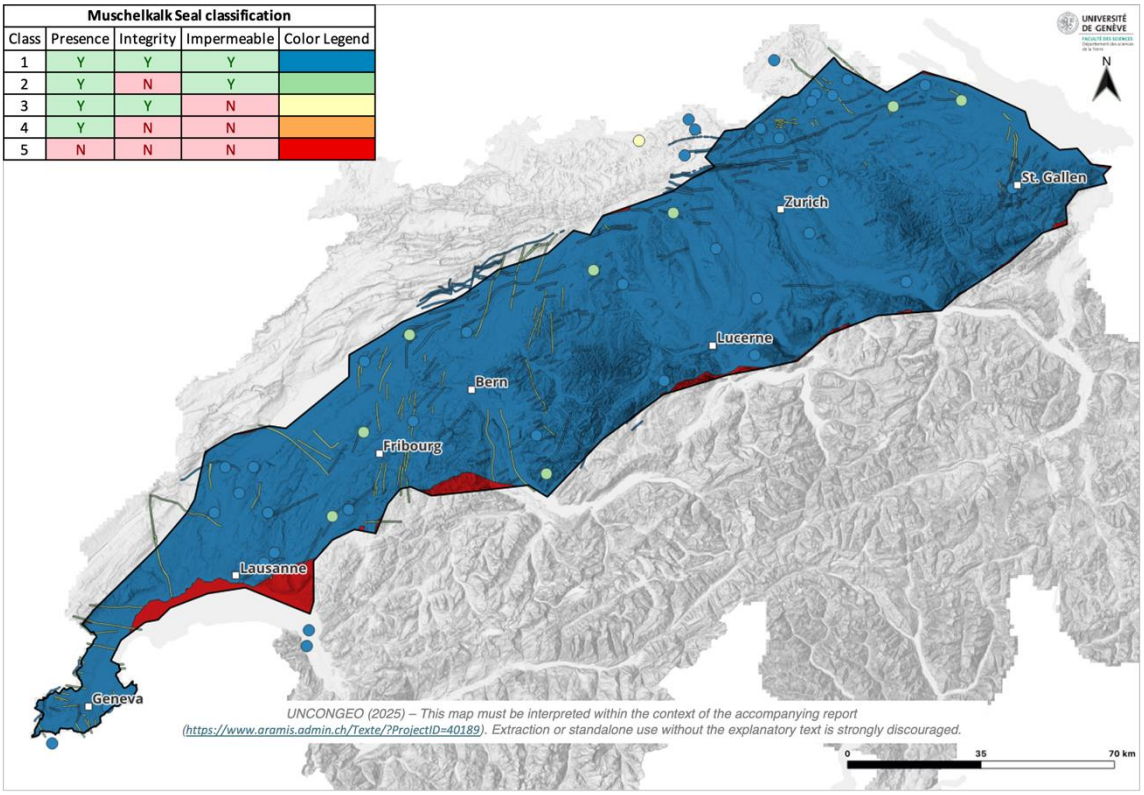


Fig. 147: Permo-Carboniferous seal (Muschelkalk unit) assessement and classification.

The CRS map of the Permo-Carboniferous play is shown in Fig. 148. The risk to encounter hydrocarbons is medium-high in the areas where the Permo-Carboniferous troughs are located, and low in the rest of the Plateau.

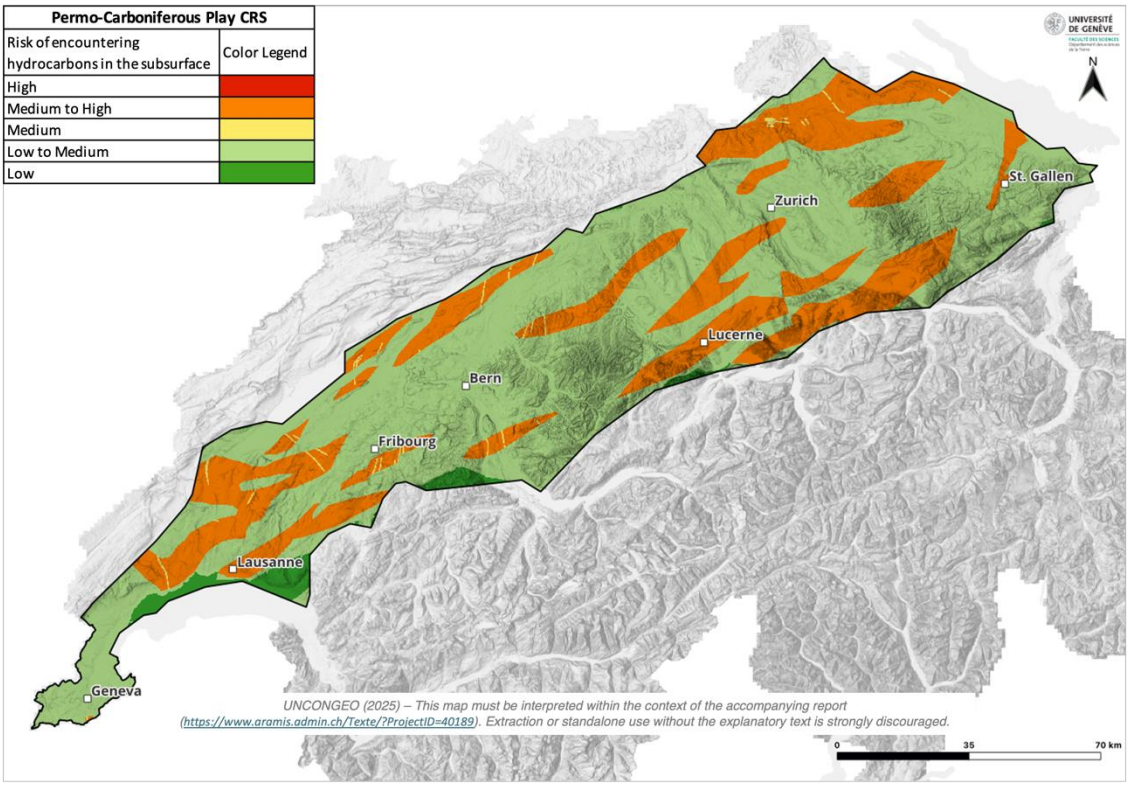


Fig. 148: CRS map for the Permo-Carboniferous play.

3.6.8 Accumulations simulated by petroleum system modelling

The results provided by the CRS maps presented above can be combined with the petroleum system modelling results, concerning the hydrocarbon accumulations simulated by the software in the different reservoir units (Fig. 149). The latter provides an estimate of the area (located along the modelled sections) where hydrocarbons could be accumulated. The accumulations shown in Fig. 149 represent the modelling results of the “open faults” scenario. This scenario shows the largest accumulations, posing the greatest risk to geothermal exploration activities. However, when consulting this data, it is essential to carefully consider all the parameters, assumptions, and uncertainties associated with the petroleum system modelling presented here. It is especially essential to consider that, in a 2D model, the potential stratigraphic and/or structural traps present in the basin cannot be properly represented. More reliable results could be provided by a regional and/or local 3D model.

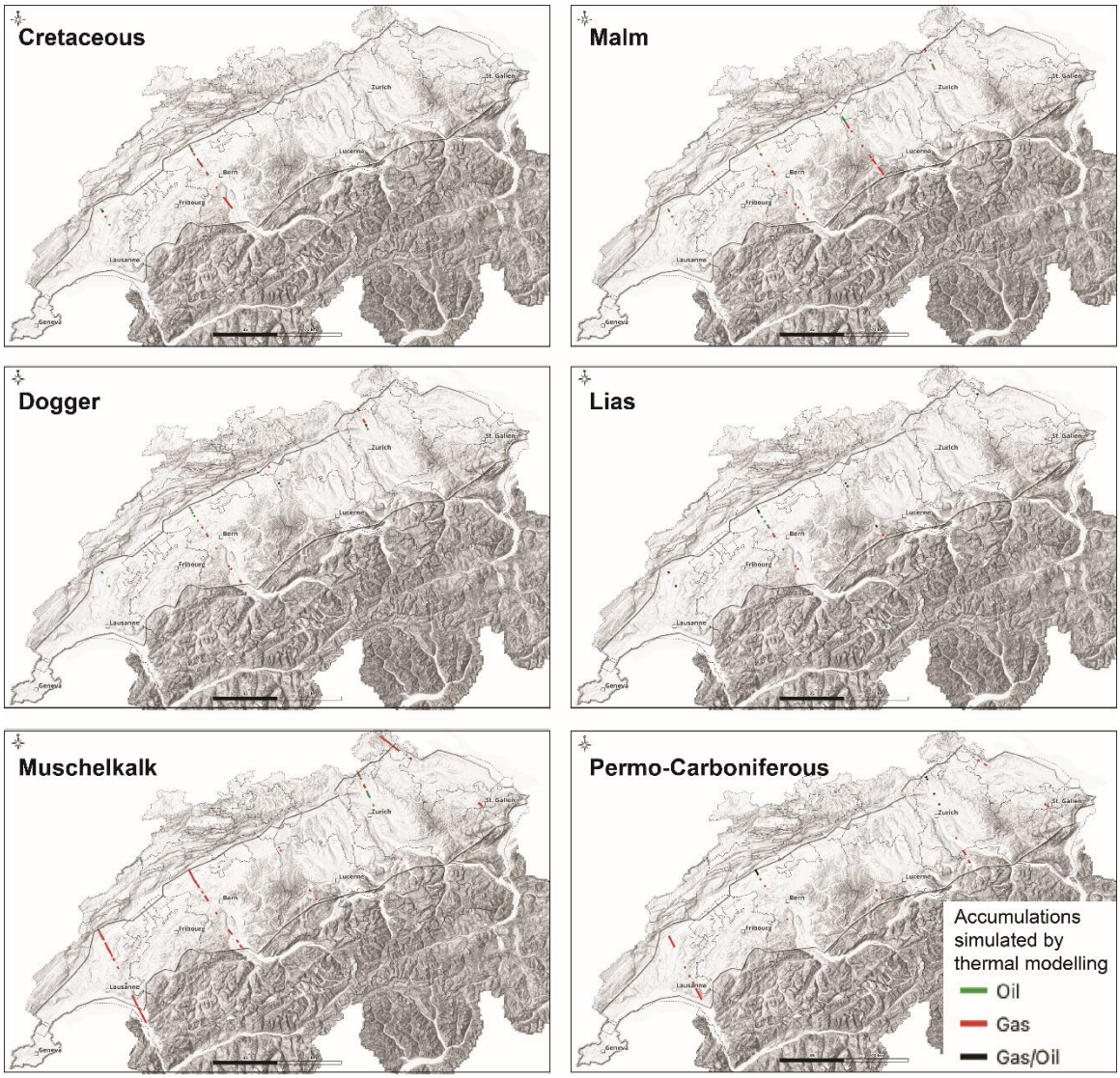


Fig. 149: Hydrocarbon accumulations simulated by thermal modelling along the five sections considered in the petroleum system modelling part of this work.

3.6.9 Data occurrence map

To visually represent the spatial distribution of the data used to build the CRS maps, a data occurrence map was produced (Fig. 150). Occurrence refers to the visual representation of the spatial distribution of areas with sufficient data density, where CRS maps have less uncertainty. This map provides critical insights into defining areas of lower certainty. Geological uncertainty related to the lack of seismic or borehole data can arise primarily due to the absence of direct subsurface information, which is crucial for understanding geological structures, formations, and rock properties (e.g. reservoir porosity, seal integrity, etc). Without accurate data inputs, geological models may rely on assumptions or extrapolations. This introduces uncertainties that can affect the reliability of predictions and decisions based on these models.

The data occurrence needs to be considered when evaluating the risk assessment and the mitigation strategies. Data occurrence should also be used as a support document to prepare data acquisition and exploration to better assess unexplored areas and further define the CRS maps.

The data occurrence map was produced using:

- Borehole data, with an effective radius of 1.5 km around the drilling site
- Seismic data (2D and 3D), with an effective radius of 2 km on each side of the seismic acquisition.

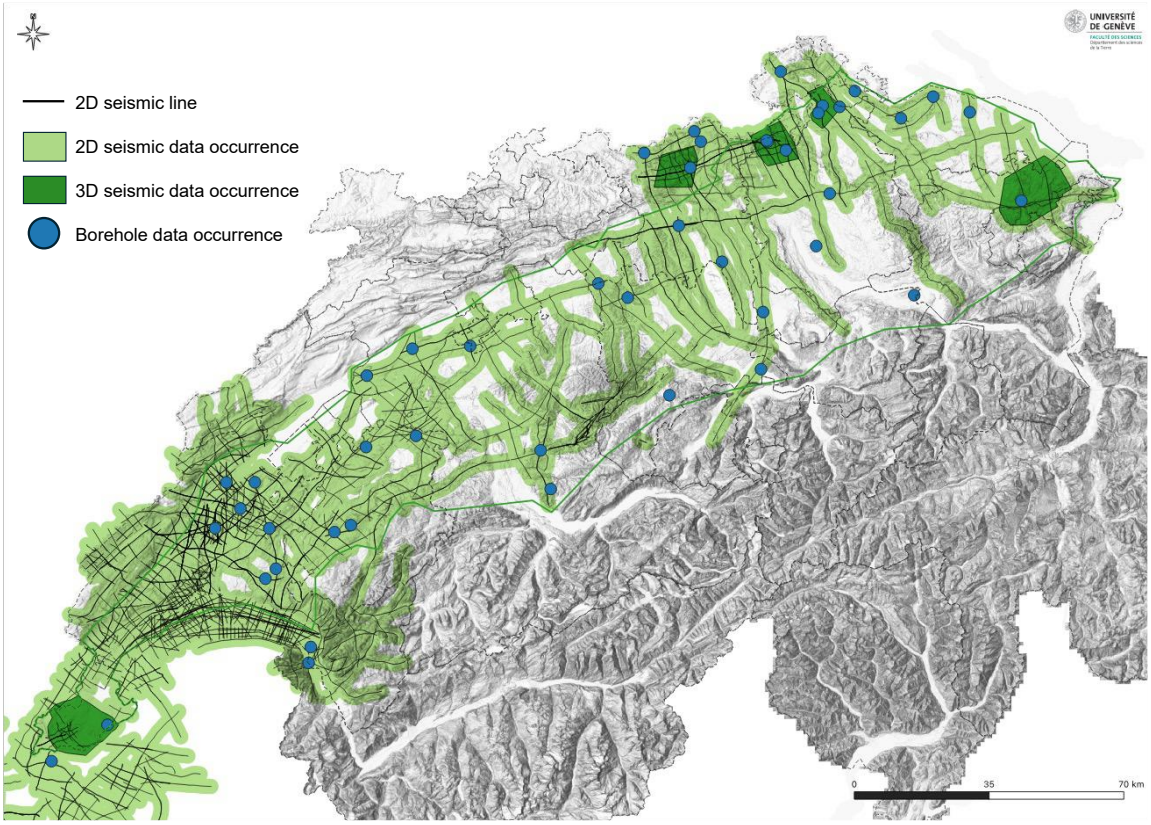


Fig. 150: Data occurrence map

4 . How to use the CRS maps: examples

This section describes how the end-user can benefit from the set of UNCONGEO CRS maps to assess the risk of encountering hydrocarbon accumulations at depth while drilling a geothermal well in a specific area located in the Swiss Plateau.

The word "risk" in this report does not refer by any means to the overall risk that a geothermal project might have if located in a zone defined as "medium/high risk" in the CRS maps, but on the likelihood that hydrocarbons are found during the exploration and exploitation activities.

The dataset used to build the CRS map was collected up to 2023. However, new data are available since the publication of this report. These new data were not included in this assessment. The map presented in this section should be regarded as evolving and subject to reassessment as new information becomes available.

The GIS database, which contains all the compiled data needed to create the CRS maps, will be made available to users with the necessary expertise upon request with the following resources:

- The CRS maps for each geothermal play,
- The play elements (reservoir, seal, source rocks) for each play,
- The data availability for each play element,
- The data coverage map.

The following provides examples of i) how to consult and read the CSR maps in different geological and geographical contexts and ii) provide possible follow up actions, which can be derived by the examination of the CSR maps in order to reduce the uncertainties and related riks associated with the presence of hydrocarbons at depth.

For this, four cases were chosen, which can be representative of real situations that a geothermal exploration project could encounter:

- Example 1 - Vertical well located in a medium to high-risk area.
- Example 2 - Vertical well located in an area with low density of data.
- Example 3 - Vertical well located in an area with medium risk and good data coverage.
- Example 4 - Deviated well into several plays, characterised by different levels of risk.

4.1 Zurich airport, example of a medium to high-risk prospect.

This example considers that a potential geothermal prospect is identified in the vicinity of Zurich's airport (Fig. 151). The defined geothermal target is the Muschelkalk reservoir.



Fig. 151: Hypothetical geothermal exploration target (violet circle) in the Zurich Airport area

The CRS map for the Muschelkalk play indicates that the identified prospect has a "Medium to High-risk" of encountering hydrocarbons when drilling (Fig. 152). The user can then consult the play elements maps used to compose the CRS map.

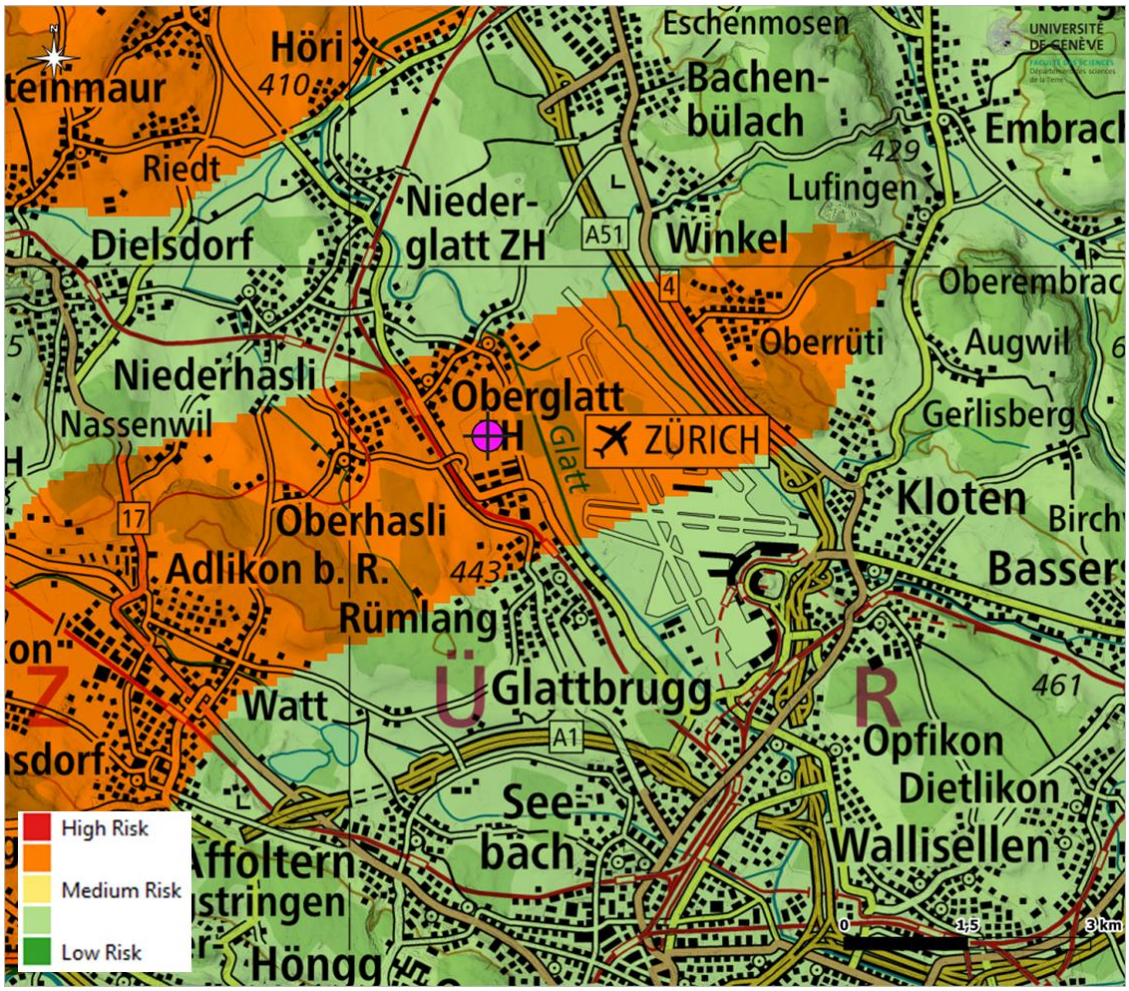


Fig. 152: CRS map for the Muschelkalk play, indicating low-high risk in the target area.

4.1.1 Source rock

The source rock element map indicates that the prospected area is in Class 1 (Fig. 153). This is because the area is on top of a Permo-Carboniferous trough, thus, it is supposed that the Permian and Carboniferous source rocks are present, with a good hydrocarbon potential.

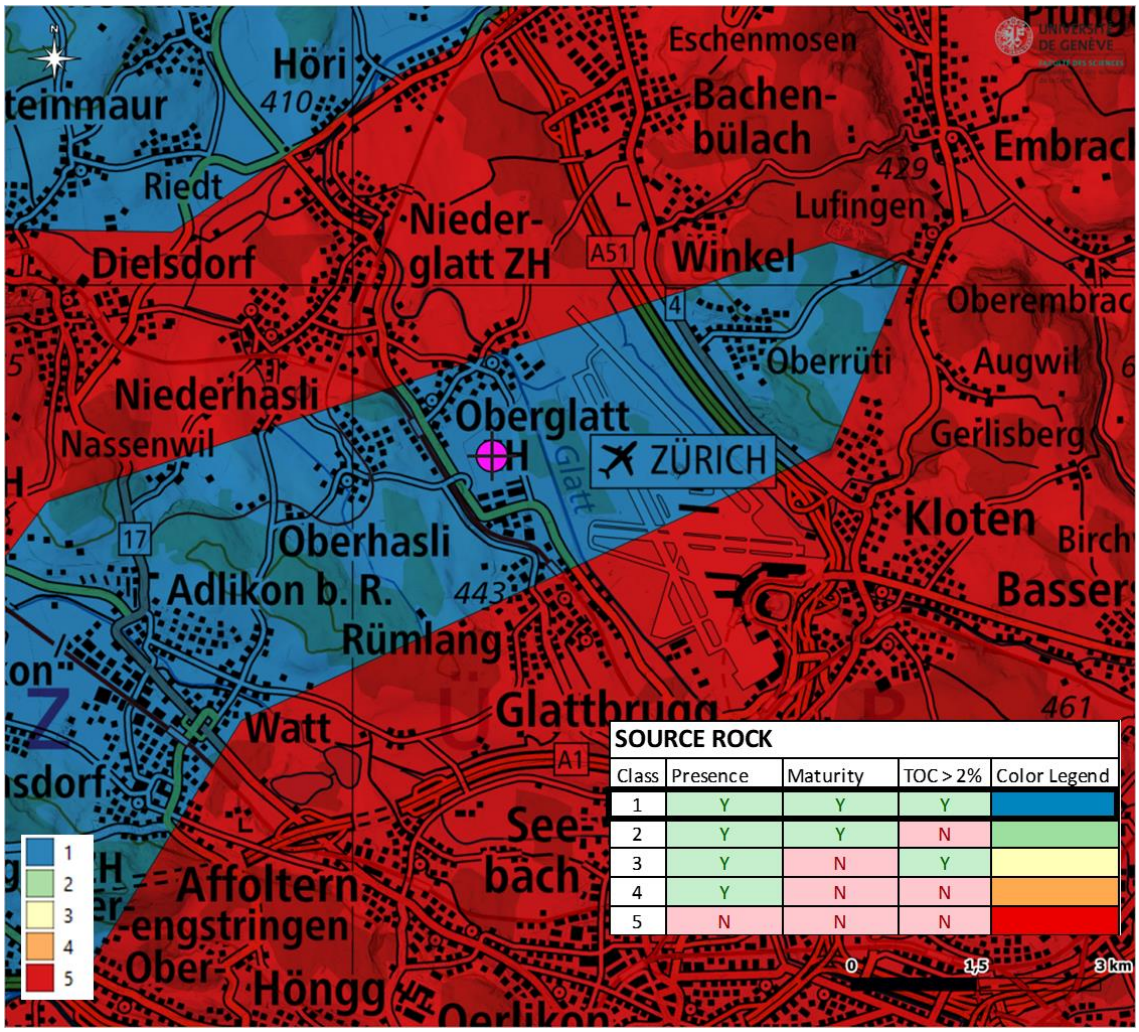


Fig. 153: Source rock assessment class resulting in the chosen target area.

4.1.2 Reservoir

The reservoir map indicates that the potential Muschelkalk reservoir is in class 4, as it is present in the area but is not considered as porous nor fractured (Fig. 154). As shown in Fig. 154, the user can display the faults on top of the map to have a better understanding of their locations.

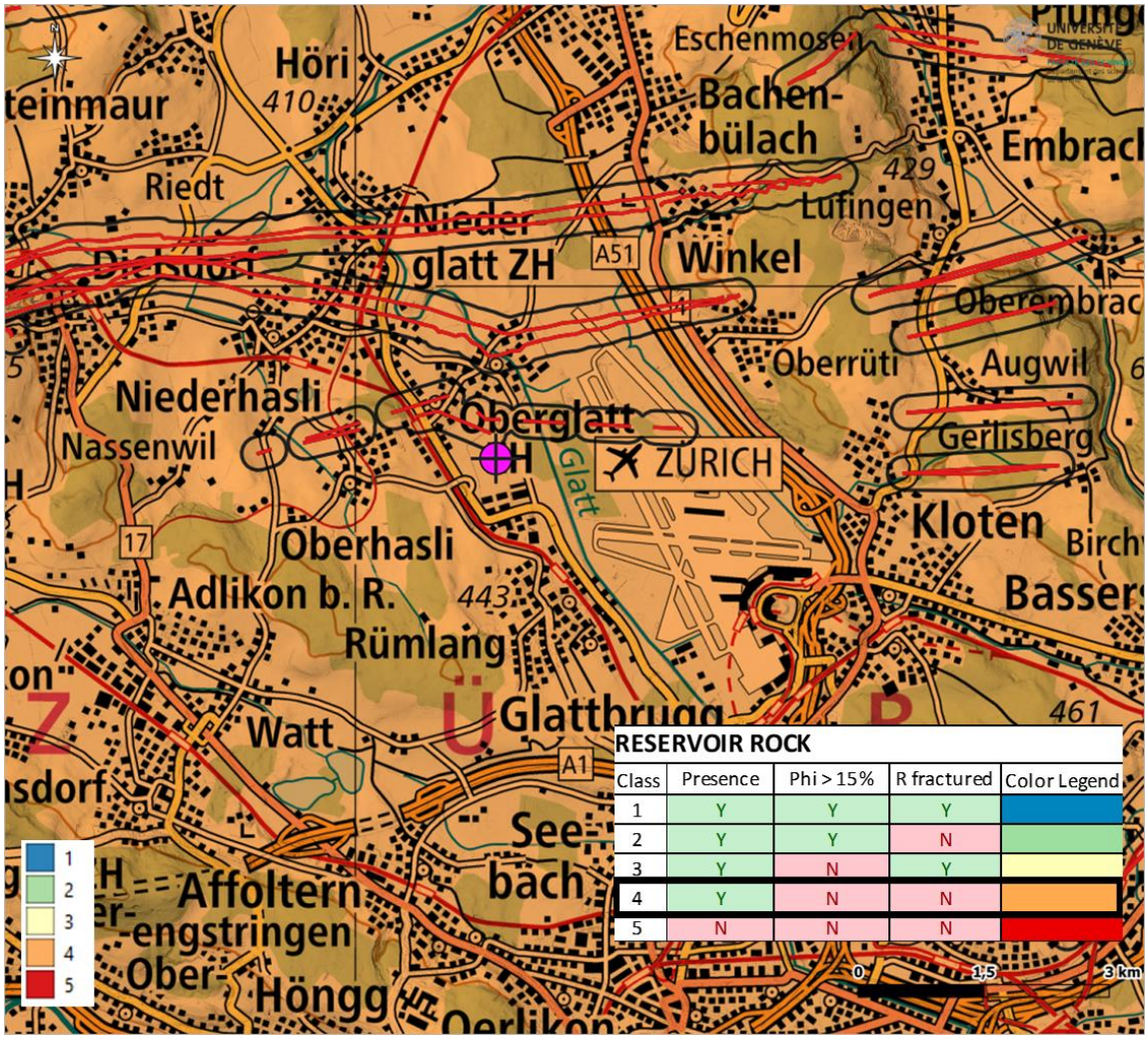


Fig. 154: Reservoir element assessment for the Muschelkalk play in the target area.

4.1.3 Seal

The seal map indicates that a seal present in this area is in Class 1, therefore it is considered to be impermeable and not fractured (Fig. 155). If hydrocarbons migration occurred, they could be sealed and trapped within the Muschelkalk reservoir.

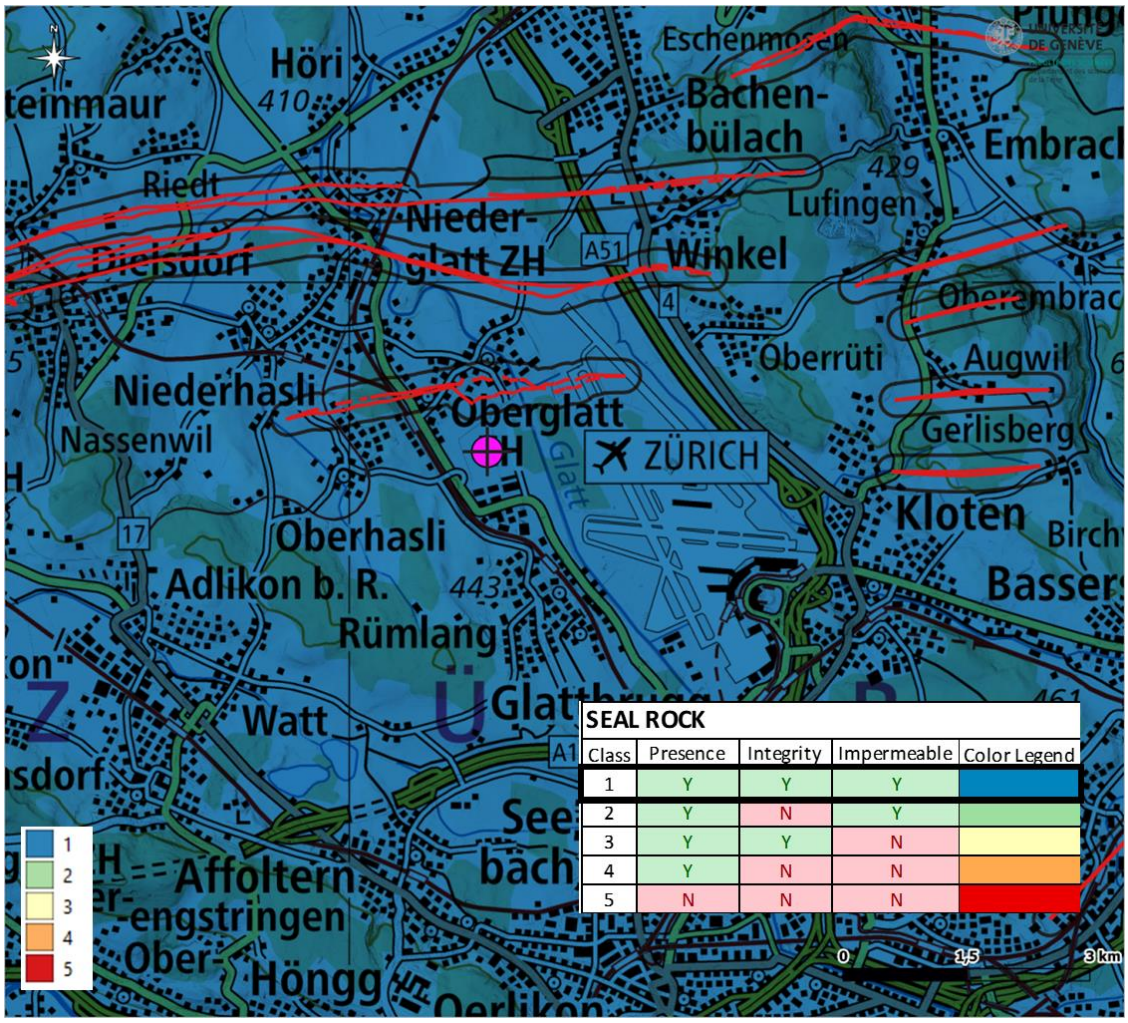


Fig. 155: Seal element assessment for the Muschelkalk play in the target area.

4.1.4 Uncertainty and data occurrence

In addition to the play elements, the user can also inquire about the density of data available in the prospected area (Fig. 156). The data occurrence map displays the density and type of subsurface data that characterise the subsurface. The prospective area has a good data density. A 2D seismic line is in proximity to the prospect, and the user can query the name of the line in the database. However, no borehole data is available close to the prospected area. The user can also refer to the data availability map of each petroleum system element (Fig. 157, Fig. 158 and Fig. 159). This information is useful to check what data is present and what type of additional data could/should be acquired.

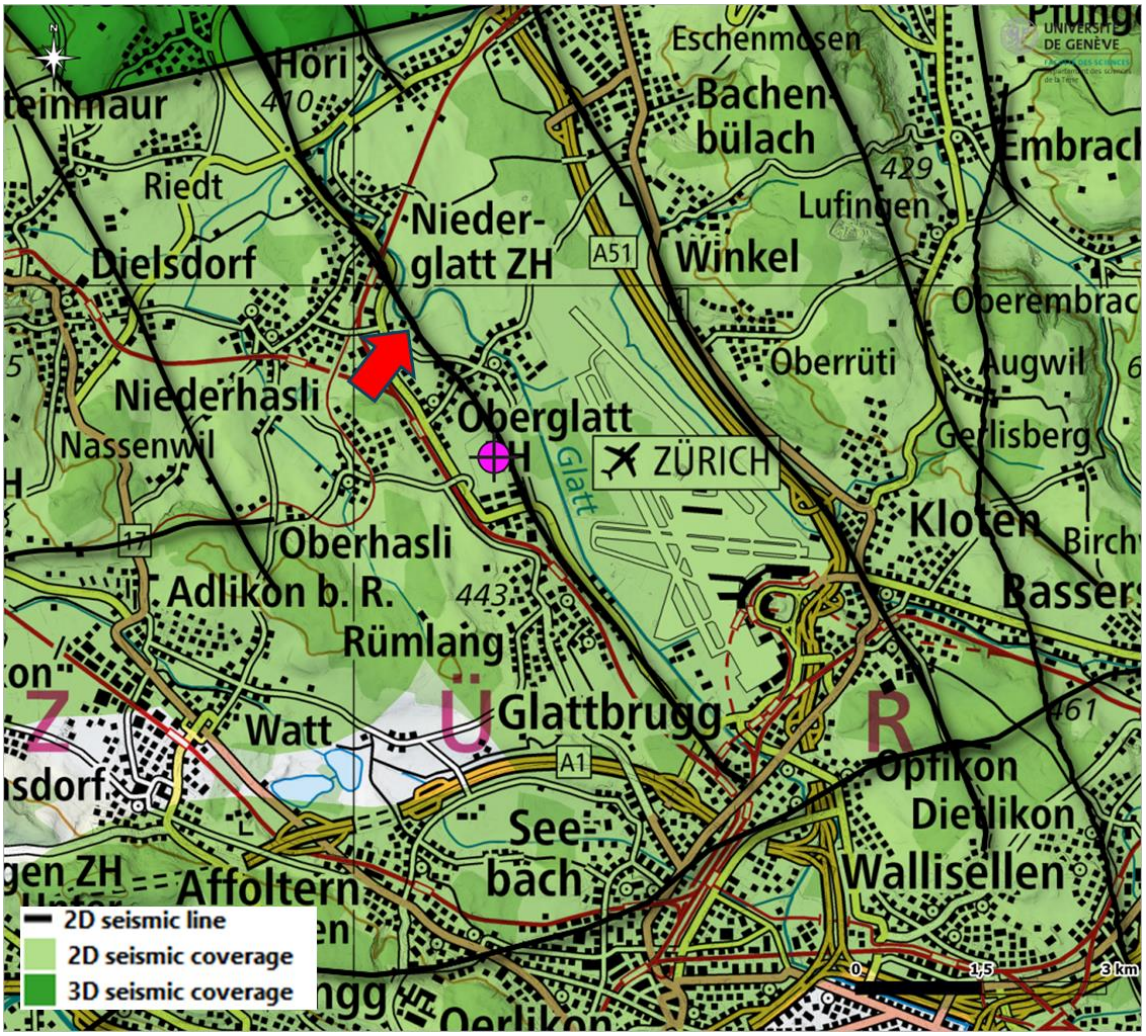
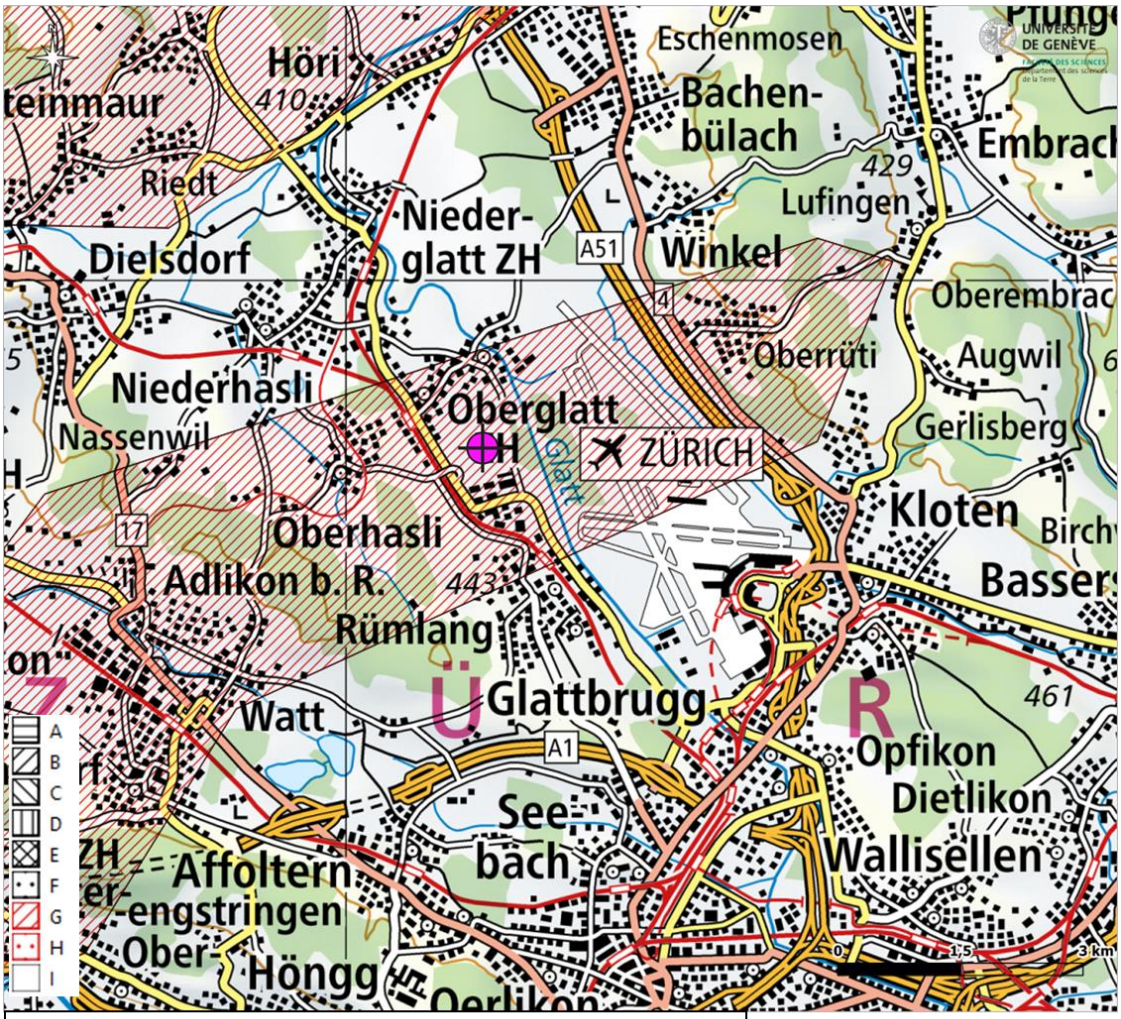
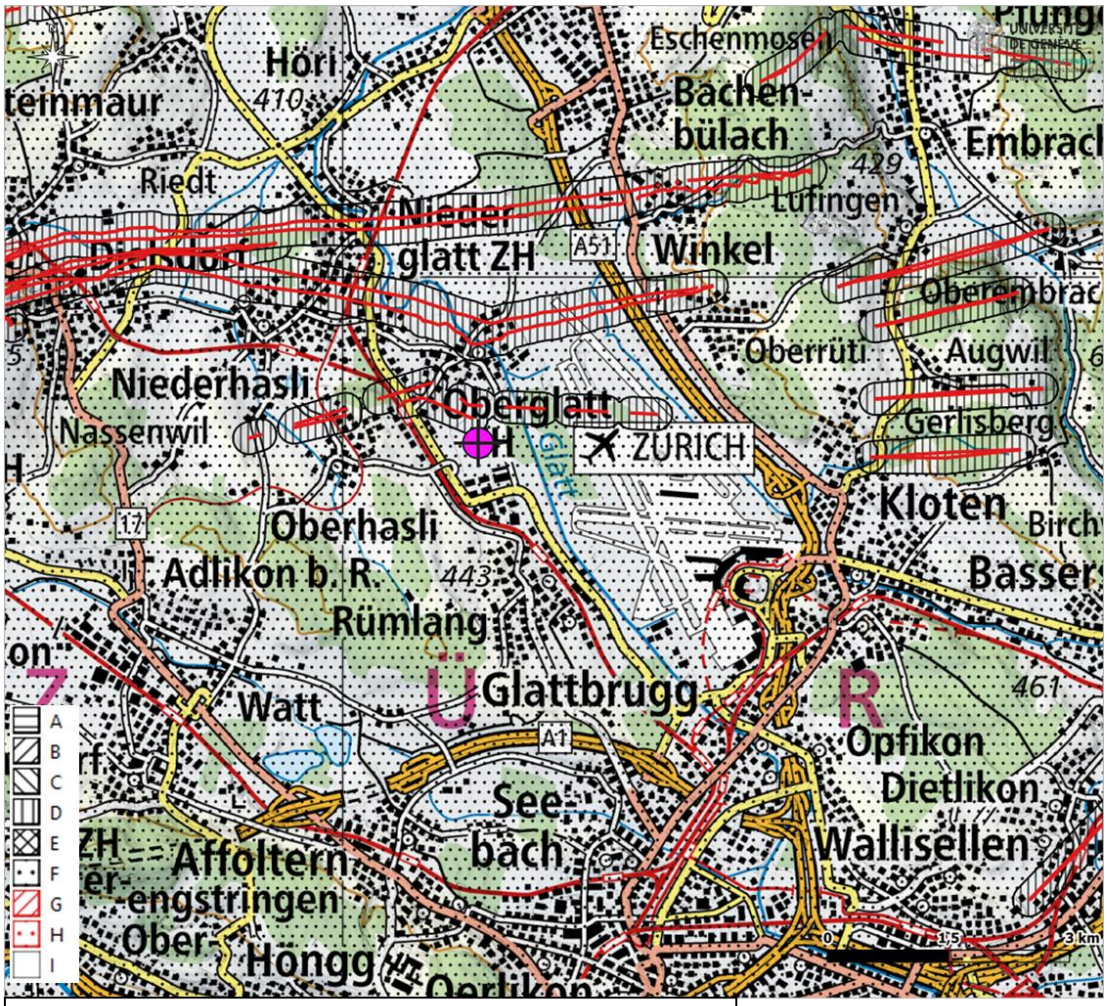


Fig. 156: Data occurrence map in the target area. The red arrow indicates the seismic line passing close to the well.



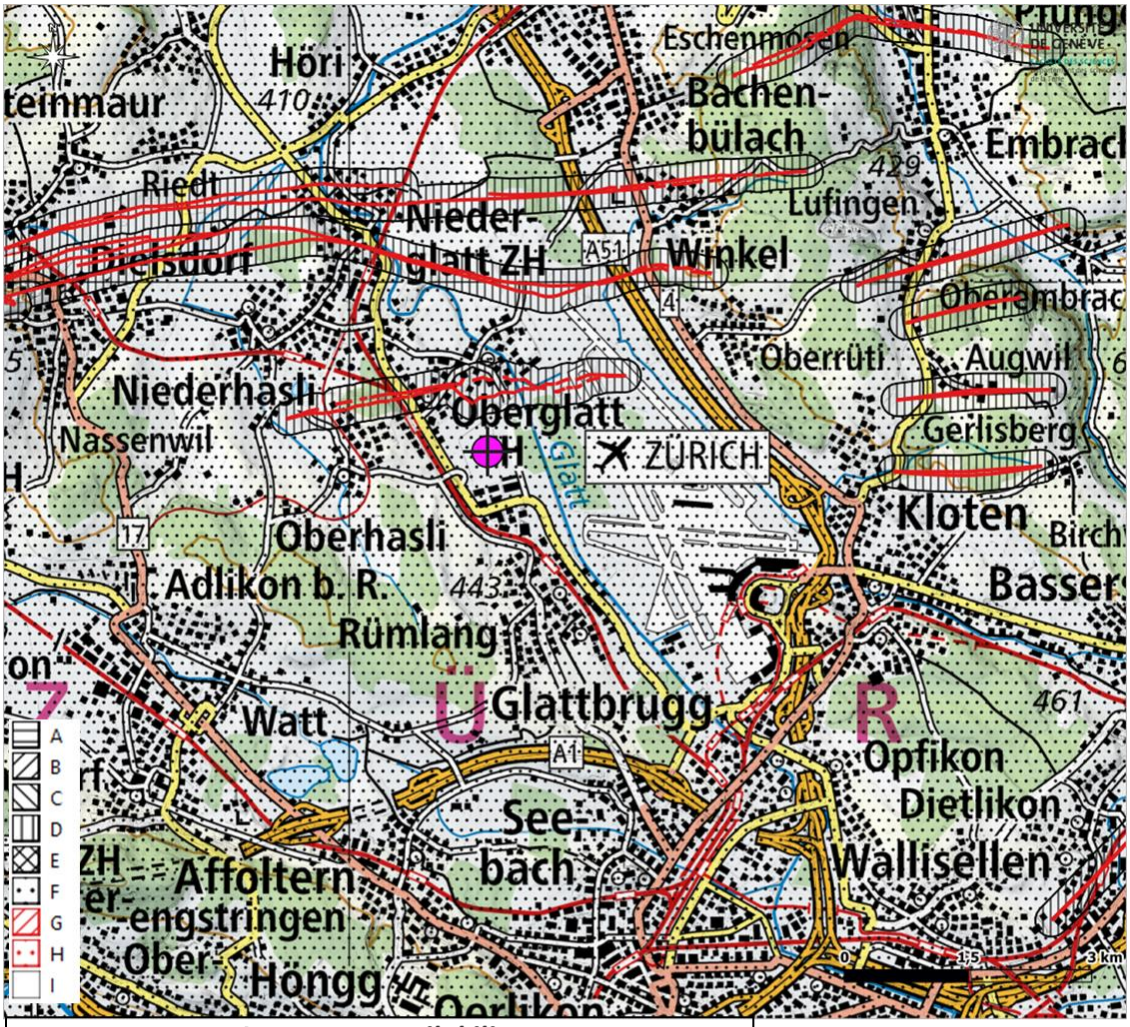
SOURCE ROCK DATA availability					
Class	Occurrence	TOC/Rock Eval	VR	Model calibration	Legend
A	Y	Y	Y	Y	
B	Y	Y	Y	N	
C	Y	N	Y	Y	
D	Y	Y	N	N	
E	Y	N	Y	N	
F	Y	N	N	Y	
G	Y	N	N	N	
H	N	N	N	Y	
I	N	N	N	N	

Fig. 157: Data availability for the Permo-Carboniferous source rock in the target area



RESERVOIR DATA availability					
Class	GeoMol Surface	GeoMol Fault	Occurrence in well	Porosity data	Legend
A	Y	Y	Y	Y	
B	Y	Y	Y	N	
C	Y	N	Y	Y	
D	Y	Y	N	N	
E	Y	N	Y	N	
F	Y	N	Y	Y	
G	Y	N	N	N	
H	N	N	Y	N	
I	N	N	N	N	

Fig. 158: Data availability for the Muschelkalk reservoir in the target area



SEAL DATA availability					
Class	GeoMol Surface	GeoMol Fault	Occurrence in well	Lithology data	Legend
A	Y	Y	Y	Y	
B	Y	Y	Y	N	
C	Y	N	Y	Y	
D	Y	Y	N	N	
E	Y	N	Y	N	
F	Y	N	Y	Y	
G	Y	N	N	N	
H	N	N	Y	N	
I	N	N	N	N	

Fig. 159: Data availability for the seal in the target area

The hypothetical case presented here for the Zürich Airport is similar to the results obtained in the St. Gallen GT-1 borehole area. In this area, the CRS map classifies the drilling location as a “Medium to High risk” of encountering hydrocarbons (Fig. 160). Thermogenic gas was indeed found during the drilling operation, carried out in 2012 at more than 4000 meters, causing an overpressured gas kick, which was controlled by emergency mud injection. The latter induced a 3.5 ML earthquake. The presence of deep gas accumulations has also been predicted by the 3D petroleum system model realised in the framework of the UNCONGEO project (Omodeo Salé et al., 2020).

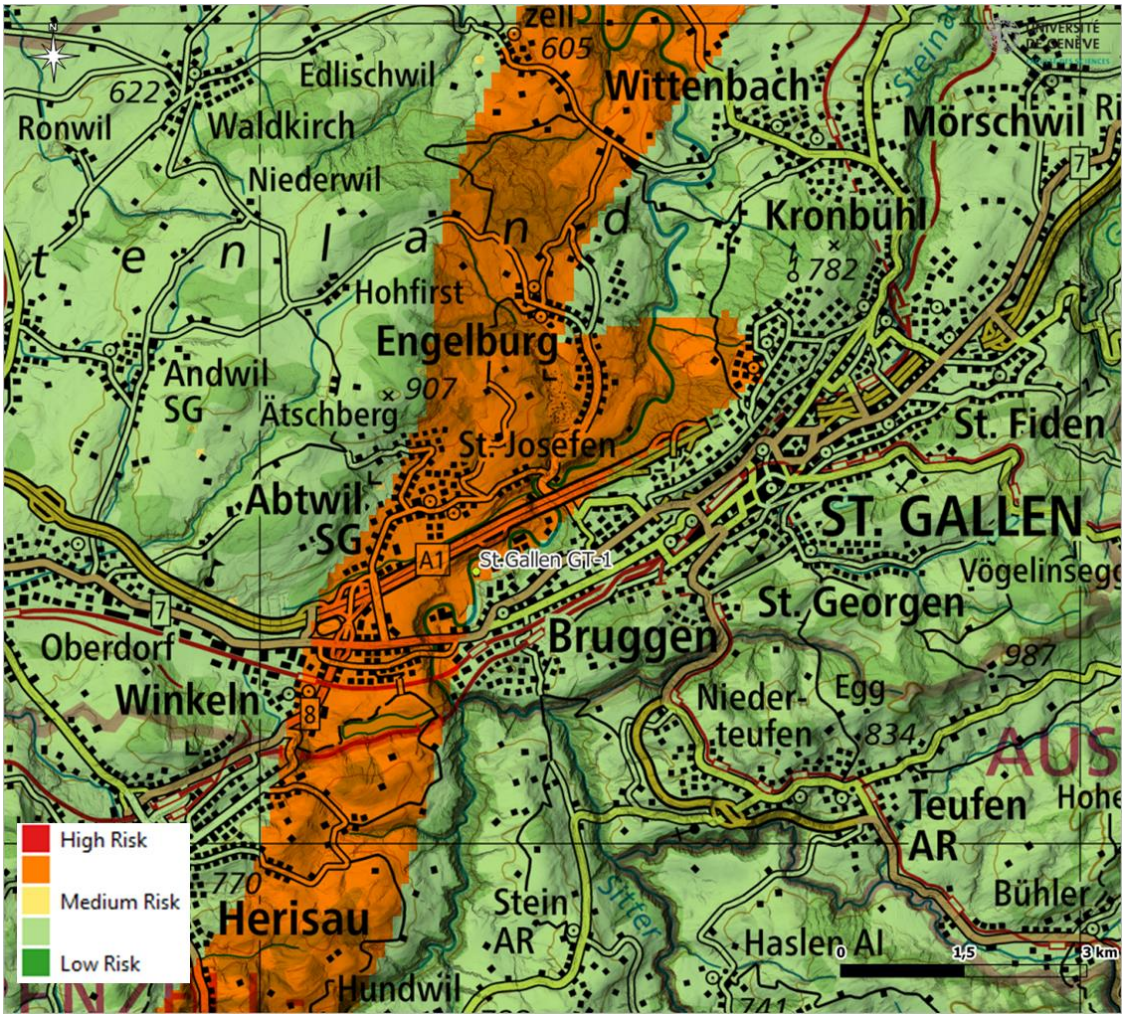


Fig. 160: CRS map for the Muschelkalk play in the St. Gallen area. The St. Gallen GT-1 well is in the medium-high risk class

4.1.5 Recommendations

In this case, several activities could be undertaken to reduce the uncertainties related to a medium to high risk of encountering hydrocarbons while drilling a deep geothermal well in this area. These mitigation activities might include:

- A complete review of the available datasets to assess the risk before drilling and identify potential hazards, especially associated with gas seepages. The user can refer to the data availability maps as well as the existing database to track and collect existing data. However, additional data might be made available which are not included in the UNCONGEO database.
- Evaluate the possibility to acquire additional 2D seismic lines or a 3D seismic survey in order to map possible hydrocarbon trapping structures and migration paths from active source rock(s) present in the area.
- Perform 2D and/or 3D petroleum generation and migration modelling across the area

- Plan for appropriate well control equipment such as BOP, chokes, kill lines and diverters systems if the risk is confirmed during operation.
- Design the well accordingly to the risk with appropriate casing and cementing programs in the concerned intervals.
- Implement real-time monitoring systems during drilling, such as LWD (logging while drilling), to detect any pressure changes during drilling operations, including seismic monitoring equipment.
- Ensure that an emergency response plan exists and that all personnel involved in the drilling is trained for gas detection, well control techniques, emergency procedures and risk awareness.

4.2 Bern, example of low data density

This example considers that a prospect has been identified in the southern part of the city of Bern, an urban area where geothermal energy could be implemented for the heating and cooling network (Fig. 161). The target is the Cretaceous geothermal play. In this case, the CRS map indicates a “Medium risk” of encountering hydrocarbons (Fig. 162). As in the previous example, the user can refer to the different play elements maps in order to assess better the risk of each element.



Fig. 161: Hypothetical geothermal exploration project in the Bern area (violet circle). The prospect is located north of Wabern, and it is marked with a violet circle.

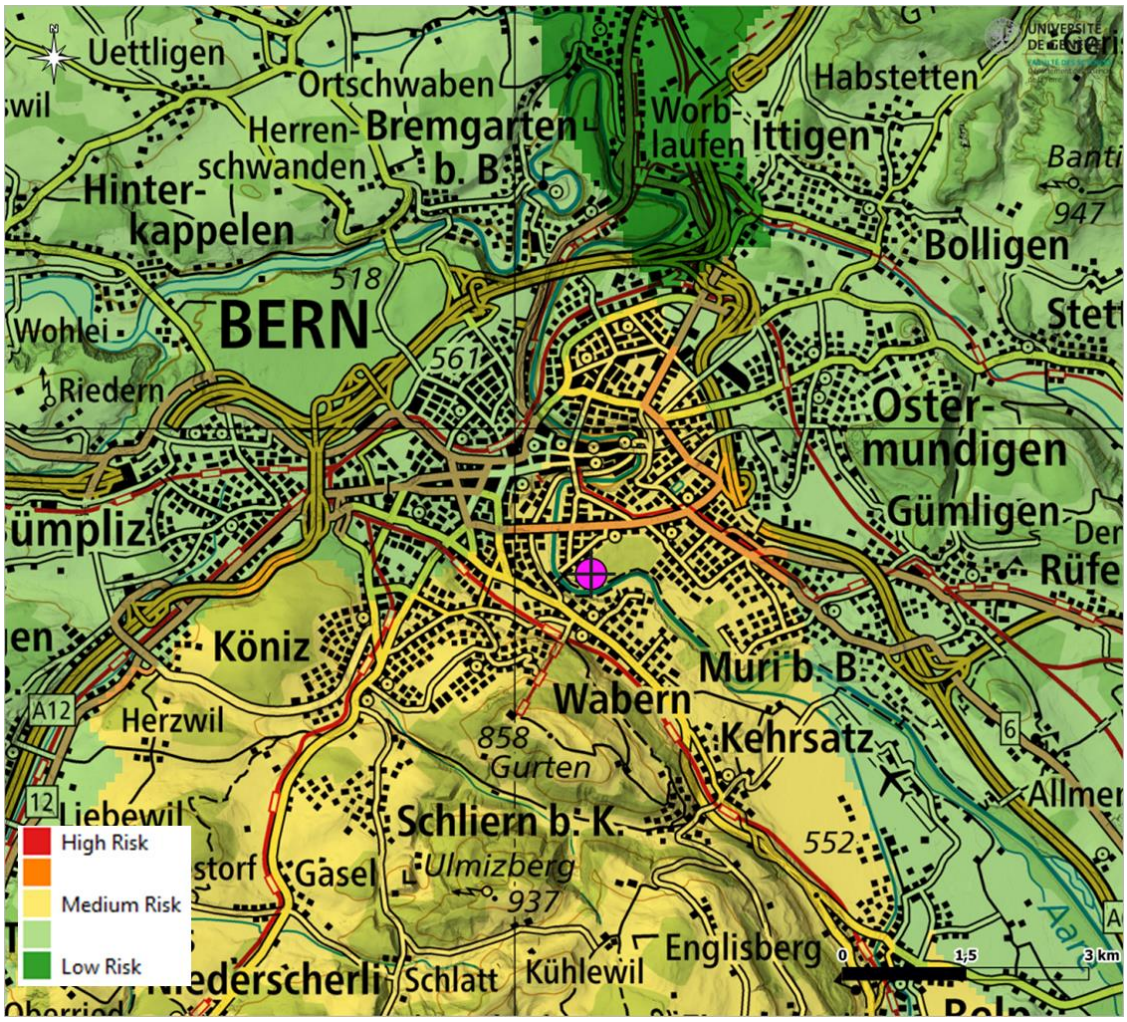
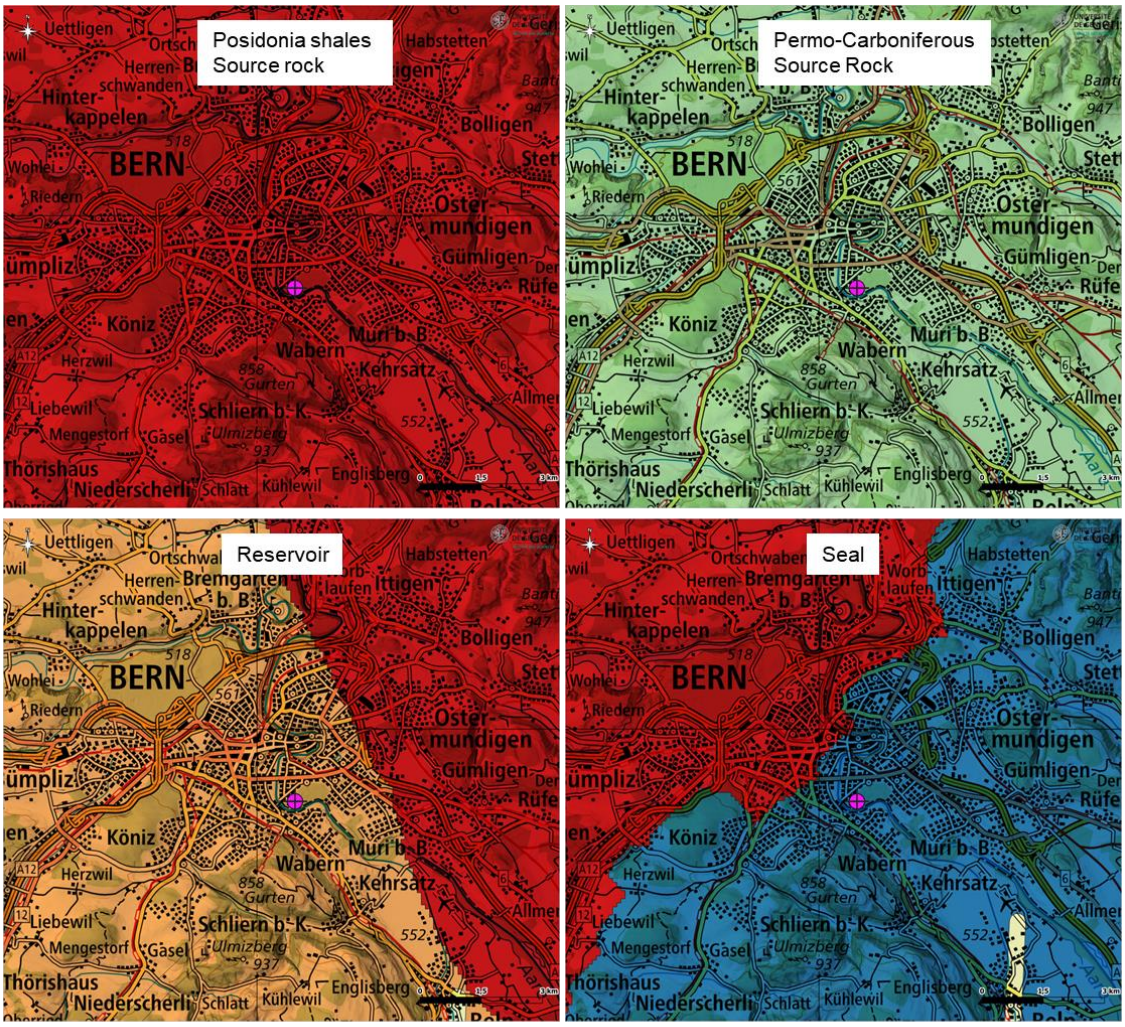


Fig. 162: CRS map for the Cretaceous play, indicating medium risk in the target area

4.2.1 Play components evaluation

The play components maps (Fig. 163) indicate that the Permo-Carboniferous source rock is classified in Class 5, as it is not present in the areas, whereas the Posidonia shale source rock is classified in Class 2, as it is supposed to be present in the area and, mature despite the TOC is expected to be less than 2%. The reservoir unit (Lower Cretaceous) is classified in Class 4, as it is expected to be neither porous nor fractured. The seal unit (Molasse) is classified in Class 1 as it is supposed to be impermeable and not fractured.



SOURCE ROCK				
Class	Presence	Maturity	TOC > 2%	Color Legend
1	Y	Y	Y	
2	Y	Y	N	
3	Y	N	Y	
4	Y	N	N	
5	N	N	N	

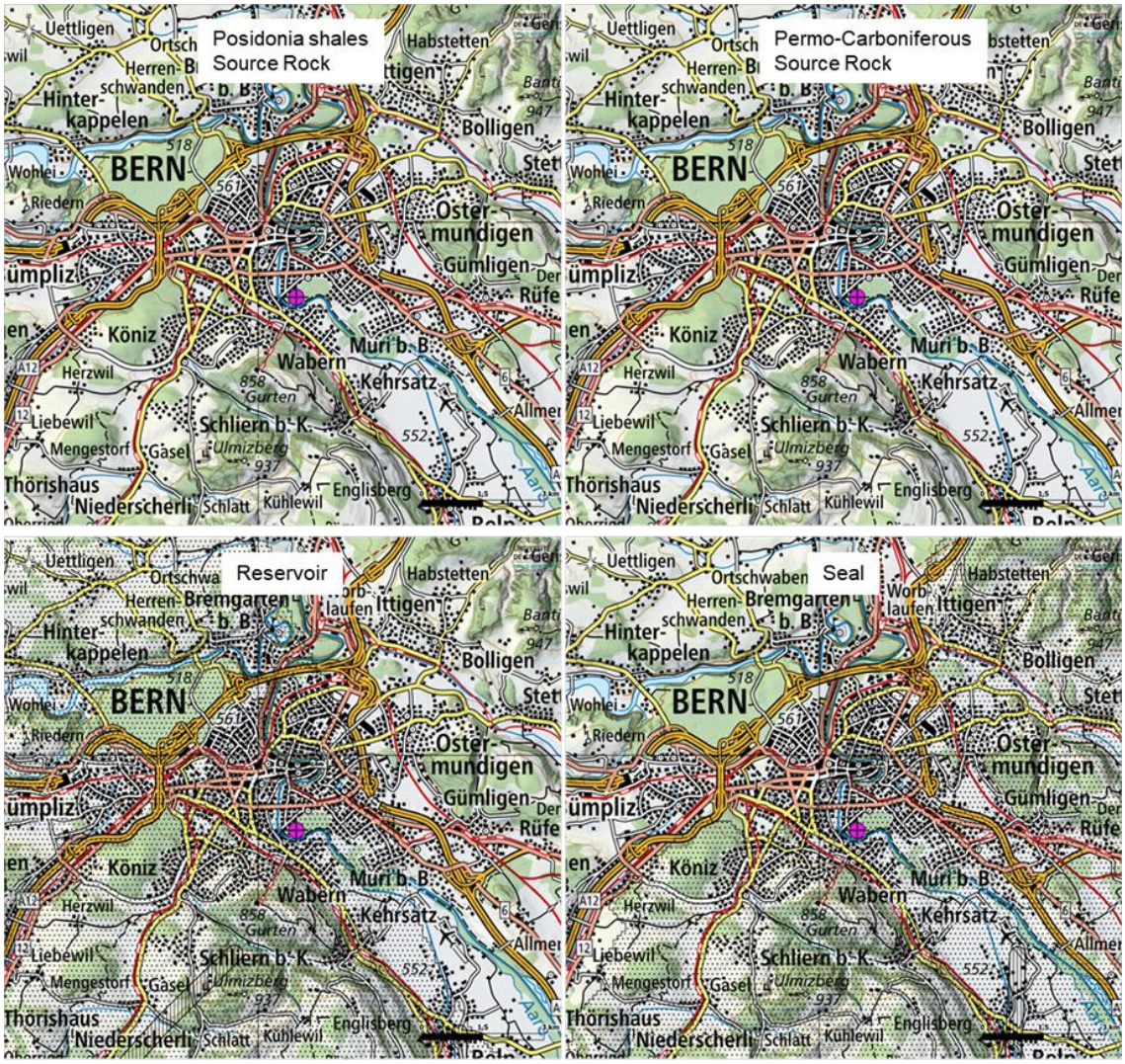
RESERVOIR ROCK				
Class	Presence	Phi > 15%	R fractured	Color Legend
1	Y	Y	Y	
2	Y	Y	N	
3	Y	N	Y	
4	Y	N	N	
5	N	N	N	

SEAL ROCK				
Class	Presence	Integrity	Impermeable	Color Legend
1	Y	Y	Y	
2	Y	N	Y	
3	Y	Y	N	
4	Y	N	N	
5	N	N	N	

Fig. 163: Play components maps of the Cretaceous play in the prospect area. Source Rock 1 refers to the Permo-Carboniferous, and Source Rock 2 refers to the Posidonia shale.

4.2.2 Data availability

To understand the uncertainties in the play elements assessment, the “Data availability” maps must be consulted (Fig. 164). In this area, little data are available for all the play elements. The data occurrence map (Fig. 165) clearly shows the poor density of data in this area. Seismic data coverage is scarce (only 2D seismic data exist), and there are no borehole data in the vicinity of the prospect.



SOURCE ROCK DATA availability

Class	Occurrence	TOC/Rock Eval	VR	Model calibration	Legend
A	Y	Y	Y	Y	
B	Y	Y	Y	N	
C	Y	N	Y	Y	
D	Y	Y	N	N	
E	Y	N	Y	N	
F	Y	N	N	Y	
G	Y	N	N	N	
H	N	N	N	Y	
I	N	N	N	N	

RESERVOIR DATA availability

Class	GeoMol Surface	GeoMol Fault	Occurrence in well	Porosity data	Legend
A	Y	Y	Y	Y	
B	Y	Y	Y	N	
C	Y	N	Y	Y	
D	Y	Y	N	N	
E	Y	N	Y	N	
F	Y	N	Y	Y	
G	Y	N	N	N	
H	N	N	Y	N	
I	N	N	N	N	

SEAL DATA availability

Class	GeoMol Surface	GeoMol Fault	Occurrence in well	Lithology data	Legend
A	Y	Y	Y	Y	
B	Y	Y	Y	N	
C	Y	N	Y	Y	
D	Y	Y	N	N	
E	Y	N	Y	N	
F	Y	N	Y	Y	
G	Y	N	N	N	
H	N	N	Y	N	
I	N	N	N	N	

Fig. 164: Data availability for each play component of the Cretaceous geothermal play in the Bern area.

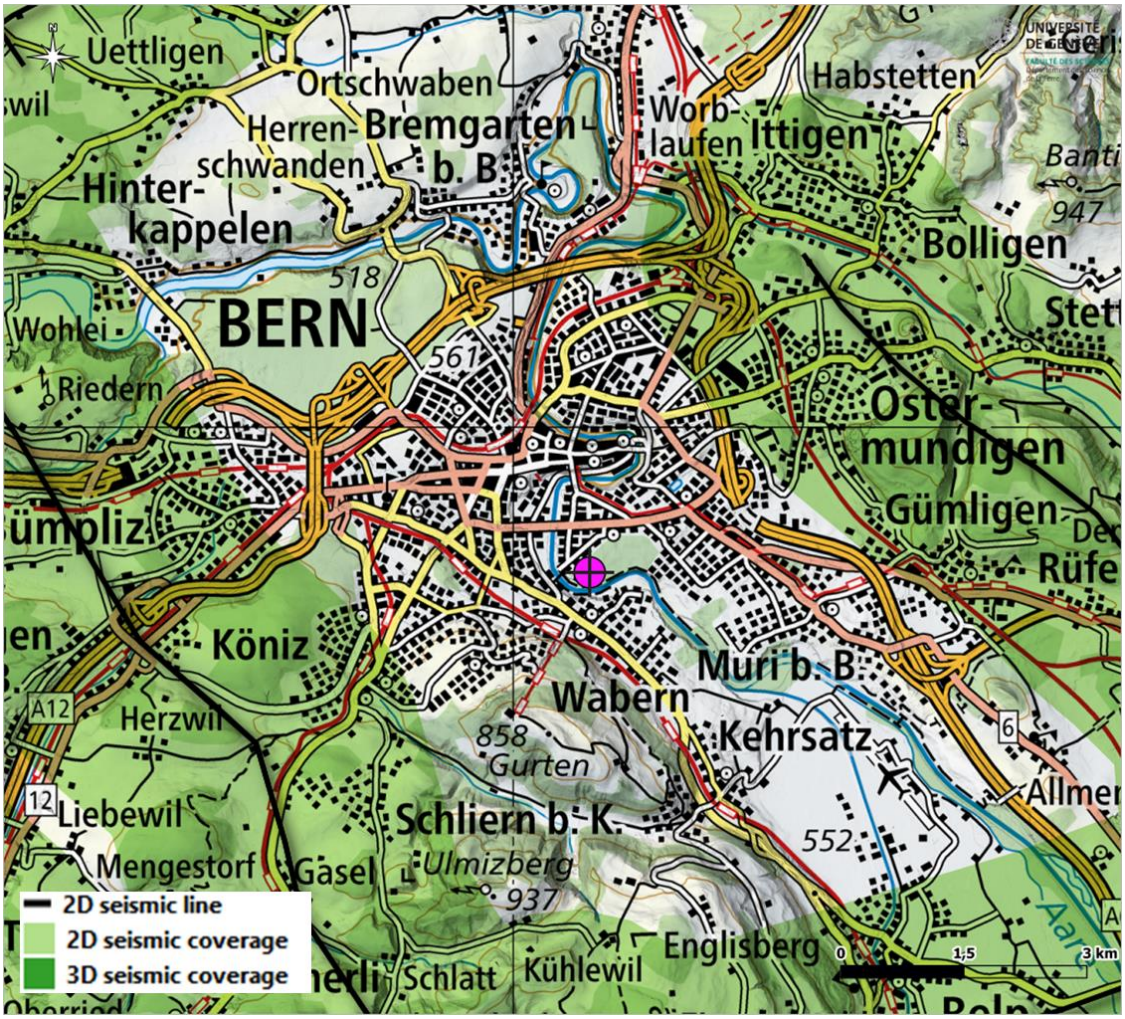


Fig. 165: Data occurrence map.

4.2.3 Recommendations

In the presented case, the user is advised to implement mitigation actions considering the data occurrence and data availability maps. This might include:

- A complete review of the available datasets to assess the risk before drilling and identify potential hazards. The user can refer to the data availability maps as well as the existing database to track and collect existing data. However, additional data might be made available which are not included in the UNCONGEO database. Plan for data acquisition to assess the lack of data coverage emphasised by the data occurrence map, i.e. evaluate the possibility to acquire 2D seismic lines or a 3D seismic survey to map possible hydrocarbon trapping structures and migration paths from active source rock(s) present in the area. Seismic data would also be useful to verify the presence and thickness of the Cretaceous unit in this area, which is in part uncertain.
- Perform 2D and/or 3D petroleum generation and migration modelling across the area
- Compare and contrast the newly acquired dataset with the existing data to further assess the inherent risks

4.3 Langenthal, example of a prospect area in the vicinity of a deep borehole

This example considers a project in the vicinity of Langenthal (Canton of Bern), with the Dogger geothermal play as a target (Fig. 166). The Dogger play CRS map indicates a “Medium risk” of encountering hydrocarbons in the subsurface (Fig. 167). As in the previous example, the user can refer to the different play elements maps in order to assess better the risk of each element.

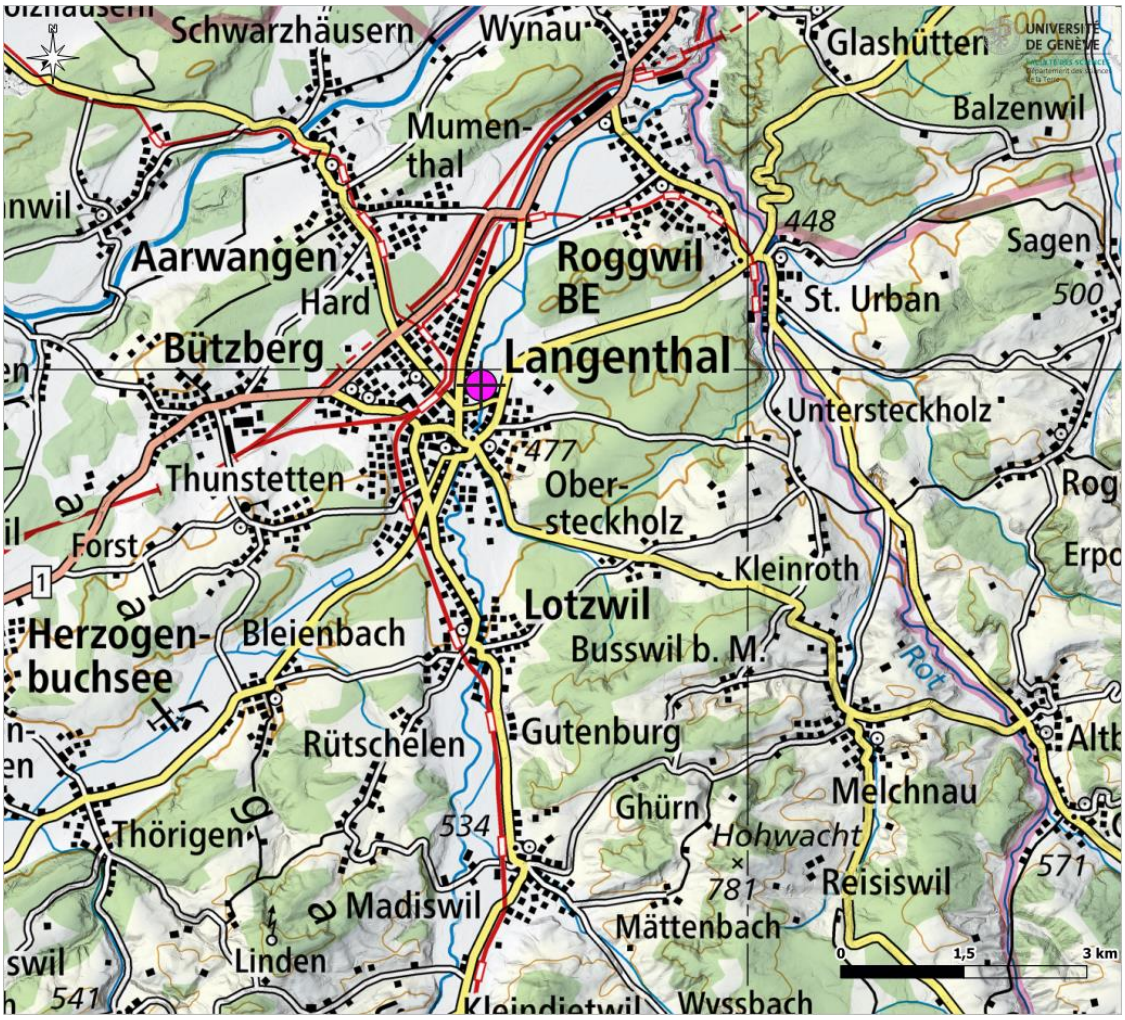


Fig. 166: Hypothetical geothermal project in the Langenthal town and its surroundings. The location of the planned well is marked in violet.

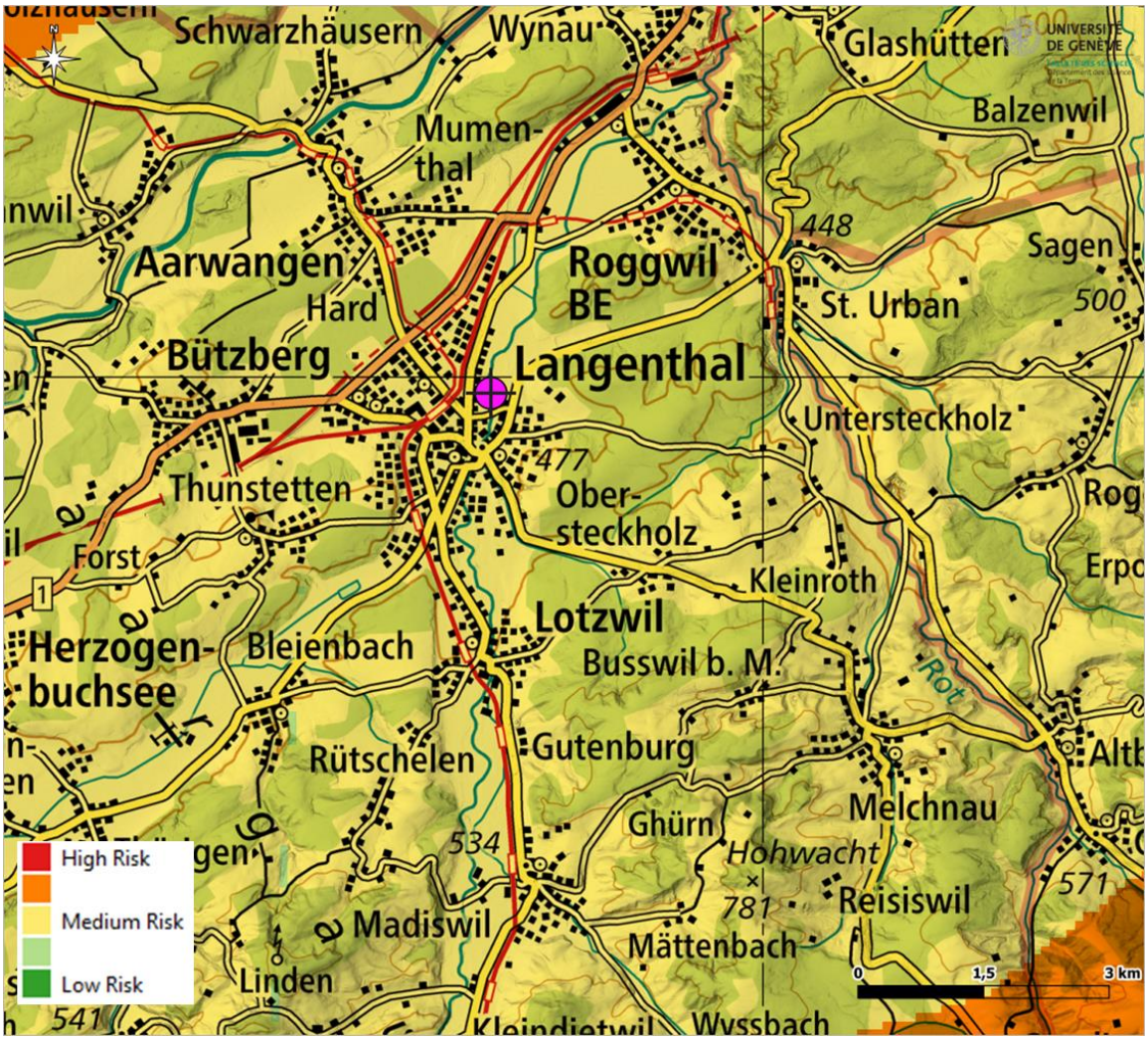
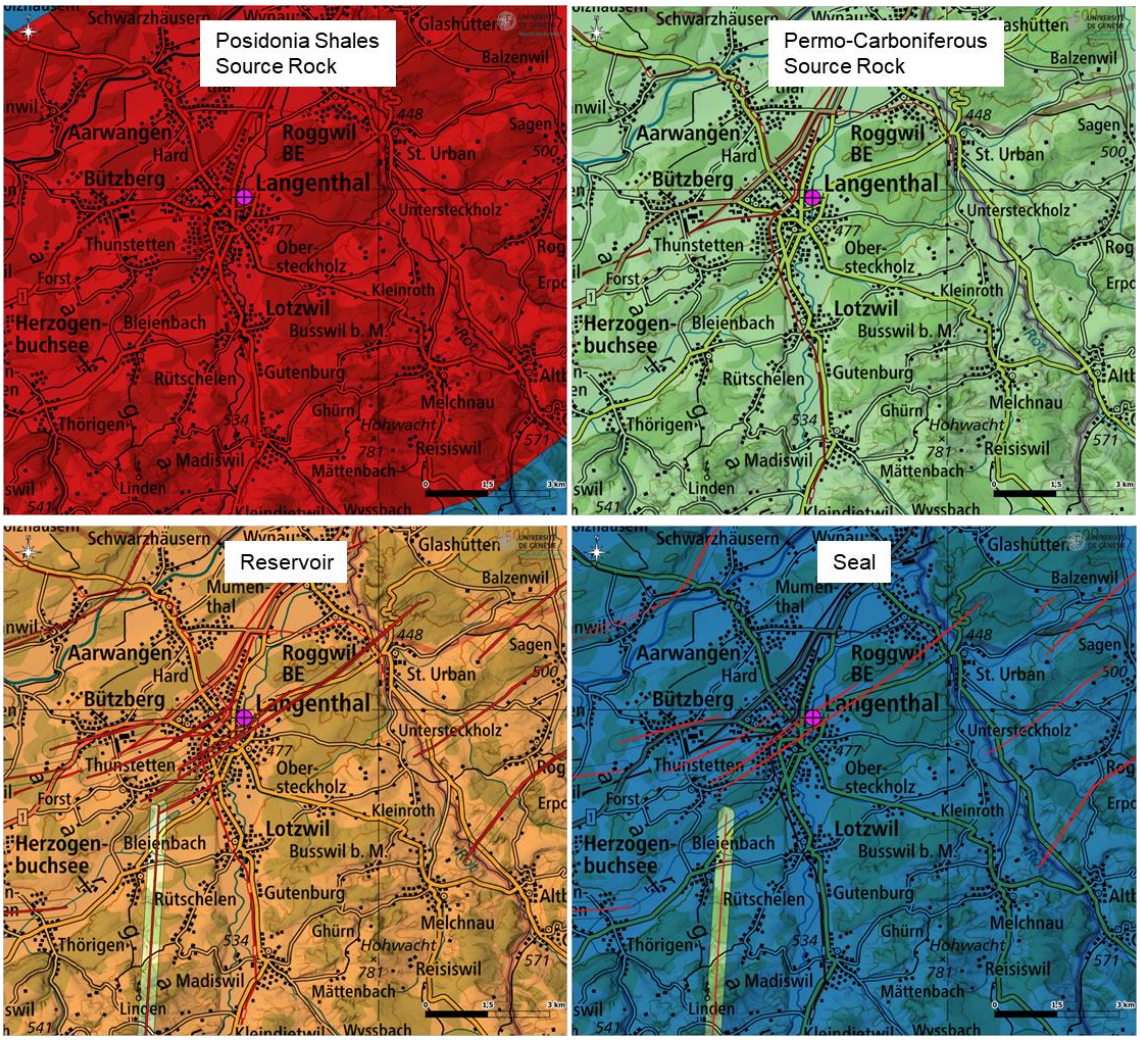


Fig. 167: CRS map for the Dogger play in the prospected area.

4.3.1 Play components evaluation

The play component maps (Fig. 168) indicate that the Permo-Carboniferous source rock is classified in Class 5, as it is not present in the areas, whereas the Posidonia shale source rock is classified in Class 2, as it is supposed that is present in the area and that, mature, with at TOC less than 2%. The reservoir unit (Dogger) is classified in Class 4 as it is present, not porous and most likely not fractured. However, in the southern part of the Langenthal town, there is a fault which might be associated with open fractures. The seal unit (Lower Malm) is present and effective (i.e. impermeable) but potentially disrupted locally by an N-S fault in the southern part of the study area.



SOURCE ROCK				
Class	Presence	Maturity	TOC > 2%	Color Legend
1	Y	Y	Y	
2	Y	Y	N	
3	Y	N	Y	
4	Y	N	N	
5	N	N	N	

RESERVOIR ROCK				
Class	Presence	Phi > 15%	R fractured	Color Legend
1	Y	Y	Y	
2	Y	Y	N	
3	Y	N	Y	
4	Y	N	N	
5	N	N	N	

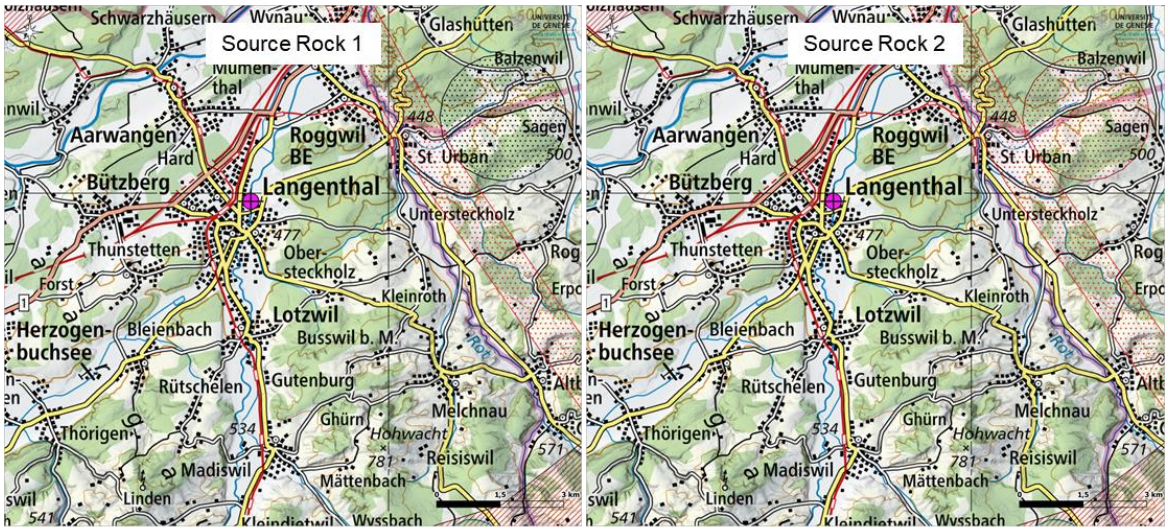
SEAL ROCK				
Class	Presence	Integrity	Impermeable	Color Legend
1	Y	Y	Y	
2	Y	N	Y	
3	Y	Y	N	
4	Y	N	N	
5	N	N	N	

Fig. 168: Play elements maps for the Dogger in the prospect area. The Reservoir and Seal CRS map shows the presence of an N-S oriented fault which affects both the reservoir (class 3) and seal (class 2).

4.3.2 Data availability

To understand the uncertainties in the play elements assessment, the “data availability” map for each play element must be consulted (Fig. 169). Several data are available in the area, including the petroleum system modelling results, as one of the modelled sections (Section 4) passes very close to the area (see Source rock data availability area, class H). The data occurrence map shows that this area benefits from a good data density, as 2D seismic lines and the Pfaffnau-1 borehole

are close to the prospected area (Fig. 170). The user can consult the database to gain more information on the available datasets during the planning phase of the project.



SOURCE ROCK DATA availability					
Class	Occurrence	TOC/Rock Eval	VR	Model calibration	Legend
A	Y	Y	Y	Y	
B	Y	Y	Y	N	
C	Y	N	Y	Y	
D	Y	Y	N	N	
E	Y	N	Y	N	
F	Y	N	N	Y	
G	Y	N	N	N	
H	N	N	N	Y	
I	N	N	N	N	

RESERVOIR DATA availability					
Class	GeoMol Surface	GeoMol Fault	Occurrence in well	Porosity data	Legend
A	Y	Y	Y	Y	
B	Y	Y	Y	N	
C	Y	N	Y	Y	
D	Y	Y	N	N	
E	Y	N	Y	N	
F	Y	N	Y	Y	
G	Y	N	N	N	
H	N	N	Y	N	
I	N	N	N	N	

SEAL DATA availability					
Class	GeoMol Surface	GeoMol Fault	Occurrence in well	Lithology data	Legend
A	Y	Y	Y	Y	
B	Y	Y	Y	N	
C	Y	N	Y	Y	
D	Y	Y	N	N	
E	Y	N	Y	N	
F	Y	N	Y	Y	
G	Y	N	N	N	
H	N	N	Y	N	
I	N	N	N	N	

Fig. 169: Data availability in the area for the Dogger geothermal play

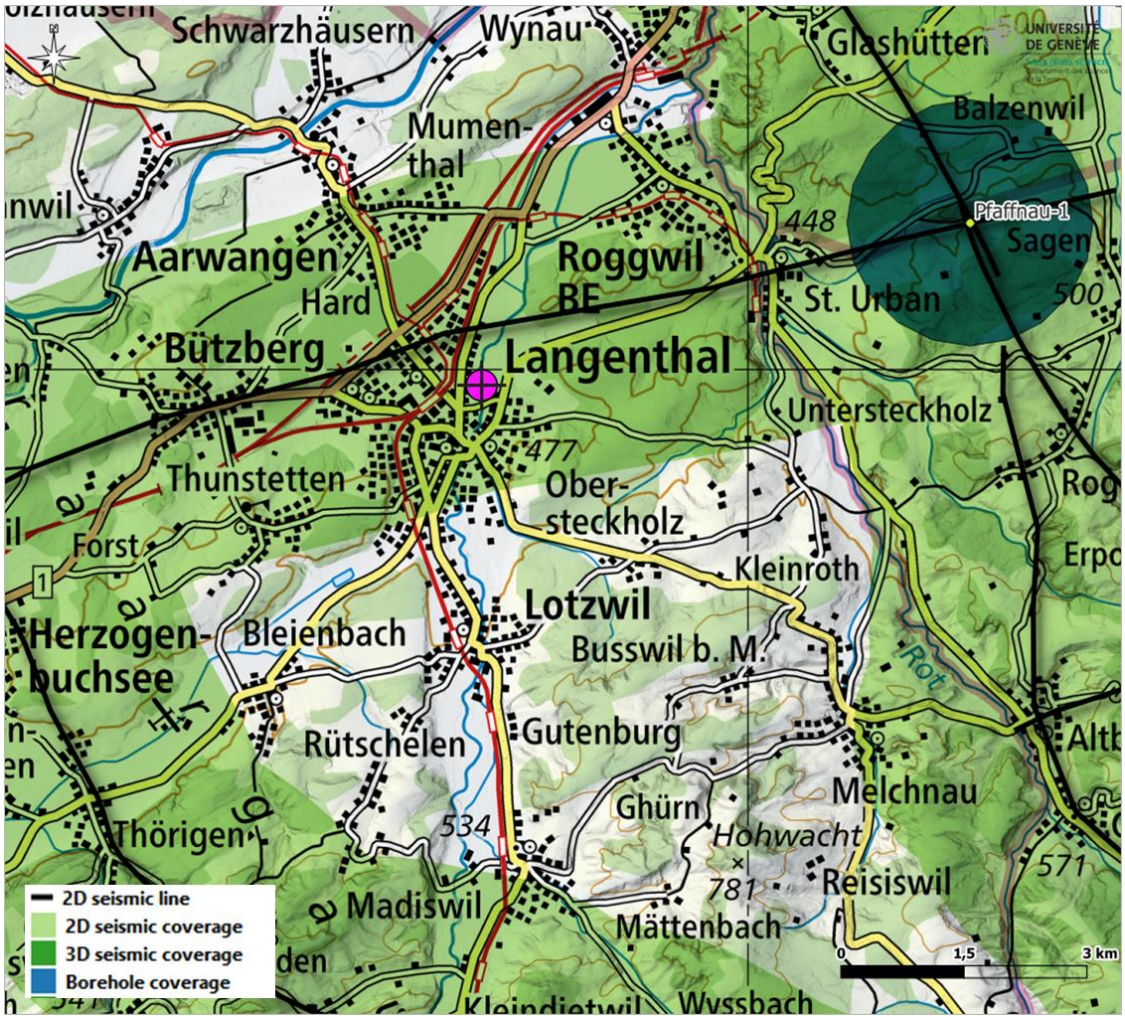


Fig. 170: Data coverage in the prospected area with indication of the data availability (2D seismic lines and deep boreholes).

4.3.3 Recommendations

In the presented case, characterised by good data coverage and availability, the user is recommended to ensure that mitigation actions related to a medium risk of encountering hydrocarbons while drilling are put in place. This could include:

- Well design tailored to hydrocarbon risk management (BOP, kill lines, diverters, etc).
- Plan for data acquisition to assess the lack of data coverage emphasized by the data occurrence map, i.e. evaluate the possibility to acquire a 3D seismic survey in order to map possible hydrocarbon trapping structures and migration paths from active source rock(s) present in the area.
- Perform 2D and/or 3D petroleum generation and migration modelling (across the area
- Monitoring before, during and after drilling, such as seismic monitoring, air and water quality around the drilling site monitoring, etc...
- Ensure that the drilling personnel are aware, trained and prepared in case of gas or oil seepages.

4.4 Yverdon-Les-Bains, example of deviated well into a medium to high-risk area.

This example considers a hypothetical existing project located in the Yverdon-Les-Bains area, in an advanced drilling planning phase (Fig. 171). The goal of the project is to drill a deviated well across two faults. The targets are the Dogger geothermal play and then the underlying Muschelkalk reservoir.

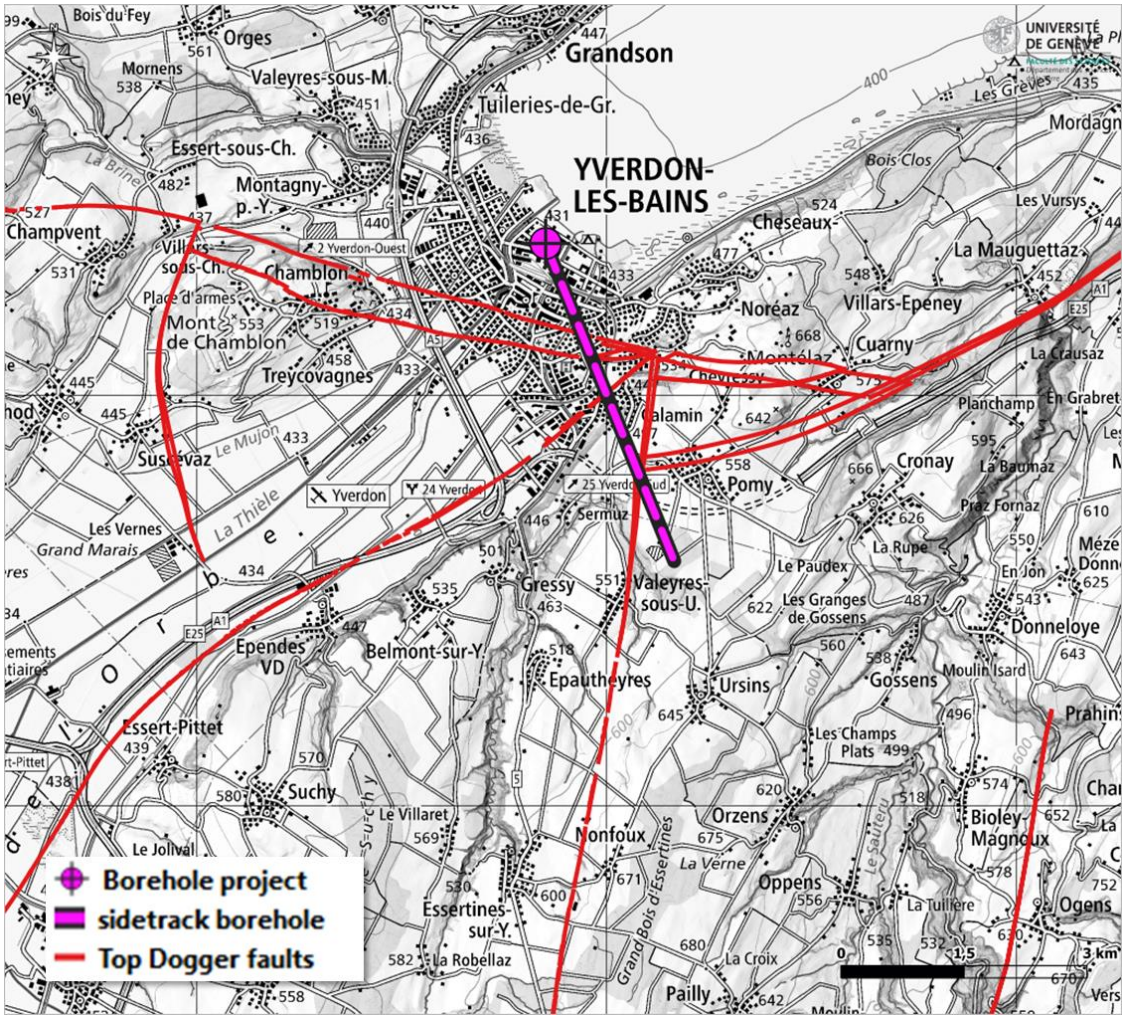


Fig. 171: Hypothetical geothermal exploration project in Yverdon-les-Bains, which considers a sidetrack through a set of faults.

Due to the sidetrack, the user must consult all CRS maps of the plays which will be encountered during the drilling operation, which are: the Cretaceous, the Dogger and the Muschelkalk plays (Fig. 171). The main relevant information provided by these maps is the following:

- The high-angle well section penetrates the Cretaceous play. This is located in a “low to medium” risk area, while the deviated track towards the SSE will penetrate a “medium risk area”. The drilling platform is in a low-risk area, therefore, there is little risk in the first stages of the drilling operations.
- In a second phase, the Dogger play will be encountered. The well crosses the targeted fault systems, which are in a “medium to high-risk” area. The targeted fault system in the Dogger, according to this CRS map, indicates that there is little risk of encountering hydrocarbons.
- Finally, the well crosses the Muschelkalk reservoir, which is in a “medium to high-risk” area. The “medium risk” zone (yellow band) is related to the presence of a fault which, based on its orientation and stress direction, is thought to be likely to seal. Therefore, the overall risk of encountering hydrocarbons during the drilling phase can be considered relatively low.

This example demonstrates how the user should consider all the CRS maps for each play crossed by the well during drilling operations. As for the other examples, in order to deeply understand the risk in the study area, the user is advised to consult the assessment of each play element, the data availability and the data coverage associated with these maps.

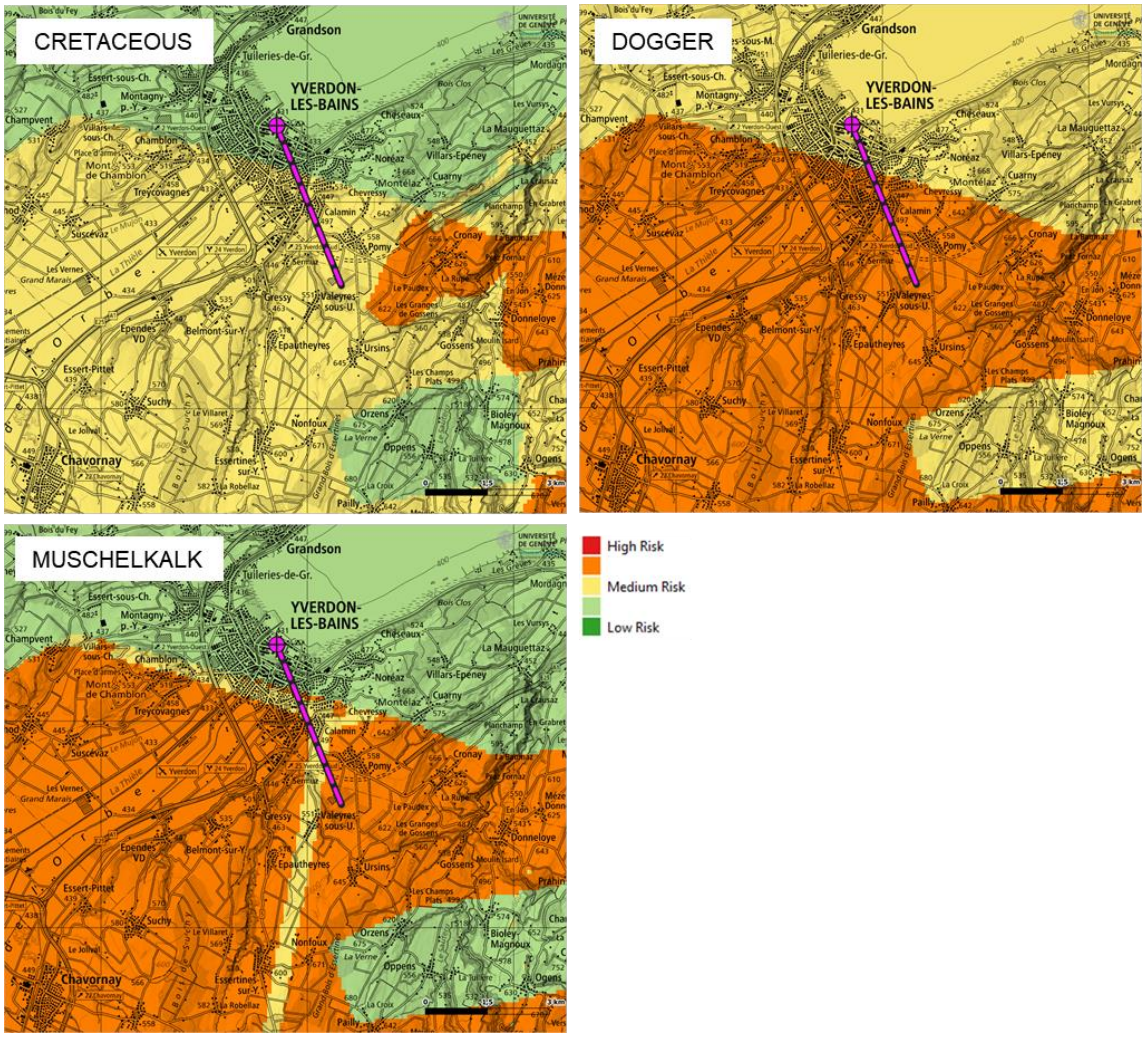


Fig. 172: Cretaceous, Dogger, and Muschelkalk CRS maps for the prospected area.

In this example, the area benefits from a high data density consisting of several 2D seismic lines and three boreholes (Fig. 173). Therefore, because of the high data density in the area, the resulting CRS maps can be considered reliable.

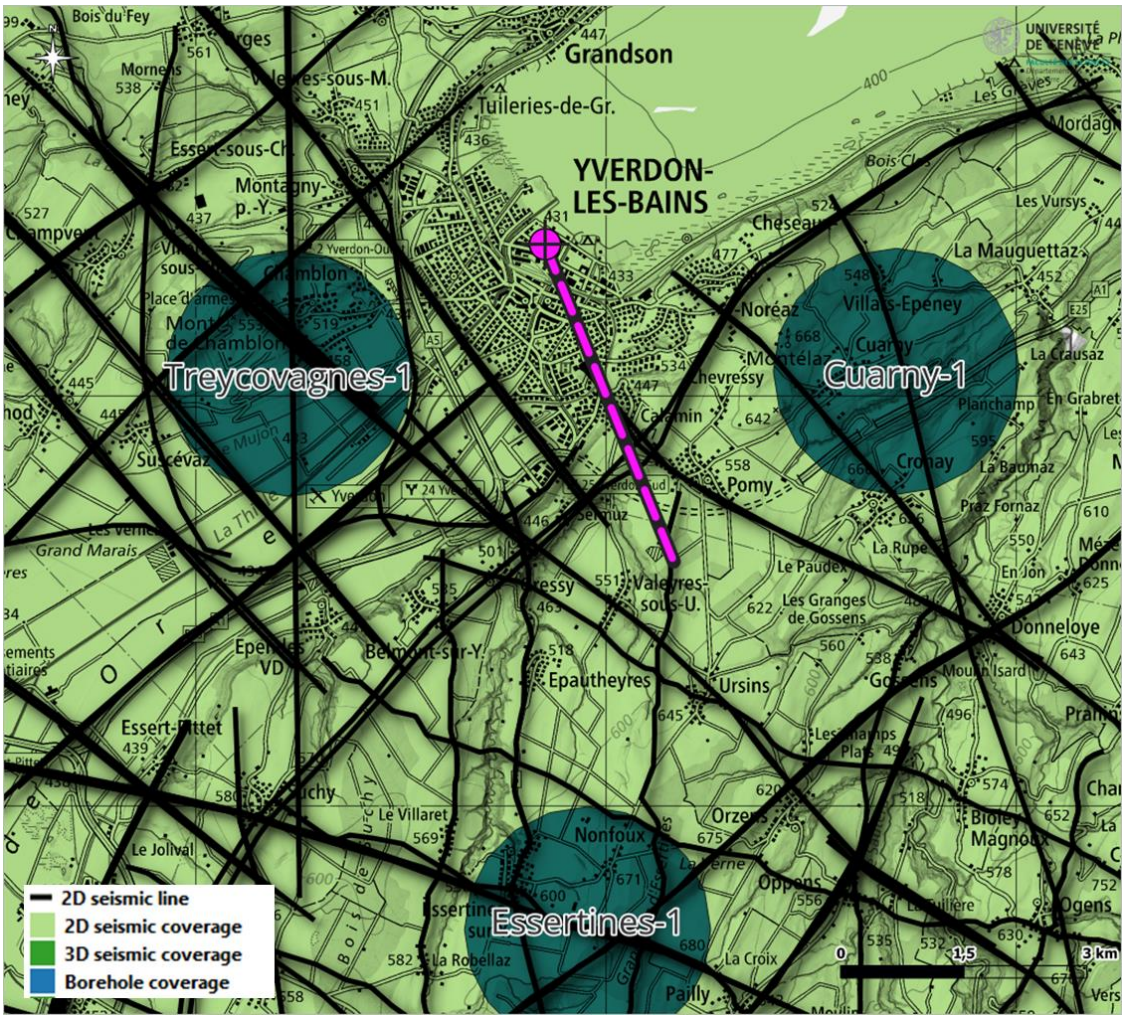


Fig. 173: Data coverage in the prospected area.

4.4.1 Recommendations

In this example, where good data coverage and data availability are present, the user should consider the risk and benefit of the well design plan. The CRS map can be used to redesign the sidetrack towards less risky areas. As for the previous examples, the user is advised to take mitigation actions related to a medium to medium-high risk of encountering hydrocarbons while drilling is in place. This could include:

- Plan for data acquisition to improve the understanding of the fault geometry by acquiring a 3D seismic survey to map possible hydrocarbon trapping structures and migration paths from active source rock(s) present in the area.
- Perform 2D and/or 3D petroleum generation and migration modelling across the area
- Well design tailored to hydrocarbon risk management (BOP, kill lines, diverters, etc).
- Monitoring before, during and after drilling, such as: seismic monitoring, air and water quality around the drilling site monitoring, etc...

Ensure that the drilling personnel are aware, trained and prepared in case of gas or oil seepages.

5 Results summary and discussion

5.1 Petroleum system modelling part

2D petroleum system models were realised along five geological sections, considered representative of the tectonic structure and stratigraphy of the entire Swiss Plateau and passing through the areas with the highest data density. In the thermal models, variations over time of the temperature and other properties, such as porosity, permeability and thermal maturity, were calculated along the section. These results were validated by calibration data (porosity, present-day temperature and vitrinite reflectance) measured in the wells located close to the model sections. The Posidonia shale source rock (Toarcian in age), mostly present in the northern part of the basin, is generally in the oil window thermal conditions. The Autunian shales source rock (Permian in age) is in the late oil window to wet gas window thermal conditions in the Permo-Carboniferous grabens located in the northern sector of the basin, and in the wet to dry gas window conditions in the grabens located toward the south. The Carboniferous coal and shales source rocks (Carboniferous in age) are in the gas windows conditions throughout the entire basin, with some local exceptions in the northern part of the basin, where the uppermost layers can still be in the late oil window conditions. By modelling, the areas along the sections where hydrocarbons can migrate and accumulate were determined. Hydrocarbons generated by the Posidonia shale source rock (mostly oil) generally accumulated in the Upper Jurassic and/or Cretaceous units, in structural traps formed in the latest Alpine deformation phases. Hydrocarbons generated by the Permian and Carboniferous source rocks (mostly gas) accumulate in the upper Permian and lower Mesozoic sandy deposits (mainly Buntsandstein and Muschelkalk units), sealed by the evaporitic Triassic units. Hydrocarbons mostly migrate along deep faults, connecting the Permo-Carboniferous grabens to the Mesozoic cover. Throughout the entire basin, several hydrocarbon migration paths formed in the Mesozoic and Cenozoic (Molasse) units, mainly along faults and permeable facies.

The petroleum system modelling generally reconstructs more hydrocarbon accumulations than what effectively found along the modelled sections. That is because we assign in the model the most favourable conditions to generate and accumulate hydrocarbons in the basin, to simulate the worst-case scenario (highest risk) for the geothermal exploration. However, due to the numerous assumptions made in constructing the petroleum system models presented in this work, a significant level of uncertainties in the results must be considered (see “Uncertainties and assumptions paragraph). In the future, additional data acquisition will be needed to improve the reliability of the modelling results.

5.2 Common Risk Segment Mapping

Common Risk Segment (CRS) maps were generated for the entire Swiss Plateau, which illustrate the spatial distribution of geological risk associated with a "working petroleum system" within a wider active Petroleum Play. In this study, the resulting CRS maps are of qualitative nature and aim to propose a graphic representation of the likelihood of encountering an accumulation of hydrocarbon in the Swiss Plateau where a future deep (> 0.5 km) geothermal well could be drilled. A CRS map was obtained for selected key potential geothermal Plays by assessing the quality of the respective source rocks, reservoir, and seal. In addition to the CRS maps, a set of data assessment and data availability maps is also provided. These maps illustrate the type of data used to produce the CRS map and how they have been interpreted. The data availability maps are key to highlighting the data gaps where acquisition is required to assess the risk of further subsurface projects, and they also highlight where the results from the CRS maps are associated with greater uncertainty.

To simplify, in the CRS maps oil and thermogenic gas accumulations were not differentiated, whereas the general hydrocarbons notion was used. Potential biogenic gas accumulations in the shallower deposits are not represented because of the lack of data concerning the organic-rich facies distribution in the shallower Quaternary and Molasse units.

The Cretaceous play is present only in the western sector of the Plateau. The source rocks of this play are both the Posidonia shale and the Permo-Carboniferous units. The reservoir is represented by the karstified and/or fractured limestones and marls composing the Lower Cretaceous unit (Early Cretaceous in age), and the seal is represented by the shales and marls composing the Molasse units (Cenozoic in age). Data and interpretations demonstrate that the quality of the reservoir (Lower Cretaceous unit) is poor in most of the Plateau, whereas the quality of the seal (Molasse unit) is good in the central part of the Plateau and poor at the borders. The resulting CRS map indicates that most of the Plateau displays medium-low risk. This risk increases to “medium to high” on top of the known Permo-Carboniferous troughs.

The Malm play is present in the entire Plateau. The source rocks of this play are both the Posidonia shale and the Permo-Carboniferous units. The reservoir is represented by Karstified and/or fractured micritic limestones and reef composing the Upper Malm unit (Late Jurassic in age) and the seal is represented by the argillaceous limestones intercalated in the Malm (not representable at a regional scale), the Cretaceous marls, or the shales and marls composing the Molasse units when the Cretaceous is not present. Data and interpretations indicate that the quality of the reservoir (Malm unit) is poor throughout the entire Plateau, whereas the quality of the seal (Molasse or Lower Cretaceous units) is very good. The resulting CRS map shows that most of the western and central sector of the Plateau displays a medium risk. This risk increases to “medium to high” on top of the Permo-Carboniferous troughs. The south-eastern part of the Swiss Plateau exhibits the lowest risk associated with the absence (non -non-deposition) of the Posidonia shale and with the poor reservoir properties.

The Dogger play is present in mostly the entire Plateau. The source rocks of this play are both the Posidonia shale and the Permo-Carboniferous units. The reservoir is represented by oolitic limestones composing the Dogger unit (Middle Jurassic in age), and the seal is represented by marly and shaly limestones composing the Lower Malm unit (Late Jurassic in age). Data and interpretations indicate that the quality of the reservoir (Dogger unit) is poor throughout the entire Plateau, whereas the quality of the seal (Lower Malm unit) is very good. The resulting CRS map shows that in the western sector of the Plateau, an extended area results in the medium risk class. This risk increases on top of the Permo-Carboniferous troughs. In the areas located in the south-eastern part of the Swiss Plateau, the result is low risk, due to the non-deposition of the Posidonia shale and an overall poor reservoir property.

The Lias play is present in mostly the entire Plateau. The source rocks of this play are both the Posidonia shale and the Permo-Carboniferous units. The reservoir is represented by sandstones, forming the Rhaetian and/or Lias units (Late Triassic, Early Jurassic in age), and the seal is represented by superimposed shale deposits, included in the same Lias unit and/or in the Dogger unit (Opalinus Clays). Data and interpretations indicate that the quality of the reservoir (Rhaetian and/or Lias unit) is poor throughout the entire Plateau, whereas the quality of the seal (Lias and/or Dogger) is very good. The resulting CRS map shows that in the west-central part of the Plateau, an extended area displays medium risk, which increases to high on top of the Permo-Carboniferous troughs. The south-eastern part of the Swiss Plateau exhibits low risk associated with a non-deposition of the Posidonia shale and overall poor reservoir properties, except for areas on the top of the Permo-Carboniferous troughs, where the risk is medium. In the north-eastern sector, the risk is medium to high, because of that both Posidonia shale and Permo-Carboniferous source rocks are present.

The Muschelkalk play is present in the entire Plateau. The source rock of this play is only the Permo-Carboniferous unit. The reservoir is represented by the Trigonodus dolomite and the Melser sandstone deposits, composing the Muschelkalk unit (Middle Triassic in age), as well as the Buntsandstein (Early Triassic in age). The seal is represented by anhydrite and salt, alternated with shales and marls, composing the Middle Muschelkalk and Keuper units (middle to late Triassic in age). Data and interpretations indicate that the quality of the reservoir (Muschelkalk and Bundsandstein units) is poor throughout the entire Plateau, except for a few areas, where medium to high porosity has been measured. The quality of the seal (Keuper and middle Muschelkalk units) is very good. The resulting CRS map shows that the risk is low to medium throughout the entire

Swiss Plateau. Medium to high-risk areas are located on the top of the Permo-Carboniferous troughs and in the proximity of certain faults, where the risk is medium to medium-high.

The Permo-Carboniferous play is present only in the areas where Permo-Carboniferous troughs are present. The source rock of this play is only the Permo-Carboniferous units. The reservoir is represented by the Permian and Carboniferous units, composed of sandstones, and the seal is represented by anhydrite and shales, composing the Mushelkalk and Keuper units, middle to late Triassic in age. Data and interpretations indicate that the quality of the reservoir (Permian and Carboniferous units) is poor throughout the entire Plateau, whereas the quality of the seal (Keuper and Muschelkalk units) is very good. The resulting CRS map shows that the risk of encountering hydrocarbons is medium-high in the areas where the Permo-Carboniferous troughs are located, and low in the rest of the Plateau. However, it is relevant to stress that the spatial distribution of the PC troughs is still poorly understood, and in some areas, their presence remains highly speculative.

Finally, to represent visually the spatial distribution of the data used to generate the CRS maps, data occurrence maps were produced. Occurrence refers to the visual representation of the spatial distribution of areas with sufficient data density, where CRS maps have less uncertainty. This map provides critical insights into defining areas of lower certainty. Geological uncertainty related to the lack of seismic or borehole data can arise primarily due to the absence of direct subsurface information, which is crucial for understanding geological structures, formations, and rock properties (e.g. reservoir porosity, seal integrity, etc). Without accurate data inputs, geological models rely on assumptions or extrapolations. This introduces uncertainties that can affect the reliability of predictions and decisions based on these models.

5.3 Uncertainties and assumptions

Petroleum system modelling simulates that the largest accumulations form in the upper Permian and lower Mesozoic sandy deposits (mainly Buntsandstein and Muschelkalk units). These hydrocarbon accumulations are most likely generated by the Permian and Carboniferous source rocks, which are, in most cases, in the late oil and gas windows. Hydrocarbons migrate along deep faults, bounding the Permo-Carboniferous grabens and accumulate in the overlying Triassic units in stratigraphic and/or structural traps. In these units, hydrocarbons were effectively found in the Noville-1, Weiach-2 and most likely also in the St. Gallen-GT-1 wells. Therefore, the areas close to the Permo-Carboniferous grabens present medium to high risk of encountering hydrocarbon accumulations. Thus, in the CRS maps, medium to high risk is most likely encountered on the top of the Permo-Carboniferous grabens for most of the Plays. As the foreland basin is dipping southward, hydrocarbons migration north and upwards can also be envisaged. However, it is relevant to emphasise that, as the infill of these grabens is in most cases unknown and their exact location and geometry are uncertain, the risk assigned in these areas could be overestimated. Permian and Carboniferous oil/gas-prone source rocks could be absent in the grabens or have an insufficient hydrocarbon potential to be able to generate enough hydrocarbons to form relevant accumulations. Further studies, based on new 3d seismic data and/or the processing of existing 2D seismic data, would enable us to constrain the exact location, thickness and infill content of these grabens.

In this study, the Keuper and Muschelkalk anhydrite facies are generally considered to be a good seal of the Permian and Triassic deep reservoirs throughout most of the Plateau. This is because in the wells where these units have been encountered, lithologic and thickness data indicate that these units could represent an impermeable barrier, able to seal hydrocarbon accumulations. However, further away from these few wells where the presence of the salt and anhydrite facies is proved, the spatial distribution and thickness variation of these facies remain unknown. In addition, recent 3D seismic data from the Geneva area undoubtedly demonstrate the connection between deep-seated faults and the shallower Mesozoic and Cenozoic overburden in locations where salt collapse structure can be identified, as well as possible migration routes from deep Palaeozoic source rocks to shallower reservoirs. This points toward a much more complex structural configuration than usually believed by following the well-consolidated thin-skin tectonic model (Moscariello et al., 2024).

Salt and anhydrite facies not identified in seismic data were not mapped in the GeoMol project. When Triassic salt/anhydrite facies are absent or very thin, hydrocarbons generated by the Permian and Carboniferous source rocks could migrate to the uppermost units and/or seep to the surface. Further studies, focused on the detailed mapping of these impermeable facies, would constrain the presence of efficient seals and traps throughout the Plateau. These data would improve the risk evaluation of gas accumulations in the stratigraphic units below the salt/anhydrite facies.

According to the model, smaller accumulations, dominantly composed of oil and subsequently of gas, are also simulated in the Jurassic and Cretaceous units, and accumulated in structural traps formed in the latest Alpine deformation phases. Oil and gas traces have been found frequently in these units in several wells throughout the entire Plateau. In particular, an economic gas accumulation was found in the Malm reservoir in the Entlebuch-1 well. These hydrocarbons could be generated by the Posidonia shale source rock, especially where it is present, in the western-northern sector of the Plateau, as well as by the deeper Permian and Carboniferous source rocks. Hydrocarbon accumulations in the Jurassic and Cretaceous units can differ from what is simulated by the model and estimated in the CRS maps because of several uncertainties on the hydrocarbon potential of the source rocks as well as on the reservoir and seal properties. Porosity data indicate low reservoir properties for most of the Mesozoic units. Make exceptions for some high porosity values measured in the Muschelkalk and Buntsandstein units; despite that, the average of the measured data in the well for the entire unit is always < 15%. Furthermore, these data are too scattered to extrapolate to the rest of the Plateau. This is why in the CRS maps, the reservoir quality is poor in most of the Plays.

The facies distribution represented in the model along the sections and in the CRS maps was extrapolated from the wells' data. Wells with lithological data are few and scattered across the Plateau. Therefore, when far from the wells, the facies lateral variation of both reservoir and seal units cannot be properly represented. Thus, their permeability and integrity properties could be different from what is simulated by the model and considered in the CRS maps. Furthermore, the model does not take into account the diagenetic processes that occurred during the basin evolution, which could considerably decrease or increase reservoir permeability by secondary pore-plugging cement precipitation or dissolution processes, respectively.

Faults have a key role in forming and preserving hydrocarbon accumulations. They may represent fluid conduits facilitating hydrocarbon migration from the source rocks to the reservoirs. If the faults are sealed by cement or clay smear, fluids cannot circulate, thus, they are considered closed. Cementation is controlled by structural stress and diagenetic processes, which must be considered to estimate the risk of encountering hydrocarbons in a fault area. In this study, the petroleum system modelling considered a first scenario where faults were not cemented (open fault scenario). This scenario simulates the maximum hydrocarbon circulation efficiency, thus a maximum risk of encountering hydrocarbons during geothermal exploration activity. A second scenario with all faults cemented (closed faults scenario) was tested. In this case, hydrocarbons generated by the source rocks remain mostly trapped in the closest reservoir units, and fewer hydrocarbons circulate in the basin, which results in a lower risk for geothermal exploration activity than in the open fault scenario.

The nature and behaviour of the deep basement faults bounding the Permo-Carboniferous grabens are not well constrained. To simulate the most efficient migration from the Permian and Carboniferous source rocks, this study has considered that faults extended to the Mesozoic cover and were reactivated during the Alpine collisional phase. Therefore, they could be efficient fluid conduits, permitting the migration of hydrocarbons generated by the deep Palaeozoic source rock to the shallower stratigraphic units. Another hypothesis is that these deep basement faults may not have been reactivated during the Alpine collision phase, thus not extending to the Mesozoic cover. In this case, the hydrocarbons generated from the Permian and Carboniferous source rocks would hardly migrate to the uppermost stratigraphic units, resulting in fewer accumulations in the Mesozoic and Cenozoic sequences. More data and further simulations would be necessary to test properly these different scenarios.

Regional stress has a strong impact on the hydrocarbon accumulation and preservation processes, as it controls the fracturing of the reservoir and seal rocks. In the case of the Swiss Plateau, where

most of the potential reservoirs have very low porosity because of the diagenetic processes related to deep burial, natural fracturing could have improved the reservoir properties by increasing their permeability. On the other hand, fracturing of a seal unit can damage its integrity and induce the leakage of possible trapped fluids, thus a secondary migration of hydrocarbons to shallower layers and/or to the surface (seepages). The structural stress factor, together with the sealing property of the faults, was implemented in the CRS maps. In this part of the study, it was considered that the faults oriented ± 45° to the regional maximum regional stress direction (sigma 1), i.e. oriented perpendicular to the Alpine thrusting direction, are closed. As a consequence, it was supposed that this family of faults preserves the seal integrity while reducing the possibility of enhanced reservoir porosity by fracture. On the other hand, it was considered that the faults oriented ± 45° to the minimum regional stress direction (sigma 3), i.e. oriented parallel to the Alpine thrusting direction, are open. As a consequence, it was supposed that this family of faults favours the reservoir fracturing, whereas it reduces the seal integrity. The assumptions proposed in this study are very general, as there are very few data to constrain them. Further studies must be carried out to improve the understanding of the fault properties throughout the Plateau, thus, their efficiency in fluid migration. This purpose can be easily carried out in case of smaller-scale, high-resolution projects, where fault properties can be looked at in detail.

Hydrocarbon migration from source rocks and/or reservoirs (i.e. leakage) is not represented in the CRS maps. Lateral migration from carriers or breaching faults can occur, mostly to the top surface and north direction, as the basin is dipping southwards. Therefore, hydrocarbon flows northward of the medium-high-risk areas indicated in the CRS maps should be envisaged. In the future, contour maps of the reservoir units should be analysed to identify potential traps (i.e. 4 and 2-way dip closure anticlines) and the related migration directions. However, the reliability of the migration route and traps depends strongly on the density of data points such as wells and seismic data. The current GeoMol structural surfaces are currently based (except for a few areas such as the northern part of the Canton of Vaud) on very sparse data points. Interpolation algorithms used to produce contour maps from a low data point density could generate misleading artefacts, which could be interpreted as structures not representative of reality (4-way dip closures).

This study does not consider the risk associated with gas occurrence at shallow depths. Shallow gas is commonly found in the Quaternary and Molasse stratigraphic units. It can be biogenic in origin, produced from the decomposition of the organic matter by anaerobic microorganisms at shallow depth, or thermogenic, generated from the thermal transformation of the organic matter at depths over 1.5 kilometres and later migrated to the subsurface through faults and/or permeable units. Gas encountered at shallow subsurface can also be linked to a mix of biogenic and thermogenic sources as demonstrated in the Geneva Basin (Do Couto et al., 2021). Biogenic gas cannot be represented in the CRS maps, as well as in the petroleum system models, because at present, the distribution of the facies rich in organic matter at shallower depth (either within the Molasse units or buried organic-rich interglacial deposits) is not known. Therefore, the exact stratigraphic intervals where biogenic gas can originate cannot be predicted. On the other hand, the potential migration of the thermogenic gas to shallow depths has been simulated by the petroleum system modelling, for which the main flow paths have been graphically represented in the modelled regional sections.

In this study, the Cenozoic play was not represented in the CRS maps. The Cenozoic play reservoir consists mostly of the Molasse units, made of sandstones of marine and terrestrial origin, intercalated with shales and marls. In this context, the occurrence of intraformational seal and stratigraphic traps must be considered. However, these have not been mapped in detail across the Plateau. For this reason, it is very difficult at the time of this study to produce risk maps for the Molasse Cenozoic play.

Finally, it must be noted that several limitations are linked to the outcomes of the 2D modelling workflow. In nature, a petroleum system in a sedimentary basin operates in the three-dimensional space and is affected by the changes in physical conditions (i.e. temperature, pressure, geometry) that the basin experiences through time. Therefore, a reliable modelling exercise would consider a three-dimensional approach. However, for practical reasons (complexity, availability of data, frame), only a two-dimensional evolution of the petroleum system was carried out using a series of regional cross-sections. Due to the two-dimensional approach, traps and migration paths cannot be properly evaluated, as in reality migration can occur away from the modelled 2D plane. Similarly, traps

identified in the 2D profile might not exist. For these reasons, it was difficult to exhaustively represent petroleum systems of the Swiss Plateau by extrapolating laterally into region-wide maps the modelling results based only on five 2D profiles. In the future, the generation of a large-scale 3D model of the petroleum system of the entire Swiss Plateau would improve the reliability and representativeness of the results, allowing a better understanding of the evolution of the petroleum system, more reliable identification of migration pathways, location of traps and assessment of risks associated with geothermal exploration activities.

6 Conclusions

This study provides an overview of the petroleum system active in the Swiss Plateau and evaluates the areas where there is the highest risk of encountering hydrocarbons (thermogenic oil and gas) in the subsurface. The definition of risk, as it is intended throughout this study, when the word “risk” is used concerning the outcomes and especially the CRS maps, explicitly refers to the risk of encountering hydrocarbons in the subsurface. In the past 80 years of subsurface exploration in Switzerland, occurrences of hydrocarbons have proved to be small. **Therefore, the word “risk” in this report does not refer by any means to the overall risk that a geothermal project might have if located in a zone defined as “medium/high risk” in the CRS maps, but to the likelihood that hydrocarbons are found during the exploration and exploitation activities.** Hydrocarbons' presence can be managed if adapted technology, such as BOP and appropriate mud control at the rig side, is implemented during the critical phases of drilling operations.

The hydrocarbon source rocks, reservoir and seal elements were characterised by considering literature data as well as new data acquired during this project. The evolution of the petroleum system was determined by applying the petroleum system modelling workflow, a methodology routinely used in the oil and gas industry. The modelling software first determines the thermal maturity of the potential hydrocarbon source rocks, based on the thermal history of the basin. Based on the maturity and distribution of the source rocks, the geometry of the basin, the faults location and the reservoir and seal properties, the modelling software calculates that hydrocarbon accumulations mostly form in the following units: i) in the Permian and Muschelkalk (mostly in the Buntsandstein facies) units, close to the areas where Permo-Carboniferous grabens are present, and ii) in the upper Jurassic and Cretaceous units, where structural traps (anticlines and faults) are present. The latter are mostly located in the northern part of the basin, close to the Jura Chain, where the Mesozoic substratum of the basin is folded and thrusted. Less frequently, structural traps can also be present in the southern part of the basin, where the Subalpine Nappes overthrust the foreland basin. As the foreland basin dips to the south, hydrocarbons might tend to migrate northward. Several hydrocarbon flows are also simulated upward in the Molasse units, mostly along faults and thrust planes. The modelling results are in good agreement with the hydrocarbon findings effectively found during the hydrocarbon exploration campaigns in Switzerland. To simulate the highest risk for the geothermal exploration, it was assumed that the source rocks have a good hydrocarbon potential throughout the entire Plateau. Thus, the generated models simulate the presence of larger accumulations, which could not be realistic. Furthermore, the reservoir and seal properties are extrapolated to the entire modelled sections from the few scattered available data measured in the wells, and they may not be representative.

Common Risk Segment (CRS) maps were produced, illustrating the spatial distribution of the geological risk associated with hydrocarbons in the subsurface throughout the entire Swiss Plateau. All the data and knowledge acquired in the previous phase on the petroleum system were integrated to compute these maps. Source rock, reservoir and seal quality assessment maps were obtained for each Play and then combined to obtain a final risk map. Data availability maps were also provided, indicating the occurrence and type of data used to build the assessment maps. The data availability maps highlight the uncertainties of the calculated risk levels presented in the CRS maps concerning the identified data gaps.

CRS maps indicate that in most plays, the highest risk of encountering hydrocarbons is related to the location of source rocks. The risk is suggested to be highest on top of Permo-Carboniferous grabens and in the western and northern sectors of the Plateau, where the Posidonia shale source rock is distributed, but uncertainties in distribution, properties and thicknesses of the source rocks need to be considered. Fault zones also represent risk areas, as hydrocarbons can flow from the source rock/reservoir to the uppermost units. Understanding the cementation state of the fault is key to properly evaluating the risk in these areas.

Because of the general poor subsurface data coverage, the final CRS maps have a considerable degree of uncertainties, as frequently the data used to build them were extrapolated from other areas and/or from our geological knowledge and understanding of the petroleum system of the basin. Therefore, in a specific area of interest, special attention needs to be paid to the occurrence, density and reliability of subsurface data. Poor data coverage could tremendously increase the risk evaluation uncertainties. Thus, in most cases, further investigations and data gathering shall be put in place to improve the evaluation of the uncertainties associated with hydrocarbon occurrence.

The maps produced by this study are useful tools for planners and decision makers, as they can be used to establish a first assessment of the risk of encountering hydrocarbons at depth. These sets of maps can be further used to propose the necessary mitigation measures (i.e. further subsurface studies, reprocessing of existing seismic data, new data acquisition, etc) and to de-risk geothermal exploration activities, specifically in the vicinity of the proposed drilling sites.

7 Outlook and next steps

Several assumptions and data extrapolations were made in this study, resulting in uncertainties in the results. Further work and data acquisition are mandatory to reduce these uncertainties. The most relevant points that need improvement are the following:

- Distribution and characterisation of the Permian and Carboniferous source rocks. At present, the geometry of the Permo-Carboniferous grabens, as well as their stratigraphic infill, is very uncertain. The geometry of the graben faults and their continuity into the Mesozoic sequence is also poorly understood. The acquisition of new deep 2D and 3D seismic and/or the reprocessing of existing geophysical data could strongly improve the understanding of these data. New wells, reaching the Permian and Carboniferous sequence, at different locations of the basin, would clarify the presence and properties of potential hydrocarbon source rocks in these grabens.
- Characterisation of the reservoir properties throughout the basin. The variation in reservoir properties throughout the Plateau can be improved by analysing the existing geophysical data (logs, seismic, etc) to extract more information that can be integrated with the limited petrophysical data (porosity, permeability, etc). Lithological data can also be improved by carrying out more lithotyping and facies analyses, both on cores and outcrops. By implementing these data, a detailed stratigraphic and facies distribution framework can be reconstructed for each reservoir unit. The acquisition of new data (porosity, permeability) would also help to improve the characterisation of reservoir properties.
- 3D geometry of potential stratigraphic and structural traps throughout the basin. More detailed mapping of potential traps can be obtained by the reconstruction of a high-resolution 3D geological model in specific areas of interest. The acquisition of new deep 2D and 3D seismic and/or the reprocessing of existing geophysical data can considerably improve the reliability of the geological model.
- Update of the faults in the Swiss Plateau. Recent, ongoing and future seismic acquisition should help in improving the fault catalogue used in the current model. Understanding the kinematic regime of the faults and main stress fields would help in better assessing the faults' properties and their effect on hydrocarbon circulation. This would significantly improve the reliability of the results provided in this study, especially in the context of the geothermal energy exploration in the Swiss Plateau, where faults are a major target for resource exploration.

- Acquisition of more calibration data to constrain the erosion magnitude and timing throughout the basin. The latter is essential to calculate the maximum temperature attained by the potential source rocks, thus their maturation and ability to generate hydrocarbons. The acquisition of new calibration data, such as vitrinite reflectance, Rock-Eval, clay minerals, and apatite fission tracks, can considerably improve the thermal modelling result reliability. At present, this action is hampered by the confidentiality status of several wells penetrating the Swiss Plateau. To acquire more data, the accessibility to cuttings and cores of most of the deep wells of the basin should be envisaged.
- Realisation of a 3d petroleum system model of the entire basin. The main outputs of this model, the thermal maturity and hydrocarbon saturation maps, could be used directly to produce the CRS maps, reducing the uncertainties associated with extrapolating the results obtained along a 2D section to maps. The main complexity of constructing a 3D model is the restoration of the thrust surfaces (subalpine Nappes and Jura fold-thrusts) in a 3D geological structural model. Therefore, to realise a 3D model of the Plateau, the structural evolution of the basin should first be constrained.
- Differentiate the nature of the potential hydrocarbon accumulations (oil and/or gas) in the CRS maps, according to the maturity state of the source rocks throughout the Plateau and the potential migration paths from deeper and more distant source rocks.
- Identify potential traps (closed anticlines) by interpreting the contour map of the top of each reservoir surface and integrating this data into the CRS maps. Potential hydrocarbon migration direction could also be recognised. Because of that, contour maps are generated from the GeoMol surfaces, which result from the interpolation of 2D seismic data; each individuated area should be carefully analysed to verify that the trap geometry appearing in the contour map is not an artefact of the interpolation. Also, the density and the resolution of the seismic data used to interpolate should be considered, as they are not homogeneous throughout the Plateau.
- Include the risk associated with the presence of biogenic gas accumulations in the shallower stratigraphic units of the basin (Quaternary and Molasse) in the CRS maps. To achieve this objective, first, a detailed map of the organic-rich facies distribution in the shallowest units must be provided.

8 National and international cooperation

The UNCONGEO project has been realised thanks to the financial and scientific contribution of several partners:

- SFOE;
- Swisstopo;
- Canton of Geneva;
- Canton of Vaud;
- NAGRA.

The collaboration with these institutions has been essential to carry out this project, by sharing geological data, knowledge on the Swiss Plateau, and by discussing the most relevant objectives of the projects as well as the workflow necessary to achieve them.

Constructive discussions with the the Audit team (Dr. Werner Leu, Dr. Armelle Kloppenburg and Dr. Andy Bell), who have accompanied the project since 2020, ensured that the work carried out by the UNIGE team met the targets and, where necessary, adapted to respond adequately to sponsor's expectations and the key objectives of the project.

The petroleum system modelling task was carried out in close collaboration with the Schlumberger technical support (Dr. Teodoro Cassola), who helped to properly plan the 2D models and to overcome the technical limitations of the software (Petromod).

The analysis of the Alpine structures and their restoration to the pre-deformation phase was performed with the valuable help of Prof. Giorgio Minelli of the University of Perugia (Italy).

In order to improve the understanding of the structural evolution of the triangular zone area and to elucidate its impact on the thermal evolution of the basin, a pilot study was carried out along one simplified section of the basin, by using the Temis thermal modelling software. This work was carried out by Dr. Juliana Gonçalves and Dr. Damien Do Couto from the ISTeP University of Sorbonne (Paris, France).

The evaluation of the hydrocarbon potential of the Permian and Carboniferous source rocks was carried out in the framework of a PhD study at the University of Leoben (Dr. Stephan Ajuaba, supervised by Prof. Reinhard Sachsenhofer), by analysing the Permian and Carboniferous stratigraphic record fully penetrated in the Weiach-1 well (northeastern of Switzerland). On the same rocks, palynological studies were carried out at the Sorbonne University (France) by Dr. Johann Schnyder.

The investigatioin of source rocks and gas seepages in the Geneva Basin was carried out by Dr. Damien Do Couto, firstly when employed at the University of Geneva, and secondly at the University of Sorbonne (Paris, France), in collaboration with other colleagues.

To evaluate the petroleum system modelling uncertainties and to analyze their impact on the modelling results, a pilot study was carried out by Dr. Mathieu Ducros (Alterna). This study integrated the machine learning tool into the modelling software, which was applied to a local project carried out in the framework of the UNCONGEO project (La Côte geothermal project).

9 Authors contribution

The UNCONGEO project was carried out between 2017 and 2024 by the staff of the Geo-Energy/Reservoir Geology and Basin Analysis (GE-RGBA) Group of the Department of Earth Sciences of the University of Geneva. This project followed the previous UNCONGAS project, which ran from 2014 to 2017, which was focusing on the assessment of the hydrocarbon potential of shale gas in the Swiss Plateau (https://www.aramis.admin.ch/Texte/?ProjectID=35783). Both projects were designed and initiated by Prof. Dr. Andrea Moscariello, who secured the funding, the management and scientific quality of the projects. For the UNCONGEO project, Dr. Silvia Omodeo Salé has been the main drive of the project, carrying out the systematic data review across the Swiss Plateau, the source rocks characterization, the reconstruction of the basin thermal evolution, the structural restoration of cross sections, the 2D and 3D petroleum system modelling and the redaction of the final report. Dr. Ovie Emmanuel Eruteya contributed by providing expertise in geophysical data management and interpretation, geological modelling and well correlations across the basin. Dr. Yasin Makhloufi contributed with his expertise in reservoir geology and was responsible for the UNCONGEO GIS database design, architecture and population and the generation of the CRS maps. All authors contributed in different ways to the final report.

10 Publications

10.1 Peer-reviewed publications in international scientific journals

Makhloufi, Y., Omodeo-Salé, S., Eruteya, O.E,., Moscariello, A. (2025). Common Risk Segment mapping to de-risk geothermal exploration. Proceedings of the European Geothermal Congress 2025 Zurich (Switzerland), 1-8.

Omodeo-Salé, S., Cassola, T., Moscariello, A. (2025). Mitigation of the geothermal energy drilling risks associated to the presence of hydrocarbons: a basin scale approach applied to the eastern Swiss Plateau area (Schlattingen-1, Herdern-1 and St. Gallen-GT-1 geothermal transect). International Journal of Coal Geology. 306, 104806.

Ajuaba, S., Sachsenhofer, R. F., Meier, V., Gross, D., Schnyder, J., Omodeo-Salé, S., Moscariello, A. and Misch, D. (2023). Coaly and lacustrine hydrocarbon source rocks in Permo-Carboniferous graben deposits (Weiach well, Northern Switzerland). Marine and petroleum geology, 150, 106147.

Omodeo-Salé, S., Hamidi, Y., Villagomez, D., Moscariello, A. (2021). Quantify multiple erosion events combining thermal modelling and apatite fission tracks data: the external sector of the Northern Alpine Foreland Basin (North-eastern Switzerland). Geosciences, 11(2), 62.

Villagomez, D., Omodeo-Salé, S., Ulyanov, A., Moscariello, A. (2021). Insights into the thermal history of north-eastern Switzerland – Apatite fission track dating of deep drill core samples from the Swiss Jura mountains and the Swiss Molasse Basin. Geosciences, 11(1), 10.

Do Couto D., Garel, S., Moscariello, A., Bou Daher, S., Littke, R., Weniger, P. (2021). Origins of oil and gas seepages in the southwestern North Alpine Foreland Basin: insights from hydrocarbon and source-rock organic geochemistry. Swiss Journal of Geosciences, 114, 1-28

Omodeo-Salé, S., Eruteya, O. E., Cassola, T., Baniasad, A., Moscariello, A. (2020). A basin thermal modelling approach to mitigate geothermal energy exploration risks: The St. Gallen case study (eastern Switzerland). Geothermics, 87, 101876.

Moscariello, A., Guglielmetti, L., Omodeo-Salé, S., De Haller, A., Eruteya, O.E., Lo, H.Y., Clerc, N., Makloufhi, Y., Do Couto, D., Ferreira De Oliveira, G., Perozzi, L., Deoliveira, F., Hollmuller, P., Quiquerez, L., De Bono, C., Martin, F., Meyer, M. (2020). Heat production and storage in Western Switzerland: advances and challenges of intense multidisciplinary geothermal exploration activities, an 8-year progress report. Proceedings of the World Geothermal Congress. Reykjavik (Iceland) - April 26 – May 2, 2020, 1-12

Moscariello A. (2019). Exploring for geo-energy resources in the Geneva Basin (Western Switzerland): opportunities and challenges. Swiss Bulletin für angewandte Geologie. Vol. 24/2, S. 105–124

10.2 Reports

Gonçalves Souza, J.M., Do Couto, D. (2024). 2D basin modelling of the triangle zone in the Eastern Swiss Molasse Basin: temperature, heat flow and pressure prediction. Sciences Sorbonne Université, 59 p.

Moscariello, A., Do Couto, D., Omodeo-Salé, S. (2023). UNCONGAS Evaluation of unconventional resource potential in the Swiss Plateau: an integrated subsurface study. OFEN, SI/5001098-1. ARAMIS, 91 p.

Ducros, M., Omodeo-Salé, S. (2023). UNCONGEO, Uncertainties analysis applying machine learning: La Côte Project case study. Internal Report, GEG2022007, 12 p.

Vranovci, B. (2022). Interprétation sismo-stratigraphique des unités Permo-Carbonifère profondément enfouies dans le Bassin Genevois: implications pour l'exploration des ressources géothermiques. Master Thesis, Département des Sciences de la Terre, Université de Genève, 52 p.

Omodeo-Salé, S., and Moscariello, A., (2022). UNCONGEO intermediate report. Report of activities 2022. GEG2022006, 102 p.

Omodeo-Salé, S., Eruteya, O. E., Makhloufi, Y., Moscariello, A. (2021). UNCONGEO intermediate report. Report of activities 2021, GEG20210006, 80 p.

Omodeo-Salé, S., and Moscariello, A. (2020). UNCONGEO Audit report, GEG2020007, 18 pp.

Omodeo-Salé, S., and Moscariello, A., (2020). UNCONGEO intermediate report. Report of activities 2020, GEG2020006, 52 p.

Meftah, E. (2020). Common risk segment map (CRS) applied to the Geneva Basin. University of Geneva. Geomatic Certificate Project 2020, in prep.

Omodeo-Salé, S., Marchant, R., Moscariello, A., (2020). Hydrocarbon occurrence assessment associated with the La Côte-Vinzel geothermal project. GEG2020005, 25 pp.

Hegazy, H. (2020). Basin modelling of the foreland basin aimed at evaluating the risk for the geothermal exploration associated with the presence of hydrocarbons in the subsurface Université de la Sorbonne, Paris. Master Thesis, 2020, 39 p.

Omodeo-Salé, S., and Moscariello, A., (2020). Hydrocarbon occurrence assessment associated with the Altendorf geothermal project. GEG2020001, 19 pp.

Villagomez, D. (2019). Apatite fission track dating of core samples from the Swiss Jura Mountains and the Molasse Basin – Insights on the thermal history of northeastern Switzerland. GEG2019004, 22 p.

Omodeo-Salé, S., and Moscariello, A., (2019). UNCONGEO intermediate report. Report of activities 2019. GEG2019003, 55 pp.

Hamidi. Y. (2019). Thermal modelling of the Northern Swiss Foreland Basin: Implication on geo-energy resources, Université de la Sorbonne, Paris. Master Thesis, 2019, 41 p.

Omodeo-Salé, S., and Moscariello, A., (2018). UNCONGEO intermediate report. Report of activities 2014-2018. GEG2018002, 117 pp.

Omodeo-Salé, S., De Haller, A., Moscariello, A., (2018). Report Analytical procedures on wells material deployed in the context of the UNCONGEO project. GEG2018001, 8 pp.

Omodeo-Salé, S., Do Couto D., Moscariello, A., (2017). UNCONGEO intermediate report. Report of activities 2017. GEG2017002, 12 pp.

10.3 Contributions to international conferences

Omodeo-Salé, S., Makhloufi, Y., Eruteya, O.E., and Moscariello, A. (2023). De-Risking geothermal exploration in the Swiss Plateau: A workflow combining the petroleum system modelling (PSM) and common potential/risk segment (CPS-CRS) mapping workflow. 21th Swiss Geoscience Meeting, Mendrisio, 2023.

Moscariello, A., Omodeo-Salé, S., Gonçalves, J., and Do Couto, D. (2023). Basin modelling as a de-risking tool for deep geothermal exploration: case studies from Switzerland. EAGE annual, Vienna, 2023.

Omodeo-Salé, S., Eruteya, O.E., Cassola, T. and Moscariello, A. (2022). Petroleum system modelling applied to the geothermal energy exploration. Schlumberger geothermal energy workshop, Geneva, 2022.

Omodeo-Salé, S., and Moscariello, A. (2020). Distribution, architecture and infill of the Permo-Carboniferous throughs in Switzerland. Deep Dust ICDP program workshop, Paris, 2020.

Omodeo-Salé, S., Cassola, T., Moscariello, A. (2019). Structural evolution of the triangle zone in the eastern fold-and-thrust Swiss Alpine belt (St. Gallen): Implications for geo-energy. 17th Swiss Geoscience Meeting, Fribourg, 2019.

Omodeo-Salé, S. Cassola, T., Eruteya, O.E., Moscariello, A. (2019). Petroleum system evolution in a fold-thrust-belt triangualr zone: A case-study from the eastern Swiss Alps. AAPG ICE, Buenos Aires, 2019.

Omodeo-Salé, S., Villagomez, D., De Haller, A., Eruteya, O.E., Guglielmetti, L., Adatte, T., Cassola, T., Moscariello, A. (2019). Reconstruction of the thermal history of the western Swiss Foreland Basin: A multidisciplinary approach to prevent risk in geothermal exploration. AAPG ICE, Buenos Aires, 2019.

Omodeo-Salé, S., Eruteya, O.E., Cassola, T., Moscariello, A. (2019). De-risking geothermal play exploration in active petroleum basins: the case of the St. Gallen well (NE Switzerland). AAPG 3rd Hydrocarbon Geothermal Cross Over Technology Workshop, Geneva, 2019.

Omodeo-Salé, S., Eruteya, O.E., Cassola, T., Adatte, T., Zieger, L., Moscariello, A. (2019). Modelling of the Petroleum System in the St. Gallen Area: Implication for Geothermal Risk Assessment. AAPG Europe Regional Conference 2019, Vienna.

Eruteya, O.E., Omodeo-Salé, S., Guglielmetti, L., Moscariello, A. (2019). New insights into the configuration of Permo-Carboniferous Grabens in St Gallen, Northern Switzerland and its Implication on Geo-Energy Prospectivity. AAPG Europe Regional Conference 2019, Vienna

Omodeo-Salé, S., Eruteya, O.E., Guglielmetti, L., Moscariello, A. (2018). New insights into the thermal and petroleum system of the St. Gallen area: Implication for geothermal exploration. 16th Swiss Geoscience Meeting, Bern, 2018.

Omodeo-Salé, S., Do Couto, D., Carraro, D., Zieger, L., Moscariello, A. (2018). Thermal modelling to prevent risks in geothermal exploration: the Geneva Basin case study (Western Switzerland). 16th Swiss Geoscience Meeting, Bern, 2018.

Omodeo-Salé, S., (2018). Is vitrinite reflectance still one of the most reliable paleothermal indicators? Workshop “Advance in thermal modelling calibration: An integrated approach”, Geneva, June 2018.

Omodeo-Salé, S., Do Couto, D., Chelle-Michout, C., Moscariello, A. (2018). Coupling hydrocarbons and geothermal exploration: the Swiss Plateau case (Switzerland). AAPG 2nd Hydrocarbon Geothermal Cross Over Technology Workshop, Utrecht, 2018.

11 References

Ajuaba, S., Sachsenhofer, R.F., Meier, V., Gross, D., Schnyder, J., Omodeo-Salé, S., Moscariello, A., Misch, D., 2023. Coaly and lacustrine hydrocarbon source rocks in Permo-Carboniferous graben deposits (Weiach well, Northern Switzerland). Mar. Pet. Geol. 150, 106147. https://doi.org/10.1016/j.marpetgeo.2023.106147

Allen, P.A., Allen, J.R., 2013. Basin analysis : principles and application to petroleum play assessment, 3rd ed. Chichester : Wiley-Blackwell.

Allenbach, R., Baumberger, R., Kurmann, E., Salomé Michael, C., Reynolds, L., 2017. GeoMol: Geologisches 3D-Modell des Schweizer Molassebeckens - Schlussbericht. Swisstopo.

Bachmann, G.H., Müller, M., 1992. Sedimentary and structural evolution of the German Molasse Basin. Eclogae Geol. Helv. 85, 519–530.

Bachmann, G.H., Müller, M., Weggen, K., 1987. Evolution of the Molasse Basin (Germany, Switzerland). Tectonophysics 137, 77–92.

Behar, F., Vandenbroucke, M., Tang, Y., Marquis, F., Espitalie, J., 1997. Thermal cracking of kerogen in open and closed systems: determination of kinetic parameters and stoichiometric coefficients for oil and gas generation. Org. Geochem. 26, 321–339. https://doi.org/http://dx.doi.org/10.1016/S0146-6380(97)00014-4

Berge, T.B., Veal, S.L., 2005. Structure of the Alpine foreland. Tectonics 24, TC5011. https://doi.org/10.1029/2003TC001588

Berger, J.-P., Reichenbacher, B., Becker, D., Grimm, M., Grimm, K., Picot, L., Storni, A., Pirkenseer, C., Derer, C., Schaefer, A., 2005. Paleogeography of the Upper Rhine Graben (URG) and the Swiss Molasse Basin (SMB) from Eocene to Pliocene. Int. J. Earth Sci. 94, 697–710. https://doi.org/10.1007/s00531-005-0475-2

Brink, H.J., Burri, J.P., Lunde, A., Winhard, H., 1992. Hydrocarbon habitat and potential of Swiss and German Molasse Basin: A comparison. Eclogae Geol. Helv. 85, 715–732.

Burkhard, M., 1990. Aspects of the large-scale Miocene deformation in the most external part of the Swiss Alps (Subalpine Molasse to Jura fold belt). Eclogae Geol. Helv. 83, 559–583.

Burkhard, M., Sommaruga, A., 1998. Evolution of the western Swiss Molasse basin: structural relations with the Alps and the Jura belt. Geol. Soc. London, Spec. Publ. 134, 279–298. https://doi.org/10.1144/gsl.sp.1998.134.01.13

Capuzzo, N., Wetzel, A., 2004. Facies and basin architecture of the Late Carboniferous Salvan-Dorénaz continental basin (Western Alps, Switzerland/France). Sedimentology 51, 675–697. https://doi.org/10.1111/j.1365-3091.2004.00642.x

Cederbom, C.E., Van Der Beek, P., Schlunegger, F., Sinclair, H.D., Oncken, O., 2011. Rapid extensive erosion of the North Alpine foreland basin at 5-4 Ma. Basin Res. 23, 528–550.

Chelle-Michou, C., Do Couto, D., Moscariello, A., Renard, P., Rusillon, E., 2017. Geothermal state of the deep Western Alpine Molasse Basin, France-Switzerland. Geothermics 67, 48–65. https://doi.org/http://dx.doi.org/10.1016/j.geothermics.2017.01.004

Chevalier, G., Diamond, L., Leu, W., 2010. Potential for deep geological sequestration of CO2 in Switzerland: a first appraisal. Swiss J. Geosci. 103, 427–455. https://doi.org/10.1007/s00015-010-0030-4

Cortesogno, L., Cassinis, G., Dallagiovanna, G., Gaggero, L., Oggiano, G., Ronchi, A., Seno, S., Vanossi, M., 1998. The Variscan post-collisional volcanism in late Carboniferous–Permian sequences of Ligurian Alps, southern Alps and Sardinia (Italy): A synthesis. Lithos 45, 305–328.

Dèzes, P., Schmid, S.M., Ziegler, P.A., 2004. Evolution of the European Cenozoic Rift System: Interaction of the Alpine and Pyrenean orogens with their foreland lithosphere. Tectonophysics 389, 1–33. https://doi.org/10.1016/j.tecto.2004.06.011

Dickinson, W.R., 1974. Plate tectonics and sedimentation, in: Dickinson, W.R. (Ed.), Tectonic and Sedimentation. pp. 1–27.

Diebold, H.P., 1988. Der Nordschweizer Permokarbon-Trog und die Steinkohlenfrage der Nordschweiz. Vierteljahrsschrift der Naturforschenden Gesellschaft Zürich 133, 143–174.

Diebold, P., Naef, H., Ammann, M., 1991. Zur Tektonik der zentralen Nordschweiz, Nagra Technischer Bericht NTB.

Diehl, T., Kraft, T., Kissling, E., Wiemer, S., 2017. The induced earthquake sequence related to the St. Gallen deep geothermal project (Switzerland): Fault reactivation and fluid interactions imaged by microseismicity. J. Geophys. Res. Solid Earth 122, 7272–7290.

Do Couto, D., Garel, S., Moscariello, A., Bou Daher, S., Littke, R., Weniger, P., 2021. Origins of hydrocarbons in the Geneva Basin: insights from oil, gas and source rock organic geochemistry. Swiss J. Geosci. 114. https://doi.org/10.1186/S00015-021-00388-4

Dolivo, E., 2007. Prospectivity of the Gros-de-Vaud permit (Canton of Vaud - Switzerland). Ascent resources plc.

Eichinger, L., 2014. Hydrochemische, gasphysikalische und isotopenhydrologische Untersuchungen am Thermalwasser aus der Geothermiebohrung St. Gallen GT 1. Hydroisotop.

Elf Aquitaine, 1989a. Etudes biostratigraphiques et geochimiques de Thoune 1.

Elf Aquitaine, 1989b. Etude du gaz de Thoune 1. Pau.

Elf Aquitaine, 1983. Etude de stratigraphie, sedimentologie et geochimie organique puits Hermingen-1. Pau.

Espitalié, J., Deroo, G., Marquis, F., 1986. La pyrolyse Rock-Eval et ses applications. Troisième partie. Oil Gas Sci. Technol. 41, 73–89.

Espitalié, J., Deroo, G., Marquis, F., 1985a. La pyrolisis Rock-Eval et ses applications: Deuxième partie. Oil Gas Sci. Technol. 40, 755–784.

Espitalié, J., Deroo, G., Marquis, F., 1985b. La pyrolyse Rock-Eval et ses applications: Première Partie. Oil Gas Sci. Technol. 40, 563–580.

Greber, E., Grünenfelder, T., Keller, B., Wyss, R., 1994. Die Geothermie-Bohrung Weggis. Bull. schweiz. Ver. Pet. u. Ing. 61, 17–43.

Greber, E., Leu, W., Schegg, R., 2011. Hydrocarbon Habitat and Potential of Switzerland. An evaluation of the oil and gas potential of Switzerland based on public well data, seismic lines and basin modelling results.

Handy, M.R., Schmid, S.M., Bousquet, R., Kissling, E., Bernoulli, D., 2010. Reconciling plate-tectonic reconstructions of Alpine Tethys with the geological–geophysical record of spreading and subduction in the Alps. Earth-Science Rev. 102, 121–158.

Heuberger, S., Roth, P., Zingg, O., Naef, H., Meier, B.P., 2016. The St. Gallen Fault Zone: a long-lived, multiphase structure in the North Alpine Foreland Basin revealed by 3D seismic data. Swiss J. Geosci. 109, 83–102. https://doi.org/10.1007/s00015-016-0208-5

Homewood, P., Allen, P.A., Williams, G.D., 1986. Dynamics of the Molasse Basin of western Switzerland., in: Allen, Philip A, Homewood, Peter (Eds.), Foreland Basins. John Wiley & Sons, pp. 199–217. https://doi.org/10.1002/9781444303810.ch10

Jarvie, D.M., Claxton, B.L., Henk, F., Breyer, J.T., 2001. Oil and shale gas from the Barnett Shale, Ft. Worth basin, Texas. AAPG Natl. Conv. Denver, Color. 85, A100.

Jurisch, A., 2013. Bestimmung der gaszusammensetzung sowie 13C/12C - und D/H-isotopenanalyse an Gasproben aus dem Geothermiprojekt St. Gallen (SG-GT1). GEO-data.

Keller, B., 1992. Hydrogeologie des schweizerischen Molasse-Beckens: Aktueller Wissensstand und weiterfuhrende Betrachtungen. Eclogae Geol. Helv. 85, 611–652.

Kempter, E.H.K., 1999. Weiach: A “Tight” Gas Sandstone Play in Northern Switzerland. Bull. angew. Geol. 4, 165–170.

Kempter, E.H.K., 1994. Erdgas aus tight reservoirs. Schweizerische Tech. Zeitung 7–8, 41–45.

Kopp, J., 1937. Petrolgeologische Unter suchungen in der subalpinen Molasse zwischen Linth and Thur mit spezieller Berücksichtigung der Petrolbohrung von Tuggen.

Kuhlemann, Joachim, Kempf, O., 2002. Post-Eocene evolution of the North Alpine Foreland Basin and its response to Alpine tectonics. Sediment. Geol. 152, 45–78. https://doi.org/http://dx.doi.org/10.1016/S0037-0738(01)00285-8

Kuhlemann, J., Kempf, O., 2002. Post-Eocene evolution of the North Alpine Foreland Basin and its response to Alpine tectonics. Sediment. Geol. 152, 45–78. https://doi.org/10.1016/s0037-0738(01)00285-8

Lahusen, P.H., Wyss, R., 1995. Erdöl-und Erdgasexploration in der Schweiz: Ein Rückblick. Bull. SUISSE DES Geol. INGENIEURS DU Pet. 62, 43–72.

Laubscher, H.-P., 1965. Ein kinematisches Modell der Jurafaltung. Eclogae Geol. Helv. 58, 232–318.

Lemcke, K., 1988. Das bayerische Alpenvorland vor der Eiszeit. Geologie von Bayern I.

Lemcke, K., 1974. Vertikalbewegungen des vormesozoischen Sockels im nördlichen Alpenvorland vom Perm bis zur Gegenwart. Eclogae Geol. Helv. 67, 121–133.

Leu, W., 2012. Swiss oil/gas exploration and lessons learnt. Swiss Bull. angew. Geol. 17, 49–59.

Leu, W., 2010. Petrosvibri's project on the Chablais structure.

Leu, W., 2008. Potential der Kohlenwasserstoffressourcen Schweizer Mittelland und subalpiner Bereich, in: NAGRA (Ed.), Nagra Arbeitsbericht NAB. Wettingen, p. 15.

Leu, W., 2007. Source rock potential and 1D basin modelling Central and Western Switzerland (Hermingen-BE and Central VD).

Leu, W., Gautschi, A., 2014. The Shale Gas Potential of the Opalinus Clay and Posidonia Shale in Switzerland – A First Assessment. Swiss Bull. angew. Geol. 19, 95–107.

Leu, W., Greber, E., Schegg, R., 2001. Basin modeling NE-Switzerland, burial, erosion and temperature history of wells Benken, Weiach and Herdern-1. Unpubl. NAGRA Rep.

Link, K. 2023. Statistik der geothermischen Nutzung in der Schweiz – Ausgabe 2023. Energie Schweiz. 50 p.

Loup, B., Wildi, W., 1994. Subsidence analysis in the Paris Basin: a key to Northwest European intracontinental basins? Basin Res. 6, 159–177.

Madritsch, H., Naef, H., Meier, B., Franzke, H.J., Schreurs, G., 2018. Architecture and Kinematics of the Constance-Frick Trough (Northern Switzerland): Implications for the Formation of Post-Variscan Basins in the Foreland of the Alps and Scenarios of Their Neogene Reactivation. Tectonics 37, 2197–2220.

Magoon, L.B., Dow, W.G., 1994. The petroleum system—From source to trap. AAPG Mem. 60, 3–24.

Marchant, R., 2016. Atlas sismique du bassin molassique vaudois.

Marchant, R., Ringgenberg, Y., Stampfli, G., Birkhäuser, P., Roth, P., Meier, B., 2005. Paleotectonic evolution of the Zürcher Weinland (northern Switzerland), based on 2D and 3D seismic data. Eclogae Geol. Helv. 98, 345–362.

Matter, A., 1987. Faziesanalyse und Ablagerungsmilieus des Permokarbons im Nordschweiz Trog. Eclogae Geol. Helv. 80, 345–367. https://doi.org/10.7892/boris.90835

Mazurek, M., Hurford, A.J., Leu, W., 2006. Unravelling the multi-stage burial history of the Swiss Molasse Basin: integration of apatite fission track, vitrinite reflectance and biomarker isomerisation analysis. Basin Res. 18, 27–50. https://doi.org/10.1111/j.1365-2117.2006.00286.x

Meier, V., 2020. Hydrocarbon potential of Permo-Carboniferous rocks in borehole Weiach-1 (CH). BachelorarbeitThesis University, 31.

Misch, D., Leu, W., Sachsenhofer, R.F., Gratzer, R., Rupprecht, B., Bechtel, A., 2017. Shallow hydrocarbon indications along the Alpine thrust belt and adjacent foreland basin: distribution and implications for petroleum exploration. J. Pet. Geol. 40, 341–362.

Mitra, S., Namson, J.S., 1989. Equal-area balancing. Am. J. Sci. 289, 563–599.

Moeck, I., Bloch, T., Graf, R., Heuberger, S., Kuhn, P., Naef, H., Sonderegger, M., Uhlig, S., Wolfgramm, M., 2015. The St. Gallen project: development of fault controlled geothermal systems in urban areas, in: Proceedings World Geothermal Congress. pp. 1–5.

Monnier, F., 1982. Thermal diagenesis in the Swiss Molasse Basin: implications for oil generation. Can. J. Earth Sci. 19, 328–342. https://doi.org/10.1139/e82-025

Moscariello, A., Eruteya, O.E., Mondino, F., 2024. New insight on the structural framework of the Geneva Basin and its impact on the structuration of the Swiss foreland and geothermal exploration., in: AAPG Europe Region Symposium "Cross Regional Carbonates and Mixed

Carbonate Systems”.

Naef, H., Schlanke, S., 2014. Geothermieprojekt St.Gallen schlussbericht geologie tiefbohrung St. Gallen GT-1. Geosfer ag.

NAGRA, 2008. Vorschlag geologischer Standortgebiet für SMA- und HAA-Lager. NAGRA Tech. Rep. NTB 08-04.

NAGRA, 2002. Technischer Bericht 02-03 - Project Opalinuston, Synthese der geowissenschaftlichen Unersuchungsergebnisse. Wettingen, Switzerland.

Omodeo-Salé, S., Eruteya, O.E., Cassola, T., Beniasad, A., Moscariello, A., 2020. A basin thermal modelling approach to mitigate geothermal energy exploration risks: the St. Gallen study-case (eastern Switzerland). Geothermics 87, 101876.

Omodeo-Salé, S., Hamidi, Y., Villagomez, D., Moscariello, A., 2021. Quantifying multiple erosion events in the distal sector of the northern alpine foreland basin (North-eastern switzerland), by combining basin thermal modelling with vitrinite reflectance and apatite fission track data. Geosci. 11, 1–29. https://doi.org/10.3390/geosciences11020062

Omodeo-Salé, S., Moscariello, A., 2020. UNCONGEO: Report of activities 2020, Internal Report.

Omodeo-Salé, S., Moscariello, A., 2019. UNCONGEO: Report of activities 2019, Internal Report.

Ortner, H., Aichholzer, S., Zerlauth, M., Pilser, R., Fügenschuh, B., 2015. Geometry, amount, and sequence of thrusting in the Subalpine Molasse of western Austria and southern Germany, European Alps. Tectonics 34, 1–30. https://doi.org/10.1002/2014TC003550

Pepper, A.S., Corvi, P.J., 1995. Simple kinetic models of petroleum formation. Part I: oil and gas generation from kerogen. Mar. Pet. Geol. 12, 291–319. https://doi.org/http://dx.doi.org/10.1016/0264-8172(95)98381-E

Peters, K.E., Walters, C.C., Moldowan, J.M., 2005. The biomarker guide: biomarkers and isotopes in the environment and human history. Cambridge University Press.

Pfiffner, O.A., 2014. Geology of the Alps. John Wiley & Sons.

Pfiffner, O.A., 1986. Evolution of the North Alpine Foreland Basin in the Central Alps, in: Foreland Basins. Blackwell Publishing Ltd., pp. 219–228. https://doi.org/10.1002/9781444303810.ch11

Philippe, Y., Colletta, B., Deville, E., Mascle, A., 1996. The Jura fold-and-thrust belt: a kinematic model based on map-balancing, in: Ziegler, P.A., Horvath, F. (Eds.), Memoires Du Museum National d’Histoire Naturelle. pp. 235–261.

Poelchau, H.S., Baker, D.R., Hantschel, T., Horsfield, B., Wygrala, B., 1997. Basin simulation and the design of the conceptual basin model, in: Welte, D.H., Horsfield, B., Baker, D.R. (Eds.), Petroleum and Basin Evolution. Springer, pp. 3–70.

Price, R.A., 1973. Large-scale gravitational flow of supracrustal rocks, southern Canadian Rockies. Gravity and tectonics 491–502.

Rouby, D., Fossen, H., Cobbold, P.R., 1996. Extension, displacement, and block rotation in the larger Gullfaks area, northern North Sea: determined from map view restoration. AAPG Bull. Assoc. Pet. Geol. 80, 875.

Royden, L., Keen, C.E., 1980. Rifting process and thermal evolution of the continental margin of eastern Canada determined from subsidence curves. Earth Planet. Sci. Lett. 51, 343–361.

Rybach, L., 1992. Geothermal potential of the Swiss Molasse Basin. Eclogae Geol. Helv. 85, 733–744.

Rybach, L., Eugster, W., Griesser, J., 1987. Die geothermischen Verhältnisse in der Nordschweiz. Eclogae Geol. Helv. 80, 521–534.

Schegg, R., 1992. Thermal maturity of the Swiss Molasse Basin: indications for paleogeothermal anomalies? Eclogae Geol. Helv. 85, 745.

Schegg, R., Cornford, C., Leu, W., 1999. Migration and accumulation of hydrocarbons in the Swiss Molasse Basin: implications of a 2D basin modeling study. Mar. Pet. Geol. 16, 511–531. https://doi.org/http://dx.doi.org/10.1016/S0264-8172(99)00018-5

Schegg, R., Leu, W., 1998. Analysis of erosion events and palaeogeothermal gradients in the North Alpine Foreland Basin of Switzerland. Geol. Soc. London, Spec. Publ. 141, 137–155. https://doi.org/10.1144/gsl.sp.1998.141.01.09

Schegg, R., Leu, W., Cornford, C., Allen, P.A., 1997. New coalification profiles in the Molasse Basin of Western Switzerland: Implications for the thermal and geodynamic evolution of the Alpine Foreland. Eclogae Geol. Helv. 90, 79–96.

Schlunegger, F., Jordan, T.E., Klaper, E.M., 1997. Controls of erosional denudation in the orogen on foreland basin evolution: The Oligocene central Swiss Molasse Basin as an example. Tectonics 16, 823–840. https://doi.org/10.1029/97TC01657

Schlunegger, F., Willett, S., 1999. Spatial and temporal variations in exhumation of the central Swiss Alps and implications for exhumation mechanisms. Geol. Soc. London, Spec. Publ. 154, 157–179.

Schönlaub, H.P., 1997. The biogeographic relationships of the Carboniferous of Austria. Ber Geol BA 40, 60–73.

Sclater, J.G., Christie, Paf., 1980. Continental stretching: An explanation of the post-Mid-Cretaceous subsidence of the central North Sea Basin. J. Geophys. Res. Solid Earth 85, 3711–3739.

SEAG, 2012. Aktivitäten der SEAG in der Schweiz. Intern. Rep. 4.

Sommaruga, A., Eichenberger, U., Mariller, F., 2012. Seismic atlas of the Swiss Molasse Basin. Swisstopo.

Stampfli, G.M., 1993. Le Briançonnais, terrain exotique dans les Alpes? Eclogae Geol. Helv. 86, 1–45.

Stampfli, G.M., Borel, G.D., Marchant, R., Mosar, J., 2002. Western Alps geological constraints on western Tethyan reconstructions. J. Virtual Explor. 8, 75–104. https://doi.org/10.3809/jvirtex.2002.00057

Stoneley, R., 1995. North Sea petroleum plays, in: Introduction to Petroleum Exploration for Non-Geologists. p. 106.

Suppe, J., 1983. Geometry and kinematics of fault-bend folding. Am. J. Sci. 283, 684–721.

Taylor, G.H., Teichmüler, M., Davis, A., Diessel, C.F.K., Littke, R., Robert, P., 1998. Organic petrology. Gebrüder Borntraeger, Berlin, Stuttgart.

Tissot, B.P., Pelet, R., Ungerer, P.H., 1987. Thermal history of sedimentary basins, maturation indices, and kinetics of oil and gas generation. AAPG Bull.;(United States) 71.

Todorov, I., Schegg, R., Wildi, W., 1993. Thermal maturity and modelling of Mesozoic and Cenozoic sediments in the south of the Rhine Graben and the eastern Jura (Switzerland). Eclogae Geol. Helv. 86, 667–692.

Trümpy, R., Aubert, D., Bernoulli, D., 1980. Geology of Switzerland: Geological excursions. Wepf.

Turcotte, D., Schubert, G., 2014. Geodynamics. Cambridge university press.

Villagomez, D., Omodeo-Salé, S., Ulyanov, A., Moscariello, A., 2021. Insights into the thermal history of north-eastern Switzerland – Apatite fission track dating of deep drill core samples from the Swiss Jura mountains and the Swiss Molasse Basin. Geosciences 11, 10.

Vollmayr, T., 1983. Temperaturmessungen in Erdölbohrungen der Schweiz. Bull. der schweizerischen Vereinigung Pet. und-Ingenieure 49, 15–27.

Vollmayr, T., Wendt, A., 1987. Die Erdgasbohrung Entlebuch 1 , ein Tiefenaufschluss am

Alpennordrand Die Erdgasbohrung Entlebuch 1 , ein Tiefenaufschluß am Alpennordrand. Bull. Ver. schweiz. Pet. u. -Ing. 53, 67–79.

Von Hagke, C., Cederbom, C.E., Oncken, O., Stöckli, D.F., Rahn, M.K., Schlunegger, F., 2012. Linking the northern Alps with their foreland: The latest exhumation history resolved by low-temperature thermochronology. Tectonics 31.

von Hagke, C., Malz, A., 2018. Triangle zones–Geometry, kinematics, mechanics, and the need for appreciation of uncertainties. Earth-Science Rev. 177, 24–42.

Von Raumer, J.F., 1998. The Palaeozoic evolution in the Alps: from Gondwana to Pangea. Geol. Rundschau 87, 407–435.

Von Raumer, J.F., Neubauer, F., 1993. Late Precambrian and Palaeozoic evolution of the Alpine basement—an overview, in: Pre-Mesozoic Geology in the Alps. Springer, pp. 625–639.

Welte, D.H., Horsfield, B., Baker, D.R., 1997. Petroleum and basin evolution: insights from petroleum geochemistry, geology and basin modeling, Springer. ed. Springer, Verlag, Berlin, Berlin.

Welte, D.H., Yalcin, M.N., 1988. Basin modelling—a new comprehensive method in petroleum geology. Org. Geochem. 13, 141–151.

Welte, D.H., Yalcin, M.N., 1987. Formation and occurrence of petroleum in sedimentary basins as deduced from computer-aided basin modelling. Pet. geochemistry Explor. Afro-Asian Reg. Balkema, Rotterdam 17–23.

Welte, D.H., Yukler, M.A., 1981. Petroleum origin and accumulation in basin evolution--a quantitative model. Am. Assoc. Pet. Geol. Bull. 65, 1387–1396.

Wersin, P., Mazurek, M., Waber, H.N., Mäder, U.K., Gimmi, T., Rufer, D., de Haller, A., 2013. Rock and porewater characterisation on drillcores from the Schlattingen borehole. Nagra Arbeitsbericht NAB 12–54, 343.

Wildi, W., Funk, H., Loup, B.F.R., Amato, E., Huggenberger, P., 1989. Mesozoic subsidence history of the European marginal shelves of the alpine Tethys (Helvetic realm, Swiss Plateau and Jura). Eclogae Geol. Helv. 82, 817–840.

Wolfgramm, M., Bloch, T., Bartels, J., Heuberger, S., Kuhn, P., Naef, H., Voigt, H., Seibt, P., Sonderegger, M., Steiger, T., 2015. Reservoir-geological characterization of a fractured limestone: Results obtained from the geothermal well St. Gallen GT-1 (Switzerland), in: Proceedings of the World Geothermal Congress.

Wygrala, B.P., 1988. Integrated computer-aided basin modeling applied to analysis of hydrocarbon generation history in a Northern Italian oil field. Org. Geochem. 13, 187–197.

Yalçin, M.N., 1991. Basin modeling and hydrocarbon exploration. J. Pet. Sci. Eng. 5, 379–398.

Yalçin, M.N., Littke, R., Sachsenhofer, R.F., 1997. Thermal history of sedimentary basins, in: Welte, D.H., Horsfield, B., Baker, D.R. (Eds.), Petroleum and Basin Evolution. Springer, pp. 71–167.

Yalçin, M.N., Welte, D.H., 1988. The thermal evolution of sedimentary basins and significance for hydrocarbon generation. Bull. Turkish Pet. Geol. Ankara, 1, 12–26.

Ziegler, P.A., Bertotti, G., Cloetingh, S., 2002. Dynamic processes controlling foreland development–the role of mechanical (de) coupling of orogenic wedges and forelands. EGU Stephan Mueller Spec. Publ. Ser. 1, 17–56.

Ziegler, P.A., Schumacher, M.E., Dèzes, P., Van Wees, J.-D., Cloetingh, S., 2004. Post-Variscan evolution of the lithosphere in the Rhine Graben area: constraints from subsidence modelling. Geol. Soc. London, Spec. Publ. 223, 289–317.

12 Appendixes

12.1 Lias Rock-Eval data

Wells	Depth (m)	Unit	TOC (%)	HI (mg /g TOC)	OI (mg CO_2/g TOC)	Tmax (°C)	S1 (mg HC/g)	S2 (mg HC/g)	S3 (mg CO_2/g)
Eclépens-1	1695	Lias Zeta+Epsilon	0.54	92	195	435	0.05	0.49	1.05
	1700	Lias Zeta+Epsilon	0.47	88	62	433	0.04	0.41	0.29
	1705	Lias Zeta+Epsilon	0.39	57	72	435	0.02	0.22	0.28
	1710	Lias Zeta+Epsilon	2.32	369	24	436	0.24	8.56	0.55
	1715	Lias Zeta+Epsilon	1.95	408	21	436	0.23	7.97	0.41
	1720	Lias Delta	1.84	424	30	432	0.24	7.78	0.55
	1725	Lias Delta	2.37	493	15	437	0.48	11.70	0.36
	1730	Lias Delta	0.84	231	42	436	0.07	1.93	0.35
	1735	Lias Delta	0.68	112	39	435	0.04	0.76	0.27
	1775	Lias Delta	1.79	449	16	437	0.37	8.05	0.28
	1836	Lias Gamma	0.61	58	50	430	0.04	0.36	0.30
	1888	Lias Gamma	0.49	92	36	435	0.04	0.46	0.18
	2037.5	Lias Alpha	0.72	115	38	440	0.11	0.83	0.28
	2043	Lias Alpha	0.73	112	33	435	0.05	0.81	0.24
	2044	Lias Alpha	0.42	90	58	437	0.07	0.38	0.24
	2066	Lias Alpha	0.50	95	55	438	0.08	0.47	0.27
	2068.7	Lias Alpha	2.35	192	10	444	0.50	4.52	0.23
	2070.4	Lias Alpha	1.91	330	11	443	0.25	6.30	0.22
	2081.3	Lias Alpha	1.53	283	15	439	0.22	4.32	0.23
Essertines-1	1904	Toarcian	0.68	116	42	434	0.05	0.79	0.29
	1906	Toarcian	0.70	112	54	435	0.06	0.78	0.38
	1908	Toarcian	0.64	174	41	432	0.04	1.11	0.26
	1910	Toarcian	0.55	138	65	435	0.05	0.76	0.36
	1912	Toarcian	0.55	87	74	432	0.03	0.47	0.41
	1914	Toarcian	0.62	111	55	435	0.04	0.68	0.34
	1916	Toarcian	0.33	98	103	429	0.03	0.32	0.34
	1918	Toarcian	0.53	113	68	435	0.04	0.60	0.36
	1920	Toarcian	0.47	103	69	434	0.03	0.49	0.33
	1922	Toarcian	0.37	130	75	435	0.05	0.47	0.28
	1924	Toarcian	0.33	178	89	432	0.06	0.60	0.30
	1926	Toarcian	0.63	89	49	435	0.04	0.56	0.31
	1928	Toarcian	0.52	108	63	432	0.06	0.56	0.33
	1930	Toarcian	0.49	136	69	434	0.08	0.66	0.34
	1932	Toarcian	0.44	113	65	435	0.04	0.50	0.29
	1934	Toarcian	0.73	104	47	436	0.03	0.76	0.35
	1936	Toarcian	0.55	128	66	437	0.04	0.71	0.37
	1938	Toarcian	0.58	156	65	434	0.05	0.90	0.38
	1940	Toarcian	0.52	126	60	436	0.04	0.66	0.32
	1942	Toarcian	0.64	121	53	439	0.04	0.77	0.34
	1944	Toarcian	0.66	122	51	436	0.06	0.81	0.34

Wells	Depth (m)	Unit	TOC (%)	HI (mg /g TOC)	OI (mg CO_2/g TOC)	Tmax (°C)	S1 (mg HC/g)	S2 (mg HC/g)	S3 (mg CO_2/g)
Essertines-1	1946	Toarcian	0.67	140	50	439	0.04	0.94	0.34
	1948	Toarcian	0.71	150	46	436	0.07	1.07	0.33
	1950	Toarcian	0.55	113	66	432	0.03	0.63	0.37
	1952	Toarcian	0.67	99	74	435	0.03	0.66	0.49
	1954	Toarcian	0.61	84	65	429	0.04	0.52	0.40
	1956	Toarcian	0.57	122	50	435	0.04	0.69	0.29
	1958	Toarcian	0.62	113	58	434	0.04	0.70	0.35
	1960	Toarcian	0.58	119	61	434	0.04	0.69	0.36
	1962	Toarcian	0.60	116	63	434	0.05	0.69	0.37
	1964	Toarcian	0.69	120	52	435	0.05	0.82	0.35
	1966	Toarcian	0.50	129	65	434	0.07	0.64	0.33
	1968	Toarcian	0.45	116	74	437	0.04	0.52	0.33
	1970	Toarcian	0.43	111	78	431	0.04	0.48	0.33
	1972	Toarcian	0.56	107	49	434	0.04	0.60	0.28
	1974	Toarcian	0.49	96	65	433	0.03	0.47	0.31
	1976	Toarcian	0.43	110	79	435	0.05	0.48	0.34
	1978	Toarcian	0.54	125	64	437	0.06	0.68	0.34
	1980	Toarcian	2.14	388	19	438	0.26	8.31	0.41
	1982	Toarcian	2.69	479	15	439	0.62	12.87	0.41
	1984	Toarcian	2.69	474	14	436	0.61	12.74	0.38
	1986	Toarcian	3.23	478	14	437	0.50	15.43	0.44
	1988	Toarcian	0.55	143	64	430	0.05	0.79	0.35
	1990	Toarcian	0.81	313	46	432	0.12	2.55	0.37
	1992	Toarcian	0.51	151	55	438	0.04	0.78	0.28
	1994	Toarcian	0.62	116	50	436	0.04	0.72	0.31
	1996	Toarcian	0.39	121	64	436	0.04	0.48	0.25
	2000	Toarcian	1.05	288	29	435	0.08	3.03	0.30
Riniken-1	435.88	Lias	0.85	124	51	435	0.05	1.05	0.43
	435.9	Lias	0.83	114	46	433	0.03	0.95	0.39
	436.35	Lias	0.87	118	51	435	0.05	1.03	0.44
	436.98	Lias	0.94	130	53	434	0.04	1.23	0.51
	437.07	Lias	0.79	111	52	434	0.04	0.88	0.41
	455.99	Lias	4.10	546	18	427	0.39	22.39	0.75
	456.29	Lias	2.10	409	26	432	0.17	8.60	0.54
	456.41	Lias	1.74	321	26	430	0.13	5.60	0.45
	456.83	Lias	3.30	474	20	429	0.32	15.66	0.65
	457.12	Lias	2.39	472	21	429	0.23	11.30	0.51
	457.65	Lias	5.97	657	15	430	0.95	39.23	0.89
	458.46	Lias	5.45	628	13	429	0.70	34.20	0.72
	458.98	Lias	4.16	673	18	426	0.82	27.98	0.75
	459.11	Lias	8.07	666	14	423	2.06	53.79	1.17
	459.45	Lias	4.59	542	15	424	0.47	24.87	0.70
	459.85	Lias	4.92	598	13	429	0.44	29.41	0.62
	460	Lias	0.61	149	45	426	0.06	0.91	0.28
	460.14	Lias	0.35	75	77	423	0.05	0.27	0.27

Wells	Depth (m)	Unit	TOC (%)	HI (mg /g TOC)	OI (mg CO_2/g TOC)	Tmax (°C)	S1 (mg HC/g)	S2 (mg HC/g)	S3 (mg CO_2/g)
Riniken-1	460.62	Lias	0.30	78	72	425	0.04	0.24	0.22
Schafisheim-1	1079.86	Toarcian	0.85	128	28	431	0.04	1.09	0.24
Schlattingeng-1	960.38	Toarcian	7.42	668	4	428	1.34	49.54	0.30
Treyçovagnes-1	1370	Toarcian	0.49	81	69	431	0.03	0.40	0.34
	1410	Toarcian	0.73	135	47	433	0.05	0.98	0.34
	1435	Toarcian	0.58	121	45	435	0.03	0.70	0.26
Weiach-1	666.99	Toarcian	0.34	112	85	425	0.05	0.39	0.29
	672.06	Toarcian	4.83	578	20	426	0.42	27.90	0.96
	672.33	Toarcian	6.05	585	18	428	0.48	35.39	1.09
	672.51	Toarcian	6.04	589	20	427	1.01	35.55	1.19
	672.88	Toarcian	3.65	530	23	425	0.31	19.33	0.85
	673.08	Toarcian	5.05	598	19	425	0.47	30.21	0.98
	673.46	Toarcian	3.55	484	23	426	0.24	17.21	0.81
	674.06	Toarcian	3.95	540	22	424	0.29	21.30	0.85
	674.24	Toarcian	2.68	428	26	428	0.17	11.46	0.69
	674.71	Toarcian	5.51	593	18	428	0.59	32.65	1.01
	675.05	Toarcian	4.74	631	20	427	0.47	29.93	0.96
	675.46	Toarcian	6.46	673	19	425	0.81	43.45	1.26
	675.96	Toarcian	3.23	464	21	413	0.43	14.96	0.67
	676.37	Toarcian	3.32	422	22	425	0.24	14.03	0.72
	676.72	Toarcian	6.88	642	18	424	0.84	44.23	1.21
	677.07	Toarcian	5.39	547	20	422	0.55	29.51	1.06
	677.21	Toarcian	10.08	671	14	420	1.83	67.71	1.45
	677.85	Toarcian	9.70	668	13	426	1.13	64.84	1.30
	678.04	Toarcian	5.22	534	17	424	0.40	27.89	0.90
	678.23	Toarcian	6.10	556	17	426	1.12	33.89	1.04

Appendix 1: Rock-Eval data measured for the Lias stratigraphic intervals measured in the Canton of Vaud and north-eastern Switzerland areas. Rock-Eval analyses were carried out at the Department of Earth Sciences at the University of Lausanne, in the framework of the UNCONGEO project. Makes an exeception the data measured in the Schlattingen-1 well, which is from Wersin et al. (2013).

12.2 Permian and Carboniferous Rock-Eval data (Weiach-1 well)

Well	Unit	Depth	Lithology	TOC [%]	HI [mg HC/g TOC]	Tmax [°C]	S1 [mg HC/g]	S2 [mg HC/g]
Weiach-1	Permian	1194.08	Shale	0.16	16	488?	0	0.03
		1194.5	Shale	0.17	21	487?	0.01	0.04
		1194.58	Shale	0.21	19	480?	0.01	0.04
		1310.08	Shale	2.97	51	447	0.11	1.52
		1310.58	Shale	3.26	65	441	0.11	2.12
		1310.8	Shale	2.89	43	444	0.12	1.26
		1311.55	Shale	3.39	82	435	0.13	2.78
		1312.95	Shale	10.25	488	440	3.31	50.07
		1313.37	Shale	5.31	382	440	1.57	20.28
		1314.16	Shale	3.33	60	447	0.22	1.99
		1314.23	Driftwood	51.2	155	445	5.95	79.12
		1316.88	Shale	1.33	26	451	0.05	0.34
		1317.25	Shale	1.51	24	442	0.04	0.36
		1326.95	Shale	1.07	27	451	0.05	0.29
		1327.67	Shale	1.04	53	443	0.04	0.55
		1328.1	Shale	0.95	35	441	0.04	0.34
		1328.65	Shale	1.18	49	440	0.04	0.58
		1328.85	Shale	1.57	110	442	0.13	1.73
		1329.35	Shale	8.44	404	439	2.31	34.08
		1329.71	Shale	3.54	229	441	0.46	8.11
		1330.15	Shale	2.83	178	440	0.31	5.05
		1330.7	Shale	3.35	252	440	0.45	8.43
		1331.1	Shale	4.91	289	441	0.86	14.2
		1331.66	Shale	4.34	250	438	0.69	10.84
		1332.43	Shale	3.62	245	439	0.56	8.86
		1333.1	Shale	4.56	273	440	0.87	12.48
		1333.3	Shale	4.86	299	440	1.02	14.53
		1333.85	Shale	2.92	231	440	0.44	6.76
		1334.22	Shale	4.07	243	439	0.61	9.88
		1334.85	Shale	3.29	238	438	0.57	7.83
		1335.3	Shale	2.44	210	441	0.3	5.12
		1335.75	Shale	2.06	88	440	0.21	1.82
		1336.12	Shale	4.45	268	439	0.8	11.92
		1336.9	Shale	5.35	295	439	1.09	15.81
		1337.4	Shale	5.25	351	438	1.18	18.46
		1338	Shale	7.19	382	436	1.73	27.46
		1338.35	Shale	9.89	480	441	2.99	47.52
		1339.2	Shale	3.3	210	438	0.67	6.93
		1341.2	Shale	3.18	54	446	0.26	1.73
		1345	Shale	1.23	26	460	0.08	0.32
		1350	Shale	1.39	91	441	0.05	1.27
		1350.3	Shale	1.82	52	439	0.11	0.94

Well	Unit	Depth	Lithology	TOC [%]	HI [mg HC/g TOC]	Tmax [°C]	S1 [mg HC/g]	S2 [mg HC/g]
Weiach-1	Permian	1350.7	Shale	2.41	175	439	0.14	4.21
		1350.95	Shale	3.72	291	437	0.33	10.84
		1358.9	Shale	2.35	34	457	0.14	0.81
		1391	Shale	0.13	22	442?	0.01	0.03
	Carboniferous	1486.4	Coal	62.93	143	459	6.26	89.97
		1494.74	Coal	69.33	195	450	5.75	135.12
		1494.82	Shale	4.98	75	449	0.24	3.72
		1556	Shale	3.79	54	466	0.24	2.04
		1557.1	Shale	2.78	53	455	0.16	1.48
		1557.4	Shale	3.79	74	450	0.24	2.81
		1558.37	Shale	6.8	124	443	0.54	8.45
		1558.5	Coal # 5	70.51	261	440	12.3	184
		1559.4	Shale	7.29	89	457	0.61	6.5
		1560	Coal # 5	72.19	233	448	10.15	168.32
		1560.65	Shale	4.35	81	447	0.27	3.54
		1561.95	Shale	5.82	99	452	0.48	5.74
		1562.4	Coal #?	66.14	219	450	10.56	144.69
		1566.5	Shale	2.01	25	459	0.09	0.5
		1585.1	Coal # 6	57.06	222	447	8.39	126.56
		1585.5	Shaly coal #6	33.52	205	448	5.57	68.75
		1586	Coal # 6	51.47	227	451	7.38	116.89
		1586.7	Coal # 6	54.81	212	449	7.34	116.43
		1586.95	Coal # 6	74.78	207	451	9.83	154.6
		1587.35	Coal # 6	69.53	209	448	9.35	145.63
		1587.48	Coal # 6	65.27	226	453	10.01	147.23
		1587.7	Coal # 6	74.51	231	447	10.48	171.9
		1588.1	Coal # 6	53.38	222	448	7.11	118.34
		1588.4	Coal # 6	69.54	236	448	9.56	164.43
		1588.63	Coal # 6	66.1	245	448	9.52	162.03
		1590.95	Coal # 6	75.69	220	451	9.64	166.55
		1591.19	Coal # 6	76.95	204	448	10.14	156.86
		1591.25	Shale	1.98	58	457	0.14	1.15
		1617.6	Coaly Shale	17.05	181	448	1.54	30.83
		1620.99	Shaly coal	28.84	182	451	3.06	52.49
		1621.5	Shale	5.31	75	460	0.42	3.98
		1623	Shale	3.17	52	465	0.22	1.66
		1623.8	Shale	8.05	98	449	0.61	7.89
		1654.04	Shale	6.31	84	462	0.55	5.33
		1656.45	Shale	7.04	84	451	0.51	5.94
		1656.67	Shale	3.69	45	457	0.19	1.67
		1701.3	Coal # 9	75.52	208	459	11.75	157.21
		1702	Shale # 9	5.7	98	451	0.55	5.57
		1703	Coaly shale	12.72	149	457	1.53	19

Well	Unit	Depth	Lithology	TOC [%]	HI [mg HC/g TOC]	Tmax [°C]	S1 [mg HC/g]	S2 [mg HC/g]
Weiach-1	Carboniferous	1738.46	Coal # 10	68.55	193	455	9.4	132.37
		1739.9	Coal # 10	65.31	202	461	8.28	132.08
		1742.3	Shale	3.51	37	488	0.21	1.29
		1834.15	Shale	5.1	95	456	0.37	4.82

Appendix 2: Rock-Eval data measured for the Permian and Carboniferous source rocks in the Northeastern Switzerland (Weiach-1 well). Data extracted from Ajuaba et al. (2023).

12.3 List of the wells and data used in this study

							DATA AVAILABILITY									
Wells	**Datum_ Elev**	**TD**	**Formation at bottom**	**Owner**	**Confidentiality**	**Accessibility**	**Well Report**	**Stratigraphic log**	**Lithologic data**	**Porosity data**	**Temperature data**	**VR data**	**Others thermal data**	**Rock-Eval data**	**Used for modelling**	**Modelled Section**
Altishofen-1	478	2166	Malm	Ing. E. Gutzwiller			No	Yes	Yes	No	No	No	AFT	No	No	Non
Benken	404.3	1007	Basement	NAGRA	Partially confidential	Not accessibile	Yes	Yes	Yes	Yes	Yes	Yes	AFT	No	Yes	2 and 6
Berlingen-1	594	2310.7	Permian	SEAG	Confidential	Not accessibile	Yes	Yes	Yes	No	No	No	No	No	Yes	6
Boswil-1	647.5	1836.2	Malm	SEAG	Confidential	Not accessibile	Yes	No	Yes	No	No	No	AFT	No	Yes	5
Bottstein	347.46	1501	Basement	NAGRA	Partially confidential	Partially accessibile	Yes	Yes	Yes	Yes	Yes	Yes	AFT	No	No	None
Bozberg-1	513.29	1037.39	Permian	NAGRA	Public	Public	Yes	Yes	Yes	Yes	No	No	No	No	No	None
Bulach-1	389.62	1370.19	Permian	NAGRA	Public	Public	Yes	Yes	Yes	Yes	No	No	No	No	No	None
Chapelle-1	764	1530.8	Cretaceous	SEAG	Confidential	Not accessibile	No	Yes	No	No	Yes	Yes	AFT	No	Yes	2
Chessel-1	380	615	Keuper	Petrosvibri	Partially confidential	Partially accessibile	No	No	No	No	No	No	No	No	No	None
Courtion-1	594	3084	Muschelkalk	NAGRA	Public	not accessibile	No	No	No	No	No	No	No	No	No	None
Cuarny-1	562	2229	Lias	SEAG	Confidential	not accessibile	No	No	No	No	No	No	No	No	No	None
Eclepens-1	515	2150	Keuper	Vaud	Public	accessibile	Yes	Yes	Yes	Yes	Yes	Yes	No	Yes	Yes	2
Entlebuch-1	1080	5289	Carboniferous	SEAG	Confidential	Not accessibile	No	Yes	Yes	Yes	Yes	No	AFT	No	Yes	4
Essertines-1	660	2936.1	Keuper	Vaud	Public	accessibile	Yes	Yes	Yes	No	Yes	Yes	No	Yes	Yes	2

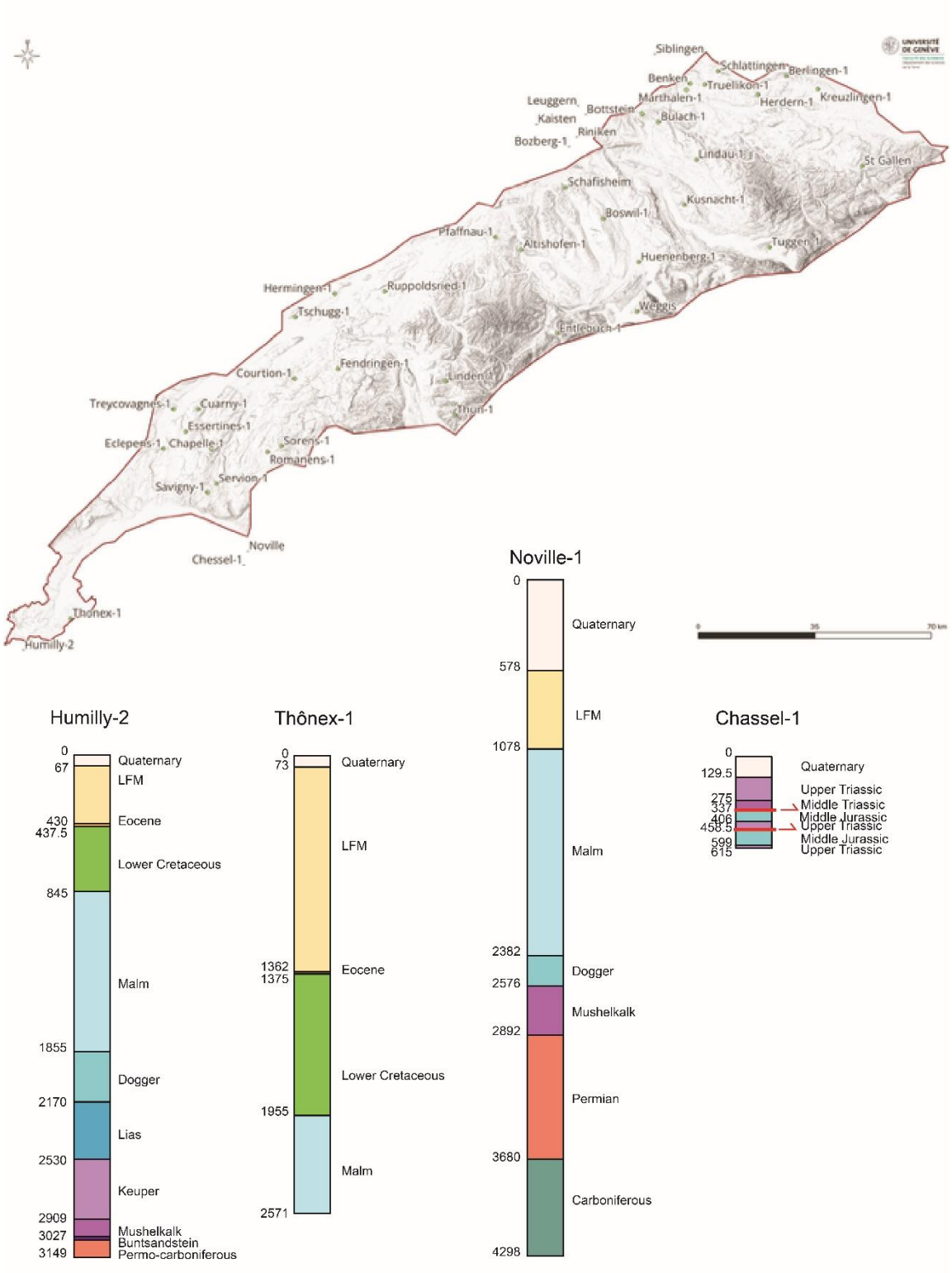
Wells	Datum_ Elev	TD	Formation at bottom	Owner	Confidentiality	Accessibility	Well Report	Stratigraphic log	Lithologic data	Porosity data	Temperature data	VR data	Others thermal data	Rock-Eval data	Used for modelling	Modelled Section
Fendringen-1	603	1970	Lower Cretaceous	BP	Public	not accessibile	No	No	No	No	No	No	No	No	No	None
Herdern-1	527.25	2154.5	Basement	SEAG	Partially confidential	Partially accessibile	Yes	yes	Yes	No	Yes	Yes	AFT	No	Yes	6
Hermingen-1	542	2425	Muschelkalk	SEAG & swissto po	Public	Partially accessibile	No	Yes	Yes	Yes	Yes	Yes	TAI	Yes	Yes	3
Humilly-2	499.56	3051	Carboniferous	TOTAL	Public	Partially accessibile	Yes	Yes	Yes	Yes	Yes	Yes	Clay	Yes	No	None
Hünenberg-1	461	3288	Malm	SEAG & swissto po	Public	Partially accessibile	Yes	yes	Yes	Yes	Yes	No	AFT	No	Yes	4 and 5
Kaisten-1	320	1306	Basement	NAGRA	Partially confidential	Partially accessibile	Yes	Yes	Yes	No	No	No	AFT	No	No	None
Kreuzlingen-1	539	2550	Permian	SEAG & swissto po	Public	Partially accessibile	Yes	yes	Yes	Yes	Yes	No	No	No	Yes	6
Kusnacht-1	641.96	2692.5	Malm	SEAG	Public	Not accessibile	Yes	yes	Yes	No	No	Yes	No	No	Yes	5
Leuggern-1	358.8	1688.9	Basement	NAGRA	Partially confidential	Partially accessibile	Yes	Yes	Yes	No	No	No	AFT	No	No	None
Lindau-1	516	2377.2	Basement	SEAG	Confidential	Not accessibile	Yes	yes	Yes	No	Yes	No	AFT	No	Yes	5
Linden-1	886	5447.5	Keuper	SEAG	Confidential	Not accessibile	No	Yes	Yes	No	Yes	No	AFT	No	Yes	3
Marthalen-1	399.48	1099.25	Basement	NAGRA	Public	Public	Yes	Yes	Yes	Yes	No	No	No	No	No	None

Wells	Datum_ Elev	TD	Formation at bottom	Owner	Confidentiality	Accessibility	Well Report	Stratigraphic log	Lithologic data	Porosity data	Temperature data	VR data	Others thermal data	Rock-Eval data	Used for modelling	Modelled Section
Noville-1	372.8	4298	Carboniferous	SEAG/ Vaud	Public	Accessibile	Yes	Yes	Yes	No	Yes	Yes	No	No	Yes	2
Pfaffnau-1	500	1843	Basement	SEAG & swissto po	Public	Partially accessibile	Yes	Yes	Yes	No	Yes	No	AFT	No	Yes	4
Riniken-1	385.07	1804.7	Permian	NAGRA	Partially confidential	Partially accessibile	Yes	Yes	Yes	Yes	Yes	Yes	AFT	Yes	Yes	5
Romanens-1	947	4022	Keuper	SEAG	Confidential	Not accessibile	Yes	Yes	Yes	Yes	No	No	AFT	No	Yes	2
Ruppoldsried-1	481	985.6	Malm	SEAG	Confidential	Not accessibile	No	Yes	Yes	No	Yes	No	No	No	Yes	3
Savigny-1	214	2435	Cretaceous	SEAG & swissto po	Public	Partially accessibile	Yes	Yes	Yes	No	Yes	Yes	AFT	No	Yes	2
Schafisheim	421.2	2006	Basement	NAGRA	Partially confidential	Partially accessibile	Yes	Yes	Yes	Yes	Yes	Yes	AFT	No	Yes	4
Schlattingen	416.7	1508	Basement	NAGRA	not available	Not accessibile	No	No	Yes	No	No	No	No	No	Yes	6
Servion-1	765	1432.45	Aquitanian	Büro für Bergbau	Confidential	not accessibile	No	No	No	No	No	No	No	No	No	None
Siblingen	574.35	1522	Basement	NAGRA	Partially confidential	not accessibile	Yes	Yes	Yes	No	No	No	No	No	No	None
Sorens-1	1019.67	3165.3	Cretaceous	SEAG	Confidential	not accessibile	Yes	Yes	Yes	No	No	No	No	No	No	None
St Gallen	579.2	4253	Dogger	St. Gallen city	Public	Partially accessibile	Yes	yes	Yes	Yes (calculated)	Yes	Yes	No	Yes	Yes	6
Thônex-1	428.35	2571	Malm	Geneve	Public	accessibile	Yes	Yes	Yes	Yes	Yes	Yes	Clay	No	No	None

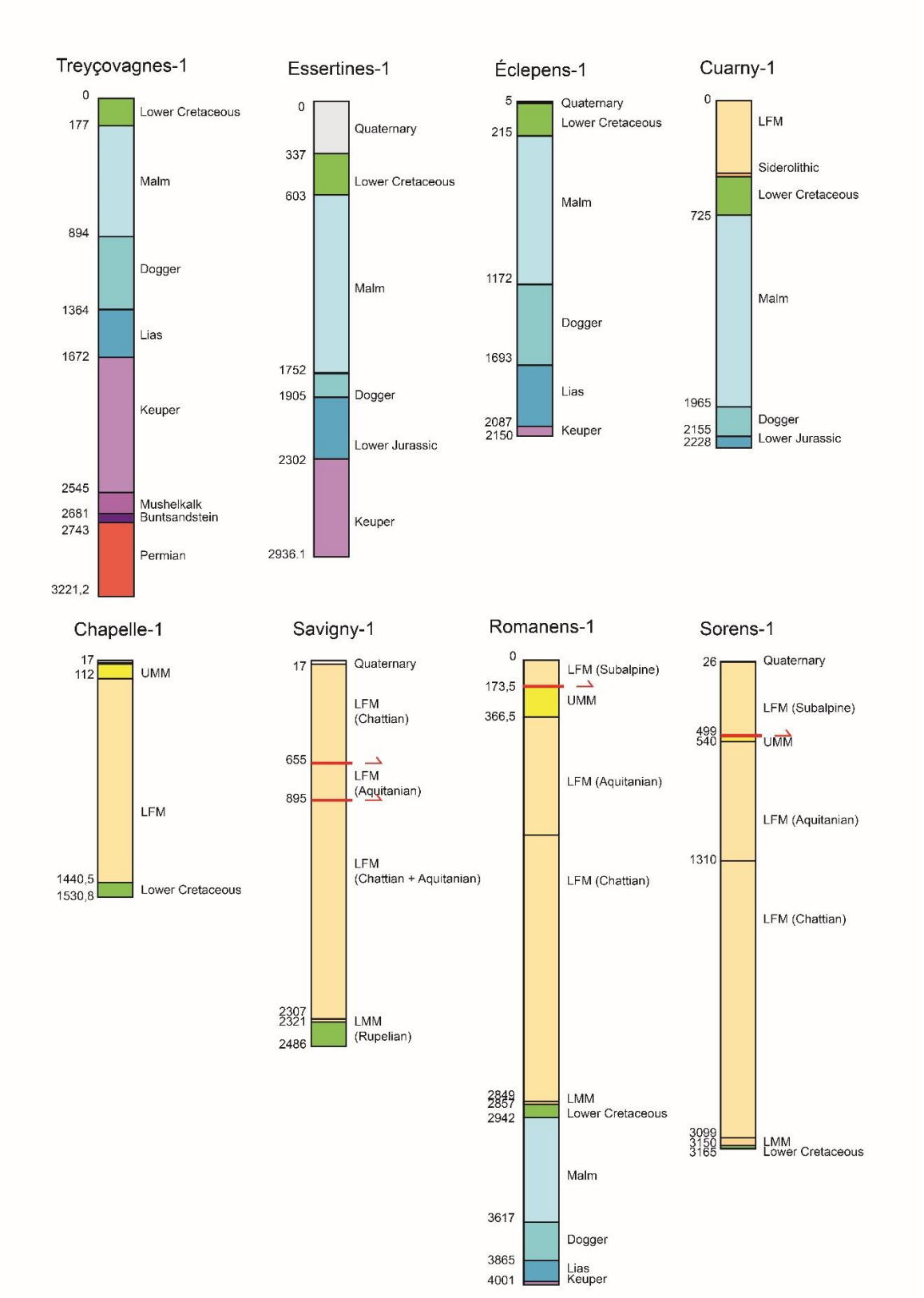
Wells	Datum_ Elev	TD	Formation at bottom	Owner	Confidentiality	Accessibility	Well Report	Stratigraphic log	Lithologic data	Porosity data	Temperature data	VR data	Others thermal data	Rock-Eval data	Used for modelling	Modelled Section
Thun-1	1077	5951.5	Lias	SEAG & swissto po	Public	Partially accessibile	Yes	Yes	Yes	Yes	Yes	No	TAI	Yes	Yes	3
Treycovagnes-1	477.9	3221	Permian	Vaud	Public	accessibile	Yes	Yes	Yes	Yes	Yes	Yes	No	Yes	Yes	2
Truellikon-1	475.07	1310	Basement	NAGRA	Public	Public	Yes	Yes	Yes	Yes	No	No	No	No	No	None
Tschugg-1	462	704	Malm	Konsortium für Untertagespeicher	Partially confidential	Not accessibile	No	Yes	Yes	No	Yes	No	No	No	Yes	3
Tuggen-1	408	1634.75	LFM	?	Partially confidential	Not accessibile	Yes	yes	Yes	No	No	No	No	No	Yes	5
Weggis-1	457.3	2302	LFM	MAGMA	Public	Not accessibile	No	Yes	No	No	Yes	No	AFT	No	Yes	4 and 5
Weiach-1	368.7	2477.5	Basement	NAGRA	Partially confidential	Partially accessibile	Yes	yes	Yes	Yes	Yes	Yes	AFT	Yes	Yes	5
Weiach-2	368	2008.5	?	SEAG	Confidential	not accessibile	No	No	No	No	No	No	No	No	No	No

Appendix 3: List of the wells used in this work and main data available (VR = vitrinite reflectance; AFT = apatite fission tracks; TAI = thermal alteration index). The wells used for the petroleum system modelling work are indicated. For the CRS map work all the wells listed in this table were used.

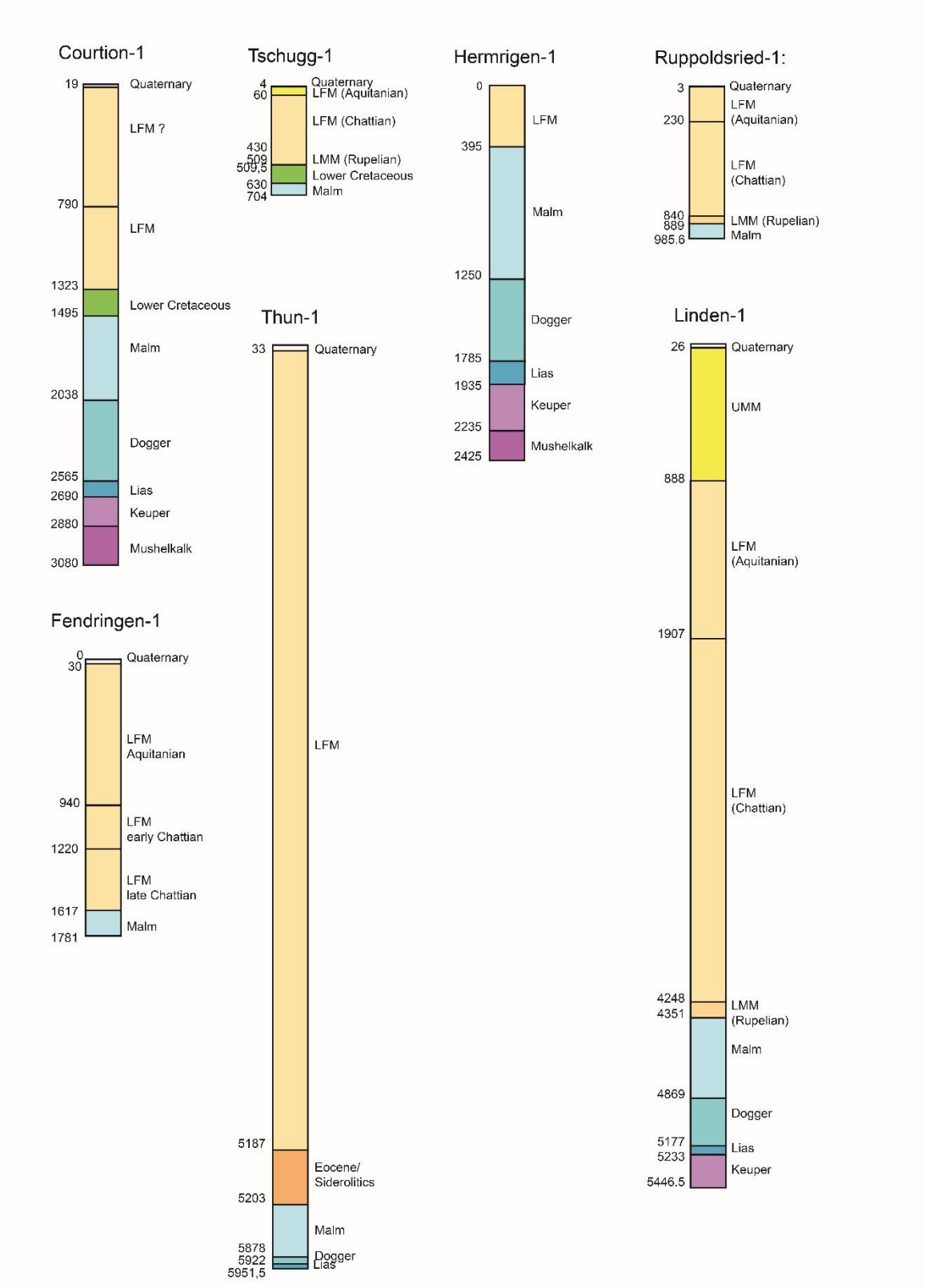
12.4 Wells stratigraphy



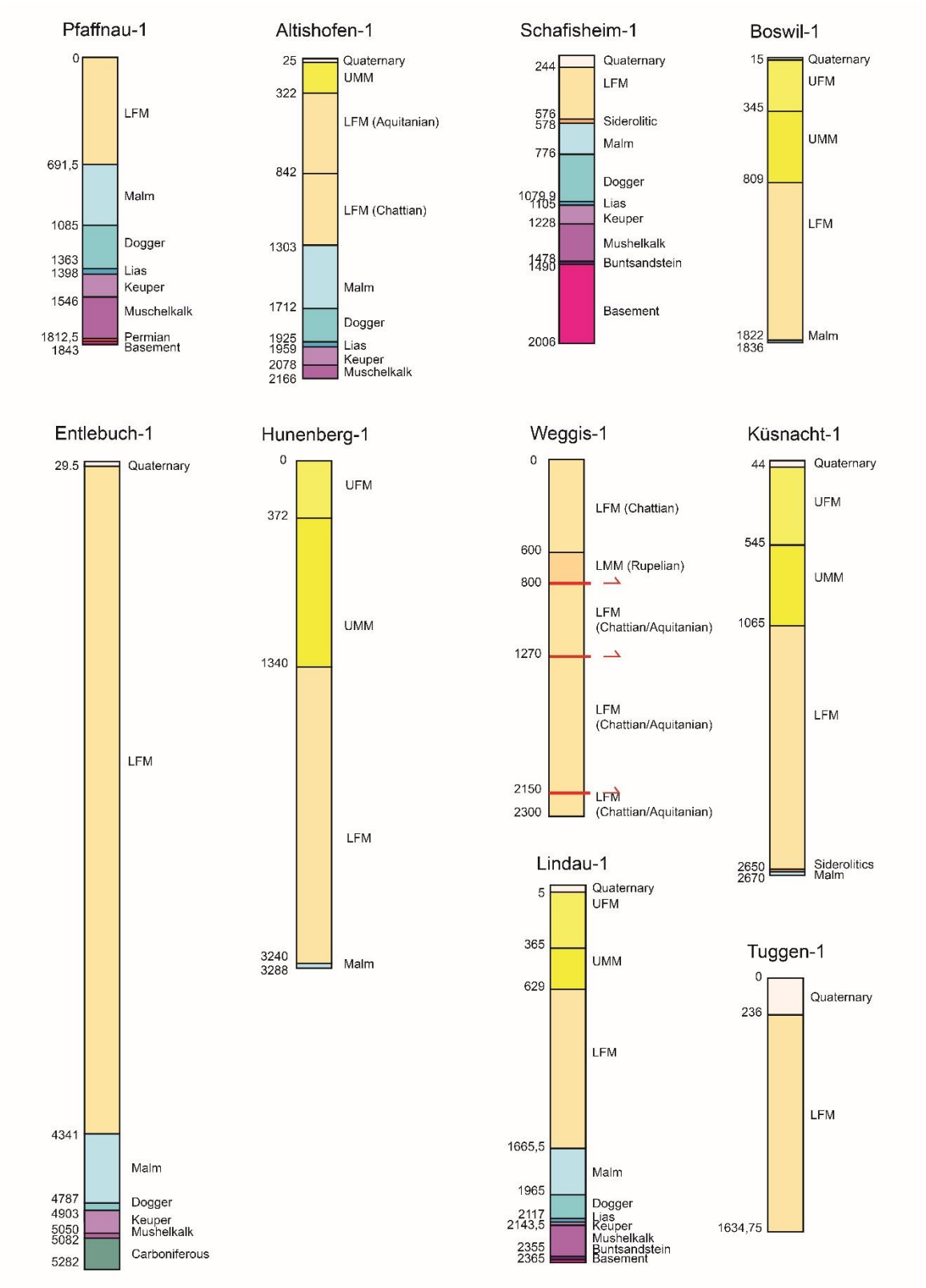
Appendix 4: Stratigraphy of the most relevant wells of the Swiss Plateau (continues)



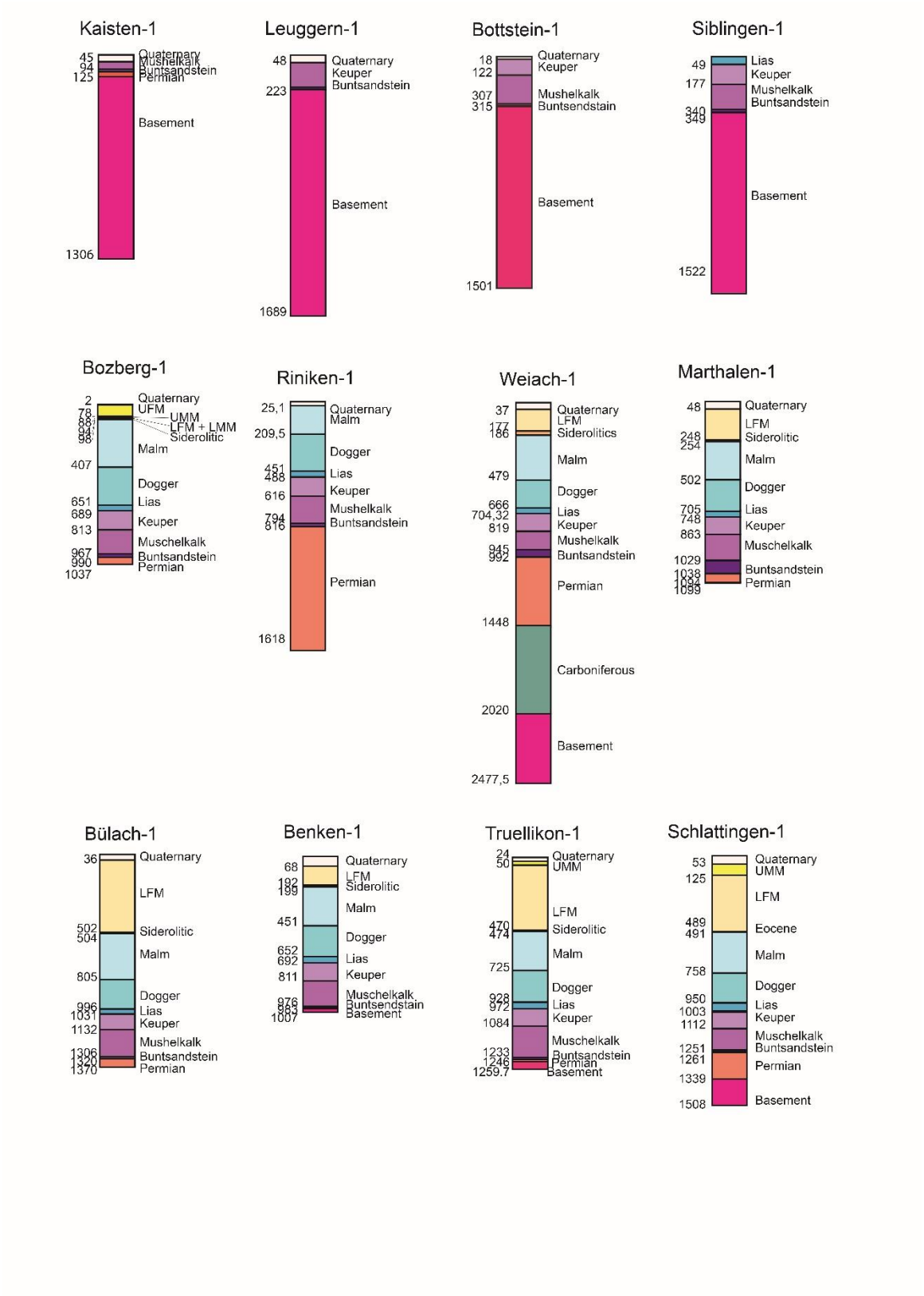
Appendix 4: Stratigraphy of the most relevant wells of the Swiss Plateau (continues)



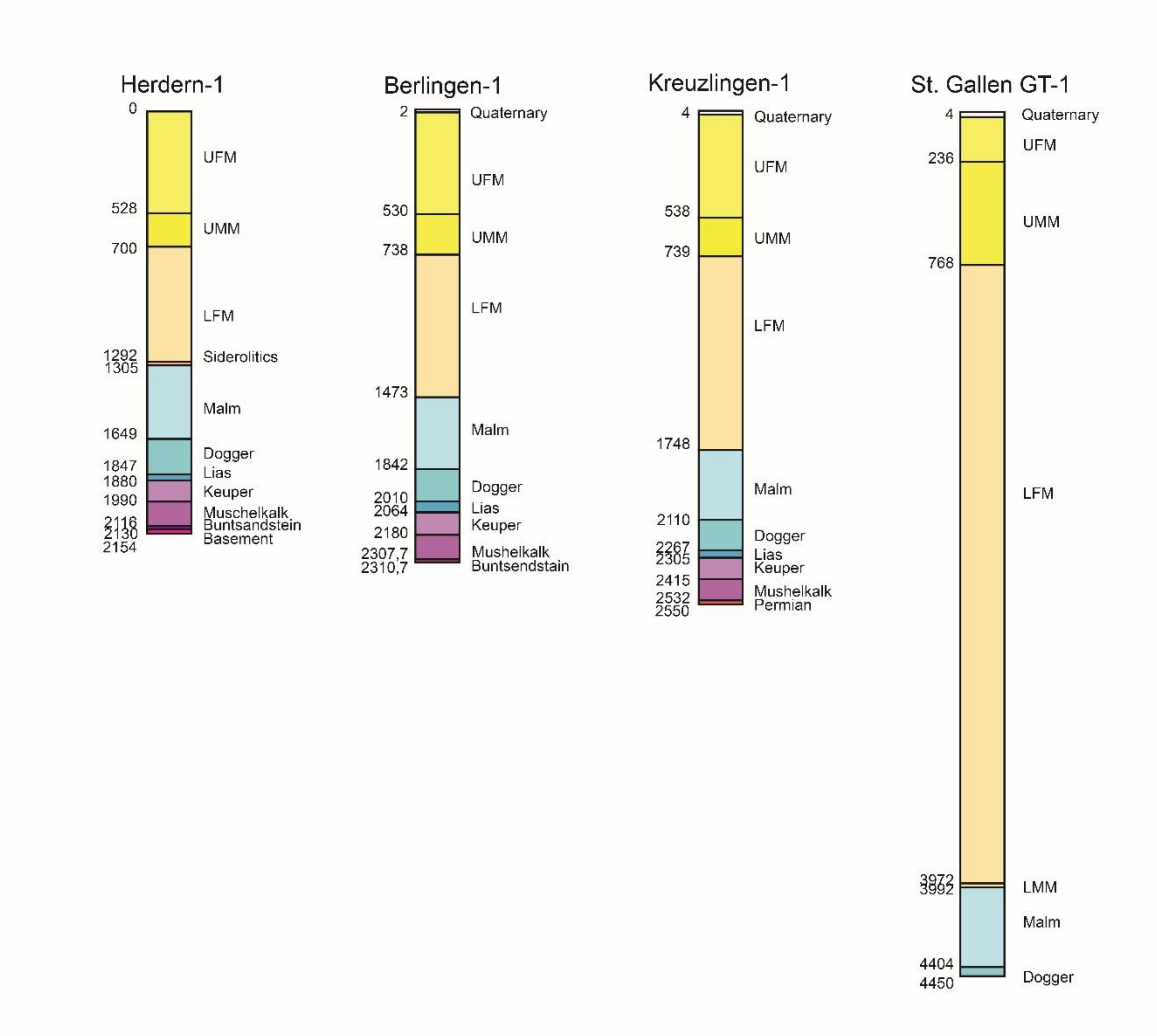
Appendix 4: Stratigraphy of the most relevant wells of the Swiss Plateau (continues)



Appendix 4: Stratigraphy of the most relevant wells of the Swiss Plateau (continues)



Appendix 4: Stratigraphy of the most relevant wells of the Swiss Plateau (continues)



Appendix 4: Stratigraphy of the most relevant wells of the Swiss Plateau

12.5 Wells facies

Well	Top Depth	Unit	Lithology	Source
Benken-1	0	Quaternary	50% gravel; 25% sandstones; 25% shales	Nagra, 2001
	68	LFM	30% sandstones; 40% shales; 30% marls	
	199	Upper Malm	80% limestones; 20% marls	
	437	Lower Malm	55% shale; 45% limestones	
	451	Dogger	80% shales; 15% limestones; 5% sandstones	
	652	Lias	50% marls; 20% limestone; 30% shales	
	692	Keuper	20% dolomite; 40% shales; 10% anhydrite; 30% marls	
	736	Gypskeuper	20% anhydrite; 50% shales; 30% marls	
	811	Upper Muschelkalk	50% dolomite; 50% limestones	
	874	Middle Muschelkalk	15% salt; 30% anhydrite; 30% dolomite; 25% shales	
	942	Lower Mushelkalk	60% marls; 40% dolomite	
	976	Buntsandstein	100% sandstones	
	983	Basement	Gneiss	
Berlingen-1	0	Quaternary	100% gravel	Well stratigraphic section
	2	UFM	60% marls; 30% sandstones; 10% conglomerate; 10% shales	
	530	UMM	60% sandstones; 40% marls	
	738	LFM	50% marls; 30% shales; 20% sandstones	
	1473	Upper Malm	80% limestones; 20% marls	
	1810	Lower Malm	80% marls; 20% limestones	
	1842	Dogger	70% marls; 20% limestones; 10% sandstones	
	2010	Lias	60% shales; 20% limestones; 20% sandstones	
	2079.5	Keuper	40% shales; 30% sandstones; 30% marls	
	2140	Gipskeuper	20% shales; 30% marls; 30% anhydrite; 20% dolomite	
	2180	Up Muschelkalk	30% anhydrite; 50% dolomite; 20% shales	
	2246	Anhy Muschelkalk	95% anhydrite; 5% shales	
	2286	Lower Muschelkalk	20% marls; 10% dolomite; 40% shales; 30% sandstones	
	2307	Buntsandstein	80% shales; 20% sandstones	
Chapelle-1	0	Quaternary	95% conglomerate; 5% sandstones	Well Report
	17	UMM	90% sandstones; 10% marls	
	112	LFM	5% limestones; 60% marls; 35% sandstones	
	1440.5	Barremian	90% limestones; 10% shales	
Eclépens	0	Quaternary	50% sandstone 50% conglomerate	Well Report
	5	Barremian	50% marls 50% limestone	
	50	Hauterivian	50% marls 50% limestone	
	136	Valanginian	100% limestones	
	215	Berriasian	100% limestones	
	268	Tithonian	70% limestone 30% dolomie	

Well	Top Depth	Unit	Lithology	Source
Eclépens	369	Kimmeridgian	70% limestone 30% dolomie	
	749	Oxfordian	90% marly limestones 10% marls	
	1061	Callovian	100% marls	
	1150	Bathonian	50% marly limestone 50% marls	
	1318	Bajocian	75% limestones 20% carbonaceous sandstones 5% marls	
	1526	Aalenian	50% marls 50% shales	
	1693	Toarcian	40% marls 50% shales 10% limestones	
	1720	Pliensbachian	50% marls 50% shales	
	1833	Pliensbachian2	50% marls 50% shales	
	1899	Sinemurian	50% marls 50% shales	
	1968	Sinem-Hettangian	50% limestone 50% marls	
	2087	Rhetian	50% shales 30% dolomie 20% sandstones	
	2106	Keuper	50% marls 30% shales 20% dolomie	
Entlebuch-1	0	Quaternary	30% shales; 50% gravel; 20% silt	
	29.5	LFM I-II granitic Molasse	40% arkosic sandstones; 30% siltstones; 30% coloured mudstones	
	3995	LFM III carbonate Molasse	40% carbonatic sandstones; 30% siltstones; 30% coloured mudstones;	
	4341	Upper Malm	100% limestones	
	4698	Lower Malm	70% limestones; 30% marls	
	4787	Dogger	70% shales; 30% limestones	
	4844	Lias	80% sandstones; 10% shales; 10% limestones	
	4910	Keuper	45% anhydrit; 40% dolomite; 10% shales; 5% sandstones	
	5050	Muschelkalk	5% anhydrite; 35% shales; 60% dolomite	
	5082	Carboniferous	20% carbonaceous sandstones; 30% sandstones; 5% coal;45% shales	
Essertines-1	0	Chattian - LFM	50% Marls; 50% Sandstones	Well Report
	337	Barremian	100% Limestone	
	360	Hauterivian	100% Limestone	
	430	Valanginian	100% Limestone	
	531	Berriasian	100% Marly limestone	
	603	Tithonian-Kimmerid	100% Limestone	
	925	Oxfordian	100% Marly limestone	
	1347	Callovian	80% Limestone; 20% Marls	
	1375	Bathonian-Bajocian	80% Limestone; 20% Marls	
	1752	Aalenian	80% Shales; 20% Marls	
	1905	Toarcian	50% Shales; 50% Marls	
	2002	Pliensbachian	50% Limestones; 50% Marls	
	2199	Hettangian-Sinem	80% Shales; 20% Limestones	
	2302	Rhetian	50% Shales; 50% Sandstone	
	2322	Upper Keuper	25% Shales; 25% Dolomite; 25% Anhydrites; 25% marls	
	2553	Gypskeuper	30% Shales; 30% Anhydrites; 40% Salt	
Herdern-1	0	Quaternary	50% gravel; 25% sandstones; 25% shales	
	2	UFM	70% marls; 20% shales; 10% sandstones	
	528	UMM	40% marls; 20% siltstones; 40% sandstones	

Well	Top Depth	Unit	Lithology	Source
Herdern-1	700	LFM	20% sandstones; 30% shales; 50% marls	
	1305	Upper Malm	85% limestones; 15% marls	
	1602	Lower Malm	35% shales; 65% limestones	
	1649	Dogger	85% shales; 15% limestones	
	1847.5	Lias	95% shales; 5% limestone	
	1949	Keuper	40% shales; 30% sandstones; 30% dolomite	
	1990	Gipskeuper	30% shales; 20% anhydrite; 20% dolomite; 20% limestones; 10% marls	
	2054	Upper Muschelkalk	60% limestones; 30% dolomite; 10% shales	
	2100	Mid Muschelkalk	40% dolomite; 30% limestones; 20% shales; 5% anhydrite; 5% halite	
	2116.5	Lower Muschelkalk	15% salt; 30% anhydrite; 30% dolomite; 25% shales	
	2130	Buntasandstein	100% sandstones	
	2154.5	Basement	100% gneiss	
Hermingen-1	0	UFM marls	60% shales; 35% marls; 5% sandstone	Stratigraphic log from well report
	267	UFM sand	50% sandstones; 30% limestones; 20% shales	
	395	Lower Cretaceous	100% limestone, packstone-wackstone	
	402	Kimmeridgian	100% limestone, grainstone	
	610	Oxfordian limestone	100% limestone, grainstone	
	900	Oxfordian marls	50% marls; 50% limestone	
	1250	Callovian	70% limestones; 30% marls	
	1310	Bathonian	100% limestone, packstone-wackstone	
	1350	Bajocian	60% limestones packstone-wackstone; 40% marls	
	1685	Aalanian	50% marls; 50% shales	
	1785	Lias	75% limestones; 20% black shales; 5% sandstones	
	1935	Keuper	40% dolomite; 20% shales; 40% anydrite	
	2085	Keuper anhydrite	78% anhydrite; 20% shales; 2% halite	
	2235	Muschelkalk	80% dolomite; 20% limestones	
	2313	Muschelkalk salt	95% Halite 5% anhydrite	
Hünenberg-1	0	Quaternary	30% shales; 50% gravel; 20% silt	Well Report
	2	UFM	75% marls; 15% sandstones; 10% calcareous sandstones	
	372	UMM	10% conglomerate; 60% sandstones; 30% marls	
	1340	LFM	50% marls; 30% sandstones; 20% shales	
	3259	Malm	70% limestones; 30% marls	
Kreuzlingen-1	0	Quaternary	70% shales; 30% sandstones	Well Report
	4	UFM	70% marls; 30% sandstones	
	538	UMM	80% sandstones; 20% marls	
	739	LFM	60% marls; 25% sandstones; 3% shales; 2% limestones	
	1748	Upper Malm	100% limestones	
	2075	Lower Malm	9o% limestones; 10% marls	
	2110	Dogger	50% marls; 30% limestones; 10% shales; 10% sandstones	
	2267	Lias	85% shales; 10% marl% 5% limestones	
	2314	Keuper	70% shales; 20% marls; 5% sandstones; 5% limestones	

Well	Top Depth	Unit	Lithology	Source
Kreuzlingen-1	2407	Gypskeuper	50% dolomite; 10% sanstone; 10% marls; 30% shales	
	2415	Upper Muschelkalk	60% shales; 15% dolomite; 5% sandstones; 20% limestones	
	2480	Middle Muschelkalk	70% shales; 20% anhydrite; 10% dolomite	
	2524	Lower Muschelkalk	20% marls; 5% anhydrite; 75% shales	
	2532	Permian Carboniferous	100% breccia	
Kusnacht-1	0	Quaternary	50% gravel; 50% shales	Stratigraphic log from well report
	44	UFM	85% marls; 9% sandstones; 1% limestones; 5% shales	
	545	UMM	70% sandstones; 20% marls; 10% shales	
	1065	LFM	50% marls; 20% sandstones; 25% shales; 5% limestones	
	2480	Alpine LFM	70% marls; 30% sandstones	
	2670	Malm	80% limestones; 20% marls	
Lindau-1	0	Quaternary	50% gravel; 50% shales	Stratigraphic log from well report
	5	UFM	70% marls; 30% sandstones	
	365	UMM	60% sandstones; 40% marls	
	629	LFM	70% marls; 30% sandstones	
	1665.5	Upper Malm	90% limestone; 10% marls	
	1935	Lower Malm	90% marls; 10% limestones	
	1965	Dogger	70% marls; 30% limestones	
	2117	Lias	30% limestones; 40% shales; 30% sandstones	
	2141	Rhatian	100% shales	
	2143.5	Keuper	50% dolomite; 30% marls; 20% shales	
	2173	Gipskeuper	50% anhydrite; 20% shales; 30% marls	
	2225	Upper Muschelkalk	80% dolomite; 10% marls; 10% anhydrite	
	2286	Anhy Muschelkalk	60% anhydrite; 40% marls	
	2340	Lower Muschelkalk	70% marls; 10% anhydrite; 20% marls	
	2355	Buntsandstein	80% marls; 20% sandstones	
	2365	Basement	granite	
Linden-1	0	Quaternary	30% conglomerate; 30% sandstones; 40% shales	Stratigraphic log from well report
	26	UMM	70% conglomerate; 20% sandstones; 10% shales	
	888	LFM Aquitanian	80% shales; 15% sandstones; 5% conglomerates	
	1907	LFM Chattian	60% shales; 40% sandstones	
	4248	LMM	50% shales; 40% sandstones; 10% limestones	
	4350.5	Upper Malm	100% limestones (micrite)	
	4688	Lower Malm	100% limestones (micrite)	
	4869	Dogger	100% limestones (micrite)	
	5102	Aalenian	60% black shales; 40% marls	
	5135	Opalinus	100% sandstones	
	5177	Lias+Rhetian	50% sandstones; 40% shales; 10% limestones	

Well	Top Depth	Unit	Lithology	Source
Linden-1	5233	Keuper	60% anhydrite; 35% shales; 5% dolomestones	
	5320	Gipskeuper	70% anhydrite; 20% shales; 5% dolomestones; 5% halite	
Noville-1	0	Quaternary	30% conglomerate; 40% sandstones; 30% shales	Well Report
	578	Paleogene	65% shales; 25% sandstones; 5% marls; 5% silstones	
	1078	Portlandian	100% limestones	
	1230	Kimmeridgian	100% limestones	
	1790	Oxfordian	70% marls; 20% limestones; 10% shales	
	2382	Dogger	40% marls; 20% limestones; 20% siltstones; 20% shales	
	2576	Upper-Middle Muschelkalk	50% limestones; 40% dolomite; 10% marls	
	2685	Lower Muschelkalk	70% sandstones; 24% shales; 5% dolomite; 1% gypsum	
	2808	Buntsandstein	93% sandstones; 7% shales	
	2892	Permian Verrucano	85% sandstones; 15% shales	
	3185	Permian	40% shales; 10%limestones; 20% sandstones; 30% silstones	
	3680	Autunian	20% sandstones; 60% silstones; 40% shales	
	3760	Carboniferous	20% sandstones; 60% silstones; 40% shales	
Pfaffnau-1	0	LFM	70% marls; 20% sandstones; 10% shales	Well Report
	691.5	Kimmeridgian	90% limestones; 5% sandstones; 5% marls	
	855	Oxfordian	80% marly limestones; 20% marls	
	1085	Callovian	70% marls; 30% limestones	
	1090	Bathonian + Bajocian	85% limestones; 15% marls	
	1250	Opalinus	100% marly limestones	
	1363	Lias	50% limestones; 50% sandstones	
	1408	Upper Keuper	10% dolomestones; 40% marls; 50% anydrite	
	1429.5	Gipsum keuper	10% dolomestones; 40% marls; 50% anydrite	
	1538.5	Lower Keuper	10% dolomestones; 40% marls; 50% anydrite	
	1546	Upper Muschelkalk	20% dolomestones; 10% limestones; 10% gypsum; 60% marls	
	1610	Middle Muschelkalk	80% salt; 20% marls	
	1772	Lower Muschelkalk	70% anydrite; 20% marls; 5% limestones; 5% dolomestones	
	1807	Permian	60% sandstones; 40% shales	
	1824	Basement	Gneiss	
Riniken-1	0	Quaternary	100% sandstones	Stratigraphic log from well report
	25	Malm	50% shale, 40% Marly-shale 10 % Limestone	
	210	Dogger	85 % Shales, 15% micritic limestone	
	451	Lias	50% shale, 40% Marly-shale 10 % Limestone	
	489	Keuper	42% marly-dolomit, 39% marly-shale, 4%silt, 15% anhydrit	
	616	Muschelkalk	39% Dolomite, 14% marly-shale, 20 % marly-limestone , 22% anhydrite, 5% salt	
	794	Buntsandstein	100% sandstones	
	816	Permian	48 % cristalline Breccia, 16% shaly-sandstone, 36% sandstone	

Well	Top Depth	Unit	Lithology	Source
Romanens-1	0	Chattian	40% sandstone 35% marls 20% shales 5% conglomerate	Well report
	173.5	Burdigalian	40% sandstone 35% marls 20% shales 5% conglomerate	
	366.5	Aquitanian	40% sandstone 35% marls 20% shales 5% conglomerate	
	1129.5	Chattian	40% sandstone 35% marls 20% shales 5% conglomerate	
	2849	Rupelian	40% sandstone 35% marls 20% shales 5% conglomerate	
	2857	Valanginian	100% limestones	
	2942	Kimmeridgian	100% limestones	
	3289	Oxfordian	100% limestones	
	3617	Callovian	100% limestones	
	3785	Bajocian	100% shaly limestones	
	3865	Aalanian	100% shales	
	3876	Toarcian	100% shales	
	3986	Rhetian	100% shales	
	4001	Keuper	30% anhydrite 70% shales	
Ruppoldsdried-1	0	Quaternary	100% sandstones	Stratigraphic log from well report and Schlanke et al., 1978
	3	LFM Aquitanian	60% marls; 39% sandstones; 1% coal	
	230	LFM Chattian	60% marls; 38% sandstones; 1% coal; 1% evaporite	
	840	LMM Rupelian	80% marls; 20% silt	
	889	Tithonian	100% limestones micritic	
Savigny-1	0	Quaternary	50% sandstone; 25% conglomerate; 25% shales	Well Report
	17	Early Chattian thrusted	50% sandstone; 50% marls	
	655	Aquitanian thrusted	50% sandstone; 50% marls	
	895	Late Chattian	50% sandstone; 50% marls	
	2307	Rupelian	40% marls; 60% sandstones	
	2321	Cenomanian	80% limestones; 20% marls	
	2338	Albian	70% sandstones; 30% marls	
	2353	Aptian	60% limestone; 25% marls; 15% sandstones	
	2367	Upper Barremian	50% sandstone; 50% marls	
	2435	Lower Barrem-Hauteriv	50% sandstone; 50% marls	
Schafisheim-1	0	Quaternary	75% Sandstone, 25% shales	Well Report
	244	LFM	50% Sandstone, 20% shale, 30% siltstone	
	566	Eocene	100% shales	
	576	Malm	75% limestone, 10% marls; 10% shales	
	840	Dogger	25% limestones, 50% shales, 25% marly limestone	
	1080	Lias	94% Shales, 5% limestone, 1% marls	
	1106	Keuper	10% Dolomit, 40% shaly dolomit, 15% anhydrite, 35% shale	
	1228	Muschelkalk	55% dolomite, 5% shales; 5% marls, 20% anhydrite, 15% Salt	
	1478	Buntsandstein	100% sandstones	
	1490	Basement	100% granite	

Well	Top Depth	Unit	Lithology	Source
St-Gallen GT-1	0	Quaternary	100% breccia	Naef and Schalnke, 2014
	4	UFM	10% sandstones; 90% marls	
	236	UMM	30% sandstones; 10% conglomerate; 30% marls; 30% silstone	
	768	LFM upper	75% marls; 20% sandstones; 5% limestones;	
	2436	LFM triangle	30% sandstones; 55% marls; 15% limestones	
	3315	LFM lower	13% sandstones; 85% marls; 2% limestones	
	3791	LMM	40% sandstones; 10% shales; 50% marls	
	3810	Malm	100% limestones	
	4207	Dogger	20% sandstones; 50% shales; 30% limestones	
Thun-1	0	Quaternary	100% conglomerate	Stratigraphic log from well report
	33	LFM 1 thrust	80% conglomerate; 20% shales	
	1359	LFM 2 thrust	80% sandstones; 20% shales	
	2750	LFM authochtone	80% sandstones; 20% shales	
	5187	Syderolithic	100% limestones	
	5203	Tithonian	80% limestones; 20% dolomestones	
	5309	Kimmeridgian	80% limestones; 20% dolomestones	
	5540	Oxfordian	80% limestones; 20% dolomestones	
	5878	Callov-Bathonian	80% limestones; 20% marls	
	5894	Bajocian	80% limestones; 20% shales	
	5914	Aalanian (Opalinus)	100% black shales	
	5922	Toarcian	50% sandstones; 50% limestones	
Treyçovagnes-1	0	Hauterivian	80% limestones; 20% shaly limestones	Well Report
	89	Valanginian	60% oolitic limestone; 40% limestone	
	160	Barriasian	60% grainstone; 40% limestone	
	177	Tithonian	100% limestone	
	305	Kimmeridgian	100% limestone	
	450	Oxfordian	30% limestone; 40% marls; 30% shales	
	894	Callovian	70% marls; 30% limestone	
	996	Bathonian	70% marls; 30% shales	
	1090	Bajocian	100% limestone	
	1278	Aalenian	50% shales; 50% limestone	
	1364	Toarcian	90% shales; 10% limiestones	
	1444	Pliensbachian	50% shales; 50% limestone	
	1672	Rhaetian	10% dolomite; 50% shales; 40% sandstone	
	1696	Upper Keuper	40% anhydrite; 30% dolomite; 30% shales	
	2324	Middle Keuper	10% shales; 50% anhydrite; 40% dolomite	
	2374	Lower Keuper	40% salt; 30% shales; 30% anhydrite	
	2530	Letthenkhole	50% dolomite; 50% anhydrite	
	2545	Muschelkalk	10% sandstones; 30% dolomite; 20% limestone; 20% anhydrite; 20% shales	
	2681	Buntsandstein	80% sandstone; 20% shales	
	2743	Permian	50% conglomerate; 40% sandstone; 10% shales	

Well	Top Depth	Unit	Lithology	Source
Tschugg-1	0	Quaternary	50% shales; 40% sandstones; 10% conglomerates	Stratigraphic log from well report and Schlanke et al., 1978
	4	LFM Aquitanian	60% sandstones; 40% marls	
	60	LFM Chattian	10% limestones; 40% marls; 47% sandstones; 1% gypsum; 2% coal	
	150	LFM Chattian 2	70% marls; 30% sandstones	
	430	LMM	70% marls; 10% sandstones; 17% shales; 3% gypsum	
	509	Siderolitic	100% shales	
	509.5	Barremian	100% limestones	
	535	Hauterivian	60% limestones; 40% marly limestones	
	594	Valanginian	100% limestones	
	630	Tithonian	100% limestones micritic	
Tuggen-1	0	Quaternary	50% sandstones; 50% shales	Stratigraphic log from well report
	236	Chattian	85% marls; 15% sandstones (oil)	
Weiach-1	0	Quaternary	50% gravel; 50% shales	Stratigraphic log from well report
	37	LFM	70% sandstones; 20% silt; 10% shales	
	186	Upper Malm	70% limestones; 30% marls	
	391	Lower Malm	70% marls; 30% limestones	
	479	Dogger	40% shales; 30% limestones; 30% marls	
	666	Lias	60% marls; 30% shales; 10% limestones	
	704.32	Keuper	40% dolomite; 50% mergel; 10% shales	
	740	Gypskeuper	30% Anhydrite; 20% dolomite; 30% mergel; 20% shales	
	819	Upper Muschelkalk	70% dolomite; 30% limestone	
	888	Mid Muschelkalk	40% anhydrite; 40% dolomite; 20% shales	
	945	Lower Muschelkalk	60% shales; 30% dolomite; 10% marls	
	982	Buntsandstein	80% sandstein; 20% shales	
	992	Permian	40% sandstones; 15% congl; 35% shales	
	1448	Carboniferous	25% silt; 33% shales; 40% sandstones; 2% coal	
		Basement	Gneiss and granite	

Appendix 5: Facies described as litologies percentages assigned to each stratigraphic units described in the wells of the Swiss Plateau used for thermal modelling

12.6 Porosity data

Well	Unit	Depth	Porosity mean (%)	Stratigraphic unit average	Source
Benken-1	Malm	401.68	3.40		Well report
	Dogger	454.95	9.90		
	Dogger	519.96	9.10		
	Dogger	545.16	11.30		
	Dogger	555.31	10.40		
	Dogger	571.55	7.40		
	Dogger	576.9	11.50		
	Dogger	582.09	8.80		
	Dogger	586.61	10.80		
	Dogger	601.04	13.10		
	Dogger	613.48	12.50		
	Dogger	637.01	10.00		
	Dogger	645.05	12.40	10.05	
	Lias	657.62	2.20		
	Lias	678.26	13.40		
	Lias	683.27	13.20	9.60	
	Keuper	702.37	15.00		
	Keuper	712.76	0.60		
	Keuper	734.18	14.30		
	Gypskeuper	755.83	12.10	10.50	
	Upper Muschelkalk	821.52	24.50	9.53	
	Upper Muschelkalk	853.98	3.30		
	Lower Muschelkalk	951.13	3.30	10.37	
	Buntsandstein	979.34	7.00	7.00	
Böttstein-1	Keuper	44	21.60		Well report
	Keuper	93	9.90		
	Keuper	101	7.60		
	Keuper	110	1.50		
	Keuper	114	6.20		
	Keuper	118	24.20	11.83	
	Muschelkalk	123	21.00		
	Muschelkalk	127	22.20		
	Muschelkalk	131	20.90		
	Muschelkalk	135	13.00		
	Muschelkalk	143	15.00		
	Muschelkalk	145	28.30		
	Muschelkalk	148	14.70		
	Muschelkalk	153	8.00		
	Muschelkalk	161	5.60		
	Muschelkalk	178	5.30		

Well	Unit	Depth	Porosity mean (%)	Stratigraphic unit average	Source
Böttstein-1	Muschelkalk	192	15.00		
	Muschelkalk	192	14.00		
	Muschelkalk	198	25.00		
	Muschelkalk	210	10.00		
	Muschelkalk	221	3.80		
	Muschelkalk	225	1.30		
	Muschelkalk	237	4.10		
	Muschelkalk	241	2.50		
	Muschelkalk	249	7.10		
	Muschelkalk	252	1.30		
	Muschelkalk	264	8.90		
	Muschelkalk	274	7.50		
	Muschelkalk	280	8.90		
	Muschelkalk	281	4.60		
	Muschelkalk	282	9.80		
	Muschelkalk	288	4.50		
	Muschelkalk	294	7.70	10.74	
	Buntsandstein	309	14.00		
	Buntsandstein	310	15.00		
	Buntsandstein	310	8.00		
	Buntsandstein	310	10.00		
	Buntsandstein	311	9.00		
	Buntsandstein	312	9.00		
	Buntsandstein	312	9.00		
	Buntsandstein	312	13.00		
	Buntsandstein	314	16.00		
	Buntsandstein	315	15.00	11.80	
Bozberg-1	Malm		7.40	7.40	Well report
	Dogger (Passwang Fm)		9.00		
	Dogger (Ifenthal to Klingau)		7.60	8.30	
	Muschelkalk		14.00	14.00	
	Buntsandstein		12.20	12.20	
	Rotligend		5.80	5.80	
Bulach-1	Malm		3.40	3.40	Well report
	Dogger		13.00	13.00	
	Muschelkalk		12.00	12.00	
	Buntsandstein		9.50	9.50	
	Rotligend		10.30	10.30	
Eclépens-1	Malm	237	4.00		Well report
	Malm	237.85	3.50		
	Malm	238.125	2.25		
	Malm	238.725	3.60		
	Malm	239.2	2.50		
	Malm	239.6	2.45		

Well	Unit	Depth	Porosity mean (%)	Stratigraphic unit average	Source
Eclépens-1	Malm	239.85	4.25		
	Malm	240.05	8.00		
	Malm	540.1	0.50		
	Malm	540.6	0.75		
	Malm	540.58	0.85		
	Malm	541.1	1.00		
	Malm	541.6	1.00		
	Malm	541.95	0.90		
	Malm	542.41	1.00		
	Malm	542.73	0.80		
	Malm	543.4	1.10		
	Malm	543.75	0.75		
	Malm	544.1	0.50		
	Malm	544.65	0.80		
	Malm	545	1.00		
	Malm	545.5	1.00		
	Malm	546.16	1.00		
	Malm	546.45	0.50		
	Malm	546.95	0.30		
	Malm	547.45	0.20		
	Malm	548	0.20		
	Malm	548.4	2.00		
	Malm	548.7	1.00		
	Malm	549	0.50		
	Malm	549.5	0.75		
	Malm	549.9	0.40		
	Malm	554.5	2.00		
	Malm	555.8	1.50		
	Malm	556.4	0.90		
	Malm	556.9	0.20		
	Malm	557.5	0.90		
	Malm	557.7	0.50		
	Malm	558.1	1.00		
	Malm	558.5	0.50		
	Malm	558.8	0.40		
	Malm	559.3	0.85		
	Malm	559.6	0.90		
	Malm	559.9	0.10		
	Malm	560.3	0.10		
	Malm	560.7	0.20		
	Malm	561.3	0.20		
	Malm	561.7	0.80		
	Malm	562.3	0.80		
	Malm	562.42	0.50		

Well	Unit	Depth	Porosity mean (%)	Stratigraphic unit average	Source
Eclépens-1	Malm	562.8	1.00		
	Malm	563.4	2.50		
	Malm	563.9	3.00		
	Malm	564.3	2.50		
	Malm	564.8	2.50		
	Malm	655.1	1.10		
	Malm	565.6	1.00		
	Malm	566	0.20		
	Malm	566.4	0.30		
	Malm	566.7	0.70		
	Malm	567	1.00		
	Malm	567.57	0.20		
	Malm	568	0.30	1.24	
	Lias	2063.1	1.50		
	Lias	2064.4	1.00		
	Lias	2065.4	0.90		
	Lias	2066.4	2.00		
	Lias	2066.9	1.00		
	Lias	2069	0.75		
	Lias	2070	1.00		
	Lias	2071.2	0.50		
	Lias	2072.3	0.90		
	Lias	2073.15	1.20		
	Lias	2074	1.00		
	Lias	2074.9	1.00		
	Lias	2074.4	1.20		
	Lias	2076.8	1.20		
	Lias	2077.6	1.10		
	Lias	2078.4	1.00		
	Lias	2078.8	1.10		
	Lias	2079.7	1.00		
	Lias	2080.1	1.00		
	Lias	2080.5	1.00		
	Lias	2081.5	0.90		
	Lias	2081.7	1.00		
	Lias	2082.3	1.10		
	Lias	2082.6	1.50		
	Lias	2082.9	1.10		
	Lias	2083.2	1.80		
	Lias	2083.5	1.30		
	Lias	2083.7	1.20		
	Lias	2084.2	1.00		
	Lias	2089.5	1.00		
	Lias	2089.7	1.00	1.10	

Well	Unit	Depth	Porosity mean (%)	Stratigraphic unit average	Source
Eclépens-1	Rhetian	2090	3.20		
	Rhetian	2090.2	2.00		
	Rhetian	2090.5	4.00		
	Rhetian	2091	8.00		
	Rhetian	2091.6	6.50		
	Rhetian	2093.1	1.20		
	Rhetian	2096.3	3.00		
	Rhetian	2097.1	2.00		
	Rhetian	2097.5	2.00		
	Rhetian	2098.4	3.00		
	Rhetian	2104.25	2.50		
	Keuper	2107.7	0.50	3.16	
Essertines-1	USM	150	17.80		Greber et al., 2007
	USM	250	9.70	13.75	
	Cretaceous	400	2.50	2.50	
	Malm	1000	1.00	1.00	
	Dogger	1700	1.70	1.70	
	Lias	2000	1.60		
	Lias	2100	1.30	1.45	
	Keuper	2300	3.50		
	Keuper	2600	48.70	26.10	
Hermingen-1	USM	350	15.00	15.00	Greber et al., 2007
	Malm	450	10.00		
	Malm	620	6.50		
	Malm	700	6.00	7.5	
	Dogger	1300	5.00		
	Dogger	1330	7.00		
	Dogger	1420	17.00		
	Dogger	1500	10.00		
	Dogger	1550	13.00	10.4	
	Lias	1810	5.00		
	Lias	1910	8.50	6.75	
	Keuper	1980	8.50		
	Keuper	2080	10.00		
	Keuper	2150	2.00	6.8	
Humilly-2	Kimmeridgian	1015.5	12.91		Russilon Thesis
	Kimmeridgian	1020.5	13.65		
	Oxfordian	1852.4	0.96		
	Oxfordian	1854.6	2.75	7.57	
	Bathonian	1857.3	2.44		
	Bathonian	1860.8	2.77		
	Bajocian	1997.3	1.89		
	Bajocian	2001.2	2.10		
	Bajocian	2003.5	1.49	2.24	

Well	Unit	Depth	Porosity mean (%)	Stratigraphic unit average	Source
Humilly-2	Liassic	2469.3	0.83	0.83	
	Raethian	2529.1	1.65		
	Raethian	2529.3	1.87		
	Lettenkohle	2907	1.91		
	Lettenkohle	2907.4	0.92		
	Lettenkohle	2908	1.54	1.58	
	Muschelkalk	2910	2.96		
	Muschelkalk	2916.6	1.52		
	Muschelkalk	2922.5	2.60		
	Muschelkalk	2930.3	0.87		
	Muschelkalk	2951.4	1.27		
	Muschelkalk	2958.5	1.92		
	Muschelkalk	2966.1	0.64	1.68	
	Buntsandstein	3028.3	2.83		
	Buntsandstein	3035	4.34		
	Buntsandstein	3037.4	1.89	3.02	
	Carboniferous	3039.3	0.62	0.62	
Hünenmberg-1	USM	2400	4.1		Greber et al., 2007
	USM	2700	<5		
	USM	3000	3.1	4.00	
Kreuzlingen-1	Malm	1780	1.1	1.1	Greber et al., 2007
	Dogger	2150	5.9	5.9	
	Lias	2250	3.9	3.9	
	Keuper	2310	2.6		
	Keuper	2400	2.5	2.40	
	Muschelkalk	2500	8.2	8.20	
Marthalen-1	Malm		2.90	2.90	Well report
	Dogger		9.10	9.10	
	Muschelkalk		15.00	15.00	
	Buntsandstein		10.00	10.00	
	Rotligend		5.90	5.90	
Pfaffnau-1	LFM	450	17		Greber et al., 2007
	Malm	750	1.9		
	Lias	1380	5.4		
	Keuper	1510	7.6		
	Muschelkalk	1810	8.1		
	LFM	474	22.60		Well report
	LFM	475	20.90		
	LFM	476	7.20		
	LFM	476	6.60		
	LFM	476	8.70		
	LFM	477	14.90		
	LFM	477	19.70		

Well	Unit	Depth	Porosity mean (%)	Stratigraphic unit average	Source
Pfaffnau-1	LFM	477	22.40		
	LFM	478	25.20		
	LFM	478	22.00		
	LFM	478	21.20		
	LFM	479	20.40		
	LFM	479	20.50		
	LFM	480	17.90		
	LFM	480	14.10		
	LFM	480	19.60		
	LFM	481	6.40		
	LFM	481	21.10		
	LFM	481	18.10		
	LFM	482	23.30		
	LFM	482	4.30	17.34	
	Upper Malm	748	1.90		
	Upper Malm	748	2.50		
	Upper Malm	748	2.40		
	Upper Malm	749	2.10		
	Upper Malm	749	1.80		
	Upper Malm	750	2.40		
	Upper Malm	750	2.40		
	Upper Malm	751	2.80		
	Upper Malm	751	2.70		
	Upper Malm	752	0.70		
	Upper Malm	752	0.40		
	Upper Malm	753	0.20	1.68	
	Lias	1366	5.00		
	Lias	1367	1.60		
	Lias	1367	2.30		
	Lias	1368	5.00		
	Lias	1368	4.10		
	Lias	1368	2.80		
	Lias	1369	7.60		
	Lias	1369	3.00		
	Lias	1370	2.40		
	Lias	1370	1.40		
	Lias	1370	2.10		
	Lias	1371	1.80		
	Lias	1372	2.00		
	Lias	1372	1.40		
	Lias	1372	1.80		
	Lias	1373	1.60		
	Lias	1373	2.50		
	Lias	1374	1.50		

Well	Unit	Depth	Porosity mean (%)	Stratigraphic unit average	Source
Pfaffnau-1	Lias	1374	1.70		
	Lias	1375	0.90		
	Lias	1375	0.80		
	Lias	1376	1.20		
	Lias	1377	1.70		
	Lias	1377	1.50		
	Lias	1377	1.60		
	Lias	1378	1.80		
	Lias	1378	2.10		
	Lias	1379	2.20		
	Lias	1379	1.20		
	Lias	1380	1.20		
	Lias	1380	2.00		
	Lias	1380	1.80		
	Lias	1381	1.30		
	Lias	1381	2.10		
	Lias	1382	1.20		
	Lias	1382	2.10		
	Lias	1383	1.30		
	Lias	1383	1.60		
	Lias	1383	4.10		
	Lias	1384	4.30		
	Lias	1384	1.80		
	Lias	1384	3.90		
	Lias	1385	10.20		
	Lias	1385	6.20		
	Lias	1385	2.60		
	Lias	1385	9.20		
	Lias	1386	8.90		
	Lias	1386	9.40		
	Lias	1387	4.10		
	Lias	1387	10.10		
	Lias	1387	8.10		
	Lias	1387	8.50		
	Lias	1388	9.80		
	Lias	1388	4.00		
	Lias	1388	7.50		
	Lias	1389	4.60		
	Lias	1389	4.80		
	Lias	1389	6.00		
	Lias	1390	5.30		
	Lias	1390	4.40		
	Lias	1390	5.00		
	Lias	1390	5.00		

Well	Unit	Depth	Porosity mean (%)	Stratigraphic unit average	Source
Pfaffnau-1	Lias	1391	3.40		
	Lias	1391	4.20		
	Lias	1391	3.80		
	Lias	1392	5.30		
	Lias	1392	3.70		
	Lias	1392	1.20		
	Lias	1393	4.20		
	Lias	1393	8.30		
	Lias	1393	1.90		
	Lias	1393	4.10		
	Lias	1394	4.70		
	Lias	1394	5.30		
	Lias	1394	5.40		
	Lias	1395	1.50		
	Lias	1395	5.20		
	Lias	1395	4.90		
	Lias	1396	4.30		
	Lias	1396	4.30		
	Lias	1396	2.40		
	Lias	1396	3.40		
	Lias	1397	2.70		
	Lias	1397	2.00		
	Lias	1397	1.20		
	Lias	1398	7.60		
	Lias	1398	1.70		
	Lias	1399	7.80		
	Lias	1399	11.00		
	Lias	1400	10.70		
	Lias	1400	11.10		
	Lias	1400	12.30	4.11	
	Keuper	1401	9.50		
	Keuper	1401	10.70		
	Keuper	1402	11.70		
	Keuper	1403	10.90		
	Keuper	1403	11.60		
	Keuper	1404	12.60		
	Keuper	1404	13.40		
	Keuper	1404	14.50		
	Keuper	1405	14.30		
	Keuper	1405	12.70		
	Keuper	1405	12.50		
	Keuper	1406	12.80		
	Keuper	1406	12.90		
	Keuper	1406	12.60		

Well	Unit	Depth	Porosity mean (%)	Stratigraphic unit average	Source
Pfaffnau-1	Keuper	1406	13.60		
	Keuper	1407	11.30		
	Keuper	1408	8.50		
	Keuper	1408	7.90	11.89	
	Muschelkalk	1544	2.00		
	Muschelkalk	1544	2.30		
	Muschelkalk	1544	2.30		
	Muschelkalk	1545	1.10		
	Muschelkalk	1545	1.70		
	Muschelkalk	1546	14.90		
	Muschelkalk	1546	15.90		
	Muschelkalk	1546	20.30		
	Muschelkalk	1547	13.10		
	Muschelkalk	1547	13.30		
	Muschelkalk	1547	10.50		
	Muschelkalk	1547	8.90		
	Muschelkalk	1548	9.80		
	Muschelkalk	1548	8.30		
	Muschelkalk	1548	6.30		
	Muschelkalk	1549	8.30		
	Muschelkalk	1549	6.10		
	Muschelkalk	1549	5.40		
	Muschelkalk	1550	8.00		
	Muschelkalk	1550	4.70		
	Muschelkalk	1550	5.70		
	Muschelkalk	1551	6.70		
	Muschelkalk	1551	3.00		
	Muschelkalk	1551	8.60		
	Muschelkalk	1551	7.60		
	Muschelkalk	1552	5.00		
	Muschelkalk	1552	7.60		
	Muschelkalk	1553	9.20		
	Muschelkalk	1553	5.10		
	Muschelkalk	1553	6.00		
	Muschelkalk	1553	5.80		
	Muschelkalk	1554	8.10		
	Muschelkalk	1554	5.30		
	Muschelkalk	1554	6.20		
	Muschelkalk	1555	6.30		
	Muschelkalk	1555	7.10		
	Muschelkalk	1555	12.20		
	Muschelkalk	1555	10.40		
	Muschelkalk	1556	9.40		
	Muschelkalk	1556	10.20		

Well	Unit	Depth	Porosity mean (%)	Stratigraphic unit average	Source
Pfaffnau-1	Muschelkalk	1556	4.50		
	Muschelkalk	1557	9.50		
	Muschelkalk	1557	10.20		
	Muschelkalk	1557	7.90		
	Muschelkalk	1557	5.20		
	Muschelkalk	1558	5.10		
	Muschelkalk	1558	6.70		
	Muschelkalk	1808	4.90		
	Muschelkalk	1809	5.20		
	Muschelkalk	1809	3.80		
	Muschelkalk	1809	6.10		
	Muschelkalk	1810	12.30		
	Muschelkalk	1810	8.00		
	Muschelkalk	1810	8.20		
	Muschelkalk	1818	11.10		
	Muschelkalk	1811	7.90		
	Muschelkalk	1811	5.60		
	Muschelkalk	1812	8.80		
	Muschelkalk	1812	4.80		
	Muschelkalk	1812	8.50		
	Muschelkalk	1812	13.10		
	Muschelkalk	1813	2.30		
	Muschelkalk	1813	4.50		
	Muschelkalk	1813	9.20		
	Muschelkalk	1814	11.00		
	Muschelkalk	1814	9.60		
	Muschelkalk	1814	12.60		
	Muschelkalk	1814	23.50		
	Muschelkalk	1814	15.60		
	Muschelkalk	1815	3.60		
	Muschelkalk	1815	6.00		
	Muschelkalk	1815	9.60		
	Muschelkalk	1816	0.00		
	Muschelkalk	1816	10.60		
	Muschelkalk	1816	18.80		
	Muschelkalk	1817	9.60		
	Muschelkalk	1817	11.20		
	Muschelkalk	1817	8.20		
	Muschelkalk	1818	4.20		
	Muschelkalk	1818	3.60		
	Muschelkalk	1818	5.90		
	Muschelkalk	1818	11.70		
	Muschelkalk	1819	6.30		
	Muschelkalk	1819	6.10		

Well	Unit	Depth	Porosity mean (%)	Stratigraphic unit average	Source
Pfaffnau-1	Muschelkalk	1820	7.40		
	Muschelkalk	1820	7.90		
	Muschelkalk	1820	10.50		
	Muschelkalk	1820	7.40		
	Muschelkalk	1821	7.40		
	Muschelkalk	1821	10.00		
	Muschelkalk	1822	8.60		
	Muschelkalk	1822	0.00		
	Muschelkalk	1822	8.40		
	Muschelkalk	1823	7.00		
	Muschelkalk	1823	12.00		
	Muschelkalk	1823	11.00		
	Muschelkalk	1824	4.20		
	Muschelkalk	1824	6.60		
	Muschelkalk	1826	5.40		
	Muschelkalk	1828	3.50		
	Muschelkalk	1830	5.00		
	Muschelkalk	1833	1.90		
	Muschelkalk	1836	1.60		
	Muschelkalk	1839	1.70	7.67	
Riniken-1	Dogger	327	3.40		Well report
	Dogger	327	4.70		
	Dogger	330	5.90		
	Dogger	342	9.40		
	Dogger	396	2.20		
	Dogger	397	3.00	4.77	
	Lias	452	4.80	4.80	
	Muschelkalk	625	20.00		
	Muschelkalk	627	29.00		
	Muschelkalk	628	22.00		
	Muschelkalk	700	8.00		
	Muschelkalk	703	6.00		
	Muschelkalk	715	11.00		
	Muschelkalk	728	4.50		
	Muschelkalk	737	1.20		
	Muschelkalk	740	4.00		
	Muschelkalk	744	8.00		
	Muschelkalk	754	4.90		
	Muschelkalk	796	18.30		
	Muschelkalk	801	3.80		
	Muschelkalk	807	16.30	11.21	
	Permian	828	4.40		
	Permian	842	9.60		
	Permian	904	6.30		

Well	Unit	Depth	Porosity mean (%)	Stratigraphic unit average	Source
Riniken-1	Permian	922	6.00		
	Permian	932	8.40		
	Permian	943	10.00		
	Permian	952	5.40		
	Permian	973	6.00		
	Permian	987	7.60		
	Permian	998	12.50		
	Permian	1011	10.00		
	Permian	1045	7.10		
	Permian	1048	13.90		
	Permian	1065	8.80		
	Permian	1121	5.60		
	Permian	1156	8.30		
	Permian	1191	7.30		
	Permian	1295	9.00		
	Permian	1382	2.50		
	Permian	1428	5.40		
	Permian	1492	1.00		
	Permian	1502	3.80		
	Permian	1563	6.00		
	Permian	1617	6.00		
	Permian	1631	7.00		
	Permian	1654	6.20		
	Permian	1673	10.30		
	Permian	1695	4.60		
	Permian	1712	2.90		
	Permian	1729	5.80		
	Permian	1737	6.40		
	Permian	1750	4.00		
	Permian	1764	6.60		
	Permian	1771	3.90		
	Permian	1784	4.80		
	Permian	1795	5.00	6.62	
Romanens-1	Malm	3239	1.20		Well report
	Malm	3239.5	1.00		
	Malm	3240	1.10		
	Malm	3240.5	1.00		
	Malm	3241	0.60		
	Malm	3241.5	0.40		
	Malm	3242	0.50		
	Malm	3242.5	0.30		
	Malm	3243	0.20		
	Malm	3243.5	0.60		
	Malm	3244	0.60		

Well	Unit	Depth	Porosity mean (%)	Stratigraphic unit average	Source
Romanens-1	Malm	3244.5	0.70		
	Malm	3245	0.60	0.68	
	Lias	3872.35	1.10		
	Lias	3872.7	1.10		
	Lias	3873.15	0.90		
	Lias	3873.5	0.70		
	Lias	3873.75	1.20		
	Lias	3874.1	1.20		
	Lias	3874.5	0.90		
	Lias	3874.9	0.80		
	Lias	3875.35	0.80		
	Lias	3875.6	0.80		
	Lias	3875.9	0.70		
	Lias	3876.15	0.70	0.91	
Schafisheim-1	USM	280	7-10.3	8.50	Greber et al., 2007
	Malm	600	0.9	0.90	
	Dogger	1080	5		
	Dogger	1090	1.3	3.15	
	Keuper	1150	6		
	Keuper	1210	7.5	6.75	
	Muschelkalk	1300	1		
	Muschelkalk	1400	1		
	Muschelkalk	1490	2.5	1.5	
Schlattingen-1	Lower Malm	735	7.14		Ciemat, Physical Porosity calculated from density, Well Report
	Lower Malm	742	7.20	7.17	
	Dogger	765	9.64		
	Dogger	780	11.44		
	Dogger	817	9.90		
	Dogger	833	12.14		
	Dogger	861	13.40		
	Dogger	880	10.59		
	Dogger	898	10.77		
	Dogger	916	12.24		
	Dogger	929	9.31		
	Dogger	939	13.26	11.27	
	Lias	972	10.79		
	Lias	988	11.06	10.93	
	Lower Malm	735	8.81		UniBern, Phyisical Porosity calculated from density, Well report
	Lower Malm	742	7.76		
	Lower Malm	751	10.07	8.88	
	Dogger	759	15.94		
	Dogger	765	9.13		

Well	Unit	Depth	Porosity mean (%)	Stratigraphic unit average	Source
Schlattingen-1	Dogger	769	11.93		
	Dogger	779	11.20		
	Dogger	779	12.93		
	Dogger	787	11.76		
	Dogger	795	4.74		
	Dogger	800	12.94		
	Dogger	812	13.07		
	Dogger	816	13.90		
	Dogger	823	14.29		
	Dogger	825	15.26		
	Dogger	833	10.29		
	Dogger	845	9.22		
	Dogger	852	10.56		
	Dogger	858	11.56		
	Dogger	861	12.25		
	Dogger	872	8.90		
	Dogger	880	11.36		
	Dogger	888	11.78		
	Dogger	898	11.44		
	Dogger	908	13.83		
	Dogger	916	11.91		
	Dogger	921	11.45		
	Dogger	929	11.77		
	Dogger	938	12.21		
	Dogger	939	12.87		
	Dogger	949	10.65	11.76	
	Lias	960	12.04		
	Lias	972	12.82		
	Lias	981	15.06		
	Lias	988	14.08	13.50	
	Dogger	762	10.59		Porosity plug, Nagra Report
	Dogger	766	8.56		
	Dogger	773	9.61		
	Dogger	774	11.51		
	Dogger	812	13.53		
	Dogger	827	1.92		
	Dogger	835	13.51		
	Dogger	886	1.98		
	Dogger	930	11.09		
	Dogger	946	11.39		
	Dogger	856	5.03	8.97	
St. Gallen GT-1	Malm	4100	0.07		Naef and Shlanke, 2014
	Malm	4120	1.79		
	Malm	4223	2.43		

Well	Unit	Depth	Porosity mean (%)	Stratigraphic unit average	Source
St. Gallen-GT-1	Malm	4290	2.07		
	Malm	4297	2.31		
	Malm	4364	5.40		
	Malm	4380	5.82		
	Malm	4387	5.86		
	Malm	4399	4.75	3.39	
	Dogger	4419	5.12	5.12	
	UFM	120	18.3		Average estimated from logs
	UMM	290	9.5		
	LFM1	550	5		
	LFM Triangle	2040	14		
	LFM 2	3650	18		
	LMM	3980	3.6		
	UFM	20	31.91		
	UFM	100	19.98		
	UFM	200	27.96		
	UFM	236	2.95		
	UMM	300	5.95		
	UMM	400	17.56		
	UMM	500	8.87		
	UMM	600	6.61		
	UMM	700	7.41		
	UMM	768	0.24		
	LFM1	800	2.00		
	LFM1	900	5.40		
	LFM1	1000	4.36		
	LFM1	1100	1.57		
	LFM1	1200	3.74		
	LFM1	1300	1.28		
	LFM1	1400	1.00		
	LFM1	1500	2.00		
	LFM1	1600	2.92		
	LFM1	1700	8.59		
	LFM1	1800	5.60		
	LFM1	1900	10.07		
	LFM1	2000	10.00		
	LFM1	2100	12.12		
	LFM1	2200	1.22		
	LFM1	2300	8.27		
	LFM1	2400	5.65		
	LFM1	2420	6.88		
	LFM Triangle	2500	6.81		
	LFM Triangle	2600	5.79		
	LFM Triangle	2700	13.12		

Well	Unit	Depth	Porosity mean (%)	Stratigraphic unit average	Source
St. Gallen-GT-1	LFM Triangle	2800	8.34		
	LFM Triangle	2900	3.75		
	LFM Triangle	3000	19.66		
	LFM Triangle	3100	18.47		
	LFM Triangle	3200	8.28		
	LFM Triangle	3300	19.21		
	LFM2	3400	20.21		
	LFM2	3500	17.28		
	LFM2	3600	20.64		
	LFM2	3700	19.34		
	LFM2	3800	18.83		
	LFM2	3900	18.95		
	LFM2	3970	10.49		
	LMM	3986	2.34		
	LMM	3993	4.69	9.96	
Thun-1	USM	2850	10.00		Greber et al., 2007
	UMM	5195	6.50	8.25	
	Malm	5600	5.00		
	Malm	5900	3.00	4.00	
Treyçovagnes-1	Dogger	902	5		Well Report- Petrophysical evaluation
	Dogger	916	5		
	Dogger	1090	3	4.3	
	Lias	1308	3	3.00	
	Muschelkalk	2548	2.3		
	Muschelkalk	2560	1.8		
	Muschelkalk	2603	1.8	5.9	
	Buntsandstein	2688	5.60		
	Buntsandstein	2739	5.60	5.60	
	Permian	2800	1.80	1.8	
	Buntsandstein	2722.6	3.10		Well Report-Geological Investigation of cores
	Buntsandstein	2722.9	2.80		
	Buntsandstein	2723.3	3.30		
	Buntsandstein	2723.6	3.30		
	Buntsandstein	2723.8	3.10		
	Buntsandstein	2724.2	5.70		
	Buntsandstein	2724.6	2.20		
	Buntsandstein	2724.9	2.80		
	Buntsandstein	2725.2	3.60		
	Buntsandstein	2725.3	3.60		
	Buntsandstein	2725.5	5.50		
	Buntsandstein	2725.9	5.40		
	Buntsandstein	2726.2	5.50		
	Buntsandstein	2726.3	4.00		

Well	Unit	Depth	Porosity mean (%)	Stratigraphic unit average	Source
Treyçovagnes-1	Buntsandstein	2726.5	3.20		
	Buntsandstein	2726.7	5.80		
	Buntsandstein	2727	5.30		
	Buntsandstein	2727.2	4.60		
	Buntsandstein	2727.5	2.50		
	Buntsandstein	2727.9	3.60		
	Buntsandstein	2728.3	4.70		
	Buntsandstein	2728.5	4.50		
	Buntsandstein	2728.9	3.30		
	Buntsandstein	2729	4.70		
	Buntsandstein	2729.2	5.40		
	Buntsandstein	2729.8	4.10	4.06	
	Permian	3215.1	1.80		
	Permian	3215.5	2.10		
	Permian	3215.8	2.00		
	Permian	3216.2	1.60		
	Permian	3216.5	1.60		
	Permian	3216.8	2.10		
	Permian	3217.2	1.70		
	Permian	3217.5	2.10		
	Permian	3217.9	2.20		
	Permian	3218.2	1.90		
	Permian	3218.5	1.90		
	Permian	3218.8	1.60		
	Permian	3219.2	1.80		
	Permian	3219.6	1.80		
	Permian	3219.9	1.70		
	Permian	3220.3	2.10		
	Permian	3220.7	2.60	1.92	
Truillikon-1	Malm		4.10	4.10	Well report
	Dogger		9.10	9.10	
	Muschelkalk		10.00	10.00	
	Buntsandstein		12.50	12.50	
	Rotligend		7.00	7.00	
Weiach-1	Chattian	52	12.50		Well report
	Chattian	53	27.00		
	Chattian	60	20.00		
	Chattian	68	0.00		
	Chattian	77	3.20		
	Chattian	103	26.50		
	Chattian	111	19.00		
	Chattian	136	28.00		
	Chattian	172	7.50	15.97	
	Upper Malm	200	1.00		

Well	Unit	Depth	Porosity mean (%)	Stratigraphic unit average	Source
Weiach-1	Upper Malm	212	0.40		
	Upper Malm	237	1.80		
	Upper Malm	252	0.75		
	Upper Malm	264	1.25		
	Upper Malm	279	1.00		
	Upper Malm	290	0.60		
	Upper Malm	320	1.40		
	Upper Malm	340	2.75		
	Upper Malm	357	1.50		
	Upper Malm	371	0.75		
	Upper Malm	386	2.75		
	Lower Malm	421	1.00	1.30	
	Dogger	503	7.00		
	Dogger	527	3.00		
	Dogger	538	7.50		
	Dogger	548	7.50		
	Dogger	553	12.50		
	Dogger	560	2.70		
	Dogger	566	11.50		
	Dogger	579	12.00		
	Dogger	588	3.70		
	Dogger	596	8.00		
	Dogger	613	11.80		
	Dogger	625	8.00		
	Dogger	633	9.00		
	Dogger	640	12.50		
	Dogger	649	7.60		
	Dogger	656	9.00	8.33	
	Lias	661	11.20		
	Lias	670	3.50		
	Lias	675	6.00		
	Lias	683	8.20		
	Lias	689	8.30		
	Lias	696	2.25	6.58	
	Keuper	706	7.50		
	Keuper	713	8.60		
	Keuper	717	7.40		
	Keuper	722	10.00		
	Keuper	727	13.40		
	Keuper	733	8.20		
	Gypskeuper	755	2.80		
	Gypskeuper	760	3.30		
	Gypskeuper	779	2.50		
	Gypskeuper	785	2.00		

Well	Unit	Depth	Porosity mean (%)	Stratigraphic unit average	Source
Weiach-1	Gypskeuper	798	7.60		
	Gypskeuper	808	1.10		
	Gypskeuper	811	2.00	5.88	
	Upper Muschelkalk	821	25.00		
	Upper Muschelkalk	824	30.00		
	Upper Muschelkalk	831	7.70		
	Upper Muschelkalk	837	7.50		
	Upper Muschelkalk	841	5.00		
	Upper Muschelkalk	847	4.20		
	Upper Muschelkalk	853	7.40		
	Upper Muschelkalk	863	0.80		
	Upper Muschelkalk	867	0.50		
	Upper Muschelkalk	869	4.50		
	Upper Muschelkalk	876	2.50		
	Upper Muschelkalk	881	2.20		
	Upper Muschelkalk	886	5.30		
	Middle Mushcelkalk	891	7.60		
	Middle Mushcelkalk	898	1.20		
	Middle Mushcelkalk	908	1.20		
	Middle Mushcelkalk	912	1.40		
	Middle Mushcelkalk	925	1.80		
	Middle Mushcelkalk	930	1.00		
	Middle Mushcelkalk	933	2.30		
	Middle Mushcelkalk	942	5.00		
	Lower Muschelkalk	947	5.10		
	Lower Muschelkalk	957	0.80		
	Lower Muschelkalk	960	4.20		
	Lower Muschelkalk	965	3.80		
	Lower Muschelkalk	979	4.40	5.48	
	Buntsandstein	984	7.50		
	Buntsandstein	985	18.00		
	Buntsandstein	988	3.50	9.67	
	Permian	1002	7.50		
	Permian	1014	7.00		
	Permian	1032	5.50		
	Permian	1044	7.00		
	Permian	1056	5.00		

Well	Unit	Depth	Porosity mean (%)	Stratigraphic unit average	Source
Weiach-1	Permian	1062	5.00		
	Permian	1073	13.50		
	Permian	1083	12.00		
	Permian	1097	29.00		
	Permian	1100	12.20		
	Permian	1105	19.00		
	Permian	1110	0.00		
	Permian	1118	15.00		
	Permian	1120	18.30		
	Permian	1135	5.70		
	Permian	1140	6.00		
	Permian	1150	8.20		
	Permian	1157	7.00		
	Permian	1170	13.50		
	Permian	1180	16.50		
	Permian	1187	12.50		
	Permian	1192	4.10		
	Permian	1204	11.00		
	Permian	1205	12.50		
	Permian	1219	14.50		
	Permian	1221	14.50		
	Permian	1228	0.00		
	Permian	1234	11.50		
	Permian	1247	13.20		
	Permian	1267	15.40		
	Permian	1285	4.50		
	Permian	1295	12.60		
	Permian	1299	0.00		
	Permian	1301	13.00		
	Permian	1302	7.00		
	Permian	1307	9.40		
	Permian	1318	5.70		
	Permian	1325	9.80		
	Permian	1341	6.50		
	Permian	1343	5.50		
	Permian	1366	6.50		
	Permian	1369	6.40		
	Permian	1390	8.20		
	Permian	1401	8.60		
	Permian	1409	8.00		
	Permian	1413	4.70		
	Permian	1422	12.50		
	Permian	1435	6.70	9.54	
	Carboniferous	1448	6.20		

Well	Unit	Depth	Porosity mean (%)	Stratigraphic unit average	Source
Weiach-1	Carboniferous	1458	10.00		
	Carboniferous	1470	6.00		
	Carboniferous	1484	7.00		
	Carboniferous	1502	11.00		
	Carboniferous	1510	6.50		
	Carboniferous	1530	1.80		
	Carboniferous	1549	5.10		
	Carboniferous	1570	8.50		
	Carboniferous	1581	10.50		
	Carboniferous	1598	6.50		
	Carboniferous	1604	13.50		
	Carboniferous	1609	10.10		
	Carboniferous	1636	7.50		
	Carboniferous	1660	8.50		
	Carboniferous	1675	8.10		
	Carboniferous	1695	9.50		
	Carboniferous	1727	5.80		
	Carboniferous	1761	5.00		
	Carboniferous	1774	4.10		
	Carboniferous	1800	3.50		
	Carboniferous	1821	6.00		
	Carboniferous	1845	10.00		
	Carboniferous	1885	4.00		
	Carboniferous	1890	10.00		
	Carboniferous	1915	7.70		
	Carboniferous	1935	7.50		
	Carboniferous	1940	2.50		
	Carboniferous	1970	4.50		
	Carboniferous	1994	0.70		
	Carboniferous	2002	6.00		
	Carboniferous	2015	2.30		
	Carboniferous	2019	10.00		
	Carboniferous	2144	1.40		
	Carboniferous	2227	0.00		
	Carboniferous	2026	3.00		
	Carboniferous	2042	2.00		
	Carboniferous	2060	2.60		
	Carboniferous	2077	2.00	6.07	
	Basement	2192	2.00		
	Basement	2271	0.00		
	Basement	2097	12.90		
	Basement	2220	3.40		
	Basement	2064	3.50		
	Basement	2257	4.40	4.37	

Appendix 6: Porosity data measured in the most relevant wells of the Swiss Plateau. For each well, the average for stratigraphic unit is indicated.

12.7 Temperature data

Well	Unit	Depth	Temperature	Source
Benken-1	LFM	100	15.2	Nagra, 2001
	LFM	150	16.9	
	Malm	200	18.6	
	Malm	250	20.1	
	Malm	300	21.4	
	Malm	350	22.9	
	Malm	400	24.3	
	Malm	450	26.3	
	Dogger	500	28.5	
	Dogger	550	31	
	Dogger	600	34.4	
	Dogger	650	38	
	Lias	700	41.1	
	Lias	750	43.3	
	Keuper	800	45.5	
	Mushelkalk	850	46.6	
	Mushelkalk	900	48	
	Mushelkalk	950	49.7	
	Basement	1000	51.5	
Chapelle-1	Chattian	480	33	Vollmayr, 1983
	Lower Cretaceous	1500	58	
Eclépens	Lower Cretaceous	192	45	Vollmayr, 1983
	Malm	1061	55.7	
	Keuper	2142	97.6	
	Lias	2038	106.4	
	Lower Cretaceous	201	48.1	Well Report
	Lower Cretaceous	203	47.9	
	Lower Cretaceous	203	48.1	
	Malm	1066	52.9	
	Malm	1070	55.4	
	Malm	1070	54.9	
	Lias	1784	66.6	
	Lias	1881	67	
	Lias	2049	78.7	
	Lias	2048	86.7	
	Lias	2046	82.7	
	Keuper	2108	80.7	
	Keuper	2147	87.3	
	Keuper	2150	94.3	
Entlebuch-1	LFM	294	28.9	Vollymar, 1983
	LFM	2210	71.9	
	LFM	3990	116.1	

Well	Unit	Depth	Temperature	Source
Entlebuch-1	Malm	4501	144.9	
	Lias	4852	156.6	
	Carboniferous	5289	160	
Essertines-1	Quaternary	500	38.5	Vollmayr, 1983
	Malm	1000	57	
	Lias	2000	93.5	
Herdern-1	UFM	100	14.4	Vollmayr, 1983
	UFM	200	18.1	
	UFM	300	21.7	
	UFM	400	25.5	
	UFM	479	39.1	
	UFM	480	28.6	
	Malm	1306	57.2	
	Mushelkalk	2154	87.6	
	Quaternary	0	10	Nagra, 2002
	OMM	528	38	
	Eocene	1305	60	
	Malm	1649	70	
	Dogger	1847	80	
	Lias	1879	82	
	Keuper	1950	85	
	Muschelkalk	2130	89	
Hermingen-1	Cretaceous	420.8	36	Vollmayr, 1983; Elf-Aquitaine, 1982
	Malm	879	47.5	
	Lias	1818	60	
	Muschelkalk	2297.5	85	
	Muschelkalk	2425	93	
Hunenberg-1	UMM	725	38	Vollmayr, 1983
	LFM	2150	64	
	Malm	3288	96	
Kreuzlingen-1	UMM	594	45	Vollmayr, 1983
	LFM	1730	72	
	Muschelkalk	2517	114	
Linden-1	LFM	2226.5	64.4	Well Report
	LFM	3406.6	95.5	
Noville-1	Quaternary	10	20.86	Well Report
	Quaternary	50	20.48	
	Quaternary	250	18.06	
	Quaternary	500	21.16	
	LFM	750	29.17	
	LFM	1000	36.65	
	Malm	1250	40.62	
	Malm	1500	1500	
	Malm	1750	50.72	

Well	Unit	Depth	Temperature	Source
Noville-1	Malm	2000	60.08	
	Malm	2250	68.77	
	Dogger	2500	75.75	
	Muschelkalk	2750	85.48	
	Permian	3000	95.46	
	Permian	3044	97.68	
Pfaffnau-1	LFM	442	20	Vollymar, 1983
	Malm	752	39	
	Lias	1386	65	
	Keuper	1408	52	
	Muschelkalk	1820	72	
Ruppoldsdried-1	LFM	300	25	Vollmayr, 1983
	LFM	800	44	
	Malm	890	46	
	Malm	980	48	
Savigny-1	Quaternary	201	30.4	Well Report
	Rupelian	991	51.6	
	Rupelian	992	44.6	
	Albian	2339	84.4	
	Hauterivian	2430	92.3	
	Hauterivian	2486	89	
Schafisheim-1	Quaternary	0	10	Well Report
	Quaternary	200	17	
	LFM	301	20.5	
	LFM	400	23	
	Malm	600	31	
	Malm	710	36	
	Malm	800	38	
	Dogger	971	46	
	Dogger	1000	48	
	Dogger	1016	49	
	Keuper	1103	53	
	Keuper	1137	55.9	
	Keuper	1200	59	
	Keuper	1226	58	
	Muschelkalk	1400	65	
	Muschelkalk	1446	67	
	Muschelkalk	1469	68.7	
	Basement	1517	70.8	
	Basement	1600	72	
	Basement	1718	78.7	
	Basement	2000	86	
	Basement	2005	90.5	
St-Gallen GT-1	Quaternary	0	30	Naef and Shlanke, 2014

Well	Unit	Depth	Temperature	Source
St. Gallen-GT-1	UFM	100	39	
	UFM	200	45	
	UMM	450	50	
	UMM	650	54	
	LFM	1000	60	
	LFM	1300	68	
	LFM	1800	71	
	LFM	2400	83	
	LFM	2800	91	
	LFM	3200	101	
	LFM	3700	114	
	Malm	4100	124	
	Dogger	4430	144	
Thun-1	LFM	2175	65	Rybach, 1989
	LFM	2175.1	70	
	LFM	4736	139	
	LFM	4736	150	
	Malm	5561	185	
	Dogger	5911	188	
	Dogger	5911.1	197	
	Lias	5945	195	
Treyçovagnes-1	Dogger	881	48.2	Vollmayr, 1983
	Keuper	2244	91.6	
	Keuper	2395	98	
	Permian	2800	109.3	
	Permian	3210	125.6	
	Malm	879	50.3	Well Report
	Malm	880	50.5	
	Malm	886	50.3	
	Keuper	2242	85.7	
	Keuper	2246	89	
	Keuper	2395	89.1	
	Muschelkalk	2800	108.1	
	Permian	3210	120.8	
Tschugg-1	LFM	280	20	Vollmayr, 1983
	Malm	700	32	
Weiach-1	Malm	195	27.5	Matter et al., 1988
	Malm	255	34.7	
	Malm	479	26.4	
	Dogger	550	27	
	Lias	699	43.1	
	Keuper	728	34.6	
	Muschelkalk	859	43.8	
	Muschelkalk	859	50	

Well	Unit	Depth	Temperature	Source
Weiach-1	Muschelkalk	926	41.6	
	Buntsandstein	984	51.9	
	Buntsandstein	985	35	
	Permian	1111	55.3	
	Permian	1118	54.3	
	Permian	1240	53.6	
	Permian	1303	58.1	
	Permian	1369	62.5	
	Permian	1411	64.1	
	Carboniferous	1457	64.8	
	Carboniferous	1603	68.4	
	Carboniferous	1881	91.3	
	Carboniferous	1965	87.4	

Appendix 7: Temperature data measured in the most relevant wells of the Swiss Plateau

12.8 Vitrinite Reflectance (%Ro) data

Well	Unit	Depth	%Ro value	%Ro Min	%Ro Max	Source
Benken-1	Malm	220	0.48			Nagra,2001 - New Castle University
	Malm	400	0.55			
	Dogger	540	0.51			
	Dogger	550	0.56			
	Dogger	570	0.59			
	Lias	660	0.61			
	Keuper	810	0.65			
	Muschelkalk	950	0.71			
	Malm	228	0.48			Nagra, 2001 - RGCI Koldingen
	Malm	402	0.55			
	Dogger	543.97	0.55			
	Dogger	543.97	0.5			
	Dogger	543.97	0.52			
	Dogger	550.48	0.68			
	Dogger	550.48	0.66			
	Dogger	550.48	0.56			
	Dogger	586.99	0.43			
	Dogger	586.99	0.58			
	Dogger	586.99	0.56			
	Dogger	586.99	0.62			
	Lias	677.97	0.63			
	Lias	677.97	0.85			
	Muschelkalk	810.59	0.63			
	Muschelkalk	810.59	0.65			
	Muschelkalk	968.01	0.71			
	Muschelkalk	968.01	0.88			
Chapelle-1	UMM	53	0.41	0.32	0.48	Schegg et al., 1997
	UMM	78	0.43	0.33	0.56	
	LFM	600	0.5	0.39	0.62	
	LFM	1366	0.7	0.64	0.75	
	Lower Cretaceous	1437	0.69	0.6	0.81	
	Lower Cretaceous	1504	0.72	0.51	0.92	
Eclépens	Malm	770	0.5	0.4	0.55	Schegg et al., 1997
	Malm	815	0.49	0.39	0.63	
	Malm	1050	0.62	0.57	0.67	
	Dogger	1220	0.58	0.48	0.67	
	Posidonia shale	1705	0.73	0.65	0.83	
	Lias	1908	0.66	0.56	0.7	

Well	Unit	Depth	%Ro value	%Ro Min	%Ro Max	Source
Eclépens	Lias	2002	0.76	0.61	0.86	
	Keuper	2056	0.75	0.61	0.89	
Essertines-1	Lower Cretaceous	310	0.43	0.38	0.52	Schegg et al., 1997
	Lower Cretaceous	315	0.49	0.42	0.6	
	Lower Cretaceous	406	0.68	0.5	0.73	
	Lower Cretaceous	562	0.74	0.63	0.82	
	Malm	1062	0.69	0.64	0.9	
	Malm	1246	0.72	0.65	0.9	
	Malm	1698	0.88	0.65	0.9	
	Posidonia shale	1976	0.88	0.61	0.89	
	Lias	2080	0.89	0.69	1.02	
	Lias	2234	0.84	0.72	0.91	
Herdern-1	Oligocene	170	0.42			Leu et al., 2001; Nagra 2002
	Oligocene	350	0.23			
	Oligocene	650	0.56			
	Oligocene	670	0.54			
	Oligocene	1150	0.52			
	Oligocene	1210	0.48			
	Malm	1450	0.55			
	Malm	1580	0.7			
	Dogger	1720	0.75			
	Dogger	1730	0.74			
	Lias	1850	0.58			
	Lias	1875	0.72			
	Upper Muschelkalk	1990	0.75			
	Buntsandstein	2120	0.82			
Hermrigen-1	Molasse	320	0.24			Leu, 2007 (Stratochem)
	Dogger	1539	1.13			
	Dogger	1540	1.15			
	Dogger	1589	1.24			
	Dogger	1650	1.15			
	Dogger	1707	1.29			
	Molasse	400	0.88			Converted from TAI, Elf-Aquitaine, 1983
	Malm	694	0.88			
	Malm	871	0.88			
	Malm	1009	0.63			
	Malm	1009	0.88			
	Dogger	1309	0.35			
	Dogger	1617	0.88			
	Dogger	1782.5	0.88			

Well	Unit	Depth	%Ro value	%Ro Min	%Ro Max	Source
Hermrigen-1	Lias	1882.7	0.88			
	Lias	1893.26	0.88			
	Lias	1902.85	0.75			
	Lias	1919.95	0.75			
	Lias	1931	0.88			
	Muschelkalk	2259.65	1.13			
	Muschelkalk	2275.45	1			
Kusnacht-1	UFM	350	0.45			Rybach and Bodmer, 1980
	UFM	500	0.5			
	UMM	800	0.45			
	LFM	1890	0.6			
Noville-1	LFM	620	1.43			Geoform, 2010
	LFM	740	1.41			
	LFM	994	1.65			
	LFM	1050	1.49			
	LFM	1069	1.65			
	Dogger	2478	2.81			
	Muschelkalk	2626	2.8			
	Permian	3350	3.1			
	Permian	3399	2.7			
	Carboniferous	3690	2.74			
	Carboniferous	3876	3.2			
	Carboniferous	3871	2.79			
	Carboniferous	3934	2.83			
	Carboniferous	3944	2.76			
	Carboniferous	4100	2.92			
	Carboniferous	4212	2.89			
	Carboniferous	4274	2.99			
	Carboniferous	4294	3.21			
Riniken	Malm	50	0.37			Matter et al., 1987
	Dogger	350	0.4			
	Dogger	385	0.44			
	Dogger	390	0.4			
	Dogger-Lias	450	0.43			
	Keuper	600	0.4			
	Muschelkalk	700	0.44			
Savigny-1	LFM	540	0.85	0.77	1.13	Schegg et al., 1997
	LFM	695	0.67	0.58	0.74	
	LFM	745	0.7	0.66	0.98	
	LFM	810	0.65	0.64	0.66	
Schafisheim-1	LFM	847	0.63	0.59	0.69	
	LFM	1087	0.7	0	0	
	LFM	1110	0.68	0.65	0.7	

Well	Unit	Depth	%Ro value	%Ro Min	%Ro Max	Source
Schafisheim-1	LFM	1247	0.63	0.46	0.75	
	LFM	1602	0.5	0.42	0.63	
	LFM	2087	0.75	0	0	
	LFM	2187	0.77	0.68	0.89	
Schlattingen-1	Lower Malm	735	0.4			%Ro converted from Tmax, Nagra Report
	Lower Malm	751	0.36			
	Dogger	765	0.5			
	Dogger	768	0.51			
	Dogger	787	0.54			
	Dogger	816	0.49			
	Dogger	823	0.53			
	Dogger	833	0.56			
	Dogger	852	0.6			
	Dogger	880	0.6			
	Dogger	915	0.6			
	Dogger	929	0.62			
	Lias	960	0.54			
	Lias	987	0.62			
Schafisheim-1	Malm	710	0.39			NAGRA, 1992; Matter et al., 1988
	Dogger	971	0.45			
	Dogger	1016	0.5			
	Lias	1104	0.46			
	Keuper	1226	0.6			
	Muschelkalk	1446	0.47			
	Muschelkalk	1446	0.92			
St-Gallen GT-1	UFM	140	0.5	0.45	0.65	Omodeo-Salé et al., 2020
	UMM	320	0.57	0.45	0.75	
	UMM	470	0.55	0.4	0.65	
	UMM	635	1.7	1.35	1.8	
	LFM	2480	1.67	1.6	1.75	
	LFM	2530	1.3	1.3	1.85	
	LMM	3985	2	1.8	2.25	
	Dogger	4423	2.15	1.7	2.6	
	Dogger	4430	2.3	2.1	2.7	
	Dogger	4445	2.6	1.8	2.95	
Thun-1	Syderolitique	5102-5198	1-1.7			Converted from TAI, Elf-Aquitaine, 1989
	Malm	5198-5204	3.0-4.0			
	Malm	5904	3.0-4.0			
	Malm	5222	3.0-4.0			
	Malm	5338	3.0-4.0			
	Malm	5473	3.0-4.0			

Well	Unit	Depth	%Ro value	%Ro Min	%Ro Max	Source
Thun-1	Malm	5610	3.0-4.0			
	Malm	5710	3.0-4.0			
	Malm	5806	3.0-4.0			
	Malm	5836	3.0-4.0			
	Dogger	5878	3.0-4.0			
	Dogger	5912	3.0-4.0			
Treyçovagnes-1	Lower Cretaceous	40	0.45	0.41	0.66	Schegg et al., 1997
	Malm	765	0.54	0.46	0.63	
	Malm	835	0.62	0.49	0.68	
	Posidonia shale	1440	0.54	0.48	0.59	
	Keuper	1687	0.65	0.54	0.84	
	Keuper	2260	0.82	0.77	0.85	
	Keuper	2395	0.89	0.75	0.99	
Weiach-1	Malm	365	0.45			Matter, 1987; Nagra 2002
	Dogger	501	0.53			
	Dogger	575	0.57			
	Dogger	632	0.57			
	Keuper	818	0.59			
	Muschelkalk	947	0.59			
	Muschelkalk	965	0.66			
	Permian	1314	0.64			
	Permian	1363	0.65			
	Permian	1403	0.7			
	Carboniferous	1481	0.78			
	Carboniferous	1542	0.86			
	Carboniferous	1542	0.81			
	Carboniferous	1542	0.85			
	Carboniferous	1560	0.85			
	Carboniferous	1562	0.84			
	Carboniferous	1562	0.91			
	Carboniferous	1585	0.86			
	Carboniferous	1585	0.85			
	Carboniferous	1585	0.86			
	Carboniferous	1587	0.87			
	Carboniferous	1588	0.87			
	Carboniferous	1590	0.87			
	Carboniferous	1590	0.87			
	Carboniferous	1623	0.91			
	Carboniferous	1700	0.98			
	Carboniferous	1740	1.02			
	Carboniferous	1749	1.03			
	Carboniferous	1772	1.15			
	Carboniferous	1772	1.14			

Well	Unit	Depth	%Ro value	%Ro Min	%Ro Max	Source
Weiach-1	Carboniferous	1838	1.06			
	Carboniferous	1871	1.18			
	Carboniferous	1871	1.21			
	Carboniferous	1949	1.24			
	Carboniferous	1949	1.28			

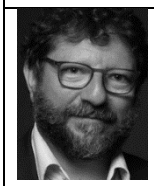
Appendix 8: Vitrinite reflectance (%Ro) data measured in the most relevant wells of the Swiss Plateau. The minimum (min) and maximum (max) measured values are indicated, when available.

12.9 TOC data (Hermrigen-1 and Thun-1 wells)

Well	Depth	Unit	Lithology	TOC	Source
Hermrigen-1	308.4	LFM Oligocene	Shale	0.97	Elf Aquitaine, 1983
Hermrigen-1	313.4	LFM Oligocene	Shale	0.17	Elf Aquitaine, 1983
Hermrigen-1	403.2	Valanginian	limestone	0.25	Elf Aquitaine, 1983
Hermrigen-1	413.7	Upper Jurassic	limestone	0.44	Elf Aquitaine, 1983
Hermrigen-1	425.7	Upper Jurassic	limestone	0.26	Elf Aquitaine, 1983
Hermrigen-1	696	Upper Jurassic	limestone	0.42	Elf Aquitaine, 1983
Hermrigen-1	873	Upper Jurassic	limestone	0.14	Elf Aquitaine, 1983
Hermrigen-1	1014	Oxfordian	limestone	0.15	Elf Aquitaine, 1983
Hermrigen-1	1163	Oxfordian	limestone	0.13	Elf Aquitaine, 1983
Hermrigen-1	1312	Callovian	shale	0.94	Elf Aquitaine, 1983
Hermrigen-1	1476	Bathonian-Bajocian	limestone	0.22	Elf Aquitaine, 1983
Hermrigen-1	1620	Bathonian-Bajocian	limestone	0.08	Elf Aquitaine, 1983
Hermrigen-1	1783	Aalenian	limestone	0.06	Elf Aquitaine, 1983
Hermrigen-1	1882	Pliensbachian	limestone	0.03	Elf Aquitaine, 1983
Hermrigen-1	1893	Lias Alpha	Unknown	0.09	Elf Aquitaine, 1983
Hermrigen-1	1902	Lower Lias	Unknown	0.17	Elf Aquitaine, 1983
Hermrigen-1	1919	Lower Lias	Unknown	0.09	Elf Aquitaine, 1983
Hermrigen-1	1931	Rhetian	Unknown	0.04	Elf Aquitaine, 1983
Hermrigen-1	2259.65	Muschelkalk	Unknown	0.07	Elf Aquitaine, 1983
Hermrigen-1	2275.45	Muschelkalk	Unknown	0.17	Elf Aquitaine, 1983
Thun-1	5222	Upper Jurassic	limestone	0.05	Elf Aquitaine, 1989
Thun-1	5338	Upper Jurassic	limestone	0.05	Elf Aquitaine, 1989
Thun-1	5473	Upper Jurassic	limestone	0.02	Elf Aquitaine, 1989
Thun-1	5610	Upper Jurassic	limestone	0.03	Elf Aquitaine, 1989
Thun-1	5710	Upper Jurassic	limestone	0.16	Elf Aquitaine, 1989
Thun-1	5806	Upper Jurassic	limestone	0.1	Elf Aquitaine, 1989
Thun-1	5836	Upper Jurassic	limestone	0.22	Elf Aquitaine, 1989
Thun-1	5878	Dogger Opalinus	limestone	0.14	Elf Aquitaine, 1989
Thun-1	5912	Dogger Opalinus	Shale	0.5	Elf Aquitaine, 1989

Appendix 9: TOC data measured in the wells Hermrigen-1 and Thun-1

13 Authors short biography

	Dr. Silvia Omodeo Salé has a PhD from the University of Madrid (Spain) and is a Snr Researcher at the University of Geneva in Department of Earth sciences. She is a sedimentologist by background and developed a strong expertise in organic petrography and petroleum system analysis and thermal modelling. She spent more than 15-years in academia in top research centres (Parma, Madrid, Barcelona, Oviedo, Nancy, Potsdam, IFPEN-Rueil Malmaison). Silvia has a large expertise in basin analysis and she develops integrated workflow that maximises the value of organic geochemistry data from source rock, to establish sound petroleum system models, to assist exploration of hydrocarbons and the risk that their occurrence could cause to geothermal and CO2 storage projects.
	Dr. Yasin Makhloufi has a PhD from the Sorbonne University (France) and is Snr Researcher at the University of Geneva in the Department of Earth sciences. He is a carbonate reservoir geologist with 12-years of experience and a reference for carbonate petrography and diagenesis. Yasin has been exposed to critical integrated study and complex project management where subsurface data including core, petrophysics, geochemistry and mineralogy have been integrated with outcrop and used to build a comprehensive understanding of the subsurface. Yasin is specialised in developing integrated workflows, for risk evaluation, using multi criteria analysis, providing a comprehensive approach for VOI evaluation and quantification of exploration risks including CRS mapping. Yasin is also specialised in geodatabase design, architecture framework and management.
	Dr. Ovie Emmanuel Eruteya has a PhD from the University of Haifa (Israel) and is Snr Researcher at the University of Geneva in the Department of Earth sciences. Ovie is global energy geoscientist specializing in the use of subsurface geological and geophysical dataset, for oil and gas exploration, geothermal energy exploration and geological storage. Ovie has 10+ years of experience in several geothermal, CCS and hydrocarbon projects onshore Europe and offshore areas in the eastern Mediterranean, Offshore Norway, Iceland, offshore South Africa, West Africa and western Australia. His expertise spans from time-depth conversion, well to seismic ties, seismic geomorphology, attribute analysis, spectral decomposition and 3D reservoir modelling. Ovie also delivers courses on 2D-3D seismic interpretation, petrophysical analysis and 3D geological modelling.
	Prof. Dr. Andrea Moscariello is Full Professor head of the Geo-Energy / Reservoir Geology and Basin Analysis group at the University of Geneva in the Department of Earth sciences. Andrea is a sedimentologist by background who developed a both reservoir characterization, seismic interpretation and play analysis expertise over 15 years of career spent in the hydrocarbon industry on both development and exploration projects worldwide. Since his appointment at the University of Geneva in 2011, Andrea and his group are carrying out numerous applied and fundamental research projects, focused on the understanding of multi-scale geological processes controlling geo-energy resources generation, accumulation and storage. Andrea provides his expertise on technical boards of geo-energy companies and international organisations such as the World Bank and United Nations.